UC Berkeley
UC Berkeley Electronic Theses and Dissertations

Title

Investigations into the Reactivities of Transition Metal Fluoroalkyl Complexes for the Formation of Fluoroalkylarenes

Permalink

https://escholarship.org/uc/item/85m6n7k1

Author

Kalkman, Eric Daniel

Publication Date

2022

Peer reviewed|Thesis/dissertation

eScholarship.org Powered by the California Digital Library
University of California

Investigations into the Reactivities of Transition Metal Fluoroalkyl Complexes for the Formation of Fluoroalkylarenes

by

Eric Daniel Kalkman

A dissertation submitted in partial satisfaction of the

requirements for the degree of

Doctor of Philosophy

in

Chemistry

in the

Graduate Division

of the

University of California, Berkeley

Committee in Charge:
Professor John F. Hartwig, Chair
Professor F. Dean Toste
Professor Alexis Bell

Spring 2022

Abstract

Investigations into the Reactivities of Transition Metal Fluoroalkyl Complexes for the Formation of Fluoroalkylarenes

by

Eric Daniel Kalkman

Doctor of Philosophy in Chemistry

University of California, Berkeley

Professor John F. Hartwig, Chair

The following Dissertation discusses mechanistic investigations into reactions of organometallic complexes that contain fluoroalkyl ligands. In particular, this work focuses on elucidating electronic and stereochemical effects of cross-coupling reactions in which the aforementioned complexes are putative intermediates.

Chapter 1 reviews the reactivities of fluoroalkylcopper and -palladium complexes involved in cross-coupling reactions with a focus on the formation of fluoroalkylarenes. Common challenges encountered in fluoroalkylation reactions are discussed in the context of the fundamental reactivity of intermediate fluoroalkyl complexes, and mechanistic insights into these systems are collected and summarized. Areas in need of further study are highlighted, and the author's recommendations for the development of new metal-mediated fluoroalkylation reactions are provided.

Chapter 2 describes mechanistic investigations into the unprecedented electronic effect of ancillary bipyridine ligands on the copper-mediated pentafluoroethylation of aryl halides. A survey of electronically varied bipyridine ligands revealed that reactions of complexes containing less electron-donating bipyridine ligands proceeded faster than those of complexes containing more electron-donating bipyridine ligands. Kinetic and computational studies revealed that this effect is due a difference in rate of oxidative addition of the aryl halide to the pentafluoroethylcopper center.

Chapter 3 describes investigations into the origins of enantioselectivity of the palladium-catalyzed asymmetric α-arylation of 3-fluorooxindoles. The putative intermediate diastereomeric arylpalladium fluoroenolate complexes were independently synthesized and characterized, and upon heating yielded arylated 3-fluorooxindoles in high yields with enantioselectivities that matched those of the corresponding catalytic reactions.

Chapter 4 describes preliminary investigations into the development of a palladium-catalyzed trifluoromethylation of aryl bromides. Side-reactions of the sole reported palladium-catalyzed trifluoromethylation of aryl chlorides were examined, and new ancillary phosphine ligands were evaluated for their ability to promote the challenging transmetallation and reductive elimination steps of the reaction. Trifluoromethylcopper reagents also were evaluated as sources of nucleophilic CF_3, and in most cases were found to undergo exchange of ancillary ligands with the Pd center, resulting in the formation of aryl(trifluoromethyl)palladium species that were unable to undergo reductive elimination to form trifluoromethylarene.

Chapter 5 describes computational investigations into the reductive elimination of fluoroalkylarenes from aryl(fluoroalkyl)palladium complexes. Complexes containing more electron-withdrawing fluoroalkyl ligands generally were calculated to have higher barriers to reductive elimination than complexes containing less electron-withdrawing fluoroalkyl ligands. However, complexes containing the fluoroalkyl ligands -CF_2CN and -CF_2Ph were calculated to have lower barriers to reductive elimination than expected based on the electronegativities of these fluoroalkyl ligands. IGMH and NBO analyses revealed that these complexes were stabilized in the transition state by interactions with the filled *d* orbitals of the Pd center and the π^* orbitals of the CN or Ph fragments of the CF_2CN or CF_2Ph ligands, respectively. Deletion of these interactions by NBO analysis reestablished the trend that complexes containing more electronegative fluoroalkyl ligands underwent reductive elimination with higher barriers than complexes containing less electronegative fluoroalkyl ligands (adjusted barriers for $CF_2CN > CF_3 > CF_2Ph > CF_2H > CFH_2 > CH_3$).

Table of Contents

Chapter 1. **Copper and Palladium Fluoroalkyl Complexes in the Formation of Fluoroalkylarenes** 1

1.1 Introduction 2
1.2 Complexes of Copper 3
1.2.1 Perfluoroalkylcopper(I) Complexes 3
1.2.1.1 Trifluoromethylcopper(I) Complexes Not Containing Ancillary Ligands 4
1.2.1.2 Higher Perfluoroalkylcopper(I) Complexes Not Containing Ancillary Ligands 9
1.2.1.3 Perfluoroalkylcopper(I) Complexes Containing Ancillary Ligands 10
1.2.2 Difluoromethylcopper(I) Complexes 12
1.2.3 Fluoroalkylcopper(I) Complexes of Carboxylic Acid Derivatives 14
1.2.4 Other Fluoroalkylcopper(I) Complexes 16
1.2.5 Fluoroalkylcopper(III) Complexes 17
1.3 Complexes of Palladium 20
1.3.1 Perfluoroalkylpalladium(II) Complexes 20
1.3.1.1 Trifluoromethylpalladium(II) Complexes Containing Diphosphine Ligands 21
1.3.1.2 Perfluoroalkylpalladium(II) Complexes Containing Monophosphine Ligands 25
1.3.2 Pd^{II}–CF_2R and Pd^{II}–CFRR' Complexes 29
1.3.2.1 Difluoromethylpalladium(II) Complexes 29
1.3.2.2 Other Pd^{II}–CF_2R and Pd^{II}–CFRR' Comoplexes 35
1.3.3 Pd=CF_2 Complexes 37
1.3.4 Palladium(IV) Complexes 39
1.4 Outlook on Cu- and Pd-Mediated Fluoroalkylation Reactions 41
1.4.1 Cu-Mediated Fluoroalkylation Reactions 41
1.4.2 Pd-Mediated Fluoroalkylation Reactions 43
1.5 References 45

Chapter 2. **Unusual Electronic Effects of Ancillary Ligands on the Perfluoroalkylation of Aryl Iodides and Bromides Mediated by Copper(I) Pentafluoroethyl Complexes of Substituted Bipyridines** 58

2.1 Introduction 59
2.2 Preparation of Bipyridine-Ligated Pentafluoroethylcopper(I) Complexes 60
2.3 Reactivity of Bipyridine-Ligated Pentafluoroethylcopper(I) Complexes with Aryl Halides 61

2.4 Computational Investigations into the Origin of the Electronic Effect of the Ancillary Ligand 66
2.5 Conclusion 68
2.6 Footnotes 68
2.7 Supplementary Experimental Information 69
2.8 References 115

Chapter 3. Direct Observation of Diastereomeric *α*-C-Bound Enolates during Enantioselective *α*-Arylations: Synthesis, Characterization, and Reactivity of Arylpalladium Fluorooxindole Complexes 120

3.1 Introduction 121
3.2 Synthesis and Reactivity of (*S*)-SEGPHOS-Ligated Arylpalladium Fluorooxindole Complexes 122
3.3 Analysis of the Electronic Effect of the Eliminating Aryl Ligand 125
3.4 Computational Modeling and the Origins of Enantioselectivity 127
3.5 Kinetic Analysis of the Catalytic Reaction 131
3.6 Conclusions 134
3.7 Footnotes 135
3.8 Supplementary Experimental Information 135
3.9 References 191

Chapter 4. Investigations into the Formation, Speciation, and Reactivity of Aryl(trifluoromethyl)palladium Complexes toward the Development of a Robust Palladium-Catalyzed Trifluoromethylation of Aryl Bromides 197

4.1 Introduction 198
4.2 Investigations of the Trifluoromethylation of Aryl Halides Catalyzed by Pd Complexes Containing BrettPhos 200
4.3 Investigations of Other Ligand Scaffolds 205
4.4 Trifluoromethylcopper Reagents as Sources of Nucleophilic CF_3 210
4.5 Conclusions 213
4.6 Footnotes 214
4.7 Supplementary Experimental Information 214
4.8 References 268

Chapter 5. Computational Studies of the Electronic Effects of the Participating Ligands on the Reductive Elimination of Fluoroalkylarenes from Several Aryl(fluoroalkyl)palladium Complexes 273

5.1 Introduction 274
5.2 Results and Discussion 274
5.3 Conclusions 281

5.4 Footnotes 281
5.5 Computational Methods 282
5.6 Optimized Structures and Energies 282
5.7 References 363

Acknowledgements

It is an honor to be receiving a PhD from UC Berkeley, and I would like to highlight some of the people that have supported me throughout my journey towards this distinction. First and foremost, I must thank my parents Dan and Lisa Kalkman. Since my childhood, they have tirelessly fostered my desire to learn about the natural world, with topics ranging from meteorology to microbiology to, of course, chemistry. The love, stability, and financial support that they have provided, though perhaps not appreciated at the time and likely still underappreciated now, are the foundation upon which my entire education has been based. I must also thank my late grandparents Daniel Brott and Donald and Rosemary Kalkman, who all sadly passed away within the last year, but who were always thrilled to hear about the latest nonsense that I'd gotten up to. Grandma and Grandpa Brott, as teachers and researchers themselves, also have always encouraged my curiosity about all types of green things around me.

In terms of scholarly support, I must thank all the teachers and mentors who set me on this path. In particular, thank you to Jennifer Caskey, whose chemistry and physics classes set me up for higher study; Professor David Blank, who helped me navigate curricula for two majors and subsequent career paths; Professor Tom Hoye, who sparked my interest in organic chemistry research and the wonders of NMR spectroscopy; and Professor Ian Tonks and my "overgrad" Dr. Abby Smith, who not only gave me the opportunity to explore academic research and organometallic chemistry, but who also encouraged me to "go big" when applying for graduate school. I do not exaggerate when I say that my life would have gone in any number of different directions without their influences.

Of course, I must also thank my PhD advisor Professor John Hartwig for his mentorship. The sheer wealth of knowledge and experience that John brings to any discussion, while in some cases terrifying, has been foundational in my development as a chemist, as a teacher, and as a scientific communicator. The rigor and no-nonsense skepticism that he fosters have kept me grounded (or at least, more grounded than not) in my studies, and have become central to how I approach problems. While certain global events haven't been especially conducive to academic research or teaching, John's careful considerations of all group members and the resources available have maintained a productive and educational laboratory environment. For this, I am sincerely grateful.

I also would like to thank the amazingly intelligent and talented members of the Hartwig group, both past and present, for making it such a great place to work. In particular, I am grateful to Drs. Taegyo Lee and Chen Cheng, who mentored me while I was working as an undergraduate scholar in John's lab as part of the Amgen program; Dr. Mike Mormino, who has been extremely helpful from the beginning in navigating graduate school and fluoroorganometallic chemistry, and who always has a dry quip ready; Dr. Trevor Butcher, whose wide knowledge of organic chemistry and enthusiasm for cute molecules have made for invaluable and entertaining discussions; Dr. Steven Hanna, for offering kind and down-to-earth advice on both my chemistry and graduate school; my yearmate Brandon Boomer, for chemical discussions and solid friendship, and for often silly yet still earnest and profound insights; Dr. Masha Elkin, who gave solid advice for job applications and interviews and has tolerated my embarrassingly frequent questions about named reactions; and Dr. Connor Delaney, who shares my delight for mechanistic edge cases and can always be counted on for helpful discussions speculating what is *actually* going on in a reaction. I would also like to thank the past and present denizens of 702 Latimer for the constant dialogue on Making the Chemistry Work and for tolerating my histrionics when it often did not: Drs. Taegyo

Lee, Matt Peacock, Yumeng Xi, and Alex Fawcett (sorry, I still don't have any good suggestions for incorporating drones into synthetic chemistry), and current students Jason Ma, Isaac Yu, and Jenna Manske. Finally, thank you to everyone whom I've come up to with a vial and asked, "what color is this?" for being patient with me. Colors are hard.

Thank you to Hasan Celik for maintaining our NMR facility, for always being willing to discuss the best way to take advantage of the facility's capabilities, for always being available to debug problems with the instruments, and for the miraculously high success rate for getting grants funded. Thank you as well to Dave Small and Kathy Durkin at the MGCF for ready advice on methods, functionals, and further capabilities to computationally explore my synthetic transformations. Without the resources that these people have provided, many of the results of this Dissertation would only have been won after much greater difficulty, or not at all.

Finally, thank you to the College of Chemistry for administering the work environment. While my graduate career has had its ups and downs, Latimer Hall has been an often-unexpected source of vertical stability. For this, I am duly grateful.

Chapter 1

Copper and Palladium Fluoroalkyl Complexes in the Formation of Fluoroalkylarenes

1.1 Introduction

The construction of fluorinated organic molecules is a topic of immense interest, especially for the development of biologically active molecules, such as pharmaceuticals and agrochemicals.[1–10] However, most fluorine-containing organic molecules are produced on large scales industrially under harsh reaction conditions or with toxic reagents, such as the strongly acidic reaction of trichloromethylarenes with HF to form trifluoromethylarenes in the Swarts processs.[11–14] Such reaction conditions are incompatible with a wide range of functional groups, and thus fluorinated moieties are often incorporated into molecules at early stages of the synthesis from fluorinated building blocks. The development of mild, selective, and functional-group-tolerant methods for the introduction of fluorinated moieties allows for installation at later stages of the synthesis. These factors allow for the rapid preparation of many variants of the target molecule during, *e.g.*, drug discovery.

To this end, cross coupling reactions catalyzed by transition-metal complexes, especially those of Pd or Cu, have become an invaluable tool for the selective incorporation of fluoroalkyl motifs into organic molecules and have expanded access significantly to fluorine-containing aromatic compounds.[13,15,16] However, fluoroalkyl ligands often impart reactivity (or a lack thereof) to the putative organometallic intermediates that is different from that of their non-fluorinated counterparts. Complexes containing fluoroalkyl ligands in many cases are less reactive than analogous complexes containing non-fluorinated alkyl ligands.[13,17–19] Representative examples of this lower reactivity include a) oxidative addition of CH_3I to *trans*-$(P(CH_3)_2(C_6H_5))_2Pt(R)(I)$ proceeding more readily than oxidative addition of CF_3I;[20,21] b) facile insertion of CO into the Mn–C(sp^3) bond of $Mn(CO)_5(CH_3)$ to form $Mn(CO)_5(C(O)CH_3)$, but a lack of insertion of CO into the analogous bond in $Mn(CO)_5(CF_3)$, even at elevated temperatures and pressures of CO;[22] and c) more facile reductive elimination from arylpalladium α-fluoroenolate complexes containing a lower degree of fluorination at the α-carbon than from complexes containing a higher degree of fluorination at the same carbon.[23] Overall, fluoroalkylmetal complexes appear to follow the general trend in organometallic chemistry that metal–carbon bonds containing more electron-poor carbon atoms are more stable than those containing more electron-rich carbon atoms. Despite their electron-withdrawing nature, however, perfluoroalkyl ligands remain strong σ-donors.[13] In fact, the *trans* influence of CF_3, C_2F_5, and *n*-C_3F_7 ligands were shown to be comparable to that of CH_3 or Ph ligands in related complexes.[18,19,24–26] The high stability of metal–R^F bonds (R^F = fluoroalkyl) and the strong σ-donation of fluoroalkyl ligands have been cited as reasons for the sluggish reactivity of organometallic intermediates in cross-coupling reactions and the high stability of high-valent copper, palladium, and silver complexes containing fluoroalkyl ligands.[13]

However, the stability of a metal–R^F bond does not necessary imply the stability of the metal complex as a whole. For example, a common pathway for the decomposition of fluoroalkylmetal complexes, especially trifluoromethylmetal complexes, is the decomposition of the fluoroalkyl ligand into a carbenoid species and a metal fluoride *via* intra- or intermolecular α-fluoride elimination.[13,18,19,27] Especially for complexes of late transition metals with occupied *d* orbitals, α-elimination can occur readily due to stabilization of the resulting carbene *via* π back-bonding and is promoted by hard Lewis acids like H^+, Li^+, or SbF_5.[27] The resulting carbene can undergo a variety of insertion reactions to form, *e.g.*, higher fluoroalkyl homologues or undergo further decomposition. The stability of the metal–R^F bond and the potential instability of the complex to salt additives present two competing challenges for the development of fluoroalkylation reactions catalyzed by transition-metal complexes.

This Chapter reviews the reactivities of copper (Section 1.2) and palladium (Section 1.3)

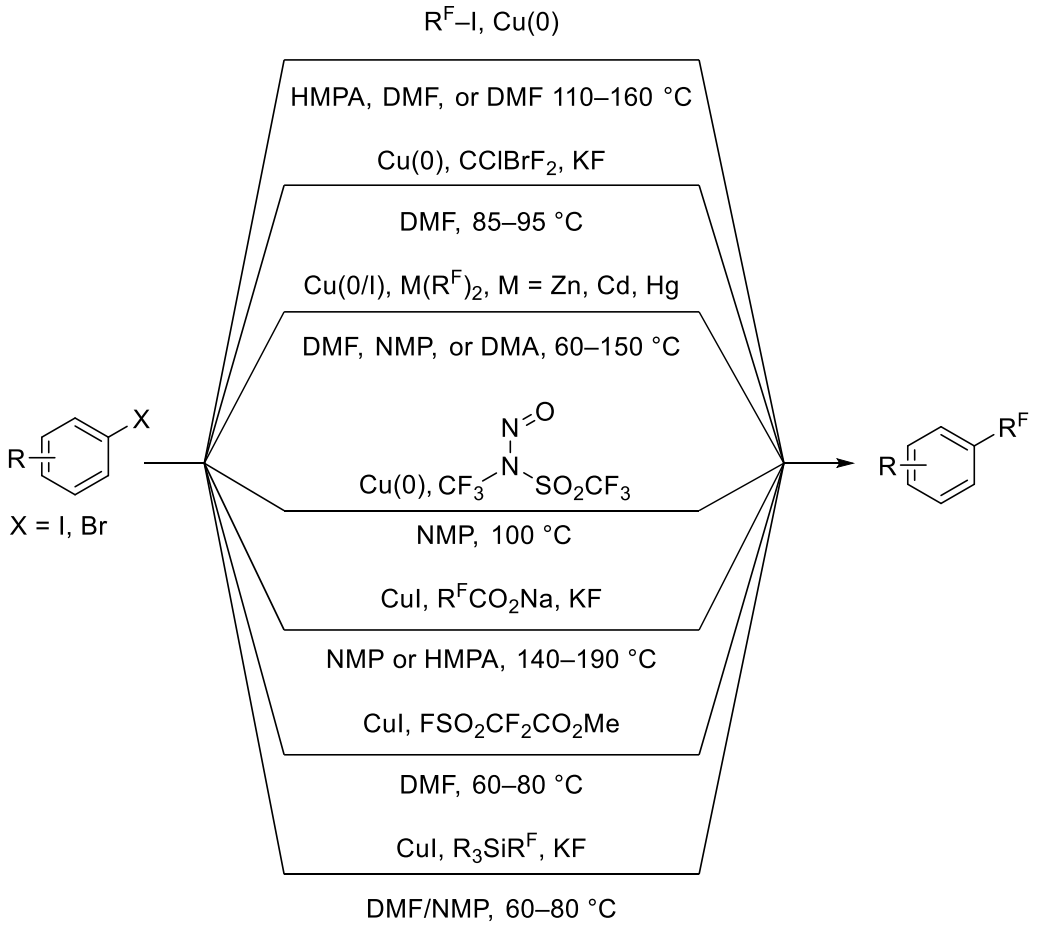
complexes containing fluoroalkyl ligands that function either as intermediates along a putative catalytic route or as reagents in their own right for the formation of fluoroalkylarenes. Special attention is paid to trends in the reactivity of these complexes along both productive and non-productive pathways, as well as to challenges in the development of fundamental reactions into useful synthetic methods. These two metals were chosen at the exclusion of others due to their prevalence in fluoroalkylation reactions and their relevance to the other Chapters of this dissertation. While recent reports considering the reactivity of complexes of Ni and Au are extremely important towards the development of useful synthetic methods, they are nonetheless beyond the scope of this Dissertation.

1.2 Complexes of Copper

Fluoroalkylation reactions either mediated or catalyzed by copper(I) complexes constitute the majority of metal-mediated fluoroalkylations of arenes. The greatest focus in the literature has been placed on developing methods for trifluoromethylation. Few studies have probed the putative fluoroalkylcopper intermediates. This Section focuses on fluoroalkylation reactions for which the identification and reactivity of fluoroalkylcopper intermediates have been reported.

1.2.1 Perfluoroalkylcopper(I) Complexes

Copper(I)-mediated perfluoroalkylation reactions comprise the majority of metal-mediated fluoroalkylation reactions.[13] These reactions can be traced to the pioneering work of McLoughlin and Thrower[28] and later Kobayashi,[29] who reported methods to generate solutions of putative Cu–R^F species (including R^F = CF_3, C_3F_7, C_7F_{15}) from the corresponding perfluoroalkyl iodides and copper bronze in DMSO or DMF. While the perfluoroalkylcopper complexes were not rigorously characterized, the authors demonstrated that solutions of the putative perfluoroalkylcopper species constituted stable reagents for the perfluoroalkylation of aryl iodides among many other organic electrophiles. In refluxing DMSO, these compounds were shown to liberate perfluoroalkyl radicals that reacted with arenes to form the corresponding perfluoroalkylarenes.[30] Other early examples of the formation of putative perfluoroalkylcopper species for the perfluoroalkylation of haloarenes include reduction of $Hg(CF_3)_2$[31] or an *N*-nitrosylsulfonamide[32] with copper metal, decarboxylation of perfluorocarboxylate salts in the presence of CuX,[33,34] transmetallation from perfluoroalkylzinc or -cadmium reagents[35,36] or organosilanes[37] to copper(I) halides, and decarbonylation/desulfonylation of $FSO_2CF_2CO_2CH_3$[38] (Scheme 1.2.1). Commonalities among all methods are the application of polar aprotic solvents and hierarchical reactivities of different classes of aryl halides in these systems (ArI > ArBr >> ArCl). In general, copper-mediated perfluoroalkylation reactions of aryl halides only proceed in high yields for aryl iodides and electron-poor aryl bromides. Reactions of perfluoroalkylcopper(I) reagents with other organic substrates have been reviewed elsewhere.[13,15,39–41]

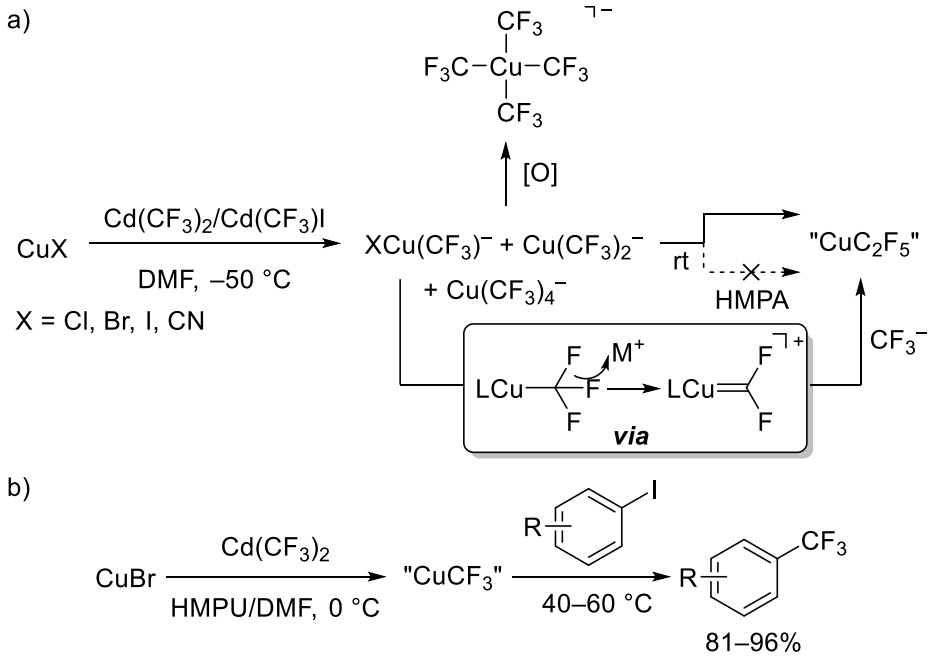


Scheme 1.2.1 Conditions for generating putative perfluoroalkylcopper species for the formation of perfluoroalkylarenes

1.2.1.1 Trifluoromethylcopper(I) Complexes Not Containing Ancillary Ligands

Many of the perfluoroalkylcopper complexes involved in trifluoromethylation reactions are generated *in situ* from the combination of commonly available copper(I) complex and various sources of nucleophilic equivalents of CF_3. These reagents are characterized by the formation of anionic cuprates, especially the heteroleptic cuprate $XCu(CF_3)^-$ containing the X ligand of the CuX precursor. Burton and co-workers were the first to explore the speciation of these reagents by NMR spectroscopy. Trifluoromethylcopper species were generated by the treatment of CuX salts (X = Cl, Br, I, CN) at –50 °C in DMF solution with a mixture of $Cd(CF_3)_2$ and $Cd(CF_3)X$ (X = Cl or Br) and formed trifluoromethylarenes from aryl iodides in good yields (Scheme 1.2.2).[36] ^{19}F NMR spectroscopy revealed the formation of a single new trifluoromethylcopper species (–28.8 ppm), which upon warming to room temperature partially converted into two other trifluoromethylcopper species (–32.3 and –35.4 ppm), as well as a pentafluoroethylcopper species.[36,42] The pentafluoroethylcopper species was the sole perfluoroalkylcopper species present in solution after 11 h at room temperature and was proposed to form by α-fluoride elimination from $Cu–CF_3$. The addition of HMPA to the mixture before warming forestalled this decomposition. Of the three trifluoromethylcopper species, the one initially formed at –50 °C was proposed to be the species that reacted with aryl iodides to form trifluoromethylarenes based on the rapid consumption of this species in trifluoromethylation reactions. The authors later proposed that the active species was

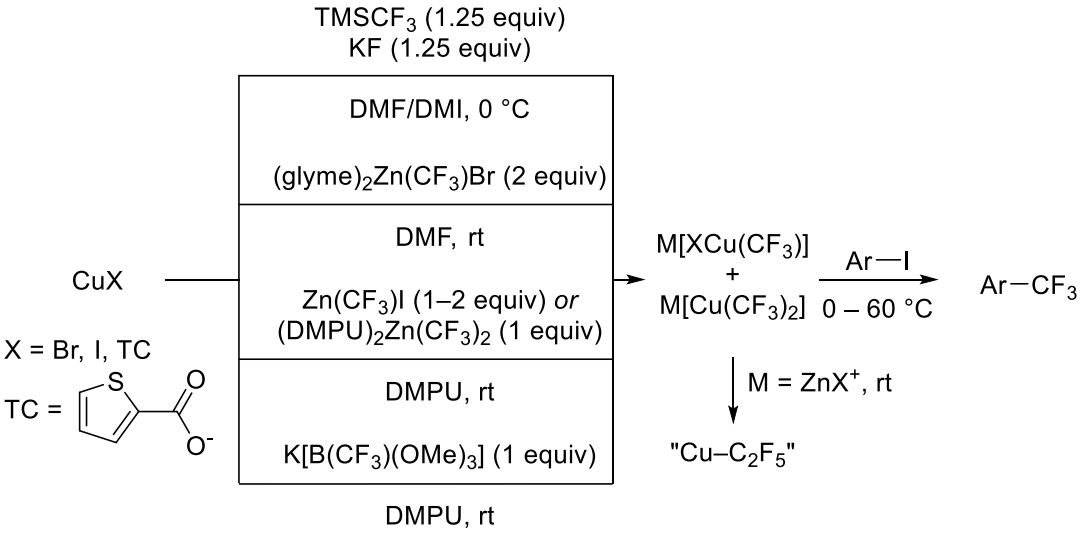
$Cu^{I}(CF_3)X^-$ (X = halide) and that the other two resonances in the NMR spectrum corresponded to $Cu^{I}(CF_3)_2^-$ (–32.3 ppm) and $Cu^{III}(CF_3)_4^-$ (–35.4 ppm).[43] It was demonstrated further that $Cu(CF_3)_2^-$ oxidized to Cu(III) species in the presence of oxygen, elemental halogens, or disulfiram ($[Et_2NC(S)S]_2$).[43,44]



Scheme 1.2.2 Generation of trifluoromethylcopper species from $Cd(CF_3)_2$ and subsequent reactivity

Kolomeitsev,[45] Kremlev[46] and Mikami,[47,48] and Gooßen[49] have since characterized by NMR spectroscopy similar trifluoromethylcopper species formed by the treatment of copper(I) salts with sources of nucleophilic CF_3 (Scheme 1.2.3). In addition to the trifluoromethylcadmium reagents discussed above, the trifluoromethylzinc reagents $(glyme)Zn(CF_3)Br\cdot(DMF)$,[46] "$Zn(CF_3)I$",[47] and $(DMPU)Zn(CF_3)_2$[48] all generated organocopper reagents that formed pentafluoroethylcopper species gradually upon standing at room temperature for several hours. In contrast, the trifluoromethylcopper reagent generated from $K[B(CF_3)(OMe)_3]$ did not form pentafluoroethylcopper species under similar conditions.[49] Overall, trifluoromethylcopper species generated from group 12 trifluoromethylmetal reagents appear especially prone to decomposition to pentafluoroethylcopper species, possibly facilitated by the Lewis acidity of the zinc halide byproducts of transmetallation. Regardless of the method of generation, all of the trifluoromethylcopper reagents facilitated the trifluoromethylation of aryl iodides at mild temperatures (ambient to 60 °C), which were proposed to occur through reactions with the heteroleptic cuprate $XCu(CF_3)^-$ (though recent work by Shen has contested this assertion; *vide infra*).[50] However, none of these studies reported the trifluoromethylation of aryl bromides or chlorides. Because none of the homoleptic cuprate $Cu(CF_3)_2^-$ remained after reactions with aryl halides, it was proposed to serve as a reservoir of "$Cu(CF_3)$" in equilibrium with the heteroleptic cuprate. Of the sources of nucleophilic CF_3 for the generation of Cu–CF_3 species, only $(DMPU)_2Zn(CF_3)X$ (X = Br, I) has been incorporated into a trifluoromethylation reaction catalytic in copper without also including an ancillary ligand (most catalytic methods require an ancillary

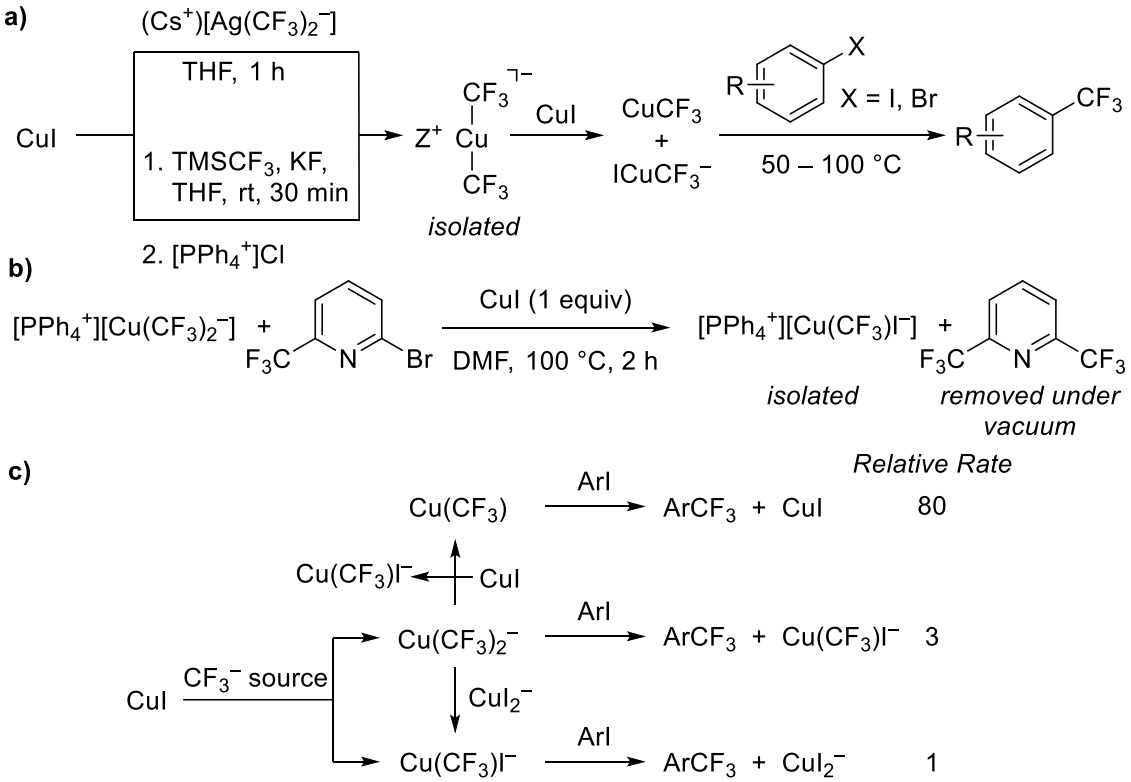
ligand; *vide infra*).[46,47,47]



Scheme 1.2.3 Other methods shown to generate $XCu(CF_3)^-$ and $Cu(CF_3)_2^-$ from copper(I) salts

Reports by Vicic[15,51,52] and more recently Pérez-Temprano[53] and Shen[50,54] have sought to explore the roles of the hetero- and homoleptic cuprates $XCu(CF_3)^-$ (X = halide) and $Cu(CF_3)_2^-$ in trifluoromethylation reactions derived from "CF_3^-" and copper(I) halide salts. In back-to-back reports in 2019, Pérez-Temprano and Shen independently reported for the first time the isolation of $[Z^+][Cu(CF_3)_2^-]$ (Z = Cs,[53] PPh_4[54]) by treating copper(I) halides with either $(Cs^+)[Ag(CF_3)_2^-]$[53] or a large excess of $TMSCF_3$ and KF followed by salt metathesis with PPh_4Cl (Scheme 1.2.4a).[54] Both groups found that, in agreement with previous proposals, $Cu(CF_3)_2^-$ reacted sluggishly with aryl iodides, and that the addition of CuI greatly accelerated the reaction, presumably through the formation of $ICu(CF_3)^-$ and the much more reactive "ligandless" $Cu(CF_3)$ species (*vide infra*). To complete the analysis, Shen reported in 2021 a deep mechanistic investigation into the trifluoromethylcopper species involved in CuX-mediated trifluoromethylation reactions. As part of this work, Shen isolated for the first time the heteroleptic cuprate $[PPh_4^+][Cu(CF_3)I^-]$ (Scheme 1.2.4b) and showed through a set of kinetic experiments and comparisons to reactions containing $[PPh_4^+][Cu(CF_3)_2^-]$ and $[NBu_4^+][CuI_2]$ that the rate of reaction of aryl iodide with $[PPh_4^+][Cu(CF_3)I^-]$ was *slower* than the reaction of aryl halide with $[PPh_4^+][Cu(CF_3)_2^-]$. The rate of reaction of aryl iodide with "ligandless" $Cu(CF_3)$ was more than 20 times faster than reactions with either cuprate. This result contrasts the aforementioned proposals about the species that reacts with the aryl halide, particularly those claiming the innocence of the homoleptic cuprate. For reactions of trifluoromethylcopper species generated from copper(I) halides and nucleophilic CF_3, the authors proposed instead that a) the presence of excess copper(I) halide facilitated the formation of the active "ligandless" $Cu(CF_3)$ species from the cuprates and b) in cases where all of the CuX precursor was converted completely to cuprate species, the reaction with $Cu(CF_3)_2^-$ with the aryl halide predominated. A summary of Shen's mechanistic conclusions is shown in Scheme 1.2.4c, highlighting the complex interplay between the different copper species.

To identify more economical sources of fluoroalkylcopper reagents, Grushin reported several studies aimed at the generation of perfluoroalkylcopper species *via* deprotonation of the corresponding $C_nF_{2n+1}H$ compounds and conducted detailed mechanistic investigations of perfluoroalkylation reactions involving these reagents (Scheme 1.2.5).[41,55–57] The authors found

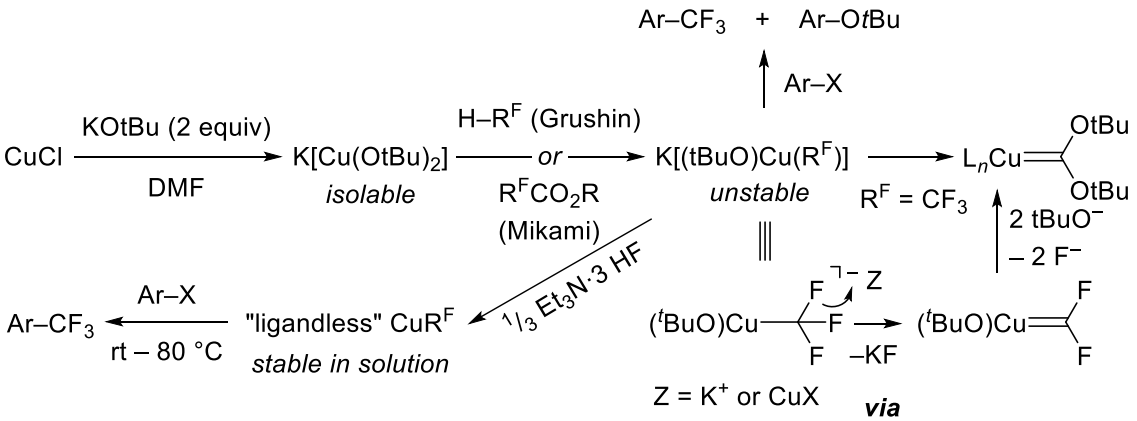


Scheme 1.2.4 a) Syntheses of $[Z^+][Cu(CF_3)_2^-]$ for isolation (Z = Cs, PPh_4); b) Synthesis of $[PPh_4^+][Cu(CF_3)I^-]$; c) Summary of the mechanism for the Cu-mediated trifluoromethylation of aryl halides

that $K[Cu^I(OtBu)_2]$ was sufficiently basic to deprotonate CHF_3 (Scheme 1.2.5) or CHF_2CF_3 in DMF solution to form the heteroleptic cuprates (*t*BuO)CuR^{F-} (R^F = CF_3, C_2F_5). Identical species were accessed by treating $K[Cu(OtBu)_2]$ with 2,2,2-trifluoroacetophenone[58] or ethyl pentafluoropropionate,[59] although neither of these routes led to perfluoroalkylcopper species containing heavier perfluoroalkyl homologues than C_2F_5. In contrast to the aforementioned heteroleptic cuprates containing halides, the cuprates (tBuO)CuR^{F-} facilitated the perfluoroalkylation of aryl halides in many cases at room temperature, although the formation of aryl ether also was observed due to competitive coupling with the O*t*Bu$^-$ moiety. (*t*BuO)$Cu(CF_3)^-$ decomposed upon standing *via* *α*-fluoride elimination pathways over several hours, while (*t*BuO)$Cu(C_2F_5)^-$ was stable for days at room temperature, demonstrating the higher stability of pentafluoroethyl complexes toward *α*-fluoride elimination. However, treatment of the heteroleptic cuprates with $Et_3N{\cdot}3$ HF formed neutral CuR^F species lacking any X-type ligand and presumably coordinated only by DMF solvent. Reactions of a wide range of aryl iodides with 1.2–2 equivalents of these "ligandless" perfluoroalkylcopper species in most cases led to nearly quantitative yields of perfluoroalkylarene at room temperature. Trifluoromethylation of activated aryl bromides (*e.g.*, 2-bromopyridines and arenes with carboxylate groups at the *ortho* position) using "ligandless" $Cu(CF_3)$ also proceeded in high yields with gentle heating (50–80 °C), although yields were usually lower than those from reactions of aryl iodides and were limited by the instability of the reagent to the CuBr byproduct.[41,60] Even a few examples of very electron-poor aryl chlorides underwent trifluoromethylation, albeit in low yields.

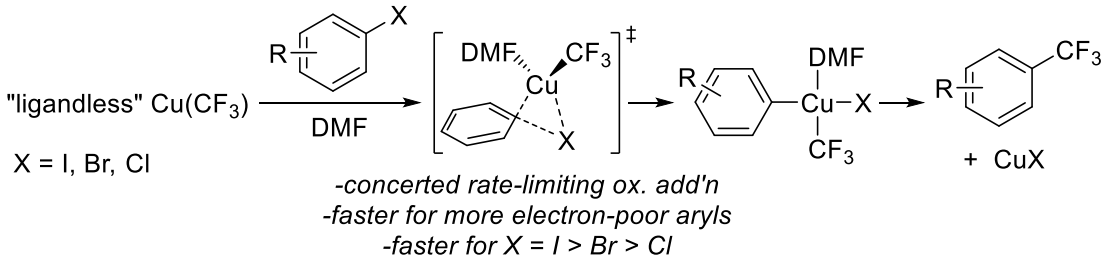
Grushin[57] and Mikami[59] later reported that the reaction of aryl bromides with the analogous

"ligandless" Cu(C_2F_5) gave high yields of electron-rich and electron-poor pentafluoroethylarenes from reactions at remarkably mild temperatures (50–90 °C). This method is one of few to convert an aryl bromide into a perfluoroalkylarene with Cu.[61] Overall, these "ligandless" perfluoroalkylcopper reagents enabled the perfluoroalkylation of haloarenes with a larger scope under milder conditions than any other copper-mediated or -catalyzed method.



Scheme 1.2.5 Synthesis and stability of "ligandless" perfluoroalkylcopper(I) species

Grushin also has conducted mechanistic investigations on trifluoromethylation reactions enabled by "ligandless" Cu(CF_3) (Scheme 1.2.6).[41] Radical clock and kinetic experiments, as well as DFT calculations, suggested that the rate-limiting step in the reaction was a concerted oxidative addition to (DMF)Cu(CF_3) to form the corresponding copper(III) species (DMF)Cu(CF_3)(aryl)X, consistent with the higher temperatures required for aryl bromides and chlorides compared to aryl iodides. DFT calculations further suggested the energetic barrier to oxidative addition of iodobenzene to Cu$(CF_3)_2^-$ was significantly higher than that to the solvent-coordinated "ligandless" species (28.1 kcal/mol *vs* 21.9, respectively), consistent with claims by Vicic,[15,51,52] Pérez-Temprano,[53] and Shen[50,54] that the homoleptic cuprate Cu$(CF_3)_2^-$ is not the species that reacted with the aryl halide (*vide supra*). The authors also observed that trifluoromethylation reactions of more electron-poor aryl iodides proceeded with faster rates than reactions of more electron-rich aryl iodides. A Hammett study revealed that the relative rates of these reactions exhibited a strong positive correlation with the σ_p^- substituent parameter, suggesting an accumulation of resonance-stabilized negative charge on the aryl fragment in the transition state. These findings are consistent with the long-proposed rate-limiting oxidative addition of aryl halide to the trifluoromethylcopper species.



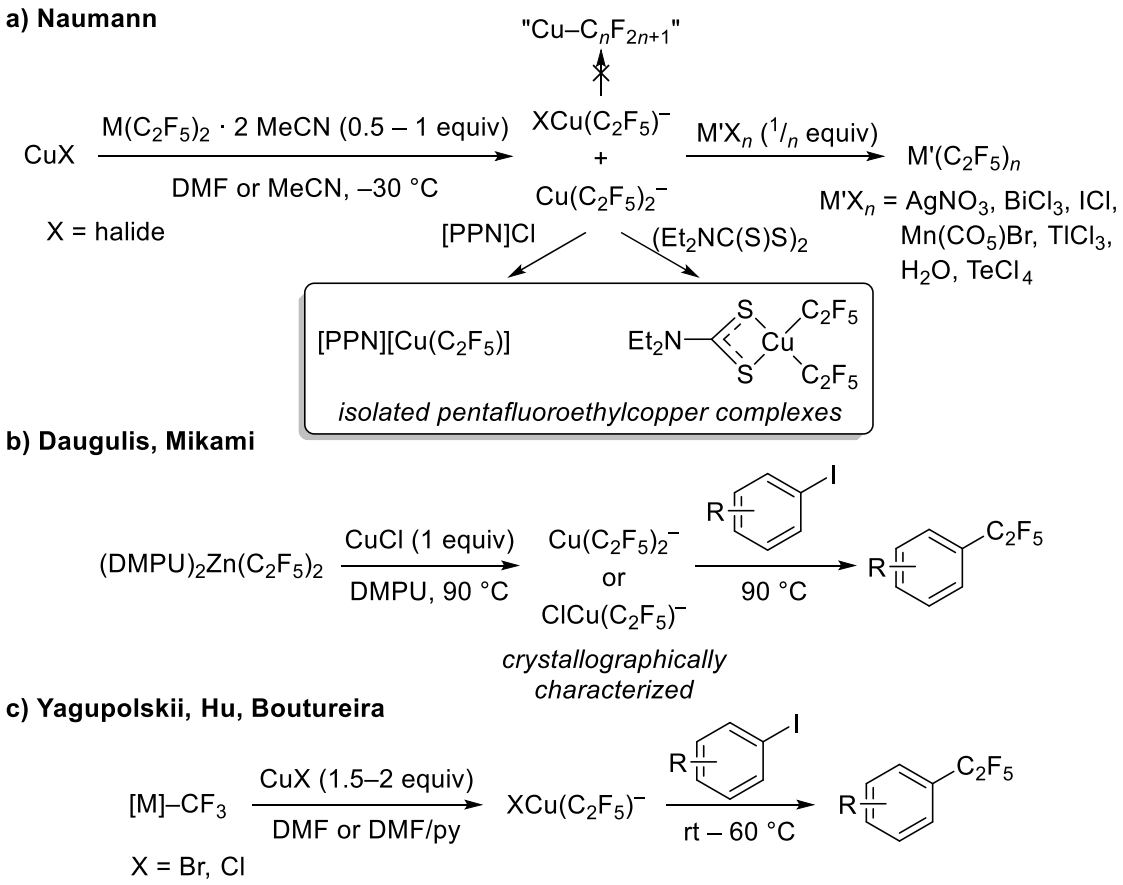
Scheme 1.2.6 Mechanism of the trifluoromethylation of aryl halides mediated by "ligandless" Cu(CF_3)

1.2.1.2 Higher Perfluoroalkylcopper(I) Complexes Not Containing Ancillary Ligands

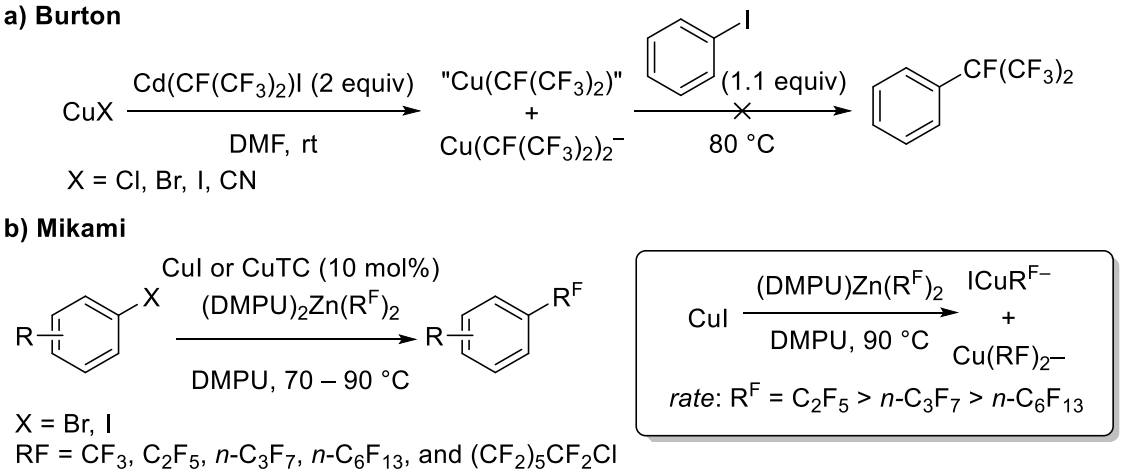
Preparations of analogous perfluoroalkylcopper(I) containing perfluoroalkyl homologues of trifluoromethyl in most cases rely on reactions with group 12 pentafluoroethylmetal complexes or by the reaction of copper(0) with the corresponding iodoperfluoroalkanes.[28,29] Inspired by Burton's work with trifluoromethylcadmium species, Naumann and co-workers first prepared pentafluoroethylcopper reagents *via* the reaction of $M(C_2F_5)_2 \cdot 2\,CH_3CN$ (M = Cd, Zn) with copper(I) halides in DMF at –30 °C and characterized them spectroscopically (Scheme 1.2.7a).[62] The pentafluoroethyl analogs of the trifluoromethylcuprates $XCu(CF_3)^-$ and $Cu(CF_3)_2^-$ discussed above, $XCu(C_2F_5)^-$ and $Cu(C_2F_5)_2^-$, were identified by ^{19}F NMR spectroscopy. However, unlike the Cu–CF_3 species, the Cu–C_2F_5 species did not undergo decomposition to heavier perfluoroalkylcopper species (*e.g.*, Cu–*n*-C_3F_7) upon standing in solution at room temperature, demonstrating the greater resilience of heavier perfluoroalkylmetal species toward α-fluoride elimination. The authors also isolated $Cu(C_2F_5)_2^-$ as its PPN salt, characterized this species crystallographically, and showed that it could transfer a C_2F_5 group to a variety of inorganic electrophiles. Direct oxidation of this salt with disulfiram formed the air-stable copper(III) complex $(edtc)Cu(C_2F_5)_2$ (edtc = $SC(S)NEt_2$), although oxidation with O_2 simply formed C_4F_{10}.

While Naumann did not report reactions of the pentafluoroethylcopper reagents with organic electrophiles, others have shown that these reagents enable the pentafluoroethylation of aryl halides in high yields. Daugulis[63] and Mikami[48] showed that Cu–C_2F_5 reagents generated from $(DMPU)_2Zn(C_2F_5)_2$ and CuX (X = I, Cl) enabled the pentafluoroethylation of model aryl iodides (Scheme 1.2.7b). Daugulis further elucidated the structure of the heteroleptic cuprate $ClCu(C_2F_5)^-$ by single-crystal X-ray diffraction and confirmed Naumann's spectroscopic assignments of $XCu(C_2F_5)^-$ and $Cu(C_2F_5)_2^-$. In a separate approach, Yagupolskii,[46] Hu,[64] and Boutureira[65] prepared Cu–C_2F_5 species by leveraging the tendency of Cu–CF_3 species to undergo α-fluoride elimination in the presence of excess CuCl or CuBr,[60] and showed that reactions of these reagents with aryl iodides afforded high yields of pentafluoroethylarenes at moderate temperatures (Scheme 1.2.7c). Despite reports detailing the preparation of pentafluoroethyl analogues of all of the trifluoromethylcopper species studied by Shen (*vide supra*), there have been no studies comparing the reactivities of "ligandless" $Cu(C_2F_5)$, $XCu(C_2F_5)_2^-$, and $Cu(C_2F_5)_2^-$.

Reports of heavier perfluoroalkylcopper homologues are scarcer. Burton reported the preparation of $XCu(i\text{-}C_3F_7)^-$ and $Cu(i\text{-}C_3F_7)^-$, again by treating copper(I) halide salts with the corresponding cadmium reagent in DMF (Scheme 1.2.8a).[66] In contrast to the corresponding trifluoromethylcopper reagents, the heptafluoroisopropylcopper reagents were stable at room temperature but decomposed slowly at 80 °C and did not undergo reactions with aryl halides to form heptafluoroisopropylarenes. Mikami also has reported the preparation of a series of $(DMPU)_2Zn(R^F)_2$ reagents (R^F = CF_3, C_2F_5, C_3F_7, C_6F_{13}, and $(CF_2)_5CF_2Cl$) that underwent salt metathesis with CuI or copper(I) thiophene-2-carboxylate (CuTC) to form the corresponding $XCuR^{F-}$ and $CuR^F{}_2^-$ cuprates (Scheme 1.2.8b).[48] The authors found that longer-chain perfluoroalkylzinc reagents underwent slower salt metathesis with CuI to form fluoroalkylcopper species than did shorter-chain fluoroalkylzinc reagents, and all transmetallation reactions required heating to proceed. These systems were translated into a set of reaction conditions for copper-catalyzed fluoroalkylations that afforded high yields of perfluoroalkylarenes from aryl iodides and some electron-poor aryl bromides ($R^F \neq CF_3$).



Scheme 1.2.7 Formation and reactivity of perfluoroalkylcopper(I) complexes

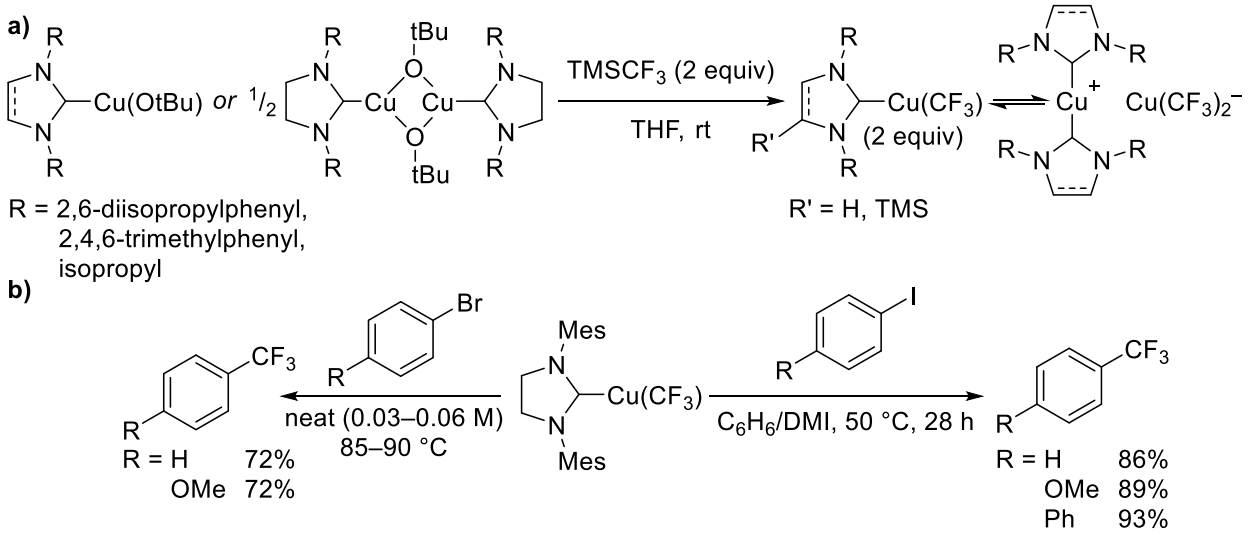


Scheme 1.2.8 Preparation and reactivity of higher perfluoroalkylcopper homologues

1.2.1.3 Perfluoroalkylcopper(I) Complexes Containing Ancillary Ligands

Interest in the development of more convenient perfluoroalkylcopper reagents has led to the isolation of several stable perfluoroalkylcopper species bearing ancillary ligands. Vicic and co-workers prepared and characterized the first examples of isolable trifluoromethylcopper(I) complexes (Scheme 1.2.9a), which were supported by ancillary *N*-heterocyclic carbene (NHC)

ligands.[51,52] These complexes reacted with excess aryl iodide in DMF at ambient or 50 °C to form high yields of trifluoromethylarenes. Trifluoromethylation of two bromoarenes also occurred with these reagents but required higher temperatures (85–90 °C) and solvent quantities of the bromoarene to limit competitive decomposition of the reagent. The authors showed that (SIMes)Cu(CF_3) existed in solution in a Schlenk-like equilibrium between neutral (NHC)Cu(CF_3) and ionic [$(NHC)_2Cu^+$][$Cu(CF_3)_2^-$] forms and concluded, based on the concentration dependence of the rate of the trifluoromethylation reaction, that the neutral form, not the ionic form, reacted with the aryl halides to form trifluoromethylarenes (see Section 1.2.1.1).



Scheme 1.2.9 a) Preparation of NHC-ligated $CuCF_3$ species b) Reactions of these complexes with aryl halides

Following Amii's seminal report[67] and several subsequent reports[47,49,68] of CuX-catalyzed trifluoromethylations of aryl iodides with $TESCF_3$ enabled by phenanthroline (phen) as an ancillary ligand, Hartwig,[69–71] Grushin,[72,73] Huang,[74] and Ohashi and Ogoshi[75] reported the preparation of perfluoroalkylcopper complexes supported by phen, bipyridine (bpy), and phosphine ligands (Chart 1.2.1).

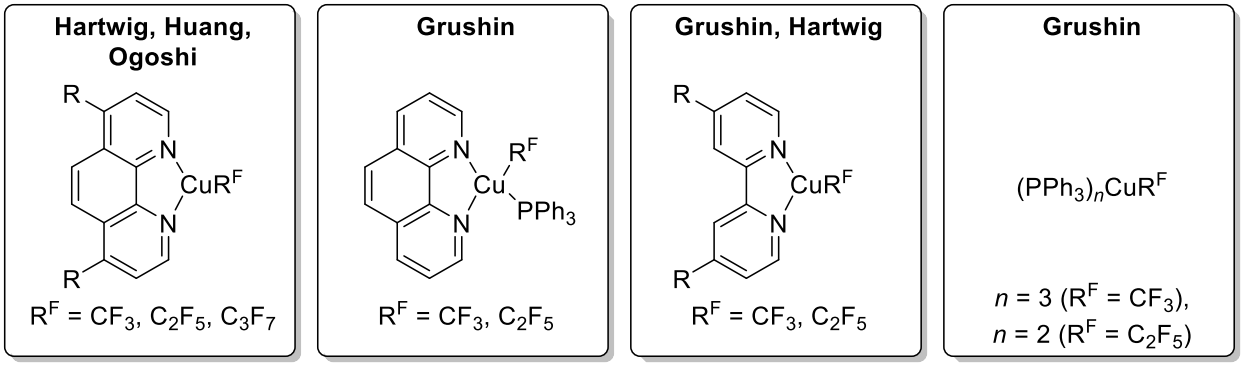
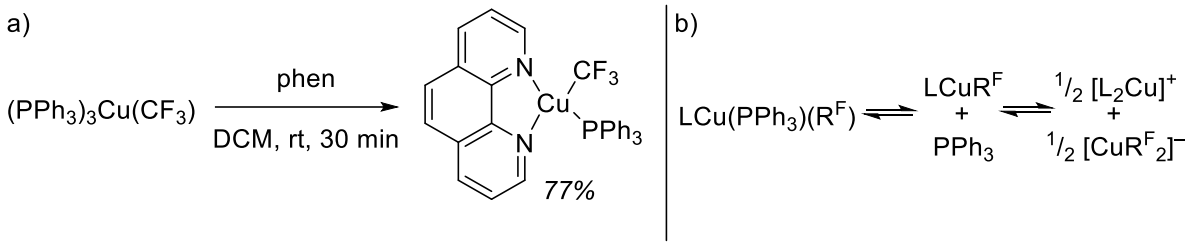


Chart 1.2.1 Isolable perfluoroalkylcopper reagents bearing ancillary ligands

For all these complexes, ligand exchange was shown to be facile. For example, EXSY experiments showed that $(PPh_3)_3Cu(CF_3)$ underwent exchange with free PPh_3 at –90 °C with a rate

on the order of 1 s^{-1}.[72] This exchange was exploited for the synthesis of (phen)Cu(PPh_3)(CF_3) (Scheme 1.2.10a). The resulting complex, like the aforementioned (NHC)Cu(CF_3) complexes and related $LCuR^F$ complexes (L = phen or bpy derivative), was shown to participate in a Schlenk-like equilibrium with the corresponding ionic form [L_2Cu^+][$CuR^F{}_2^-$] (Scheme 1.2.10b).[69–74] The ionic form of these complex was found to exist as a solvent-separated ion pair in DMF.[71]



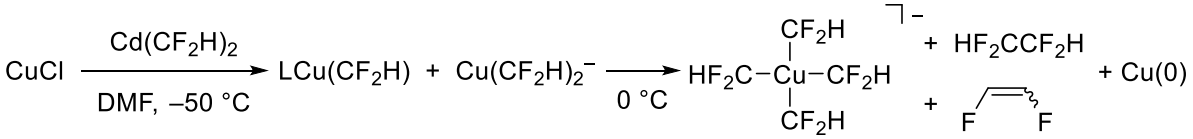
Scheme 1.2.10 a) Formation of (phen)Cu(PPh_3)(CF_3) from (PPh_3)$_3$Cu(CF_3); b) Equilibria governing the solution-state speciation of isolable LCu(PPh_3)(R^F) and $LCuR^F$ reagents (L = phen or bpy derivative)

While the phen- and bpy-ligated perfluoroalkylcopper species are convenient, isolable reagents for the perfluoroalkylation of a wide range of aryl iodides, they do not appear appreciably more stable toward nonproductive decomposition or more reactive toward aryl halides than Grushin's "ligandless" CuR^F reagents derived from R^F–H.[41,55–57,60,73] For example, the trifluoromethylation of aryl iodides and electron-poor aryl bromides with both Grushin's "ligandless" $CuCF_3$ derived from CHF_3 and Hartwig's (phen)Cu(CF_3) proceeded in high yields (generally >85%) overnight in DMF at mild temperatures. However, the trifluoromethylation of electron-neutral or electron-rich aryl bromides proceeded in low yields in reactions with either reagent and required a significant excess of one of the components and reaction temperatures ranging from 80 to 110 °C.[60,69] In fact, the rate constants of perfluoroalkylation of aryl iodides with "ligandless" CuC_2F_5 and bipyridine-ligated (R_2bpy)Cu(C_2F_5) were measured and found to differ by less than an order of magnitude (see Chapter 2 for a detailed discussion on the effect of the bpy ancillary ligand).[71] Thus, the origin of the observed beneficial effect of ancillary ligands in copper-catalyzed perfluoroalkylation reactions remains unclear.[67]

1.2.2 Difluoromethylcopper(I) Complexes

While the development of *per*fluoroalkylation reactions constitutes the majority of the literature on copper-mediated fluoroalkylation, some reports have focused on fluoroalkyl groups containing other substituents besides fluorine. The simplest of these is the difluoromethyl group, which has been studied recently because of its ability to act as a weak hydrogen-bond donor and its potential utility as lipophilic bioisosteres for alcohols and thiols.[10,76] Inspired by the success of Cd(CF_3)$_2$ and Cu(CF_3) reagents, Eujen reported in 1996 the first example of the corresponding Cd(CF_2H)$_2$ reagent (Scheme 1.2.11).[77] Upon treating CuCl with M(CF_2H)$_2$ (M = Cd, Zn) at low temperature in DMF or DMSO, the authors observed by NMR spectroscopy the formation of new difluoromethylcopper(I) species assigned as LCu(CF_2H) (L = halide or solvent) and Cu(CF_2H)$_2^-$. The rate of transmetallation from Cd(CF_2H)$_2$ to copper was found to be significantly faster than from Zn(CF_3)$_2$. However, the Cu–CF_2H species thus generated were significantly less thermally stable than the corresponding Cu(CF_3) species, with Cu(CF_2H)$_2^-$ disproportionating to Cu^{III}(CF_2H)$_4^-$ and copper metal upon warming to 0 °C. Alternatively, when the neutral species

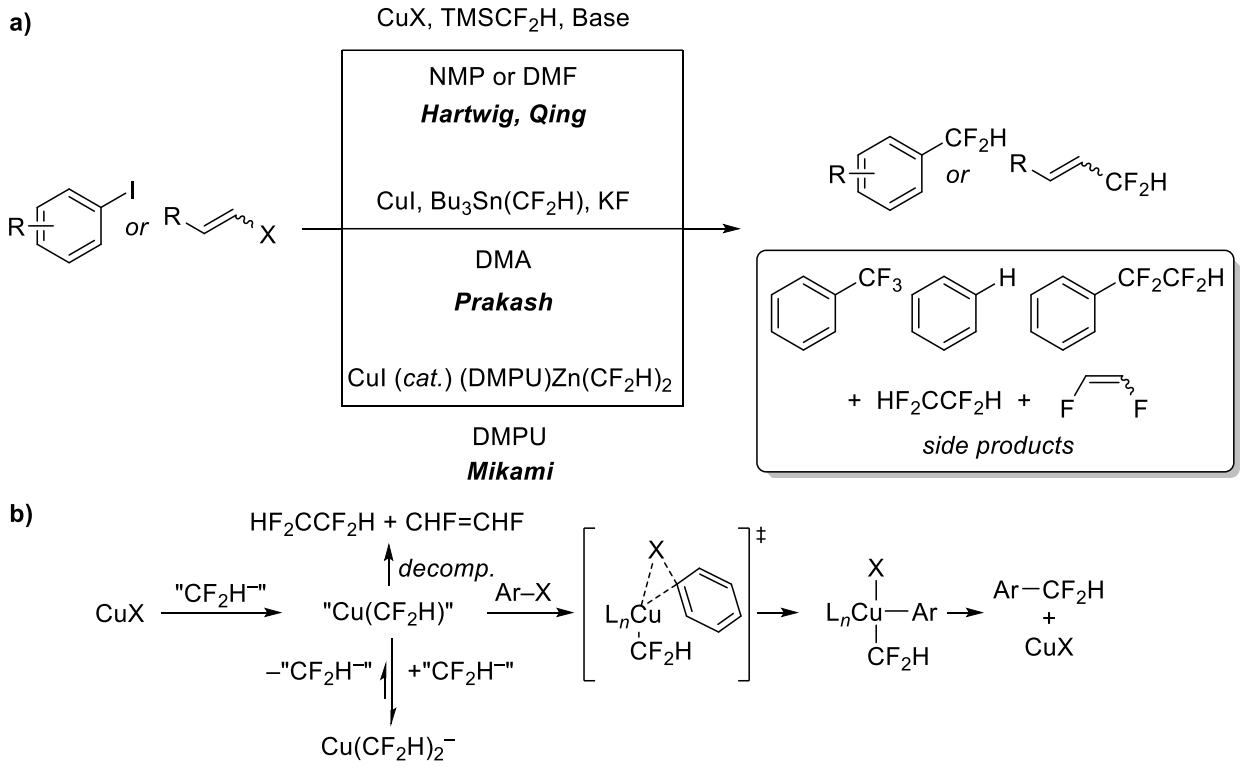
$Cu(CF_2H)$ was stabilized by adding HMPA to the mixture, slower thermal decomposition resulted in the formation of HF_2CCF_2H and 1,2-difluoroethylene, resulting from reductive coupling and the formation of fluorocarbene, respectively.[77,78] None of these difluoromethylcopper(I) species were isolated. The difluoromethylcopper reagent reacted with carbon electrophiles including allyl, propargyl, and benzyl halides as well as propargyl sulfonates to form good yields of difluoromethylated products. Eujen also showed that oxidation of the mixture with oxygen, iodine or disulfiram led to the formation of the air-stable complex $Cu^{III}(CF_2H)_4^-$, which was isolated as a PNP salt and characterized by single-crystal X-ray diffraction.



Scheme 1.2.11 Preparation of Cu–CF_2H species from $Cd(CF_2H)_2$

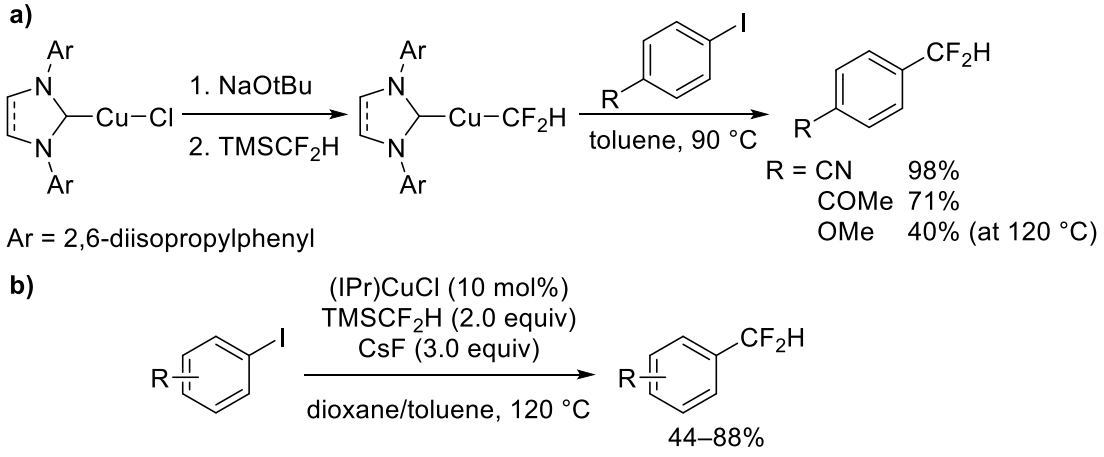
The copper-mediated difluoromethylation of aryl and vinyl iodides was reported first by both Hartwig and Prakash in 2012 using a combination of stoichiometric CuI, $TMSCF_2H$, and CsF,[79] or CuI, $Bu_3Sn(CF_3)$, and KF (Scheme 1.2.12), respectively.[80] Qing reported a system similar to Hartwig's that enabled the reaction of electron-poor aryl iodides in higher yields,[81] and Mikami reported the first copper-catalyzed difluoromethylation of aryl iodides using a combination of CuI and $(DMPU)_2Zn(CF_2H)_2$.[82] Hartwig and Prakash proposed that the formation of difluoromethylarene occurred through a concerted reaction with an unobserved "$Cu(CF_2H)$" species based on radical trapping studies[79] and DFT calculations.[80] In contrast to more typical Ullmann-type cross-coupling reactions, in which reactions of more electron-poor aryl halides proceed more quickly and in higher yields than reactions of more electron-rich aryl halides, Hartwig found that reactions of more electron-rich aryl iodides gave higher yields of difluoromethylarene than did reactions of more electron poor aryl iodides. For electron-poor aryl iodides, hydrodehalogenated and trifluoromethyl- and tetrafluoroethylarene products were observed, resulting from hydride transfer from $TMSCF_2H$ (or some product derived therefrom) and the formation of difluorocarbene, respectively. In contrast to the aforementioned thermal instability of Cu–CF_2H species generated from $Cd(CF_2H)_2$, Hartwig and Mikami both observed the accumulation of $Cu(CF_2H)_2^-$ in the absence of haloarene at high temperature, although Mikami showed that such a species generated from $(DMPU)Zn(CF_2H)_2$ decomposed slowly over several hours to tetrafluoroethane and 1,2-difluoroethylene, even at room temperature.[79,82] Detailed mechanistic investigations into the identities and reactivities of the difluoromethylcopper species have not been undertaken.

Inspired by Vicic's preparation of of $(NHC)Cu(CF_3)$ species, Sanford reported in 2017 the isolation of $(IPr)Cu(CF_2H)$ and $(SIPr)Cu(CF_2H)$ by treating the corresponding (NHC)CuCl complexes with $TMSCF_2H$ and NaOtBu (Scheme 1.2.13).[83] These complex represent the first examples of isolated difluoromethylcopper(I) species. In contrast to Vicic's $(NHC)Cu(CF_3)$ species, which exist in solution either exclusively or partially as the ionic $[(NHC)_2Cu^+][Cu(CF_3)_2^-]$ pair, $(IPr)Cu(CF_2H)$ and $(SIPr)Cu(CF_2H)$ were found to exist exclusively as the neutral species in solution. These $(NHC)Cu(CF_2H)$ complexes demonstrated high thermal stability and reacted with diaryliodonium salts at room temperature and aryl iodides at 90 °C to afford difluoromethylarene, with the reaction of $(IPr)Cu(CF_2H)$ with 4-iodobenzonitrile occurring in nearly quantitative yield. Reactions of more electron-rich aryl iodides occurred in lower yields and required higher temperatures than reactions of electron-poor aryl iodides, suggesting that oxidative



Scheme 1.2.12 a) Copper-mediated and copper-catalyzed difluoromethylation of aryl and vinyl halides; b) Proposed (incomplete) mechanism for copper-mediated difluoromethylation

addition to (NHC)Cu(CF_2H) is the rate-limiting step. The authors translated these stoichiometric experiments into a set of catalytic reactions, affording a range of electron-poor and electron-rich difluoromethylarenes in moderate to good yields.



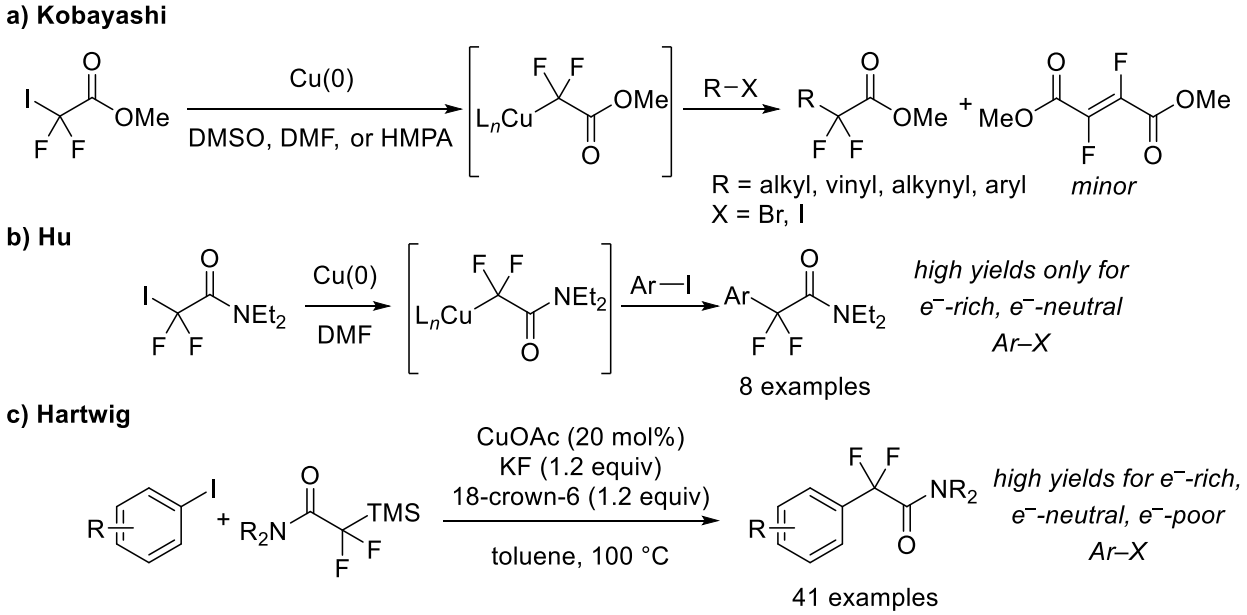
Scheme 1.2.13 Synthesis and reactivity of discrete (NHC)Cu(CF_2H) complexes

1.2.3 Fluoroalkylcopper(I) Complexes of Carboxylic Acid Derivatives

Copper-mediated α-arylations of α-fluorocarboxylic acid derivatives to form α-fluoroketones, esters, amides,[84–86] nitriles,[87] have all been reported. However, studies on the

identities and reactivities of the putative fluoroalkylcopper intermediates are rare, and isolable complexes containing these fluoroalkyl moieties have not been reported. Kobayashi first reported the preparation of methyl α-hydrocarbyl-α,α-difluoroesters by the reaction of superstoichiometric copper powder with methyl 2,2-difluoro-2-iodoacetate and alkyl, allyl, vinyl, alkynyl, or aryl iodides or bromides in a reductive coupling (Scheme 1.2.14a).[88,89] The reactions proceeded in moderate to good yields in DMSO at mild temperatures (ambient to 70 °C) and with short reaction times (generally less than 1 h). The identity of the putative copper enolate species was investigated by ^{19}F NMR spectroscopy and found to vary depending on the solvent. In DMF and DMSO, the NMR spectrum contained two coupled resonances in a 1:2 ratio, suggesting the formation of a cluster containing multiple inequivalent fluoroenolate moieties, while in HMPA only a single resonance was observed. The species were moderately stable at room temperature, gradually decomposing in several hours to dimethyl difluorofumarate, presumably formed from dimerization of the carbene resulting from formal α-fluoride elimination of the enolate. Further characterization of these species was not reported.

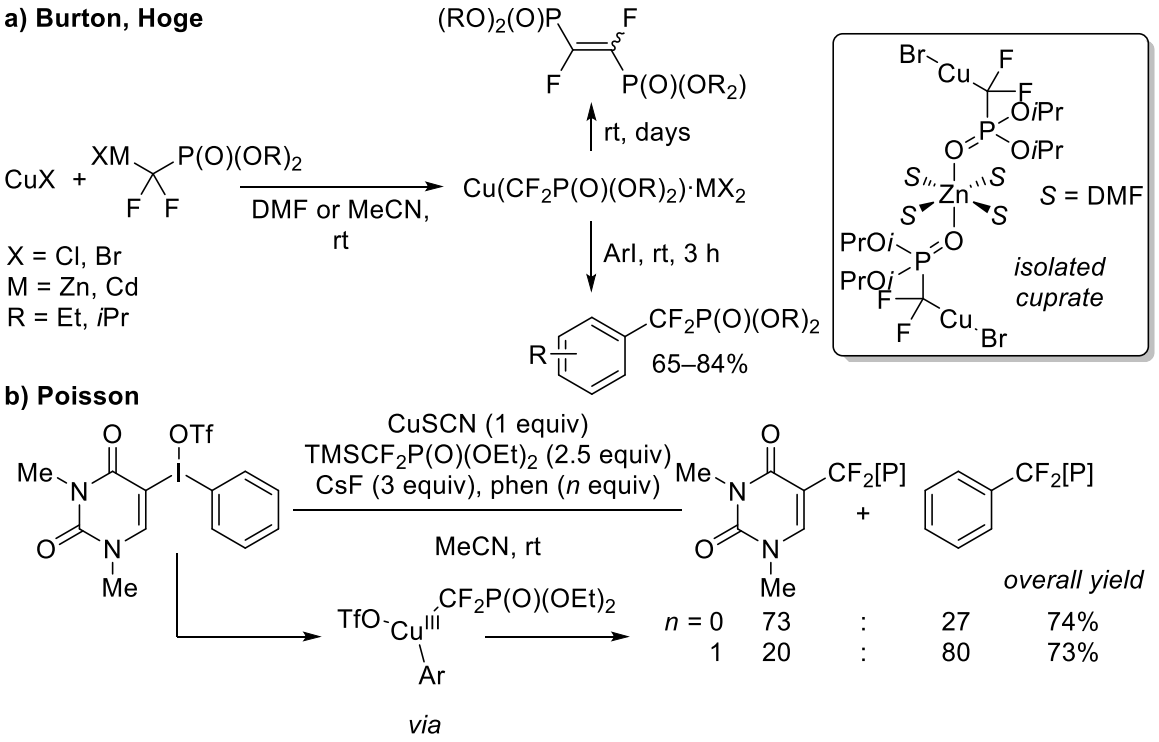
Hu reported that the reaction of copper(0) with diethyl 2,2-difluoro-2-iodoacetamide in DMF likewise resulted in the appearance of two resonances corresponding to a putative $L_nCuCF_2CONEt_2$ species (Scheme 1.2.14b).[84,85] The resulting reagent formed aryldifluoroacetamides from a limited scope of electron-poor and electron-neutral aryl iodides, but no further attempt was made to characterize the copper fluoroenolate intermediate. Hartwig recently reported a copper-catalyzed α-arylation of α-silyldifluoroamides which presumably proceeds through a common fluoroalkylcopper intermediate (Scheme 1.2.14 c).[86] However, despite this shared intermediate, the cross-coupling reactions of aryl iodides with α-silyldifluoroamides proceeded with higher yields for a much wider range of (hetero)aryl halides (18 examples of (hetero)aryl iodide coupling partners) than did Hu's reactions involving diethyl 2,2-difluoro-2-iodoacetamide (8 examples). Much work remains to be done to elucidate the identity of the copper fluoroenolate species in solution and to explore the differences in reactivity between these systems.



Scheme 1.2.14 Formation of α-aryl-α,α-difluorocarboxylic acid derivatives *via* copper fluoroenolate species

1.2.4 Other Fluoroalkylcopper(I) Complexes

Methods for the copper-mediated α-arylation of α,α-difluoromethylphosphonates[90–94] also have been reported. Burton reported that the reaction of CuCl with $M(CF_2P(O)(OEt)_2)X$ reagents (M = Zn, Cd) in DMF formed a copper-containing species according to ^{19}F NMR spectroscopy,[92,95] which was proposed to be $Cu(CF_2P(O)(OEt)_2)\cdot MX_2$ (Scheme 1.2.15a).[90,92,95,96] The presence of the MX_2 adduct recently was confirmed in the solid state by Hoge and co-workers, who characterized the heteroleptic cuprate resulting from a 1:1 mixture of CuBr $Zn(CF_2P(O)(OiPr)_2)Br$ in DMF as $[Zn\{BrCu(CF_2P(O)(OiPr)_2)\}_2\{DMF\}_4]$ by single-crystal X-ray diffraction.[97] Treatment of the mixture with electron-poor or electron-neutral aryl iodides at room temperature generated the corresponding aryl phosphonates in high yields. Reactions at higher temperatures for a wider variety of substrates were presumably hindered by the stability of the $Cu(CF_2P(O)(OEt)_2)$ species, which decomposed over several days at ambient temperature to $(EtO)_2P(O)F$, $(EtO)_2P(O)CF_2H$, a new $(EtO)_2P(O)C_2F_4Cu$ species, and $(EtO)_2P(O)CF{=}CFP(O)(OEt)_2$. The last two species were proposed to form from the ejection of $P(O)(OEt)_2^-$ to form difluorocarbene (or a complex containing it) and α-fluoride elimination to form a carbenoid species of the form $(EtO)_2P(O)C(:)F$, respectively. Decomposition of $[Zn\{[(iPrO)_2P(O)CF_2]CuBr\}_2\{DMF\}_4]$ was found to be first order in cuprate.[97]

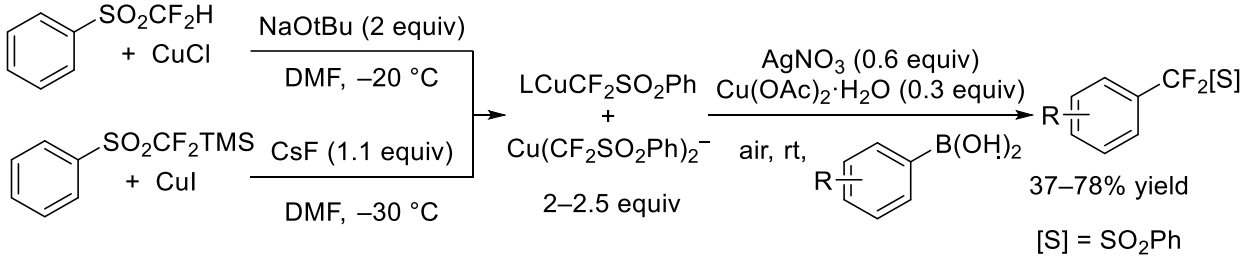


Scheme 1.2.15 Reactions of $Cu(CF_2P(O)(OR)_2)$ species

Similar "$Cu(CF_2P(O)(OEt)_2)$" species that were generated from a combination of CuSCN, $TMSCF_2P(O)(OEt)_2$, and CsF in acetonitrile (Scheme 1.2.15b) were also reported recently by Poisson.[98,99] While characterization of the copper species was not reported, the reagent solution thus generated reacted with a wide range of organic electrophiles, including aryldiazonium salts and λ^3-iodanes, to afford a wide range of electron-poor and electron-rich arenes and heteroarenes in moderate to good yields. The authors conducted mechanistic investigations and found that the

reactions of λ^3-iodanes likely involved a concerted oxidative addition at the copper center, while the reactions of aryldiazonium salts proceeded through the usual SET pathways. The addition of phenanthroline to the reaction generally did not affect yields, but the presence or absence of phenanthroline greatly affected the selectivity toward different aryl groups in unsymmetrical λ^3-iodanes, suggesting that including a ligand changes the speciation of the reagent. The iodoarene byproducts from the reactions of the λ^3-iodanes were found to be unreactive under the reaction conditions.

Finally, Hu reported in 2011 the only example of a $CuCF_2SO_2Ph$ species (Scheme 1.2.16).[100,101] While the reaction of $PhSO_2CF_2I$ and copper powder yielded none of the desired organocopper species, treatment of CuI with $PhSO_2CF_2TMS$ and CsF at –30 °C in DMF led to the appearance of two new resonances in the ^{19}F NMR spectrum of the reaction, which were tentatively assigned as $LCu(CF_2SO_2Ph)$ (L = solvent or iodide) and $Cu(CF_2SO_2Ph)_2^-$, in analogy to other fluoroalkylcopper complexes (*vide supra*). The authors described the generation of the same species in a subsequent report by the deprotonation of $PhSO_2CF_2H$ with $Na[Cu(O\textit{t}Bu)_2]$ generated *in situ*.[101] In both reports, the fluoroalkylcopper reagent decomposed over two hours at room temperature, with the putative homoleptic cuprate decomposing more quickly. The addition of phenanthroline did not stabilize the copper species, although the addition of 18-crown-6 slightly reduced the rate of decomposition, suggesting that the alkali cation was involved in the degradation of the reagent. While the sensitivity of the reagent to temperature precluded reactions with aryl halides to form aryldifluorosulfonates, reactions with electron-rich and electron-poor aryl- and heteroarylboronic acids containing halogen, alkyl, ether, aldehyde, nitrile, and nitro functional groups under air proceeded in moderate yields to afford the corresponding fluoroalkylarene products.



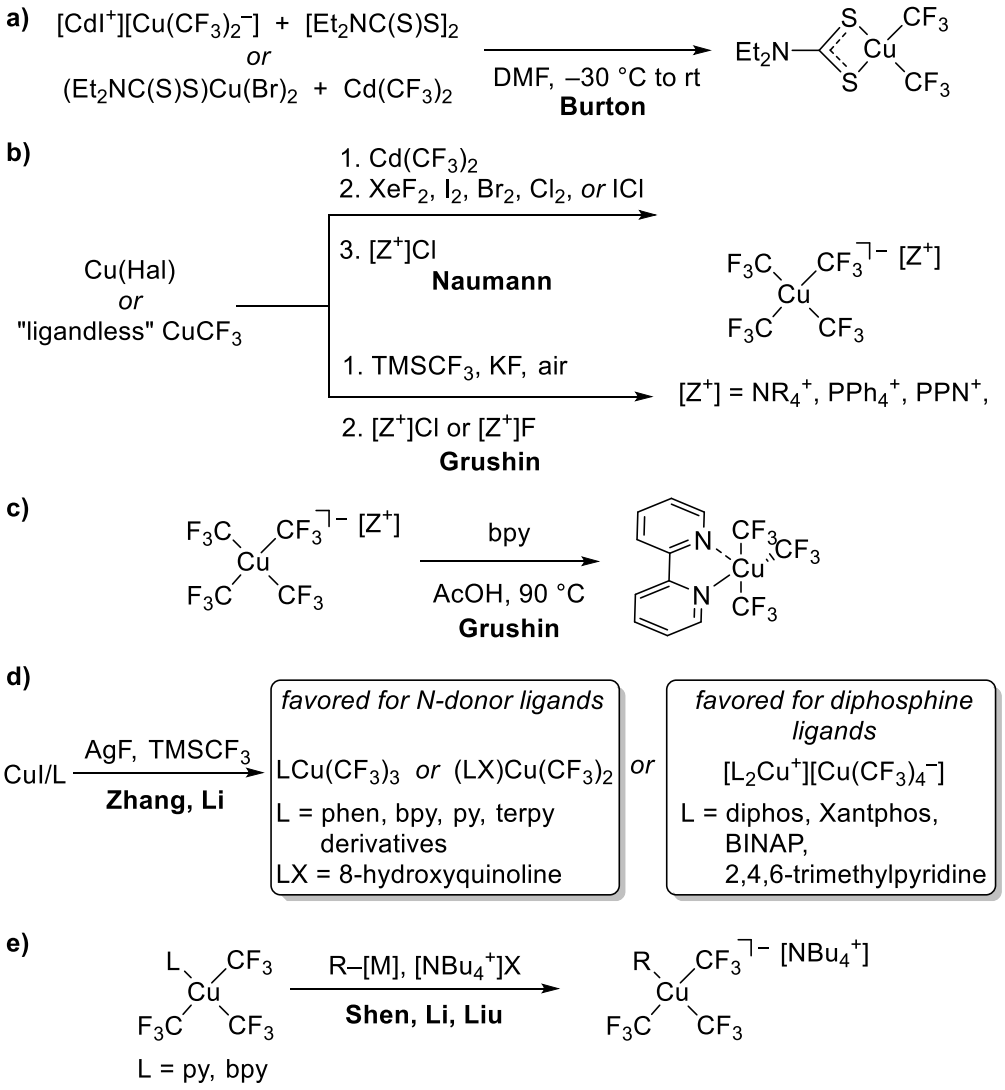
Scheme 1.2.16 Synthesis and reactivity of $Cu(CF_2SO_2Ph)$ species

1.2.5 Fluoroalkylcopper(III) Complexes

Of the handful of reported stable Cu(III) species, polyperfluoroalkylcopper(III) complexes constitute a significant subset and have been investigated as reagents and as putative intermediates in perfluoroalkylation reactions.[102] Tetrakis(perfluoroalkyl)copper(III) is prepared by oxidation of fluoroalkylcopper(I) species, as first demonstrated by Burton and co-workers and later by Naumann, Grushin, and Eujen (Scheme 1.2.17a-b).[36,44,77,103] Eujen also reported that the reaction of $Cu(CF_2H)_4^-$ and $(CF_3)_2Cu^{III}(S_2CNEt_2)$ generated all combinations of fluoroalkylcopper(III) species $Cu(CF_3)_n(CF_2H)_{4-n}$ in a roughly statistical mixture, showing that two fluoroalkylcopper(III) can exchange ligands.[77] Overall, these complexes exhibited remarkable stability to light, air, moisture, chromatography, and heating, and showed no tendency to form Cu–C_2F_5 species by α-fluoride elimination pathways. Ligand substitution of $Cu(CF_3)_4^-$ by the protonolysis of a single CF_3 group was achieved only after heating at 90 °C in acetic acid in the presence of bpy derivatives, forming the discrete, air- and moisture-stable complex $(bpy)Cu(CF_3)_3$

(Scheme 1.2.17c).[44,104] Zhang has reported the syntheses of several $LCu^{III}(CF_3)_n$ complexes (n = 2–3, L = bpy, phen, pyridine, hydroxyquinoline, and terpyridine derivatives) and $[L_2Cu^+][Cu(CF_3)_4]$ ion pairs (L = phen, diphos, BINAP, Xantphos, 2,4,6-trimethylpyridine) by treatment of copper(I) iodide with a mixture of the desired ligand, silver fluoride, and $TMSCF_3$ (Scheme 1.2.17d).[105–108] Finally, Li,[109] Liu,[110] and Shen[111] have reported the syntheses of several $Cu^{III}(CF_3)(R)^-$ (R = alkyl, fluoroaryl) species *via* the transmetallation of organometallic reagents (Scheme 1.2.17e).

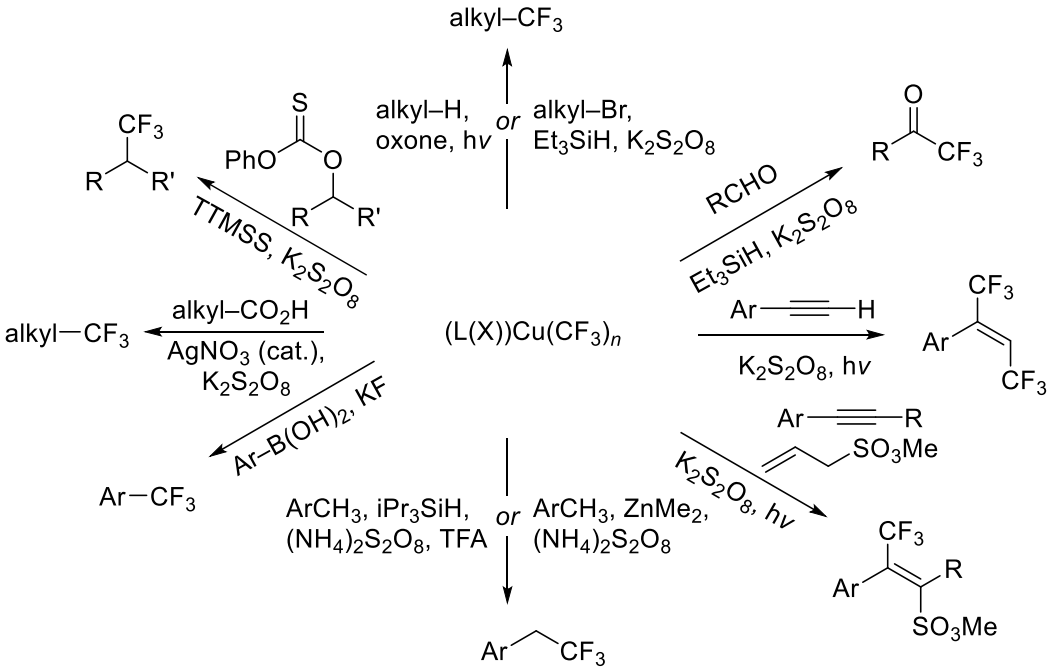
Despite the remarkable stability of polyfluoroalkylcopper(III) complexes, $L_nCu(CF_3)_m$ complexes have been used as sources of trifluoromethyl radical in trifluoromethylation reactions, although generally not for the formation of fluoroalkylarenes (Scheme 1.2.18). Alkyl halides,[112] carboxylic acids,[109] and aldehydes[113], arylalkanes,[104,114] unactivated alkanes,[115] alkenes,[116] alkynes,[117–119] and *O*-alkylthiocarbonates[120] all underwent trifluoromethylation in the presence of $(bpy)Cu(CF_3)_3$ or $(phen)Cu(CF_3)_3$, following the formation of alkyl, acyl, or vinyl radicals. Although the mechanisms of these transformations have not been studied in detail, the proposed



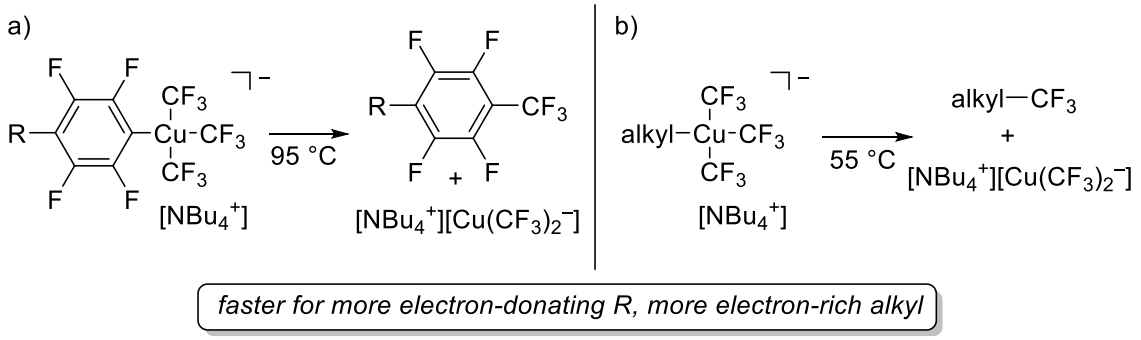
Scheme 1.2.17 Syntheses of polytrifluoromethylcopper(III) complexes

mechanisms have common features. Radical trapping experiments have shown that $LCu^{III}(CF_3)_3$ complexes undergo photolytic or thermal homolysis to liberate a trifluoromethyl radical and a putative $LCu^{II}(CF_3)_2$ species.[112–114,117,120,121] Combination of the latter with an alkyl radical to form a copper(III) species, followed by facile product-forming reductive elimination has been proposed in several cases.[61,109,113,114,117,120,122] Zhang also showed that most of the complexes in Scheme 1.2.17d undergo reactions with arylboronic acids to form trifluoromethyl arenes, although the mechanisms of these transformations and the speciation of the copper complexes under these conditions have not been investigated in depth.[105–108]

Investigations into the two-electron chemistry of copper(III) species are more limited but are relevant to the proposed intermediacy of $Cu^{III}(aryl)(R^F)$ species in perfluoroalkylation reactions of aryl halides. To this end, Shen recently reported the synthesis and reactivity of several air-stable and moisture-stable $Cu(Ar^F)(CF_3)_3^-$ complexes (Ar^F = 4-R-C_6F_4) as the first examples of isolated copper complexes containing both an aryl group and a trifluoromethyl group bound to Cu (Scheme 1.2.19a).[111] These complexes underwent clean reductive elimination upon heating at 95 °C in a wide array of solvents to form trifluoromethylarene products. The authors ruled out radical processes through spin trapping experiments and proposed that product formation occurs through a concerted three-centered transition state. This proposal was supported further by comparing the measured activation parameters to those estimated by density functional theory. Reductive elimination from complexes containing more electron-rich Ar^F was faster than that from complexes containing more electron-poor Ar^F. This trend matches that observed for the non-fluorinated components in reductive eliminations from (benzyl)$Cu(CF_3)_3^-$ to form trifluoroethylbenzenes (Scheme 1.2.19b) and from arylpalladium difluoromethyl and fluoroenolate complexes to form α-arylated fluoroenolates (see Section 1.3.2 and Chapter 3).[23,123,124]



Scheme 1.2.18 Reactions using discrete polytrifluoromethylcopper(III) species as sources of CF_3



Scheme 1.2.19 Reductive elimination from isolated $RCu(CF_3)_3^-$ species

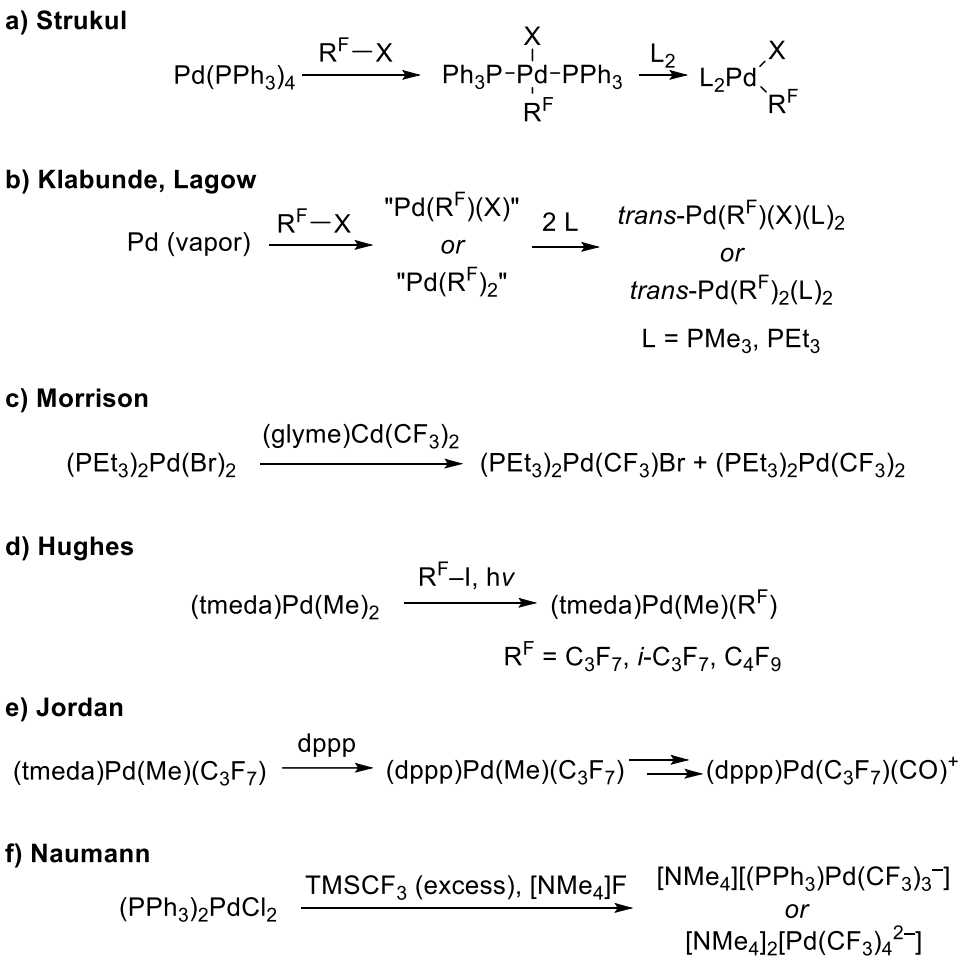
1.3 Complexes of Palladium

Despite the lower cost and wider availability of copper for synthetic transformations, the high, often stoichiometric, loadings of copper complexes in copper-mediated perfluoroalkylation reactions and the narrow scope of aryl electrophiles that react with these copper complexes has prompted investigations into fluoroalkylation reactions catalyzed by palladium. Whereas copper-mediated fluoroalkylations are typically limited to aryl iodides and some activated aryl bromides, due to the high barrier to oxidative addition of aryl halides to the corresponding Cu–R^F species, palladium complexes supported by appropriate ancillary ligands are known to react with a wide range of aryl–X bonds. This Section describes investigations into the fundamental reactivity of fluoroalkylpalladium complexes as well as efforts to develop these findings into catalytic fluoroalkylation reactions.

1.3.1 Perfluoroalkylpalladium(II) Complexes

While early examples of palladium complexes containing perfluoroalkyl ligands were not investigated in the context of perfluoroalkylations of arenes, they do highlight some import trends in fluoroalkylpalladium chemistry. Like the first perfluoroalkylcopper complexes, the first fluoroalkylpalladium(II) species were generated by the reaction of metal(0) with perfluoroalkyl halides (or, in some cases, perfluoroalkyl radicals generated therefrom) (Scheme 1.3.1a-b)[125–128] and, later, by reaction of palladium(II) halide complexes with (glyme)$Cd(CF_3)_2$ (Scheme 1.3.1c).[19,129,130] However, the exploration of the reactivities of the resulting fluoroalkylpalladium complexes was generally superficial. Hughes reported that the reaction of perfluoroalkyl iodides with (TMEDA)$Pd(Me)_2$ (TMEDA = *N,N,N',N'*-tetramethylethylenediamine) resulted in the formation of stable (TMEDA)Pd(R^F)(Me) species and iodomethane (Scheme 1.3.1c).[25,26] While such species were proposed to form from decomposition of the transient Pd(IV) compound (TMEDA)Pd(R^F)(I)$(Me)_2$, side products from the reductive elimination of the R^F fragment were never observed, demonstrating the greater reactivity of the Pd–alkyl moiety, relative to the Pd–perfluoroalkyl moiety. Jordan reported the first examples of diphosphine-ligated palladium(II) complexes containing one fluoroalkyl group and one hydrocarbyl group by treating (TMEDA)Pd(C_3F_7)(Me) with 1,3-*bis*(disphenylphosphino)propane (dppp) to form (dppp)Pd(C_3F_7)(Me) (Scheme 1.3.1d).[131,132] The authors further showed that, while the complex did not undergo C–C reductive elimination, protonolysis of the methyl ligand and treatment of the resulting complex with carbon monoxide led to the formation of (dppp)Pd(*n*-C_3F_7)$(CO)^+$. However, in contrast to the non-fluorinated methyl complex (dppp)Pd(Me)$(CO)^+$, the perfluoropropyl complex did not undergo migratory insertion to form an acyl species, as was the

case for the $Mn(CO)_5CF_3/Mn(CO)_5Me$ pair discussed in the Introduction.[22] Naumann first showed that $[NMe_4^+][Pd(PPh_3)(CF_3)_3^-]$ and $[NMe_4^+]_2[Pd(CF_3)_4^{2-}]$ could be generated from the reaction of $(PPh_3)_2Pd(Cl)_2$, $TMSCF_3$, and $[NMe_4]F$, showing that "CF_3^-" could easily displace ancillary phosphine ligands to form polytrifluoromethylpalladate species.[133]

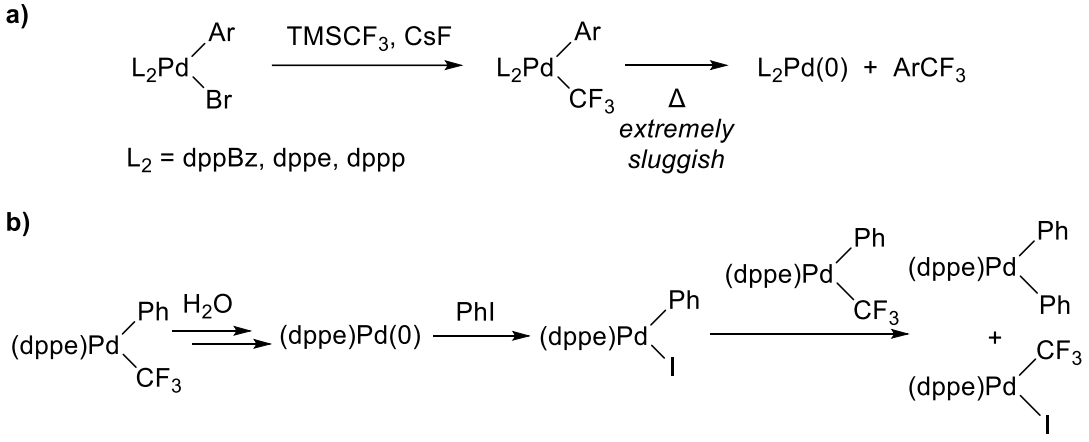


Scheme 1.3.1 Syntheses of early examples of perfluoroalkylpalladium(II) complexes

1.3.1.1 Trifluoromethylpalladium(II) Complexes Containing Diphosphine Ligands

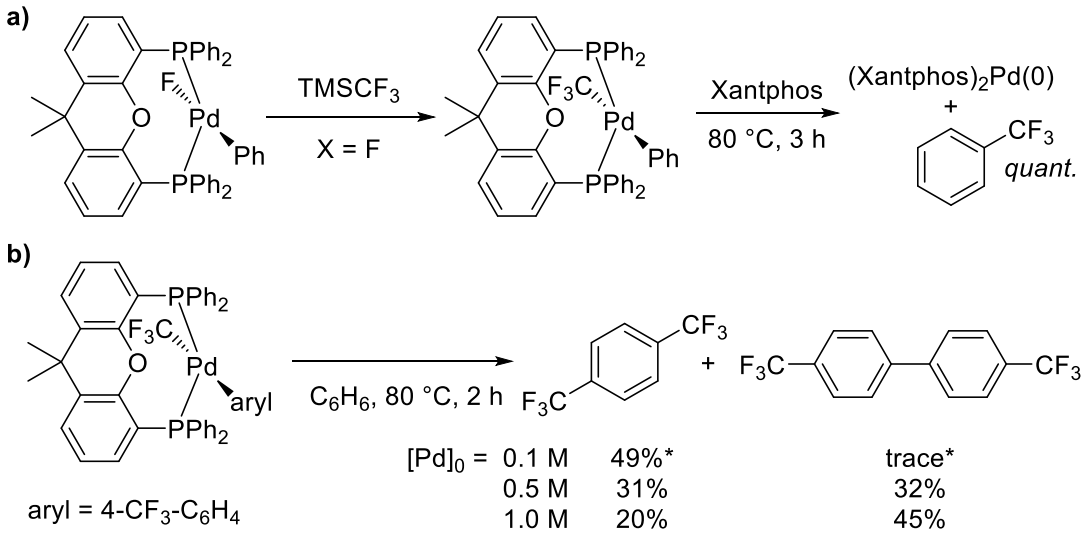
Although the first reports of Pd-*catalyzed* perfluoroalkylation reactions involved complexes containing monophosphine ligands (*vide infra*), much of the foundational work focused on aryl(perfluoroalkyl)palladium containing diphosphine ligands. In a comparative study on a series of (dppBz)Pd(aryl)(alkyl) complexes (dppBz = 1,2-*bis*(diphenylphosphino)benzene), Hartwig reported the synthesis of (dppBz)Pd(*o*-CH_3-C_6H_4)(CF_3) by treating the corresponding arylpalladium bromide complex with a combination of $TMSCF_3$ and CsF (Scheme 1.3.2a). This complex constitutes the first example of a phosphine-ligated aryl(trifluoromethyl)palladium(II) species. Such species are of interest as intermediates in the Pd-catalyzed trifluoromethylation of arenes, as such species could conceivably undergo reductive elimination to form trifluoromethylarenes.[132] However, while (dppBz)Pd(aryl)(alkyl) complexes containing alkyl ligands besides trifluoromethyl (alkyl = methyl, benzyl, -C(O)R, -CH_2CN, and -CH_2CF_3) underwent reductive elimination upon heating to form alkyl–aryl bonds, the trifluoromethyl

complex was uniquely stable, undergoing no decomposition when heated at 130 °C for several days.



Scheme 1.3.2 Seminal examples of aryl(trifluoromethyl)palladium(II) complexes containing ancillary diphosphine ligands

Two years later, Grushin prepared (DPPE)Pd(Ph)(CF_3) and (DPPP)Pd(Ph)(CF_3) (DPPE = 1,2-bis(diphenylphosphino)ethane, DPPP = 1,3-bis(diphenylphosphino)propane) by a similar route, and these complexes were shown to undergo very slow reductive elimination at 145 °C under rigorously anhydrous conditions to form trifluoromethylarene (~10 and ~60% yield after 64 hours for the complexes containing DPPE and DPPP, respectively).[134,135] For comparison, the related complex (DPPE)Pd(Ph)(Me) was shown to undergo facile reductive elimination at 35 °C in benzene.[136] Further evaluation of the reactivities of these complexes revealed that trace water could reduce these complexes, likely through a series of α-fluoride eliminations of the trifluoromethyl group and oxidation of the arylphosphine ligand, resulting in the formation of $L_2Pd(0)$ species. This $L_2Pd(0)$ species was then shown to react with aryl iodide to form $L_2Pd(Ar)(I)$, which catalyzed the decomposition of the remaining $L_2Pd(Ph)(CF_3)$ to form

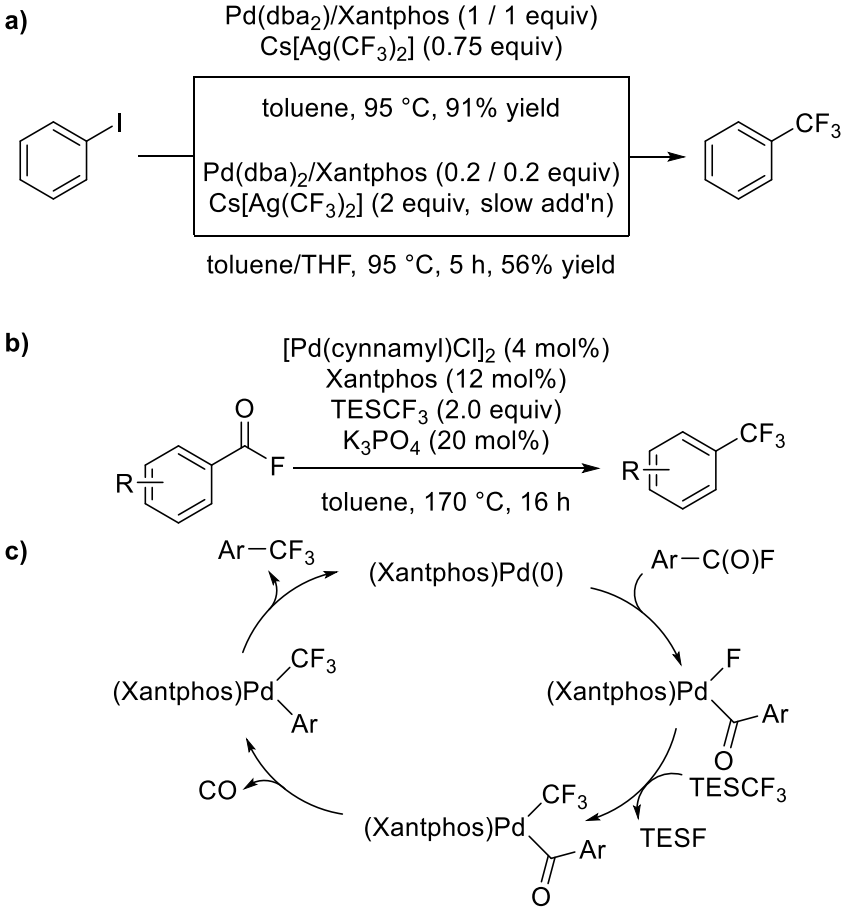


Scheme 1.3.3 Pd-mediated trifluoromethylation reactions facilitated by Xantphos

$L_2Pd(CF_3)I$ and biaryl (Scheme 1.3.2b), highlighting the myriad possible side reactions of phosphine-ligated aryl(trifluoromethyl)palladium(II) species.

A subsequent report by Grushin disclosed the synthesis of (Xantphos)Pd(Ph)(CF_3) (Scheme 1.3.3a).[137] Whereas previous examples of aryl(trifluoromethyl)palladium complexes containing diphosphine ligands were synthesized from the corresponding arylpalladium halide complexes, Grushin observed the displacement of the ancillary phosphine ligands when the halide complexes were treated with $TMSCF_3$ and CF_3, resulting in low yields of the desired aryl(trifluoromethyl)palladium complexes. However, the authors found that treatment of the preformed arylpalladium fluoride complex (Xantphos)Pd(Ph)(F) with $TMSCF_3$ cleanly afforded the desired complex (Xantphos)Pd(Ph)(CF_3). Upon heating at 80 °C for 3 hours, (Xantphos)Pd(Ph)(CF_3) underwent clean reductive elimination to afford quantitative yields of trifluoromethylbenzene with no side-products;[135,137] however, later work by Zhang showed that these complexes form biaryl at higher concentrations due to bimolecular ligand exchange (Scheme 1.3.3b).[138] Nevertheless, this complex represents the first example of an aryl(perfluoroalkyl)palladium(II) complex that undergoes clean reductive elimination at mild temperatures. The origin of the more rapid reductive elimination from the Xantphos-ligated complex than from complexes containing other diphosphines was studied computationally by Schoenebeck and was attributed to greater steric interactions between the arylphosphine moieties of Xantphos and the eliminating aryl and CF_3 ligands.[139]

Despite the ability of Xantphos to facilitate the reductive elimination of trifluoromethyl-

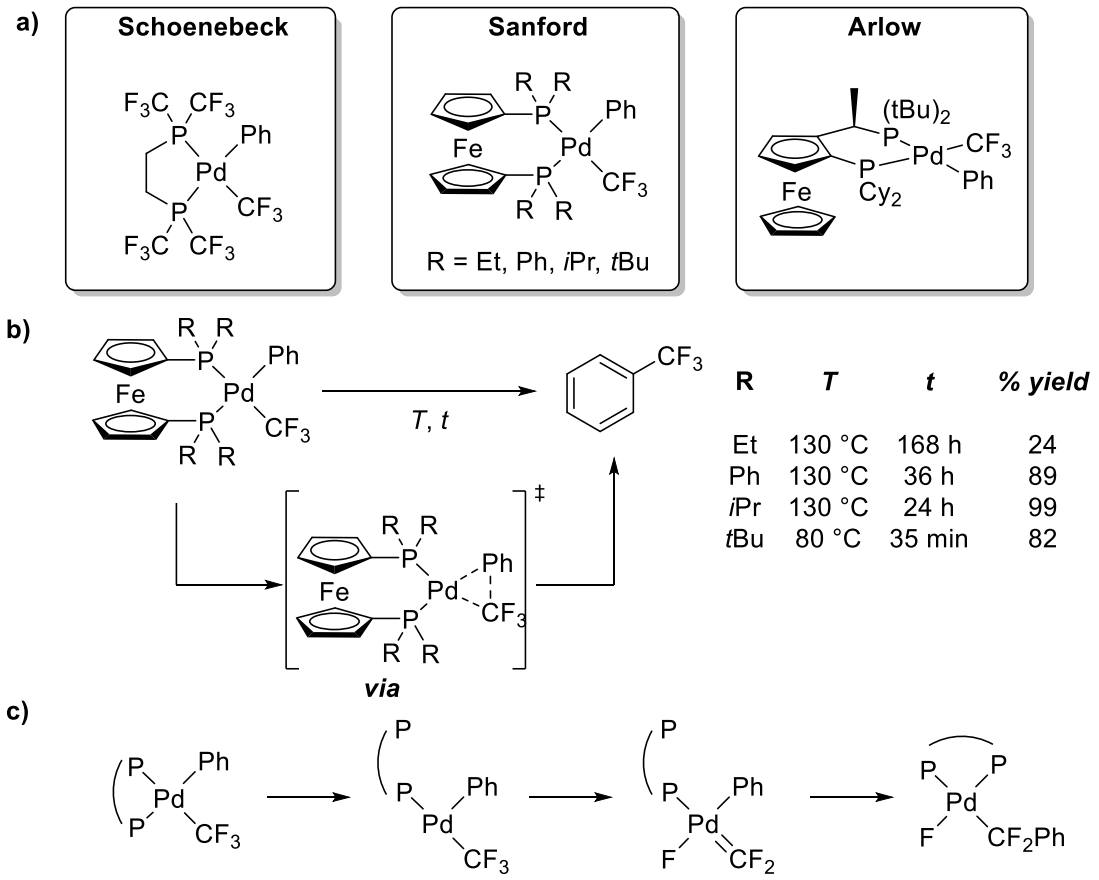


Scheme 1.3.4 Pd-catalyzed trifluoromethylations of aryl electrophiles enabled by Xantphos

arene at mild temperatures, attempts to develop catalytic trifluoromethylations of aryl halides with this ligand have been mostly unsuccessful, likely due to the facile displacement of the ligand by excess "CF_3^-".[137] Pérez-Temprano has reported a single example of the catalytic trifluoromethylation of iodobenzene in 56% yield in which Xantphos served as the ancillary ligand and $Cs[Ag(CF_3)_2]$ as the source of nucleophilic CF_3 (Scheme 1.3.4a).[140] However, the reaction required high loadings of Pd precatalyst (20 mol%) and slow addition of the temperature-sensitive silver reagent, and it occurred to less than three turnovers of the Pd catalyst.

To circumvent the displacement of the Xantphos ligand, Schoenebeck reported a method involving the Pd-catalyzed decarbonylative trifluoromethylation of aroyl fluorides (Scheme 1.3.4b).[141] In this reaction, oxidative addition of the aroyl fluoride to the Pd(0) center resulted in the formation of an intermediate acylpalladium fluoride complex, which reacted with $TMSCF_3$ to form the corresponding aroylpalladium trifluoromethyl complex (Scheme 1.3.4c). This clever approach obviates the need for exogenous base to activate the $TESCF_3$ reagent and avoids the generation of CF_3^- equivalents or fluorotrimethylsilicates at concentrations that exceed those of the palladium catalyst and lead to displacement of the ancillary ligand. By a combination of experimental and computational studies, the authors found that decarbonylation of the acyl(trifluoromethyl)palladium species was likely the turnover-limiting step of the catalytic reaction.

Several recent studies have identified other ancillary diphosphine ligands that facilitate the



R	T	t	% yield
Et	130 °C	168 h	24
Ph	130 °C	36 h	89
*i*Pr	130 °C	24 h	99
*t*Bu	80 °C	35 min	82

Scheme 1.3.5 a) Diphosphine ligands that support reductive elimination of trifluoromethylarene; b) Reductive elimination from *bis*(phosphino)ferrocene-ligated aryl(trifluoromethyl)palladium complexes; c) Hypothetical (though unobserved) pathway involving α-fluoride elimination

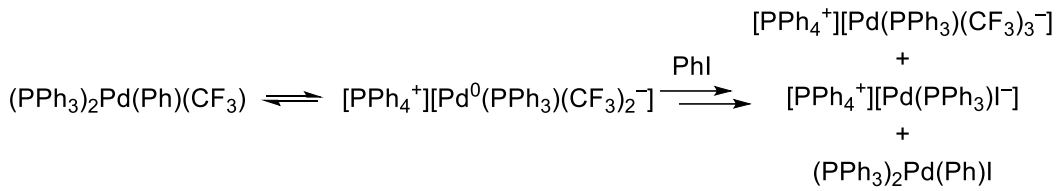
reductive elimination of perfluoroalkylarenes from Pd (Scheme 1.3.5). Based on DFT and molecular mechanics models of several (diphosphine)Pd(Ph)(CF_3) complexes,[139] Schoenebeck identified 1,2-*bis*(*bis*(trifluoromethyl)phosphino)ethane (DFMPE) as a ligand with a small bite angle that could promote reductive elimination of trifluoromethylarenes and demonstrated that (DFMPE)Pd(Ph)(CF_3) underwent reductive elimination of trifluorotoluene. The authors proposed that the strong electrostatic repulsion between the trifluoromethyl groups of the phosphine ligand and the trifluoromethyl ligand of Pd destabilized the ground state, resulting in lower barriers to elimination than for complexes containing phosphines lacking fluoroalkyl groups. We note that stabilization of the increasing Pd(0) character of the transition state by this strongly electron-withdrawing perfluoroalkylphosphine is also a compelling rationalization for the lower energetic barriers and faster rates of reductive elimination than from complexes containing non-fluorinated phosphines.

In an effort to identify properties of ancillary ligands that might facilitate the challenging aryl–perfluoroalkyl reductive elimination from Pd, Sanford prepared a series of aryl(trifluoromethyl)palladium(II) complexes containing 1,1'-*bis*(dihydrocarbylphosphino)ferrocene ligands (hydrocarbyl = Et, Ph, *i*Pr, *t*Bu; DEPF, DPPF, DiPPF, and DTBPF, respectively; Scheme 1.3.5b) with varying degrees of steric bulk.[142] In most cases, L_2Pd(Ph)(CF_3) complexes containing these ligands underwent concerted reductive elimination in high yields. Predictably, the rate of reductive elimination of trifluoromethylbenzene increased with increasingly bulky hydrocarbyl groups on the phosphine ligand (rate of Et < Ph < *i*Pr << *t*Bu). Spectroscopic and computational investigations revealed that reductive elimination from these complexes occurred from four-coordinate Pd complexes without dissociation of one of the phosphine arms. For the complex containing DTBPF, DFT calculations suggested that dissociation of one phosphine arm and subsequent α-fluoride elimination (Scheme 1.3.5c) could occur with only a slightly higher barrier than reductive elimination of trifluoromethylarene ($\Delta\Delta G^{\ddagger}$ = 1.2 kcal/mol), although no byproducts consistent with a pathway occurring by α-fluoride elimination were observed experimentally. Despite the propensity of these ligands to promote the reductive elimination step, especially DTBPF, no catalytic reactions supported by these ligands have been disclosed.

Finally, Arlow conducted a survey of a variety of mono- and bisphosphine ligands in which the labile precursor (3-fluoropyridine)$_2$Pd(Ph)(CF_3)[143] was treated with the desired phosphine and heated. The diphosphine-ligated aryl(trifluoromethyl)palladium complexes thus formed were not characterized. Of many ligands tested, only the complex containing the Josiphos derivative CyPF-*t*Bu formed high yields of trifluoromethylarene upon heating (Scheme 1.3.5a, right). Again, no catalytic reactions with this ligand were reported.

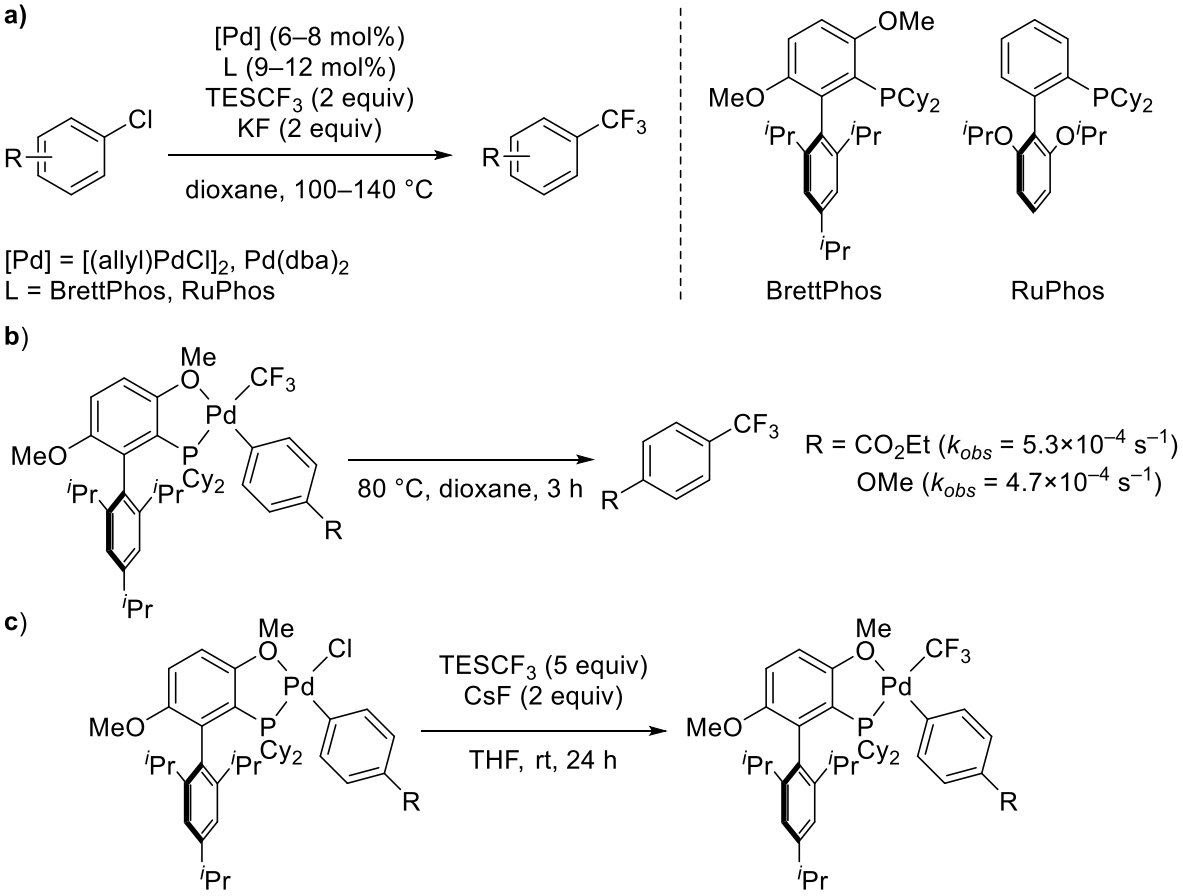
1.3.1.2 Perfluoroalkylpalladium(II) Complexes Containing Monophosphine Ligands

(PPh_3)$_2$Pd(Ph)(CF_3) is the first example of an aryl(trifluoromethyl)palladium complex containing monophosphine ligand and was prepared by Grushin by treating the corresponding arylpalladium fluoride complex with $TMSCF_3$.[137] As previously observed by Naumann, displacement of the triphenylphosphine ligands was observed when treating the corresponding arylpalladium iodide with a combination of CsF and $TMSCF_3$. However, upon heating in the presence of iodobenzene, this complex did not undergo reductive elimination to form trifluoromethylarene. Instead, it decomposed through a series of bimolecular ligand exchanges and ultimately formed several anionic palladate species (Scheme 1.3.6).



Scheme 1.3.6 Decomposition of $(PPh_3)_2Pd(Ph)(CF_3)$

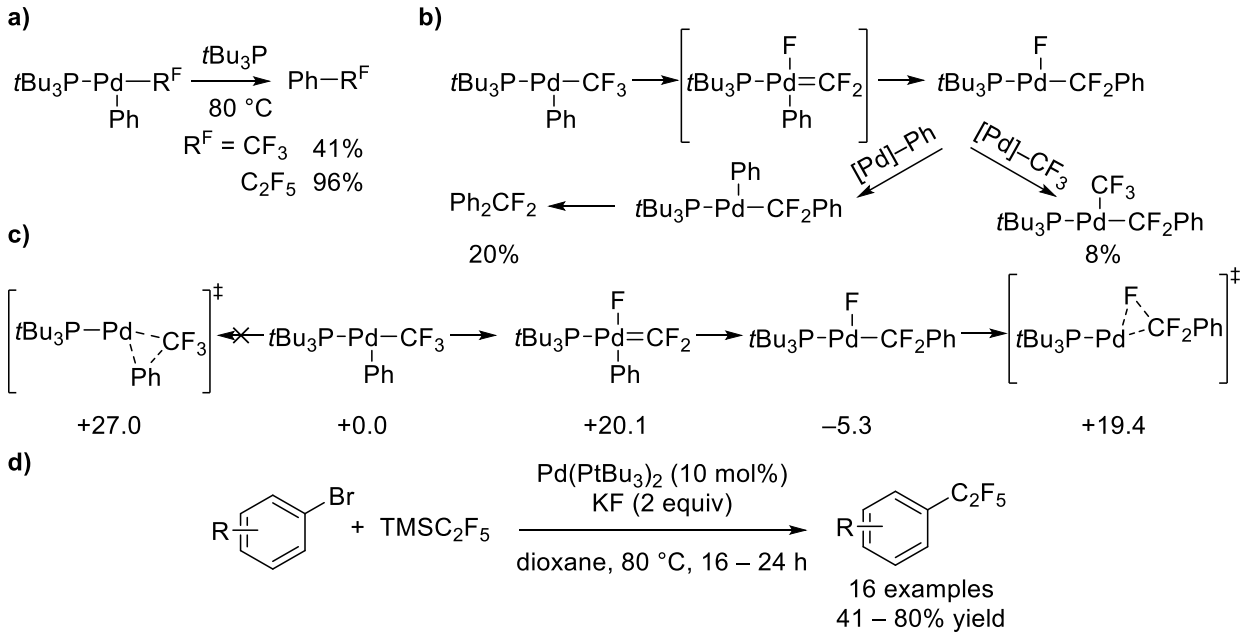
The first examples of aryl(perfluoroalkyl)palladium complexes containing a monophopshine and undergoing reductive elimination were reported by Buchwald in 2010. The authors described the first and only example of a general Pd-catalyzed trifluoromethylation of aryl chlorides (Scheme 1.3.7a).[132] BrettPhos and RuPhos were identified as two ligands that facilitated the typically slow reductive elimination step. After screening a variety of CF_3 sources, the authors found that the slow release of CF_3^- from the reaction of $TESCF_3$ and KF was crucial for catalysis. The catalytic method afforded moderate to good yields (70 – 74%) of trifluoromethylarenes from a wide range of aryl chlorides, although the reaction required high temperatures (> 120 °C) and catalyst loadings (6–9 mol% Pd, 9–12 mol% ligand). As part of their study, the authors also isolated two aryl(trifluoromethyl)palladium complexes ligated by Brettphos that underwent smooth reductive elimination at 80 °C to afford quantitative yields of trifluoromethylarene, demonstrating that these complexes were kinetically competent intermediates in the catalytic



Scheme 1.3.7 Pd-catalyzed and -mediated perfluoroalkylation of aryls with RuPhos and BrettPhos as supporting ligands

reaction (Scheme 1.3.7b). A significant difference in the rate of reductive elimination from complexes containing electron-rich and electron-poor aryl groups was not observed. During the preparation of these complexes (Scheme 1.3.7c), the authors observed the accumulation of free BrettPhos, which was tentatively attributed to the displacement of the ancillary ligand by excess CF_3^-.

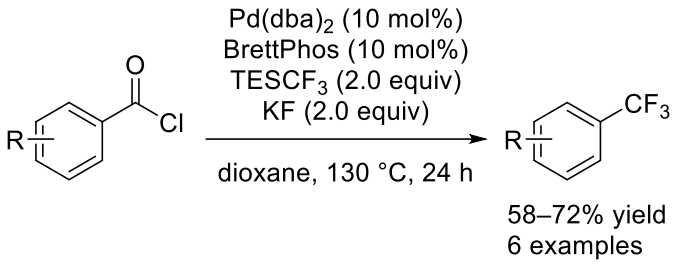
Sanford recently published a study on the reductive elimination of perfluoroalkylarenes from aryl(perfluoroalkyl)palladium(II) complexes ligated by tri-*tert*-butylphosphine (Scheme 1.3.8).[144] The three-coordinate complex (*t*Bu$_3$P)Pd(Ph)(CF$_3$) formed low yields of trifluoromethylbenzene upon heating due to competitive α-fluoride elimination (Scheme 1.3.8a), and organic and organometallic byproducts resulting from the insertion of difluorocarbene into the Pd–aryl bond were observed and characterized (Scheme 1.3.8b). In addition, DFT calculations suggested that the concerted reductive elimination of the aryl and CF$_3$ ligands was not the lowest-energy path to the formation of trifluoromethylarene. Instead, the authors proposed that the trifluoromethylarene formed by reductive elimination from (*t*Bu$_3$P)Pd(F)(CF$_2$Ph), which formed by α-fluoride elimination, and insertion of the resulting carbene into the Pd–aryl bond (Scheme 1.3.8c).[135,145] In contrast, the corresponding pentafluoroethyl complex (*t*Bu$_3$P)Pd(Ph)(C$_2$F$_5$) was predicted to undergo concerted reductive elimination with a lower energetic barrier than α-fluoride elimination. Consistent with this proposal, the pentafluoroethyl complex underwent reductive elimination upon heating at 80 °C for 10 minutes to form pentafluoroethylbenzene in quantitative yields without pentafluoroethylarene or diaryldifluoromethane products that would have resulted from α-fluoride elimination. This result is consistent with the higher calculated barrier for α-fluoride elimination from the C$_2$F$_5$ group relative to reductive elimination, whereas the CF$_3$ group



Scheme 1.3.8 Reactions of aryl(perfluoroalkyl)palladium complexes containing P*t*Bu$_3$ as an ancillary ligand. a) Reductive elimination from isolated complexes; b) Pathways to observed side-products from the thermal decomposition of (tBu$_3$P)Pd(aryl)(CF$_3$). The numbers below each structure represent the relative free energies of the species in kcal/mol; c) Mechanistic proposal for reductive elimination from (tBu$_3$P)Pd(aryl)(CF$_3$); d) Pd-catalyzed pentafluoroethylation of aryl bromides

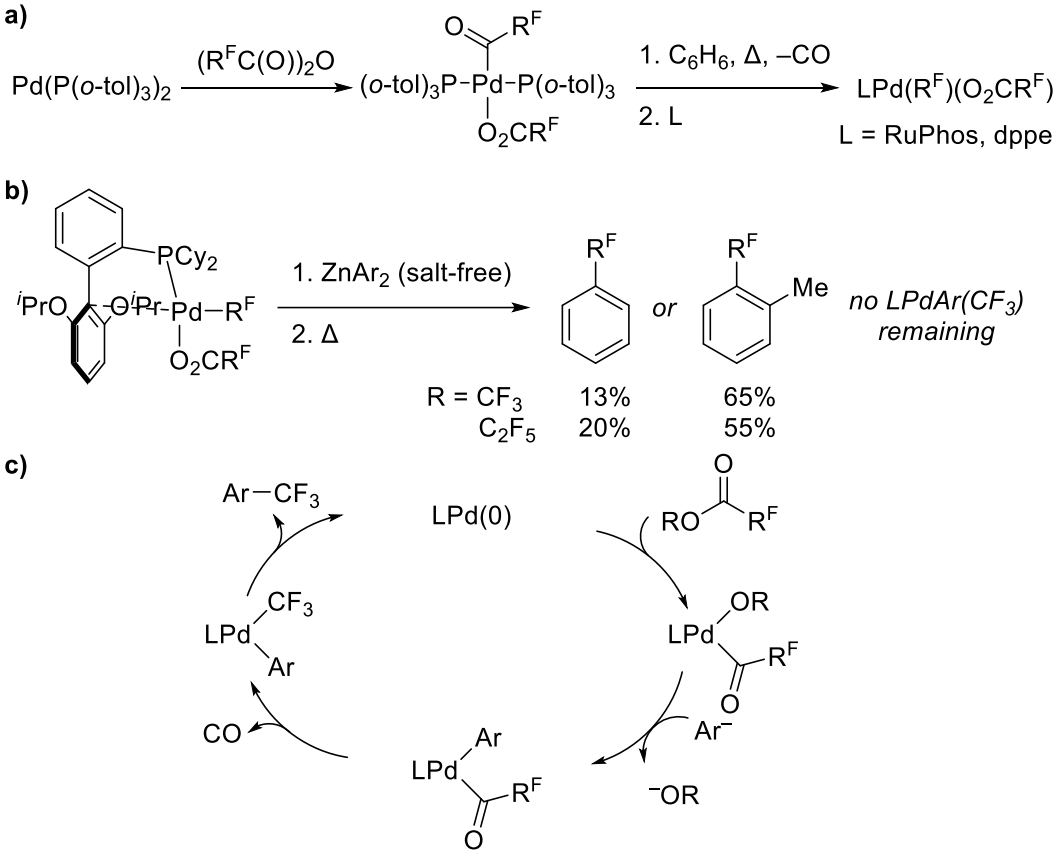
was calculated to have a slightly lower barrier to α-fluoride elimination relative to reductive elimination. A set of conditions for the catalytic pentafluoroethylation of aryl bromides was thus developed, constituting the first example of a Pd-catalyzed pentafluoroethylation of aryl halides and the first Pd-catalyzed perfluoroalkylation of aryl bromides (Scheme 1.3.8d).[144] The two aryl(perfluoroalkyl)phosphine complexes of this report constitute the only isolated examples of this class of complex supported by monodentate phosphine ligands that undergo reductive elimination to form perfluoroalkylarenes.

Although no Pd-catalyzed trifluoromethylations of other classes of aryl halides besides aryl chlorides have been reported, Sanford demonstrated that electron-poor and electron-neutral aroyl chlorides were suitable coupling partners under conditions similar to those reported by Buchwald for the trifluoromethylation of aryl chlorides (Scheme 1.3.9).[146] The reaction of aroyl chloride with a combination of $TESCF_3$, KF, and catalytic $Pd(dba)_2$ and BrettPhos formed generally modest yields of trifluoromethylarene, and the reaction required even higher loadings of palladium catalyst (10 mol%) than the trifluoromethylation of aryl chlorides (6 mol%). Although the mechanism of this transformation was not investigated in depth, the reaction presumably proceeds through the same (BrettPhos)Pd(aryl)(CF_3) complexes that were reported by Buchwald.



Scheme 1.3.9 Pd-catalyzed trifluoromethylation of aroyl chlorides

Sanford also has explored decarbonylation as a strategy for polarity-reversed perfluoroalkylations of arylboronic acids in which the electrophilic component was a perfluoroalkyl fragment. In a pair of publications in 2014, the authors showed that treating the Pd(0) complex $Pd(P(o\text{-tol})_3)_2$ with perfluoroalkylcarboxylic acid anhydrides formed perfluoroacylpalladium salts that underwent decarbonylation upon heating and subsequent facile ligand substitution to form (RuPhos)Pd(R^F)(O_2CR^F) (R^F = CF_3, C_2F_5, n-C_3F_7, C_6F_5) (Scheme 1.3.10a).[147,148] The trifluoromethyl complex (RuPhos)Pd(CF_3)(OTFA) also was prepared by the direct reaction of CpPd(allyl), RuPhos, and trifluoroacetic anhydride. Tracing a hypothetical catalytic cycle, the authors treated these complexes with salt-free diarylzinc to form (RuPhos)Pd(aryl)(R^F) complexes, which upon heating underwent reductive elimination of perfluoroalkylarenes (Scheme 1.3.10b). However, reductive elimination from the (RuPhos)Pd(aryl)(R^F) was high-yielding only when the aryl group was hindered at the *ortho* position (Scheme 1.3.7c-d). This result agrees with the scope reported by Buchwald for the trifluoromethylation of aryl chlorides in which the complex containing the less-hindered ligand RuPhos catalyzed trifluoromethylations of aryl chlorides that are very sterically hindered and for which systems containing the bulkier ligand BrettPhos were ineffective. While the individual steps of a putative catalytic reaction involving this decarbonylative perfluoroalkylation of aryl nucleophiles were evaluated (Scheme 1.3.10c),[147,149] no such catalytic reaction has been reported, although conclusions from these studies assisted the development of a Pd-catalyzed difluoromethylation of arylboronic acids (see Section 1.3.2).

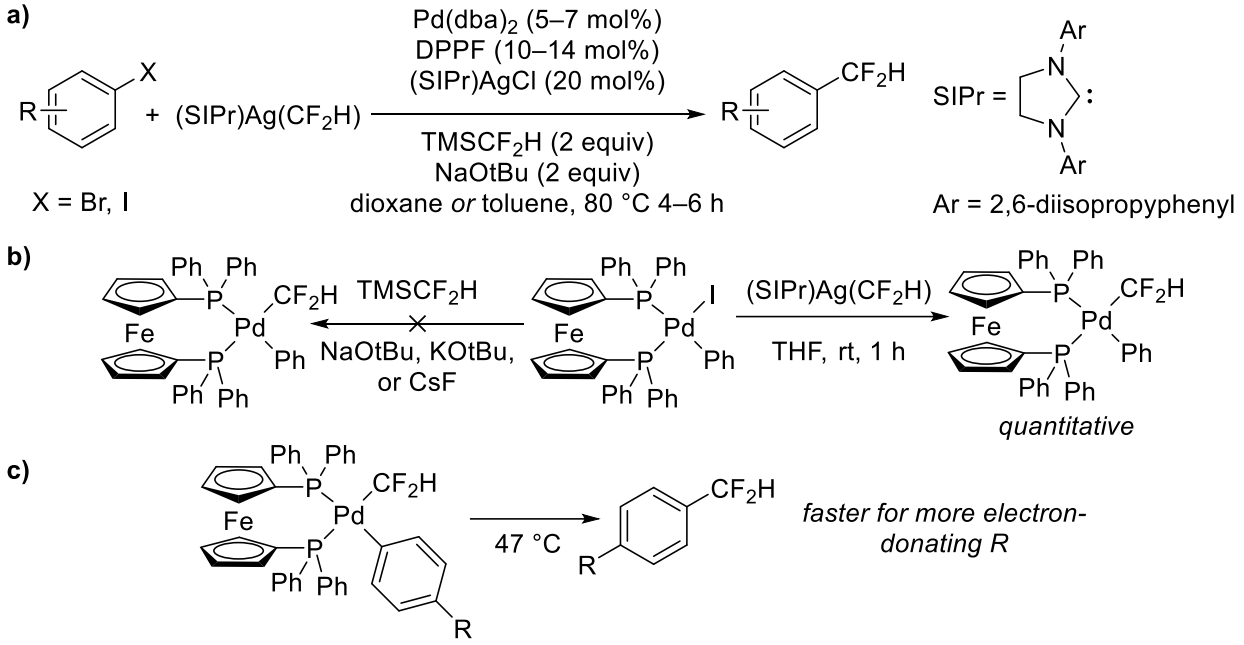


Scheme 1.3.10 Synthesis and reactivity of fluoroalkylpalladium complexes generated from acid anhydrides and a putative catalytic cycle for the perfluoroalkylation of aryl nucleophiles

1.3.2 Pd^{II}–CF_2R and Pd^{II}–CFRR' Complexes

1.3.2.1 Difluoromethylpalladium(II) Complexes

While numerous methods for the cross-coupling of partially fluorinated alkyl groups have been reported and reviewed[150] and many mechanisms for these transformations proposed, investigations of the putative intermediate fluoroalkylpalladium(II) in these studies are rare. Shen[151,152] and Mikami[153] recently disclosed similar methods for the Pd-catalyzed difluoromethylation of aryl and vinyl electrophiles as well as studies on the reactivity of aryl(difluoromethyl)palladium(II) species, which are putative intermediates (Scheme 1.3.11 and Scheme 1.3.12). Key to both the methods and the generation of these complexes for stoichiometric studies was the inclusion of a second metal, either as a co-catalytic shuttle for or as a source of nucleophilic CF_2H .

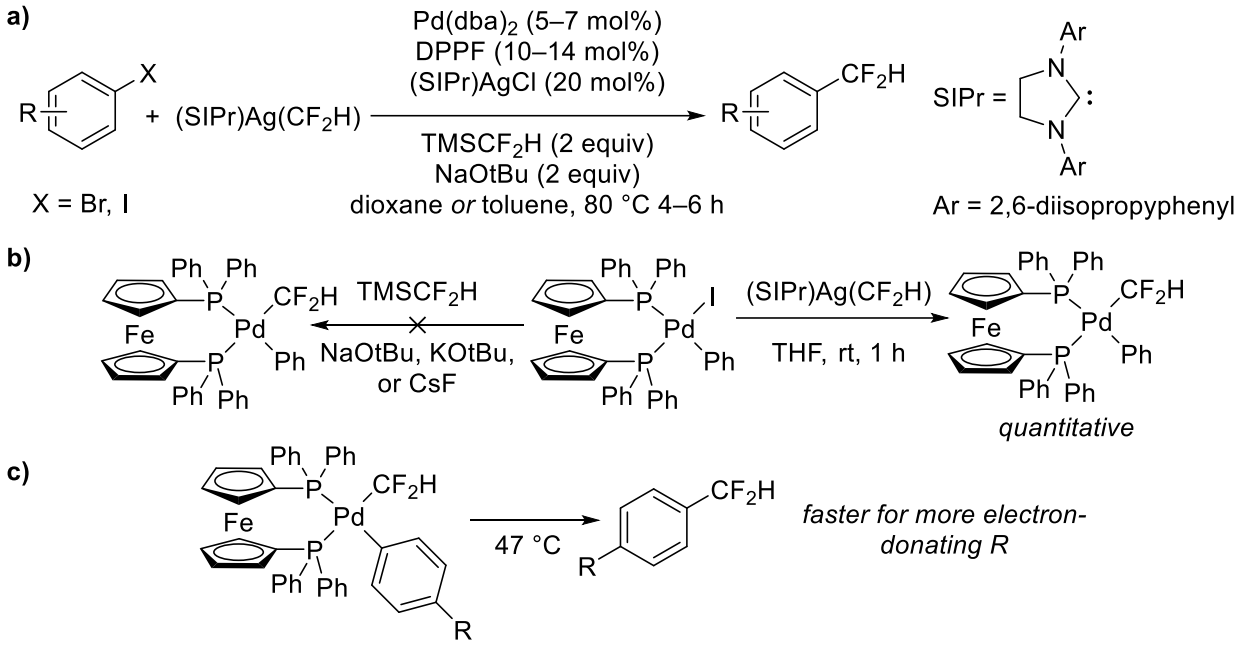


Scheme 1.3.11 Pd-catalyzed difluoromethylation of aryl halides and accompanying stoichiometric studies

Shen reported that stoichiometric reactions of (DPPF)Pd(Ph)I with $TMSCF_2H$ and a Lewis basic activator resulted in the formation of "self-decomposition side products from difluoromethyl trimethylsilane," indicating that decomposition of "CF_2H^-" outpaced transmetallation to the Pd center (Scheme 1.3.11b).[151,152] However, analogous transmetallation reactions of $TMSCF_2H$ and (SIPr)AgCl afforded high yields of the air-stable reagent (SIPr)Ag(CF_2H). (SIPr)Ag(CF_2H) was shown to transfer the CF_2H group cleanly to (DPPF)Pd(aryl)I complexes to form high yields of the corresponding aryl(difluoromethyl)palladium complex (DPPF)Pd(aryl)(CF_2H). Upon heating, this complex underwent smooth reductive elimination at 47 °C to form difluoromethylarene in quantitative yields. These reaction conditions are much milder than those required for reductive elimination from the analogous (DPPF)Pd(aryl)(CF_3) complexes, which required a temperature of 130 °C (see Section 1.3.1.1). The relative rates of reductive elimination from (DPPF)Pd(aryl)(CF_2H) complexes containing substituted aryl groups correlated inversely with the substituent constants of substituted aryl groups in a Hammett study (ρ = –0.9, R^2 = 0.961), demonstrating that reductive eliminations from complexes containing more electron-rich aryl ligands proceeded with faster rates than reductive eliminations from complexes containing more electron-poor aryl ligands (Scheme 1.3.11c). This electronic effects contrasts that of the participating aryl group in most other classes of reductive eliminations to form aryl–carbon or –heteroatom bonds from Pd(II) centers.[154]

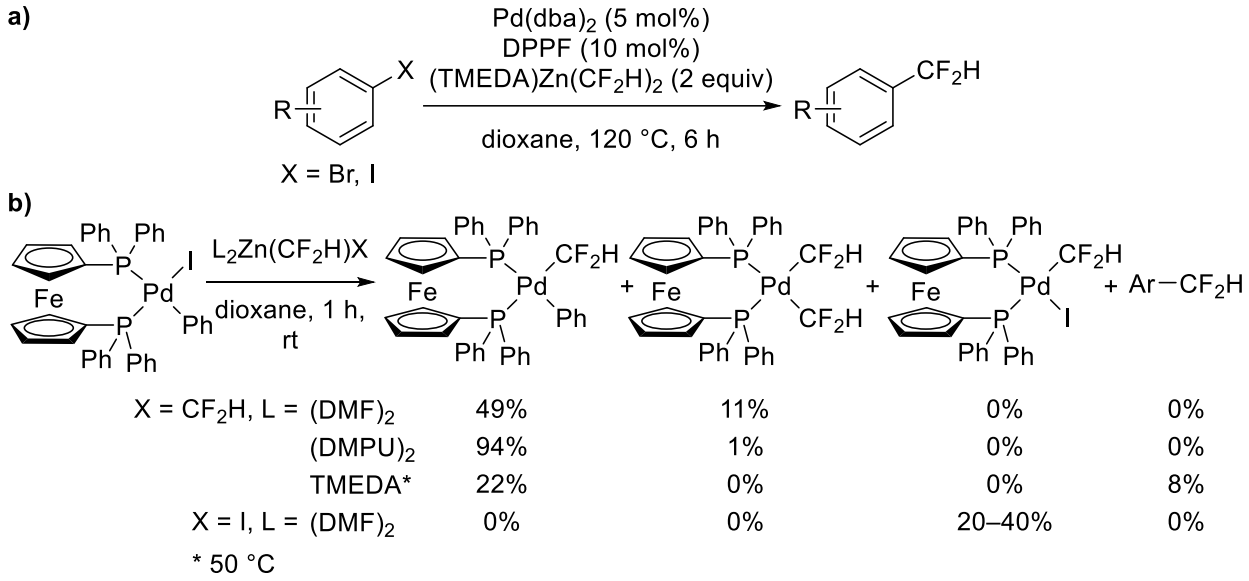
Ultimately, these stoichiometric reactions were translated into a Pd/Ag co-catalyzed difluoromethylation of aryl halides with $TMSCF_2H$ as the terminal source of nucleophilic CF_2H and NaO*t*Bu as the activator for the silane (Scheme 1.3.11a). Reactions containing Xantphos, DPEPhos, or BINAP instead of DPPF as the ancillary ligand for Pd also afforded difluoromethylarene, albeit in much lower yields than reactions containing DPPF, suggesting that reductive elimination from aryl(difluoromethyl)palladium complexes containing these ligands is also likely facile. In contrast to Buchwald's conditions for trifluoromethylation,[132] Shen's method for difluoromethylation did not form difluoromethylarenes from aryl chlorides, but gave high

yields of difluoromethylarenes from a variety of aryl bromides and iodides. However, subsequent reports disclosed similar methods for the difluoromethylation of (hetero)aryl chlorides, bromides, iodides, and sulfonates and reductive eliminations from $L_2Pd(aryl)(CF_2H)$ complexes that occurred within an hour at room temperature.[155,156] In comparison, similar *bis*-phosphinoferrocene- or Xantphos-ligated $L_2Pd(aryl)(CF_3)$ complexes required much higher temperatures (80–150 °C) to form trifluoromethylarenes, demonstrating that a lower degree of fluorination of the fluoroalkyl ligand greatly accelerates reductive elimination from these complexes.



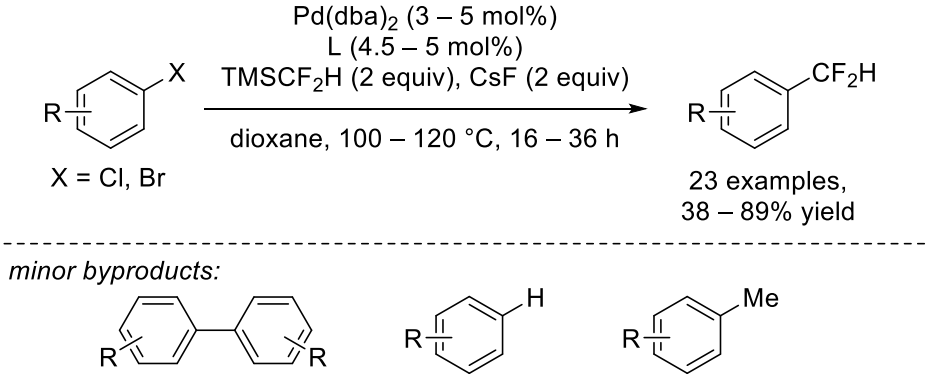
Scheme 1.3.12 Pd/Ag co-catalyzed difluoromethylation of aryl halides

One year after Shen's initial report, Mikami disclosed the Pd-catalyzed difluoromethylation of aryl iodides and bromides in which $L_2Zn(CF_2H)_n$ reagents were the source of nucleophilic CF_2H (Scheme 1.3.13a).[153] In contrast to Shen's reactions of (DPPF)Pd(Ph)I with (SIPr)Ag(CF_2H), Mikami's reactions of (DPPF)Pd(Ph)I with a variety of $L_2Zn(CF_2H)_2$ and $L_2Zn(CF_2H)I$ complexes (L = DMF, DMPU, TMEDA) resulted in both the formation of the desired difluoromethylpalladium complex (DPPF)Pd(Ph)(CF_2H) and variable amounts of (DPPF)Pd(CF_2H)$_2$, depending on the ancillary ligand of the zinc reagent (Scheme 1.3.13b). The reaction of (DPPF)Pd(Ph)I with the heteroleptic complex $(DMF)_2Zn(CF_2H)I$ resulted in the exclusive formation of (DPPF)Pd(CF_2H)I and none of the desired aryl(difluoromethyl)palladium complex. These results suggested that, in contrast to Shen's (SIPr)AgX complexes, the Zn complexes facilitate exchange of X-type ligands of the Pd complexes. Perfluoroalkylzinc complexes containing chelating diamine ligands suppressed the formation of the *bis*(difluoromethyl)palladium complex, and thus were used as reagents in the catalytic reaction.



Scheme 1.3.13 Pd-catalyzed difluoromethylation of aryl halides with (TMEDA)Zn(CF_2H)$_2$

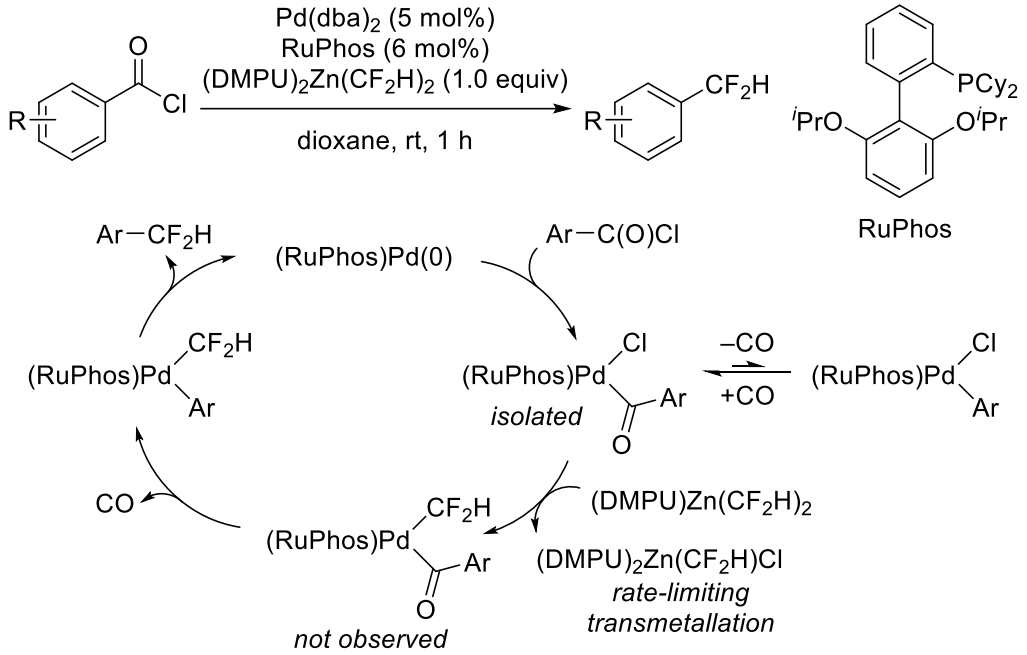
In spite of the difficulties observed by Shen using $TMSCF_2H$ directly as a source of nucleophilic CF_2H without Ag– or Zn–CF_2H complexes as intermediaries, Sanford reported in 2019 the Pd-catalyzed difluoromethylation of aryl halides with $TMSCF_2H$ and CsF. Both BrettPhos and tri-*tert*-butylphosphine enabled the transformation when included as ancillary ligands (Scheme 1.3.14).[157] In contrast to the aforementioned catalytic difluoromethylation reactions containing DPPF as the ancillary ligand for Pd, in which only aryl iodides and bromides reacted in high yields, the conditions reported by Sanford afforded moderate to good yields of difluoromethylarenes from several aryl chlorides and bromides. While the authors did not conduct in-depth investigations into the speciation of the Pd catalyst, they noted that the transfer of CH_3 from $TMSCF_2H$ competed with the transfer of CF_2H in some cases. The authors also noted the formation of biaryl as a minor byproduct, suggesting that exchange of X-type ligands between Pd centers also can occur in the absence of metal shuttles.



Scheme 1.3.14 Pd-catalyzed difluoromethylation of aryl halides with $TMSCF_2H$ and CsF in the absence of secondary metal co-catalysts or reagents

Inspired by Sanford's Pd-catalyzed decarbonylative trifluoromethylation of aroyl chlorides,[146] Ritter recently reported a Pd-catalyzed decarbonylative difluoromethylation of these

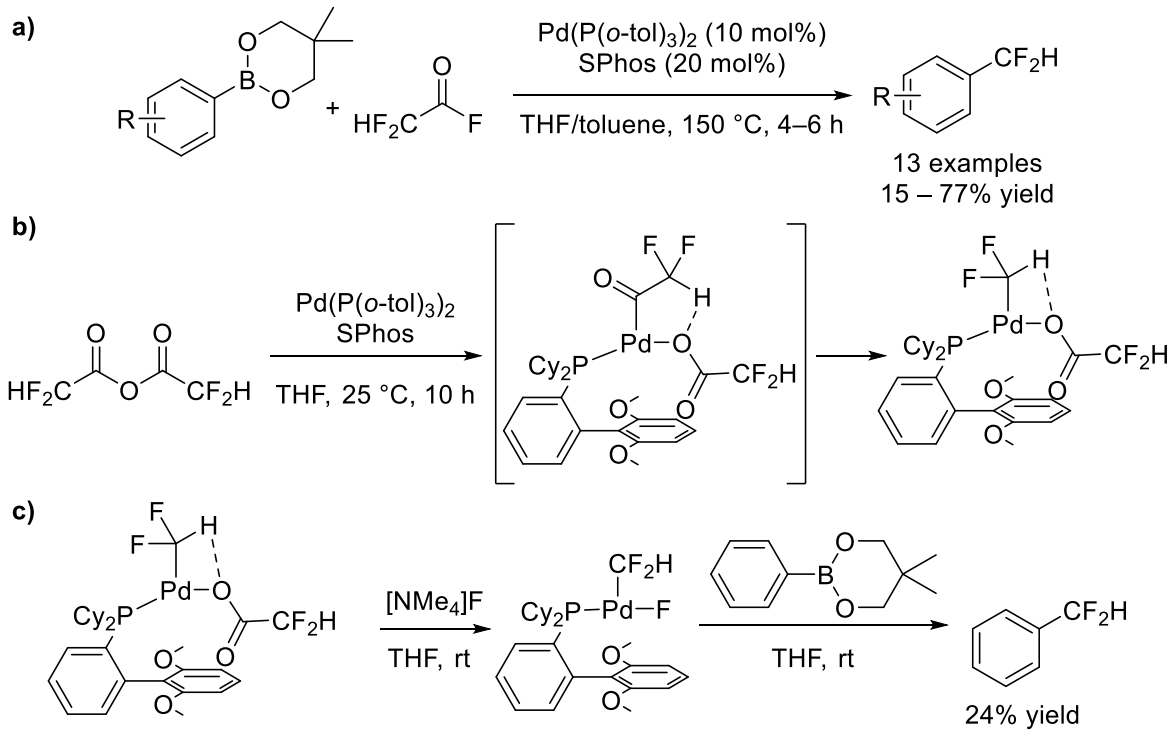
precursors enabled by RuPhos and one of Mikami's *bis*(difluoromethyl)zinc reagents as a source of nucleophilic CF_2H (Scheme 1.3.15).[158] The decarbonylation of the aroylpalladium chloride complex was found to be reversible and energetically unfavorable. The subsequent, rate-limiting transmetallation of CF_2H^- to form the corresponding aroyl(difluoromethyl)palladium complex was followed by fast decarbonylation and reductive elimination to furnish the difluoromethylarene product. In sharp contrast to previous examples of decarbonylative *tri*fluoromethylation, the decarbonylative *di*fluoromethylation reaction proceeded at room temperature and is the mildest Pd-catalyzed nucleophilic fluoroalkylation of any aryl electrophile to date, suggesting that both the decarbonylation and reductive elimination steps are significantly faster for difluoromethylpalladium species than for trifluoromethylpalladium species.



Scheme 1.3.15 Pd-catalyzed difluoromethylation of aroyl chlorides and the proposed mechanism

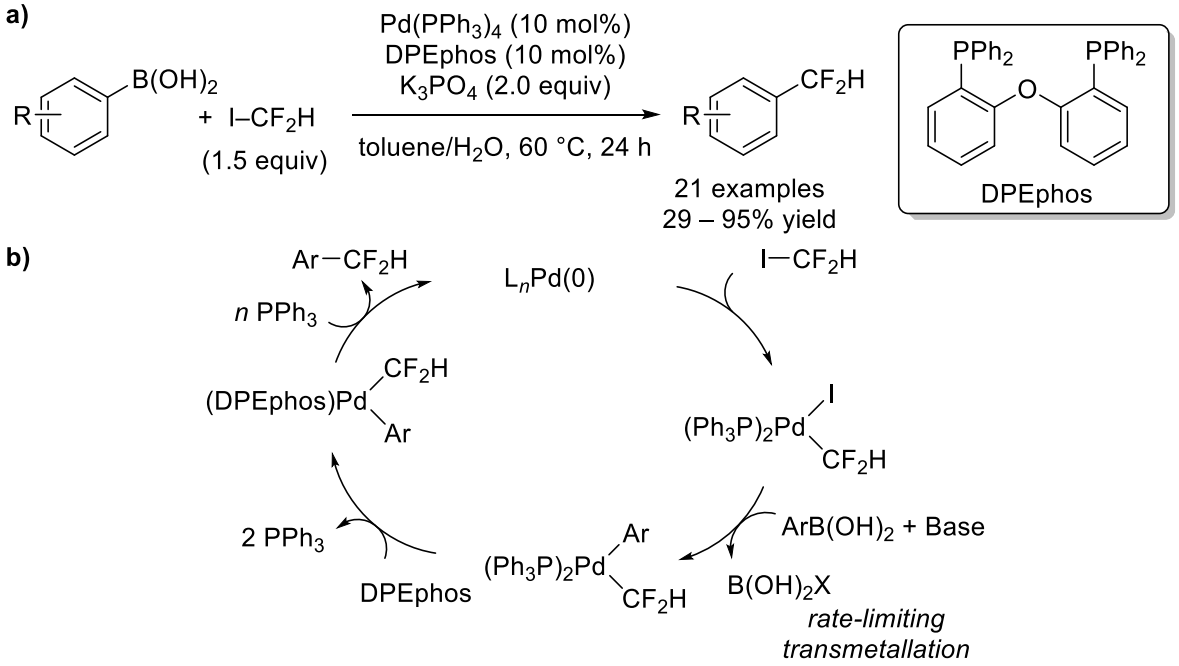
In a continuation of the group's work on the oxidative addition of fluoroalkylcarboxylic acid anhydrides to Pd(0), Sanford recently reported a polarity-reversed Pd-catalyzed decarbonylative difluoromethylation of arylboronic esters enabled by the ligand SPhos (Scheme 1.3.16a).[147–149] The less sterically hindered ligand SPhos (relative to RuPhos in the prior reports) was chosen to facilitate the oxidative addition of difluoroacetic anhydride to the Pd center, and an SPhos-ligated difluoromethylpalladium difluoroacetate complex was prepared for mechanistic study (Scheme 1.3.16b). Based on computational and crystallographic evidence, the authors postulated that the faster decarbonylation of the difluoroacetylpalladium trifluoroacetate species, relative to that of the analogous trifluoroacetylpalladium complex, was facilitated by a hydrogen bonding interaction between the H of the CF_2H group and the oxygen of the difluoroacetate ligand. The difluoroacetate group on the fluoroalkyl complex could be displaced by fluoride to form the difluoromethyl palladium fluoride complex, which reacted an arylboronic ester at room temperature to form difluoromethylarene (Scheme 1.3.16c). These findings were translated into a base-free Pd-catalyzed decarbonylative difluoromethylation of neopentyl glycol esters of electron-poor arylboronic acids in which difluoroacetyl fluoride served as both a source of electrophilic CF_2H and a built-in activator for the arylboronic ester. The higher temperatures required in the

catalytic reaction relative to the reactions conducted with the difluoromethyl complexes were proposed to be the result of removing the difluoroacetate group, resulting in less favorable decarbonylation of the acyl species.



Scheme 1.3.16 Pd-catalyzed decarbonylative difluoromethylation of arylboronic esters

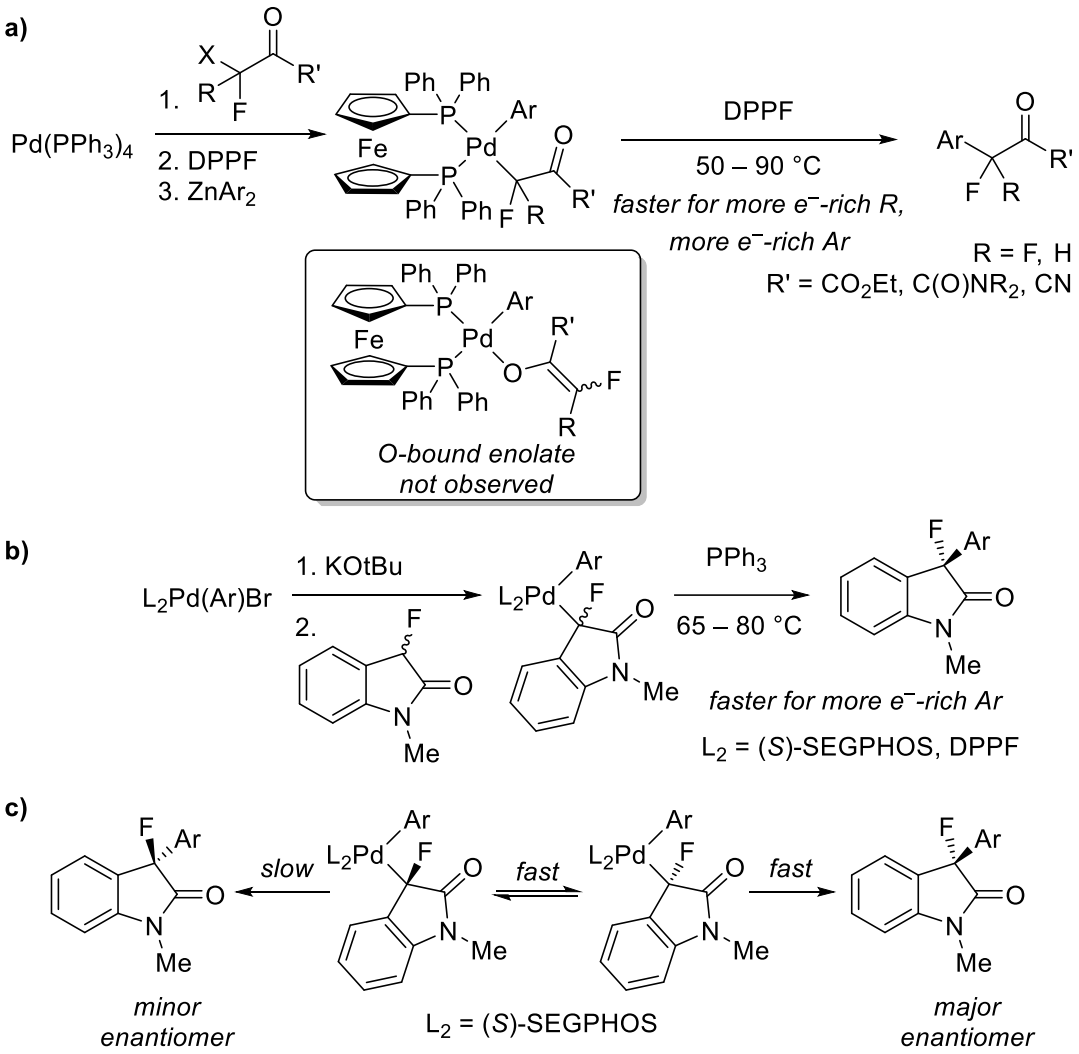
Finally, two recent reports describe the Pd-catalyzed difluoromethylation of arylboronic acids in which CHF_2X (X = Cl, I) served as the electrophilic component as well as accompanying mechanistic investigations to elucidate the structures of the organopalladium intermediates.[159,160] While Zhang showed that the reaction of CHF_2Cl likely proceeded *via* the *in-situ* formation of difluorocarbene and subsequent insertion into the Pd–aryl bond (*vide infra*),[159] Mikami and co-workers demonstrated that CHF_2I underwent facile oxidative addition to Pd(0) complexes (Scheme 1.3.17a).[160] Although Xantphos or DPEPhos were added to form the palladium catalyst, Mikami found that the reaction of CHF_2I, $Pd(PPh_3)_4$ and ancillary diphosphine ligand formed $(PPh_3)_2Pd(CF_2H)I$, instead of the analogous Pd complexes containing the diphosphines. The *bis*(triphenylphosphine) complex was stable to the exchange of ancillary phosphine ligands even at elevated temperatures. Only after transmetallation of an aryl group to form $(PPh_3)_2Pd(CF_2H)$(aryl) did ligand substitution with the bidentate ligand occur to form $L_2Pd(CF_2H)$(aryl) (L_2 = DPEPhos, Xantphos), which underwent facile reductive elimination to form difluoromethylarene (Scheme 1.3.17b). The reason the two palladium species preferentially bind different ligands is unclear.



Scheme 1.3.17 Pd-catalyzed difluoromethylation of arylboronic acids with I–CF_2H

1.3.2.2 Other Pd^{II}–CF_2R and Pd^{II}–CFRR' Complexes (R ≠ H)

Pd complexes also catalyze cross-coupling reactions to construct α-aryl-α-fluorocarboxylic acid derivatives,[161–168] but only two studies on the reactivity of the putative intermediate arylpalladium fluoroenolate complexes have been published (Scheme 1.3.21).[23,124] Hartwig reported the first examples of arylpalladium fluoroenolate complexes in 2017.[23] These mono- and difluoroester, difluoroamide, and difluoronitrile complexes were prepared by oxidative addition of the corresponding halofluorocarbonyl compounds to $Pd(PPh_3)_4$, followed by ligand substitution with DPPF and treatment with diarylzinc to form the corresponding (DPPF)Pd(Ph)(CF_2R) and (DPPF)Pd(Ph)(CHFR) complexes (Scheme 1.3.18a). While the mechanism of oxidative addition was not investigated in this work, radical trapping studies by Zhang on the catalytic cross-coupling of arylboronic acids with bromodifluorocarbonyl compounds suggested the intermediacy of free *α*,*α*-difluorocarbonyl radicals.[165] It was shown previously that complexes containing non-fluorinated *α*,*α*-disubstituted enolates bound to the Pd center through the enolate oxygen instead of the *α*-carbon, due to steric effects.[154,169,170] However, all of the *α*-fluorinated enolates in this work bound to the Pd center through the *α*-carbon, likely due to the small steric profile and the electron-withdrawing property of the fluorine substituents. Each of these fluoroenolate complexes underwent smooth reductive elimination upon heating to form *α*-aryl carbonyl compounds, and complexes containing more electron-rich carbonyl derivatives underwent faster reactions than complexes containing more electron-poor carbonyl derivatives (CHFC(O)OEt >> $CF_2C(O)NR_2$ > $CF_2C(O)OEt$ > CF_2CN). The effect of the aryl ligand on the rate of reductive elimination from (DPPF)Pd(aryl)($CF_2C(O)OEt$) was evaluated for three *para*-substituted aryl groups, revealing the tentative trend that complexes containing more electron-rich aryl groups underwent faster reductive elimination than complexes containing less electron-rich aryl groups. This trend contrasts the trend observed in the reductive elimination from arylpalladium complexes of non-fluorinated enolates, in which complexes containing more electron-poor ligands underwent faster reductive elimination than complexes containing more electron-rich aryl ligands.[154]

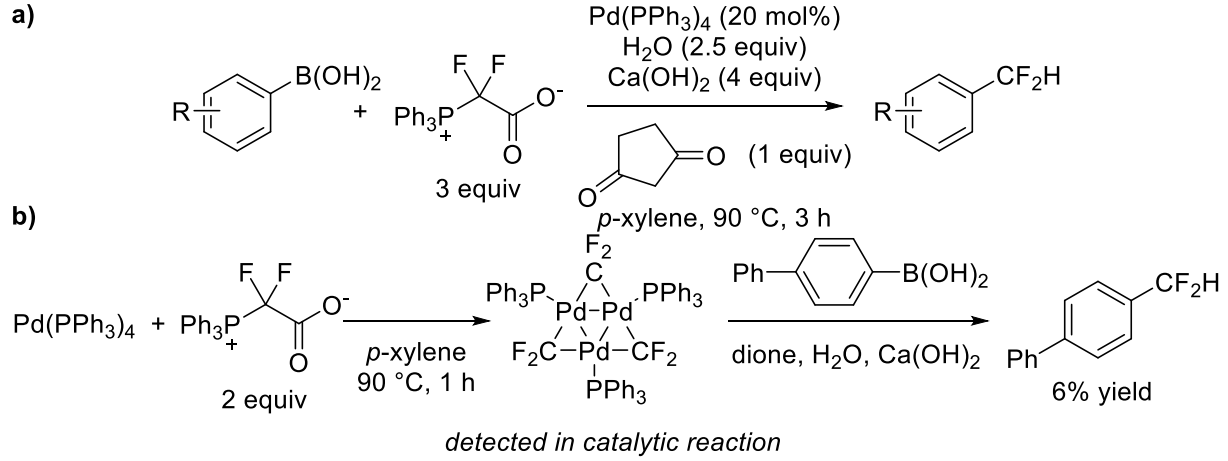


Scheme 1.3.18 Syntheses of arylpalladium fluoroenolate complexes

A similar electronic trend was observed for a wider range of aryl ligands by Hartwig in 2021, as part of a report studying the enantioselective α-arylation of 3-fluorooxindoles.[124] The authors prepared a series of arylpalladium fluorooxindole complexes containing DPPF or (*S*)-SEGPHOS as the ancillary ligand and found that heating these complexes formed α-arylated-α-fluorooxindoles with faster rates for complexes containing more electron-rich aryl ligands than for complexes containing more electron-deficient aryl ligands (Scheme 1.3.18b, $\rho = -1.0$, $R^2 = 0.79$). Diastereomeric mixtures of the (*S*)-SEGPHOS-ligated complexes formed the α-arylated products upon heating with high enantioselectivities and were shown through a series of kinetic and spectroscopic experiments to be competent intermediates in the Pd-catalyzed asymmetric α-arylation of 3-fluorooxindoles.[167] The authors also evaluated the origins of enantioselectivity of the arylation reaction by kinetic and computational studies and found that, while the diastereomeric (SEGPHOS)Pd(aryl)(fluorooxindole) complexes interconverted sluggishly, the largest influence on enantioselectivity was the difference in energies between the transition states for reductive elimination from the two diastereomeric fluoroenolate complexes (Scheme 1.3.18c, see Chapter 3 for a more thorough discussion).

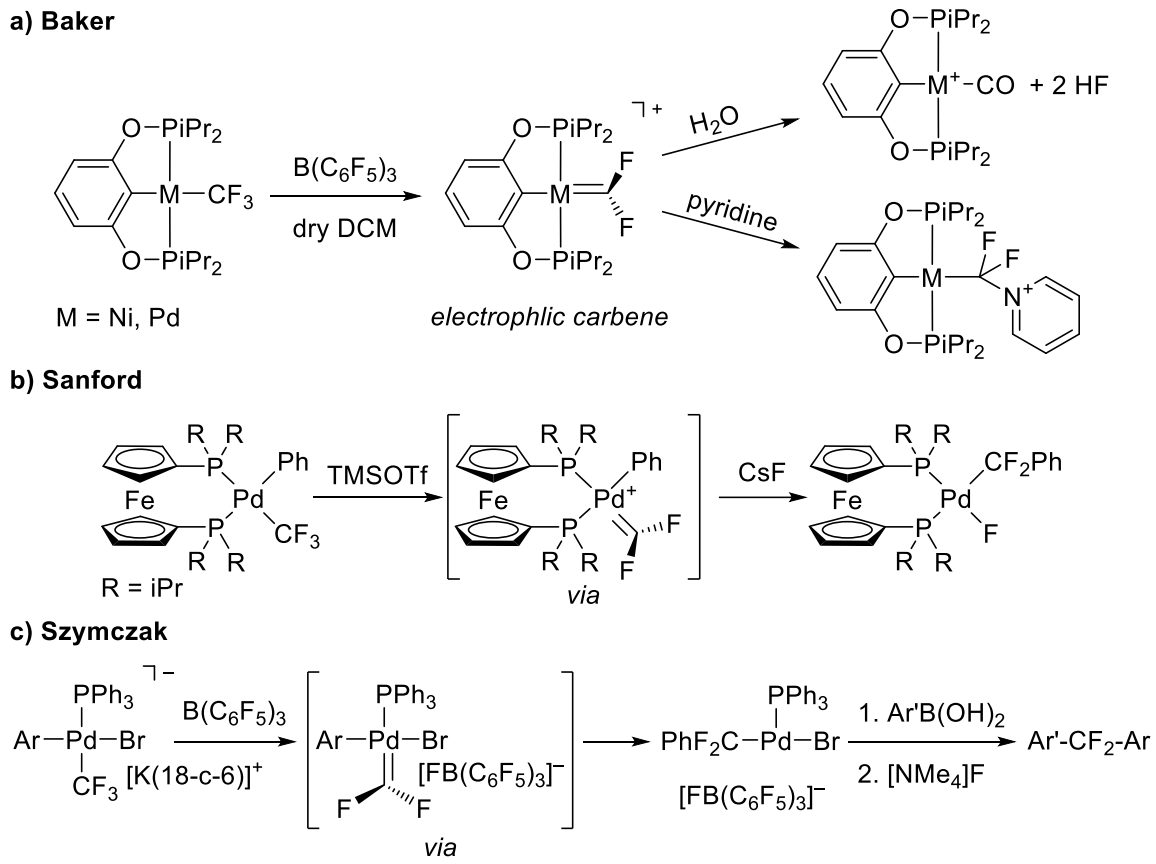
1.3.3 Pd=CF_2 Complexes

As alluded to in Section 1.3.2.2, another strategy toward the formation of CF_2H and of some CF_2R compounds involves the generation of Pd=CF_2 species, which can form fluoroalkylpalladium complexes by carbene insertion reactions.[171,172] The reactivity of these complexes is governed by the oxidation state of the Pd center, with Pd^0=CF_2 species reacting as nucleophiles at the carbene and Pd^{II}=CF_2 species reacting as strong electrophiles.[173] Although Pd=CF_2 intermediates had been invoked previously in the Pd-catalyzed difluoromethylation of arylboronic acids,[171,172] the first observation and characterization of a palladium difluorocarbene complex was reported by Xiao in 2016 (Scheme 1.3.19).[172] As part of the group's development of a Pd-catalyzed difluoromethylation of arylboronic acids, the authors observed the formation of $[Pd(PPh)_3(\mu^2\text{-}CF_2)]_3$ in the catalytic reaction mixture and prepared it independently (Scheme 1.3.19a). However, the complex itself was poorly reactive toward the difluoromethylation of arylboronic acids in a stoichiometric experiment (Scheme 1.3.19b), suggesting that it is not an intermediate in the catalytic reaction.



Scheme 1.3.19 Formation of a Pd=CF_2 complex in the Pd-catalyzed difluoromethylation of arylboronic acids

In 2017, Baker reported the first example of an isolated, monomeric Pd=CF_2 complex and a related Ni=CF_2 complex (Scheme 1.3.20a).[173] The authors initially prepared the parent trifluoromethyl complexes (^{iPr}POCOP)M(CF_3) (M = Ni, Pd; ^{iPr}POCOP = $\kappa^P,\kappa^C,\kappa^P$-(2,6-(*i*$Pr_2PO)_2$-$C_6H_3$) from the reaction of (^{iPr}POCOP)MCl, $TMSCF_3$, and CsF. Exploiting the facile fluoride abstraction from trifluoromethylmetal species, the authors showed that treatment of these complexes with the fluorophilic Lewis acids $SiMe_3OTf$ or $B(C_6F_5)_3$ formed the corresponding cationic difluorocarbene complexes (POCOP)M$(CF_2)^+$, which were isolated and characterized. These d^8 difluorocarbene complexes were extremely electrophilic at the carbene moiety, reacting with pyridine to form *N*-difluoromethylenyl complexes or decomposing to HF and CO in the presence of trace water.

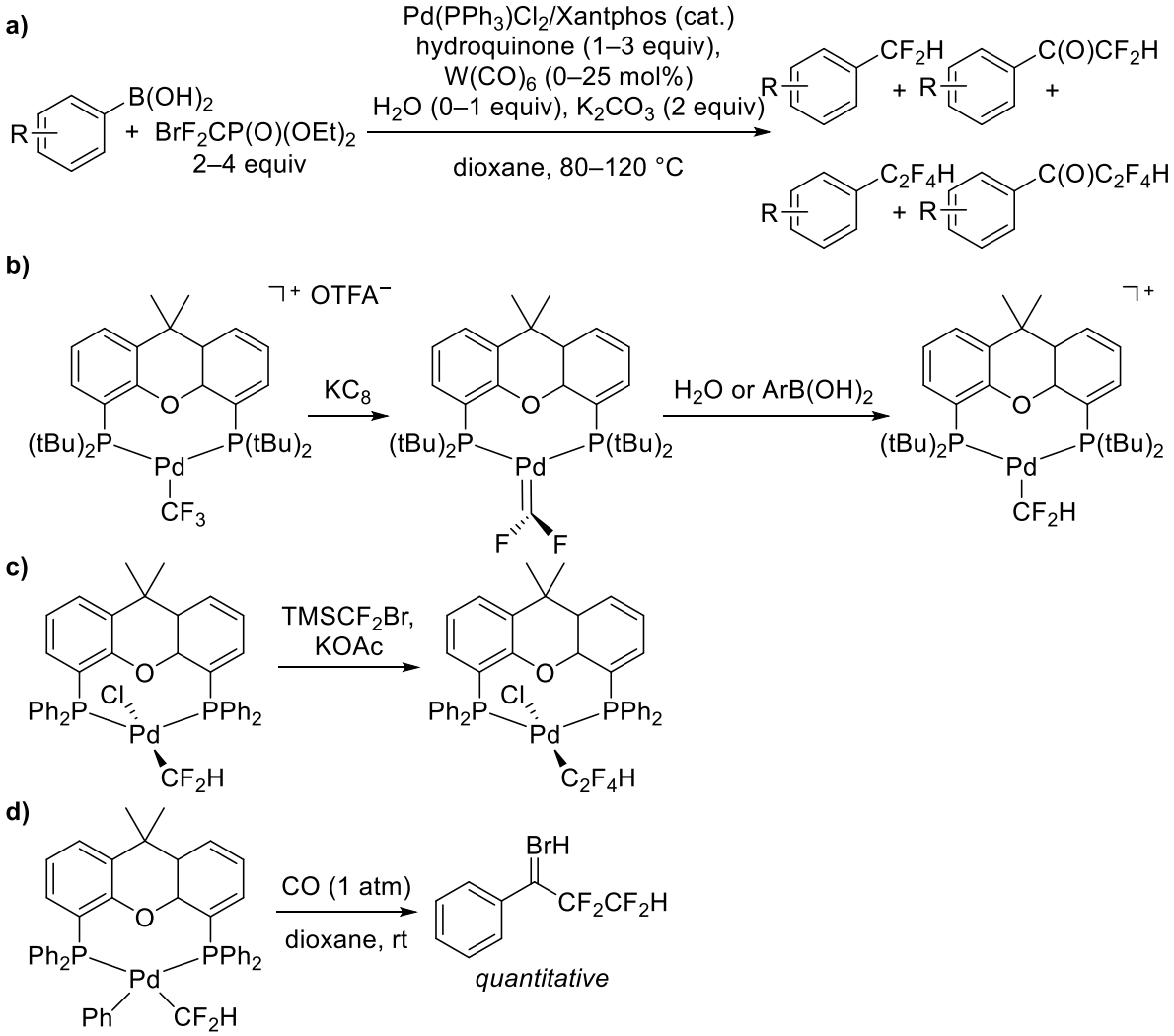


Scheme 1.3.20 Reactions of electrophilic Pd(II) difluorocarbene species

The electrophilicity of $Pd^{II}=CF_2$ complexes resulting from Lewis acid-mediated fluoride abstraction from aryl(trifluoromethyl)palladium(II) complexes (Scheme 1.3.20b-c) was demonstrated in subsequent reports by Sanford[142] and Szymczak.[174] Although the putative $Pd^{II}=CF_2^+$ species were not observed directly, the transient carbene units underwent migratory insertion into the Pd–aryl bond to form aryldifluoromethylpalladium(II) species. Szymczak further developed this process into a method to form unsymmetrical difluorodiarylmethanes by treatment of the aryldifluoromethyl complexes with arylboronic acids (Scheme 1.3.20c).

Zhang reported a series of studies involving Pd-catalyzed couplings of aryl nucleophiles and difluorocarbene generated from a variety of common RCF_2X precursors (X = halide) in which both nucleophilic and electrophilic $Pd=CF_2$ species were proposed as intermediates.[159,171,175] In a recent in-depth study,[175] the authors demonstrated that subtle changes to the reaction conditions enabled selective formation of aryl–CF_2H, aryl–$C(O)CF_2H$, aryl–C_2F_4H, or aryl–$C(O)C_2F_4H$ products from the reaction of palladium catalyst, diethyl bromodifluoromethylphosphonate, arylboronic acid, and hydroquinone (Scheme 1.3.21a). The authors found that fast generation of large amounts of difluorocarbene favored the formation of products containing a tetrafluoroethyl unit over a difluoromethyl unit, while addition of water or the incorporation of $W(CO)_6$ as a source of CO led to the carbonylated products. To model individual steps of the proposed mechanism, the authors prepared the reported first example of an isolated d^{10} Pd difluorocarbene complex, (^{tBu}Xantphos)$Pd=CF_2$, by reduction of the corresponding trifluoromethylpalladium(II) complex with KC_8 (Scheme 1.3.21b). Similar to Baker's d^{10} $Ni=CF_2$ complexes,[176] this "Pd^0" carbene complex was nucleophilic at the carbene and was readily protonated by arylboronic acid or water

to form (^{tBu}Xantphos)Pd^{II}–CF_2H^+, which was proposed to react with the arylboronic acid to form difluoromethylarene. Alternatively, the authors demonstrated experimentally and computationally that complexes of the type (Xantphos)Pd(CF_2H)X (X = Cl, OH) could react with another equivalent of difluorocarbene to form the tetrafluoroethyl complex (Xantphos)Pd(C_2F_4H)X by a coordination-insertion mechanism (Scheme 1.3.21c). The carbonylated products arose from the insertion of CO into the Pd–R^F bond (Scheme 1.3.21d). For reactions in which no source of CO was added to the catalytic reaction, the authors proposed that CO was generated *in situ* by the hydrolysis of the intermediate Pd^{II}=CF_2 species, as proposed by Baker (*vide supra*).

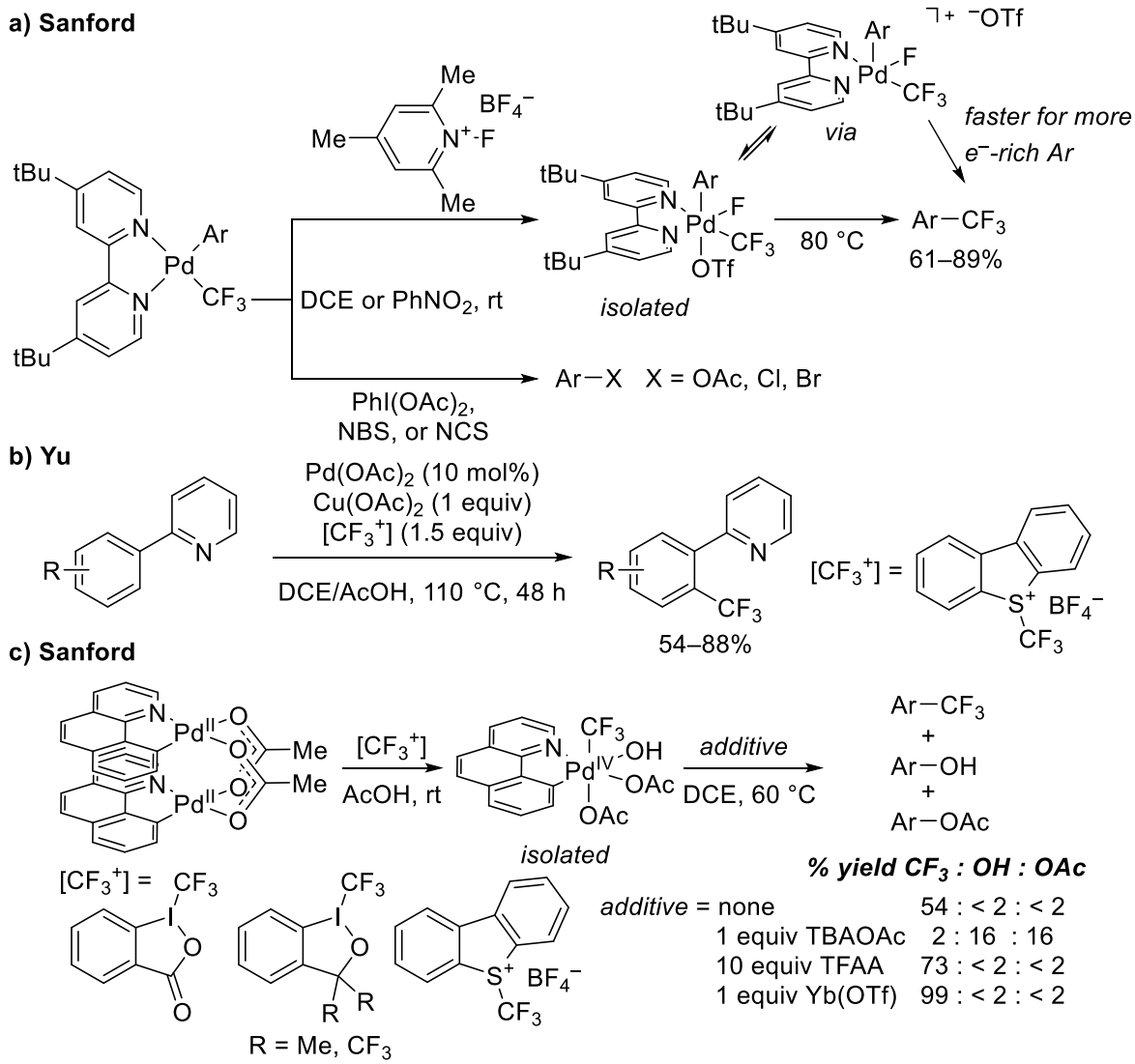


Scheme 1.3.21 Pd-catalyzed cross-coupling of difluorocarbene with arylboronic acids and stoichiometric experiments involving Pd=CF_2 species

1.3.4 Palladium(IV) Complexes

The challenge of achieving reductive elimination from LPd^{II}(aryl)(CF_3) complexes that would occur during in a typical Pd(0/II) catalytic cycle to form trifluoromethlarenes has prompted a few investigations into the formation and reactivity of high-valent Pd(IV) species. Such species would be expected to undergo facile reductive elimination because of the high oxidation state of

the metal. In this vein, Sanford reported in 2010 a model system in which the treatment of (dtbbpy)Pd(aryl)(CF_3) (dtbbpy = 4,4'-di-*tert*-butyl-2,2'-bipyridine, aryl = 4-F-C_6H_4) with *N*-fluoro-2,4,6-trimethylpyridinium triflate (NFTPT) formed (dtbbpy)Pd^{IV}(aryl)(CF_3)(F)(OTf), the first example of an isolable Pd(IV)–CF_3 species (Scheme 1.3.22a).[177] Whereas the parent Pd(II) complex did not undergo reductive elimination to form trifluoromethylarene, even after 3 days at 130 °C, the Pd(IV) complex underwent clean reductive elimination after just 3 hours at 80 °C in nitrobenzene, constituting the first example of reductive elimination to form the aryl–CF_3 bond from a well-defined Pd^{IV}(aryl)(CF_3) complex. The identity of the oxidant was crucial; reactions of (dtbbpy)Pd(aryl)(CF_3) with $PhI(OAc)_2$, NCS, or NBS led to the formation of halogenated or oxygenated arene byproducts.[177,178]



Scheme 1.3.22 Oxidative aromatic trifluoromethylation *via* Pd(IV) complexes

The mechanism of this transformation was investigated in a subsequent study by a series of kinetic and computational methods, which revealed that reversible dissociation of the triflate anion to form a five-coordinate Pd(IV) species preceded rate-limiting reductive elimination to form trifluoromethylarene.[178] Lower yields of trifluoromethylarene products were obtained from

reactions involving more electron-poor aryl groups due to the competing formation of biaryl. In agreement with the aforementioned studies of reductive elimination to form aryl–R^F compounds from Pd^{II}(aryl)(fluoroalkyl) and Cu^{III}(aryl)(CF_3) complexes (see Sections 1.3.2 and 1.2.5, respectively), the reductive elimination from (dtbbpy)Pd(aryl)(CF_3)(F)(OTf) complexes containing more electron-rich aryl ligands proceed more quickly than that of complexes containing more electron-poor aryl ligands. The enthalpies of activation for the reductive elimination from the five-coordinate complex were calculated by DFT and found to correlate more strongly with the σ^+ substituent parameters of the aryl ligands than with σ or σ^-, suggesting the accumulation of positive charge on the aryl ring in the transition state. The authors identified TMEDA as a ligand that facilitated the dissociation of the triflate anion and showed that (TMEDA)Pd(aryl)(CF_3)(F)(OTf) underwent facile reductive elimination at room temperature. A few L_2Pd^{IV}(aryl)(CF_3)$(X)_2$ complexes also were prepared in studies probing the ability of Pd(IV) complexes to facilitate C–H activation reactions; however, in these studies, the CF_3 ligand was simply a spectator ligand that stabilized the Pd(IV) complex.[179]

Yu reported in 2009 the first example of a Pd-catalyzed oxidative *ortho*-C–H trifluoromethylation of 2-pyridyl arenes in which 5-(trifluoromethyl)dibenzothiophenium tetrafluoroborate served as a source of "CF_3^+" (Scheme 1.3.22b).[180] While the authors proposed several tentative mechanisms for the formation of trifluoromethylarene, a 2010 report by Sanford gave a detailed account of the mechanism of this transformation, including the characterization of a key reaction intermediate (Scheme 1.3.22c).[181] Starting from the model complex $[(bzq)Pd(OAc)]_2$ (bzq = benzo[*h*]quinoline), the authors showed that reactions with several sources of electrophilic CF_3 led to the formation of the monomeric Pd(IV) complex (bqz)Pd(CF_3)$(OAc)_2(OH_2)$, which was isolated and characterized by X-ray crystallography. This oxidation step was shown later to occur directly to $[(bzq)Pd(OAc)]_2$ to form a formally Pd^{III}–Pd^{III} dimeric species, which underwent heterolytic cleavage to yield the oxidized Pd(IV) species and one equivalent of a Pd(II) complex.[182] While the Pd(IV) complex underwent reductive elimination to form trifluoromethylarene in moderate yields upon heating at 60 °C, quantitative yields and faster rates of formation of trifluoromethylarene were observed when Brønsted- or Lewis-acidic additives, such as trifluoroacetic acid or $Yb(OTf)_3$, were included in the reaction. These additives were proposed to facilitate dissociation of an acetate ligand from the Pd(IV) complex to form a five-coordinate species, which was proposed to undergo facile reductive elimination.

1.4 Outlook on Cu- and Pd-Mediated Fluoroalkylation Reactions

1.4.1 Cu-Mediated Fluoroalkylation Reactions

While most fluoroalkylation reactions involving copper have been adopted more widely than those involving palladium, many limitations of copper-mediated fluoroalkylation reactions remain to be overcome. The biggest limitation of copper-catalyzed and copper-mediated fluoroalkylations of aryl halides is the restricted scope of aryl halides. Especially for methods catalytic in copper, the fluoroalkylation of aryl bromides or chlorides remains a significant challenge. Only copper-mediated pentafluoroethylation with "ligandless" Cu(C_2F_5) gave high yields of pentafluoroethylarenes from a wide range of aryl bromides.[57] While the oxidative addition of aryl halides is known to be rate-limiting in Ullmann- and Goldberg-type cross-coupling reactions and is prohibitively slow for most aryl chlorides and bromides, the fluoroalkylcopper reagents are also unstable and decompose at room temperature after generation *in situ*. Nevertheless, a series of studies investigating trifluoromethylcopper species has led to the

development of Cu–CF_3 reagents that are much more stable than those in Burton's original work, so it is reasonable to expect that similar developments of other fluoroalkylcopper reagents might result in more stable reagents requiring lower temperatures to react with aryl halides.

In this vein, the structures of Cu–R^F complexes in which R^F is a partially fluorinated alkyl fragment scarcely have been investigated, in part due to the sensitivity of these reagents to temperature. In particular, it is unclear whether the reagents formed by treatment of Cu(I) complexes with "R^F–" form the heteroleptic cuprates XCuR^F– *in situ*, or whether the "X" ligand on copper is displaced by *e.g.*, solvent molecules. It is also unclear what relevance such species might have to the formation of fluoroalkylarenes, as Shen showed that Cu(CF_3), Cu$(CF_3)_2^-$, and X$Cu(CF_3)^-$ all can form trifluoromethylarene from reactions with aryl halides, albeit with significantly different rates. For example, the putative Cu–R^F species have been generated for R^F = CF_2H, CF_2SO_2Ph, $CF_2P(O)(OEt)_2$, and $CF_2C(O)R$, and, in most cases, multiple ^{19}F NMR resonances corresponding to fluoroalkylcopper complexes were observed by ^{19}F NMR spectroscopy; however, assignments of these resonances is currently tentative and are based on analogies to perfluoroalkylcopper species. Conclusive identification of these species may provide a foundation to develop more stable or more reactive reagents.

One obvious approach to enhancing the rate of the oxidative addition and increasing the stability of the organocopper reagents is the inclusion of ancillary ligands. 1,10-phenanthroline has been use commonly for copper-catalyzed trifluoromethylations of aryl iodides, and 2,2'-bipyridine ligands form isolable perfluoroalkylcopper complexes. However, stoichiometric perfluoroalkylations of aryl halides are conducted at similar temperatures in both the presence and absence of ancillary ligands, and recent work by our group showed that the rates of reactions of "ligandless" and ligated pentafluoroethylcopper species differed by less than an order of magnitude. Thus, these ligands do not appear to affect the rate of perfluoroalkylation significantly. On the other hand, reactions of partially fluorinated alkylcopper species are often conducted in the absence of ancillary ligands, and the addition of phen to many of these reactions did not lead to new reactivity. Further studies are needed to establish the effect of these ligands on both stoichiometric and catalytic reactions and to identify other classes of ancillary ligands that more greatly increase the rate of the oxidative addition step. Recent work by Ma has led to the development of oxalamide ligands that enable Ullmann-type cross-coupling reactions of aryl bromides and even some reactions of aryl chlorides in catalytic etherification and amination reactions.[183–185] While current ligands are likely unsuitable for fluoroalkylation reactions due to the presence of acidic protons in the ligand scaffold, it is possible that other strongly donating X-type ligands could increase the rate of oxidative addition in fluoroalkylation reactions.

Incorporating ancillary ligands into copper-mediated fluoroalkylation reactions may also increase the stability of the intermediate fluoroalkylcopper reagents at higher temperatures and enable the fluoroalkylation of less reactive aryl coupling partners. Grushin showed that the copper halide byproducts of fluoroalkylation reactions facilitate the decomposition of trifluoromethylcopper reagents. On the other hand, Burton showed that the addition of HMPU stabilized a variety of Cu–R^F species, possibly by quenching the Lewis acidity of the byproduct CuX species. By judicious choice of an ancillary ligand, Lewis acidic species such as CuX may be quenched while still allowing for the conversion of less reactive species such as X$Cu(R^F)^-$ or $Cu(R^F)_2^-$ into more active "ligandless" or ligated Cu–CF_3 species, allowing for higher overall stability of the reagent and shorter reaction times. The incorporation of ancillary ligands into the aforementioned Cu–CF_2R complexes may also render them isolable for study, as was observed the case (NHC)$Cu(R^F)$ (RF = CF_3, CF_2H).[83]

The application of fluoroalkylcopper(III) species toward perfluoroalkylation reactions besides trifluoromethylation is also underexplored. Under similar reaction conditions to the original synthesis of and (edtc)Cu(CF_3)$_2$ and Cu(CF_3)$_4^-$ by Burton and Naumann,[36,43,103] $Cu^{III}R^F$ complexes were reported for R^F = CF_2H, C_2F_5, including the direct difluoromethyl analogue Cu(CF_2H)$_4^-$ of the widely used Cu(CF_3)$_4^-$.[77] However, reactions of these species with organic substrates are rare overall, especially reactions that form fluoroalkylarenes. Eujen also showed that Cu(R^F)$_4^-$ can undergo ligand exchange with other fluoroalkyl groups to form mixed cuprates, and Grushin recently reported a simple and accessible synthesis of Cu(CF_3)$_4^-$,[44,77] and this chemistry of Cu(CF_3)$_4^-$ could constitute entry points for studies of other fluoroalkylcopper(III) reagents.

1.4.2 Pd-Mediated Fluoroalkylation Reactions

Several opportunities are available to develop Pd-catalyzed fluoroalkylation reactions further. Despite several recent studies on the formation and reactivity of aryl(trifluoromethyl)palladium complexes,[135,139,140,142–144,147] Buchwald's twelve-year-old report remains the sole example of a Pd-catalyzed trifluoromethylation reaction that forms a wide range of trifluoromethylarenes from any class of aryl (pseudo)halide,[14,132] though reactions of aroyl halides as electrophiles have been published in recent years.[141,146,158] The conditions in Buchwald's report were only suitable for aryl or aroyl[146] chlorides; the authors noted that, for unknown reasons, trifluoromethylations of aryl bromides under the reported conditions generally occurred in low yields. While reductive elimination from the intermediate aryl(trifluoromethyl)palladium complexes traditionally has been seen as the challenging step in the catalytic reaction, Buchwald and others have reported numerous examples of ancillary ligands that promote high-yielding reductive elimination of trifluoromethylarene at mild temperatures.[87,135,137,139,142–144,147,149] Many of these ligands are well known to promote the oxidative addition of aryl (pseudo)halides to form the intermediate arylpalladium (pseudo)halide complexes. By process of elimination, this leaves the conversion of the arylpalladium (pseudo)halide into the aryl(trifluoromethyl)palladium species or deleterious side reactions of these species as the primary hurdles facing the further development of Pd-catalyzed trifluoromethylation reactions.

In this vein, the potential interplay between Pd(aryl)R^F species and the Pd(aryl)X species formed from oxidative addition of the aryl electrophile should be explored.[135] Grushin and Zhang showed that X-type ligand exchange occurred readily between (L)Pd(aryl)(CF_3) and (L)Pd(aryl)I to form (L)Pd(CF_3)I and biaryl (L = DPPE, Xantphos).[134,138] Mikami also showed that X-type ligand exchange of (DPPF)Pd(aryl)I was facilitated by zinc in the Pd-catalyzed difluoromethylation of aryl halides, resulting in the formation of catalytically inactive (DPPF)Pd(CF_3)$_2$ and (DPPF)Pd(CF_3)I. Nevertheless, the stoichiometric studies of Pd(aryl)R^F complexes typically are conducted in the absence of aryl halide complexes, and such reactivity remains poorly explored for the few systems that enable the fluoroalkylation of aryl halides.

In the design or assessment of ligands for new Pd-catalyzed trifluoromethylation reactions, there are some useful trends that may guide future study. Almost all of the ancillary phosphine ligands that facilitate aryl–R^F reductive elimination are bidentate, either as chelating bisphosphines or, in the case of the dialkylbiarylphosphine ligands BrettPhos, RuPhos, and SPhos, κ^2-P,C or κ^2-P,O binding. Of the competent ligands, the only truly monodentate supporting ligand, P*t*Bu$_3$, formed aryl(trifluoromethyl)palladium complexes that underwent deleterious side reactions, due to the presence of an open coordination site (though the analogous Pd–C_2F_5 complexes underwent clean reductive elimination). Bidentate binding of the ancillary ligand leads to the absence of an open coordination site that would be involved in α-fluoride elimination. Likewise, bidentate

ligands (except for perhaps DFMPE) impart a high degree of steric hindrance to the Pd center. Such steric crowding is certainly necessary to facilitate the challenging aryl–perfluoroalkyl reductive elimination; however, a possible secondary effect of this steric crowding is to suppress bimolecular reactivity, especially X-type ligand exchanges that form catalytically inert species.

Perfluoroalkylsilanes are the most common, nucleophilic perfluoroalkyl reagent used to form Pd(aryl)R^F species in Pd-catalyzed perfluoroalkylations of aryl electrophiles. However, these reagents can require external, typically insoluble, fluoride activators, making the release of perfluoroalkyl anion equivalents difficult to control. If too much "R^{F-}" is released at once, the fluoroalkyl nucleophiles may displace both the desired (pseudo)halide ligand and the ancillary phosphine ligand, generating unreactive $Pd(R^F)_n^{m-}$ species.[133,137] Grushin showed that multiple additions of CF_3^- to $(PPh_3)_2Pd(Ph)I$ occurred, even at low conversion, suggesting that the aryl(perfluoroalkyl)palladium species may be more electrophilic than the parent halide complex. At present, the only strategies to mitigate this undesirable process, while still employing fluoroalkylsilanes as sources of nucleophilic R^F, are to employ less reactive silanes (such as the more sterically shielded $TIPSCF_3$) instead of the more conventional $TMSCF_3$ or $TESCF_3$ in trifluoromethylation reactions, to use less soluble activators, or to add the silane slowly. On the other hand, silanes containing partially fluorinated R^F groups are rarer and tend to require much stronger activators, like CsF or NaOtBu.[123,186] In addition, $TMSCF_2H$ has been shown to transfer non-fluorinated spectator alkyl groups, instead of the fluoroalkane, suggesting that organosilanes may not be suitable reagents for fluoroalkyl groups that are less electron-poor than CF_2H.[157] Thus, alternative reagents that cause slow release of R^{F-} or reduce its nucleophilicity are needed.

For this reason, other fluoroorganometallic reagents besides the fluoroalkylsilanes have been developed in an attempt to facilitate transmetallation of nucleophilic fluoroalkyl equivalents. While early examples of fluoroalkylmercury and -cadmium complexes are undesirable, due to their toxicity and tendency to detonate,[31,77] recently developed fluoroalkylzinc and fluoroalkylsilver reagents attenuate the extreme nucleophilicity of "R^{F-}" and could prevent the transfer of multiple fluoroalkyl equivalents to an arylpalladium halide complex.[48,82,153] Such reagents have been applied in Pd-catalyzed difluoromethylations of aryl halides, but not in trifluoromethylations or pentafluoroethylations, even though the analogous trifluoromethylmetal reagents have been shown to transmetallate to arylpalladium halide complexes selectively and in high yields.[48] Perfluoroalkylcopper species also remain underexplored as shuttles for nucleophilic perfluoroalkyl equivalents, even though they are more thermally stable than their perfluoroalkylsilver counterparts[140] and are easily accessible from a wide range of copper salts and reagents (see Section 1.2). Thus, it seems prudent to examine these species, either as co-catalysts or reagents in their own right, in transmetallation reactions. Chapter 4 of this Dissertation contains preliminary investigations into the reactions of arylpalladium halides with such reagents.

Decarbonylative methods to form fluoroalkylarenes are present an opportunity for developing new catalytic fluoroalkylation reactions. In an elegant approach that achieved the controlled release of CF_3^-, Schoenebeck's decarbonylative trifluoromethylation of aroyl fluorides generated a Pd–F species that reacted with $TESCF_3$ to form the aryl(trifluoromethyl)palladium complex, obviating the need for an exogenous activator for the silane and preventing displacement of the ancillary ligand by excess "CF_3^-".[141] However, reactions with aryl halides do not generate these key palladium fluoride intermediates, making this mechanism inaccessible for the trifluoromethylation of aryl halides. Catalytic polarity-reversed decarbonylative difluoromethylations of arylboronic acids in which fluorocarboxylic anhydrides served as electrophiles were reported by Sanford, and the individual steps of putative catalytic

perfluoroalkylations have been studied.[147,149] However, no analogous catalytic decarbonylative *per*fluoroalkylation reactions have been reported, possibly due to much higher barriers to rate-limiting decarbonylation. Necessary for study is this decarbonylation step: work by both Schoenebeck and Sanford showed that decarbonylation of the intermediate acylpalladium species was extremely sluggish in multiple systems for perfluoroalkylation, and in Schoenebeck's case decarbonylation was turnover-limiting and the main reason for the extremely high temperatures of the reaction (> 150 °C). The identification of ligand scaffolds or exogenous reagents to facilitate decarbonylations in systems containing fluoroalkyl moieties, therefore, is desirable.

Finally, greater effort should be made to synthesize, characterize, and study the reactivity of fluoroalkylmetal complexes. Few examples of aryl(fluoroalkyl)palladium complexes containing partially fluorinated fluoroalkyl groups have been reported, although it is not clear if this dearth of complexes is due to the lack of methods to prepare them or their inherent lack of stability. Attractive targets for fluoroalkyl ligands include CF_2Ph, CF_2CN, CF_2SO_2R, and $CF_2P(O)(OEt)_2$ moieties because few investigations into complexes containing these fragments have been reported despite reports of arylation reactions forming the corresponding fluoroalkylarenes.[87,165,186] In this context, one trend that should be examined more widely is the relationship between the electronic properties of the aryl fragment and the rate of reductive eliminations from $Pd^{II/IV}(aryl)R^F$ complexes. Arylpalladium complexes containing difluoromethyl and fluoroenolate ligands were shown to exhibit an unusual dependence on the electronic properties of the aryl group in which eliminations from complexes containing more electron-rich aryl ligands proceeded with faster rates than eliminations from complexes containing more electron-poor aryl ligands. However, it is unclear whether the electronic effect of the aryl group on the rates of reductive elimination from complexes containing other classes of fluoroalkyl ligands is the same as that observed in reactions of the Pd–CF_2H and Pd–CFRC(O)R' complexes. This effect for complexes containing difluoromethyl and fluorocarboxylic acid derivatives is the opposite of what was observed for reductive elimination of alkylarenes from the corresponding complexes containing non-fluorinated alkyl groups, and merits further study to understand the origin of this fundamental organometallic reactivity.

1.5 References

(1) Jeschke, P. The Unique Role of Fluorine in the Design of Active Ingredients for Modern Crop Protection. *ChemBioChem* **2004**, *5*, 570–589.

(2) Böhm, H.-J.; Banner, D.; Bendels, S.; Kansy, M.; Kuhn, B.; Müller, K.; Obst-Sander, U.; Stahl, M. Fluorine in Medicinal Chemistry. *ChemBioChem* **2004**, *5*, 637–643.

(3) Purser, S.; Moore, P. R.; Swallow, S.; Gouverneur, V. Fluorine in Medicinal Chemistry. *Chem. Soc. Rev.* **2008**, *37*, 320–330.

(4) Kirk, K. L. Fluorination in Medicinal Chemistry: Methods, Strategies, and Recent Developments. *Org. Process Res. Dev.* **2008**, *12*, 305–321.

(5) Gillis, E. P.; Eastman, K. J.; Hill, M. D.; Donnelly, D. J.; Meanwell, N. A. Applications of Fluorine in Medicinal Chemistry. *J. Med. Chem.* **2015**, *58*, 8315–8359.

(6) Dolbier, W. R. Fluorine Chemistry at the Millennium. *J. Fluor. Chem.* **2005**, *126*, 157–163.

(7) Yamazaki, T.; Taguchi, T.; Ojima, I. Unique Properties of Fluorine and Their Relevance to Medicinal Chemistry and Chemical Biology. In *Fluorine in Medicinal Chemistry and Chemical Biology*; John Wiley & Sons, Ltd, 2009; pp 1–49.

(8) Wang, J.; Sanchez-Rosello, M.; Acena, J. L.; del Pozo, C.; Sorochinsky, A. E.; Fustero, S.; Soloshonok, V. A.; Liu, H. Fluorine in Pharmaceutical Industry: Fluorine-Containing Drugs

Introduced to the Market in the Last Decade (2001-2011). *Chem. Rev.* **2014**, *114*, 2432–2506.
(9) Inoue, M.; Sumii, Y.; Shibata, N. Contribution of Organofluorine Compounds to Pharmaceuticals. *ACS Omega* **2020**, *5*, 10633–10640.
(10) Meanwell, N. A. Synopsis of Some Recent Tactical Application of Bioisosteres in Drug Design. *J. Med. Chem.* **2011**, *54*, 2529–2591.
(11) Swarts, F. Fluorine Derivatives of Toluene. *Bull Acad R Belg* **1898**, *35*, 375.
(12) Daudt, H. W.; Youker, M. A. Preparation of Carbon Compounds Containing Fluorine. U.S. Patent 2005705, 1935.
(13) Tomashenko, O. A.; Grushin, V. V. Aromatic Trifluoromethylation with Metal Complexes. *Chem. Rev.* **2011**, *111*, 4475–4521.
(14) Albéniz, A. C.; Casares, J. A. Chapter One - Palladium-Mediated Organofluorine Chemistry. In *Advances in Organometallic Chemistry*; Pérez, P. J., Ed.; Academic Press, 2014; Vol. 62, pp 1–110.
(15) Wang, H.; Vicic, D. A. Organometallic Aspects of Fluoroalkylation Reactions with Copper and Nickel. *Synlett* **2013**, *24*, 1887–1898.
(16) Chen, B.; Vicic, D. A. Transition-Metal-Catalyzed Difluoromethylation, Difluoromethylenation, and Polydifluoromethylenation Reactions. In *Organometallic Fluorine Chemistry*; Braun, T., Hughes, R. P., Eds.; Topics in Organometallic Chemistry; Springer International Publishing: Cham, 2014; Vol. 52, pp 113–141.
(17) García-Monforte, M. A.; Martínez-Salvador, S.; Menjón, B. The Trifluoromethyl Group in Transition Metal Chemistry. *Eur. J. Inorg. Chem.* **2012**, *2012*, 4945–4966.
(18) Hughes, R. P. Organo-Transition Metal Compounds Containing Perfluorinated Ligands. In *Advances in Organometallic Chemistry*; Stone, F. G. A., West, R., Eds.; Academic Press, 1990; Vol. 31, pp 183–267.
(19) Morrison, J. A. Trifluoromethyl-Containing Transition Metal Complexes. In *Advances in Organometallic Chemistry*; Stone, F. G. A., West, R., Eds.; Academic Press, 1993; Vol. 35, pp 211–239.
(20) Appleton, T. G.; Berry, R. D.; Hall, J. R.; Neale, D. W. Oxidative Addition to Bis(Trifluoromethyl)Platinum(II) Complexes with N-Donor Ligands. *J. Organomet. Chem.* **1988**, *342*, 399–422.
(21) Appleton, T. G.; Clark, H. C.; Manzer, L. E. Oxidative Addition, Reductive Elemination, and Isomerization Reactions of Organoplatinum Complexes. *J. Organomet. Chem.* **1974**, *65*, 275–287.
(22) Connor, J. A.; Zafarani-Moattar, M. T.; Bickerton, J.; El Saied, N. I.; Suradi, S.; Carson, R.; Al Takhin, G.; Skinner, H. A. Enthalpy of Formation of Acyl-, Alkyl- and Hydridopentacarbonyl-Manganese Complexes. The Enthalpy Contributions of Manganese-Hydrogen and Manganese-Carbon Bonds in These Molecules. Thermochemical Aspects of Models in Fischer-Tropsch Reactions. *Organometallics* **1982**, *1*, 1166–1174.
(23) Arlow, S. I.; Hartwig, J. F. Synthesis, Characterization, and Reactivity of Palladium Fluoroenolate Complexes. *J. Am. Chem. Soc.* **2017**, *139*, 16088–16091.
(24) Bennett, M. A.; Chee, H.-K.; Robertson, G. B. Comparison of .Sigma.-Alkyl and .Sigma.-Perfluoroalkyl Groups as Ligands. 1. Crystal and Molecular Structures of the Methyl-, (Trifluoromethyl)-, and (Pentafluoroethyl)Platinum(II) Complexes Trans-PtClR(PMePh2)2 (R = Methyl, Trifluoromethyl, Pentafluoroethyl). *Inorg. Chem.* **1979**, *18*, 1061–1070.

(25) Hughes, R. P.; Overby, J. S.; Williamson, A.; Lam, K.-C.; Concolino, T. E.; Rheingold, A. L. Synthesis, Molecular Structures, and Dynamics of Primary and Secondary Fluoroalkyl Complexes of Palladium(II) with Tetramethylethylenediamine (TMEDA) Ligands. Evaluation of the Structural Trans-Influences of Methyl and Fluoroalkyl Groups as Ligands within the Same Coordination Sphere. *Organometallics* **2000**, *19*, 5190–5201.
(26) Hughes, R. P.; Meyer, M. A.; Tawa, M. D.; Ward, A. J.; Williamson, A.; Rheingold, A. L.; Zakharov, L. N. Does α-Fluorination Affect the Structural Trans-Influence and Kinetic Trans-Effect of an Alkyl Ligand? Molecular Structures of Pd(TMEDA)(CH3)(RF) and a Kinetic Study of the Trans to Cis Isomerization of Pt(TMEDA)(CH3)2I(RF) [RF = CF2CF3, CFHCF3, CH2CF3]. *Inorg. Chem.* **2004**, *43*, 747–756.
(27) Brothers, P. J.; Roper, W. R. Transition-Metal Dihalocarbene Complexes. *Chem. Rev.* **1988**, *88*, 1293–1326.
(28) McLoughlin, V. C. R.; Thrower, J. A Route to Fluoroalkyl-Substituted Aromatic Compounds Involving Fluoroalkylcopper Intermediates. *Tetrahedron* **1969**, *25*, 5921–5940.
(29) Kobayashi, Y.; Kumadaki, I. Trifluoromethylation of Aromatic Compounds. *Tetrahedron Lett.* **1969**, *10*, 4095-+.
(30) Coe, P. L.; Milner, N. E. (Perfluoroalkyl)Copper(I) Compounds III. Reaction of (Perfluoroalkyl)Copper(I) Compounds with Aromatic Hydrocarbons. *J. Fluor. Chem.* **1972**, *2*, 167–172.
(31) Kondratenko, N. V.; Vechirko, E. P.; Yagupolskii, L. M. A Convenient Method for the Introduction of Trifluoromethyl Groups into Organic Compounds. *Synthesis* **1980**, *1980*, 932–933.
(32) Umemoto, T.; Ando, A. Synthesis and Reactivity of N-Trifluoromethyl-N-Nitrosotrifluoromethanesulfonamide as a New Type of Trifluoromethylating Agent. *Bull. Chem. Soc. Jpn.* **1986**, *59*, 447–452.
(33) Matsui, K.; Tobita, E.; Ando, M.; Kondo, K. A Convenient Trifluoromethylation of Aromatic Halides with Sodium Trifluoroacetate. *Chem. Lett.* **1981**, *10*, 1719–1720.
(34) Suzuki, H.; Yoshida, Y.; Osuka, A. Copper(i) Iodide Assisted Reaction of Nonactivated Iodoarenes with Sodium Trifluoroacetate in Hexamethylphosphoric Triamide. Nuclear Trifluoromethylation and Diaryl Ether Formation. *Chem. Lett.* **1982**, *11*, 135–136.
(35) Burton, D. J.; Wiemers, D. M. A Remarkably Simple Preparation of (Trifluoromethyl)Cadmium and -Zinc Reagents Directly from Difluorodihalomethanes. *J. Am. Chem. Soc.* **1985**, *107*, 5014–5015.
(36) Wiemers, D. M.; Burton, D. J. Pregeneration, Spectroscopic Detection and Chemical Reactivity of (Trifluoromethyl)Copper, an Elusive and Complex Species. *J. Am. Chem. Soc.* **1986**, *108*, 832–834.
(37) Urata, H.; Fuchikami, T. A Novel and Convenient Method for Trifluoromethylation of Organic Halides Using CF3SiR'3/KF/Cu(I) System. *Tetrahedron Lett.* **1991**, *32*, 91–94.
(38) Chen, Q.-Y.; Wu, S.-W. Methyl Fluorosulphonyldifluoroacetate; a New Trifluoromethylating Agent. *J. Chem. Soc. Chem. Commun.* **1989**, No. 11, 705.
(39) McClinton, M. A.; McClinton, D. A. Trifluoromethylations and Related Reactions in Organic Chemistry. *Tetrahedron* **1992**, *48*, 6555–6666.
(40) Burton, D. J.; Yang, Z.-Y. Fluorinated Organometallics: Perfluoroalkyl and Functionalized Perfluoroalkyl Organometallic Reagents in Organic Synthesis. *Tetrahedron* **1992**, *48*, 189–275.

(41) Konovalov, A. I.; Lishchynskyi, A.; Grushin, V. V. Mechanism of Trifluoromethylation of Aryl Halides with $CuCF_3$ and the Ortho Effect. *J. Am. Chem. Soc.* **2014**, *136*, 13410–13425.
(42) Nair, H. K.; Morrison, J. A. Formation of Group 11 Trifluoromethyl Derivatives by Reaction of Cd(CF3)2·glyme with Representative Au, Ag, and Cu Complexes: Isolation of Au(CF3)3(PMe3), Au(CF3)3(PEt3), AuI(CF3)2(PMe3), AuCF3(PMe3), AuCF3(PEt3) and AgCF3(PMe3); Observation of CuCF3(PMe3). *J. Organomet. Chem.* **1989**, *376*, 149–164.
(43) Willert-Porada, M. A.; Burton, D. J.; Baenziger, N. C. Synthesis and X-Ray Structure of Bis(Trifluoromethyl)(N,N-Diethyldithiocarbamato)-Copper; a Remarkably Stable Perfluoroalkylcopper(III) Complex. *J. Chem. Soc. Chem. Commun.* **1989**, No. 21, 1633–1634.
(44) Romine, A. M.; Nebra, N.; Konovalov, A. I.; Martin, E.; Benet-Buchholz, J.; Grushin, V. V. Easy Access to the Copper(III) Anion [Cu(CF3)4](-). *Angew. Chem. Int. Ed. Engl.* **2015**, *54*, 2745–2749.
(45) Kütt, A.; Movchun, V.; Rodima, T.; Dansauer, T.; Rusanov, E. B.; Leito, I.; Kaljurand, I.; Koppel, J.; Pihl, V.; Koppel, I.; Ovsjannikov, G.; Toom, L.; Mishima, M.; Medebielle, M.; Lork, E.; Röschenthaler, G.-V.; Koppel, I. A.; Kolomeitsev, A. A. Pentakis(Trifluoromethyl)Phenyl, a Sterically Crowded and Electron-Withdrawing Group: Synthesis and Acidity of Pentakis(Trifluoromethyl)Benzene, -Toluene, -Phenol, and -Aniline. *J. Org. Chem.* **2008**, *73*, 2607–2620.
(46) Kremlev, M. M.; Tyrra, W.; Mushta, A. I.; Naumann, D.; Yagupolskii, Y. L. The Solid Complex Zn(CF3)Br·2DMF as an Alternative Reagent for the Preparation of Both, Trifluoromethyl and Pentafluoroethyl Copper, CuCF3 and CuC2F5. *J. Fluor. Chem.* **2010**, *131*, 212–216.
(47) Nakamura, Y.; Fujiu, M.; Murase, T.; Itoh, Y.; Serizawa, H.; Aikawa, K.; Mikami, K. Cu-Catalyzed Trifluoromethylation of Aryl Iodides with Trifluoromethylzinc Reagent Prepared in Situ from Trifluoromethyl Iodide. *Beilstein J. Org. Chem.* **2013**, *9*, 2404–2409.
(48) Aikawa, K.; Nakamura, Y.; Yokota, Y.; Toya, W.; Mikami, K. Stable but Reactive Perfluoroalkylzinc Reagents: Application in Ligand-Free Copper-Catalyzed Perfluoroalkylation of Aryl Iodides. *Chem. Eur. J.* **2015**, *21*, 96–100.
(49) Knauber, T.; Arikan, F.; Roschenthaler, G. V.; Goossen, L. J. Copper-Catalyzed Trifluoromethylation of Aryl Iodides with Potassium (Trifluoromethyl)Trimethoxyborate. *Chem. Eur. J.* **2011**, *17*, 2689–2697.
(50) Liu, H.; Wu, J.; Jin, Y.; Leng, X.; Shen, Q. Mechanistic Insight into Copper-Mediated Trifluoromethylation of Aryl Halides: The Role of CuI. *J. Am. Chem. Soc.* **2021**, *143*, 14367–14378.
(51) Dubinina, G. G.; Furutachi, H.; Vicic, D. A. Active Trifluoromethylating Agents from Well-Defined Copper(I)-CF_3 Complexes. *J. Am. Chem. Soc.* **2008**, *130*, 8600–8601.
(52) Dubinina, G. G.; Ogikubo, J.; Vicic, D. A. Structure of Bis(Trifluoromethyl)Cuprate and Its Role in Trifluoromethylation Reactions. *Organometallics* **2008**, *27*, 6233–6235.
(53) Martínez de Salinas, S.; Mudarra, Á. L.; Odena, C.; Martínez Belmonte, M.; Benet-Buchholz, J.; Maseras, F.; Pérez-Temprano, M. H. Exploring the Role of Coinage Metalates in Trifluoromethylation: A Combined Experimental and Theoretical Study. *Chem. – Eur. J.* **2019**, *25*, 9390–9394.
(54) Liu, H.; Shen, Q. Bistrifluoromethylated Organocuprate $[Ph_4P]^+[Cu(CF_3)_2]^-$: Synthesis, Characterization and Its Application for Trifluoromethylation of Activated Heteroaryl Bromides, Chlorides and Iodides. *Org. Chem. Front.* **2019**, *6*, 2324–2328.

(55) Zanardi, A.; Novikov, M. A.; Martin, E.; Benet-Buchholz, J.; Grushin, V. V. Direct Cupration of Fluoroform. *J. Am. Chem. Soc.* **2011**, *133*, 20901–20913.
(56) Konovalov, A. I.; Benet-Buchholz, J.; Martin, E.; Grushin, V. V. The Critical Effect of the Countercation in the Direct Cupration of Fluoroform with [Cu(OR)2](-). *Angew. Chem. Int. Ed. Engl.* **2013**, *52*, 11637–11641.
(57) Lishchynskyi, A.; Grushin, V. V. Cupration of C_2F_5H: Isolation, Structure, and Synthetic Applications of $[K(DMF)_2][(t\text{-BuO})Cu(C_2F_5)]$. Highly Efficient Pentafluoroethylation of Unactivated Aryl Bromides. *J. Am. Chem. Soc.* **2013**, *135*, 12584–12587.
(58) Serizawa, H.; Aikawa, K.; Mikami, K. Direct Synthesis of a Trifluoromethyl Copper Reagent from Trifluoromethyl Ketones: Application to Trifluoromethylation. *Chemistry* **2013**, *19*, 17692–17697.
(59) Serizawa, H.; Aikawa, K.; Mikami, K. Direct Synthesis of Pentafluoroethyl Copper from Pentafluoropropionate as an Economical C_2F_5 Source: Application to Pentafluoroethylation of Arylboronic Acids and Aryl Bromides. *Org. Lett.* **2014**, *16*, 3456–3459.
(60) Lishchynskyi, A.; Novikov, M. A.; Martin, E.; Escudero-Adan, E. C.; Novak, P.; Grushin, V. V. Trifluoromethylation of Aryl and Heteroaryl Halides with Fluoroform-Derived $CuCF_3$: Scope, Limitations, and Mechanistic Features. *J. Org. Chem.* **2013**, *78*, 11126–11146.
(61) Le, C.; Chen, T. Q.; Liang, T.; Zhang, P.; MacMillan, D. W. C. A Radical Approach to the Copper Oxidative Addition Problem: Trifluoromethylation of Bromoarenes. *Science* **2018**, *360*, 1010–1014.
(62) Naumann, D.; Roy, T.; Caeners, B.; Hütten, D.; Tebbe†, K.-F.; Gilles, T. Synthesen und Eigenschaften von Pentafluorethylkupfer(I)- und -(III)-Verbindungen: Cu(C2F5) · D, [Cu(C2F5)2]– und (C2F5)2CuSC(S)N(C2H5)2. *Z. Für Anorg. Allg. Chem.* **2000**, *626*, 999–1003.
(63) Popov, I.; Lindeman, S.; Daugulis, O. Copper-Catalyzed Arylation of 1H-Perfluoroalkanes. *J. Am. Chem. Soc.* **2011**, *133*, 9286–9289.
(64) Xie, Q.; Li, L.; Zhu, Z.; Zhang, R.; Ni, C.; Hu, J. From C1 to C2: TMSCF3 as a Precursor for Pentafluoroethylation. *Angew. Chem. Int. Ed.* **2018**, *57*, 13211–13215.
(65) Mestre, J.; Castillón, S.; Boutureira, O. "Ligandless" Pentafluoroethylation of Unactivated (Hetero)Aryl and Alkenyl Halides Enabled by the Controlled Self-Condensation of TMSCF3-Derived CuCF3. *J. Org. Chem.* **2019**, *84*, 15087–15097.
(66) Nair, H. K.; Burton, D. J. Perfluoroisopropylcadmium and Copper: Preparation, Stability and Reactivity. *J. Fluor. Chem.* **1992**, *56*, 341–351.
(67) Oishi, M.; Kondo, H.; Amii, H. Aromatic Trifluoromethylation Catalytic in Copper. *Chem. Commun.* **2009**, No. 14, 1909–1911.
(68) Kondo, H.; Oishi, M.; Fujikawa, K.; Amii, H. Copper-Catalyzed Aromatic Trifluoromethylation via Group Transfer from Fluoral Derivatives. *Adv. Synth. Catal.* **2011**, *353*, 1247–1252.
(69) Morimoto, H.; Tsubogo, T.; Litvinas, N. D.; Hartwig, J. F. A Broadly Applicable Copper Reagent for Trifluoromethylations and Perfluoroalkylations of Aryl Iodides and Bromides. *Angew. Chem. Int. Ed.* **2011**, *50*, 3793–3798.
(70) Litvinas, N. D.; Fier, P. S.; Hartwig, J. F. A General Strategy for the Perfluoroalkylation of Arenes and Arylbromides by Using Arylboronate Esters and $[(Phen)CuR^F]$. *Angew. Chem. Int. Ed.* **2012**, *51*, 536–539.

(71) Kalkman, E. D.; Mormino, M. G.; Hartwig, J. F. Unusual Electronic Effects of Ancillary Ligands on the Perfluoroalkylation of Aryl Iodides and Bromides Mediated by Copper(I) Pentafluoroethyl Complexes of Substituted Bipyridines. *J. Am. Chem. Soc.* **2019**, *141*, 19458–19465.
(72) Tomashenko, O. A.; Escudero-Adan, E. C.; Belmonte, M. M.; Grushin, V. V. Simple, Stable, and Easily Accessible Well-Defined $CuCF_3$ Aromatic Trifluoromethylating Agents. *Angew. Chem. Int. Ed.* **2011**, *50*, 7655–7659.
(73) Panferova, L. I.; Miloserdov, F. M.; Lishchynskyi, A.; Martinez Belmonte, M.; Benet-Buchholz, J.; Grushin, V. V. Well-Defined CuC_2F_5 Complexes and Pentafluoroethylation of Acid Chlorides. *Angew. Chem. Int. Ed.* **2015**, *54*, 5218–5222.
(74) Weng, Z. Q.; Lee, R.; Jia, W. G.; Yuan, Y. F.; Wang, W. F.; Feng, X.; Huang, K. W. Cooperative Effect of Silver in Copper-Catalyzed Trifluoromethylation of Aryl Iodides Using Me_3SiCF_3. *Organometallics* **2011**, *30*, 3229–3232.
(75) Ohashi, M.; Ishida, N.; Ando, K.; Hashimoto, Y.; Shigaki, A.; Kikushima, K.; Ogoshi, S. Cu(I) -Catalyzed Pentafluoroethylation of Aryl Iodides in the Presence of Tetrafluoroethylene and Cesium Fluoride: Determining the Route to the Key Pentafluoroethyl Cu(I) Intermediate. *Chem. Eur. J.* **2018**, *24*, 9794–9798.
(76) Erickson, J. A.; McLoughlin, J. I. Hydrogen Bond Donor Properties of the Difluoromethyl Group. *J. Org. Chem.* **1995**, *60*, 1626–1631.
(77) Eujen, R.; Hoge, B.; Brauer, D. J. Synthesis and Properties of Donor-Free Bis(Difluoromethyl) Cadmium, (CF2H)2Cd NMR Spectroscopic Detection and Structure of Tetrakis(Difluoromethyl) Cuprate(III) and Related Compounds. *J. Organomet. Chem.* **1996**, *519*, 7–20.
(78) Burton, D. J.; Hartgraves, G. A. The Preparation of HCF2CdX and HCF2ZnX via Direct Insertion into the Carbon Halogen Bond of CF2HY (Y=Br, I). *J. Fluor. Chem.* **2007**, *128*, 1198–1215.
(79) Fier, P. S.; Hartwig, J. F. Copper-Mediated Difluoromethylation of Aryl and Vinyl Iodides. *J. Am. Chem. Soc.* **2012**, *134*, 5524–5527.
(80) Prakash, G. K. S.; Ganesh, S. K.; Jones, J.-P.; Kulkarni, A.; Masood, K.; Swabeck, J. K.; Olah, G. A. Copper-Mediated Difluoromethylation of (Hetero)Aryl Iodides and β-Styryl Halides with Tributyl(Difluoromethyl)Stannane. *Angew. Chem. Int. Ed.* **2012**, *51*, 12090–12094.
(81) Jiang, X.-L.; Chen, Z.-H.; Xu, X.-H.; Qing, F.-L. Copper-Mediated Difluoromethylation of Electron-Poor Aryl Iodides at Room Temperature. *Org. Chem. Front.* **2014**, *1*, 774–776.
(82) Serizawa, H.; Ishii, K.; Aikawa, K.; Mikami, K. Copper-Catalyzed Difluoromethylation of Aryl Iodides with (Difluoromethyl)Zinc Reagent. *Org. Lett.* **2016**, *18*, 3686–3689.
(83) Bour, J. R.; Kariofillis, S. K.; Sanford, M. S. Synthesis, Reactivity, and Catalytic Applications of Isolable (NHC)Cu(CHF2) Complexes. *Organometallics* **2017**, *36*, 1220–1223.
(84) Zhu, J.; Zhang, W.; Zhang, L.; Liu, J.; Zheng, J.; Hu, J. Copper-Mediated Fluoroalkylation Reactions with Iododifluoroacetamides: Controlling the Selectivity among Cross-Coupling, Intramolecular Cyclization, and Homocoupling Reactions. *J. Org. Chem.* **2010**, *75*, 5505–5512.
(85) Zhu, J.; Ni, C.; Gao, B.; Hu, J. Copper(0)-Mediated Fluoroalkylation of Iodobenzene with 2-Bromo-1,1,2,2-Tetrafluoroethyl Compounds: Investigation on the Influence of R Substituent on the Reactivity of RCF2Cu Species. *J. Fluor. Chem.* **2015**, *171*, 139–147.

(86) Arlow, S. I.; Hartwig, J. F. Synthesis of Aryldifluoroamides by Copper-Catalyzed Cross-Coupling. *Angew. Chem. Int. Ed.* **2016**, *55*, 4567–4572.
(87) Arlow, S. I. The Development of Transition Metal-Catalyzed Fluoroalkylation and Fluoroenolate Arylation Reactions. Ph.D. Thesis, University of California, Berkeley, 2018.
(88) Taguchi, T.; Kitagawa, O.; Morikawa, T.; Nishiwaki, T.; Uehara, H.; Endo, H.; Kobayashi, Y. Synthesis of 2,2-Difluoroesters by Iododifluoroacetate-Copper with Organic Halides. *Tetrahedron Lett.* **1986**, *27*, 6103–6106.
(89) Kitagawa, O.; Taguchi, T.; Kobayashi, Y. (Methyl Difluoroacetate)Copper Reagent. Remarkable Solvent Effect on the 19F-NMR Spectrum, Stability and Reactivity. *Chem. Lett.* **1989**, *18*, 389–392.
(90) Yokomatsu, T.; Murano, T.; Suemune, K.; Shibuya, S. Facile Synthesis of Aryl(Difluoromethyl)Phosphonates through CuBr-Mediated Cross Coupling Reactions of [(Diethoxyphosphinyl)Difluoromethyl]Zinc Bromide with Aryl Iodides. *Tetrahedron* **1997**, *53*, 815–822.
(91) Weiming Qiu; Burton, D. J. A Facile and General Preparation of α,α-Difluoro Benzylic Phosphonates by the CuCl Promoted Coupling Reaction of the (Diethylphosphonyl)Difluoromethylcadmium Reagent with Aryl Lodides. *Tetrahedron Lett.* **1996**, *37*, 2745–2748.
(92) Qiu, W.; Burton, D. J. Cuprous Chloride Promoted Coupling Reaction of Diethoxyphosphinyldifluoromethylcadmium Reagent with Aryl Iodides: A Practical and Convenient Preparation of α,α-Difluoro Benzylic Phosphonates. *J. Fluor. Chem.* **2013**, *155*, 45–51.
(93) Feng, Z.; Chen, F.; Zhang, X. Copper Catalyzed Cross-Coupling of Iodobenzoates with Bromozinc-Difluorophosphonate. *Org. Lett.* **2012**, *14*, 1938–1941.
(94) Jiang, X.; Chu, L.; Qing, F.-L. Copper-Mediated Oxidative Difluoromethylenation of Aryl Boronic Acids with α-Silyldifluoromethylphosphonates: A New Method for Aryldifluorophosphonates. *New J. Chem.* **2013**, *37*, 1736–1741.
(95) Sprague, L. G.; Burton, D. J.; Guneratne, R. D.; Bennett, William. E. Synthesis and Characterization of (E) and (Z)-1,2-Difluoroethenediylbisphosphonates. *J. Fluor. Chem.* **1990**, *49*, 75–85.
(96) Yokomatsu, T.; Kato, J.; Sakuma, C.; Shibuya, S. Stereoselective Synthesis of Highly-Functionalized Cyclohexene Derivatives Having a Diethoxyphosphoryldifluoromethyl Functionality from Cyclohex-2-Enyl-1-Phosphates. *Synlett* **2003**, *2003*, 1407–1410.
(97) Alter, C.; Neumann, B.; Stammler, H.-G.; Weber, L.; Hoge, B. Solid-State Structure of a Bromo(Difluoromethylenephosphonato)Cuprate – a Key Intermediate for the Synthesis of α,α-Difluoromethylenephosphonates. *Eur. J. Inorg. Chem.* **2017**, *2017*, 3489–3493.
(98) Ivanova, M. V.; Bayle, A.; Besset, T.; Pannecoucke, X.; Poisson, T. Copper-Mediated Introduction of the CF2PO(OEt)2 Motif: Scope and Limitations. *Chem. – Eur. J.* **2017**, *23*, 17318–17338.
(99) Ivanova, M. V.; Bayle, A.; Besset, T.; Poisson, T.; Pannecoucke, X. Copper-Mediated Formation of Aryl, Heteroaryl, Vinyl and Alkynyl Difluoromethylphosphonates: A General Approach to Fluorinated Phosphate Mimics. *Angew. Chem.* **2015**, *127*, 13604–13608.
(100) Zhu, J.; Wang, F.; Huang, W.; Zhao, Y.; Ye, W.; Hu, J. Copper-Mediated Fluoroalkylation Reactions with [(Phenylsulfonyl)-Difluoromethyl]Trimethylsilane: Synthesis of PhSO2CF2-Containing Allenes and Alkynes. *Synlett* **2011**, *2011*, 899–902.

(101) Li, X.; Zhao, J.; Hu, M.; Chen, D.; Ni, C.; Wang, L.; Hu, J. Copper-Mediated Aerobic (Phenylsulfonyl)Difluoromethylation of Arylboronic Acids with Difluoromethyl Phenyl Sulfone. *Chem. Commun.* **2016**, *52*, 3657–3660.
(102) Liu, L.; Xi, Z. Organocopper(III) Compounds with Well-Defined Structures Undergo Reductive Elimination to Form C—C or C–Heteroatom Bonds. *Chin. J. Chem.* **2018**, *36*, 1213–1221.
(103) Naumann, D.; Roy, T.; Tebbe, K.-F.; Crump, W. Synthesis and Structure of Surprisingly Stable Tetrakis(Trifluoromethyl)Cuprate(III) Salts. *Angew. Chem. Int. Ed. Engl.* **1993**, *32*, 1482–1483.
(104) Paeth, M.; Carson, W.; Luo, J.-H.; Tierney, D.; Cao, Z.; Cheng, M.-J.; Liu, W. Copper-Mediated Trifluoromethylation of Benzylic Csp3−H Bonds. *Chem. – Eur. J.* **2018**, *24*, 11559–11563.
(105) Zhang, S.-L.; Bie, W.-F. Isolation and Characterization of Copper(III) Trifluoromethyl Complexes and Reactivity Studies of Aerobic Trifluoromethylation of Arylboronic Acids. *RSC Adv.* **2016**, *6*, 70902–70906.
(106) Xiao, C.; Zhang, S.-L. Isolation of OH-Bridged Ag(I)/Cu(III) and Ion-Pair Cu(I)/Cu(III) Trifluoromethyl Complexes with Monophosphines. *Dalton Trans.* **2019**, *48*, 848–853.
(107) Zhang, S.-L.; Xiao, C.; Wan, H.-X. Diverse Copper(III) Trifluoromethyl Complexes with Mono-, Bi- and Tridentate Ligands and Their Versatile Reactivity. *Dalton Trans.* **2018**, *47*, 4779–4784.
(108) Zhang, S.-L.; Bie, W.-F. Ligand-Dependent Formation of Ion-Pair CuI/CuIII Trifluoromethyl Complexes Containing Bisphosphines. *Dalton Trans.* **2016**, *45*, 17588–17592.
(109) Tan, X.; Liu, Z.; Shen, H.; Zhang, P.; Zhang, Z.; Li, C. Silver-Catalyzed Decarboxylative Trifluoromethylation of Aliphatic Carboxylic Acids. *J. Am. Chem. Soc.* **2017**, *139*, 12430–12433.
(110) Paeth, M.; Tyndall, S. B.; Chen, L.-Y.; Hong, J.-C.; Carson, W. P.; Liu, X.; Sun, X.; Liu, J.; Yang, K.; Hale, E. M.; Tierney, D. L.; Liu, B.; Cao, Z.; Cheng, M.-J.; Goddard, W. A.; Liu, W. Csp3–Csp3 Bond-Forming Reductive Elimination from Well-Defined Copper(III) Complexes. *J. Am. Chem. Soc.* **2019**, *141*, 3153–3159.
(111) Lu, Z.; Liu, H.; Liu, S.; Leng, X.; Lan, Y.; Shen, Q. A Key Intermediate in Copper-Mediated Arene Trifluoromethylation, [NBu4N][Cu(Ar)(CF3)3]: Synthesis, Characterization, and C(Sp2)−CF3 Reductive Elimination. *Angew. Chem. Int. Ed.* **2019**, *58*, 8510–8514.
(112) Shen, H.; Liu, Z.; Zhang, P.; Tan, X.; Zhang, Z.; Li, C. Trifluoromethylation of Alkyl Radicals in Aqueous Solution. *J. Am. Chem. Soc.* **2017**, *139*, 9843–9846.
(113) Zhang, P.; Shen, H.; Zhu, L.; Cao, W.; Li, C. Radical C(Sp2)–H Trifluoromethylation of Aldehydes in Aqueous Solution. *Org. Lett.* **2018**, *20*, 7062–7065.
(114) Guo, S.; AbuSalim, D. I.; Cook, S. P. Aqueous Benzylic C–H Trifluoromethylation for Late-Stage Functionalization. *J. Am. Chem. Soc.* **2018**, *140*, 12378–12382.
(115) Choi, G.; Lee, G. S.; Park, B.; Kim, D.; Hong, S. H. Direct C(Sp3)−H Trifluoromethylation of Unactivated Alkanes Enabled by Multifunctional Trifluoromethyl Copper Complexes. *Angew. Chem. Int. Ed.* **2021**, *60*, 5467–5474.
(116) Zhang, H.-R.; Xiao, C.; Zhang, S.-L.; Zhang, X. Radical C−H Bond Trifluoromethylation of Alkenes by High-Valent Copper(III) Trifluoromethyl Compounds. *Adv. Synth. Catal.* **2019**, *361*, 5305–5310.

(117) Guo, S.; AbuSalim, D. I.; Cook, S. P. 1,2-(Bis)Trifluoromethylation of Alkynes: A One-Step Reaction to Install an Underutilized Functional Group. *Angew. Chem. Int. Ed.* **2019**, *58*, 11704–11708.
(118) Zhang, S.-L.; Wan, H.-X.; Bie, W.-F. Syn-Fluoro- and -Oxy-Trifluoromethylation of Arylacetylenes. *Org. Lett.* **2017**, *19*, 6372–6375.
(119) Dong, J.-J.; Zhang, S.-L. Synthesis of 2,2,2-Trifluoroethyl Oxazoles, Oxazolines and Furans via Alkyne Oxytrifluoromethylation. *Adv. Synth. Catal.* **2020**, *362*, 795–800.
(120) Liu, Z.-Y.; Cook, S. P. Interrupting the Barton–McCombie Reaction: Aqueous Deoxygenative Trifluoromethylation of O-Alkyl Thiocarbonates. *Org. Lett.* **2021**, *23*, 808–813.
(121) Dong, X.; Jiang, W.; Hua, D.; Wang, X.; Xu, L.; Wu, X. Radical-Mediated Vicinal Addition of Alkoxysulfonyl/Fluorosulfonyl and Trifluoromethyl Groups to Aryl Alkyl Alkynes. *Chem. Sci.* **2021**, *12*, 11762–11768.
(122) Nebra, N.; Grushin, V. V. Distinct Mechanism of Oxidative Trifluoromethylation with a Well-Defined Cu(II) Fluoride Promoter: Hidden Catalysis. *J. Am. Chem. Soc.* **2014**, *136*, 16998–17001.
(123) Gu, Y.; Leng, X.; Shen, Q. Cooperative Dual Palladium/Silver Catalyst for Direct Difluoromethylation of Aryl Bromides and Iodides. *Nat. Commun.* **2014**, *5*, 5405.
(124) Kalkman, E. D.; Hartwig, J. F. Direct Observation of Diastereomeric α-C-Bound Enolates during Enantioselective α-Arylations: Synthesis, Characterization, and Reactivity of Arylpalladium Fluorooxindole Complexes. *J. Am. Chem. Soc.* **2021**, *143*, 11741–11750.
(125) Firsich, D. W.; Lagow, R. J. Novel Synthesis of σ-Bonded Palladium and Nickel Compounds by Co-Condensation of Metal Vapour with Alkyl Free Radicals. *J. Chem. Soc. Chem. Commun.* **1981**, No. 24, 1283–1284.
(126) Klabunde, K. J. Organic Chemistry of Metal Vapors. *Acc. Chem. Res.* **1975**, *8*, 393–399.
(127) Klabunde, K. J.; Low, J. Y. F. Synthesis Employing Oxidative Insertion of Palladium Atoms into Aryl, Alkyl, and Acyl Carbon-Halogen Bonds. Properties of and Phosphine Trapping of the Nonligand Stabilizer RPdX and PCOPdX Intermediates. *J. Am. Chem. Soc.* **1974**, *96*, 7674–7680.
(128) Strukul, G.; Ros, R.; Michelin, R. A. Preparation and Oxygen-Transfer Properties of Novel Palladium(II) and Platinum(II) Hydroperoxo and Alkylperoxo Complexes. *Inorg. Chem.* **1982**, *21*, 495–500.
(129) Krause, L. J.; Morrison, J. A. Trifluoromethyl Group 2B Compounds: Bis(Trifluoromethyl)Cadmium.Base. New, More Powerful Ligand-Exchange Reagents and Low-Temperature Difluorocarbene Sources. *J. Am. Chem. Soc.* **1981**, *103*, 2995–3001.
(130) Krause, L. J.; Morrison, J. A. Trifluoromethyl Group 2B Compounds: Formation of Mono- and Bis-(Trifluoromethyl)–Platinum, –Palladium, and –Nickel Trialkylphosphine Complexes from the Reaction of (CF3)2Cd·glyme [Glyme =(CH2OMe)2] with the Diligand Metal Dihalides. *J. Chem. Soc. Chem. Commun.* **1981**, No. 24, 1282–1283.
(131) Foley, S. R.; Shen, H.; Qadeer, U. A.; Jordan, R. F. Generation and Insertion Reactivity of Cationic Palladium Complexes That Contain Halogenated Alkyl Ligands. *Organometallics* **2004**, *23*, 600–609.
(132) Cho, E. J.; Senecal, T. D.; Kinzel, T.; Zhang, Y.; Watson, D. A.; Buchwald, S. L. The Palladium-Catalyzed Trifluoromethylation of Aryl Chlorides. *Science* **2010**, *328*, 1679–1681.

(133) Naumann, D.; Kirij, N. V.; Maggiarosa, N.; Tyrra, W.; Yagupolskii, Y. L.; Wickleder, M. S. Synthesen und Charakterisierungen der ersten Tris- und Tetrakis(trifluormethyl)palladate(II) und -platinate(II), [M(CF3)3(PPh3)]— und [M(CF3)4]2— (M = Pd, Pt). *Z. Für Anorg. Allg. Chem.* **2004**, *630*, 746–751.
(134) Grushin, V. V.; Marshall, W. J. Unexpected H2O-Induced Ar−X Activation with Trifluoromethylpalladium(II) Aryls. *J. Am. Chem. Soc.* **2006**, *128*, 4632–4641.
(135) Bakhmutov, V. I.; Bozoglian, F.; Gómez, K.; González, G.; Grushin, V. V.; Macgregor, S. A.; Martin, E.; Miloserdov, F. M.; Novikov, M. A.; Panetier, J. A.; Romashov, L. V. CF3–Ph Reductive Elimination from [(Xantphos)Pd(CF3)(Ph)]. *Organometallics* **2012**, *31*, 1315–1328.
(136) Ozawa, F.; Kurihara, K.; Fujimori, M.; Hidaka, T.; Toyoshima, T.; Yamamoto, A. Mechanism of the Cross-Coupling Reaction of Phenyl Iodide and Methylmagnesium Iodide Catalyzed by Trans-PdPh(I)(PEt2Ph)2. *Organometallics* **1989**, *8*, 180–188.
(137) Grushin, V. V.; Marshall, W. J. Facile Ar-CF3 Bond Formation at Pd. Strikingly Different Outcomes of Reductive Elimination from [(Ph3P)2Pd(CF3)Ph] and [(Xantphos)Pd(CF3)Ph]. *J. Am. Chem. Soc.* **2006**, *128*, 12644–12645.
(138) Zhang, S.-L.; Deng, Z.-Q. Synthesis and Reductive Elimination of ArylPd(II) Trifluoromethyl Complexes: A Remarkable Concentration Effect on Chemoselectivity. *Phys. Chem. Chem. Phys.* **2016**, *18*, 32664–32667.
(139) Anstaett, P.; Schoenebeck, F. Reductive Elimination of ArCF3 from Bidentate PdII Complexes: A Computational Study. *Chem. – Eur. J.* **2011**, *17*, 12340–12346.
(140) Martínez de Salinas, S.; Mudarra, Á. L.; Benet-Buchholz, J.; Parella, T.; Maseras, F.; Pérez-Temprano, M. H. New Vistas in Transmetalation with Discrete "AgCF3" Species: Implications in Pd-Mediated Trifluoromethylation Reactions. *Chem. – Eur. J.* **2018**, *24*, 11895–11898.
(141) Keaveney, S. T.; Schoenebeck, F. Palladium-Catalyzed Decarbonylative Trifluoromethylation of Acid Fluorides. *Angew. Chem. Int. Ed. Engl.* **2018**, *57*, 4073–4077.
(142) Ferguson, D. M.; Bour, J. R.; Canty, A. J.; Kampf, J. W.; Sanford, M. S. Aryl–CF3 Coupling from Phosphinoferrocene-Ligated Palladium(II) Complexes. *Organometallics* **2019**, *38*, 519–526.
(143) Nielsen, M. C.; Bonney, Karl. J.; Schoenebeck, F. Computational Ligand Design for the Reductive Elimination of ArCF3 from a Small Bite Angle PdII Complex: Remarkable Effect of a Perfluoroalkyl Phosphine. *Angew. Chem. Int. Ed.* **2014**, *53*, 5903–5906.
(144) Ferguson, D. M.; Bour, J. R.; Canty, A. J.; Kampf, J. W.; Sanford, M. S. Stoichiometric and Catalytic Aryl-Perfluoroalkyl Coupling at Tri-Tert-Butylphosphine Palladium(II) Complexes. *J. Am. Chem. Soc.* **2017**, *139*, 11662–11665.
(145) Zhang, S.-L.; Huang, L.; Sun, L.-J. The Mechanism, Electronic and Ligand Effects for Reductive Elimination from ArylPd(II) Trifluoromethyl Complexes: A Systematic DFT Study. *Dalton Trans.* **2015**, *44*, 4613–4622.
(146) Malapit, C. A.; Ichiishi, N.; Sanford, M. S. Pd-Catalyzed Decarbonylative Cross-Couplings of Aroyl Chlorides. *Org. Lett.* **2017**, *19*, 4142–4145.
(147) Maleckis, A.; Sanford, M. S. Catalytic Cycle for Palladium-Catalyzed Decarbonylative Trifluoromethylation Using Trifluoroacetic Esters as the CF3 Source. *Organometallics* **2014**, *33*, 2653–2660.
(148) Maleckis, A.; Sanford, M. S. Synthesis of Fluoroalkyl Palladium and Nickel Complexes via Decarbonylation of Acylmetal Species. *Organometallics* **2014**, *33*, 3831–3839.

(149) Lalloo, N.; Malapit, C. A.; Taimoory, S. M.; Brigham, C. E.; Sanford, M. S. Decarbonylative Fluoroalkylation at Palladium(II): From Fundamental Organometallic Studies to Catalysis. *J. Am. Chem. Soc.* **2021**, *143*, 18617–18625.
(150) Belhomme, M.-C.; Besset, T.; Poisson, T.; Pannecoucke, X. Recent Progress toward the Introduction of Functionalized Difluoromethylated Building Blocks onto C(Sp2) and C(Sp) Centers. *Chem. – Eur. J.* **2015**, *21*, 12836–12865.
(151) Gu, Y.; Leng, X.; Shen, Q. Cooperative Dual Palladium/Silver Catalyst for Direct Difluoromethylation of Aryl Bromides and Iodides. *Nat. Commun.* **2014**, *5*, 5405.
(152) Chang, D.; Gu, Y.; Shen, Q. Pd-Catalyzed Difluoromethylation of Vinyl Bromides, Triflates, Tosylates, and Nonaflates. *Chem. – Eur. J.* **2015**, *21*, 6074–6078.
(153) Aikawa, K.; Serizawa, H.; Ishii, K.; Mikami, K. Palladium-Catalyzed Negishi Cross-Coupling Reaction of Aryl Halides with (Difluoromethyl)Zinc Reagent. *Org. Lett.* **2016**, *18*, 3690–3693.
(154) Culkin, D. A.; Hartwig, J. F. Carbon−Carbon Bond-Forming Reductive Elimination from Arylpalladium Complexes Containing Functionalized Alkyl Groups. Influence of Ligand Steric and Electronic Properties on Structure, Stability, and Reactivity. *Organometallics* **2004**, *23*, 3398–3416.
(155) Lu, C.; Lu, H.; Wu, J.; Shen, H. C.; Hu, T.; Gu, Y.; Shen, Q. Palladium-Catalyzed Difluoromethylation of Aryl Chlorides and Triflates and Its Applications in the Preparation of Difluoromethylated Derivatives of Drug/Agrochemical Molecules. *J. Org. Chem.* **2018**, *83*, 1077–1083.
(156) Lu, C.; Gu, Y.; Wu, J.; Gu, Y.; Shen, Q. Palladium-Catalyzed Difluoromethylation of Heteroaryl Chlorides, Bromides and Iodides. *Chem. Sci.* **2017**, *8*, 4848–4852.
(157) Ferguson, D. M.; Malapit, C. A.; Bour, J. R.; Sanford, M. S. Palladium-Catalyzed Difluoromethylation of Aryl Chlorides and Bromides with TMSCF2H. *J. Org. Chem.* **2019**, *84*, 3735–3740.
(158) Pan, F.; Boursalian, G. B.; Ritter, T. Palladium-Catalyzed Decarbonylative Difluoromethylation of Acid Chlorides at Room Temperature. *Angew. Chem.* **2018**, *130*, 17113–17118.
(159) Feng, Z.; Min, Q.-Q.; Fu, X.-P.; An, L.; Zhang, X. Chlorodifluoromethane-Triggered Formation of Difluoromethylated Arenes Catalysed by Palladium. *Nat. Chem.* **2017**, *9*, 918–923.
(160) Hori, K.; Motohashi, H.; Saito, D.; Mikami, K. Precatalyst Effects on Pd-Catalyzed Cross-Coupling Difluoromethylation of Aryl Boronic Acids. *ACS Catal.* **2019**, *9*, 417–421.
(161) Guo, Y.; M. Shreeve, J. Effect of Fluorine on Palladium-Catalyzed Cross-Coupling Reactions of Aryl Bromides with Trifluoromethyl Aryl Ketones via Difluoroenol Silyl or Monofluoroenol Silyl Ethers. *Chem. Commun.* **2007**, *0*, 3583–3585.
(162) Ge, S.; Arlow, S. I.; Mormino, M. G.; Hartwig, J. F. Pd-Catalyzed α-Arylation of Trimethylsilyl Enolates of α,α-Difluoroacetamides. *J. Am. Chem. Soc.* **2014**, *136*, 14401–14404.
(163) Ge, S.; Chaładaj, W.; Hartwig, J. F. Pd-Catalyzed α-Arylation of α,α-Difluoroketones with Aryl Bromides and Chlorides. A Route to Difluoromethylarenes. *J. Am. Chem. Soc.* **2014**, *136*, 4149–4152.
(164) Xia, T.; He, L.; Liu, Y. A.; Hartwig, J. F.; Liao, X. Palladium-Catalyzed Cross-Coupling of Ethyl Bromodifluoroacetate with Aryl Bromides or Triflates and Cross-Coupling of Ethyl Bromofluoroacetate with Aryl Iodides. *Org. Lett.* **2017**, *19*, 2610–2613.

(165) Feng, Z.; Min, Q.-Q.; Xiao, Y.-L.; Zhang, B.; Zhang, X. Palladium-Catalyzed Difluoroalkylation of Aryl Boronic Acids: A New Method for the Synthesis of Aryldifluoromethylated Phosphonates and Carboxylic Acid Derivatives. *Angew. Chem. Int. Ed.* **2014**, *53*, 1669–1673.
(166) Jiao, Z.; Beiger, J. J.; Jin, Y.; Ge, S.; Zhou, J. S.; Hartwig, J. F. Palladium-Catalyzed Enantioselective α-Arylation of α-Fluoroketones. *J. Am. Chem. Soc.* **2016**, *138*, 15980–15986.
(167) Jin, Y.; Chen, M.; Ge, S.; Hartwig, J. F. Palladium-Catalyzed, Enantioselective α-Arylation of α-Fluorooxindoles. *Org. Lett.* **2017**, *19*, 1390–1393.
(168) Reina, A.; Krachko, T.; Onida, K.; Bouyssi, D.; Jeanneau, E.; Monteiro, N.; Amgoune, A. Development and Mechanistic Investigations of a Base-Free Suzuki–Miyaura Cross-Coupling of α,α-Difluoroacetamides via C–N Bond Cleavage. *ACS Catal.* **2020**, *10*, 2189–2197.
(169) Culkin, D. A.; Hartwig, J. F. C−C Bond-Forming Reductive Elimination of Ketones, Esters, and Amides from Isolated Arylpalladium(II) Enolates. *J. Am. Chem. Soc.* **2001**, *123*, 5816–5817.
(170) Culkin, D. A.; Hartwig, J. F. Palladium-Catalyzed α-Arylation of Carbonyl Compounds and Nitriles. *Acc. Chem. Res.* **2003**, *36*, 234–245.
(171) Feng, Z.; Min, Q.-Q.; Zhang, X. Access to Difluoromethylated Arenes by Pd-Catalyzed Reaction of Arylboronic Acids with Bromodifluoroacetate. *Org. Lett.* **2016**, *18*, 44–47.
(172) Deng, X. Y.; Lin, J. H.; Xiao, J. C. Pd-Catalyzed Transfer of Difluorocarbene. *Org. Lett.* **2016**, *18*, 4384–4387.
(173) Lee, G. M.; Korobkov, I.; Baker, R. T. D8 Nickel and Palladium Difluorocarbenes Derived from Trifluoromethyl POCOP-Type Pincer Complexes. *J. Organomet. Chem.* **2017**, *847*, 270–277.
(174) Wade Wolfe, M. M.; Shanahan, J. P.; Kampf, J. W.; Szymczak, N. K. Defluorinative Functionalization of Pd(II) Fluoroalkyl Complexes. *J. Am. Chem. Soc.* **2020**, *142*, 18698–18705.
(175) Fu, X.-P.; Xue, X.-S.; Zhang, X.-Y.; Xiao, Y.-L.; Zhang, S.; Guo, Y.-L.; Leng, X.; Houk, K. N.; Zhang, X. Controllable Catalytic Difluorocarbene Transfer Enables Access to Diversified Fluoroalkylated Arenes. *Nat. Chem.* **2019**, *11*, 948–956.
(176) Harrison, D. J.; Daniels, A. L.; Korobkov, I.; Baker, R. T. D10 Nickel Difluorocarbenes and Their Cycloaddition Reactions with Tetrafluoroethylene. *Organometallics* **2015**, *34*, 5683–5686.
(177) Ball, N. D.; Kampf, J. W.; Sanford, M. S. Aryl−CF3 Bond-Forming Reductive Elimination from Palladium(IV). *J. Am. Chem. Soc.* **2010**, *132*, 2878–2879.
(178) Ball, N. D.; Gary, J. B.; Ye, Y.; Sanford, M. S. Mechanistic and Computational Studies of Oxidatively-Induced Aryl−CF3 Bond-Formation at Pd: Rational Design of Room Temperature Aryl Trifluoromethylation. *J. Am. Chem. Soc.* **2011**, *133*, 7577–7584.
(179) Racowski, J. M.; Ball, N. D.; Sanford, M. S. C–H Bond Activation at Palladium(IV) Centers. *J. Am. Chem. Soc.* **2011**, *133*, 18022–18025.
(180) Wang, X.; Truesdale, L.; Yu, J. Q. Pd(II)-Catalyzed Ortho-Trifluoromethylation of Arenes Using TFA as a Promoter. *J. Am. Chem. Soc.* **2010**, *132*, 3648–3649.
(181) Ye, Y.; Ball, N. D.; Kampf, J. W.; Sanford, M. S. Oxidation of a Cyclometalated Pd(II) Dimer with "CF3+": Formation and Reactivity of a Catalytically Competent Monomeric Pd(IV) Aquo Complex. *J. Am. Chem. Soc.* **2010**, *132*, 14682–14687.

(182) Powers, D. C.; Lee, E.; Ariafard, A.; Sanford, M. S.; Yates, B. F.; Canty, A. J.; Ritter, T. Connecting Binuclear Pd(III) and Mononuclear Pd(IV) Chemistry by Pd–Pd Bond Cleavage. *J. Am. Chem. Soc.* **2012**, *134*, 12002–12009.
(183) Fan, M.; Zhou, W.; Jiang, Y.; Ma, D. CuI/Oxalamide Catalyzed Couplings of (Hetero)Aryl Chlorides and Phenols for Diaryl Ether Formation. *Angew. Chem. Int. Ed.* **2016**, *55*, 6211–6215.
(184) Gao, J.; Bhunia, S.; Wang, K.; Gan, L.; Xia, S.; Ma, D. Discovery of N-(Naphthalen-1-Yl)-N′-Alkyl Oxalamide Ligands Enables Cu-Catalyzed Aryl Amination with High Turnovers. *Org. Lett.* **2017**, *19*, 2809–2812.
(185) Bhunia, S.; Pawar, G. G.; Kumar, S. V.; Jiang, Y.; Ma, D. Selected Copper-Based Reactions for C-N, C-O, C-S, and C-C Bond Formation. *Angew. Chem. Int. Ed.* **2017**, *56*, 16136–16179.
(186) Mormino, M. The Development of Transition Metal-Catalyzed Fluoroalkylation Reactions of Aryl Electrophiles. Ph.D. Thesis, University of California, Berkeley, 2017.

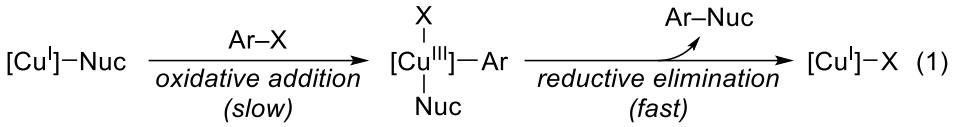
Chapter 2

Unusual Electronic Effects of Ancillary Ligands on the Perfluoroalkylation of Aryl Iodides and Bromides Mediated by Copper(I) Pentafluoroethyl Complexes of Substituted Bipyridines

2.1 Introduction

The relationship between the properties of the ancillary ligands and the reactivity of complexes of these ligands in elementary reactions must be understood to select or design catalysts for valuable transformations. While the properties of phosphines and their influence on reactivity has been studied extensively,[1–13] the properties of nitrogen-based ligands and their influence on reactions of organometallic complexes are less studied.[14,15] One class of reactions that is sensitive to the electronic properties of ancillary ligands is oxidative addition. Often, oxidative addition is faster for more electron-rich complexes, and thus complexes containing strongly donating ancillary ligands,[4–7,14,16,17] but exceptions to these trends are known, and one such exception of the reactions of the reactions of three-coordinate Ir(I)–X complexes with C–H and N–H bonds was recently studied in detail.[18]

Previous studies of the mechanism of Cu(I)-based cross coupling reactions of aryl halides have provided strong evidence that oxidative addition of an aryl halide to a Cu(I) complex to form a formally Cu(III) intermediate is rate-limiting and is followed by facile reductive elimination to furnish the coupled product (eq 1).[17,19–28]



Often, electron-donating ancillary ligands, which increase the electron density at the metal center, facilitate oxidative addition. Consistent with this hypothesis, our group previous reported that reactions of aryl halides with copper(I) amidate and imidate complexes were faster for complexes ligated by more electron-donating *bis*-amine ligands than those ligated by less electron-donating ligands based on phenanthroline or pyridine structures or than ligandless systems.[17] These data suggest that more electron-rich ligands cause these types of complexes to react faster, but amine and pyridine ligands differ by more than just their electron-donating abilities. Consistent with this trend, Taillefer showed that yields of a Cu-catalyzed arylation of phenols correlated positively with the electron-donating properties of ancillary bipyridine ligands,[29] but many factors besides reaction rate can affect the yield of a catalytic reaction. Thus, the scope of the trend of electronic properties on the reactivity of Cu(I) complexes has been assessed in only a cursory fashion and has not been studied for reactions of perfluoroalkylcopper complexes.

Several discrete perfluoroalkylcopper(I) complexes bearing ancillary dative ligands, including *N*-heterocyclic carbenes,[21,30] 1,10-phenanthrolines (phen),[31–35] 2,2'-bipyridine (bpy),[32] and triphenylphosphine,[31,32] have been isolated (Chart 2.1.1), but studies on the effects of the properties on Cu-mediated perfluoroalkylation reactions of aryl halides have not been reported. Several groups have reported that the inclusion of an ancillary ligand (usually phen) in the Cu-catalyzed perfluoroalkylation of aryl iodides is vital to achieve catalytic turnover at moderate reaction temperatures,[28,35–38] but others have developed Cu-catalyzed reactions that occur in the absence of ancillary ligands under otherwise similar reaction conditions.[39,40] In addition, Grushin and co-workers even reported that addition of phenanthroline, pyridine, or phosphine ligands to "ligandless" $CuCF_3$ diminished the reactivity of this reagent.[41] Thus, the effect of the ancillary ligand on the reactivity of Cu-based perfluoroalkylation reactions is particularly ambiguous.

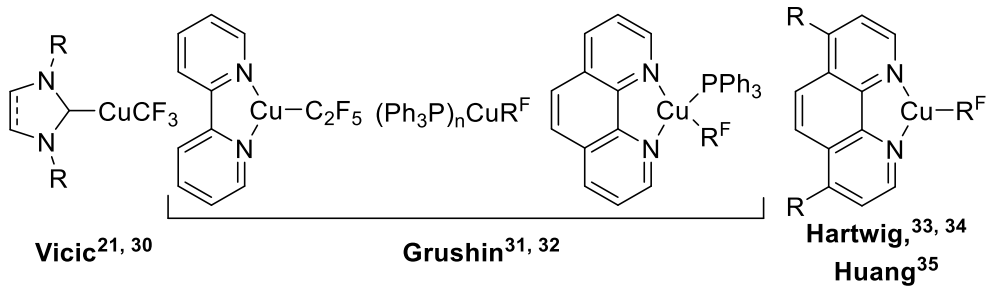


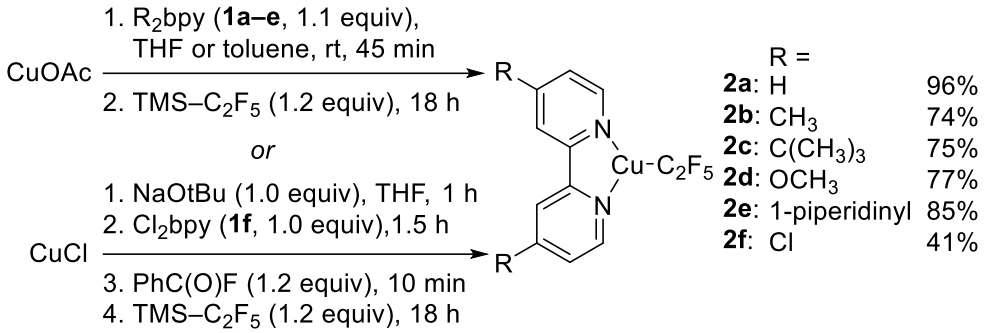
Chart 2.1.1 Discrete perfluoroalkylcopper(I) complexes

We report the synthesis of a series of pentafluoroethylcopper(I) complexes containing bipyridine (bpy) ligands with varied electronic properties that react with aryl halides to form perfluoroalkylarenes. We have measured the effects of the electronic properties of these bpy ligands on the speciation of perfluoroalkylcopper(I) complexes between neutral and ionic forms, the effect of these properties on the rates of the reaction of these complexes with aryl halides, and the effect of the ligands on selectivity. Combined, these data suggest that the reactions of the aryl halides with perfluoroalkylcopper complexes bearing less electron-donating bpy ligands are faster than with those containing more electron-donating bpy ligands. These data contrast with the common effects of electronic properties on the rate of oxidative addition of aryl halides.

2.2 Preparation of Bipyridine-Ligated Pentafluoroethylcopper(I) Complexes

Our investigations began with the preparation of a series of pentafluoroethylcopper(I) complexes ligated by 4,4'-homodisubstituted derivatives of 2,2'-bipyridine (**1a–f**, Scheme 2.2.1). Complexes **2a–e** containing electron-donating groups on the bpy scaffold were prepared in good yields by treating a mixture of ligands **1a–e** and anhydrous copper(I) acetate in THF or toluene with trimethyl(pentafluoroethyl)silane (TMS–C_2F_5). While we were unable to prepare complexes containing bpy ligands with strongly electron-withdrawing groups by this procedure, we did prepare (Cl_2bpy)CuC_2F_5 by treating CuO*t*Bu generated *in situ* with dichlorobipyridine **1f**, followed by benzoyl fluoride[42] and then TMS–C_2F_5.

Consistent with previous reports of perfluoroalkylcopper(I) complexes,[31–35,42,43] the ^{19}F NMR spectra of complexes **2a–f** in DMF solution all consisted of four resonances, two corresponding to the ethyl group in the neutral [(R_2bpy)CuC_2F_5] form and two to those in the ionic [(R_2bpy)$_2$Cu][Cu(C_2F_5)$_2$] form (eq 2). The equilibrium between the neutral and ionic species was reached within 5 min at 65 °C and remained unchanged at different total concentrations of perfluoroalkylcopper species, suggesting that the ionic components exist as solvent-separated ions as opposed to a tight ion pair[17] (see Section 2.7.3). While more electron-donating ligands might be expected to stabilize the cationic [(R_2bpy)$_2$Cu]$^+$ species more effectively than would more electron-poor ligands, the equilibria of compounds **2a–f** instead generally favored the neutral [(R_2bpy)CuC_2F_5] form more strongly for complexes of more electron-donating R_2bpy than for those of less electron-donating R_2bpy ligands (*K*, Table 2.3.1). Indeed, at 65 °C, the system containing the most electron-donating ligand 4,4'-di(1-piperidinyl)-2,2'-bipyridine (**1e**) comprised a 9:91 ratio of the ionic to neutral forms, while the system containing the least electron-donating ligand 4,4'-dichloro-2,2'-bipyridine (**1f**) comprised a 30:70 ratio. A similar trend was observed at 90 °C. A Hammett plot of the equilibrium constants governing the relative populations of the two forms displayed a loose positive correlation ($\rho \approx 1.3$) with the σ_p[26,44] values of the substituents on the bpy ligands (Figure 2.2.1).



Scheme 2.2.1 Preparation of $(R_2bpy)CuC_2F_5$ complexes **2a–f**

$$2\ (R_2bpy)CuCF_2CF_3 \underset{65\ °C}{\overset{K}{\rightleftharpoons}} [(R_2bpy)_2Cu]^+ + [Cu(CF_2CF_3)_2]^- \quad (2)$$

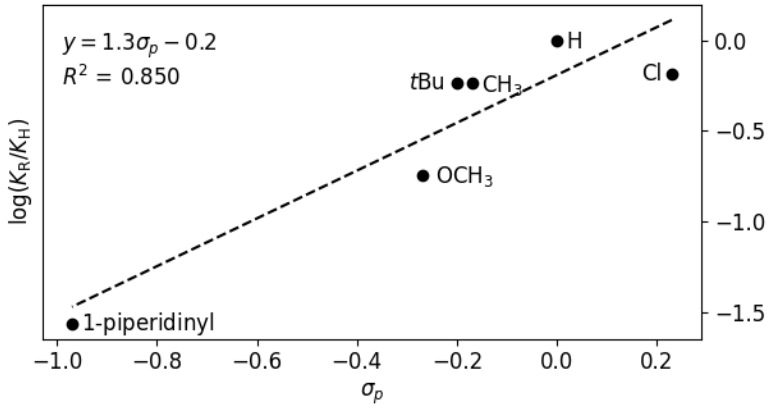


Figure 2.2.1 Hammett plot of the equilibrium constants governing the relative populations of neutral and ionic forms of **2a–f** at 65 °C[Note 1]

2.3 Reactivity of Bipyridine-Ligated Pentafluoroethylcopper(I) Complexes with Aryl Halides

To assess the effect of the electronic properties of the bpy ligand on perfluoroalkylation reactions with aryl halides, complexes **2a–f** were treated with excess 1-butyl-4-iodobenzene (**3a**) or 1-bromo-4-butylbenzene (**4**) in DMF at 65 °C or 90 °C, respectively (eq 3). The formation of pentafluoroethyl arene **5a** was followed by ^{19}F NMR spectroscopy, and rate constants for these reactions were determined from first-order exponential fits (Table 2.3.1, k_{obs}^{I}) or initial rates (k_{init}^{Br}) of the formation of **5a**. These data provide the surprising result that reactions of aryl iodide **3a** with complexes containing the less electron-donating bpy ligands were generally faster than those containing the more electron-donating bpy ligands, with dichlorobipyridine complex **2f** reacting ~4 times faster than di(piperidinyl)bipyridine complex **2e**. A Hammett plot of these rate constants *vs* σ_p revealed a small but positive correlation ($\rho \approx 0.5$, Figure 2.3.1a).

Reactions of **2a–f** with aryl bromide **4** at 90 °C proceeded much more slowly than reactions with aryl iodides **3** and in lower yields, complicating analysis of the full reaction profiles. However, the initial rates of reaction, determined from linear fits of the first 5–10% formation of **5a** (Table 2.3.1, k_{init}^{Br}), followed the same trend of electronic effects on reaction rates as was observed for

reactions with aryl iodides **3** (ρ ≈ 0.4, Figure 2.2.1b).

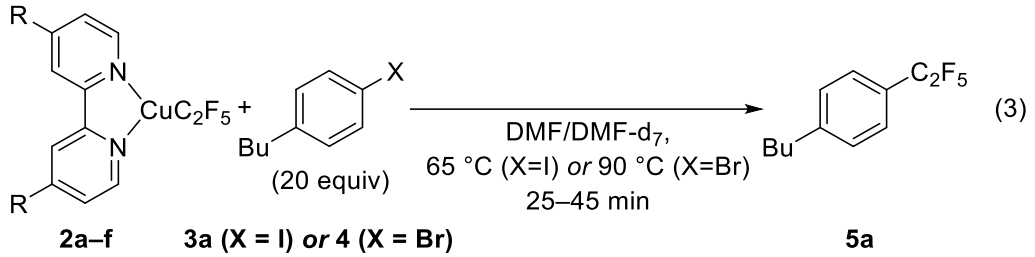


Table 2.3.1 Equilibrium constants for complexes **2a–f** in DMF and rate constants for the pentafluoroethylation of aryl halides **3a** and **4** by reaction with complexes **3a–f**

Complex	R	K (65 °C)[a]	k_{obs}^{I} (± 0.2)[b,c]	k_{corr}^{I} (± 0.3)[c,d,e]	K (90 °C)[a]	k_{init}^{Br} (± 0.2)[f,g]	k_{corr}^{Br} (± 0.5)[f,h,i]
2a	H	2.8×10^{-1}	3.2	6.3	1.9×10^{-1}	2.9	11
2b	CH_3	1.6×10^{-1}	2.6	4.8	1.4×10^{-1}	2.4	8.3
2c	*t*Bu	1.6×10^{-1}	2.2	4.0	1.4×10^{-1}	2.6	9.1
2d	OCH_3	5.1×10^{-2}	2.5	3.7	4.8×10^{-2}	2.7	7.7
2e	1-piperidinyl	7.7×10^{-3}	1.2	1.4	8.1×10^{-3}	1.5	3.6
2f	Cl	1.8×10^{-1}	4.7	8.8	7.8×10^{-2}	5.4	17

[a] $K = [[Cu(C_2F_5)_2]^-]^2/[(R_2bpy)CuC_2F_5]^2$; relative concentrations determined by ^{19}F NMR spectroscopy in DMF. [b]Rate constants given in units of $\times10^{-3}$ s^{-1}. [c]Reaction conditions: **2** (0.0500 M) and aryl iodide **3a** (1.00 M) in 5:1 DMF:DMF-d_7 at 65 °C for 45 min; k_{obs}^{I} derived from exponential fit of formation of **5a**. [d]Rate constants given in units of $\times10^{-3}$ $M^{-1}\cdot s^{-1}$. . [e]$k_{corr} = k_{obs}(1 + 2\sqrt{K})/[\mathbf{3a}]_0$. [f]Reaction conditions: **2** (0.0500 M) and aryl bromide **4** (1.00 M) in 5:1 DMF:DMF-d_7 at 90 °C for 30 min; k_{init}^{Br} determined from linear fit of formation of **5a**. [g]Rate constants given in units of $\times10^{-5}$ $M^{-1}\cdot s^{-1}$. [h]Rate constants given in units of $\times10^{-5}$ $M\cdot s^{-1}$. [i]$k_{corr} = k_{init}(1 + 2\sqrt{K})/[\mathbf{2}]_0[\mathbf{4}]_0$ (see Section 2.7.4 for derivations of k_{corr}).

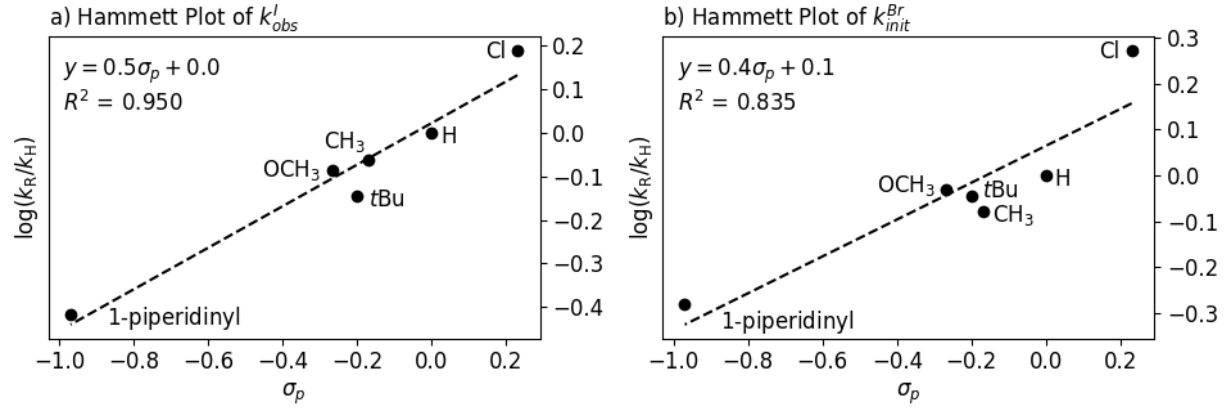


Figure 2.3.1 Hammett plots (*vs* σ_p) of a) k_{obs}^{I} for the pentafluoroethylation of aryl iodide **3a** by reactions with complexes **2a–f**; and b) k_{init}^{Br} for the pentafluoroethylation of aryl bromide **4** by reactions with complexes **2a–f**.[*Note 1*]

The results in Table 2.3.2 show the effect of varying the electronic properties of the aryl iodide on the rate of the reaction with pentafluoroethylcopper complexes **2a** and **2e** (eq 4).

Reactions of electron-neutral and electron-rich complexes **2a** and **2e** with electron-poor aryl iodide 4-iodobenzonitrile (**3b**) occurred more readily than those with more electron-rich 4-butyl iodobenzene (**3a**) or 4-iodoanisole (**3c**), proceeding at 27 °C at rates that were similar to those of reactions of the same complexes with **3a** or **3c** at the higher temperature of 65 °C. This trend is in agreement with the trend in the rates of reaction of electronically varied aryl halides with "ligandless" $CuCF_3$,[26] wherein more electron-poor aryl iodides reacted more quickly than more electron-rich iodides, and is consistent with commonly-observed effects of the electronic nature of the aryl halide on rate-limiting oxidative addition.[26,45] However, the effect of the bpy ligand on the reactions of complexes **2a** and **2e** with aryl iodides **3b** and **3c** remained the same as those for reactions with **3a**: reactions of the more electron-poor complex **2a** proceeded more rapidly than reactions involving more electron-rich complex **2e**. Thus, the unusual electronic effects of the ancillary ligand on the rate of the reaction between the perfluoroalkyl copper complex and the aryl halide are not compensated by a balancing trend in electronic effects of the aryl halide.

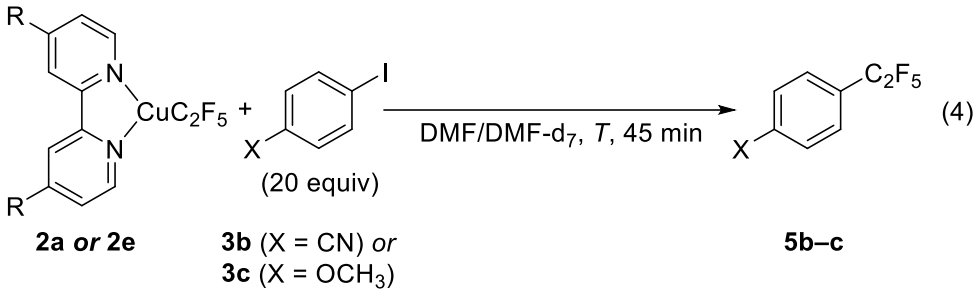


Table 2.3.2 Rate constants for the reaction of electron-neutral and electron-rich complexes **2a** and **2e** with electronically varied aryl iodides

Complex	R	X	*T* (°C)	k_{obs}^{I} ($\pm$ 0.2×10^{-3} s^{-1})
2a	H	CN	27	3.1
2a	H	Bu	65	3.2
2a	H	OCH_3	65	3.1
2e	1-piperidinyl	CN	27	1.8
2e	1-piperidinyl	Bu	65	1.2
2e	1-piperidinyl	OCH_3	65	1.3

Reaction conditions: **2** (0.0500 M) and **3b** or **3c** (1.00 M) in 5:1 DMF:DMF-d_7 at the specified temperature for 45 min.

The rates of reaction of **2a** with varying concentrations of aryl iodide **3a** revealed the reaction order in aryl halide. The rates of the reactions of **2a** in the presence of 0.500, 1.00, 1.50, and 2.00 M **3a** (eq 5) displayed a strong linear correlation with the initial concentration of **3a** ([**3a**]$_0$), implying that the reaction is first order in in aryl iodide (Figure 2.3.2). Combined with the first-order behavior in the concentration of complexes **2** (revealed by the first-order exponential fits of product formation in reactions with a large excess of **3a**), these findings are consistent with rate-limiting oxidative addition of aryl halide to complexes **2**.

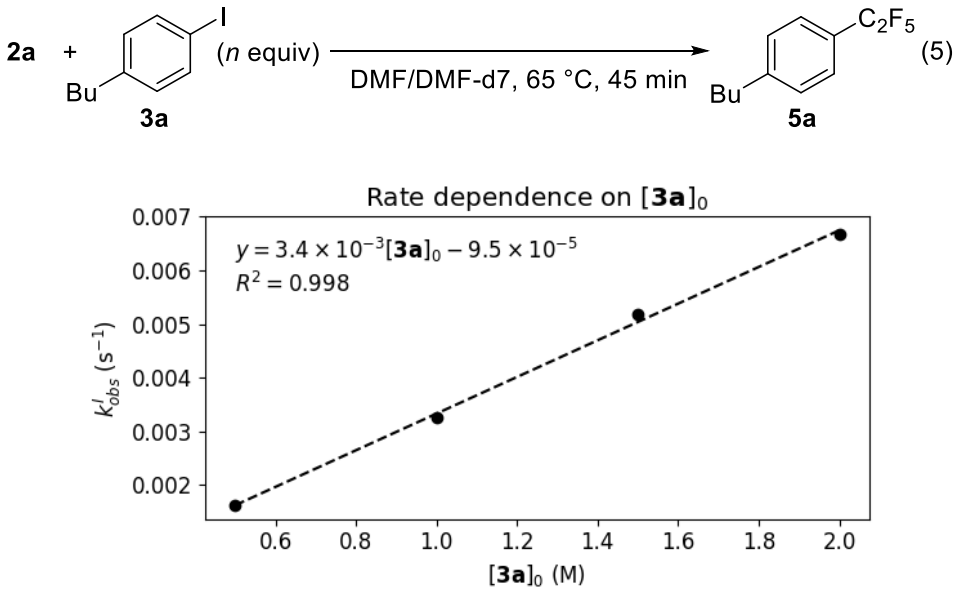


Figure 2.3.2 Dependence of the rate of the reaction of **2a** with **3a** on the initial concentration of **3a** ([**3a**]$_0$). Reaction conditions: **2a** (0.0500 M) and aryl iodide **3a** (0.500–2.00 M, *n* = 10–40) in 5:1 DMF:DMF-d$_7$ at 65 °C for 45 min.

Because the neutral form of perfluoroalkylcopper species, not the ionic form, is known to be the component that reacts with aryl halides,[21,46] it is necessary to account for the equilibrium between these forms of the CuC_2F_5 reagents to determine the effect of the bpy ligands on the rate of reaction of [(R_2bpy)CuC_2F_5] with aryl halides **3a** and **4**. Given the first-order dependence of the rate on both **2** and the aryl halide, the rate constants k_{corr} obtained after correcting k_{obs}^{I} and k_{init}^{Br} for the relative equilibrium population of the [(R_2bpy)CuC_2F_5] species are given by eq 6 and eq 7, respectively (see Section 2.7.4). The values for k_{corr} are given in Table 2.3.1.

$$k_{corr}^{I} = \frac{(1+2\sqrt{K})k_{obs}^{I}}{[\mathbf{3}]_0} \quad (6) \qquad k_{corr}^{Br} = \frac{(1+2\sqrt{K})k_{init}^{Br}}{[\mathbf{2}]_0[\mathbf{4}]_0} \quad (7)$$

Hammett plots of k_{corr} *vs* σ_p for the reactions with aryl iodide **3a** and bromide **4** (Figure 2.3.3) provided positive correlations between the rate constants and σ_p that were more linear than those obtained from the raw rate constants k_{obs}^{I} and k_{init}^{Br}. The substituent effects on k_{corr} were also slightly stronger than on k_{obs}^{I} and k_{init}^{Br} ($\rho \approx 0.7$ for k_{corr}^{I} and $\rho \approx 0.5$ for k_{corr}^{Br}). Assuming rate-limiting oxidative addition of the aryl halides to the neutral [(R_2bpy)CuC_2F_5] complex (*vide supra*), this result suggests that oxidative addition is faster to the complexes of *less* electron-donating bpy ligands than to complexes of *more* electron-donating bpy ligands. This trend is the opposite of what is observed most commonly for oxidative addition to a metal center.[4–7,14,16]

An alternative hypothesis to account for this trend of ligand electronic effects on the rate of the reaction of aryl halides with[(R_2bpy)CuC_2F_5] is that the bpy ligand initially dissociates from the Cu center to generate a small amount of free "CuC_2F_5" (**6**), which then reacts more rapidly with the aryl halide than the ligated species (eq 8). Because more electron-rich σ-donor ligands generally bind more strongly to metal centers, complexes of more electron-rich bpy ligands would generate smaller quantities of free CuC_2F_5 than complexes of more electron-poor ligands. Moreover, Mikami and Grushin have both shown that solutions of "ligandless" CuC_2F_5 in DMF react with aryl iodides and bromides at temperatures similar to or lower than those in this work to

form pentafluoroethyl arenes.[43,47] Thus, a "ligandless" complex, instead of [(R$_2$bpy)CuC$_2$F$_5$], could be the species that reacts with aryl halides during our studies.

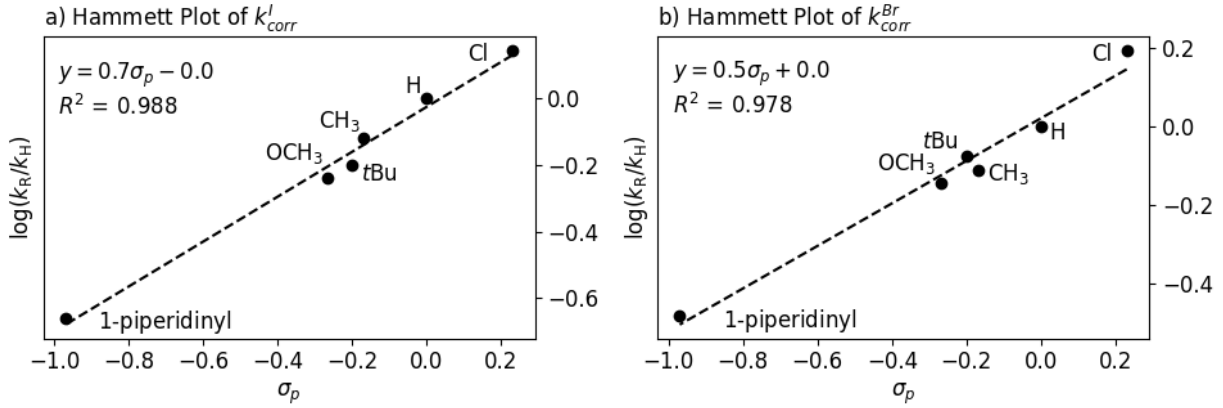
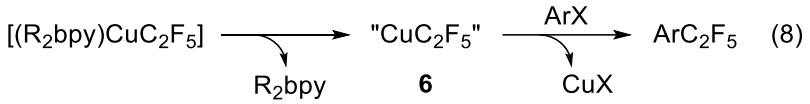


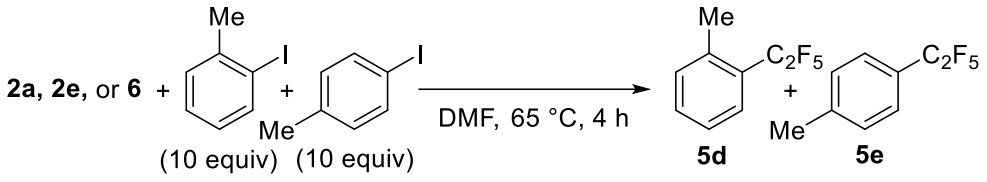
Figure 2.3.3 Hammett plots (*vs* σ_p) of equilibrium-adjusted rate constants k_{corr} for the pentafluoroethylation of a) **3a** and b) **4** by reaction with complexes **2a-f**.[Note 1]



To evaluate this hypothesis, a solution of "ligandless" CuC$_2$F$_5$ (**6**) in DMF was prepared by treatment of a solution of K(DMF)[Cu(O*t*Bu)$_2$][48] in DMF with ethyl pentafluoropropionate, followed by neutralization with 3HF·NEt$_3$.[47] The formation of pentafluoroethyl arene **5a** by reaction of **6** with excess aryl iodide **3a** at 65 °C was monitored by ^{19}F NMR spectroscopy and was found to occur with a rate constant of 9.7×10^{-4} s^{-1}. While this value is similar to the rate constant of reactions of **3a** with piperidinyl-substituted **2e** ($k_{obs}^I = 1.4\times10^{-3}$ s^{-1}), which is the slowest-reacting of complexes **2a–f**, reactions of **2a–d** and **2f** with **3a** proceeded at least 2.5 times faster than the reactions of "ligandless" CuC$_2$F$_5$ reagent **6** with **3a** (Table 2.3.1, k_{obs}^I). This result shows that "ligandless" CuC$_2$F$_5$ is not kinetically competent to be an intermediate in the reactions of complexes **2a–d** and **2f** with aryl halides.

To assess the potential reactivity through the "ligandless" complex **6** further, we conducted a competition experiment, whereby complexes **2a**, **2e**, or **6** were allowed to react with an equimolar mixture of 2- and 4-iodotoluene (**3d** and **3e**, Scheme 2.3.1). The ratio of pentafluoroethyl toluene products **5d**:**5e** formed from the reactions with **2a** and **2e** (44:56 and 39:61, respectively) were different from that with ligandless **6** (68:32), implying that the steric environment of the Cu center that reacts with the aryl halide starting from **2a** and **2e** is different from that starting from **6**,[Note 2] and is, therefore, not the "ligandless" copper complex.

Finally, the possibility of reactions of **2a–f** through the ligandless complex was assessed by measuring the rate of reaction of **2a** with **3a** in the presence of 2 equiv added bpy. The rates of reaction in the presence and absence of added ligand were indistinguishable ($k_{obs}^I = 3.0\times10^{-3}$ s^{-1} with 2 equiv of added bpy *vs* 3.2×10^{-3} s^{-1} without), implying that the overall effect of a pathway involving reaction with the ligandless species must be minor and that the electronic effect of the ligand on the rate of reaction is not due to dissociation of R$_2$bpy from [(R$_2$bpy)CuC$_2$F$_5$] prior to reaction with the aryl halide.



2a	44%	:	56%
2a + 2 bpy	40%	:	60%
2a + 15 bpy	39%	:	61%
2e	39%	:	61%
2e + 2 pip_2bpy	37%	:	63%
2e + 15 pip_2bpy	37%	:	63%
6	68%	:	32%

Scheme 2.3.1 Competition reactions of pentafluoroethyl complexes with aryl iodides **7a** and **7b**.

2.4 Computational Investigations into the Origin of the Electronic Effect of the Ancillary Ligand

These experimental results were consistent with DFT calculations (see the Section 2.7.5 for computational details, structures, and tabulated energies). The computed free energy barriers of concerted oxidative addition of unsubstituted iodobenzene (**3f**) to the neutral forms of **2a**, **2d**, and **2f** ($\Delta G_{calc}^{\ddagger}$ = 24–25 kcal/mol; Table 2.4.1; eq 9) were similar in magnitude to those determined experimentally from k_{obs}^{I} ($\Delta G_{expt}^{\ddagger}$ = 23–24 kcal/mol). However, no clear trend was observed between the computed free energies of activation and the σ_p values of the substituents on the bpy ligand (Table 2.4.1). Nevertheless, a clear trend was observed between the *enthalpies* of activation $\Delta H_{calc}^{\ddagger}$ and the σ_p values of the substituents on the bpy ligand, and this trend was consistent with the trend observed experimentally; the enthalpies of activation for oxidative addition of iodobenzene to complexes of the more electron-poor bpy ligands were computed be lower than those to complexes of the more electron-rich ligands. These calculated values for $\Delta H_{calc}^{\ddagger}$ are significantly lower than those for $\Delta G_{calc}^{\ddagger}$, highlighting a large entropic contribution to $\Delta G_{calc}^{\ddagger}$ ($\Delta S_{calc}^{\ddagger}$ = –40 – –52 cal/mol·K), which has been measured experimentally[45] and calculated previously for other reactions of copper complexes with aryl halides.[17,23] The observation of a trend in $\Delta H_{calc}^{\ddagger}$ but not in $\Delta G_{calc}^{\ddagger}$ likely results from the large uncertainties introduced in implicit solvation models and calculated entropies.[49] These calculations, therefore, support our hypothesis that the effect of the ancillary ligand on the experimental rates is due to modulation of the barrier to the rate-limiting elementary step of oxidative addition.

The observed trends in the rates of reaction of complexes **2** with aryl halides and in $\Delta H_{calc}^{\ddagger}$ could be explained by an accumulation of negative charge around the Cu center during the oxidative addition step, which would be stabilized by more electron-poor ligands. Indeed, the natural atomic charges on the Cu centers determined through natural population analysis[50] of the optimized transition state structures $\mathbf{TS_R}$ in all cases decreased relative to those of the $\mathbf{GS_R}$ structures (Δq_{Cu} = –0.02 – –0.04), although all of the net charges were positive (q_{Cu} = +0.44 – +0.56; see Table 2.7.5 and Table 2.7.6 in Section 2.7 for a list of natural atomic charges of specific atoms and fragments of the computed structures). Such a decrease in charge could result from the aryl halide attacking an electrophilic Cu center during the oxidative addition step. In such a pathway, more electron-rich aryl halides would be expected to react more quickly with compounds **2** than electron-poor aryl iodides due to better stabilization of a partial positive charge on the arene.

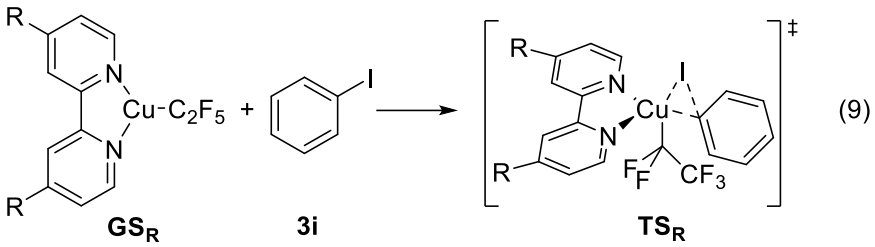
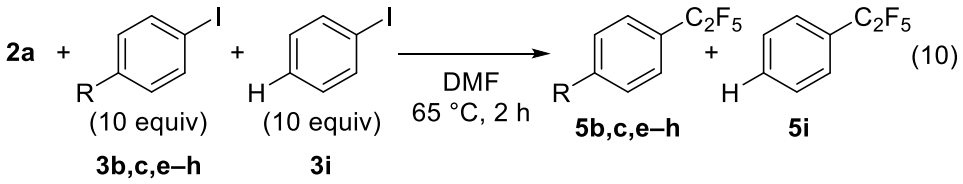


Table 2.4.1 Computed energies of activation for the oxidative addition of iodobenzene to $(R_2bpy)CuC_2F_5$.

R	σ_p	$\Delta G_{calc}^{‡}$ (kcal/mol)	$\Delta H_{calc}^{‡}$ (kcal/mol)	$\Delta S_{calc}^{‡}$ (cal/mol·K)
$N(CH_3)_2$	–0.83	24.5	9.5	–41
OCH_3 (**2d**)	–0.27	23.9	9.4	–40
H (**2a**)	0	23.9	8.8	–42
Cl (**2f**)	0.23	25.0	8.3	–46
CN	0.66	26.1	7.5	–52

See the Section 2.7.5 for full computational details



R = CN (**3b**), OCH_3 (**3c**), CH_3 (**3e**), Cl (**3f**), CF_3 (**3g**), $COCH_3$ (**3h**)

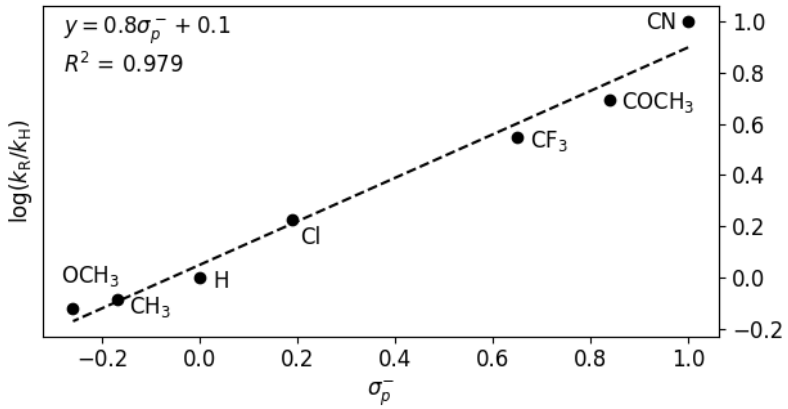


Figure 2.4.1 Hammett plot (*vs* σ_p^-) of the rates of reaction of **2a** with *para*-substituted iodobenzenes relative to unsubstituted iodobenzene as determined by competition experiments. See Section 2.7.3 for experimental details.

This prediction is inconsistent with the measured rates of reaction of aryl iodides **3a**–**c** with **2a** and **2e** (*vide supra*). To gain a more detailed view into this electronic effect, we subjected **2a** to reactions with equimolar mixtures of *para*-substituted aryl iodides **3b**, **3c**, or **3e**–**3h** and unsubstituted iodobenzene (**3i**) at 65 °C (eq 10). The rates of reaction of the substituted iodobenzenes with **2a** were determined relative to **3i** with **2a** by the final ratio of substituted

pentafluoroethylarene products **5** to pentafluoroethylbenzene (**5i**; see Section 2.7.3 for details). A Hammett plot of these relative rates revealed a strong *positive* correlation with σ_p^-[44] ($\rho = 0.8$, Figure 2.4.1), the opposite of what would be expected for a mechanism in which the copper acts as an electrophile. The positive ρ value suggests a buildup of negative charge on the arene, which is reflected by a decrease in the summed natural atomic charges of the aryl fragment in all **TS$_R$** (Δq_{aryl} = –0.06 – –0.07). This result is consistent with the results of Grushin and co-workers, who found a ρ value of +0.91 for reactions involving substituted aryl iodides with a "ligandless" $CuCF_3$ system when fitting against the σ_p^- parameters of the substituent on the arene.[26]

Despite the aforementioned decrease in positive charge on the Cu center in **TS$_R$**, relative to **GS$_R$**, the aggregate natural atomic charges of the R_2bpy fragments of the computed structures in all cases were also slightly more positive in **TS$_R$** than in **GS$_R$** (Δq_{R2bpy} = +0.02 – +0.03). Such an observation is inconsistent with the hypothesis that the bpy ligand helps to accommodate a buildup of negative charge at the Cu center, although we acknowledge that calculated localized charges (both those on the bpy ligands and those on the Cu centers) may be misleading due to the global nature of the electronic wavefunction and the fact that partitioning electron density to assign partial atomic charges is, to some degree, arbitrary. Unfortunately, further analysis of the atomic charges, computed geometries, and the frontier molecular orbitals in the context of so-called "inverted ligand field" measured for the formally Cu(III) complex $[Cu(CF_3)_4^-]$[51–54] revealed no clear trends that might explain the reactivities of complexes **2** with aryl halides. A more detailed theoretical treatment than that presented in this work is needed to elucidate the underlying effect of the bpy ligand on the reactivities of complexes **2** with aryl halides.

2.5 Conclusions

In summary, we have prepared a series of $L_2CuC_2F_5$ complexes in which L_2 are bpy ligands possessing varied electronic properties and investigated the kinetics of the reactions of these complexes with aryl halides to form pentafluoroethyl arenes. The complexes comprised an equilibrium between the neutral $[(R_2bpy)CuC_2F_5]$ and ionic $[(R_2bpy)_2Cu][Cu(C_2F5)_2]$ forms in DMF solution, which favored the neutral form more heavily for the complexes of more electron-donating bpy ligands than for complexes of less electron-donating bpy ligands. A combination of equilibrium data on this interconversion and kinetic data on the reactions with aryl halides implies that the rate-limiting oxidative addition of aryl halides to the neutral form of these complexes is, in contrast to common effects of ancillary ligands, faster for complexes of less electron-donating ligands than for those of more electron-donating ligands. This effect contrasts with the trend of the electronic effects of ligands on the rate of oxidative addition of aryl halides to amidate complexes ligated by more electron-rich alkylamines *vs* less electron-rich phenanthrolines[17] and highlights the unusual properties of complexes containing perfluoroalkyl ligands.

2.6 Footnotes

1. The Hammett σ_p value for N(*n*-propyl)$_2$ was used for 1-piperidinyl
2. The difference in ratios of **5d–e** for **2a** and **2e** suggests that ligand dissociation might be a minor pathway for **2a**. This was further assessed by addition of extra bpy to the reaction of **2a** with **3d–e** to ensure ligation of any free CuC_2F_5. The reactions involving 2 or 15 equiv added bpy resulted in the slightly smaller ratios of 40:60 and 39:61 of **5d**:**5e**, respectively, comparable to those achieved with **2e** and suggesting that the reaction of free CuC_2F_5 is an active but minor pathway.

2.7 Supplementary Experimental Information

2.7.1 General Experimental Procedure and Reagent Availability

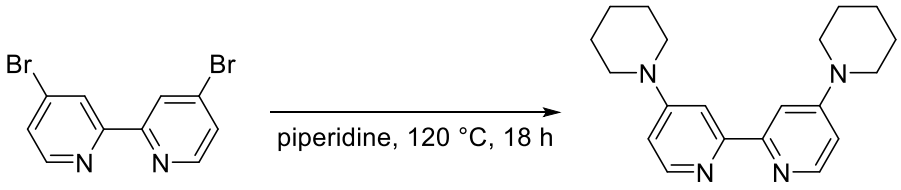
All manipulations were conducted under inert atmosphere in a nitrogen-filled glovebox equipped with oxygen and water sensors (working levels ≤ 5 ppm and 0.5 ppm, respectively) and a low-temperature refrigeration unit (–35 °C) unless otherwise noted. All glassware was flame-dried or dried overnight at 120 °C, allowed to cool under vacuum, and stored in a N_2-atomsphere drybox until use unless otherwise noted. Tetrahydrofuran, toluene, and diethyl ether were purified by passing the degassed solvents (N_2) through a column of activated alumina (solvent purification system purchased from Innovative Technologies, Newburyport, MA). Anhydrous *N*,*N*-dimethylformamide (ExtraDry) was purchased from Acros Organics and used as received. $CDCl_3$ and DMF-d_7 were purchased from Cambridge Isotope Laboratories. $CDCl_3$ was used as received, while DMF-d_7 was dried for 2 d over activated 4 Å molecular sieves, then distilled and stored over a fresh batch of sieves under N_2 atmosphere. 4,4'-dibromo-2,2'-bipyridine was purchased from Acros Organics. 4,4'-dichloro-2,2'-bipyridine was purchased from CombiBlocks or prepared according to literature procedure.[55] Trimethyl(pentafluoroethyl)silane (TMS–C_2F_5) was generously donated by Catylix. All other materials were purchased from commercial suppliers and used as received.

NMR spectra were acquired on 400, 500, 600, and 700 MHz Bruker instruments at the College of Chemistry's NMR facility at the University of California, Berkeley. NMR spectra were processed with MestreNova 11.0 (Mestrelab Research SL). Chemical shifts are reported in ppm and referenced to residual (in deuterated solvents), bulk (in non-deuterated solvents) solvent signals ($CHCl_3$ in $CDCl_3$: 7.26 ppm for ^{1}H and 77.0 ppm for ^{13}C; DMF-d_6: 8.03 ppm for ^{1}H), or an internal standard (4-(trifluoromethoxy)anisole, –58.79 ppm for ^{19}F, determined relative to the chemical shift of C_6F_6 [–164.46 ppm] in DMF[56]). Coupling constants are reported in Hz.

Elemental analyses were conducted at the Microanalysis Laboratory at the University of California, Berkeley. HR-MS analyses were conducted at the QB3/Chemistry Mass Spectrometry Facility at the University of California, Berkeley.

2.7.2 Synthetic Methods

*4,4'-di(piperidin-1-yl)-2,2'-bipyridine (**1e**)*

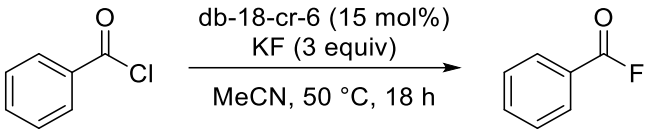


1e

To a 4 mL vial equipped with a magnetic stir bar under air were added 4,4'-dibromo-2,2'-bipyridine (150 mg, 0.478 mmol) and piperidine (1.6 mL). The headspace of the vial was purged with dry N_2, the vial was sealed, and the reaction mixture was stirred vigorously at 120 °C for 18 h. The light-yellow solution was allowed to cool to room temperature, whereupon a white precipitate formed. The mixture was then transferred to a larger vessel with the assistance of 1 M aqueous KOH and was diluted with more KOH solution (15 mL total), and the mixture was stirred

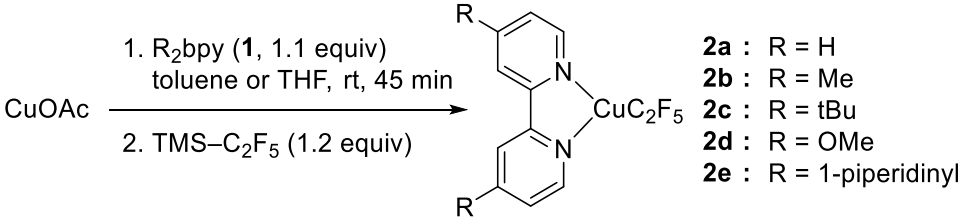
vigorously at ambient temperature for 30 min. The resulting white precipitate was collected by filtration and washed with water (3x5 mL) and dried under high vacuum to afford the title compound as a white powder (103 mg, 67% yield). Batches of piperidine discolored by age were found to afford the product without a significant decrease in yield (64%) or purity by NMR spectroscopy, though in these cases the product was slightly colored. The ^{1}H NMR spectrum matched that reported in the literature.[57]
^{1}H NMR (600 MHz, $CDCl_3$): δ 8.30 (d, *J* = 5.9 Hz, 2 H), 7.84 (d, *J* = 2.7 Hz, 2H), 6.65 (dd, *J* = 5.9, 2.8 Hz, 2H), 3.50–3.35 (m, 8 H), and 1.80–1.55 (m, 12 H) ppm.
^{13}C NMR (151 MHz, $CDCl_3$): δ 156.5 (br s), 156.1, 149.1 (br s), 108.1, 105.9, 47.6, 25.5, and 24.5 ppm.
ESI-HRMS: Calc'd (M+H): 323.223571; found: 323.2240.

Benzoyl fluoride



In an unoptimized procedure, a 20 mL vial equipped with a magnetic stir bar was charged with benzoyl chloride (581 μL, 5.00 mmol), potassium fluoride (871 mg, 15.0 mmol, 3.00 equiv), dibenzo-18-crown-6 (270 mg, 0.750 mmol, 15 mol%), and acetonitrile (10 mL). The vial was sealed and heated at 50 °C for 18 h under vigorous stirring. After full conversion of benzoyl chloride, as determined by ^{1}H NMR spectroscopy, the reaction mixture was extracted under air with pentane (5×10 mL), and the combined pentane layers were filtered to remove precipitated dibenzo-18-crown-6 and KF. The pentane layers were then concentrated under vacuum to afford benzoyl fluoride as a colorless oil (351 mg, 57% yield), which was used without further purification. We note that the product is moderately volatile and that yields likely could be improved by more careful removal of solvent. Benzoyl fluoride should be stored in a Teflon container at low temperature to avoid decomposition and the formation of HF. NMR chemical shifts matched those reported in the literature.[58]
^{1}H NMR (400 MHz, $CDCl_3$): δ 8.05 (dd, *J* = 7.7, 1.3 Hz, 2H), 7.71 (tt, *J* = 7.5, 1.3 Hz, 1 H), and 7.53 (apt t, 7.8 Hz, 2 H) ppm.
^{19}F NMR (376 MHz, $CDCl_3$, wrt $PhCF_3$ @ –62.61 ppm[56]): δ 18.2 (s, 1 F) ppm.

*General Procedure for Bipyridine-Ligated Pentafluoroethylcopper(I) Complexes **2a–e***

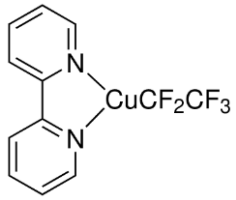


This method was developed by Michael Mormino and was reported as part of his PhD dissertation.[59] To a 20 mL vial equipped with a magnetic stir bar was added bpy ligand **1** (1.1

equiv) and THF or toluene to form a ~0.15 M solution. To the rapidly stirring solution was then added CuOAc (1.0 equiv). The vial was sealed, and the suspension was allowed to stir for 45 min. TMS–C_2F_5 (1.2 equiv) was then added dropwise to the stirring suspension, and the mixture was allowed to stir for 12 h at room temperature. The precipitated solid was collected by vacuum filtration through a fine fritted glass funnel and washed with diethyl ether until the eluent was colorless. The collected solid was then dried under vacuum to afford the pure product.

As previously reported for other Cu(I) perfluoroalkyl complexes, the prepared pentafluoroethyl complexes exist in DMF solution as an equilibrating mixture of neutral (R_2bpy)CuC_2F_5 and ionic [(R_2bpy)$_2$Cu][Cu(C_2F_5)$_2$] species.[31–35,43] Due to this dynamic behavior, broad signals were observed in the ^{1}H NMR spectra of these compounds. Likewise, characterization of these compounds by ^{13}C NMR spectroscopy was complicated by (1) the dynamic behavior of these complexes; (2) broadening of resonances by Cu–C and N–C coupling; and (3) splitting of resonances by C–F coupling, and thus was generally not performed.

*(2,2'-bipyridine)(pentafluoroethyl)copper(I) (**2a**)*



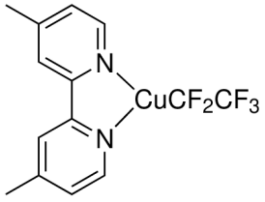
The reaction was conducted according to the general procedure in toluene on a 0.5 mmol scale. The product was obtained as an orange solid (167 mg, 93% yield). Two sets of ^{19}F NMR peaks were observed in a 44:66 ratio at ambient temperature, reflecting a 57:43 ratio of neutral to ionic forms. Despite a previous report by Grushin and co-works stating that (bpy)CuC_2F_5 (**2a**) is unstable at room temperature,[32] we found that **2a** prepared by our method that had been stored for several weeks in a N_2-atmosphere drybox at ambient temperature reacted with **3a** (limiting **2a**) in quantitative yield. The described darkening of the orange material was not observed. NMR chemical shifts matched those reported previously by Michael Mormino.[59]

^{1}H NMR (400 MHz, DMF-d_7) δ 8.77 (br s, 4H), 8.35 (br s, 2H), and 7.81 ppm (br s, 2H).

^{19}F NMR (376 MHz, DMF-d_7) δ –84.1 (s, 6F, ionic), –84.2 (s, 3F, neutral), –110.0 (s, 2F, neutral), and –117.4 ppm (s, 6F, ionic).

Anal. Calcd. for $C_{12}H_8CuF_5N_2$: C, 42.55; H: 2.38; N, 8.27; Found: C, 42.34; H, 2.61; N: 8.36.

*(4,4'-dimethyl-2,2'-dipyridyl)(pentafluoroethyl)copper(I) (**2b**)*



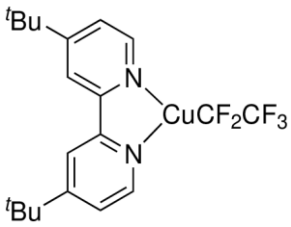
The reaction was conducted according to the general procedure in THF on a 0.4 mmol scale. The product was obtained as an orange solid (109 mg, 74%). Two sets of ^{19}F NMR peaks for the pentafluoroethyl group were observed in a 50:50 ratio at ambient temperature, reflecting a 67:33 ratio of the neutral to ionic forms. NMR chemical shifts matched those reported previously by Michael Mormino.[59]

^{1}H NMR (400 MHz, DMF-d_7) δ 8.60 (br s, 4H), 7.60 (s, 2H), and 2.56 ppm (s, 6H).

^{19}F NMR (376 MHz, DMF-d_7) δ –84.1 (s, 6F, ionic), –84.2 (s, 3F, neutral), –109.7 (s, 2F, neutral) and –117.4 (s, 4F, ionic).

Anal. Calcd. for $C_{14}H_{12}CuF_5N_2$: C, 45.84; H, 3.30; N, 7.64; Found: C, 45.53; H, 3.05; N, 7.48.

*(4,4'-di-tert-butyl-2,2'-dipyridyl)(pentafluoroethyl)copper(I) (**2c**)*



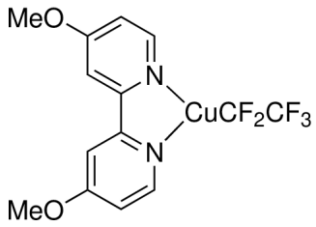
The reaction was performed according to the general procedure in THF on a 0.4 mmol scale. The product was obtained as an orange solid (135 mg, 75%). Two sets of ^{19}F NMR peaks for the pentafluoroethyl group were observed in a 57:43 ratio at ambient temperature, reflecting a 73:27 ratio of neutral to ionic forms. NMR chemical shifts matched those reported previously by Michael Mormino.[59]

^{1}H NMR (400 MHz, DMF-d_7) δ 8.45 – 9.06 (m, 4H), 7.77 (br s, 2H), and 1.46 ppm (s, 18 H).

^{19}F NMR (376 MHz, DMF-d_7) δ –84.1 (s, 6F, ionic), –84.2 (2F, neutral), –109.7 (s, 4F, neutral), and –117.4 ppm (s, 4F, ionic).

Anal. Calcd. for $C_{20}H_{24}CuF_5N_2$: C, 53.27; H, 5.36; N, 6.21; Found: C, 52.91; H, 5.44; N, 6.33.

*(4,4'-dimethoxy-2,2'-dipyridyl)(pentafluoroethyl)copper(I) (**2d**)*



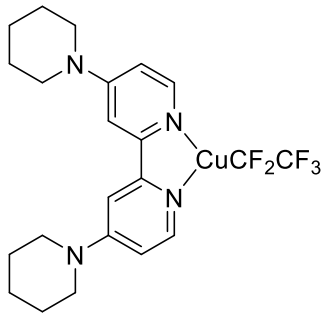
The reaction was performed according to the general procedure in THF on a 0.3 mmol scale. The product was obtained as a light orange solid (92 mg, 77%). Two sets of ^{19}F NMR peaks for the pentafluoroethyl group were observed in a 70:30 ratio at ambient temperature, reflecting an 82:18 ratio of the neutral to ionic forms. NMR chemical shifts matched those reported previously by Michael Mormino.[59]

^{1}H NMR (400 MHz, DMF-d_7) δ 8.61 (br s, 2H), 8.25 (br s, 2H), 7.35 (br s, 2H), and 4.11 ppm (s, 6H).

^{19}F NMR (376 MHz, DMF-d_7) δ –84.1 (s, 6F, ionic), –84.1 (s, 3F, neutral), –109.5 (s, 2F, neutral), and –117.4 ppm (s, 4F, ionic).

Anal. Calcd. $C_{14}H_{12}CuF_5N_2O_2$: C, 42.16; H, 3.03; N, 7.02; Found: C, 41.77; H, 2.94; N, 6.91.

*(4,4'-di(piperidin-1-yl)-2,2'-bipyridine)(pentafluoroethyl)copper(I) (**2e**)*



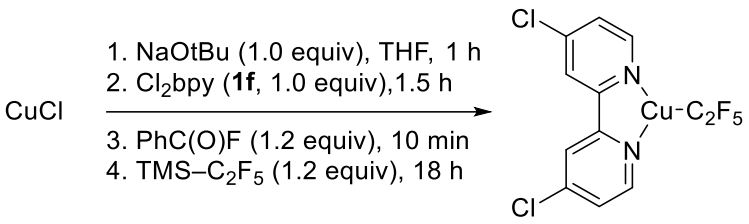
The reaction was performed according to the general procedure in THF on a 0.3 mmol scale. The product was obtained as a yellow-orange powder (128 mg, 85%). Dissolving the solid in DMF initially resulted in an orange solution, which slowly turned dark red at ambient temperature. We attribute this color change to slow equilibration between the neutral and ionic form at ambient temperature. Two sets of ^{19}F NMR peaks for the pentafluoroethyl group were observed in a 99:1 ratio at ambient temperature, corresponding to a >99:1 ratio of neutral to ionic forms. The resonance corresponding to the CF_3 peak of the ionic species was not observed due to the low abundance of this species and the proximity of the corresponding resonance to the CF_3 resonance of the neutral species.

^{1}H NMR (400 MHz, DMF-d_7): δ 8.28 (d, J = 6.3 Hz, 2H), 7.89 (d, J = 2.6 Hz, 2H), 7.04 (dd, J = 6.3, 2.6 Hz, 2H), 3.55 – 3.70 (m, 4 H), and 1.54 – 1.75 ppm (m, 12 H).

^{19}F NMR (376 MHz, DMF-d_7): δ –84.1 (s, 3H, neutral), –108.6 (s, 2H, neutral), and –117.4 ppm (s, 4H, ionic).

Anal. Calcd. $C_{22}H_{26}CuF_5N_4$: C, 52.32; H, 5.19; N, 11.09; Found: C: 51.94; H, 5.36; N, 10.80.

*(4,4'-dichloro-2,2'-bipyridine)(pentafluoroethyl)copper(I) (**2f**)*



The following procedure was partially adapted from a literature preparation of (phen)CuC_2F_5.[42] To a 4 mL vial containing a magnetic stir bar, anhydrous copper(I) chloride (19.8 mg, 0.200 mmol) and sodium *tert*-butoxide (19.3 mg, 0.201 mmol, 1.01 equiv) was added THF (0.5 mL), and the resulting suspension was stirred at ambient temperature for 1 h, over which time the mixture turned light yellow. The suspension was then filtered through a syringe filter, which was washed with THF (2×0.25 mL), and to the filtrate was added 4,4'-dichloro-2,2'-bipyridine (**1f**, 51.0 mg, 0.200 mmol, 1.00 equiv). The resulting solution was stirred for 1.5 h at ambient temperature, over which time the yellow solution darkened in color slightly. To the rapidly stirring solution was then added benzoyl fluoride (26.2 μL, 0.240 mmol, 1.20 equiv), and the solution immediately turned dark purple. The reaction mixture was stirred for 10 min, after which TMS–C_2F_5 (42.0 μL, 0.240 mmol, 1.20 equiv) was added, and the reaction mixture was allowed to stir for 18 h at ambient temperature. The red-brown reaction mixture was then concentrated under vacuum to ~0.2 mL and treated with pentane (2 mL). The resulting precipitate was collected by vacuum filtration through a fine fritted glass funnel, washed with pentane (3×5 mL), and dried under vacuum to afford the title compound as a red-brown solid (33.6 mg, 41% yield). Two sets of ^{19}F NMR peaks for the pentafluoroethyl group were observed in a 39:61 ratio at ambient temperature, reflecting a 56:44 ratio of the neutral to ionic forms.

^1H NMR (500 MHz, DMF-d_7): δ 9.01 (br s, 2 H), 8.83 (br s, 2 H), and 7.97 (br s, 2 H) ppm.

^{19}F NMR (470 MHz, DMF-d_7): δ –84.1 (s, 6 F, ionic), –84.2 (s, 3 F, neutral), –111.0 (br s, 2 F, neutral), and –117.4 (s, 4 F, ionic) ppm.

Anal. Calcd. $C_{22}H_{26}CuF_5N_4$: C, 35.36; H, 1.48; N, 6.87; Found: C: 35.01; H, 1.71; N, 7.04.

*"Ligandless" CuC_2F_5, solution in DMF (**6**)*

The following procedure was adapted from work by Mikami and co-workers.[47] To a 4 mL vial equipped with a septum cap was added K(DMF)[Cu(O*t*Bu)$_2$][13] (244.1 mg, 0.7518 mmol) and DMF (1.5 mL). After all of the K(DMF)[Cu(O*t*Bu)$_2$] had dissolved, ethyl pentafluoropropionate (118 μL, 0.795 mmol, 1.05 equiv) was added. The vial was sealed, removed from the drybox, and heated at 50 °C for 30 min. The reaction mixture was allowed to cool to room temperature, and triethylamine trihydrofluoride (41 μL, 0.25 mmol, 0.33 equiv) was added *via* microsyringe under vigorous stirring. Stirring was continued for 30 min, during which time a fine white precipitate was observed. The vial was brought back into the drybox and filtered through a syringe filter to afford a yellow solution of "ligandless" CuC_2F_5. Addition of 4-(trifluoromethoxy)anisole (9.10 μL, 0.0600 mmol) to a 50 μL aliquot revealed that the concentration of CuC_2F_5 in this solution was 0.342 M, constituting a ~95:5 ratio of neutral "CuC_2F_5" and ionic $[Cu(C_2F_5)_2]^-$ forms. The reagent solution thus obtained was stored at –35 °C under an N_2 atmosphere for at most 8 h before use. We note that only spectra of $[(tBuO)CuC_2F_5]^-$, not the HF-neutralized reagent, were reported directly in previous literature.[43,47]

^{19}F NMR (376 MHz, DMF): δ –84.1 (s, 6F, ionic), –84.3 (s, 3F, neutral), –113.9 – –111.5 (br m, 2F, neutral), and –117.3 ppm (s, 4F, ionic).

2.7.3 Studies on the Speciation and Reactivity of Pentafluoroethylcopper(I) Complexes **2a–f**

*Demonstrating Fast Equilibration of Complexes **2***

Solutions of complexes **2** were prepared by dissolving **2** (0.0300 mmol) in 600 μL DMF. 4-(trifluoromethoxy)anisole (9.10 μL, 0.0600 mmol, 2.00 equiv) was added as an internal standard. These solutions were transferred to J. Young tubes, which were cooled to –78 °C in a dry ice/acetone cold bath. Quantitative ^{19}F NMR spectra (transmitter offset centered between the two peaks of interest, calibrated 90° pulse, delay time of at least 20 s between scans) comparing the CF_2 resonances of $[(R_2bpy)CuC_2F_5]$ (~–110 ppm) and $[Cu(C_2F_5)_2]^-$ (–117.4 ppm) were integrated to determine the initial relative populations of the neutral and ionic forms of **2**, after which the J. Young tubes were replaced into the dry ice/acetone bath. The spectrometer was then warmed to 65 °C (calibrated according to a solution of 80% ethylene glycol in DMSO), and each sample was quickly warmed to room temperature and transferred to the spectrometer. Pulse lengths were quickly recalibrated, and scans were taken 5 min and 10 min after sample insertion. The spectrometer was then further warmed to 90 °C, and the relative populations of **2** were re-measured. Ratios of $[(R_2bpy)CuC_2F_5]$ and $[Cu(C_2F_5)_2]^-$ are given in the following table.

Table 2.7.1. Neutral:Ionic Ratios of Complexes **2**

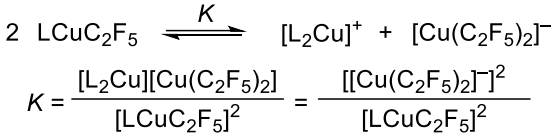
Compound	rt	65 °C (5 min)	65 °C (10 min)	90 °C (5 min)	90 °C (10 min)
2a	57:43	65:35	65:35	57:43	58:42
2b	67:33	70:30	70:30	69:31	69:31
2c	73:27	70:30	71:29	69:31	67:33
2d	82:18	81:19	81:19	80:20	80:20
2e	>99:1	91:9	91:9	92:8	92:8
2f	56:44	70:30	71:29	78:22	78:22

As can be seen in Table S1, heating at 65 °C resulted in a change in the ratio of neutral:ionic forms of complexes **2**. Equilibration appears to be fast (< 5 min), as nearly identical ratios are observed 5 and 10 min after warming to the desired temperature.

*Demonstrating the Lack of Tight Ion Pairing for the Ionic Form of Complexes **2***

Solutions of **2a** in DMF (0.0500 and 0.0167 M) were prepared by dissolving **2a** (10.2 mg, 0.0300 mmol) in DMF (600 or 1800 μL, respectively). A third solution of **2a** was prepared by adding a 200 μL aliquot of the 0.0167 M solution of **2a** to 400 μL DMF (0.00556 M). Aliquots of these solutions (600 μL each) were transferred to separate J. Young tubes, which were sealed and removed from the glove box. Quantitative ^{19}F NMR spectra of these samples at 65 °C (*vide supra*) were integrated to determine the relative equilibrium populations of the neutral and ionic forms of **2a**. The equilibrium ratios of **2a** at 0.0500 M, 0.0167 M, and 0.00556 M total concentration were determined to be 65:35, 67:33, and 66:33, respectively. This insensitivity of the relative populations of the neutral and ionic forms to the overall concentration of **2a** is consistent with solvent-separated ions $[(L_2Cu)]^+ + [Cu(C_2F_5)_2]^-$ as opposed to the tight ion pair $[L_2Cu]\cdot[Cu(C_2F_5)_2]$.

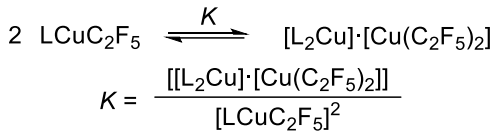
2:2 equilibrium, no concentration dependence on neutral:ionic ratio



$$2\ LCuC_2F_5 \rightleftharpoons [L_2Cu]^+ + [Cu(C_2F_5)_2]^-$$

$$K = \frac{[L_2Cu][Cu(C_2F_5)_2]}{[LCuC_2F_5]^2} = \frac{[[Cu(C_2F_5)_2]^-]^2}{[LCuC_2F_5]^2}$$

2:1 equilibrium, concentration dependence on neutral:ionic ratio



$$2\ LCuC_2F_5 \rightleftharpoons [L_2Cu]\cdot[Cu(C_2F_5)_2]$$

$$K = \frac{[[L_2Cu]\cdot[Cu(C_2F_5)_2]]}{[LCuC_2F_5]^2}$$

*Sample Preparation for Tracking the Pentafluoroethylation of Aryl Halides **3** and **4** by Complexes **2***

In a N_2-atmosphere drybox, the appropriate $(R_2bpy)CuC_2F_5$ complex **2** (0.0300 mmol) was added to a 4 mL vial, followed by a 1.00 M solution of 1-butyl-4-iodobenzene (**3a**), 4-iodobenzonitrile (**3b**), 4-iodoanisole (**3c**), or 1-bromo-4-butylbenzene (**4**) in 5:1 DMF:DMF-d_7 (v/v) (600 μL, 0.600 mmol, 20.0 equiv). 4-(trifluoromethoxy)anisole (9.10 μL, 11.5 mg, 0.0600 mmol, 2.00 equiv) was then added as an internal standard. The mixture was quickly mixed by pipette, and the resulting red solution transferred to a J. Young tube, which was sealed, removed from the drybox, and cooled to –78 °C in a dry ice/acetone cold bath until data collection could begin.

*Sample Preparation for Tracking the Pentafluoroethylation of Aryl Iodide **3a** by "Ligandless" CuC_2F_5 (**6**)*

In a N_2-atmosphere drybox, an aliquot of reagent solution **6** (86.8 μL, 0.0300 mmol) was added to a 4 mL vial, followed by DMF (213 μL), a 2.00 M solution of 1-butyl-4-iodobenzene (**3a**) 5:1 DMF:DMF-d_7 (v/v) (300 μL, 0.600 mmol, 20.0 equiv), and 4-(trifluoromethoxy)anisole (9.10 μL, 11.5 mg, 0.0600 mmol, 2.00 equiv) as an internal standard. The mixture was quickly mixed by pipette, and the light-yellow solution was transferred to a J. Young tube, which was sealed, removed from the drybox, and cooled to –78 °C in a dry ice/acetone cold bath until data collection could begin.

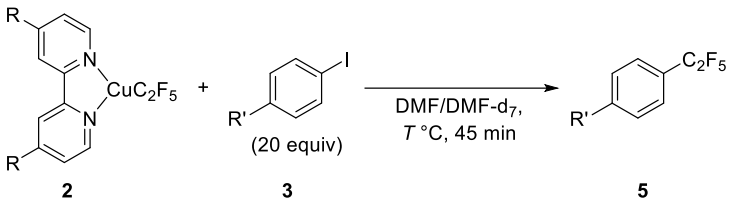
*Tracking the Pentafluoroethylation of Aryl Halides **3** and **4** by Complexes **2** or Reagent **6***

A 500 or 600 MHz NMR spectrometer was preheated to the appropriate reaction temperature (calibrated according to the spectral distance between glycol peaks in an 80% solution of ethylene glycol in DMSO-d_6). Shimming and 90° pulse calibration were performed according to the ^{19}F signals of a dummy sample (600 μL of a 1.00 M solution of **3a** in 5:1 DMF:DMF-d_7 (v/v) with 4-(trifluoromethoxy)anisole as an internal standard). The cold sample was then quickly warmed to room temperature and transferred to the instrument. After letting the sample thermally equilibrate for ~30 s, single-scan ^{19}F NMR spectra were collected at fixed time intervals for 45 min (for reactions with **3**) or 25–30 min (for reactions with **4**). After acquisition was complete, all samples were heated at the appropriate reaction temperature for 24 h, and final yields were determined by quantitative ^{19}F NMR spectroscopy. First-order exponential fits (for reactions with **3**) were determined by using Microsoft Excel's Solver (GRG Nonlinear) to minimize the total squared error between the fit and the experimental data points by varying *A*, *k*, and *c* in the first-order exponential equation $y = A\,(1 - \exp(-kt + c))$. Initial rates were determined by ordinary least-squares fit of the concentration of product **5a** *vs* time.

*NMR Chemical Shifts for Product Pentafluoroethylarenes **5***

5a: ^{19}F NMR (470 MHz, DMF): δ –85.3 (s, 3F) and –110.6 ppm (s, 2F).

5b: ^{19}F NMR (470 MHz, DMF): δ –85.2 (s, 3F) and –115.7 ppm (s, 2F).
5c: ^{19}F NMR (470 MHz, DMF): δ –85.4 (s, 3F) and –113.7 ppm (s, 2F).



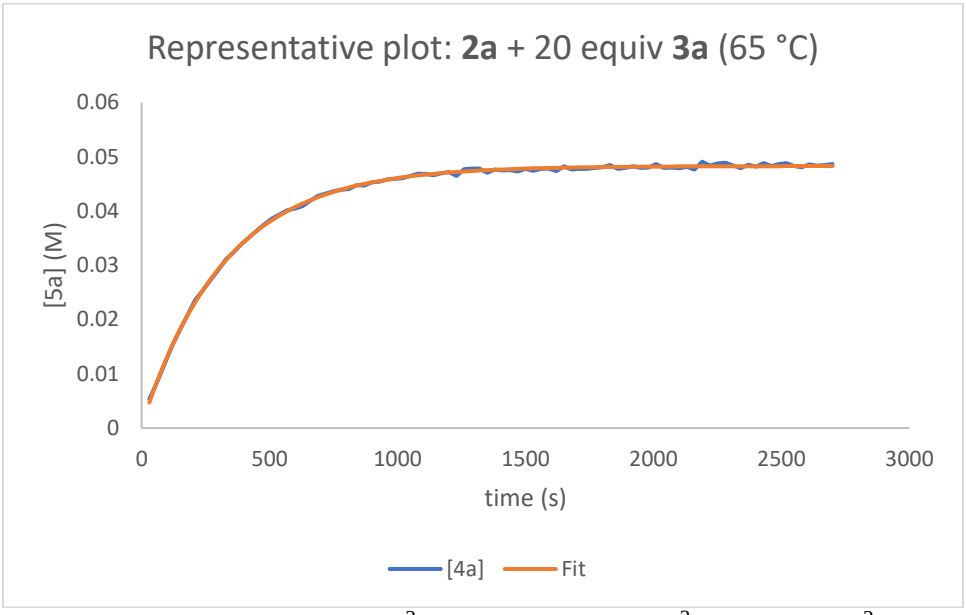


Figure 2.7.1 Fit: y = 4.83×10^{-2} (1 – exp(-3.07×10^{-3} t – 1.07×10^{-2})); Representative plot of the formation of **5a** over time in the reaction of **2a** + 20 equiv **3a** at 65 °C

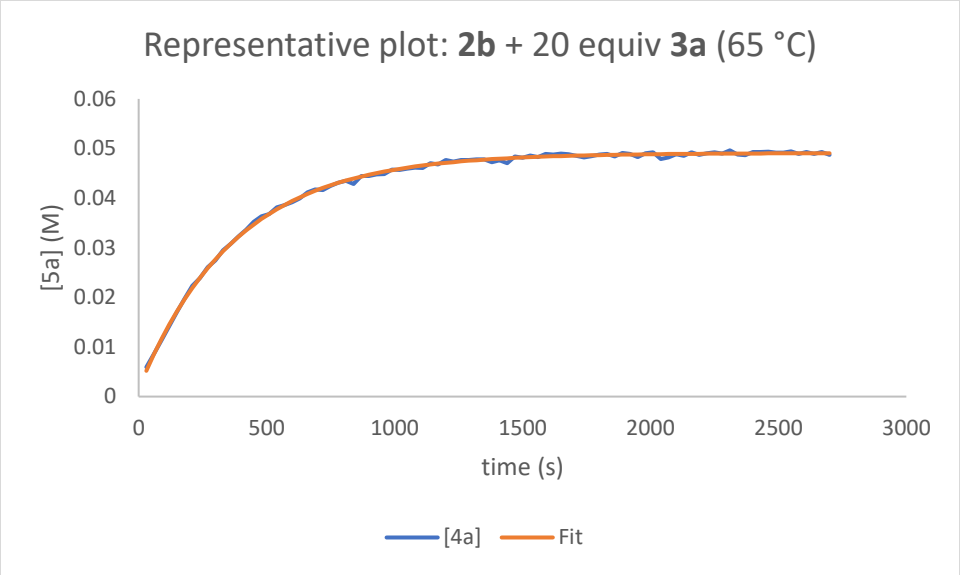


Figure 2.7.2 Fit: $y = 4.91\times10^{-2}\ (1 - \exp(-2.65\times10^{-3}\ t - 3.23\times10^{-2}))$; Representative plot of the formation of **5a** over time in the reaction of **2b** + 20 equiv **3a** at 65 °C

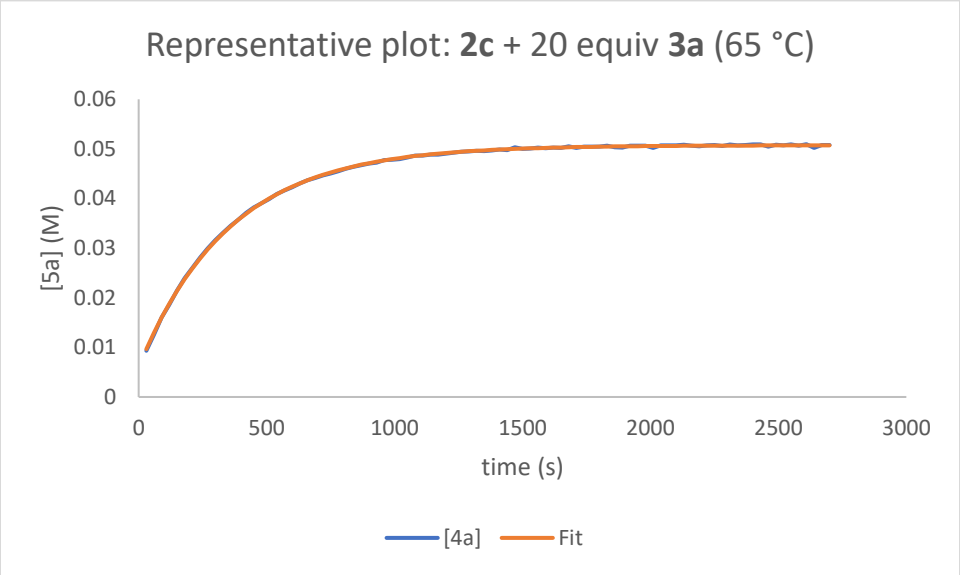


Figure 2.7.3 Fit: $y = 5.07\times10^{-2}\ (1 - \exp(-2.80\times10^{-3}\ t - 1.27\times10^{-1}))$; Representative plot of the formation of **5a** over time in the reaction of **2c** + 20 equiv **3a** at 65 °C

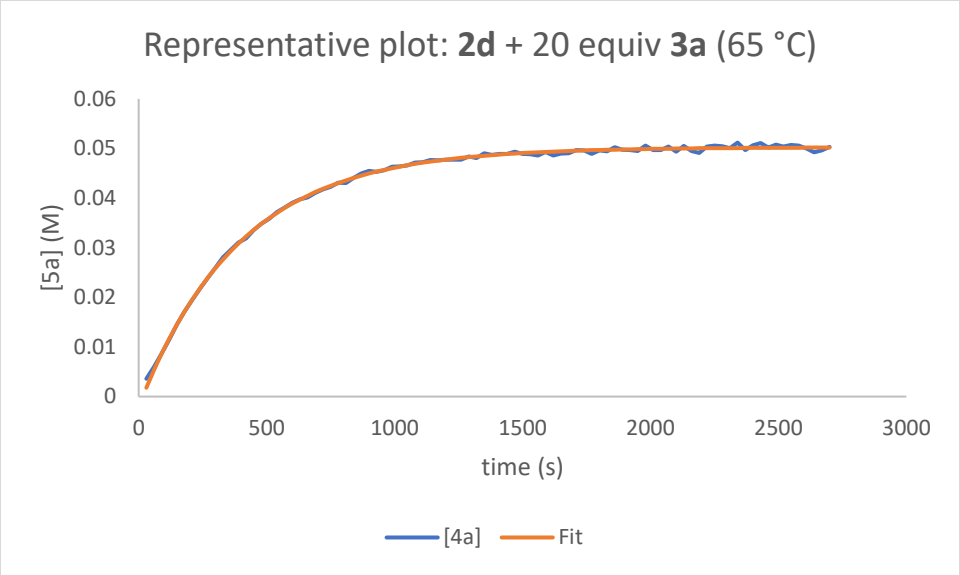


Figure 2.7.4 Fit: $y = 5.02\times10^{-2}\ (1 - \exp(-2.54\times10^{-3}\ t - 4.03\times10^{-2}))$; Representative plot of the formation of **5a** over time in the reaction of **2d** + 20 equiv **3a** at 65 °C

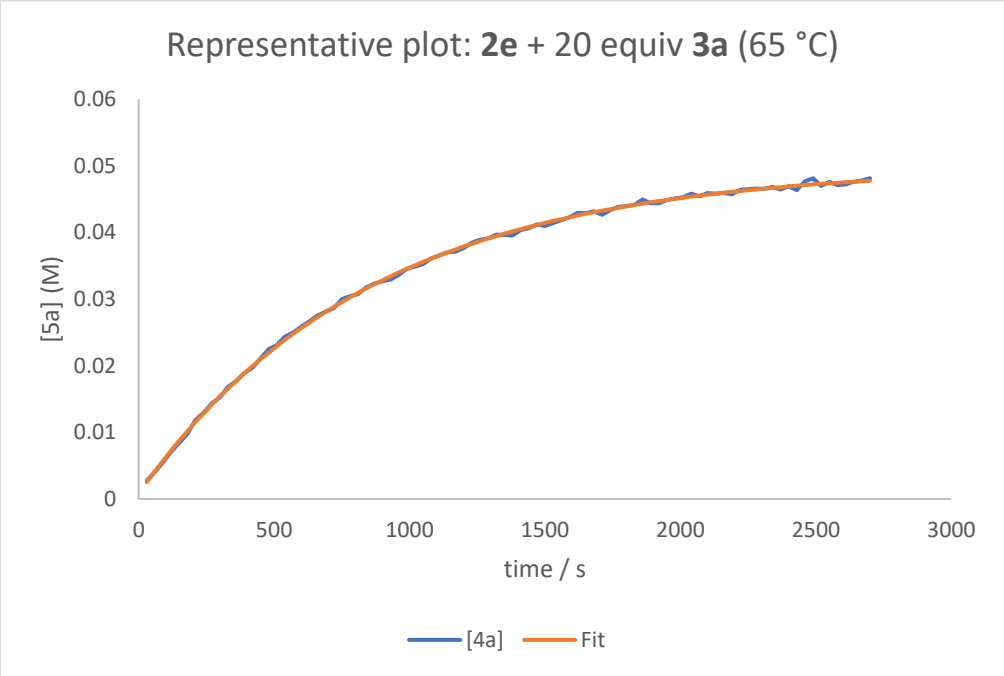


Figure 2.7.5 Fit: $y = 4.98\times10^{-2}\ (1 - \exp(-1.18\times10^{-3}\ t - 1.69\times10^{-2}))$; Representative plot of the formation of **5a** over time in the reaction of **2e** + 20 equiv **3a** at 65 °C

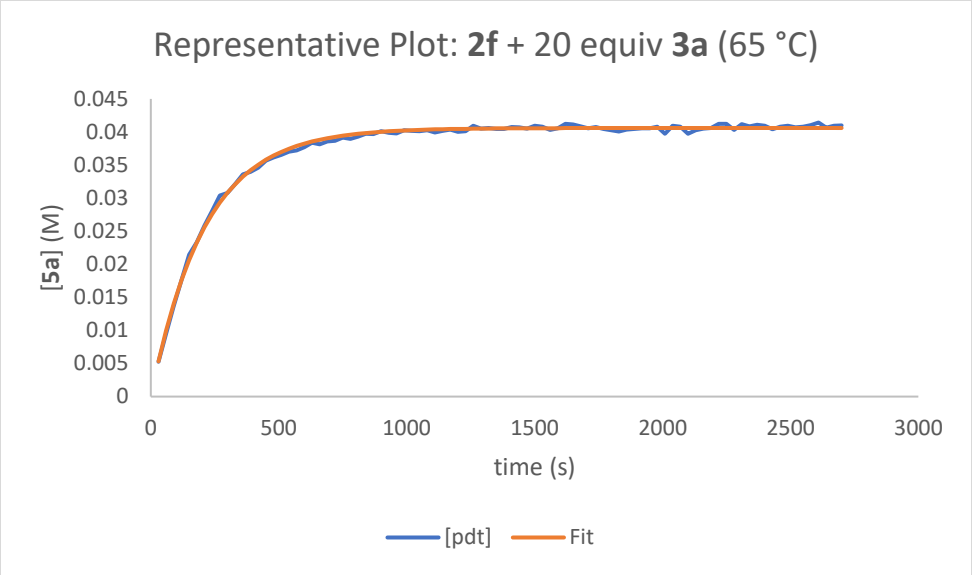


Figure 2.7.6 Fit: $y = 4.06\times10^{-2}\ (1 - \exp(-4.75\times10^{-3}\ t + 1.92\times10^{-3})$; Representative plot of the formation of **5a** over time in the reaction of **2f** + 20 equiv **3a** at 65 °C

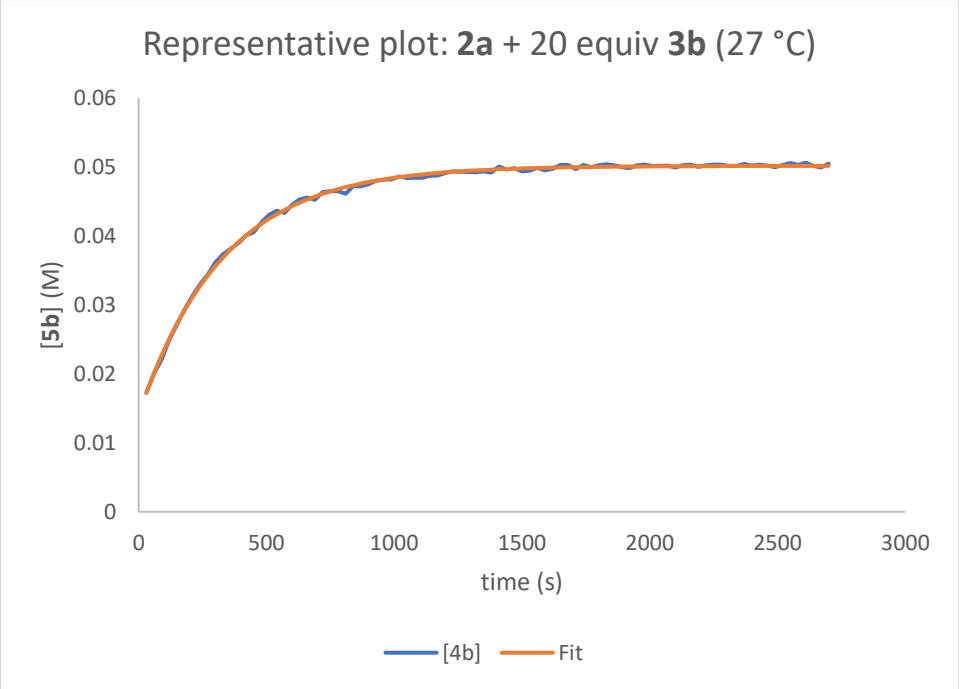


Figure 2.7.7 $y = 5.02\times10^{-2}\ (1 - \exp(-3.03\times10^{-3}\ t - 3.29\times10^{-1}))$; Representative plot of the formation of **5b** overt time in the reaction of **2a** + 20 equiv **3b** at 27 °C

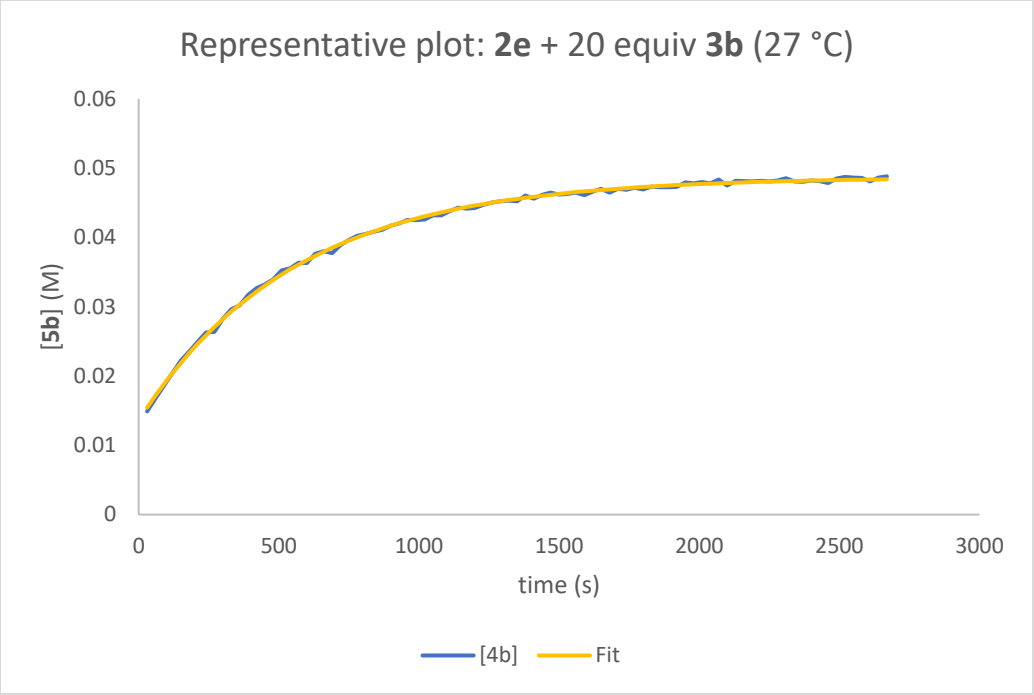


Figure 2.7.8 Fit: $y = 4.87\times10^{-2}\ (1 - \exp(-1.79\times10^{-3}\ t - 3.27\times10^{-1}))$; Representative plot of the formation of **5b** over time in the reaction of **2e** + 20 equiv **3b** at 27 °C

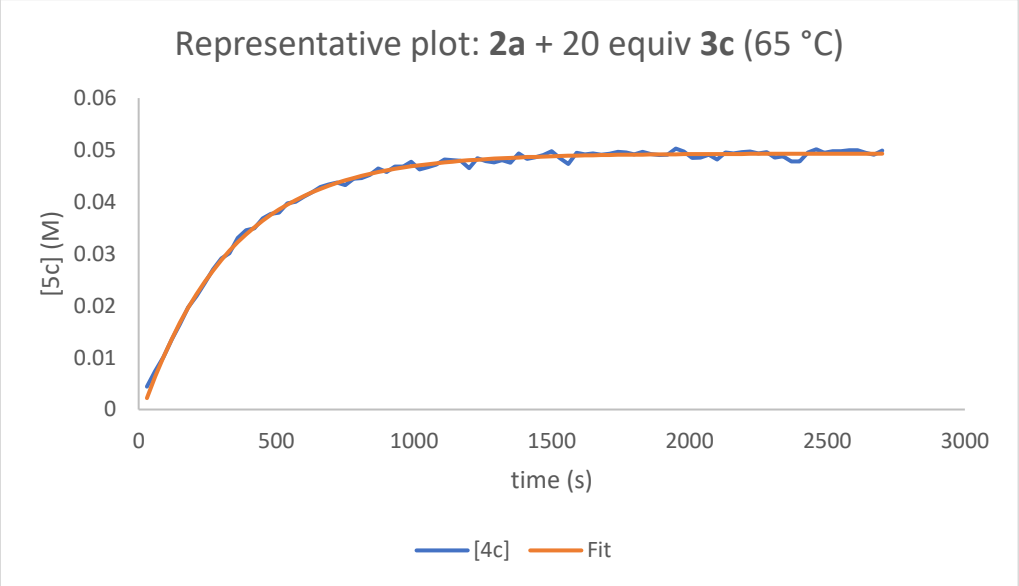


Figure 2.7.9 $y = 4.93\times10^{-2}\ (1 - \exp(-3.08\times10^{-3}\ t - 4.67\times10^{-2}))$; Representative plot of the formation of **5c** over time in the reaction of **2a** + 20 equiv **3c** at 65 °C

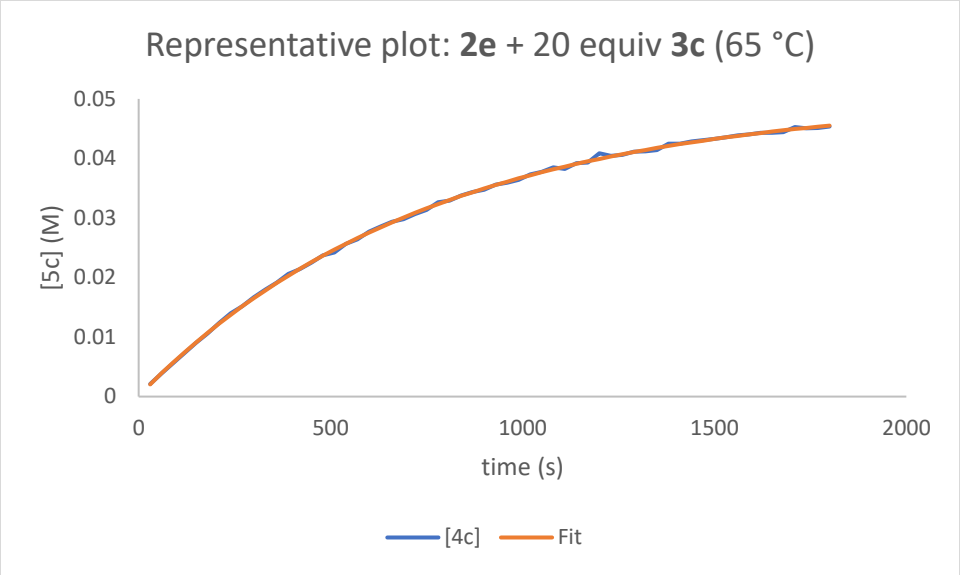
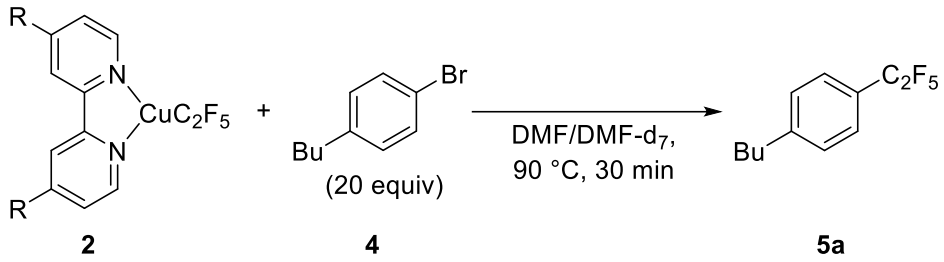


Figure 2.7.10 Fit: $y = 5.01\times10^{-2}\ (1 - \exp(-1.33\times10^{-3}\ t - 1.90\times10^{-3}))$; Representative plot of the formation of **5c** over time in the reaction of **2e** + 20 equiv **3c** at 65 °C



2 **4** **5a**

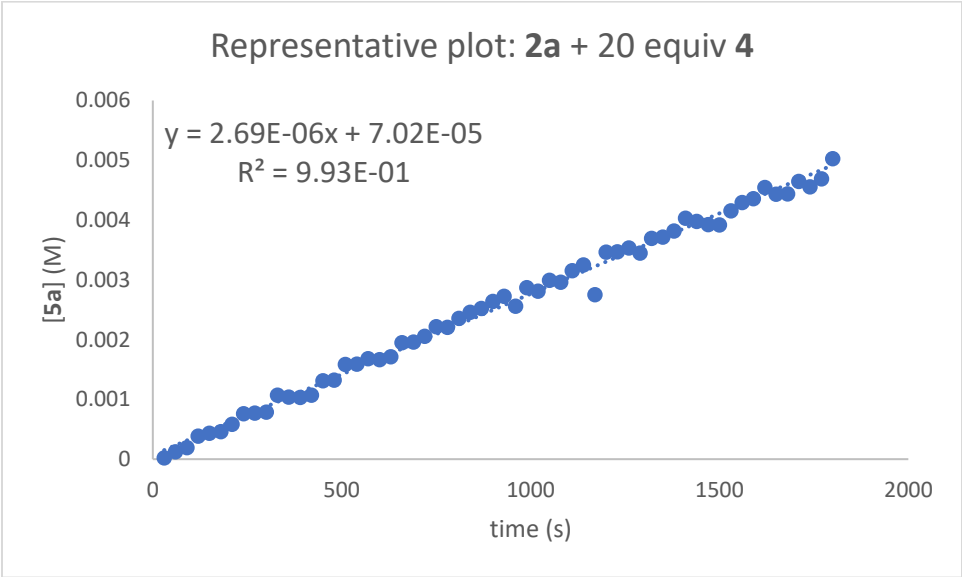


Figure 2.7.11 Representative plot of the formation of **5a** over time in the reaction of **2a** + 20 equiv **4** at 90 °C

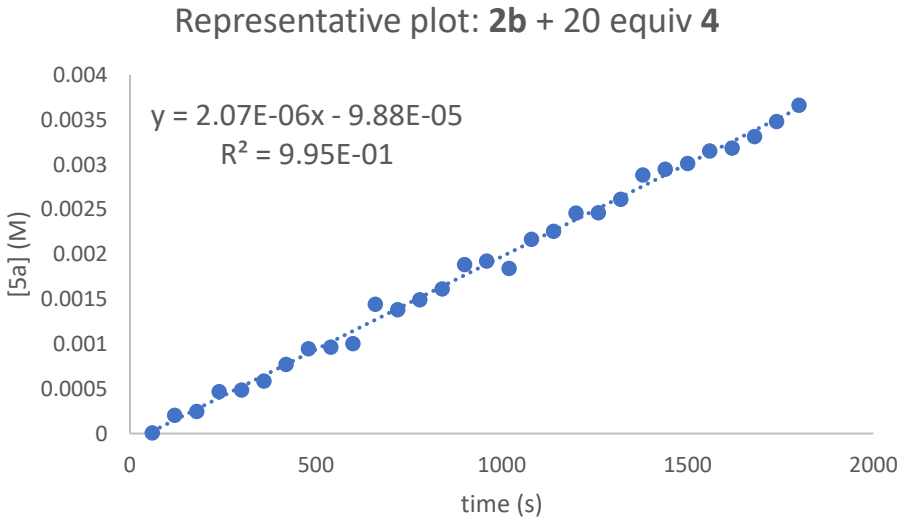


Figure 2.7.12 Representative plot of the formation of **5a** over time in the reaction of **2b** + 20 equiv **4** at 90 °C

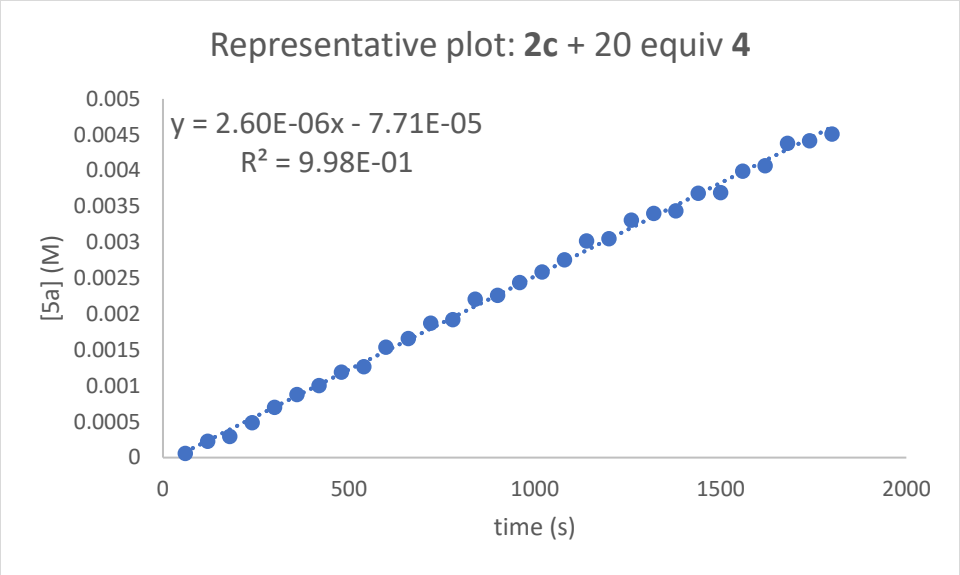


Figure 2.7.13 Representative plot of the formation of **5a** over time in the reaction of **2c** + 20 equiv **4** at 90 °C

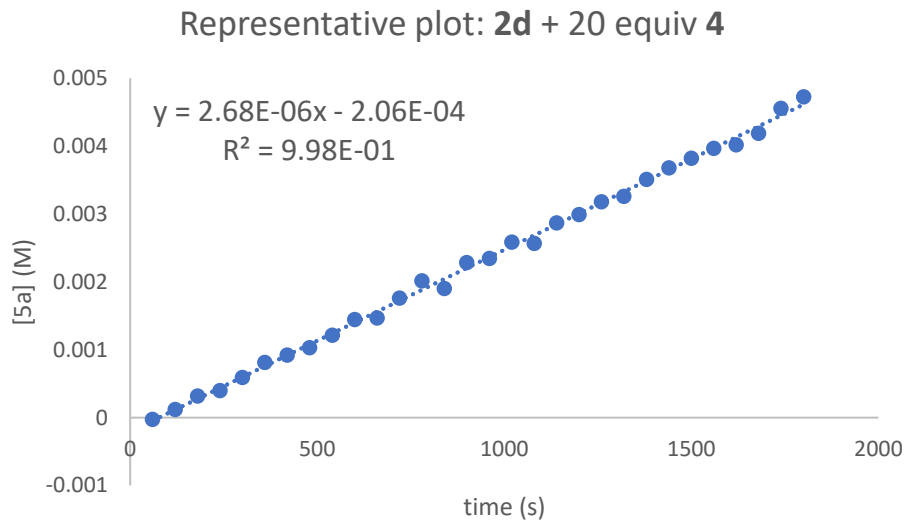


Figure 2.7.14 Representative plot of the formation of **5a** over time in the reaction of **2d** + 20 equiv **4** at 90 °C

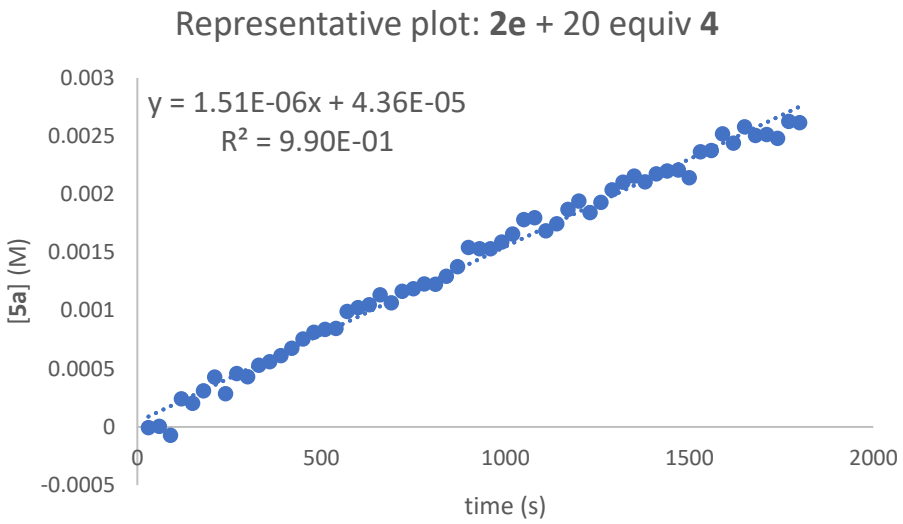


Figure 2.7.15 Representative plot of the formation of **5a** over time in the reaction of **2e** + 20 equiv **4** at 90 °C

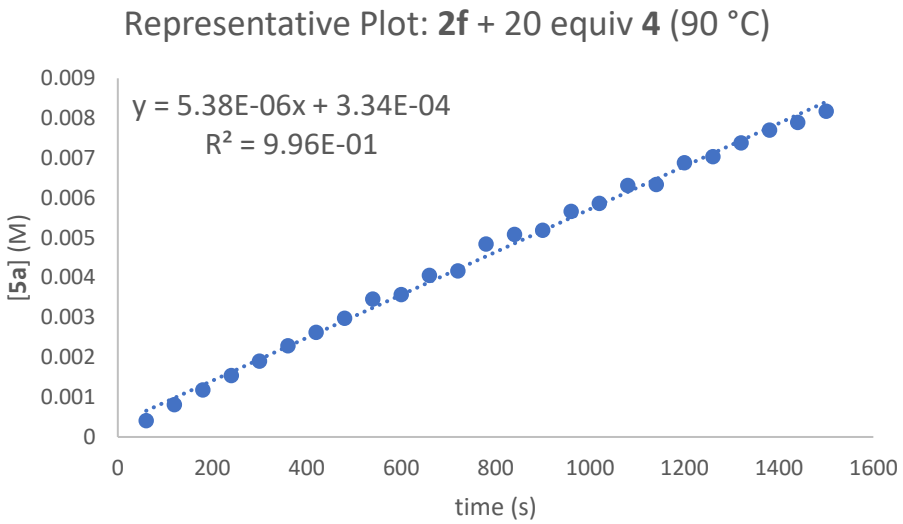
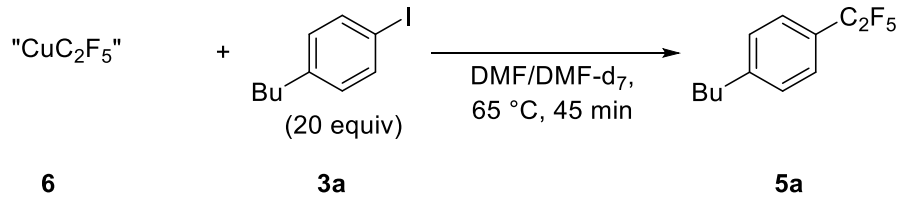


Figure 2.7.16 Representative plot of the formation of **5a** over time in the reaction of **2f** + 20 equiv **4** at 90 °C



6 **3a** **5a**

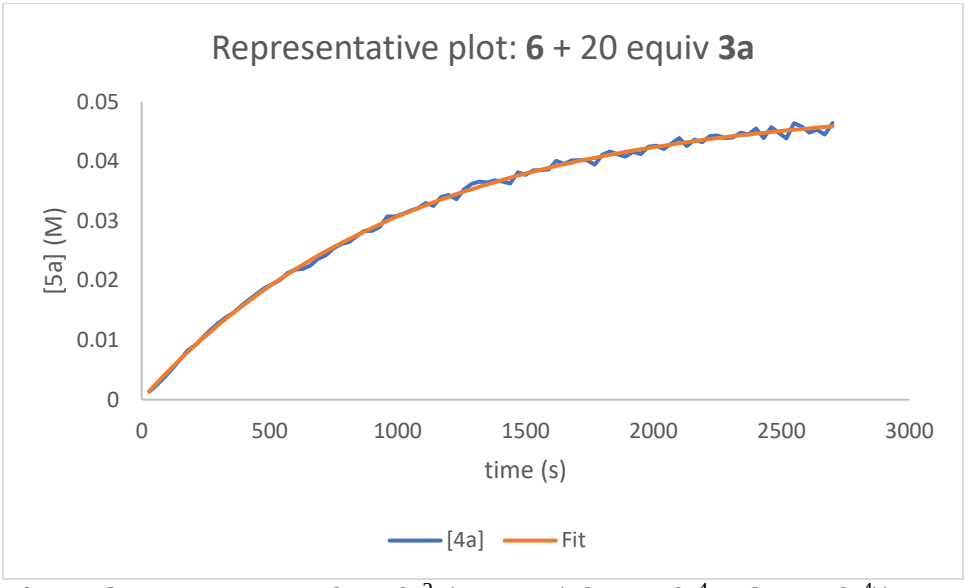
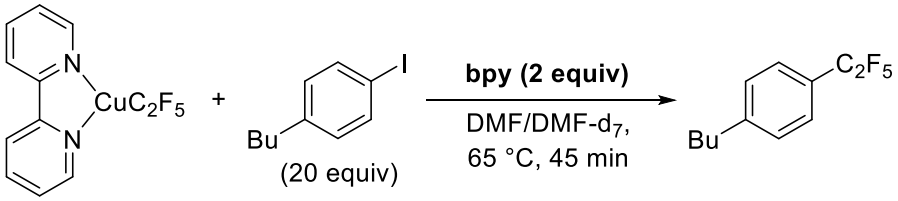


Figure 2.7.17 Fit: y = 4.95×10^{-2} (1 – exp(–9.71×10^{-4} – 6.75×10^{-4})); Representative plot of the formation of **5a** over time in the reaction of **6** + 20 equiv **3a** at 65 °C



2a **3a** **5a**

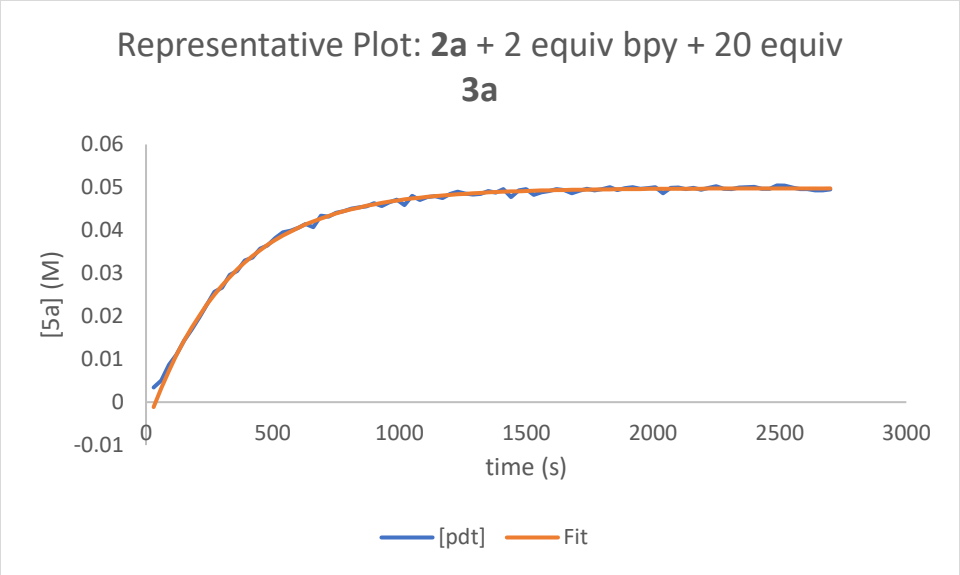


Figure 2.7.18 Fit: y = 4.98×10^{-2} (1 – exp(-3.00×10^{-3} *t* + 1.27×10^{-1})); Representative plot of the formation of **5a** over time in the reaction of **2a** + 2 equiv bpy + 20 equiv **3a** at 65 °C

*Determining the Reaction Order of **3a** in the Reaction with **2a***

In a N_2-atmosphere drybox, the appropriate **2a** (10.2 mg, 0.0300 mmol) was added to a 4 mL vial, followed by a stock solution of 1-butyl-4-iodobenzene (**3a**, 2.00 M) and 4-(trifluoromethoxy)anisole (0.218 M) in 5:1 DMF:DMF-d_7 (v/v) (150, 300, 450, or 600 µL; 0.300, 0.600, 0.900, or 1.20 mmol; 10.0, 20.0, 30.0, or 40.0 equiv) and extra DMF (450, 300, 150, or 0 µL). The mixtures were quickly mixed by pipette, and the resulting red solutions were transferred to J. Young tubes, which were sealed, removed from the drybox, and cooled to –78 °C in a dry ice/acetone cold bath until data collection could begin. Reaction monitoring was conducted as described above at 65 °C with scans collected at 30 s intervals.

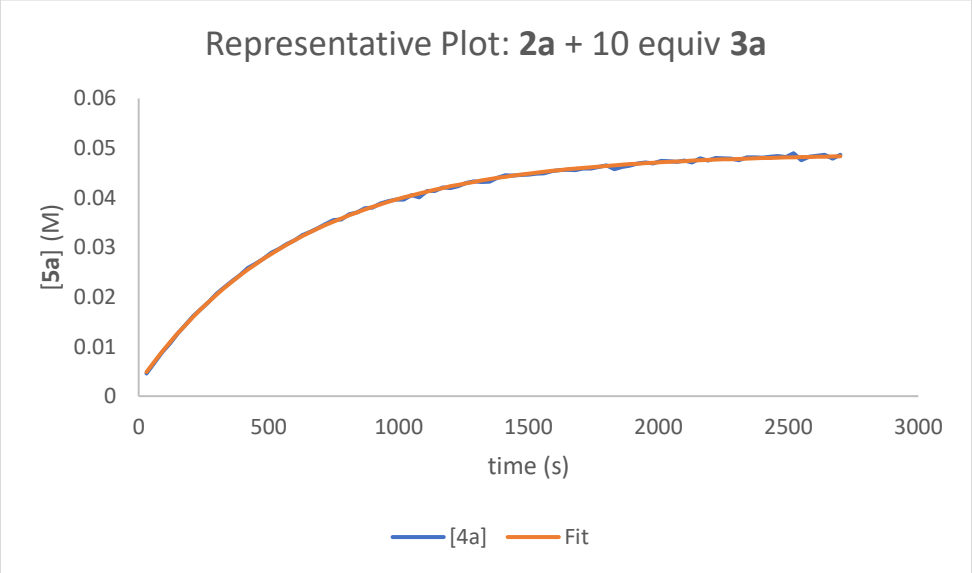


Figure 2.7.19 Fit: *y* = 4.89×10^{-2} (1 – exp(-1.62×10^{-3} *t* – 5.60×10^{-2})); Representative plot of the formation of **5a** over time in the reaction of **2a** + 10 equiv **3a** at 65 °C

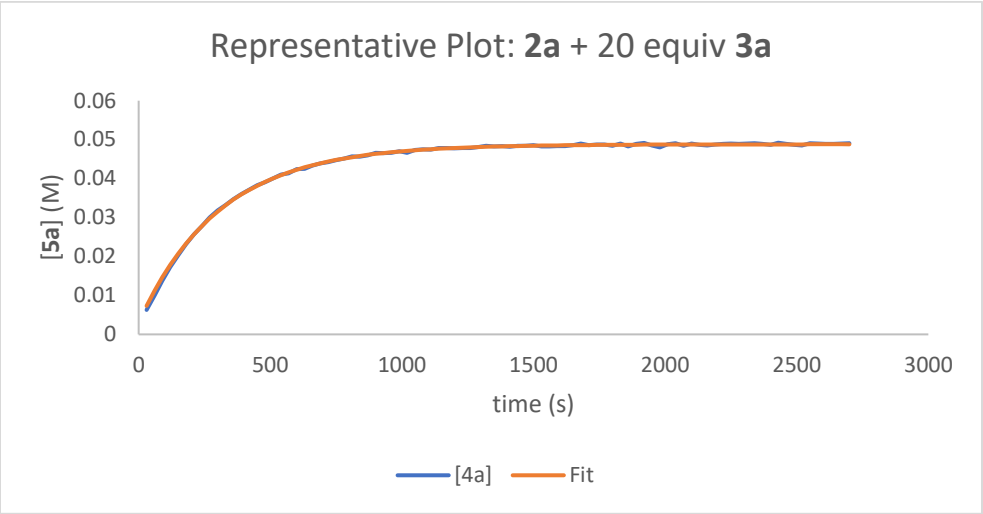


Figure 2.7.20 Fit: $y = 4.88\times10^{-2}\ (1 - \exp(-3.25\times10^{-3}\ t - 6.52\times10^{-2}))$; Representative plot of the formation of **5a** over time in the reaction of **2a** + 20 equiv **3a** at 65 °C

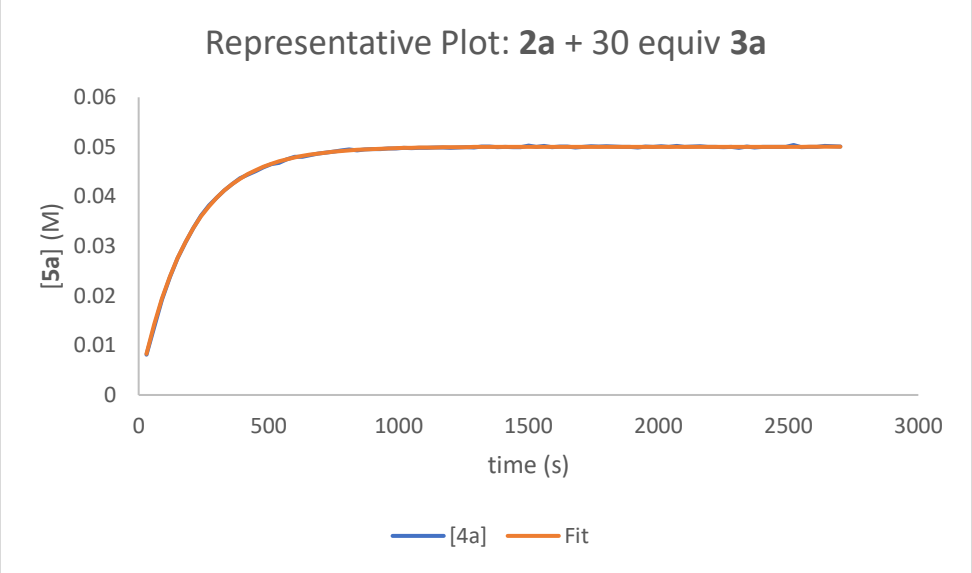


Figure 2.7.21 Fit: $y = 5.00\times10^{-2}\ (1 - \exp(-5.19\times10^{-3}\ t - 2.54\times10^{-2}))$; Representative plot of the formation of **5a** over time in the reaction of **2a** + 30 equiv **3a** at 65 °C

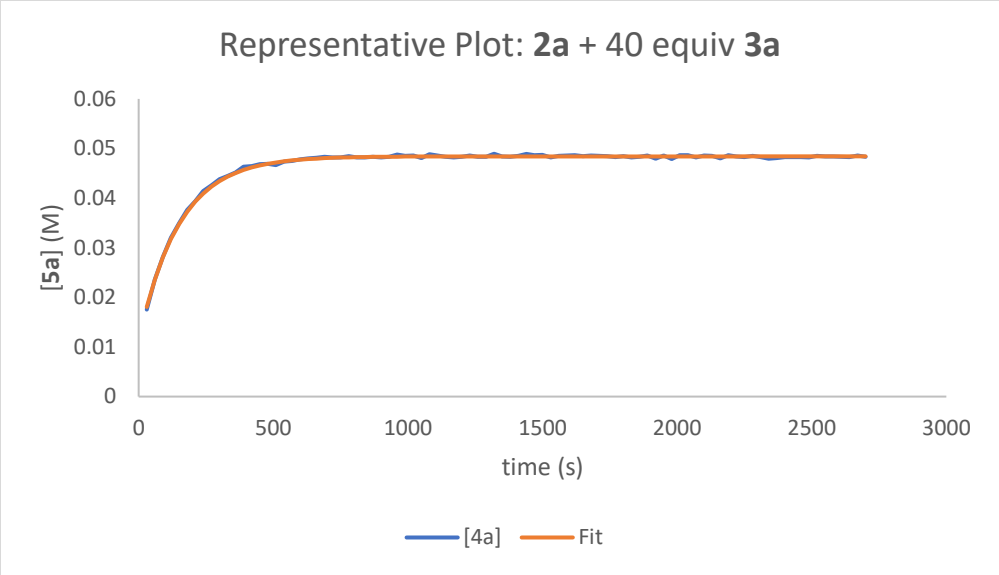
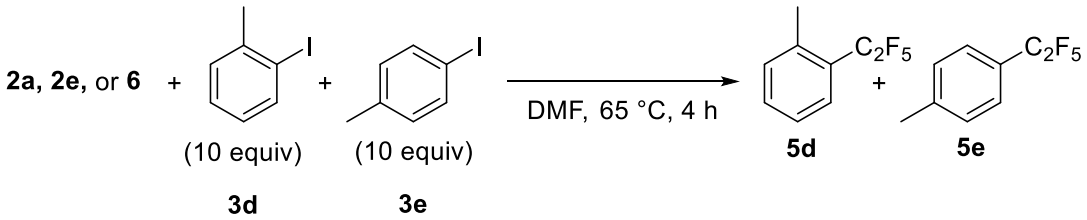


Figure S2.7.22 Fit: $y = 4.82\times10^{-2}\ (1 - \exp(-6.67\times10^{-3}\ t - 2.67\times10^{-1}))$; Representative plot of the formation of **5a** over time in the reaction of **2a** + 40 equiv **3a** at 65 °C

*Competition Experiments between Methyl-Substituted Aryl Iodides **7** (Scheme 2.3.1)*



Starting from 2a or 2e

To a 4 mL vial containing **2a** or **2e** (0.0150 mmol) and ligand **1a** or **1e**, respectively (0, 0.0300, or 0.225 mmol; 0, 2.00, or 15.00 equiv) was added 300 μL of a DMF solution of 2-iodotoluene (**3d**), 4-iodotoluene (**3e**) (0.500 M each, 10.0 equiv each) and 4-(trifluoromethoxy)anisole (0.200 M, 4.00 equiv) as an internal standard. The vial was sealed, removed from the drybox, and heated for 2 h at 65 °C. The reaction mixture was then transferred to an NMR tube and the yields and ratios of products 2-pentafluoroethyltoluene (**5d**) and 4-pentafluoroethyltoluene (**5e**) were determined by quantitative ^{19}F NMR spectroscopy.
5d: ^{19}F NMR (376 MHz, DMF): δ –84.8 (s, 3F) and –110.6 ppm (s, 2F).
5e: ^{19}F NMR (376 MHz, DMF): δ –85.4 (s, 3F) and –114.8 ppm (s, 2F).

Starting from 6

In a N_2-atmosphere drybox, an aliquot of reagent solution **6** (43.4 μL, 0.0150 mmol) was added to a 4 mL vial, followed by DMF (107 μL) and 150 μL of a DMF solution of 2-iodotoluene and 4-iodotoluene (1.00 M each, 10.0 equiv each) and 4-(trifluoromethoxy)anisole (0.200 M, 2.00 equiv) as an internal standard. The vial was sealed, removed from the drybox, and heated for 2 h at 65 °C. The reaction mixture was then transferred to an NMR tube, and the yields and ratios of products **5d–e** were determined by quantitative ^{19}F NMR spectroscopy.

Representative ^{19}F NMR Spectra for Competition Experiments

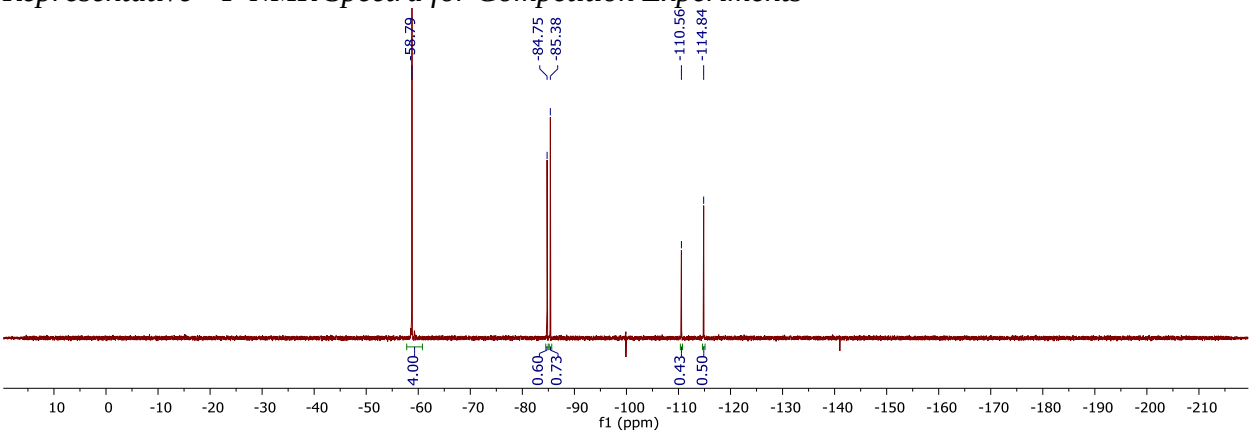


Figure 2.7.23 Full ^{19}F NMR spectrum of 4-(trifluoromethoxy)anisole (internal standard) and **5d–e** in the reaction of **2a** and **3d–e** in DMF after 2 h at 65 °C; integrals are not quantitative (pulse calibration was not performed)

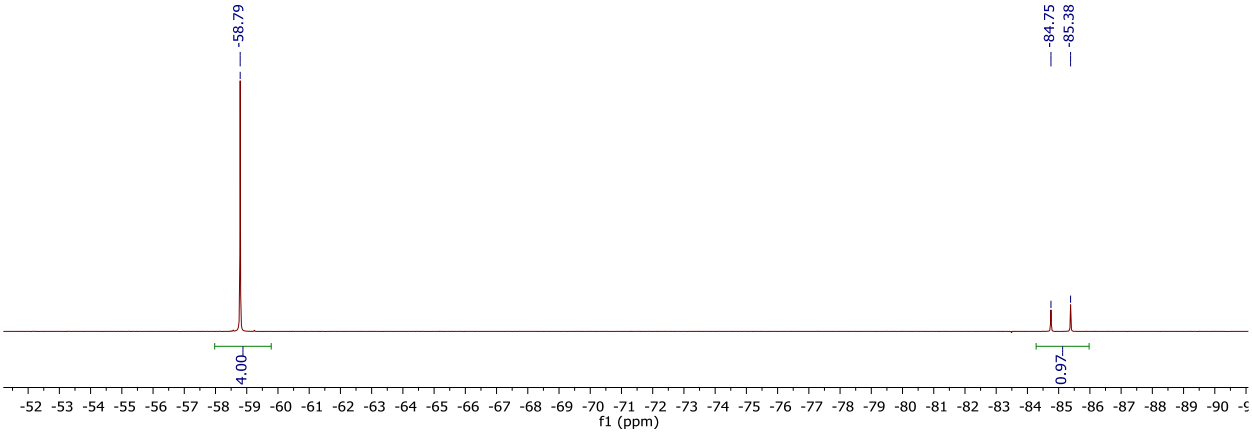


Figure 2.7.24 Quantitative ^{19}F NMR spectrum of the same sample showing 4-(trifluoromethoxy)anisole and the CF_3 peaks of **5d–e** to determine the yield of the reaction of **2a** with **3d–e**

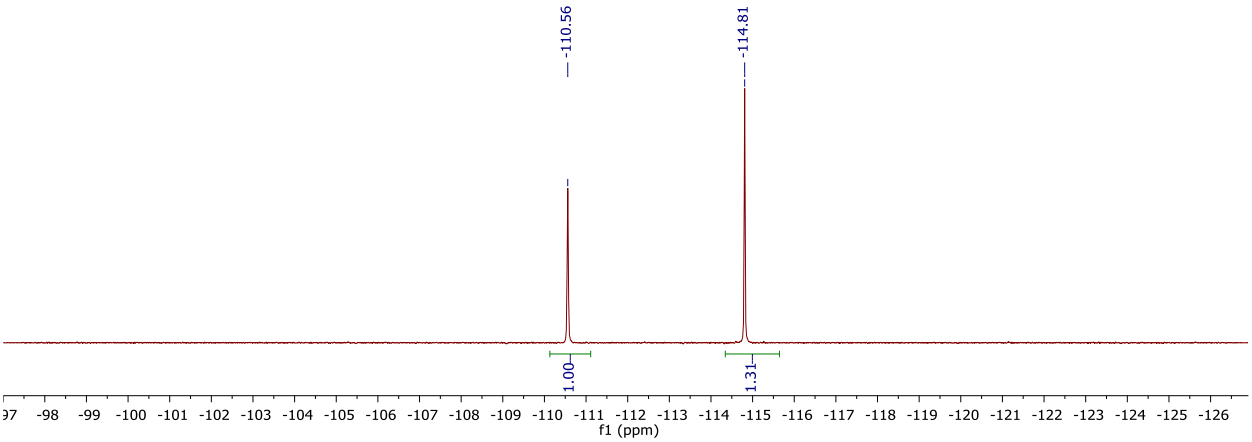
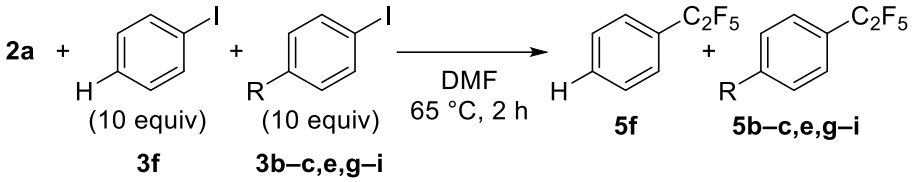


Figure 2.7.25 Quantitative ^{19}F NMR spectrum of the same sample showing only the CF_2 peaks of **5d–e** to determine the ratio of **5d** to **5e** from the reaction of **2a** with **3d–e**

Determining the Relative Rates of Reaction of para*-Substituted Aryl Iodides* ***5a–i*** *(Figure 2.4.1)*



R = CN (**3b**), OCH_3 (**3c**), CH_3 (**3e**), Cl (**3g**), CF_3 (**3h**), $COCH_3$ (**3i**)

To a 4 mL vial containing **2a** (0.0300 mmol) was added 300 μL of a DMF solution of iodobenzene (**3f**) and the *para*-substituted iodobenzene (0.500 M each, 10.0 equiv each), and 4-(trifluoromethoxy)anisole (~0.150 M, ~3.00 equiv; the exact was amount varied slightly between experiments but was measured to three significant figures) as an internal standard. The vial was sealed, removed from the drybox, and heated for 2 h at 65 °C. The reaction mixture was then transferred to an NMR tube, and the yields and ratios of the pentafluoroethylarene products were determined by quantitative ^{19}F NMR spectroscopy.

Because both aryl iodides are present in the reaction mixture at the same concentrations, the final ratios of the pentafluoroethylarene products mirror the relative rates of reaction of the two aryl iodides with **2a**. Thus, k_R / k_H is the final ratio [$RPhC_2F_5$] / [PhC_2F_5]. We note that Grushin and co-workers also found a more linear correlation with σ_p^- than with σ_p for a related "ligandless" $CuCF_3$ system, and that no difference was observed in relative rates determined by same-flask competition experiments (as presented here) *vs* relative rates determined by directly measuring the rate constants for each aryl iodide.[26]

Table 2.7.2 Chemical shifts of pentafluoroethylarene products, Hammett σ_p and σ_p^- values of the substituent at the *para* position of the starting aryl iodide, and the rates of reaction of each aryl iodide relative to that of iodobenzene

R	**δ(CF_2) (ppm)**	**δ(CF_3) (ppm)**	**σ_p**[44]	**σ_p^-**[44]	**k_R / k_H**
H (**5f**)	–114.9	–85.4	0	0	1
CN (**5b**)	–115.7	–85.2	0.49	1.00	10.0
$COCH_3$ (**5i**)	–115.2	–85.2	0.50	0.84	4.95
CF_3 (**5h**)	–115.4	–85.2	0.54	0.65	3.52
Cl (**5g**)	–114.8	–85.4	0.23	0.19	1.68
CH_3 (**5e**)	–114.8	–85.4	–0.17	–0.17	0.820
OCH_3 (**5c**)	–113.7	–85.4	–0.27	–0.26	0.758

Representative ^{19}F NMR Spectra for the Competition Reactions between para*-Substituted Aryl Iodides and Iodobenzene (**3f**)*

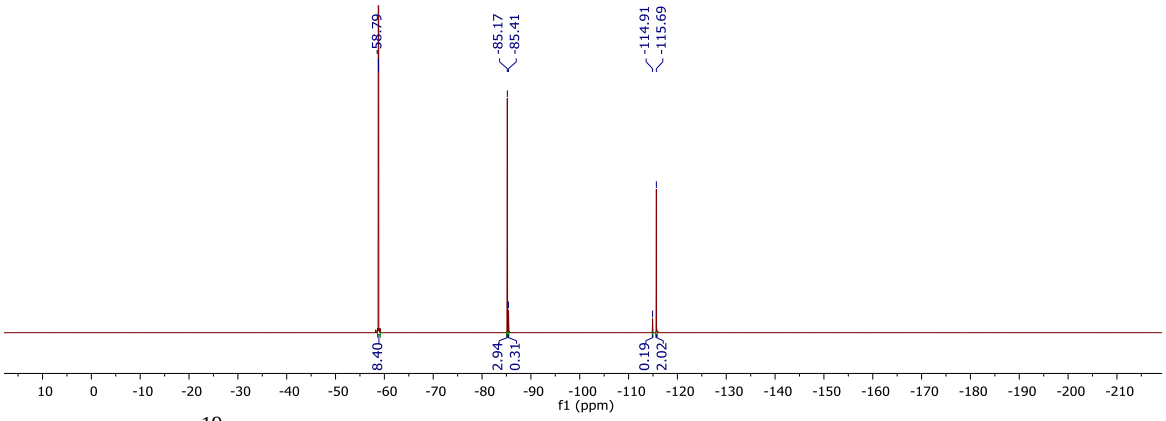


Figure 2.7.26 Full ^{19}F NMR spectrum of 4-(trifluoromethoxy)anisole, **5f**, and **5b** from the reaction of **2a**, **3f**, and **3b** in DMF after 2 h at 65 °C; integrals are not quantitative

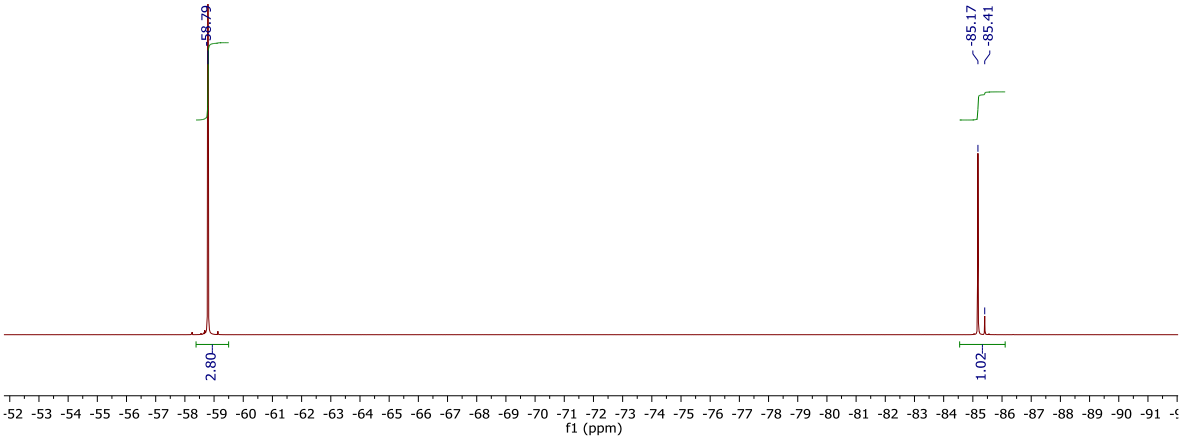


Figure 2.7.27 Quantitative ^{19}F NMR spectrum of 4-(trifluoromethoxy)anisole and the CF_3 peaks of **5f** and **5b** to determine the yield of the reaction of **2a** with **3f** and **3b**

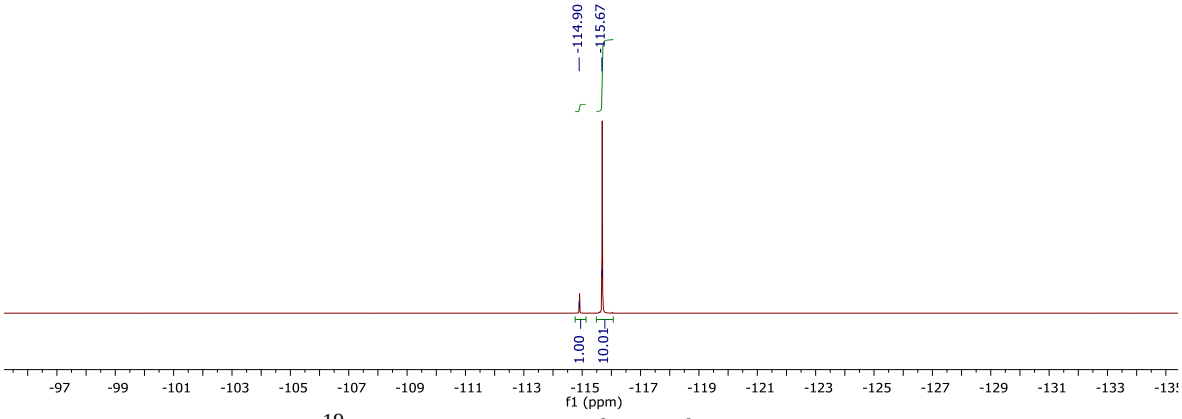


Figure 2.7.28 Quantitative ^{19}F NMR spectrum of 4-(trifluoromethoxy)anisole and the CF_2 peaks of **5f** and **5b** to determine the ratio of **5f** to **5b** from the reaction of **2a** with **3f** and **3b**

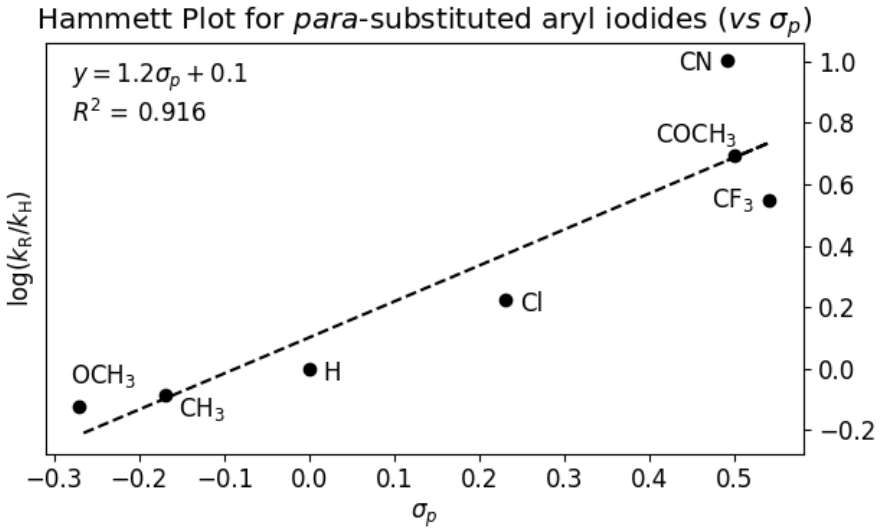


Figure 2.7.29 Hammett plot of the relative rates of reaction if *para*-substituted iodobenzenes with **2a** *vs* σ_p

Note that the fit is better for more electron-withdrawing substituents when the relative rates are plotted against the σ_p^-[44] substituent parameters than when plotted against the standard σ_p[44] substituent parameters. Grushin and co-workers previously have reported that the relative rates of reactions of substituted aryl iodides with their "ligandless" $CuCF_3$ system also fit better with σ_p^- than with σ_p.[26] They also provided extensive evidence that the poor fit with σ_p was not due to distinct mechanisms of oxidative addition for electron-rich and electron-poor aryl iodides; rather, a single, concerted, 3-center oxidative addition of the aryl halide to the Cu center was proposed for all aryl iodides. σ_p is based on the ionization of substituted benzoic acid derivatives, and σ_p^- is based on the ionization of substituted phenol derivatives. Thus, σ_p^- better takes into account the substituent's ability to stabilize negative charge through resonance.[44]

2.7.4 Derivation of the Expression for Rate Constant k_{corr} from k_{obs} (k_{obs} from first-order exponential fit)

The reaction of ligated perfluoroalkylcopper species $LCuR^F$ with aryl halide ArX to form pentafluoroalkylarene product P is expected to be first order in both $LCuR^F$ and ArX. The corresponding rate law is given as follows:

(1) $\frac{d[\mathrm{P}]}{dt} = k_{corr}[\mathrm{LCuR^F}][\mathrm{ArX}] \approx k_{corr}[\mathrm{LCuR^F}][\mathrm{ArX}]_0$

When aryl halide ArX is in excess, [ArX] does not change significantly over the course of the reaction ([ArX] = $[ArX]_0$), so the rate law becomes approximately first order. Thus, the observed formation of product was fit to a first-order exponential:

(2) $[\mathrm{P}] = [\mathrm{P}]_{\mathrm{final}}(1 - e^{-k_{obs}t+c})$

in which [P] is the concentration of perfluoroalkylarene product at time *t* and $[P]_{final}$ is the concentration of product upon completion of the reaction (i.e., final yield expressed as

concentration). The experimental rate of product formation is thus given by

(3) $rate = k_{obs}([\mathrm{P}]_{\mathrm{final}} - [\mathrm{P}]) = k_{obs}[\mathrm{P}]_{\mathrm{final}}(1 - \xi)$

in which ξ is the extent of the reaction. Assuming no side-reactions of the CuR^F reagent **2** ($[\mathbf{2}]_0 = [\mathrm{P}]_{\mathrm{final}}$), (3) can be equivalently expressed in terms of [**2**], the instantaneous total concentration of CuR^F reagent remaining in all forms (neutral + ionic):

(4) $rate = k_{obs}[\mathrm{P}]_{\mathrm{final}}(1 - \xi) = k_{obs}[\mathbf{2}]_0(1 - \xi) = k_{obs}[\mathbf{2}]$

Equating the experimental rate (4) with the proposed rate law (1) gives

(5) $k_{obs}[\mathbf{2}] = rate = \frac{d[\mathrm{P}]}{dt} = k_{corr}[\mathrm{LCuR^F}][\mathrm{ArX}]_0$

In order to proceed, we relate [**2**] to [$LCuR^F$] (the active species) by invoking the fast equilibrium of the CuR^F reagent between neutral and ionic forms (the latter as solvent-separated ions; *vide supra*):

(6) $2\ \mathrm{LCuR^F} \overset{K}{\rightleftharpoons} [\mathrm{L_2Cu}]^+ + [\mathrm{Cu(R^F)_2}]^-$

So

(7) $K = \frac{[\mathrm{L_2Cu}]^+[\mathrm{Cu(R^F)_2}]^-}{[\mathrm{LCuR^F}]^2}$

Because $[L_2Cu]^+ = [Cu(R^F)_2]^-$, we define a new constant *K*' for ease of notation:

(8) $K' = \sqrt{K} = \sqrt{\frac{[\mathrm{L_2Cu}]^+[\mathrm{Cu(R^F)_2}]^-}{[\mathrm{LCuR^F}]^2}} = \sqrt{\frac{([\mathrm{Cu(R^F)_2}]^-)^2}{[\mathrm{LCuR^F}]^2}} = \frac{[\mathrm{Cu(R^F)_2}]}{[\mathrm{LCuR^F}]}$

Note that according to the equilibrium (7) between neutral and ionic forms,

(9) $[\mathbf{2}] = [\mathrm{LCuR^F}] + 2[\mathrm{Cu(R^F)_2}]^-$

Solving for (8) for $[Cu(R^F)_2]^-$ and substituting into (9) gives

(10) $[\mathbf{2}] = [\mathrm{LCuR^F}] + 2K'[\mathrm{LCuR^F}] = (1 + 2K')[\mathrm{LCuR^F}]$

Substitution for [**2**] in (5) using (10) gives

(11) $k_{obs}(1 + 2K')[\mathrm{LCuR^F}] = k_{corr}[\mathrm{LCuR^F}][\mathrm{ArX}]_0$

Rearrangement affords the rate constant with respect to k_{obs}:

(12) $$k_{corr} = \frac{(1+2K')k_{obs}}{[\mathrm{ArI}]_0}$$

Derivation of the Expression of Rate Constant k_{corr} from k_{init} (for initial-rate measurements)

A similar analysis is applicable is applicable for initial rate conditions. We assume:

(1) $$rate = k_{init} \approx \frac{d[\mathrm{P}]}{d\mathrm{t}} \approx k_{corr}[\mathrm{LCuR_F}]_0[\mathrm{ArX}]_0$$

which, using (10), can be rewritten as

(2) $$k_{init} \approx \frac{kcorr[\mathbf{2}]_0[\mathrm{ArX}]_0}{1+2K'}$$

which affords the adjusted rate constant as

(3) $$k_{corr} \approx \frac{(1+2K')k_{init}}{[\mathbf{2}]_0[\mathrm{ArX}]_0}$$

2.7.5 Computational Details

DFT calculations were conducted at the Molecular Graphics and Computation Facility at the University of California, Berkeley using the Gaussian 16 software package.[60] All calculations, including geometry optimizations, were performed in DMF using the SMD solvent formalism reported by Truhlar and co-workers[61] with VeryTight convergence criteria for iterative calculations of polarization charges (threshold=10^{-12}; QConv=VeryTight and SC=QConv=VeryTight) and an average density of integration points of 10 $Å^{-2}$ (PDens=10). Initial geometries were constructed in GaussView[62] and optimized to stationary points (either minima or first-order saddle points) with the PBE0 functional (the hybrid functional based on the Perdew-Burke-Ernzerhof functional [PBE][63,64] as described by Adamo[65]) with Grimme's D3 dispersion correction with Becke-Johnson damping (GD3-BJ)[66] using basis sets def2-TZVPD for Cu,[67,68] def2-SVPD on all light atoms,[67,68] and def2-SVPD with the def2-ECP effective core potential on I (**BS1**).[67–69] The nature of each stationary point was verified by accompanying frequency calculations (all positive eigenvalues for minima and exactly one negative eigenvalue for transition states). Frequency calculations were performed at 1 atm at 338.15 K. Further single point energy calculations were performed on the optimized geometries with the larger def2-TZVPD basis set on all atoms using the def2-ECP effective core potential on I (**BS2**). [67–69] All basis sets and ECPs were obtained from the Basis Set Exchange website (accessed June 2019).[70–72] In all cases, Gibbs free energies and enthalpies for calculations using **BS2** were approximated by summing the internal energy calculated with **BS2** and the thermal correction from the frequency calculation on the same structure with **BS1**. Entropies were taken directly from calculations with **BS1**. Natural Population Analyses[50] were performed on the optimized structures with **BS2** to determine the natural atomic charges of each atom (NBO program version 3.0 as provided by Gaussian 16).

Table 2.7.3 Calculated barriers for oxidative addition of iodobenzene to [(R_2bpy)CuC_2F_5] (1 atm, 335 K)

R	$\Delta E^{\ddagger}$ (kcal/mol)	$\Delta G^{\ddagger}$ (kcal/mol)	$\Delta H^{\ddagger}$ (kcal/mol)	$\Delta S^{\ddagger}$ (cal/mol·K)
NMe_2	9.9	24.5	9.5	–41
OMe	9.5	23.9	9.4	–40
H	8.7	23.9	8.8	–42
Cl	8.3	25.0	8.3	–46
CN	8.3	26.1	7.5	–52

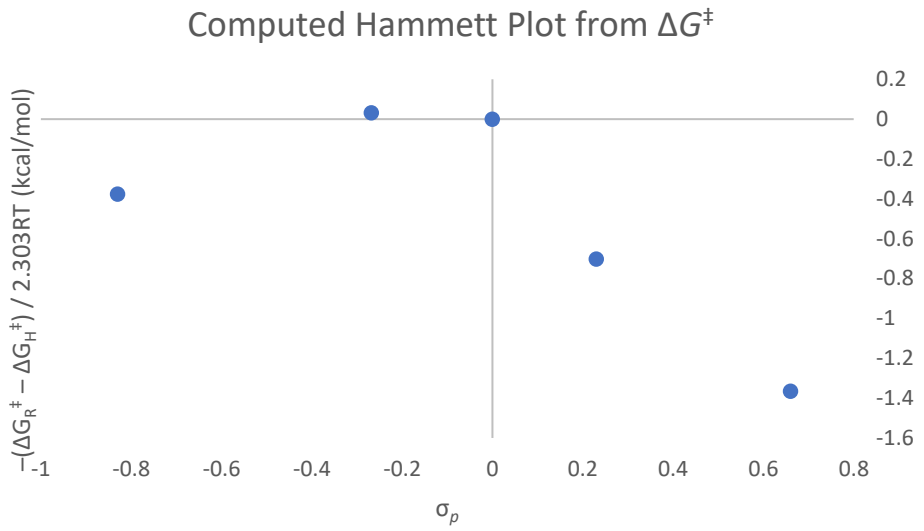


Figure 2.7.30 Hammett plot based directly on differences in $\Delta G^{\ddagger}$ for various R groups for the oxidative addition of iodobenzene to [(R_2bpy)CuC_2F_5]; T = 338.15

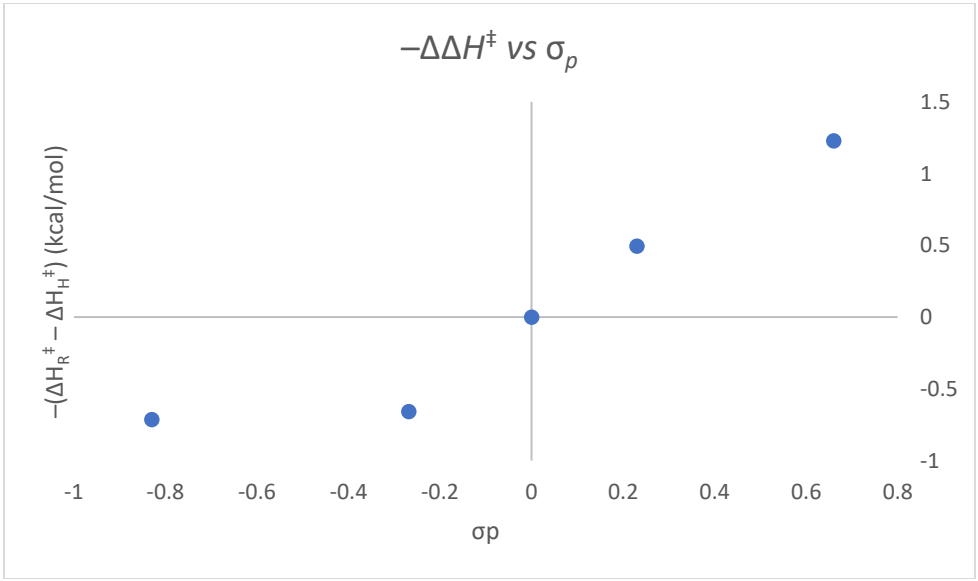
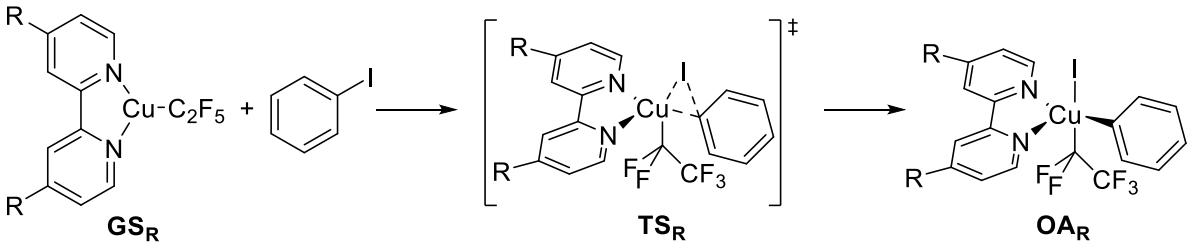


Figure 2.7.31 Relationship between the computed activation enthalpies for the oxidation of iodobenzene to [(R_2bpy)CuC_2F_5]. Note that the sign of $\Delta\Delta H^{\ddagger}$ has been inverted for a better visual

match to a Hammett plot. The trend in $\Delta H^{\ddagger}$ matches the experimentally observed trend, *i.e.*, that more electron-poor ligands result in lower activation enthalpies, corresponding to faster rates.

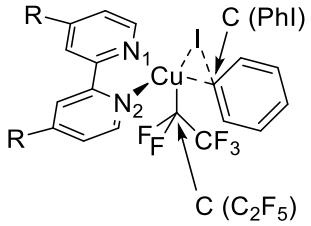
Table 2.7.4 Computed energies for optimized structures (1 atm, 338.15 K)



GS$_R$ **TS$_R$** **OA$_R$**

Structure	E (Hartree)	Gibbs Free Energy (Hartree)	Enthalpy (Hartree)	Entropy (cal/mol·K)
PhI	-529.186376602	-529.131907602	-529.087425602	79.435
GS_H	-2710.49310253	-2710.36613753	-2710.28335653	153.618
TS_H	-3239.66561055	-3239.45988955	-3239.35682555	191.257
OA_H	-3239.68441879	-3239.47491879	-3239.37288979	189.337
GS_{OMe}	-2939.40354232	-2939.21854932	-2939.12192632	179.304
TS_{OMe}	-3468.57475017	-3468.31237817	-3468.19434417	219.037
OA_{OMe}	-3468.59481729	-3468.32651229	-3468.21152129	213.390
GS_{NMe2}	-2978.25219112	-2977.99070612	-2977.88417612	197.561
TS_{NMe2}	-3507.42285081	-3507.08352981	-3506.95650781	235.716
OA_{NMe2}	-3507.44390746	-3507.09886346	-3506.97433246	231.094
GS_{Cl}	-3629.43080461	-3629.33019361	-3629.23757261	171.876
TS_{Cl}	-4158.60398363	-4158.42221463	-4158.31183063	204.84
OA_{Cl}	-4158.62202376	-4158.43613876	-4158.32673776	203.015
GS_{CN}	-2894.83403491	-2894.71924491	-2894.62283691	178.905
TS_{CN}	-3424.00712304	-3423.80963004	-3423.69826104	206.67
OA_{CN}	-3424.02488714	-3423.82328214	-3423.71169814	207.067

Table 2.7.5 Calculated natural atomic charges for selected atoms of computed structures



Structure	Cu	N_1	N_2	C (C_2F_5)	C (PhI)
GS_H + PhI	0.475	–0.471	–0.472	0.228	–0.157*
TS_H	0.458	–0.455	–0.438	0.281	–0.166
OA_H	0.557	–0.451	–0.439	0.485	–0.118
GS_{OMe} + PhI	0.462	–0.498	–0.502	0.231	–0.157*
TS_{OMe}	0.436	–0.478	–0.463	0.291	–0.154
OA_{OMe}	0.556	–0.477	–0.469	0.490	–0.118
GS_{NMe2} + PhI	0.443	–0.524	–0.526	0.233	–0.157*
TS_{NMe2}	0.427	–0.503	–0.490	0.290	–0.158
OA_{NMe2}	0.546	–0.494	–0.499	0.492	–0.120
GS_{Cl} + PhI	0.485	–0.466	–0.468	0.227	–0.157*
TS_{Cl}	0.464	–0.452	–0.432	0.281	–0.165
OA_{Cl}	0.560	–0.449	–0.435	0.483	–0.116
GS_{CN} + PhI	0.502	–0.445	–0.441	0.226	–0.157*
TS_{CN}	0.464	–0.428	–0.414	0.290	–0.161
OA_{CN}	0.568	–0.429	–0.409	0.478	–0.115

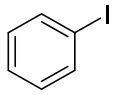
Table 2.7.6 Aggregate natural atomic charges for selected fragments of computed structures

Structure	Cu	R_2bpy	C_2F_5	C_6H_5	I
GS_H + PhI	0.475	0.182	–0.656	–0.138*	0.138*
TS_H	0.458	0.208	–0.565	–0.212	0.111
OA_H	0.557	0.295	–0.215	–0.192	–0.444
GS_{OMe} + PhI	0.462	0.196	–0.658	–0.138*	0.138*
TS_{OMe}	0.436	0.235	–0.557	–0.201	0.087
OA_{OMe}	0.556	0.306	–0.210	–0.191	–0.461
GS_{NMe2} + PhI	0.443	0.216	–0.660	–0.138*	0.138*
OA_{NMe2}	0.546	0.328	–0.216	–0.205	–0.452
TS_{NMe2}	0.427	0.250	–0.566	–0.208	0.958
GS_{Cl} + PhI	0.485	0.172	–0.657	–0.138*	0.138*
OA_{Cl}	0.560	0.278	–0.214	–0.183	–0.441
TS_{Cl}	0.464	0.197	–0.560	–0.209	0.108
GS_{CN} + PhI	0.502	0.154	–0.656	–0.138*	0.138*
TS_{CN}	0.464	0.181	–0.5440	–0.201	0.099
OA_{CN}	0.568	0.260	–0.219	–0.180	–0.430

*Values calculated for free iodobenzene

Geometries for Computed Structures (XYZ format)

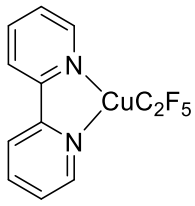
PhI



12

```
C     0.000000   -0.000000   -0.557860
C    -0.000000    1.214994   -1.243344
C    -0.000000    1.206332   -2.638730
C     0.000000   -0.000000   -3.338497
C    -0.000000   -1.206332   -2.638730
C    -0.000000   -1.214994   -1.243344
H    -0.000000    2.160665   -0.699677
H    -0.000000    2.155821   -3.178165
H     0.000000   -0.000000   -4.430032
H    -0.000000   -2.155821   -3.178165
H    -0.000000   -2.160665   -0.699677
I     0.000000    0.000000    1.549976
```

GS$_H$

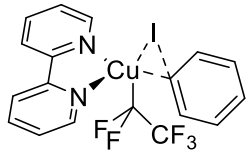


28

```
C    -1.204029    3.652170   -0.009385
C    -2.577312    3.429827    0.000172
C    -3.054420    2.123376    0.004671
C    -2.138865    1.068967   -0.000703
C    -0.358547    2.546951   -0.013857
C    -2.545184   -0.360529    0.002969
C    -3.878718   -0.773725    0.014152
C    -4.163869   -2.134907    0.017847
H    -5.200292   -2.475650    0.027156
C    -3.114945   -3.048539    0.009698
C    -1.813594   -2.556477   -0.001729
H    -0.787407    4.659394   -0.013283
H    -3.277158    4.266846    0.004097
H     0.725772    2.668694   -0.021131
H    -3.292570   -4.123996    0.012186
H    -0.957654   -3.232909   -0.008479
N    -1.541282   -1.252327   -0.004825
```

N	-0.816569	1.296800	-0.009652
Cu	0.368515	-0.435607	-0.012924
C	2.263998	-0.900630	-0.017961
C	3.220819	0.288626	0.023094
F	2.694036	-1.623778	-1.140043
F	2.685879	-1.693068	1.059728
F	3.031869	1.086579	-1.037244
F	3.019642	1.021449	1.127364
F	4.525324	-0.051083	0.020131
H	-4.688983	-0.046944	0.020363
H	-4.126452	1.934309	0.012008

TS_H

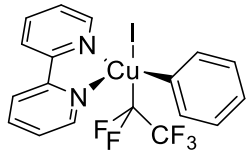


40

C	3.082858	1.010057	-2.823736
C	4.236106	0.708311	-2.104830
C	4.119484	0.209476	-0.813397
C	2.845724	0.025197	-0.266077
C	1.854244	0.801066	-2.208777
C	2.625564	-0.506730	1.103353
C	3.677768	-0.745355	1.993299
C	3.390984	-1.225912	3.265307
C	2.064959	-1.454978	3.618450
C	1.078646	-1.191760	2.672730
H	3.127218	1.399045	-3.841001
H	0.920798	1.019865	-2.729390
H	1.791333	-1.827553	4.605587
H	0.026227	-1.351267	2.909913
N	1.352590	-0.739098	1.452638
N	1.745802	0.326257	-0.969551
Cu	-0.135735	-0.006054	-0.061592
C	-0.569169	1.795824	0.785578
C	-0.787503	2.987123	-0.140980
F	0.475476	2.218251	1.611729
F	-1.676233	1.804568	1.622656
F	0.296705	3.208955	-0.894534
F	-1.820849	2.777983	-0.965370
F	-1.044699	4.140935	0.510822
H	4.709287	-0.552371	1.704540
H	5.012908	-0.038030	-0.243363

C	-2.058221	-0.836376	-0.061694
C	-2.343062	-1.395412	1.191610
C	-3.023886	-0.078497	-0.739057
C	-3.560257	-1.104851	1.805934
H	-1.624413	-2.051830	1.680663
C	-4.233271	0.198808	-0.110033
H	-2.821873	0.305200	-1.738512
C	-4.507457	-0.305607	1.164607
H	-3.771004	-1.523817	2.792370
H	-4.973159	0.813359	-0.627662
H	-5.462366	-0.090277	1.647194
I	-0.708371	-2.135387	-1.436688
H	4.198795	-1.415064	3.973885
H	5.222795	0.855175	-2.546650

OA$_H$

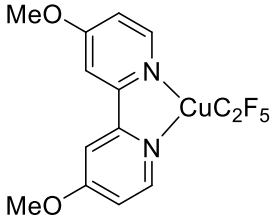


40

C	2.632749	1.226933	-2.994408
C	3.854516	1.155032	-2.332078
C	3.884830	0.749715	-1.003815
C	2.688478	0.429042	-0.358025
C	1.485237	0.884940	-2.292221
C	2.623598	-0.012285	1.056146
C	3.755104	-0.110014	1.870539
C	3.600343	-0.537200	3.184501
H	4.470086	-0.620986	3.837755
C	2.328004	-0.852912	3.650109
C	1.255548	-0.723619	2.771849
H	2.561208	1.536934	-4.036472
H	4.782345	1.409401	-2.846097
H	0.503762	0.910355	-2.765008
H	2.161070	-1.192168	4.672224
H	0.240192	-0.956721	3.094313
N	1.404825	-0.317565	1.515825
N	1.522312	0.501835	-1.016000
Cu	-0.210539	-0.028800	-0.123018
C	-0.611243	1.773827	0.608484
C	-1.534979	2.702537	-0.209090
F	0.585302	2.424165	0.668087
F	-1.074986	1.766286	1.880019

F	-1.325686	2.544162	-1.516668
F	-2.817215	2.472827	0.047019
F	-1.299094	3.989441	0.080681
H	4.743885	0.143348	1.492901
H	4.833946	0.682416	-0.476413
C	-2.058133	-0.386086	0.237878
C	-2.456927	-0.785637	1.508054
C	-2.967125	-0.337781	-0.816615
C	-3.789406	-1.150372	1.724496
H	-1.748502	-0.827131	2.335047
C	-4.297281	-0.696153	-0.589837
H	-2.653409	-0.029021	-1.814675
C	-4.710939	-1.103971	0.679299
H	-4.102142	-1.471003	2.720647
H	-5.011343	-0.657658	-1.415642
H	-5.751429	-1.385029	0.853089
I	-0.002371	-2.454958	-1.061549

GS_{OMe}

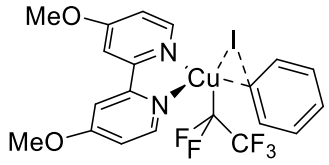


36

C	-0.158873	3.534673	-0.013457
C	-1.555245	3.441523	-0.002035
C	-2.142772	2.168829	-0.000137
C	-1.328128	1.046251	-0.009908
C	0.569692	2.352056	-0.022221
C	-1.865946	-0.341350	-0.008456
C	-3.224237	-0.620679	0.007114
C	-3.650696	-1.955901	0.010059
C	-2.683701	-2.967326	-0.005501
C	-1.348310	-2.587526	-0.021182
H	0.363959	4.488684	-0.015549
H	1.660387	2.387251	-0.030915
H	-2.942612	-4.023965	-0.005201
H	-0.568478	-3.350422	-0.033106
N	-0.940695	-1.319992	-0.022119
N	0.013920	1.143506	-0.020759
Cu	1.024968	-0.695933	-0.029483
C	2.869526	-1.330020	-0.029599
C	3.929413	-0.233463	0.047135

F	3.246147	-2.065211	-1.163577
F	3.208540	-2.180367	1.034212
F	3.826811	0.601092	-0.996810
F	3.782162	0.491157	1.165410
F	5.198087	-0.689781	0.050024
H	-3.974523	0.167569	0.018326
H	-3.228617	2.094187	0.009065
O	-2.383643	4.484220	0.007469
O	-4.965346	-2.165259	0.028251
C	-1.834787	5.792386	0.006032
H	-2.685531	6.480164	0.016466
H	-1.216443	5.959813	0.900466
H	-1.234196	5.965221	-0.899408
C	-5.445093	-3.500552	0.038848
H	-5.095155	-4.036467	0.933655
H	-6.536773	-3.432196	0.058236
H	-5.127517	-4.039477	-0.866127

TS$_{OMe}$

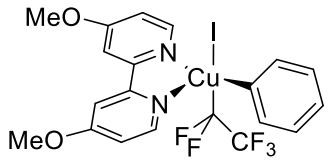


48

C	2.019706	-3.298078	0.437357
C	3.270269	-2.698164	0.243987
C	3.322379	-1.317742	0.012239
C	2.145523	-0.586338	-0.035120
C	0.896945	-2.488209	0.378486
C	2.119369	0.879972	-0.265717
C	3.275715	1.629220	-0.434009
C	3.168352	3.012524	-0.628367
C	1.892737	3.587919	-0.652105
C	0.799425	2.748145	-0.477103
H	1.904107	-4.361999	0.631052
H	-0.093266	-2.915613	0.533189
H	1.735567	4.654278	-0.797940
H	-0.208334	3.165681	-0.489743
N	0.900027	1.437933	-0.288540
N	0.951298	-1.178823	0.143545
Cu	-0.757857	-0.089775	0.080519
C	-1.045150	-0.319922	-1.867924
C	-1.899374	-1.521532	-2.326083
F	0.191194	-0.537783	-2.397705

F	-1.515492	0.775178	-2.508648
F	-1.678965	-2.580795	-1.545784
F	-3.196712	-1.241265	-2.304465
F	-1.593077	-1.877915	-3.580929
H	4.265658	1.177534	-0.414797
H	4.292362	-0.844998	-0.126142
C	-2.606530	0.411125	0.103129
C	-2.976758	1.720812	-0.179474
C	-3.549087	-0.526221	0.519962
C	-4.314134	2.101490	-0.031172
H	-2.242297	2.455788	-0.508771
C	-4.883708	-0.139884	0.656883
H	-3.257723	-1.553206	0.744616
C	-5.268526	1.173853	0.384396
H	-4.605100	3.132316	-0.245131
H	-5.624106	-0.873969	0.982982
H	-6.312448	1.473601	0.494941
I	-0.696952	0.233903	2.683542
O	4.430844	-3.346652	0.268581
O	4.306883	3.688171	-0.777479
C	4.427556	-4.748863	0.490198
H	5.474942	-5.063497	0.463886
H	3.996174	-4.989702	1.472948
H	3.867923	-5.269079	-0.301202
C	4.246553	5.092580	-0.967490
H	3.775533	5.585850	-0.104218
H	5.282158	5.432833	-1.061455
H	3.693987	5.341946	-1.885508

OA$_{OMe}$

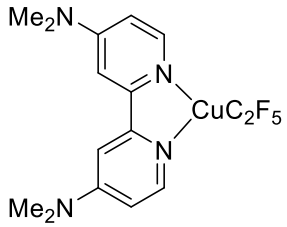


48

C	1.998633	-3.309790	0.414439
C	3.255036	-2.717443	0.236185
C	3.319176	-1.335208	0.018708
C	2.148206	-0.594491	-0.029832
C	0.882427	-2.490910	0.355569
C	2.134721	0.874207	-0.245863
C	3.297846	1.616337	-0.398224
C	3.202268	3.002287	-0.579441
C	1.931204	3.587516	-0.606647

C	0.830384	2.754324	-0.448031
H	1.873656	-4.374690	0.596587
H	-0.112062	-2.912341	0.498781
H	1.783094	4.656438	-0.742893
H	-0.174102	3.179570	-0.463783
N	0.919789	1.441568	-0.271921
N	0.948302	-1.179688	0.134201
Cu	-0.752145	-0.077177	0.069727
C	-1.026864	-0.285656	-1.882963
C	-1.886679	-1.476135	-2.359361
F	0.211664	-0.507549	-2.405925
F	-1.484287	0.819318	-2.516043
F	-1.679931	-2.544781	-1.588171
F	-3.182006	-1.186299	-2.344339
F	-1.573869	-1.822261	-3.615471
H	4.284211	1.157011	-0.376372
H	4.293658	-0.868450	-0.107874
C	-2.597132	0.437432	0.083960
C	-2.955464	1.752640	-0.188142
C	-3.549710	-0.496881	0.484502
C	-4.291005	2.141915	-0.045727
H	-2.213129	2.485299	-0.504699
C	-4.882369	-0.101855	0.615615
H	-3.267696	-1.528235	0.700931
C	-5.255334	1.217411	0.353562
H	-4.572669	3.176998	-0.251419
H	-5.630612	-0.833546	0.928939
H	-6.297765	1.523921	0.459539
I	-0.707899	0.219995	2.676246
O	4.410513	-3.374899	0.262678
O	4.346888	3.670765	-0.713492
C	4.395103	-4.779191	0.470160
H	5.440269	-5.101455	0.448285
H	3.954739	-5.026574	1.447285
H	3.837407	-5.287225	-0.330468
C	4.298467	5.077420	-0.889810
H	3.824838	5.565581	-0.025063
H	5.337250	5.410757	-0.972836
H	3.754527	5.340119	-1.809259

GS_{NMe2}

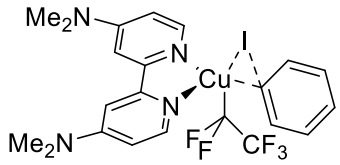


44

C	-0.098869	3.406129	-0.010376
C	-1.501591	3.207287	-0.004839
C	-1.941875	1.861182	-0.003540
C	-1.020839	0.825243	-0.008382
C	0.736472	2.306909	-0.014492
C	-1.431574	-0.608746	-0.007549
C	-2.761681	-0.998241	0.001953
C	-3.103905	-2.372689	0.004221
C	-2.020496	-3.285500	-0.005032
C	-0.729228	-2.797933	-0.014908
H	0.338579	4.401765	-0.011594
H	1.818543	2.450558	-0.018641
H	-2.178458	-4.361455	-0.004401
H	0.110655	-3.494827	-0.022194
N	-0.419181	-1.496928	-0.015996
N	0.307743	1.040797	-0.013913
Cu	1.474217	-0.678256	-0.021662
C	3.364247	-1.151482	-0.025349
C	4.328798	0.030532	0.040935
F	3.800143	-1.858503	-1.157568
F	3.780225	-1.964826	1.041510
F	4.152539	0.847553	-1.007199
F	4.126544	0.746962	1.155963
F	5.631978	-0.316895	0.040330
H	-3.543859	-0.245538	0.007623
H	-3.004724	1.640183	0.001215
C	-1.886272	5.598046	-0.002033
H	-2.737152	6.284391	0.003054
H	-1.270465	5.805827	0.887389
H	-1.279479	5.807810	-0.897188
C	-4.694178	-4.197292	0.016344
H	-4.278505	-4.697560	0.905338
H	-5.778985	-4.331836	0.023870
H	-4.291073	-4.696488	-0.878953
N	-2.374517	4.237523	-0.000982
N	-4.389955	-2.783960	0.014807
C	-3.797637	3.983838	0.003763

H	-4.331141	4.937996	0.004584
H	-4.109140	3.415344	-0.886843
H	-4.103609	3.416842	0.897257
C	-5.463471	-1.815671	0.026552
H	-6.421697	-2.341934	0.035468
H	-5.416412	-1.171988	0.919201
H	-5.434266	-1.169955	-0.865348

TS_{NMe2}

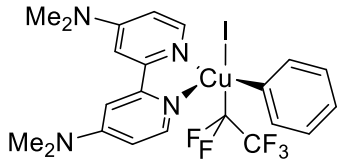


56

C	-1.670995	-3.344543	-0.277620
C	-2.958725	-2.763394	-0.159621
C	-2.998720	-1.354913	-0.022133
C	-1.827541	-0.615168	0.006306
C	-0.561041	-2.529853	-0.240966
C	-1.821047	0.867284	0.139823
C	-2.993020	1.602388	0.250585
C	-2.937503	3.011252	0.373991
C	-1.643398	3.587156	0.377572
C	-0.540565	2.763332	0.259092
H	-1.533285	-4.416097	-0.397785
H	0.434983	-2.961708	-0.337370
H	-1.494815	4.660545	0.467355
H	0.458376	3.202636	0.259846
N	-0.606785	1.436735	0.140704
N	-0.621589	-1.201462	-0.097678
Cu	1.061027	-0.108166	-0.083362
C	1.286401	-0.159223	1.888118
C	2.156568	-1.286824	2.482491
F	0.044089	-0.358951	2.410085
F	1.715305	1.004216	2.433959
F	1.976920	-2.425226	1.810501
F	3.448279	-0.980298	2.459500
F	1.831033	-1.522742	3.761590
H	-3.954379	1.098686	0.242927
H	-3.954308	-0.847549	0.059263
C	2.901204	0.426821	-0.111171
C	3.246000	1.763388	0.058350
C	3.874040	-0.527116	-0.404684
C	4.582669	2.151703	-0.074982

H	2.489675	2.514360	0.286315
C	5.207788	-0.133607	-0.528514
H	3.605920	-1.575675	-0.542569
C	5.565069	1.205955	-0.365963
H	4.851266	3.202907	0.051339
H	5.969747	-0.882377	-0.757199
H	6.608403	1.511675	-0.465632
I	1.080408	0.002394	-2.691696
C	-4.001941	-4.939046	-0.345426
H	-5.010745	-5.359903	-0.339097
H	-3.521545	-5.207542	-1.299429
H	-3.428847	-5.404085	0.471983
C	-3.958040	5.193919	0.616164
H	-3.476532	5.649957	-0.263807
H	-4.961592	5.616104	0.715374
H	-3.377336	5.474577	1.508967
N	-4.058178	3.758481	0.482304
N	-4.084851	-3.504670	-0.182088
C	-5.357570	3.126968	0.450193
H	-5.518110	2.581397	-0.493367
H	-5.483208	2.416723	1.282930
H	-6.131326	3.894495	0.536065
C	-5.377029	-2.867428	-0.058075
H	-5.560537	-2.162578	-0.884399
H	-6.157502	-3.632427	-0.079795
H	-5.462159	-2.315063	0.890896

OA$_{NMe2}$

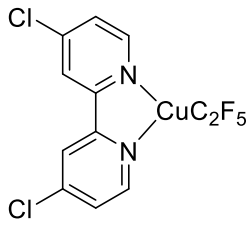


56

C	-1.670995	-3.344543	-0.277620
C	-2.958725	-2.763394	-0.159621
C	-2.998720	-1.354913	-0.022133
C	-1.827541	-0.615168	0.006306
C	-0.561041	-2.529853	-0.240966
C	-1.821047	0.867284	0.139823
C	-2.993020	1.602388	0.250585
C	-2.937503	3.011252	0.373991
C	-1.643398	3.587156	0.377572
C	-0.540565	2.763332	0.259092
H	-1.533285	-4.416097	-0.397785

```
H    0.434983  -2.961708  -0.337370
H    -1.494815  4.660545  0.467355
H    0.458376  3.202636  0.259846
N    -0.606785  1.436735  0.140704
N    -0.621589  -1.201462  -0.097678
Cu    1.061027  -0.108166  -0.083362
C    1.286401  -0.159223  1.888118
C    2.156568  -1.286824  2.482491
F    0.044089  -0.358951  2.410085
F    1.715305  1.004216  2.433959
F    1.976920  -2.425226  1.810501
F    3.448279  -0.980298  2.459500
F    1.831033  -1.522742  3.761590
H    -3.954379  1.098686  0.242927
H    -3.954308  -0.847549  0.059263
C    2.901204  0.426821  -0.111171
C    3.246000  1.763388  0.058350
C    3.874040  -0.527116  -0.404684
C    4.582669  2.151703  -0.074982
H    2.489675  2.514360  0.286315
C    5.207788  -0.133607  -0.528514
H    3.605920  -1.575675  -0.542569
C    5.565069  1.205955  -0.365963
H    4.851266  3.202907  0.051339
H    5.969747  -0.882377  -0.757199
H    6.608403  1.511675  -0.465632
I    1.080408  0.002394  -2.691696
C    -4.001941  -4.939046  -0.345426
H    -5.010745  -5.359903  -0.339097
H    -3.521545  -5.207542  -1.299429
H    -3.428847  -5.404085  0.471983
C    -3.958040  5.193919  0.616164
H    -3.476532  5.649957  -0.263807
H    -4.961592  5.616104  0.715374
H    -3.377336  5.474577  1.508967
N    -4.058178  3.758481  0.482304
N    -4.084851  -3.504670  -0.182088
C    -5.357570  3.126968  0.450193
H    -5.518110  2.581397  -0.493367
H    -5.483208  2.416723  1.282930
H    -6.131326  3.894495  0.536065
C    -5.377029  -2.867428  -0.058075
H    -5.560537  -2.162578  -0.884399
H    -6.157502  -3.632427  -0.079795
H    -5.462159  -2.315063  0.890896
```

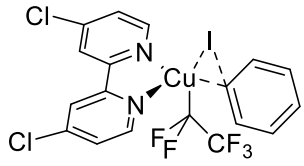
GS$_{Cl}$



28

C	-0.477592	3.483231	-0.014733
C	-1.843738	3.230355	-0.003532
C	-2.321566	1.925669	0.000576
C	-1.388959	0.888756	-0.006965
C	0.372145	2.382707	-0.021032
C	-1.779918	-0.545356	-0.004981
C	-3.110026	-0.963031	0.007893
C	-3.365165	-2.328776	0.008829
C	-2.318759	-3.242558	-0.003719
C	-1.026869	-2.729324	-0.016093
H	-0.077436	4.495924	-0.018665
H	1.453774	2.523491	-0.029658
H	-2.490453	-4.317874	-0.003810
H	-0.169097	-3.402707	-0.026008
N	-0.766558	-1.423887	-0.016433
N	-0.070654	1.128444	-0.017261
Cu	1.141761	-0.596671	-0.021890
C	3.043316	-1.037851	-0.021380
C	3.983634	0.163708	0.036481
F	3.487251	-1.744429	-1.147705
F	3.468413	-1.834912	1.050810
F	3.789410	0.969238	-1.017068
F	3.766170	0.882851	1.146601
F	5.292153	-0.158907	0.037545
H	-3.932904	-0.251652	0.017438
H	-3.392302	1.734030	0.008915
Cl	-2.965960	4.549402	0.005160
Cl	-5.002966	-2.890544	0.025590

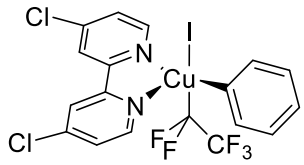
TS$_{Cl}$



40

C	2.356050	3.214444	-0.060225
C	3.532434	2.477548	-0.137909
C	3.494707	1.090973	-0.183192
C	2.247004	0.465318	-0.140957
C	1.164016	2.502790	-0.030932
C	2.096719	-1.011402	-0.175772
C	3.190289	-1.868399	-0.033556
C	2.953684	-3.235934	-0.063859
C	1.663326	-3.723784	-0.228284
C	0.642761	-2.787321	-0.353701
H	2.356944	4.302878	-0.026227
H	0.210544	3.029622	0.022233
H	1.447441	-4.790802	-0.254108
H	-0.388209	-3.121638	-0.473203
N	0.851518	-1.475234	-0.334380
N	1.113887	1.173713	-0.068024
Cu	-0.728016	0.133248	-0.046156
C	-1.039356	-0.171015	1.943833
C	-1.259136	1.066194	2.808060
F	0.061110	-0.791434	2.538190
F	-2.100912	-1.005313	2.259297
F	-0.203532	1.887001	2.741207
F	-2.335282	1.752392	2.405012
F	-1.447907	0.787890	4.114707
H	4.199082	-1.489385	0.114308
H	4.416418	0.518624	-0.262435
C	-2.652166	-0.261684	-0.741423
C	-2.830077	-1.638971	-0.929821
C	-3.664994	0.514222	-0.160741
C	-3.982480	-2.250391	-0.438125
H	-2.078894	-2.226305	-1.456830
C	-4.809099	-0.114108	0.320466
H	-3.549339	1.593689	-0.069807
C	-4.973296	-1.496407	0.191663
H	-4.108738	-3.327620	-0.566759
H	-5.585202	0.488381	0.797687
H	-5.878061	-1.979517	0.564525
I	-1.453261	0.805747	-2.432990
Cl	4.280487	-4.337142	0.111146
Cl	5.060209	3.292239	-0.189053

OA_{Cl}

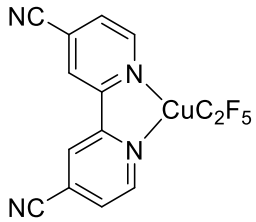


40

C	2.617552	1.245306	-2.988440
C	3.830985	1.192823	-2.312637
C	3.882584	0.788226	-0.985865
C	2.689113	0.445884	-0.351060
C	1.481254	0.883408	-2.280077
C	2.633584	-0.008725	1.059730
C	3.775962	-0.146250	1.849976
C	3.609549	-0.592106	3.154873
C	2.343496	-0.887099	3.645420
C	1.270630	-0.715374	2.776832
H	2.547298	1.553677	-4.030087
H	0.503192	0.896191	-2.759717
H	2.187023	-1.239223	4.663715
H	0.255845	-0.934306	3.110697
N	1.415170	-0.291079	1.527632
N	1.520826	0.501417	-1.004852
Cu	-0.222885	-0.026144	-0.093408
C	-0.630768	1.786243	0.602578
C	-1.514011	2.709225	-0.262755
F	0.572632	2.422764	0.685819
F	-1.132872	1.810404	1.858265
F	-1.232630	2.549068	-1.556726
F	-2.806632	2.473508	-0.076188
F	-1.299198	3.997046	0.037953
H	4.769735	0.080650	1.470454
H	4.835103	0.743660	-0.463150
C	-2.068731	-0.382344	0.258253
C	-2.479058	-0.748116	1.534420
C	-2.961562	-0.370486	-0.810576
C	-3.811256	-1.119293	1.742016
H	-1.781325	-0.754672	2.371891
C	-4.291478	-0.734386	-0.591427
H	-2.635492	-0.086597	-1.812046
C	-4.718195	-1.110936	0.683039
H	-4.135688	-1.414288	2.742332
H	-4.994734	-0.725118	-1.427289
H	-5.758382	-1.396875	0.850441
I	0.041309	-2.467525	-0.954138
Cl	4.996896	-0.782667	4.174823

Cl 5.292053 1.630492 -3.128428

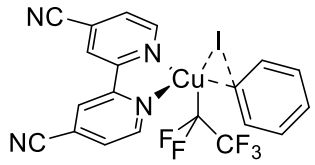
GS$_{CN}$



30

C	-0.637089	3.501315	-0.011056
C	-2.010137	3.245842	-0.004442
C	-2.472439	1.927786	-0.002057
C	-1.532403	0.899268	-0.006951
C	0.222355	2.408824	-0.015213
C	-1.908050	-0.537755	-0.006905
C	-3.231374	-0.972254	0.013103
C	-3.478059	-2.346906	0.012335
C	-2.408451	-3.244706	-0.009826
C	-1.123185	-2.716195	-0.028700
H	-0.247558	4.518144	-0.013079
H	1.303142	2.552635	-0.020498
H	-2.569050	-4.321701	-0.011657
H	-0.253849	-3.373625	-0.045831
N	-0.886594	-1.406481	-0.026780
N	-0.217053	1.153748	-0.013242
Cu	1.015309	-0.562158	-0.027945
C	2.923816	-0.984251	-0.022639
C	3.851615	0.226519	0.042044
F	3.376816	-1.683145	-1.149152
F	3.350964	-1.779940	1.048714
F	3.652328	1.033141	-1.009624
F	3.622848	0.939736	1.153625
F	5.162871	-0.083331	0.046432
H	-4.064476	-0.272898	0.030261
H	-3.541726	1.728198	0.002311
C	-2.948071	4.330676	-0.000517
C	-4.828981	-2.827360	0.034084
N	-5.918645	-3.215938	0.051739
N	-3.703448	5.207082	0.002482

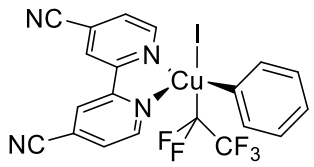
TS$_{CN}$



42

C	-2.287477	-3.146681	-0.974631
C	-3.510417	-2.503129	-0.766174
C	-3.533535	-1.157078	-0.398235
C	-2.317799	-0.491064	-0.242074
C	-1.130423	-2.401995	-0.792552
C	-2.228420	0.943496	0.129735
C	-3.349906	1.712022	0.442926
C	-3.158780	3.054707	0.773935
C	-1.869716	3.593750	0.780879
C	-0.817264	2.744905	0.460551
H	-2.237974	-4.194217	-1.267227
H	-0.149667	-2.854698	-0.939879
H	-1.690892	4.638162	1.031104
H	0.208925	3.113161	0.456156
N	-0.997244	1.466754	0.147043
N	-1.152659	-1.121410	-0.434866
Cu	0.628611	-0.022963	-0.058505
C	0.973760	-0.394559	1.912509
C	1.077446	-1.854679	2.344184
F	-0.052419	0.111413	2.711447
F	2.116318	0.194615	2.424335
F	-0.065733	-2.507455	2.103382
F	2.055948	-2.484027	1.682615
F	1.339120	-2.009307	3.658058
H	-4.354372	1.294427	0.440963
H	-4.486112	-0.654801	-0.246577
C	2.580539	0.422572	-0.609165
C	2.981613	1.687483	-0.160740
C	3.446213	-0.675726	-0.523788
C	4.225738	1.826615	0.451314
H	2.329156	2.552060	-0.281737
C	4.682328	-0.516813	0.096378
H	3.148749	-1.646582	-0.919593
C	5.079123	0.730293	0.586210
H	4.530855	2.809059	0.818195
H	5.345740	-1.379584	0.188863
H	6.055230	0.848840	1.059783
I	1.230502	0.441910	-2.529872
C	-4.741649	-3.218793	-0.932802

C	-4.287550	3.874448	1.104918
N	-5.197209	4.537884	1.371843
N	-5.734035	-3.798504	-1.066734



42

C	2.038888	3.266902	-0.754768
C	3.292452	2.699119	-0.515541
C	3.388424	1.356912	-0.148712
C	2.216888	0.612207	-0.022727
C	0.926042	2.452509	-0.610072
C	2.214856	-0.820554	0.358740
C	3.389219	-1.540102	0.578314
C	3.278174	-2.884999	0.936868
C	2.016014	-3.468481	1.067933
C	0.907302	-2.665756	0.822203
H	1.930426	4.310256	-1.045133
H	-0.075937	2.838829	-0.791919
H	1.899507	-4.513704	1.349256
H	-0.099266	-3.075187	0.907961
N	1.012408	-1.388959	0.477320
N	1.022037	1.172920	-0.253289
Cu	-0.703504	0.109094	-0.103991
C	-0.994102	0.444480	1.829338
C	-1.895749	1.623700	2.248167
F	0.236936	0.749014	2.333927
F	-1.406786	-0.641346	2.522371
F	-1.689806	2.675943	1.455162
F	-3.182799	1.303755	2.206433
F	-1.624488	2.008006	3.502968
H	4.372574	-1.087766	0.471380
H	4.364048	0.914760	0.038845
C	-2.545394	-0.403525	-0.123786
C	-2.926295	-1.688574	0.241068
C	-3.471642	0.513066	-0.614833
C	-4.265723	-2.066091	0.103439
H	-2.199992	-2.406500	0.621267
C	-4.807698	0.128378	-0.741980
H	-3.167216	1.519539	-0.905118
C	-5.206689	-1.160574	-0.385062
H	-4.568396	-3.077814	0.381959

```
H    -5.537502  0.844234  -1.126916
H    -6.251735  -1.458908  -0.488022
I    -0.576789  -0.519442  -2.623211
C    4.461910  -3.660386  1.169645
C    4.481789  3.489280  -0.645555
N    5.415691  -4.287298  1.359076
N    5.440293  4.128431  -0.750274
```

2.8 References

Portions of this chapter were reprinted with permission from "Unusual Electronic Effects of Ancillary Ligands on the Perfluoroalkylation of Aryl Iodides and Bromides Mediated by Copper(I) Pentafluoroethyl Complexes of Substituted Bipyridines," Kalkman, E. D.; Mormino, M. G.; and Hartwig, J. F. *J. Am. Chem. Soc.* **2019**, *141*, 19458–19465.

(1) Tolman, C. A. Electron Donor-Acceptor Properties of Phosphorus Ligands - Substituent Additivity. *J. Am. Chem. Soc.* **1970**, *92*, 2953–2956.

(2) Tolman, C. A. Steric Effects of Phosphorus Ligands in Organometallic Chemistry and Homogeneous Catalysis. *Chem. Rev.* **1977**, *77*, 313–348.

(3) Golovin, M. N.; Rahman, M.; Belmonte, J. E.; Giering, W. P. Quantitative Separation of S- and p-Components of Transition-Metal Phosphorus Bonding and the Application of Ligand Effects in Organometallic Chemistry. *Organometallics* **1985**, *4*, 1981–1991.

(4) Hartwig, J. F.; Paul, F. Oxidative Addition of Aryl Bromide after Dissociation of Phosphine from a Two-Coordinate Palladium(0) Complex, Bis(Tri-*o*-Tolylphosphine)Palladium(0). *J. Am. Chem. Soc.* **1995**, *117*, 5373–5374.

(5) Christmann, U.; Vilar, R. Monoligated Palladium Species as Catalysts in Cross-Coupling Reactions. *Angew. Chem. Int. Ed.* **2005**, *44*, 366–374.

(6) Surry, D. S.; Buchwald, S. L. Dialkylbiaryl Phosphines in Pd-Catalyzed Amination: A User's Guide. *Chem. Sci.* **2011**, *2*, 27–50.

(7) Stradiotto, M.; Lundgren, R. J. Application of Sterically Demanding Phosphine Ligands in Palladium-Catalyzed Cross-Coupling Leading to C(Sp^2)─E Bond Formation (E = NH_2, OH, and F). In *Ligand Design in Metal Chemistry*; John Wiley & Sons, Ltd: Chichester, UK; Hoboken, NJ, 2016; pp 104–133.

(8) Hartwig, J. F. Evolution of a Fourth Generation Catalyst for the Amination and Thioetherification of Aryl Halides. *Acc. Chem. Res.* **2008**, *41*, 1534–1544.

(9) Surry, D. S.; Buchwald, S. L. Biaryl Phosphane Ligands in Palladium-Catalyzed Amination. *Angew. Chem. Int. Ed.* **2008**, *47*, 6338–6361.

(10) Lundgren, R. J.; Stradiotto, M. Addressing Challenges in Palladium-Catalyzed Cross-Coupling Reactions through Ligand Design. *Chemistry* **2012**, *18*, 9758–9769.

(11) Chow, K. K.; Levason, W.; McAuliffe, C. A. Transition Metal Complexes Containing Phosphine Ligands. In *Transition Metal Complexes of Phosphorus, Arsenic and Antimony Ligands*; McAuliffe, C. A., Ed.; Macmillan Education UK: London, 1973; pp 33–204.

(12) Bartlett, K. L.; Goldberg, K. I.; Borden, W. T. Computational Study of Reductive Elimination Reactions to Form C–H Bonds from Platinum(II) and Platinum(IV) Centers

with Strongly Coordinating Trimethylphosphine Ligands. *Organometallics* **2001**, *20*, 2669–2678.
(13) Kaddouri, H.; Vicente, V.; Ouali, A.; Ouazzani, F.; Taillefer, M. Copper-Catalyzed Arylation of Nucleophiles by Using Butadienylphosphines as Ligands: Mechanistic Insight. *Angew. Chem. Int. Ed.* **2009**, *48*, 333–336.
(14) Rendina, L. M.; Puddephatt, R. J. Oxidative Addition Reactions of Organoplatinum(II) Complexes with Nitrogen-Donor Ligands. *Chem. Rev.* **1997**, *97*, 1735–1754.
(15) Togni, A.; Venanzi, L. M. Nitrogen Donors in Organometallic Chemistry and Homogeneous Catalysis. *Angew. Chem. Int. Ed.* **1994**, *33*, 497–526.
(16) Thompson, W. H.; Sears, C. T. Kinetics of Oxidative Addition to Iridium(I) Complexes. *Inorg. Chem.* **1977**, *16*, 769–774.
(17) Tye, J. W.; Weng, Z.; Johns, A. M.; Incarvito, C. D.; Hartwig, J. F. Copper Complexes of Anionic Nitrogen Ligands in the Amidation and Imidation of Aryl Halides. *J. Am. Chem. Soc.* **2008**, *130*, 9971–9983.
(18) Wang, D. Y.; Choliy, Y.; Haibach, M. C.; Hartwig, J. F.; Krogh-Jespersen, K.; Goldman, A. S. Assessment of the Electronic Factors Determining the Thermodynamics of "Oxidative Addition" of C–H and N–H Bonds to Ir(I) Complexes. *J. Am. Chem. Soc.* **2016**, *138*, 149–163.
(19) Cristau, H.-J.; Cellier, P. P.; Spindler, J.-F.; Taillefer, M. Highly Efficient and Mild Copper-Catalyzed N- and C-Arylations with Aryl Bromides and Iodides. *Chem. Eur. J.* **2004**, *10*, 5607–5622.
(20) Zhang, S.-L.; Liu, L.; Fu, Y.; Guo, Q.-X. Theoretical Study on Copper(I)-Catalyzed Cross-Coupling between Aryl Halides and Amides. *Organometallics* **2007**, *26*, 4546–4554.
(21) Dubinina, G. G.; Ogikubo, J.; Vicic, D. A. Structure of Bis(Trifluoromethyl)Cuprate and Its Role in Trifluoromethylation Reactions. *Organometallics* **2008**, *27*, 6233–6235.
(22) Tye, J. W.; Weng, Z.; Giri, R.; Hartwig, J. F. Copper(I) Phenoxide Complexes in the Etherification of Aryl Halides. *Angew. Chem. Int. Ed.* **2010**, *49*, 2185–2189.
(23) Yu, H.-Z.; Jiang, Y.-Y.; Fu, Y.; Liu, L. Alternative Mechanistic Explanation for Ligand-Dependent Selectivities in Copper-Catalyzed N- and O-Arylation Reactions. *J. Am. Chem. Soc.* **2010**, *132*, 18078–18091.
(24) Lefèvre, G.; Franc, G.; Tlili, A.; Adamo, C.; Taillefer, M.; Ciofini, I.; Jutand, A. Contribution to the Mechanism of Copper-Catalyzed C–N and C–O Bond Formation. *Organometallics* **2012**, *31*, 7694–7707.
(25) Lefèvre, G.; Tlili, A.; Taillefer, M.; Adamo, C.; Ciofini, I.; Jutand, A. Discriminating Role of Bases in Diketonate Copper(I)-Catalyzed C–O Couplings: Phenol versus Diarylether. *Dalton Trans.* **2013**, *42*, 5348–5354.
(26) Konovalov, A. I.; Lishchynskyi, A.; Grushin, V. V. Mechanism of Trifluoromethylation of Aryl Halides with $CuCF_3$ and the Ortho Effect. *J. Am. Chem. Soc.* **2014**, *136*, 13410–13425.
(27) Bhunia, S.; Pawar, G. G.; Kumar, S. V.; Jiang, Y.; Ma, D. Selected Copper-Based Reactions for C-N, C-O, C-S, and C-C Bond Formation. *Angew. Chem. Int. Ed.* **2017**, *56*, 16136–16179.
(28) Oishi, M.; Kondo, H.; Amii, H. Aromatic Trifluoromethylation Catalytic in Copper. *Chem. Commun.* **2009**, No. 14, 1909–1911.
(29) Ouali, A.; Spindler, J. F.; Jutand, A.; Taillefer, M. Nitrogen Ligands in Copper-Catalyzed Arylation of Phenols: Structure/Activity Relationships and Applications. *Adv. Synth. Catal.* **2007**, *349*, 1906–1916.

(30) Dubinina, G. G.; Furutachi, H.; Vicic, D. A. Active Trifluoromethylating Agents from Well-Defined Copper(I)-CF_3 Complexes. *J. Am. Chem. Soc.* **2008**, *130*, 8600–8601.
(31) Tomashenko, O. A.; Escudero-Adan, E. C.; Belmonte, M. M.; Grushin, V. V. Simple, Stable, and Easily Accessible Well-Defined $CuCF_3$ Aromatic Trifluoromethylating Agents. *Angew. Chem. Int. Ed.* **2011**, *50*, 7655–7659.
(32) Panferova, L. I.; Miloserdov, F. M.; Lishchynskyi, A.; Martinez Belmonte, M.; Benet-Buchholz, J.; Grushin, V. V. Well-Defined CuC_2F_5 Complexes and Pentafluoroethylation of Acid Chlorides. *Angew. Chem. Int. Ed.* **2015**, *54*, 5218–5222.
(33) Morimoto, H.; Tsubogo, T.; Litvinas, N. D.; Hartwig, J. F. A Broadly Applicable Copper Reagent for Trifluoromethylations and Perfluoroalkylations of Aryl Iodides and Bromides. *Angew. Chem. Int. Ed.* **2011**, *50*, 3793–3798.
(34) Litvinas, N. D.; Fier, P. S.; Hartwig, J. F. A General Strategy for the Perfluoroalkylation of Arenes and Arylbromides by Using Arylboronate Esters and [(Phen)CuR^F]. *Angew. Chem. Int. Ed.* **2012**, *51*, 536–539.
(35) Weng, Z. Q.; Lee, R.; Jia, W. G.; Yuan, Y. F.; Wang, W. F.; Feng, X.; Huang, K. W. Cooperative Effect of Silver in Copper-Catalyzed Trifluoromethylation of Aryl Iodides Using Me_3SiCF_3. *Organometallics* **2011**, *30*, 3229–3232.
(36) Kondo, H.; Oishi, M.; Fujikawa, K.; Amii, H. Copper-Catalyzed Aromatic Trifluoromethylation via Group Transfer from Fluoral Derivatives. *Adv. Synth. Catal.* **2011**, *353*, 1247–1252.
(37) Knauber, T.; Arikan, F.; Roschenthaler, G. V.; Goossen, L. J. Copper-Catalyzed Trifluoromethylation of Aryl Iodides with Potassium (Trifluoromethyl)Trimethoxyborate. *Chem. Eur. J.* **2011**, *17*, 2689–2697.
(38) Nakamura, Y.; Fujiu, M.; Murase, T.; Itoh, Y.; Serizawa, H.; Aikawa, K.; Mikami, K. Cu-Catalyzed Trifluoromethylation of Aryl Iodides with Trifluoromethylzinc Reagent Prepared in Situ from Trifluoromethyl Iodide. *Beilstein J. Org. Chem.* **2013**, *9*, 2404–2409.
(39) Chen, Q.-Y.; Wu, S.-W. Methyl Fluorosulphonyldifluoroacetate; a New Trifluoromethylating Agent. *J. Chem. Soc. Chem. Commun.* **1989**, No. 11, 705.
(40) Aikawa, K.; Nakamura, Y.; Yokota, Y.; Toya, W.; Mikami, K. Stable but Reactive Perfluoroalkylzinc Reagents: Application in Ligand-Free Copper-Catalyzed Perfluoroalkylation of Aryl Iodides. *Chem. Eur. J.* **2015**, *21*, 96–100.
(41) Lishchynskyi, A.; Novikov, M. A.; Martin, E.; Escudero-Adan, E. C.; Novak, P.; Grushin, V. V. Trifluoromethylation of Aryl and Heteroaryl Halides with Fluoroform-Derived $CuCF_3$: Scope, Limitations, and Mechanistic Features. *J. Org. Chem.* **2013**, *78*, 11126–11146.
(42) Ohashi, M.; Ishida, N.; Ando, K.; Hashimoto, Y.; Shigaki, A.; Kikushima, K.; Ogoshi, S. Cu(I) -Catalyzed Pentafluoroethylation of Aryl Iodides in the Presence of Tetrafluoroethylene and Cesium Fluoride: Determining the Route to the Key Pentafluoroethyl Cu(I) Intermediate. *Chem. Eur. J.* **2018**, *24*, 9794–9798.
(43) Lishchynskyi, A.; Grushin, V. V. Cupration of C_2F_5H: Isolation, Structure, and Synthetic Applications of $[K(DMF)_2][(t\text{-BuO})Cu(C_2F_5)]$. Highly Efficient Pentafluoroethylation of Unactivated Aryl Bromides. *J. Am. Chem. Soc.* **2013**, *135*, 12584–12587.
(44) Hansch, C.; Leo, A.; Taft, R. W. A Survey of Hammett Substituent Constants and Resonance and Field Parameters. *Chem. Rev.* **1991**, *91*, 165–195.
(45) Strieter, E. R.; Bhayana, B.; Buchwald, S. L. Mechanistic Studies on the Copper-Catalyzed N-Arylation of Amides. *J. Am. Chem. Soc.* **2009**, *131*, 78–88.

(46) Liu, H.; Shen, Q. Bistrifluoromethylated Organocuprate $[Ph_4P]^+[Cu(CF_3)_2]^-$: Synthesis, Characterization and Its Application for Trifluoromethylation of Activated Heteroaryl Bromides, Chlorides and Iodides. *Org. Chem. Front.* **2019**, *6*, 2324–2328.
(47) Serizawa, H.; Aikawa, K.; Mikami, K. Direct Synthesis of Pentafluoroethyl Copper from Pentafluoropropionate as an Economical C_2F_5 Source: Application to Pentafluoroethylation of Arylboronic Acids and Aryl Bromides. *Org. Lett.* **2014**, *16*, 3456–3459.
(48) Zanardi, A.; Novikov, M. A.; Martin, E.; Benet-Buchholz, J.; Grushin, V. V. Direct Cupration of Fluoroform. *J. Am. Chem. Soc.* **2011**, *133*, 20901–20913.
(49) Chang, C. E.; Chen, W.; Gilson, M. K. Evaluating the Accuracy of the Quasiharmonic Approximation. *J. Chem. Theory Comput.* **2005**, *1*, 1017–1028.
(50) Alan E. Reed; Robert B. Weinstock; Frank Weinhold. Natural Population Analysis. *J. Chem. Phys.* **1985**, *83*, 735–746.
(51) Snyder, J. P. Elusiveness of Cu^{III} Complexation; Preference for Trifluoromethyl Oxidation in the Formation of $[Cu^{I}(CF_3)_4]^-$ Salts. *Angew. Chem. Int. Ed.* **1995**, *34*, 80–81.
(52) Walroth, R. C.; Lukens, J. T.; MacMillan, S. N.; Finkelstein, K. D.; Lancaster, K. M. Spectroscopic Evidence for a $3d^{10}$ Ground State Electronic Configuration and Ligand Field Inversion in $[Cu(CF_3)_4]^{1-}$. *J. Am. Chem. Soc.* **2016**, *138*, 1922–1931.
(53) Hoffmann, R.; Alvarez, S.; Mealli, C.; Falceto, A.; Cahill, T. J.; Zeng, T.; Manca, G. From Widely Accepted Concepts in Coordination Chemistry to Inverted Ligand Fields. *Chem. Rev.* **2016**, *116*, 8173–8192.
(54) Baya, M.; Joven-Sancho, D.; Alonso, P. J.; Orduna, J.; Menjón, B. M−C Bond Homolysis in Coinage-Metal $[M(CF_3)_4]^-$ Derivatives. *Angew. Chem. Int. Ed.* **2019**, *58*, 9954–9958.
(55) Louërat, F.; Gros, P. C. Functional Polypyridine Ligands from Copper-Mediated Room Temperature Coupling of 4-Chloro-2-Trimethylsilylpyridine. *Tetrahedron Lett.* **2010**, *51*, 3558–3560.
(56) Rosenau, C. P.; Jelier, B. J.; Gossert, A. D.; Togni, A. Exposing the Origins of Irreproducibility in Fluorine NMR Spectroscopy. *Angew. Chem. Int. Ed.* **2018**, *57*, 9528–9533.
(57) Hue, R. J.; Vatassery, R.; Mann, K. R.; Gladfelter, W. L. Zinc Oxide Nanocrystal Quenching of Emission from Electron-Rich Ruthenium-Bipyridine Complexes. *Dalton Trans.* **2015**, *44*, 4630–4639.
(58) Beaulieu, F.; Beauregard, L. P.; Courchesne, G.; Couturier, M.; LaFlamme, F.; L'Heureux, A. Aminodifluorosulfinium Tetrafluoroborate Salts as Stable and Crystalline Deoxofluorinating Reagents. *Org. Lett.* **2009**, *11*, 5050–5053.
(59) Mormino, M. The Development of Transition Metal-Catalyzed Fluoroalkylation Reactions of Aryl Electrophiles. Ph.D. Thesis, University of California, Berkeley, 2017.
(60) Frisch, M. J.; Trucks, G. W.; Schlegel, H. B.; Scuseria, G. E.; Robb, M. A.; Cheeseman, J. R.; Scalmani, G.; Barone, V.; Petersson, G. A.; Nakatsuji, H.; Li, X.; Caricato, M.; Marenich, A. V.; Bloino, J.; Janesko, B. G.; Gomperts, R.; Mennucci, B.; Hratchian, H. P.; Ortiz, J. V.; Izmaylov, A. F.; Sonnenberg, J. L.; Williams-Young, D.; Ding, F.; Lipparini, F.; Egidi, F.; Goings, J.; Peng, B.; Petrone, A.; Henderson, T.; Ranasinghe, D.; Zakrzewski, V. G.; Gao, J.; Rega, N.; Zheng, G.; Liang, W.; Hada, M.; Ehara, M.; Toyota, K.; Fukuda, R.; Hasegawa, J.; Ishida, M.; Nakajima, T.; Honda, Y.; Kitao, O.; Nakai, H.; Vreven, T.; Throssell, K.; Montgomery, J. A.; Peralta, J. E.; Ogliaro, F.; Bearpark, M. J.; Heyd, J. J.; Brothers, E. N.; Kudin, K. N.; Staroverov, V. N.; Keith, T. A.; Kobayashi, R.; Normand, J.; Raghavachari, K.; Rendell, A. P.; Burant, J. C.; Iyengar, S. S.; Tomasi, J.; Cossi, M.;

Millam, J. M.; Klene, M.; Adamo, C.; Cammi, R.; Ochterski, J. W.; Martin, R. L.; Morokuma, K.; Farkas, O.; Foresman, J. B.; Fox, D. J. *Gaussian 16, Revision A.03*; Gaussian, Inc.: Wallingford CT, 2016.

(61) Marenich, A. V.; Cramer, C. J.; Truhlar, D. G. Universal Solvation Model Based on Solute Electron Density and on a Continuum Model of the Solvent Defined by the Bulk Dielectric Constant and Atomic Surface Tensions. *J. Phys. Chem. B* **2009**, *113*, 6378–6396.

(62) Dennington, R.; Keith, T. A.; Millam, J. M. *GaussView, Version 6.1*; Semichem Inc.: Shawnee Mission, KS, 2016.

(63) Perdew, J. P.; Burke, K.; Ernzerhof, M. Generalized Gradient Approximation Made Simple. *Phys. Rev. Lett.* **1996**, *77*, 3865–3868.

(64) Perdew, J. P.; Burke, K.; Ernzerhof, M. Generalized Gradient Approximation Made Simple. *Phys. Rev. Lett.* **1997**, *78*, 1396–1396.

(65) Adamo, C.; Barone, V. Toward Reliable Density Functional Methods without Adjustable Parameters: The PBE0 Model. *J. Chem. Phys.* **1999**, *110*, 6158–6170.

(66) Grimme, S.; Ehrlich, S.; Goerigk, L. Effect of the Damping Function in Dispersion Corrected Density Functional Theory. *J. Comput. Chem.* **2011**, *32*, 1456–1465.

(67) Weigend, F.; Ahlrichs, R. Balanced Basis Sets of Split Valence, Triple Zeta Valence and Quadruple Zeta Valence Quality for H to Rn: Design and Assessment of Accuracy. *Phys. Chem. Chem. Phys.* **2005**, *7*, 3297–3305.

(68) Rappoport, D.; Furche, F. Property-Optimized Gaussian Basis Sets for Molecular Response Calculations. *J. Chem. Phys.* **2010**, *133*, 134105.

(69) Peterson, K. A.; Figgen, D.; Goll, E.; Stoll, H.; Dolg, M. Systematically Convergent Basis Sets with Relativistic Pseudopotentials. II. Small-Core Pseudopotentials and Correlation Consistent Basis Sets for the Post-d Group 16–18 Elements. *J. Chem. Phys.* **2003**, *119*, 11113–11123.

(70) Feller, D. The Role of Databases in Support of Computational Chemistry Calculations. *J. Comput. Chem.* **1996**, *17*, 1571–1586.

(71) Schuchardt, K. L.; Didier, B. T.; Elsethagen, T.; Sun, L.; Gurumoorthi, V.; Chase, J.; Li, J.; Windus, T. L. Basis Set Exchange: A Community Database for Computational Sciences. *J. Chem. Inf. Model.* **2007**, *47*, 1045–1052.

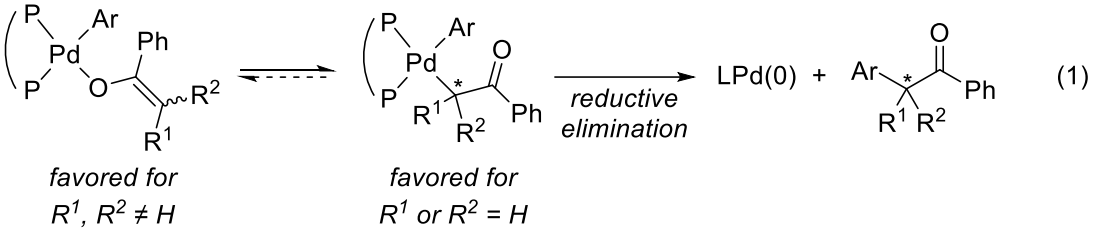
(72) Pritchard, B. P.; Altarawy, D.; Didier, B.; Gibson, T. D.; Windus, T. L. New Basis Set Exchange: An Open, Up-to-Date Resource for the Molecular Sciences Community. *J. Chem. Inf. Model.* **2019**, *59*, 4814–4820.

Chapter 3

Direct Observation of Diastereomeric α-C-Bound Enolates during Enantioselective α-Arylations: Synthesis, Characterization, and Reactivity of Arylpalladium Fluorooxindole Complexes

3.1 Introduction

The α-arylation of carbonyl compounds has become a widely practiced class of coupling reactions, and enantioselective versions of this process have been reported in both intermolecular and intramolecular forms with a range of carbonyl compounds and sp^2 electrophiles.[1–26] the intermediates in the αarylations that form the carbon-carbon bond are C-bound arylpalladium enolate complexes. Examples of arylpalladium enolate complexes have been prepared, and the rates of reductive elimination as a function of the steric and electronic properties of the enolate have been studied.[6,27,28] However, analogous enolate complexes that are putative intermediates in the enantioselective processes and that undergo reductive eliminations to form enantioenriched, chiral products have not been studied. Thus, the influence of the chiral ancillary ligand and enolate structure on the formation, speciation, and reactivity of diastereomeric arylpalladium enolate intermediates is unknown.



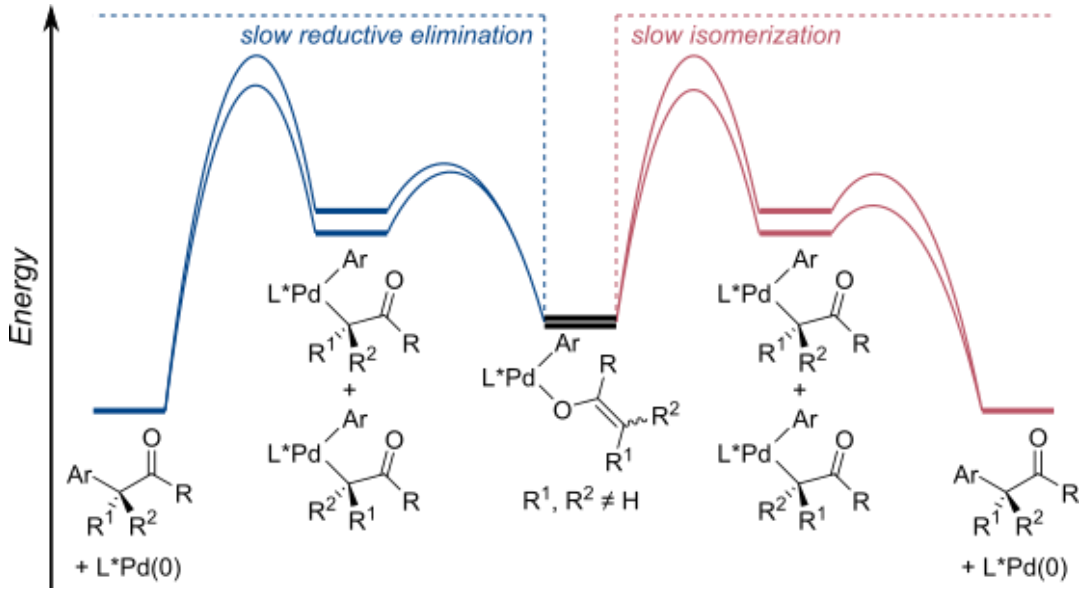


Figure 3.1.1 Conceptual energy diagram of possible epimerizations and stereoselectivity-determining steps of the formation of enantioenriched *α*-aryl carbonyl compounds from chiral arylpalladium *α*,*α*-disubstituted enolate complexes.

In particular, it is unknown whether the formation of the C-bound arylpalladium enolate complexes (Figure 3.1.1, red) or reductive elimination from these complexes (Figure 3.1.1, blue) is the stereoselectivity-determining step in the enantioselective formation of chiral products (eq 1). This information has been difficult to obtain because *α*,*α*-disubstituted enolates typically bind to the metal center through the enolate oxygen (eq 1; R^1, $R^2 \neq H$), not the *α*-carbon (R^1 or $R^2 = H$).[6,27–29] This preference for *κO* binding over *κC* binding precludes the evaluation of diastereomeric

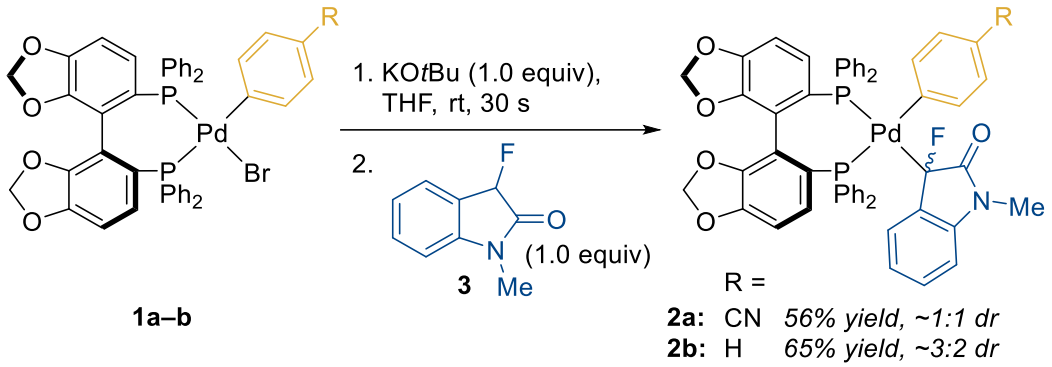
intermediates because the C-bound form is not observed. Diastereomeric C-bound enolate complexes of α-monosubstituted carbonyl compounds might be observable because the α-C-bound isomer of these complexes can be more stable than the O-bound form.[27] However, the benzylic α-C–H bond in the coupled products is more acidic than the α-C–H bonds of the starting carbonyl compounds, and this greater acidity of the product complicates analysis of the origins of enantioselectivity because racemization of the arylated products occurs under the basic reaction conditions typically employed for catalysis.[9,16,30–34] Thus, information on the origins of enantioselectivity has been limited to that from computational studies.[32,33]

We recently reported several examples of the enantioselective α-arylation of α-fluoroenolates.[18,19] We considered that these reactions might provide an opportunity to observe such diastereomeric intermediates because the fluorine atom on these enolates could lead to an electronic preference for the α-C-bound form[35–37] and the small size of fluorine would not significantly destabilize this form due to steric interactions. Because the arylated products formed from these reactions lack acidic C–H bonds at the newly formed stereocenter, they do not epimerize under catalytic conditions.[18,19] Thus, such systems provide a potential opportunity to study the reactivity of enolate complexes containing a stereogenic, palladium-bound carbon atom and a chiral ancillary phosphine ligand and to address whether the formation of these diastereomeric complexes or the reductive elimination from these complexes determines enantioselectivity.

We report the synthesis of diphosphine-ligated, chiral, arylpalladium fluoroenolate complexes derived from an α-fluorooxindole in which the enolate fragments are bound to the Pd center at a stereogenic α-carbon, including the first such complexes bearing a chiral diphosphine ligand ((*S*)-SEGPHOS). These complexes undergo reductive elimination in high yields, allowing an assessment of the relative rates of epimerization of and reductive elimination from the fluoroenolate complexes. These studies show that the fluoroenolate complexes undergo epimerization with rates that are comparable to, but slightly faster than, those of reductive elimination and that reductive elimination is the principal determinant of enantioselectivity. Studies of analogous complexes containing the chiral ligand DPPF (DPPF = 1,1'-bis(diphenylphosphino)ferrocene) enabled comparisons to prior studies of fluorinated and nonfluorinated arylpalladium enolates, and allowed further information on the electronic effects of the aryl fragment on the rates of reductive elimination to be obtained.

3.2 Synthesis and Reactivity of (*S*)-SEGPHOS-Ligated Arylpalladium Fluorooxindole Complexes

Our investigations began with the preparation of (*S*)-SEGPHOS-ligated arylpalladium fluorooxindole species that are the putative intermediates that undergo reductive elimination to form the coupled products in our previous studies on the Pd-catalyzed α-arylation of 3-fluorooxindoles.[19] Complexes **2a** and **2b** were prepared by treating arylpalladium bromide complexes **1a**–**b** with KO*t*Bu in THF to form the corresponding arylpalladium *tert*-butoxide complexes, which were combined *in situ* with 3-fluoro-*N*-methyl-oxindole (**3**) to form the desired fluoroenolate complexes as mixtures of diastereomers (Scheme 3.2.1). The diagnostic NMR signals of (4-cyanophenyl)palladium enolate complex **2a** are shown in Figure 3.2.1. The ^{19}F NMR spectra of both complexes **2a** and **2b** consist of two doublets of doublets with large coupling constants ($^{3}J_{F–P}$ = 112–115 Hz and 38–39 Hz), each of which is coupled to a pair of doublets of doublets in the $^{31}P\{^{1}H\}$ NMR spectra ($^{2}J_{P–P}$ = 27–33 Hz). These data are consistent with a mixture of diastereomeric α-C-bound enolate complexes containing a fluorine atom on the α-carbon.



Scheme 3.2.1 Preparation of (*S*)-SEGPHOS-ligated Arylpalladium Fluorooxindole Complexes **2**

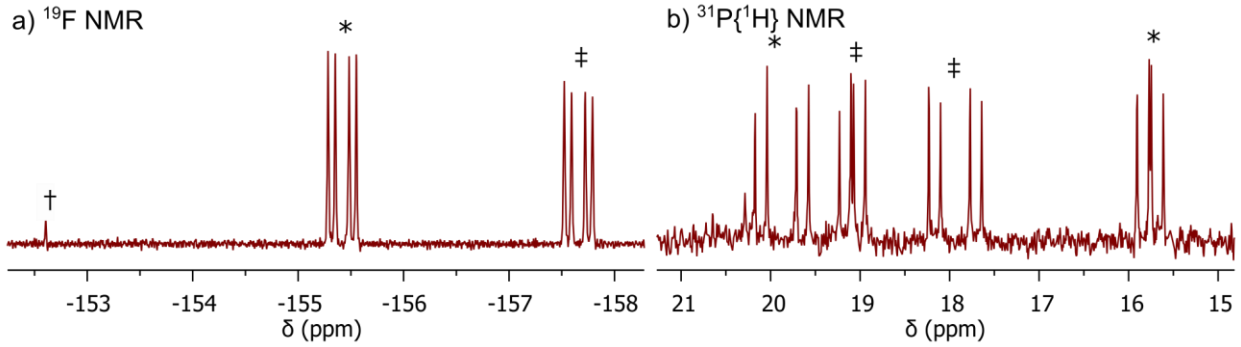


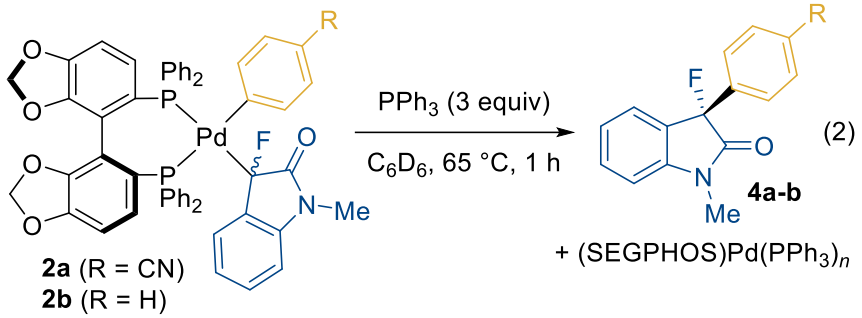
Figure 3.2.1 Diagnostic signals of **2a** in its a) ^{19}F and b) ^{31}P{^{1}H} NMR spectra (C_6D_6). (*) and (‡) indicate peaks corresponding to the two diastereomers of **2a**. (†) indicates a trace amount of coupled product **4a**.

Heating complexes **2a–b** at 65 °C in C_6D_6 in the presence of PPh_3 to trap the generated Pd(0) species (eq 2) resulted in the quantitative formation of the α-arylated products **4a–b** in high *ee*'s (93% and 95% for **4a** and **4b**, respectively; see **Table 3.2.1**). Both the formation of arylated products **4a**–**b** and the decomposition of the starting complexes **2a**–**2b** were monitored by quantitative inverse-gated ^{19}F{^{31}P} NMR spectroscopy and displayed clean first-order kinetics.

The time course for the decomposition of **2a** and the formation of **4a** is show in **Figure 3.2.2**a. For both complexes **2a** and **2b**, the concentrations of the two diastereomers quickly reached a ratio of ~3:1, and this ratio remained constant over the remainder of the reaction. While the *dr* of the unsubstituted phenylpalladium enolate complex **2b** reached its equilibrium ratio within the first minute of heating (see Section 3.8.3). the isomerization of (4-cyanophenyl)palladium enolate complex **2a** to its steady-state *dr* was slow enough to observe over the first 5 minutes of the reaction (**Figure 3.2.2**b). Because the *ee*'s of the coupled products **4a**–**b** far exceed the steady-state *dr*'s of the fluoroenolate complexes **2a**–**b**, the relative rates of reductive elimination from the two diastereomers must be the dominant contributor to the enantioselectivity of this reaction.[*Note 1*]

Table 3.2.1 Reductive Elimination from (*S*)-SEGPHOS-ligated Arylpalladium Fluoroenolate

Complexes **2a–b** at 65 °C



Complex	R	k_{obs} ($s^{-1}\times10^4$)[a]	*dr*[b]	Yield	*ee* of 4
2a	CN	8.6±0.4	3.0:1	>99%	93%
2b	H	26±2	3.2:1	>99%	95%

[a]Determined by monitoring the rate of formation of the coupled product by quantitative $^{19}F\{^{31}P\}$ NMR spectroscopy. [b]Determined as the average ratio between the two diastereomers (major:minor) during the second half-life of the reaction.

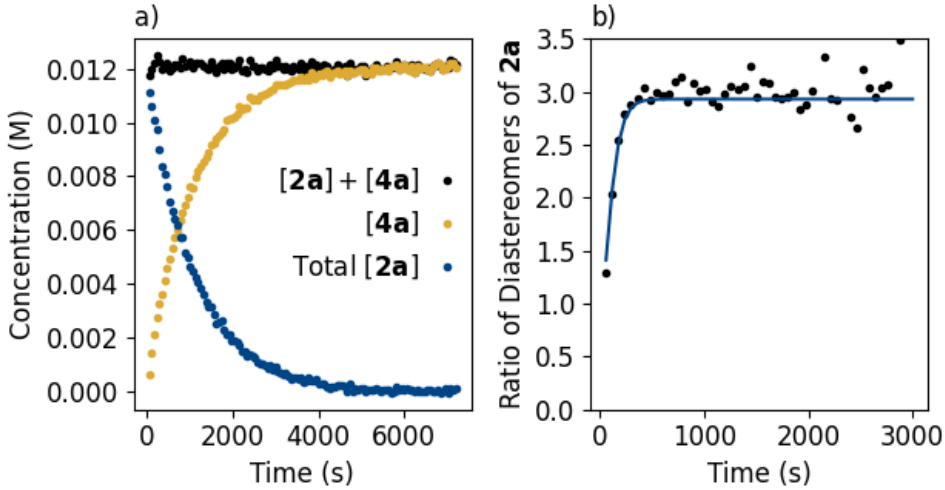
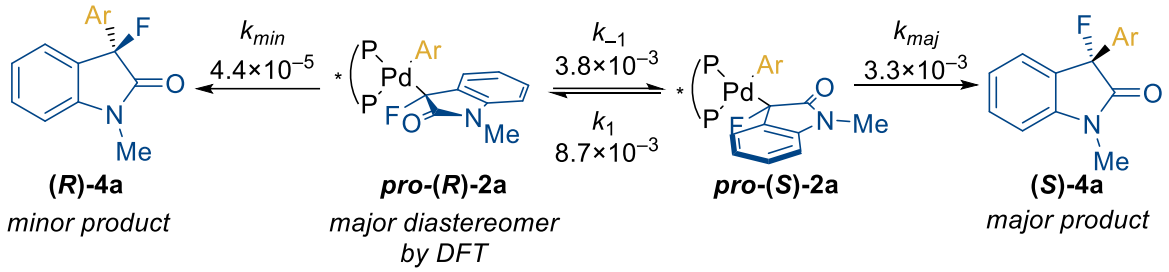


Figure 3.2.2 Time courses of the thermolysis of **2a** in C_6D_6 at 65 °C (eq 2) showing a) the concentrations of **2a** and **4a** and b) the *dr* of **2a**. Concentrations were determined by quantitative inverse-gated $^{19}F\{^{31}P\}$ NMR spectroscopy relative to an internal standard. The solid line in b) represents the simulated *dr* of **3a** according to the fitted rate constants for epimerization and thermolysis (see text).

To obtain a more complete picture of the dynamics of the reaction of **2a**, we estimated the first-order rate constants for the epimerization of and the reductive elimination from **2a** using the kinetic modeling software COPASI (Figure 3.3.2; see Section 3.8.3 for a derivation of the rate equation).[38] While isomerization from the diastereomer that gives the major product enantiomer (***pro*-(*S*)-2a**) to the diastereomer that gives the minor product enantiomer (***pro*-(*R*)-2a**) occurs with a rate constant that is significantly larger than that of the subsequent reductive elimination step by more than two orders of magnitude (k_1 = 8.7×10^{-3} s^{-1} *vs* k_{min} = 4.4×10^{-5} s^{-1}, respectively), isomerization of the diastereomer that gives the minor product to the diastereomer that gives the

major product is just barely faster than the rate of reductive elimination (k_{-1} = 3.8×10^{-3} s^{-1} *vs* k_{maj} = 3.3×10^{-3} s^{-1}, respectively). These similar rate constants for epimerization and reductive elimination are consistent with the sluggish equilibration observed in Figure 3.2.2b and highlight the large difference in rates between the two manifolds forming the two enantiomeric products. Computational modeling of the individual isomerization and reductive elimination steps by DFT, along with a discussion of the implications for the origins of enantioselectivity, are presented in Sections 3.4 and 3.6.



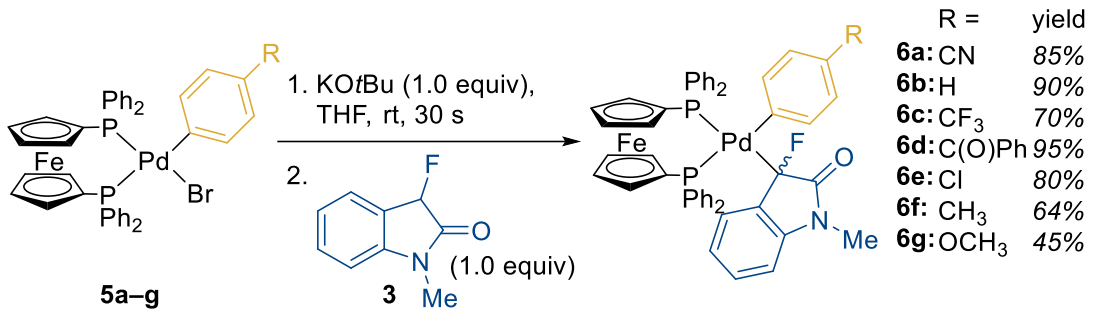
Scheme 3.2.2 Rate constants of epimerization and reductive elimination of complex **2a** as modeled by COPASI.[38] Rate constants are given in units of s^{-1}. Assignment of major and minor diastereomers of **2a** was based on DFT calculations (see Section 3.4).

3.3 Analysis of the Electronic Effect of the Eliminating Aryl Fragment

Because the rates of reductive elimination can depend on the electronic properties of the eliminating aryl group, causing the electronic properties to affect the relative rates for reductive elimination and epimerization, we also compared the rates of reductive elimination from **2b** and *para*-CN-substituted **2a**. Surprisingly, the formation of arylated **4b** from the complex containing the more electron-rich phenyl group (**2b**) occurred ~3 times faster than the formation of **4a** from the complex containing the more electron-poor 4-cyanophenyl group (**2a**). This difference is the opposite of that observed for the rates of reductive elimination from diphosphine-ligated arylpalladium complexes of nonfluorinated enolates and indeed most Pd-catalyzed reductive elimination reactions to form C–X bonds.[28] Such rates are generally faster for complexes containing more electron-poor aryl groups than for complexes containing more electron-rich aryl groups.[39–42] Two studies on the electronic effect of the aryl ligand on the rates of reductive elimination of arylpalladium(II) difluoromethyl[43] and difluoroenolate[44] complexes showed that reductive elimination occurs more rapidly from complexes containing more electron-donating aryl groups than from complexes containing less electron-donating aryl groups. Our data imply that this trend observed previously for two classes of fluoroalkyl complexes is general for a range of fluoroenolates.

In light of these results, we sought to explore further the influence of the electronic properties of the Pd-bound aryl group on the rates of reductive elimination in the absence of potentially competing stereoelectronic effects from the two diastereomers of the SEGPHOS-ligated complexes **2a**–**b**. To this end, we prepared a series of DPPF-ligated arylpalladium fluorooxindole complexes **6a–g** (DPPF = 1,1'-bis(diphenylphosphino)ferrocene). These complexes were prepared from analogous arylpalladium bromide complexes **5a–g** by a route analogous to that used to prepare SEGPHOS-ligated complexes **2a–b** (Scheme 3.3.1). The ^{19}F NMR spectra of complexes **6a–g** consist of a single doublet of doublets ($^3J_{F–P}$ = 110–112 Hz and 39–40 Hz) coupled to two doublets of doublets in the ^{31}P{^{1}H} spectra. These data indicate that the

enolates in these complexes are connected to the palladium center through the α-carbon of the enolate.



Scheme 3.3.1 Preparation of DPPF-ligated arylpalladium fluoroenolate complexes **6a–g**

We also unambiguously confirmed the α-C-bound connectivity of (4-cyanophenyl)palladium enolate complex **6a** in the solid state by single crystal X-ray diffraction (Figure 3.3.1). The Pd–C(aryl) bond of **6a** is slightly longer than Pd–C(aryl) bonds of previously reported DPPF-ligated arylpalladium fluoroenolate complexes (2.063(3) Å; literature: 2.051(2)–2.058(3) Å).[44] The Pd–C(enolate) bond (2.139(3) Å) of **6a** is longer than the Pd–C(enolate) bonds of mono- and difluoroester complexes (2.105(3) Å and 2.099(3) Å, respectively), but is shorter than that of a difluoroamide complex (2.188(3) Å).

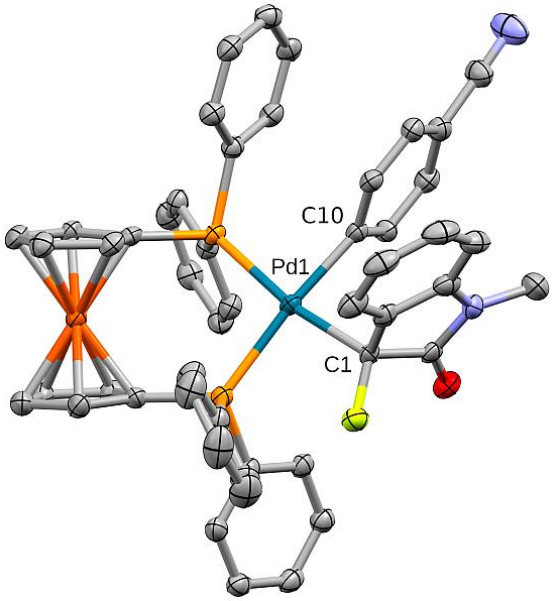


Figure 3.3.1 Thermal ellipsoid drawing of fluoroenolate complex **6a**. Ellipsoids are drawn at 50% probability, and hydrogens and crystallization solvent are omitted for clarity. Teal = Pd, light gray = C, blue = N, light green = F, light orange = P, dark orange = Fe. Selected bond lengths: Pd–C1, 2.139(3) Å; Pd–C10, 2.063(3) Å.

Heating the enolate complexes **6a–g** in C_6D_6 at 80 °C in the presence of PPh_3 afforded the corresponding arylated fluorooxindoles **4a–g** in quantitative yields. The reactions were monitored by quantitative inverse-gated $^{19}F\{^{31}P\}$ NMR spectroscopy, and the rate constants were determined from first-order exponential fits of product formation (see the SI for a table of rate constants). A

Hammett plot of the relative rates of reductive elimination *vs* the σ_p[45] substituent parameter of the R group on the aryl ring is shown in Figure 3.3.2. In contrast to previous studies on arylpalladium enolate complexes that did not contain fluorine,[28,42] the reductive elimination from fluoroenolate complexes **6a–g** containing more electron-donating aryl fragments were faster than those of complexes containing more electron-withdrawing aryl fragments (ρ = –1.0), with the electron-rich *para*-methyl-substituted complex **6f** reacting ~8 times faster than the electron-poor *para*-CF_3-substituted complex **6c**. This trend matches that observed for SEGPHOS-ligated complexes **2a–b** and that for the limited previous arylpalladium fluoroalkyl complexes shown to undergo reductive elimination[43,44] giving more evidence for the unusual effect of fluorine on the rates of reductive elimination.

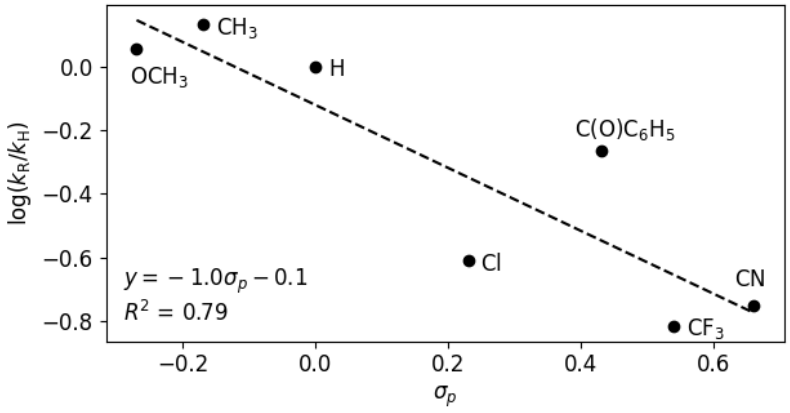


Figure 3.3.2 Hammett plot of the relative rates of thermolysis of complexes **6a–g** *vs* the σ_p parameter of the *para* substituent of the eliminating aryl group. See Table 3.8.1 in Section 3.8.3 for a list of rate constants.

To identify parameters that increase the linearity of the Hammett plot in Figure 3.3.2, we also constructed a composite substituent parameter $\bar{\sigma}$ by varying the inductive ("field") and resonance contributions of the R group on the aryl ligand (See Figure 3.8.8 and the preceding discussion). Such a treatment previously increased the linearity of the fits of the relative rates of reductive elimination reactions of arylpalladium amide,[39] thiolate,[40] and alkoxide complexes.[41,46] However, the optimal combination of field and resonance parameters ($\bar{\sigma}$ = 0.69 *F* + 0.31 *R*) only modestly increased the linearity (R^2 = 0.87) of the Hammett plot for reductive elimination from complexes **6a–g**.

3.4 Computational Modeling and the Origins of Enantioselectivity

DFT calculations of the energies of the α-C- and O-bound enolates of (*S*)-SEGPHOS-ligated arylpalladium fluoroenolate complexes **2a–b** are consistent with the observation of the C-bound connectivity in the ground state (Figure 3.4.1; see Section 3.8.5 for computational methods, structures, and energies). For both 4-cyanophenyl complex **2a** and phenyl complex **2b**, the free energy fo the diastereomer that affords the minor enantiomer (***pro*-(R)**) was found to be lower than that of the complex that affords the major enantiomer (***pro*-(S)**) for several functionals (ΔG = 0.83–1.3 kcal/mol; see Table 3.8.5). The energies of the energy-minimized O-bound isomers of

complexes **2a** and **2b** were calculated to be more than 4 kcal/mol higher than the energies of either of the two α-C-bound diastereomers. Consistent with the minor diastereomer forming the major enantiomer of the product, the free energy barriers to reductive elimination to form the major product enantiomers (*S*)-**4a** and (*S*)-**4b** from ***pro*-(*S*)-2a** and ***pro*-(*S*)-2b** were calculated to be 22.5 and 21.7 kcal/mol, respectively, while those to elimination to form the minor product enantiomers (*R*)-**4a** and (*R*)-**4b** were both calculated to be 26.2 kcal/mol. These computed barriers agree well with the experimentally determined rates of reductive elimination of **2a** ($\Delta G^{\ddagger}_{expt}$(***pro*-(*S*)-2a**) = 23.7 kcal/mol, $\Delta G^{\ddagger}_{expt}$(***pro*-(*R*)-2a**) = 26.6 kcal/mol) and support the faster rates of reductive elimination observed from phenyl complex **2b** than from 4-cyanophenyl complex **2a**.

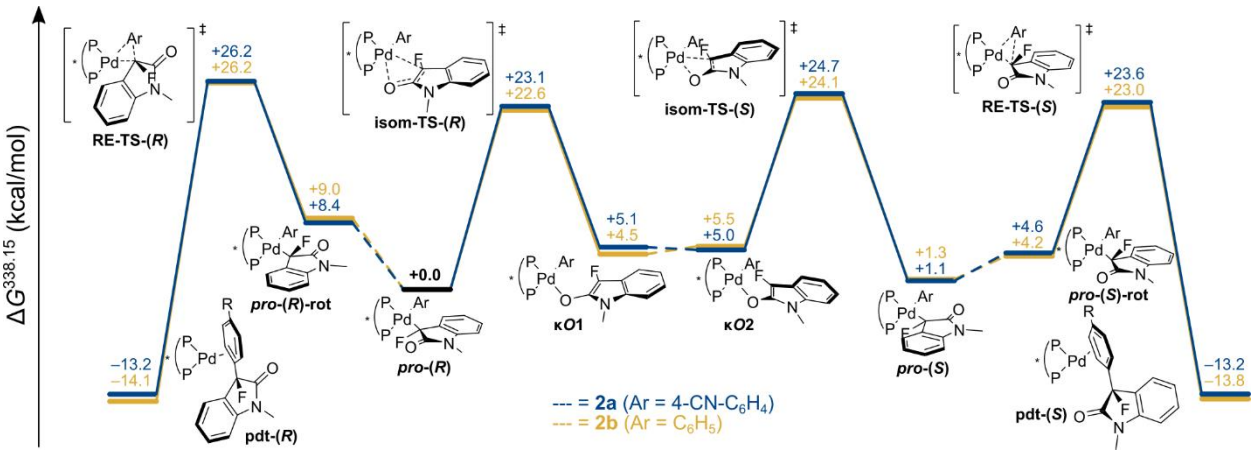


Figure 3.4.1 Energy coordinate diagram for the epimerization of and reductive elimination from (*S*)-SEGPHOS-ligated complexes **2a–b**. Free energies are given at 338.15 K in kcal/mol. See Section 3.8.5 for computational methods and structures.

The free energy barriers for the isomerization from the α-C-bound isomers ***pro*-(*R*)** and ***pro*-(*S*)** to the corresponding O-bound enolate isomers ***κO*1** and ***κO*2** were calculated to be 22–25 kcal/mol. These values are close to the calculated barriers for reductive elimination to form the major enantiomers of the products ((*S*)-**4a–b**) and are consistent with the comparable rates of epimerization and reductive elimination to form this enantiomer determined experimentally.[Note 2] Simulations were conducted to determine the *ee* values of α-aryl fluorooxindoles **4a** and **4b** that would result from the reaction of a 1:1 mixture of the corresponding diastereomeric complexes ***pro*-(*R*)-2a,b** and ***pro*-(*S*)-2a,b** with rate constants from the computed free-energy barriers of isomerization and reductive elimination. The simulated *ee* values were found to be 87% and 94% for **4a** and **4b**, respectively, which are well within error of the experimentally observed values of 93% and 95% (see Table 3.8.6 and the preceding discussion on the effects of the small differences in free energy barriers on this value). Altogether, these results support our conclusion that the reductive elimination step has the greatest influence on enantioselectivity and that the minor observed diastereomer forms the major enantiomer of the coupled product.

Further inspection of the calculated transition-state structures for reductive elimination revealed close contacts between the oxygen atom in the carbonyl of the fluorooxindole fragment and several aryl C–H bonds (r = 2.24–2.60 Å; R_{vdW}(O) + R_{vdW}(H)[47] = 2.62 Å). These contacts in the transition state to give the major product enantiomer (**RE-TS-(*S*)**; 2.24–2.33 Å; Figure 3.4.2a) were shorter than those in the transition state to give the minor enantiomer (**RE-TS-(*R*)**; 2.47–2.60 Å; Figure 3.4.2d). Zhou and co-workers previously proposed that such C(aryl)–H···O(carbonyl) interactions were stabilizing and responsible for the high enantioselectivities

observed in their Pd-catalyzed asymmetric arylation of silyl ketene acetals and enol ethers.[32,33]

To probe these close contacts further, we used Noncovalent Interaction (NCI) analysis.[48] This analysis reveals regions of a molecule engaged in noncovalent interactions when both the electron density ρ and the reduced density gradient $s = 1/(2(3\pi^2)^{1/3})|\nabla\rho|/\rho^{4/3}$ are near 0. NCI analysis further classifies these regions by the sign of the second eigenvalue λ_2 of the Hessian of ρ as stabilizing and bonding-like ($\lambda_2 < 0$, colored blue), destabilizing and nonbonded ($\lambda_2 > 0$, colored red), or due to van der Waals interactions ($\lambda_2 \approx 0$, colored green). regions with larger ρ are considered to represent stronger interactions and are represented visually by more saturated reds and blues.

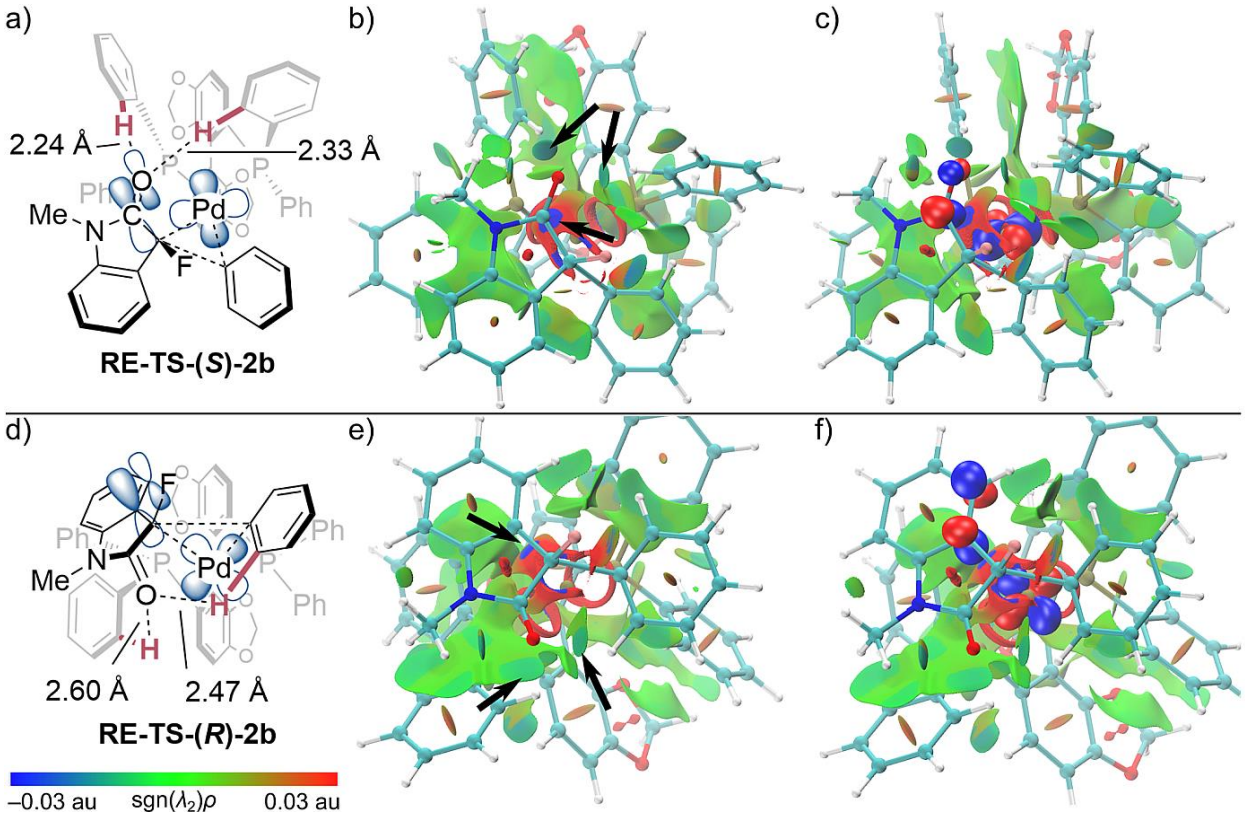


Figure 3.4.2 Schematics for the transition state structures (left), NCI plots (center), and overlays of the leading NBOS involved in the *d*(Pd) → π^* interactions (right) for a-c) **RE-TS-(*S*)-2b** and d-f) **RE-TS-(*R*)-2b**. NCI isosurfaces are drawn at $s = 0.05$ au excluding $\rho > 0.05$ au. Grid data were generated with Multiwfn 3.7[49] and visualized with VMD.[50] Black arrows highlight C(aryl)–H···O(carbonyl) and *d*(Pd) → π^* interactions. A higher resolution of this figure is available in the published manuscript.[51]

The NCI plots of structures **RE-TS-(*S*)** and **RE-TS-(*R*)** for phenylpalladium enolate complex **2b** (Figure 3.4.2b,e, respectively) display blue-green isosurfaces between the aforementioned C(aryl)–H bonds and the carbonyl oxygen atom of the fluorooxindole fragment, indicating attractive interactions. These interactions are more prominent (darker blue) in the transition state to give the major product enantiomer (**RE-TS-(*S*)-2b**) than in that to give the minor enantiomer (**RE-TS-(*R*)-2b**). While these differences may influence the relative stabilities of the two transition states, the NCI plots also reveal much more prominent, bonding-like interactions between the fluorooxindole fragment and the Pd center. In **RE-TS-(*S*)-2b**, this region is positioned

between the Pd center and the carbonyl carbon, while in **RE-TS-(*R*)-2b** it is positioned similarly between the Pd center and one of the carbons of the aryl ring of the fluorooxindole fragment. Notably, these regions were present in neither the starting nor final ground-state complexes (see Figure 3.8.37 and Figure 3.8.38). We hypothesized that these regions correspond to donor–acceptor interactions between *d* orbitals on the Pd center and the C=O* antibonding orbital of the carbonyl in the case of **RE-TS-(*S*)-2b** and a π^* orbital of the aryl ring in the case of **RE-TS-(*R*)-2b**. Because carbonyl groups are typically more electrophilic than aromatic rings, this interaction should be more stabilizing in **RE-TS-(*S*)-2b** than in **RE-TS-(*R*)-2b**.

To evaluate these hypotheses further, we analyzed the second-order Natural Bond Orbital (NBO) interactions of **RE-TS-(*S*)-2b** and **RE-TS-(*R*)-2b**.[52,53] Second-order NBO interactions quantitatively describe the electronic stabilization resulting from donation of electrons in an occupied NBO into another unoccupied NBO. Analysis of the donor–acceptor interactions between all (partially) occupied *d* orbitals of the Pd center and the NBO-localized fluorooxindole C=O* orbital (**RE-TS-(*S*)-2b**; Figure 3.4.2c) or the proximal C=C* orbital of the fluorooxindole aryl ring (**RE-TS-(*R*)-2b**; Figure 3.4.2f) revealed interaction energies of 8.7 and 3.4 kcal/mol, respectively. These energies are consistent with our hypothesis that the interaction is more stabilizing in the transition state to give the major product enantiomer than in that to give the minor product enantiomer.

This interaction is reflected further in the NAO-based Wiberg bond indices[54] (WBIs) between the Pd center and the relevant atoms of the π^* orbitals of the fluorooxindole fragment across the reaction coordinate (Figure 3.4.3, gold dotted line). As the reaction proceeds from the starting complexes ***pro*-(*S*)-rot-2b** and ***pro*-(*R*)-rot-2b**, the WBIs increase to maxima just after the transition state (WBI = 0.175 and 0.052 for **RE-TS-(*S*)-2b** and **RE-TS-(*R*)-2b**, respectively) and then decrease until they reach the product η^2-arene complexes **pdt-(*S*)-2b** and **pdt-(*R*)-2b**. Thus, these interactions arise exclusively in the transition state and are not present in the starting and product complexes. Taken together, these results strongly suggest that *d*(Pd) → π^* interactions are responsible for the stereoselectivity of the reductive elimination step in complexes **2a–b**.

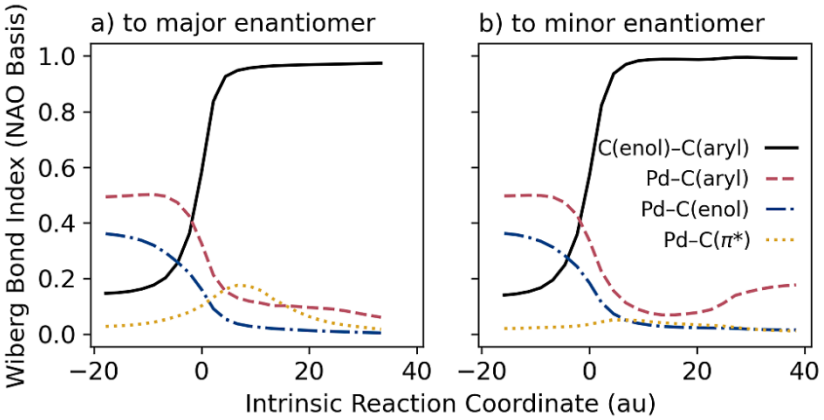
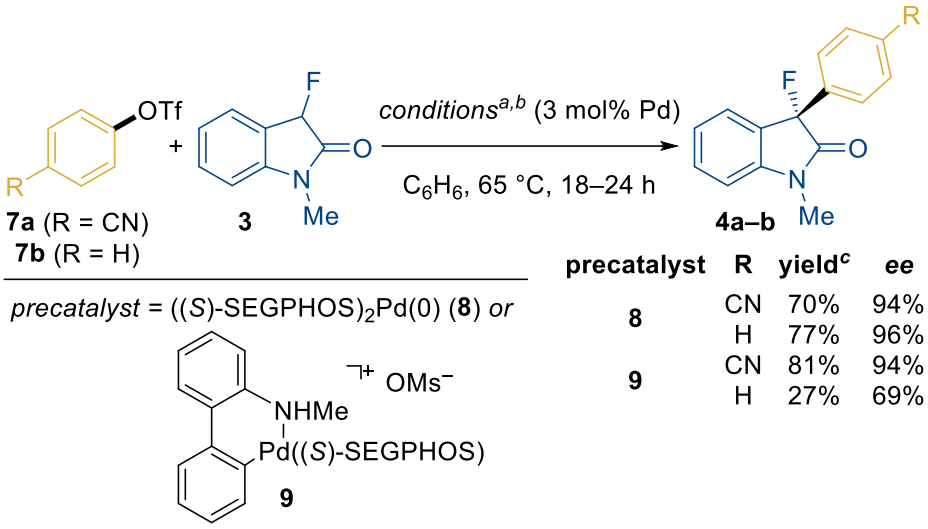


Figure 3.4.3 Wiberg bond indices across the intrinsic reaction coordinate for reductive elimination from **2b**. IRC = 0 corresponds to the transition state along the path. a) WBIs along the path to give the major product enantiomer (encountering **RE-TS-(*S*)-2b**). Pd–C(π^*) corresponds to the WBI between the Pd center and the C of the enolate C=O. b) WBIs along the path to give the minor product enantiomer (encountering **RE-TS-(*R*)-2b**). Pd–C(π^*) corresponds to the WBI between the Pd center and the nearest C of the phenyl ring of the fluorooxindole fragment. The rising Pd–

C(aryl) WBI near the end of the reaction coordinate corresponds to the formation of the product η^2-arene complexes **pdt-(*R*)-2b**.

3.5 Kinetic Analysis of the Catalytic Reaction

Having demonstrated that (*S*)-SEGPHOS-ligated fluoroenolate complexes **2a** and **2b** undergo reductive elimination to form α-arylated products in high yields and enantioselectivities, we sought to assess the intermediacy and potential accumulation of these complexes in the catalytic coupling reactions of aryl triflates **7a** and **7b** and fluorooxindole **3** with K_3PO_4 as a base (Scheme 3.5.1). When ((*S*)-SEGPHOS)$_2$Pd(0) (**8**) was used as the catalyst precursor, the enantioselectivities of the arylations with aryl triflates **7a** and **7b** (94% and 96%, respectively) matched those obtained for the stoichiometric reductive elimination reactions from **2a** and **2b** (*vide supra*).



precatalyst	R	yield[c]	ee
8	CN	70%	94%
	H	77%	96%
9	CN	81%	94%
	H	27%	69%

Scheme 3.5.1 Catalytic arylation of **3** with aryl triflates. [a]Aryl triflate (0.100 mmol), **3** (0.200 mmol), K_3PO_4 (0.300 mmol), **8** (0.0030 mmol), (*S*)SEGPHOS (0.0015 mmol). [b]Aryl triflate (0.100 mmol), **3** (0.200 mmol), K_3PO_4 (0.300 mmol), **9** (0.0030 mmol), 2,6-lutidine (0.018 mmol). [c]Yields determined by quantitative ^{19}F NMR spectroscopy.

Phenylpalladium fluoroenolate complex **2b** was not detected by $^{19}F\{^{31}P\}$ or $^{31}P\{^1H\}$ NMR spectroscopy in an aliquot of the reaction mixture of the arylation of fluorooxindole **3** with phenyl triflate (**7b**) catalyzed by *bis*-(*S*)-SEGPHOS-ligated Pd(0) complex **8** after 1 h (~4% conversion). Instead, complex **8** and free SEGPHOS were the only phosphine-containing species detected in solution by $^{31}P\{^1H\}$ NMR spectroscopy (see Section 3.8.4). This result suggests that ligand dissociation to form (SEGPHOS)Pd(0) or the subsequent oxidative addition of aryl triflate is the turnover-limiting step of the catalytic reaction when **8** is used as the precatalyst.

To probe this hypothesis further, we measured the initial rates of formation of arylated product **4b** while systematically varying the initial concentrations of each component. As shown in Figure 3.5.1, the catalytic coupling reaction was first-order in the concentrations of precatalyst **8** and aryl triflate **7b**, zero-order in the concentration of fluorooxindole **3**, and inverse order in the concentration of added (*S*)-SEGPHOS. These reaction orders are consistent with turnover-limiting oxidative addition after reversible dissociation of the diphosphine. Moreover, the initial rates of formation of product **4b** were slower than the initial rate that would be observed if reductive

elimination from phenylpalladium fluoroenolate complex **2b** were the turnover-limiting step of the reaction (hypothetical $k_{init,RE} = 1.2\times10^{-5}$ M·s^{-1} with 3.0 mol% **2b**). Thus, complex **2b** is kinetically competent to be an intermediate in the formation of **4b** under catalytic conditions, but does not accumulate in the catalytic reaction under these conditions.

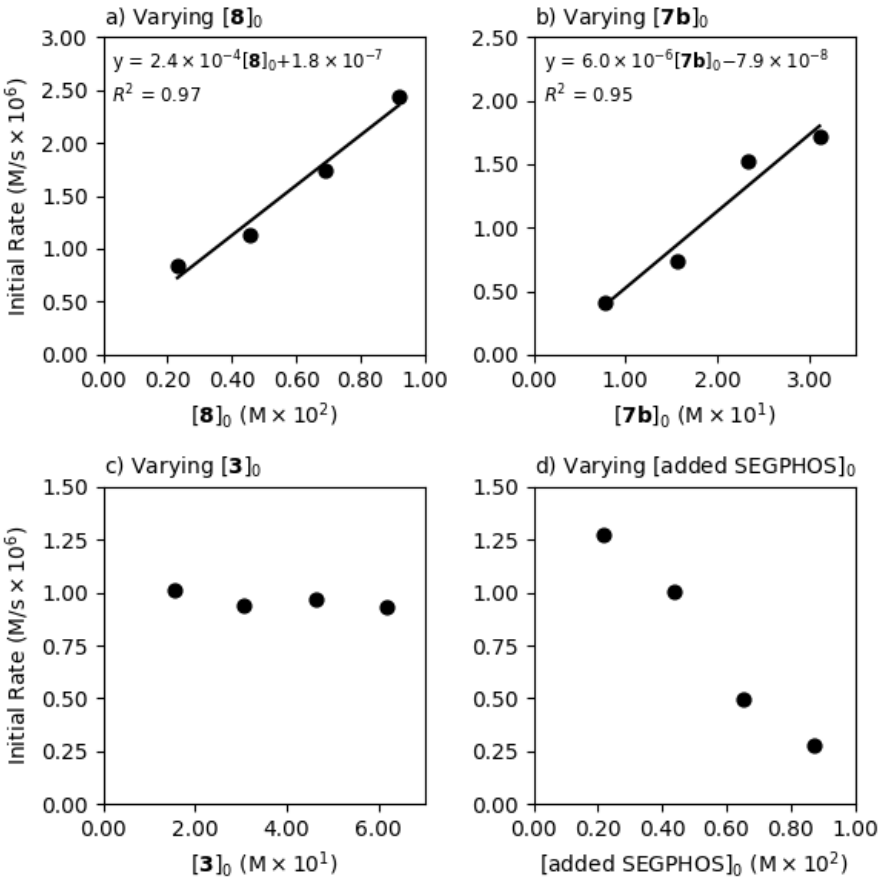


Figure 3.5.1 Initial rates of the reaction of phenyl triflate (**7b**) with fluorooxindole **3** catalyzed by ((*S*)-SEGPHOS)$_2$Pd(0) (**8**) *vs* varying initial concentrations of a) precatalyst **8**; b) aryl triflate **7b**; c) fluorooxindole **3**; and d) added (*S*)-SEGPHOS. Baseline conditions: **7b** (0.100 mmol, 0.153 M), **3** (0.200 mmol), K_3PO_4 (0.300 mmol), **8** (3.0 mol%), (*S*)-SEGPHOS (1.5 mol%). See Section 3.8.4 for details.

In contrast to phenyl complexes **2b**, the 4-cyanophenyl complex **2a** was detected in the reaction of electron-deficient 4-cyanophenyl triflate (**7a**) with Pd(0) complex **8** as the precatalyst (~50% of the loading of **8** as determined by quantitative $^{19}F\{^{31}P\}$ NMR spectroscopy). *Bis*-(*S*)-SEGPHOS complex **8** was also detected in the $^{31}P\{^{1}H\}$ spectrum of this reaction. We hypothesized that the different resting states for the reactions of aryl triflates **7a** and **7b** resulted from the faster oxidative addition of electron-deficient 4-cyanophenyl triflate (**7a**) than that of more electron-rich phenyl triflate (**7b**). While the oxidative addition step in the reaction of the more electron-rich aryl triflate **7b** was slow enough relative to the reductive elimination from the intermediate complex **2b** that oxidative addition was the turnover-limiting step in the catalytic reaction, the oxidative addition step in the reaction of the more electron-deficient aryl triflate **7a** was fast enough to be competitive with reductive elimination from the intermediate fluoroenolate complex **2a**, leading

to the observation of both the palladium(0) complex **8** and the fluoroenolate **2a** in the reaction of **7a**.

We reasoned that maintaining a 1:1 ratio of SEGPHOS and Pd would mitigate the accumulation of the *bis*-(*S*)-SEGPHOS Pd(0) complex **8** and facilitate the oxidative addition step, thereby causing reductive elimination from the fluoroenolate complex **2a** to be the turnover-limiting step in the catalytic reaction of 4-cyanophenyl triflate (**7a**). After some experimentation, we found that fluoroenolate complex **2a** was the dominant phosphine-containing species in solution for the reaction of **7a** with fluorooxindole **3**, as determined by $^{31}P\{^{1}H\}$ NMR spectroscopy, when the (*S*)-SEGPHOS-ligated palladacycle **9** was used as the precatalyst (see Section 3.8.4 for details).

Analysis of the initial rates of formation of α-aryl-oxindole **4a** during the reaction of 4-cyanophenyl triflate (**7a**), fluorooxindole **3**, and precatalyst **9** revealed a zero-order dependence of the rate of the catalytic reaction on the concentrations of aryl triflate **7a** and fluorooxindole **3** and a first-order dependence on the concentration of precatalyst **9**, consistent with turnover-limiting reductive elimination from the resting-state fluoroenolate complex **2a** (Figure 3.5.2). The k_{obs} determined from a plot of the initial rates of formation of arylated product **4a** *vs* the loading of precatalyst **9** was 6.9×10^{-4} s^{-1}, which is close to the observed rate constant for reductive elimination from **2a** measured in the stoichiometric experiments (8.6×10^{-4} s^{-1}, see Section 3.2).[*Note 3*] The *ee* value of the resulting arylated product **4a** was also 94%, which matches that obtained from the thermolysis of **2a** or in reactions catalyzed by ((*S*)-SEGPHOS)$_2$Pd(0) (**8**). Taken together, these results directly implicate arylpalladium fluoroenolate complexes **2a** and **2b** as the species that form the C–C bond and control enantioselectivity during the formation of **4a** and **4b** under catalytic conditions.[*Note 4*]

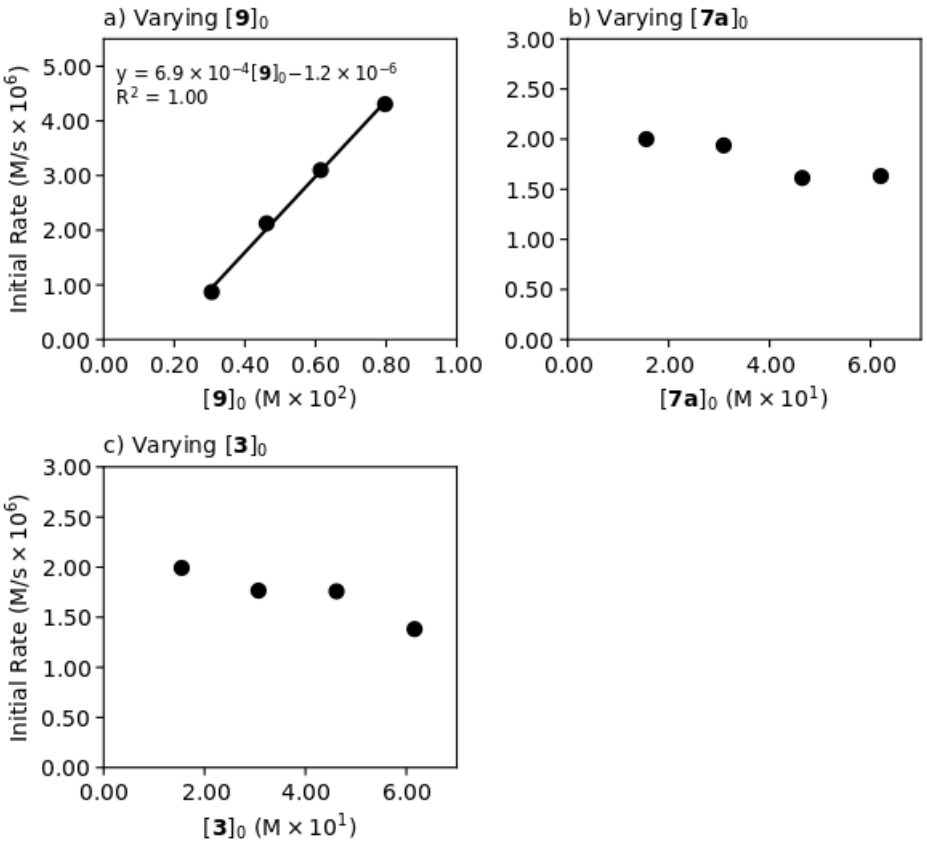


Figure 3.5.2 Initial rates of the reaction of aryl triflate **7a** with fluorooxindole **3** catalyzed by precatalyst **9** *vs* varying initial concentrations of a) precatalyst **9**; b) aryl triflate **7a**; and c) fluorooxindole **3**. Baseline conditions: **7a** (0.100 mmol, 0.153 M), **3** (0.200 mmol), K_3PO_4 (0.300 mmol), **9** (3.0 mol%), and 2,6-lutidine (12 mol%). See Section 3.8.4 for more details.

3.6 Conclusions

In summary, we have prepared a series of diphosphine-ligated arylpalladium *α*-C-bound fluorooxindole complexes, including two complexes bearing (*S*)-SEGPHOS as the ancillary ligand, that begin to reveal the origins of enantioselectivity in the enantioselective *α*-arylation of carbonyl compounds. These complexes undergo reductive elimination to form *α*-aryl-*α*-fluorooxindoles in quantitative yields. The SEGPHOS-ligated arylpalladium fluorooxindole complexes **2a–b** formed the coupled products with *ee* values that matched those obtained in the Pd-catalyzed coupling of aryl triflates with fluorooxindole **3**, and **2a** was directly observed in the crude catalytic reaction mixture. These experiments established the relevance of these complexes to catalysis and the origins of enantioselectivity. Epimerization between the two diastereomers of the SEGPHOS-ligated complexes was observed directly and was shown to be faster than reductive elimination, demonstrating that the enantioselectivity of the reaction is chiefly determined by the relative rates of reductive elimination from the two diastereomers. Computational analyses suggest that the difference in energy between the two diastereomeric transition states to reductive elimination is due to interactions between the carbonyl oxygen atom of the fluorooxindole fragment with the aryl C–H bonds of the SEGPHOS ligand, as well as donor–acceptor interactions between the Pd center and π^* orbitals of the fluorooxindole fragment.

Given that arylpalladium fluoroalkyl complexes undergo reductive elimination more slowly than their nonfluorinated counterparts,[28,37] two scenarios for the enantioselective arylation of nonfluorinated enolates are possible in light of the current work. First, if the difference in the rate of the isomerization between the O- and C-bound forms of the fluorinated and nonfluorinated enolate complexes is similar or greater than the difference in the rate of reductive elimination of the two types of complexes, then reductive elimination would remain the principal determined of enantioselectivity. In this case, enantioselectivities from the arylations of nonfluorinated enolates could be enhanced by designing systems to facilitate the aforementioned C–H···O and $d(\text{Pd}) \rightarrow \pi^*$ interactions. If isomerization between the O- and C-bound forms of the nonfluorinated enolates is significantly *slower* than reductive elimination, then the formation of the diastereomeric enolate complexes would control enantioselectivity, and factors to form one C-bound diastereomer over the other would need to be developed. To this end, increasing the size of the substituent on the α-carbon while maintaining its electron-withdrawing nature could enable the observation of both C-bound and O-bound arylpalladium enolate species and the measurement of the rates of conversion among them. Studies to assess the relationship of these conclusions to the reactions of enolates lacking fluorine and to design further enantioselective fluoroalkylations are in progress.

3.7 Footnotes

1. In the case of CN-substituted complex **2a**, the fact that equilibration is slow enough to observe over the course of the thermolysis reaction means that the reaction is not governed by traditional Curtin-Hammett kinetics, which require a fast equilibrium between diastereomers. However, the barriers to reductive elimination remain the most significant driver of enantioselectivity. See Section 3.8.3 for a more kinetic detailed treatment.
2. The higher calculated barrier of isomerization from ***pro*-(*S*)-2a** to ***pro*-(*R*)-2a** relative to the barrier of reductive elimination from ***pro*-(*S*)-2a** is within the error typically expected for DFT calculations. See Section 3.8.5 for a comparison of different functionals.
3. The negative intercept of the plot of initial rate vs [**9**] (Figure 10a) is likely due to instability of the intermediate arylpalladium triflate complexes or trace impurities in the starting materials, as suggested by the slightly downward-trending rates with increasing loadings of **7a** and **3** (Figure 10b–c).
4. Unfortunately, when palladacycle **9** was used as a precatalyst for the catalytic reaction of phenyl triflate (**7b**) with fluorooxindole **3**, the yield and *ee* of arylated product **4b** were significantly lower than those from the same reaction using Pd(0) complex **8** as the precatalyst or from thermolysis of (*S*)-SEGPHOS-ligated arylpalladium enolate complex **2b**. We hypothesize the unstable putative arylpalladium triflate complex formed by oxidative addition of **7b** to the unsaturated complex ((*S*)-SEGPHOS)Pd(0) decomposed at the start of the reaction before a sufficient amount of deprotonated **3** could be generated to quench it.

3.8 Supplementary Experimental Information

3.8.1 General Experimental Procedures and Reagent Availability

All manipulations were conducted under inert atmosphere in a nitrogen-filled glovebox equipped with oxygen and water sensors (working levels ≤ 5 ppm and 0.5 ppm, respectively) and a low-temperature refrigeration unit (–35 °C) unless otherwise noted. All glassware was flame-

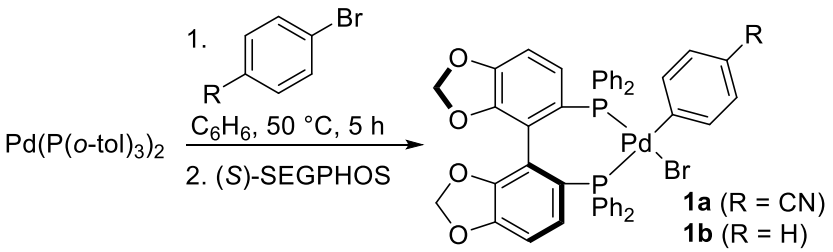
dried or dried overnight at 120 °C, allowed to cool under vacuum, and stored in a N_2-atomsphere drybox until use unless otherwise noted. Tetrahydrofuran, toluene, and diethyl ether were purified by passing the degassed solvents (N_2) through a column of activated alumina (solvent purification system purchased from Innovative Technologies, Newburyport, MA). Tetrahydrofuran was further dried for a week over activated 4 Å molecular sieves. $CDCl_3$ and C_6D_6 were purchased from Cambridge Isotope Laboratories. $CDCl_3$ was used as received. C_6D_6 was dried for 2 d over activated 4 Å molecular sieves, thrice degassed (freeze-pump-thaw under N_2), and stored over a fresh batch of activated molecular sieves under N_2. 1,1'-bis(diphenylphosphino)ferrocene (DPPF), (*S*)-SEGPHOS, and phenyl triflate were purchased from TCI. *N*-methyl-3-fluorooxindole (**3**),[55] *N*-methyl-2-aminobiphenylpalladium methanesulfonate,[56] *bis*(tri(2-methylphenyl)phosphine)palladium(0) (Pd(P(*o*-tol)$_3$)$_2$),[57] and 4-cyanophenyltriflate (**7a**)[58] were prepared according to literature procedures. All other materials were purchased from commercial suppliers and used as received. Unless otherwise specified, all manipulations were carried out in a nitrogen-atmosphere drybox (O_2 < 5 ppm, H_2O < 0.5 ppm).

NMR spectra were acquired on 400, 500, 600, and 700 MHz Bruker instruments at the College of Chemistry's NMR facility at the University of California, Berkeley. NMR spectra were processed with MestreNova >11.0 (Mestrelab Research SL). Chemical shifts are reported in ppm and referenced to residual (in deuterated solvents) or bulk (in non-deuterated solvents) solvent signals ($CDCl_3$: 7.26 ppm for ^{1}H; C_6D_6: 7.16 ppm for ^{1}H; 2.05 ppm for ^{1}H), relative to an internal standard (4,4'-difluorobiphenyl, –115.92 ppm for ^{19}F, determined relative to the chemical shift of $C_6H_5CF_3$ [–62.74 ppm][59] in C_6D_6), or relative to an external standard (TMP, 3.0 pm for ^{31}P). Coupling constants are reported in Hz. For NMR spectra collected at non-ambient temperatures, the temperature of the probe was calibrated before acquisition according to the spectral distance between the peaks of a standard 80% glycol/DMSO-d_6 sample. Quantitative ^{19}F and ^{19}F{^{31}P} spectra were acquired by first calibrating the 90° pulse of the analyte and setting the interscan delay as to 20 s, a value >5× the T_1 value of all signals of interest. Quantitative ^{19}F{^{31}P} spectra were acquired with inverse-gated decoupling to prevent NOE enhancement of the signals of interest.

Elemental analyses were conducted at the Microanalysis Laboratory at the University of California, Berkeley. HR-MS analyses were conducted at the QB3/Chemistry Mass Spectrometry Facility at the University of California, Berkeley, or at the Lawrence Berkeley National Lab Catalysis Laboratory. Single-crystal X-ray diffraction experiments were performed by Nicholas Settineri at the Small Molecular X-ray Crystallography Facility.

3.8.2 Synthetic Methods

*Preparation of (S)-SEGPHOS-ligated arylpalladium bromide complexes **1a–b***



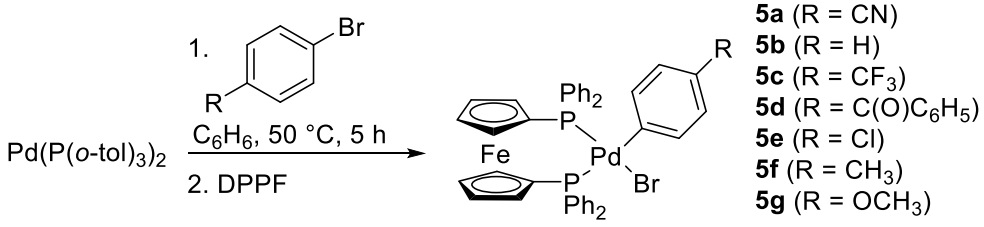
The following procedure was adapted from the literature.[13] To a 4 mL vial was added

bis(tri(2-methylphenyl)phosphine)palladium(0)[57] (75.0 mg, 0.105 mmol, 1.00 equiv), the corresponding aryl bromide (0.525 mmol, 5.00 equiv), benzene (3.0 mL), and a magnetic stir bar. The vial was sealed with a Teflon-lined cap, removed from the glove box, and the suspension was stirred at 50 °C for 5 h. During this time, the reaction mixture either clarified to a light-yellow solution (R = H) or formed a white precipitate (R = CN). The reaction mixture was allowed to cool to room temperature and returned to the glove box. (*S*)-SEGPHOS (64.5 mg, 0.107 mmol, 1.01 equiv) was added as a solid, and the mixture was stirred at room temperature for 1 h. The reaction mixture then was transferred to a 20 mL vial with the aid of 0.5 mL diethyl ether, and was concentrated to ~150 μL under vacuum. Diethyl ether (5 mL) was added, and the mixture was stirred vigorously for 20 min. The light-yellow precipitate that formed was collected by vacuum filtration on a fine frit, washed 3 times with 1.5 mL diethyl ether and once with 2 mL hexane. The collected solid was dried under high vacuum overnight to afford the corresponding arylpalladium bromide complexes as light-yellow solids.

1a: 65.1 mg, 69% yield.
^{1}H ((CD$_3$)CO, 400 MHz): δ 8.04–7.85 (m, 4 H), 7.70–7.61 (m, 2 H), 7.59–7.38 (m, 11 H), 7.26–7.07 (m, 6 H), 6.83 (dd, *J* = 8.3, 2.3 Hz, 2 H), 6.65 (dd, *J* = 8.3, 1.5 Hz, 1 H), 6.44 (dd, *J* = 8.2, 1.2 Hz, 1 H), 6.24 (t, *J* = 9.2 Hz, 1 H), 5.91 (s, 1 H), 5.89 (s, 1 H), 5.85 (s, 1 H), and 5.64 (s, 1 H).
^{31}P{^{1}H} (CDCl$_3$, 162 MHz): δ 25.8 (d, *J* = 42.0 Hz) and 11.6 (d, *J* = 42.0 Hz) ppm.
Anal. Calcd. for $C_{45}H_{32}BrNO_4P_2Pd$: C, 60.12; H, 3.59; N, 1.56; Found: C, 60.10; H 3.64; N 1.71.

1b: 62.0 mg, 68% yield.
^{1}H (C$_6$H$_6$, 600 MHz): δ 8.25 (apt t, *J* = 8.9 Hz, 2 H), 8.04–7.97 (m, 2 H), 7.97–7.87 (m, 4 H), 7.34–7.28 (m, 2 H), 7.20–7.07 (m, 3 H), 7.03–6.95 (m, 2 H), 6.94–6.90 (m, 3 H), 6.89–6.83 (m, 4 H), 6.78–6.72 (m, 4 H), 6.39 (t, *J* = 8.6 Hz, 1 H), 6.19 (dd, *J* = 8.2, 1.4 Hz, 1 H), 5.97 (d, *J* = 8.1 Hz, 1 H), 5.29–5.24 (m, 2 H), 5.10 (d, *J* = 1.5 Hz, 1 H), and 4.96 (d, *J* = 1.6 Hz, 1 H) ppm
^{31}P{^{1}H} (CDCl$_3$, 162 MHz): δ 26.1 (d, *J* = 43.8 Hz) and 10.61 (d, *J* = 44.0 Hz) ppm
Anal. Calcd. for $C_{44}H_{33}BrO_4P_2Pd$: C, 60.47; H, 3.81; Found: C, 60.58; H, 4.10.

*Preparation of DPPF-ligated arylpalladium bromide complexes **5a–g***



To a 4 mL vial was added *bis*(tri(2-methylphenyl)phosphine)palladium(0)[57] (75.0 mg, 0.105 mmol, 1.00 equiv), the corresponding aryl bromide (0.525 mmol, 5.00 equiv), benzene (3.0 mL), and a magnetic stir bar. The vial was sealed with a Teflon-lined cap, removed from the glove box, and the suspension was stirred at 50 °C for 5 h. The reaction mixture was allowed to cool to room temperature and returned to the glove box. 1,1'-bis(diphenylphosphino)ferrocene (DPPF, 58.7 mg, 0.107 mmol, 1.01 equiv) was added as a solid, and the mixture was stirred at room temperature for 1 h. The reaction mixture then was transferred to a 20 mL vial with the aid of 0.5 mL diethyl ether, and was concentrated to ~150 μL under vacuum. Diethyl ether (5 mL) was added, and the mixture was stirred vigorously for 20 min. The yellow-orange precipitate formed thereby was collected by

vacuum filtration on a fine fritted glass funnel, washed 3× with 1.5 mL diethyl ether and 1× with 2 mL hexane, and the collected solid was dried on high vacuum overnight to afford the corresponding arylpalladium bromide complexes as yellow or yellow-orange solids.

5a: 75.7 mg, 85.6% yield.
Spectroscopic characterization matched that reported in the literature.[60]
^{1}H ($CDCl_3$, 400 MHz): δ 8.08 – 7.97 (m, 4 H), 7.54 – 7.45 (m, 6 H), 7.40 – 7.30 (m, 6 H), 7.19 – 7.08 (m, 6 H), 6.80 (d, *J* = 7.8 Hz, 2 H), 4.70 (s, 2 H), 4.53 (s, 2 H), 4.17 (s, 2 H), and 3.61 (s, 2H) ppm.
^{31}P{^{1}H} ($CDCl_3$, 162 MHz): δ 30.3 (d, *J* = 31.6 Hz) and 10.0 (d, *J* = 31.6 Hz) ppm.

5b: 66.2 mg, 77.2% yield.
Spectroscopic characterization matched that reported in the literature.[60]
^{1}H ($CDCl_3$, 500 MHz): δ 8.11 – 8.01 (m, 4 H), 7.50 – 7.43 (m, 6 H), 7.37 (d, *J* = 7.7 Hz, 2 H), 7.35 (d, *J* = 7.9 Hz, 2 H), 7.29 (t, *J* = 7.4 Hz, 2 H), 7.12 (td, *J* = 7.9, 3.9 Hz, 4 H), 6.95 (td, *J* = 7.8, 2.8 Hz, 2 H), 6.56 (td, *J* = 7.6, 2.5 Hz, 2 H), 6.49 (t, *J* = 7.2 Hz, 1 H), 4.67 (s, 2 H), 4.48 (s, 2 H), 4.14 (s, 2 H), and 3.63 (s, 2H) ppm.
^{31}P{^{1}H} ($CDCl_3$, 202 MHz): δ 30.1 (d, *J* = 33.8 Hz) and 8.68 (d, *J* = 33.8 Hz) ppm.

5c: 65.8 mg, 70.8% yield.
Spectroscopic characterization matched that reported in the literature.[60]
^{1}H ($CDCl_3$, 400 MHz): δ 8.10 – 8.01 (m, 4 H), 7.51 – 7.45 (m, 6 H), 7.40 – 7.28 (m, 6 H), 7.16 – 7.07 (m, 6 H), 6.77 (d, *J* = 7.8 Hz, 2 H), 4.70 (apt q, *J* = 2.1 Hz, 2 H), 4.51 (s, 2 H), 4.16 (s, 2 H), and 3.63 (apt q, *J* = 1.9 Hz, 2 H) ppm.
^{19}F ($CDCl_3$, 376 MHz): δ –61.2 ppm.
^{31}P{^{1}H} ($CDCl_3$, 162 MHz): δ 33.3 (d, *J* = 32.6 Hz) and 9.5 (d, *J* = 33.0 Hz) ppm.

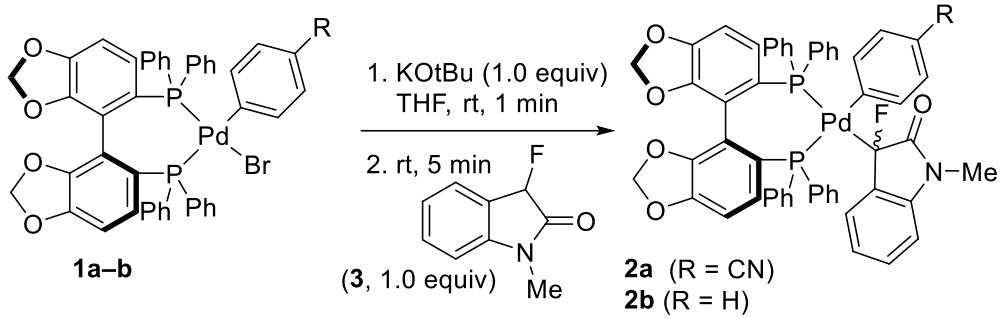
5d: 77.5 mg, 80.1% yield.
^{1}H ($CDCl_3$, 400 MHz): δ 8.12 – 8.00 (m, 4 H), 7.64 (d, *J* = 7.6 Hz, 2 H), 7.54 – 7.45 (m, 7 H), 7.44 – 7.29 (m, 8 H), 7.22 – 7.09 (m, 6 H), 7.04 (d, *J* = 7.0 Hz, 2 H), 4.71 (s, 2 H), 4.52 (s, 2 H), 4.16 (s, 2 H), and 3.62 (s, 2 H) ppm.
^{31}P{^{1}H} ($CDCl_3$, 162 MHz): δ 30.2 (d, *J* = 32.6 Hz) and 9.5 (d, *J* = 32. Hz) ppm.

5e: 61.3 mg, 69% yield.
^{1}H ($CDCl_3$, 400 MHz): δ 8.10 – 7.98 (m, 2H), 7.55 – 7.42 (m, 3H), 7.42 – 7.30 (m, 3H), 7.21 – 7.09 (m, 2H), 6.87 (t, *J* = 7.4 Hz, 1H), 6.56 (apt d, *J* = 7.2 Hz, 1H), 4.67 (s, 1H), 4.49 (s, 1H), 4.15 (s, 1H), and 3.64 (s, 1H) ppm.
^{31}P{^{1}H} ($CDCl_3$, 162 MHz): δ 30.1 (d, *J* = 32.3 Hz) and 9.42 (d, *J* = 32.5) ppm.

5f: 70.4 mg, 80.7% yield.
Spectroscopic characterization matched that reported in the literature.[61]
^{1}H ($CDCl_3$, 500 MHz): δ 8.11 – 8.01 (m, 4 H), 7.51 – 7.43 (m, 6 H), 7.40 – 7.28 (m, 6 H), 7.16 – 7.06 (m, 4 H), 6.79 (td, *J* = 8.1, 2.9 Hz, 2 H), 6.41 (d, *J* = 7.5 Hz, 2 H), 4.65 (s, 2 H), 4.47 (s, 2 H), 4.13 (s, 2 H), 3.65 (s, 2 H), and 2.00 (s, 3 H) ppm.
^{31}P{^{1}H} ($CDCl_3$, 202 MHz): 29.7 (d, *J* = 33.8 Hz) and 8.6 (d, *J* = 34.0 Hz) ppm.

5g: 59.1 mg, 66% yield. *NMR Spectra*
Spectroscopic characterization matched that reported in the literature.[60]
^{1}H ($CDCl_3$, 500 MHz): δ 8.11 – 8.00 (m, 4 H), 7.51 – 7.45 (m, 6 H), 7.40 – 7.33 (m, 4 H), 7.33–7.28 (m, 2 H), 7.13 (td, *J* = 7.8, 2.4 Hz, 4 H), 6.79 (td, *J* = 8.2, 2.6 Hz, 2 H), 6.26 (dd, *J* = 8.5, 1.8 Hz, 2 H), 4.66 (q, *J* = 2.1 Hz, 2 H), 4.47 (t, *J* = 2.0 Hz, 2H), 4.14 (t, *J* = 1.9 Hz), 3.65 (q, *J* = 1.8 Hz), and 3.56 (s, 3 H) ppm.
^{31}P{^{1}H} ($CDCl_3$, 202 MHz): δ 30.0 (d, *J* = 32.8 Hz) and 8.8 (d, *J* = 32.6 Hz) ppm.

*Preparation of ((S)-SEGPHOS)Pd(aryl)(fluorooxindole) complexes **2a–b***



To a rapidly stirring solution of the appropriate arylpalladium bromide **1** (0.030 mmol, 1.0 equiv) in THF (2.5 mL) was added potassium *tert*-butoxide in THF (300 μL, 0.10 M, 0.030 mmol, 1.0 equiv). The reaction mixture was allowed to stir for ~1 min at ambient temperature, during which time the solution darkened slightly. To the reaction mixture was then added *N*-methyl-3-fluorooxindole (**3**) in THF (300 μL, 0.10 M, 0.030 mmol, 1.0 equiv), and stirring was continued for another 5 min. The reaction mixture was then filtered through a syringe filter (VRW, PTFE < 0.2 μm), and the light-yellow solution was concentrated under vacuum to a thin film. This film was dissolved in benzene (~150 μL), and hexane (5 mL) was added to afford a yellow precipitate that was collected by vacuum filtration on a fine fritted glass funnel. The powder was washed with hexane (3×2 mL) and dried on high vacuum for 1 h to afford the product **2** as an inseparable mixture (~1:1) of diastereomers. Further purification of these compounds was hindered by their lack of thermal stability.

The purity of the solid thus obtained was determined by integrating the inverse-gated ^{19}F{^{31}P} NMR signals relative to a known amount of 4,4'-difluorobiphenyl as an internal standard.

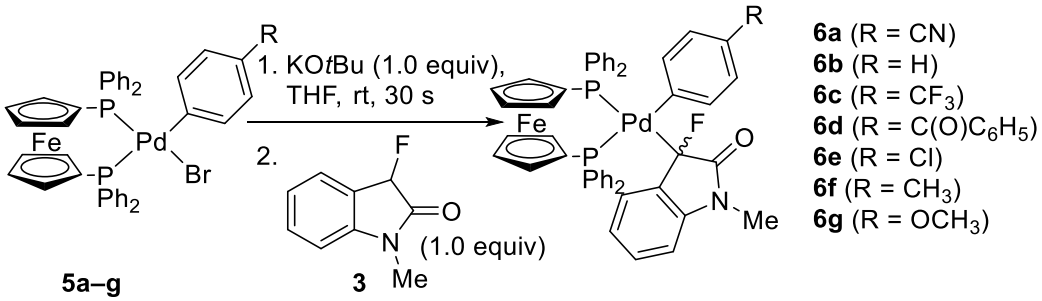
Complexes **2a–b** undergo slow decomposition at room temperature in solution (hours) and in the solid state (days) but were stored at –35 °C for 2 months without significant decomposition, as determined by ^{19}F NMR spectroscopy.

2a: Pale yellow powder, 19.1 mg, 56% yield (86% w/w), ~1:1 mixture of diastereomers.
Major diastereomer (upon heating):
^{1}H (C_6D_6, 600 MHz): δ 8.12 – 6.55 (m, 29H), 6.41 (dd, *J* = 8.1, 1.4 Hz, 1H), 6.04 (d, *J* = 8.2 Hz, 1H), 5.61 (d, *J* = 7.7 Hz, 1H), 5.24 (d, *J* = 1.8 Hz, 1H, SEGPHOS -OCH_2O-), 5.21 (d, *J* = 1.5 Hz, 1H, SEGPHOS -OCH_2O-), 4.97 (d, *J* = 1.5 Hz, 1H), 4.90 (d, *J* = 1.9 Hz, 1H), and 2.33 (s, 3H, fluorooxindole N–C*H*$_3$) ppm.
^{19}F (C_6D_6, 565 MHz): δ –157.7 (dd, $^{3}J_{F–P}$ = 112.1, 38.8 Hz) ppm.
^{31}P{^{1}H} (C_6D_6, 243 MHz): δ 19.1 (dd, $^{3}J_{P–F}$ = 38.9 Hz, $^{2}J_{P–P}$ = 31.5 Hz) and 17.9 (dd, $^{3}J_{P–F}$ = 112.1 Hz, $^{2}J_{P–P}$ = 31.6 Hz) ppm.

Minor diastereomer (upon heating):
^{1}H (C_6D_6, 600 MHz): δ 8.59 (d, *J* = 7.8 Hz, 1H), 8.57 (d, *J* = 7.7 Hz, 1H), 8.27 (t, *J* = 6.9 Hz, 1H), 8.13 – 6.54 (m, 25H), 6.36 – 6.29 (m, 1 H), 6.16 (dd, *J* = 8.3, 1.1 Hz, 1H), 6.09 (dd, *J* = 8.2, 1.1 Hz, 1H), 5.85 (d, *J* = 7.7 Hz, 1H), 5.27 (d, *J* = 1.7 Hz, 1H, SEGPHOS -OCH_2O-), 5.16 (d, *J* = 1.6 Hz, 1H, SEGPHOS -OCH_2O-), 5.14 (d, *J* = 1.7 Hz, 1H, SEGPHOS -OCH_2O-), 4.17 (d, *J* = 1.6 Hz, 1H, SEGPHOS -OCH_2O-), and 2.01 (s, 3H, fluorooxindole N–C*H*$_3$) ppm.
^{19}F (C_6D_6, 565 MHz): δ –155.4 (dd, $^3J_{F–P}$ = 112.6, 38.9 Hz) ppm.
^{31}P{^{1}H} (C_6D_6, 243 MHz): δ 19.9 (dd, $^3J_{P–F}$ = 112.4 Hz, $^2J_{P–P}$ = 33.0 Hz) and 15.8 (dd, $^3J_{P–F}$ = 38.5 Hz, $^2J_{P–P}$ = 32.6 Hz) ppm.

2b: Pale yellow powder, 22.7 mg, 65% yield (84% w/w), ~3:2 mixture of diastereomers.
The ratio of the diastereomers for **2b** changed over the course of acquisition of NMR spectra due to slow interconversion at room temperature.
Major diastereomer:
^{1}H (C_6D_6, 600 MHz): δ 8.21 – 6.63 (m, 29H), 6.56 (t, *J* = 8.4 Hz, 1H), 6.48 (dd, *J* = 8.1, 1.4 Hz, 1H), 6.00 (d, *J* = 8.2 Hz, 1H), 5.85 (d, *J* = 7.7 Hz, 1H), 5.27 (d, *J* = 1.9 Hz, 1H, SEGPHOS -OCH_2O-), 5.24 (apt s, 1 H, SEGPHOS -OCH_2O-), 5.08 (apt s, 1 H, SEGPHOS -OCH_2O-), 4.88 (d, *J* = 1.9 Hz, 1 H, SEGPHOS -OCH_2O-), and 2.48 (s, 3H, fluorooxindole N–C*H*$_3$) ppm.
^{19}F (C_6D_6, 565 MHz): δ –158.3 (dd, $^3J_{F–P}$ = 113.5, 38.6 Hz) ppm.
^{31}P{^{1}H} (C_6D_6, 243 MHz): δ 19.6 (dd, $^3J_{P–F}$ = 38.2 Hz, $^2J_{P–P}$ = 27.8 Hz) and 17.0 (dd, $^3J_{P–F}$ = 113.6 Hz, $^2J_{P–P}$ = 27.2 Hz) ppm.
Minor diastereomer:
^{1}H (C_6D_6, 600 MHz): δ 8.66 – 8.61 (m, 2H), 8.49 – 8.43 (m, 1H), 8.21 – 6.63 (m, 25H), 6.61 (t, *J* = 7.1 Hz, 1H), 6.36 – 6.30 (m, 1H), 6.15 (d, *J* = 8.3 Hz, 1H), 6.10 (d, *J* = 8.6 Hz, 1 H), 6.09 (d, *J* = 8.4 Hz, 1 H), 5.29 (d, *J* = 1.7 Hz, 1 H, SEGPHOS -OCH_2O-), 5.19 (d, *J* = 1.6 Hz, 1H, SEGPHOS -OCH_2O-), 5.15 (d, *J* = 1.8 Hz, 1H, SEGPHOS -OCH_2O-), 4.76 (apt s, 1H, SEGPHOS -OCH_2O-), and 2.18 (s, 3H, fluorooxindole N–C*H*$_3$) ppm.
^{19}F (C_6D_6, 565 MHz): δ –156.7 (dd, $^3J_{F–P}$ = 114.3, 38.9 Hz) ppm.
^{31}P{^{1}H} (C_6D_6, 243 MHz): δ 19.2 (dd, $^3J_{P–F}$ = 114.7 Hz, $^2J_{P–P}$ = 29.3 Hz) and 15.8 (dd, $^3J_{P–F}$ = 39.3 Hz, $^2J_{P–P}$ = 29.4 Hz) ppm

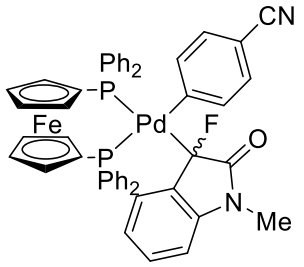
*Preparation of (DPPF)Pd(aryl)(fluorooxindole) complexes **6a–g***



To a rapidly stirring solution of the appropriate arylpalladium bromide **5** (0.0300 mmol, 1.00 equiv) in THF (2.5 mL) was added potassium *tert*-butoxide in THF (300 μL, 0.10 M, 0.030 mmol, 1.0 equiv). The reaction mixture was allowed to stir for ~1 min at ambient temperature, during which time the solution darkened from light yellow to orange. To the reaction mixture was

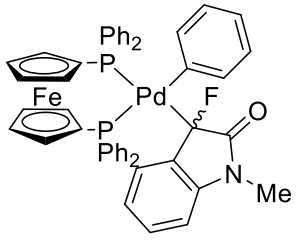
then added *N*-methyl-3-fluorooxindole (**3**) in THF (300 μL, 0.10 M, 0.030 mmol, 1.0 equiv), and stirring was continued for another 5 min. The reaction mixture was then filtered through a syringe filter (from VRW, PTFE, < 0.2 μm) into a 20 mL vial, and the light-yellow solution was concentrated under vacuum to a thin film. This film was dissolved in a minimal volume of toluene (100–300 μL), and the product complex **6** spontaneously began to crystallize upon standing at ambient temperature. The vial was cooled to –35 °C overnight to afford a yellow-orange precipitate. The mother liquor was carefully decanted, and the remaining solid was washed with hexane (3×1 mL) and dried overnight on high vacuum to afford a yellow-orange powder. The remaining toluene was removed by dissolving the powder in C_6H_6 and lyophilizing the solution under high vacuum to afford the product compound **6** as a yellow orange powder.

6a: Compound **6a** was prepared according to the general procedure and was further recrystallized from diethyl ether. Crystals suitable for XRD were obtained by allowing a saturated solution of **6a** in diethyl ether to stand at room temperature for 2 h. No, this was not intentional. Yellow-orange solid, 23.6 mg, 84.6% yield.



^{1}H NMR (600 MHz, C_6D_6): δ 8.91 (dd, *J* = 11 Hz, 7.7 Hz, 2 H), 8.07 (dd, *J* = 10.1, 8.3 Hz, 2 H), 7.70 (dd, 10.0 Hz, 8.3 Hz, 2 H), 7.53 (td, *J* = 7.8, 2.0 Hz, 2 H), 7.48 (t, *J* = 7.1 Hz, 1 H), 7.32–7.22 (m, 3 H), 7.19 (t, *J* = 7.6 Hz, 1 H), 6.96–6.87 (m, 5 H), 6.84–6.74 (m, 4 H), 6.70 (td, *J* = 7.7, 2.4 Hz, 2 H), 6.54 (dd, *J* = 7.7, 2.0 Hz, 1 H), 6.20 (dt, *J* = 7.9, 2.0 Hz, 1 H), 5.99 (t, *J* = 7.0 Hz, 1 H), 5.63 (d, *J* = 7.6 Hz), 4.60 (s, 1 H, ferrocenyl C–*H*), 4.12 (s, 1 H, ferrocenyl C–*H*), 4.08 (s, 1 H, ferrocenyl C–*H*), 3.87 (s, 1 H, ferrocenyl C–*H*), 3.81 (s, 1 H, ferrocenyl C–*H*), 3.69 (s, 1 H, ferrocenyl C–*H*), 3.54 (s, 1 H, ferrocenyl C–*H*), 3.45 (s, 1H, ferrocenyl C–*H*), and 2.07 (s, 3 H, N–C*H*$_3$) ppm.
^{19}F NMR (565 MHz, C_6D_6): δ –158.1 (dd, $^3J_{F–P}$ = 109.9, 39.6 Hz, 1 F) ppm.
^{31}P{^{1}H} NMR (243 MHz, C_6D_6): δ 20.8 (dd, $^3J_{P–F}$ = 39.4 Hz, $^2J_{P–P}$ = 27.3 Hz, 1 P) and 15.1 (dd, $^3J_{P–F}$ = 109.6 Hz, $^2J_{P–P}$ 27.0 Hz, 1 P) ppm.
Anal Calc'd for $C_{50}H_{39}FFeN_2OP_2Pd$: C, 64.78; H: 4.24; N: 3.02; Found: C, 64.54; H, 4.38; N: 2.74.

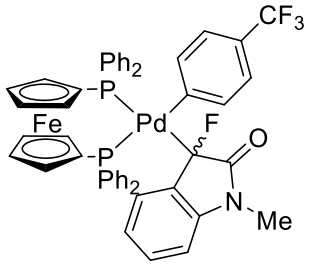
6b: Compound **6b** was prepared according to the general procedure and was recrystallized from toluene a second time. Yellow solid, 24.3 mg, 89.8% yield.



^{1}H NMR (600 MHz, C_6D_6): δ 9.00 (ddt, *J* = 10.8, 8.1, 1.4 Hz, 2 H), 8.14 (ddt, *J* = 9.6, 8.0, 1.2 Hz, 2 H), 7.87–7.79 (m, 2 H), 7.60 (ddt, *J* = 7.8, 6.5, 1.4 Hz, 1 H), 7.56 (td, *J* = 7.8, 2.0 Hz, 2 H), 7.30

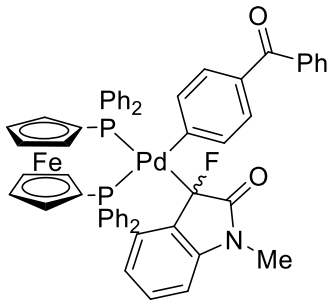
(td, *J* = 7.8, 2.0 Hz, 2 H), 7.27 (tdd, *J* = 7.4 Hz, 2.9, 1.2 Hz, 1 H), 7.20 (tq, *J* = 7.2, 1.4 Hz, 1 H), 7.06 (d, *J* = 7.1 Hz, 1 H), 7.01–6.95 (m, 3 H), 6.94–6.90 (m, 3 H), 6.87–6.81 (m, 2 H), 6.75 (td, *J* = 7.7, 2.2 Hz, 2 H), 6.55 (tt, *J* = 7.4, 1.9 Hz, 1 H), 6.40 (t, *J* = 7.2 Hz, 1 H), 6.18 (tt, *J* = 7.3, 1.9 Hz, 1 H), 6.05 (ddt, *J* = 7.7, 6.3, 1.4 Hz, 1 H), 5.84 (d, *J* = 7.6 Hz, 1 H), 4.71–4.67 (m, 1 H, ferrocenyl C–*H*), 4.16–4.12 (m, 2 H, ferrocenyl C–*H*), 3.95–3.93 (m, 1H, ferrocenyl C–*H*), 3.84–3.81 (m, 1H, ferrocenyl C–*H*), 3.73–3.70 (m, 1H, ferrocenyl C–*H*), 3.58–3.55 (m, 1 H, ferrocenyl C–*H*), 3.55–3.53 (m, 1 H, ferrocenyl C–*H*), and 2.26 (s, 3 H, N–C*H*$_3$) ppm.
^{19}F NMR (565 MHz, C_6D_6): δ –158.3 (dd, $^3J_{F–P}$ = 111.9, 39.3 Hz, 1F) ppm.
^{31}P{^{1}H} NMR (243 MHz, C_6D_6): δ 21.2 (dd, $^3J_{P–F}$ = 39.1 Hz, $^2J_{P–P}$ = 25.7 Hz, 1 P) and 14.5 (dd, $^3J_{P–F}$ = 112.3 Hz, $^2J_{P–P}$ = 25.4 Hz, 1 P) ppm.
Anal Calc'd for $C_{49}H_{40}FFeNOP_2Pd$: C, 65.24; H: 4.47; N: 1.55; Found: C, 65.34; H: 4.63; N: 1.64.

6c: Compound **6c** was prepared according to the general procedure. 23.1 mg, 80.4% yield, bright yellow solid.



^{1}H NMR (500 MHz, C_6D_6): δ 8.95 (ddt, *J* = 10.9, 7.9, 1.6 Hz, 2 H), 8.14–8.04 (m, 2 H), 7.80–7.69 (m, 2 H), 7.62 (t, *J* = 7.1 Hz, 1 H), 7.54 (td, *J* = 7.8, 2.0 Hz, 2 H), 7.36–7.16 (m, 4 H), 7.00 (d, *J* = 7.1 Hz, 1 H), 6.96–6.69 (m, 11 H), 6.40 (dt, *J* = 8.1, 2.1 Hz, 1 H), 6.08 (t, *J* = 7.1 Hz, 1 H), 5.72 (d, *J* = 7.7 Hz, 1 H), 4.67–4.60 (m, 1 H, ferrocenyl C–*H*), 4.15–4.12 (m, 1 H, ferrocenyl C–*H*), 4.12–4.09 (m, 1 H, ferrocenyl C–*H*), 3.91–3.87 (m, 1 H, ferrocenyl C–*H*), 3.84–3.80 (m, 1 H, ferrocenyl C–*H*), 3.73–3.68 (m, 1 H, ferrocenyl C–*H*), 3.57–3.53 (m, 1 H, ferrocenyl C–*H*), 3.51–3.47 (m, 1 H, ferrocenyl C–*H*), and 2.15 (s, N–C*H*$_3$) ppm.
^{19}F NMR (471 MHz, C_6D_6): δ –61.5 (s, 3 F) and –158.5 (dd, $^3J_{F–P}$ = 110.0, 39.4 Hz, 1 F) ppm.
^{31}P{^{1}H} NMR (202 MHz, C_6D_6): δ 21.1 (dd, $^3J_{P–F}$ = 39.7 Hz, $^2J_{P–P}$ = 26.3 Hz, 1 P) and 15.0 (dd, $^3J_{P–F}$ = 110.2 Hz, $^2J_{P–P}$ = 26.2 Hz, 1 P) ppm.
Anal Calc'd for $C_{50}H_{39}F_4FeNOP_2Pd$: C, 61.91; H, 4.05; N, 1.44; Found: C, 61.66; H, 3.78; N: 1.31.

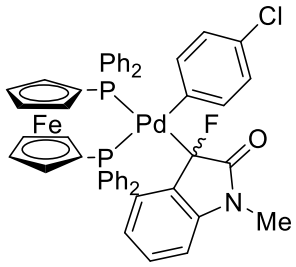
6d: Compound **6d** was prepared according to the general procedure. Pale yellow solid, 28.7 mg, 95.1% yield.



^{1}H NMR (600 MHz, C_6D_6): δ 8.97 (ddt, *J* = 11.0, 8.1, 1.4 Hz, 2 H), 8.15–8.10 (m, 2 H), 7.87–7.77 (m, 4 H), 7.66 (ddd, *J* = 7.7, 6.1, 1.3 Hz, 1 H), 7.54 (td, *J* = 7.8, 1.9 Hz, 2 H), 7.30 (td, *J* = 7.8, 2.0 Hz, 2 H), 7.27 (tdd, *J* = 7.4, 1.4, 1.2 Hz, 1 H), 7.24 (dt, *J* = 7.9, 2.1 Hz, 1 H), 7.20 (tq, *J* = 7.4, 1.5

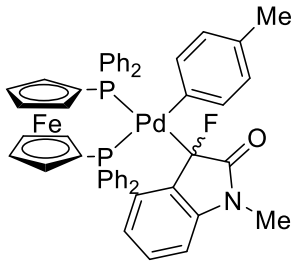
Hz, 1 H), 7.18–7.16 (m, 1 H), 7.14–7.08 (m, 2 H), 7.05 (d, *J* = 7.5 Hz, 1 H), 6.97–6.88 (m, 6 H), 6.83 (tq, *J* = 7.2, 1.3 Hz, 1 H), 6.80 (d, *J* = 7.7 Hz, 1 H), 6.77 (td, *J* = 7.9, 2.1 Hz, 1 H), 6.73 (ddd, *J* = 9.5, 7.4, 2.2 Hz, 2 H), 6.21 (ddd, *J* = 7.6, 6.0, 1.3 Hz, 1 H), 5.75 (d, *J* = 7.6 Hz, 1 H), 4.69–4.66 (m, 1 H, ferrocenyl C–*H*), 4.16–4.14 (m, 1 H, ferrocenyl C–*H*), 4.14–4.12 (m, 1 H, ferrocenyl C–*H*), 3.90–3.87 (m, 1 H, ferrocenyl C–*H*), 3.86–3.81 (m, 1 H, ferrocenyl C–*H*), 3.73–3.69 (m, 1 H, ferrocenyl C–*H*), 3.58–3.54 (m, 1 H, ferrocenyl C–*H*), 3.48–3.44 (m, 1 H, ferrocenyl C–*H*), and 2.24 (s, 3 H, N–CH_3) ppm.
^{19}F NMR (565 MHz, C_6D_6): δ –157.8 (dd, $^3J_{F–P}$ = 110.9, 39.3 Hz, 1 F) ppm.
^{31}P{^{1}H} NMR (243 MHz, C_6D_6): δ 20.9 (dd, $^3J_{P–F}$ = 38.8 Hz, $^2J_{P–P}$ = 26.1 Hz, 1 P), 14.8 (dd, $^3J_{P–F}$ = 111.1 Hz, $^2J_{P–P}$ = 26.1 Hz, 1 P) ppm.
Anal Calc'd for $C_{56}H_{44}FFeNO_2P_2Pd$: C, 65.85; H: 4.41; N: 1.39; Found: C, 66.47; H, 4.24; N: 1.43.

6e: Compound **6e** was prepared according to the general procedure. 22.6 mg, 80.4% yield, bright yellow solid.



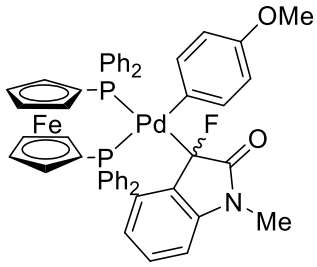
^{1}H NMR (600 MHz, C_6D_6): δ 8.95 (dd, *J* = 10.9, 7.7 Hz, 2 H), 8.10 (dd, *J* = 10.5, 7.9 Hz, 2 H), 7.76 (dd, *J* = 11.0, 7.2 Hz, 2 H), 7.54 (td, *J* = 7.8, 2.0 Hz, 2 H), 7.42 (ddd, *J* = 8.0, 6.2, 1.8 Hz, 1 H), 7.32–7.23 (m, 3 H), 7.21–7.17 (m, 1 H), 7.01–6.85 (m, 8 H), 6.83–6.76 (m, 3 H), 6.59 (dt, *J* = 8.1, 2.1 Hz, 1 H), 6.23 (dt, *J* = 8.2, 2.1 Hz, 1 H), 5.86 (ddd, *J* = 8.0, 6.1, 1.7 Hz, 1 H), 5.77 (d, *J* = 7.6 Hz, 1 H), 4.67–4.61 (m, 1 H, ferrocenyl C–*H*), 4.15–4.12 (m, 1 H, ferrocenyl C–*H*), 4.12–4.11 (m, 1 H, ferrocenyl C–*H*), 3.94–3.89 (m, 1 H, ferrocenyl C–*H*), 3.83–3.80 (m, 1 H, ferrocenyl C–*H*), 3.71–3.69 (m, 1 H, ferrocenyl C–*H*), 3.57–3.53 (m, 1 H, ferrocenyl C–*H*), 3.53–3.49 (m, 1 H, ferrocenyl C–*H*), and 2.23 (s, 3 H, N–CH_3) ppm.
^{19}F NMR (565 MHz, C_6D_6): δ –158.7 (dd, $^3J_{F–P}$ = 110.4, 40.0 Hz, 1 F) ppm.
^{31}P{^{1}H} NMR (243 MHz, C_6D_6): δ 20.7 (dd, $^3J_{P–F}$ = 39.7 Hz, $^2J_{P–P}$ = 26.3 Hz, 1 P) and 15.0 (dd, $^3J_{P–F}$ = 110.4 Hz, $^2J_{P–P}$ = 25.7 Hz, 1 P) ppm.
Anal Calc'd for $C_{49}H_{39}ClFFeNOP_2Pd$: C, 62.84; H: 4.41; N: 1.50; Found: C, 62.96; H, 4.25; N: 1.50.

6f: Compound **6f** was prepared according to the general procedure. Pale yellow solid, 17.7 mg, 64.4% yield.



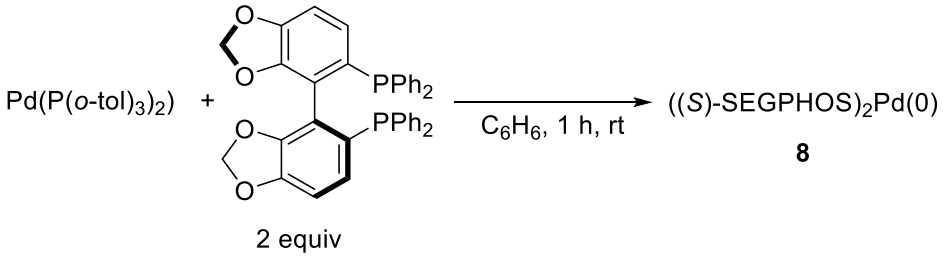
^{1}H NMR (600 MHz, C_6D_6): δ 9.00 (dd, *J* = 10.3, 8.6 Hz, 2 H), 8.14 (dd, *J* = 10.1, 8.0 Hz, 2 H), 7.84–7.78 (m, 2 H), 7.56 (td, *J* = 7.7, 1.9 Hz, 2 H), 7.47 (t, *J* = 7.0 Hz, 1 H), 7.33–7.24 (m, 3 H), 7.20 (tq, *J* = 7.4, 1.4 Hz, 1 H), 7.03 (d, *J* = 7.6 Hz 1 H), 7.01–6.88 (m, 6 H), 6.88–6.81 (m, 2 H), 6.74 (td, *J*= 7.8, 2.2 Hz, 2 H), 6.40 (dt, *J* = 7.7, 2.0 Hz, 1 H), 6.04 (dt, *J* = 7.8, 2.2 Hz, 1 H), 5.89 (ddd, *J*= 7.8, 6.2, 1.5 Hz, 1 H), 5.86 (d, *J* = 7.7 Hz, 1 H), 7.70–4.64 (m, 1 H, ferrocenyl C–*H*), 4.15–4.12 (m, 2 H, ferrocenyl C–*H*), 3.98–3.93 (m, 1 H, ferrocenyl C–*H*), 3.85–3.80 (m, 1 H, ferrocenyl C–*H*), 3.75–3.69 (m, 1 H, ferrocenyl C–*H*), 3.58–3.56 (m, 1 H, ferrocenyl C–*H*), 3.56–3.53 (m, 1 H, ferrocenyl C–*H*), 2.26 (s, 3 H, N–CH_3), and 1.95 (s, 3 H, Pd–C_6H_4–CH_3) ppm.
^{19}F NMR (565 MHz, C_6D_6): δ –158.9 (dd, $^{3}J_{F–P}$ = 111.3, 39.8 Hz, 1 F) ppm.
^{31}P{^{1}H} NMR (243 MHz, C_6D_6): δ 20.7 (dd, $^{3}J_{P–F}$ = 39.4 Hz, $^{2}J_{P–P}$ = 25.2 Hz, 1 P) and 14.5 (dd, $^{3}J_{P–F}$ = 111.0 Hz, $^{2}J_{P–P}$ = 25.4 Hz, 1 P) ppm.
Anal Calc'd for $C_{50}H_{42}FFeNOP_2Pd$: C, 65.55; H: 4.62; N: 1.53; Found: C, 65.27; H, 4.91; N: 1.52.

6g: Compound **6g** was prepared according to the general procedure. Yellow solid, 12.7 mg, 45.4% yield.



^{1}H NMR (400 MHz, C_6D_6): δ 9.01 (dd, *J* = 10.0, 8.6 Hz, 2 H), 8.14 (t, *J* = 9.0 Hz, 2 H), 7.88–7.74 (m, 2 H), 7.56 (td, *J*= 7.7, 1.9 Hz, 2 H), 7.43 (ddd, *J* = 8.1, 6.3, 1.7 Hz, 1 H), 7.36–7.23 (m, 3 H), 7.22–7.17 (m, 1 H), 7.07–6.89 (m, 7 H), 6.89–6.73 (m, 4 H), 6.28 (dt, *J* = 7.9, 1.9 Hz, 1 H), 5.96–5.91 (m, 1 H), 5.91–5.80 (m, 2 H), 4.66 (apt s, 1 H, ferrocenyl C–*H*), 4.16–4.11 (m, 2 H, ferrocenyl C–*H*), 3.96 (apt s, 1 H, ferrocenyl C–*H*), 3.87–3.79 (m, 1 H, ferrocenyl C–*H*), 3.75–3.68 (m, 1 H), 3.59–3.53 (m, 2 H, ferrocenyl C–*H*), 3.26 (s, 3 H, Pd–C_6H_4–OCH_3), and 2.31 (s, 3 H, N–CH_3) ppm.
^{19}F NMR (565 MHz, C_6D_6): δ –158.7 (dd, $^{3}J_{F–P}$ = 111.1, 39.8 Hz, 1 F) ppm.
^{31}P{^{1}H} NMR (243 MHz, C_6D_6): δ 20.9 (dd, $^{3}J_{P–F}$ = 40.7 Hz, $^{2}J_{P–P}$ = 25.1 Hz, 1 P) and 14.5 (dd, $^{3}J_{P–F}$ = 111.4 Hz, $^{2}J_{P–P}$ = 25.0 Hz, 1 P) ppm.
Anal Calc'd for $C_{50}H_{42}FFeNO_2P_2Pd$: C, 64.43; H: 4.54; N: 1.50; Found: C, 64.09; H, 4.79; N: 1.71.

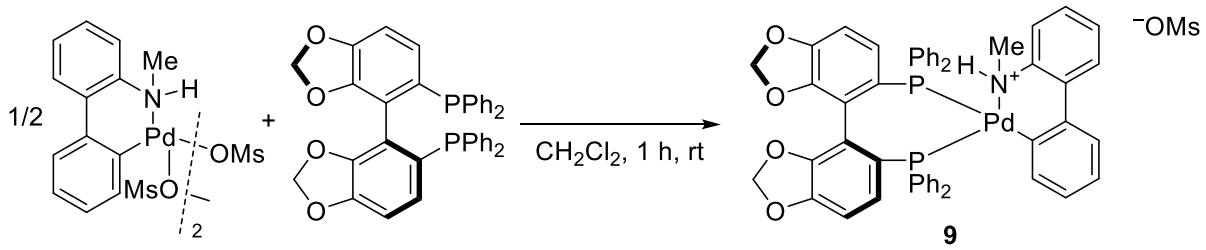
*Preparation of bis((S)-SEGPHOS)palladium(0) (**8**)*



The following procedure was adapted from previous reports for the synthesis of

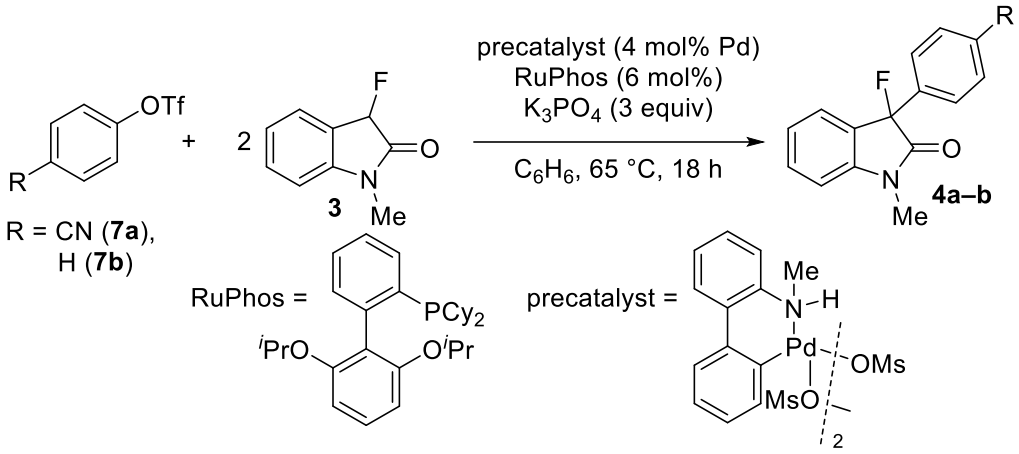
$(DPPF)_2Pd(0)$ and $(BINAP)_2Pd(0)$.[62] To a 4 mL vial containing $Pd(P(o\text{-}tol)_3)_2$ (35.8 mg, 0.0500 mmol, 1.00 equiv) and (*S*)-SEGPHOS (64.1 mg, 0.105 mmol, 2.10 equiv) was added benzene (1.5 mL), and the slurry was stirred for 1 h at ambient temperature. The reaction mixture clarified to an orange solution over this time. The solution was then filtered through a syringe filter (VRW, PTFE, 0.2 μm), and the filtrate was layered with hexane (2.5 mL) and left undisturbed at ambient temperature. After 2 d, compound **8** had precipitated on to the sides of the vial as an orange solid. The liquor was decanted, and the precipitate was triturated with hexane (3×0.5 mL) to afford product **8** as an orange solid (55.1 mg, 83.0% yield).
^{1}H NMR (C_6D_6, 500 MHz): δ 8.23–8.08 (m, 8 H), 7.80–7.73 (m, 8 H), 7.06–6.97 (m, 12 H), 6.89–6.82 (m, 4 H), 6.71 (t, *J* = 7.3 Hz, 4 H), 6.46 (t, *J* = 7.5 Hz, 8 H), 6.34 (d, *J* = 8.0 Hz, 4 H), 5.51 (s, 4 H), and 5.28 (s, 4 H) ppm.
^{31}P{^{1}H} NMR (C_6D_6, 243 MHz): δ 22.43 (s, 4 P) ppm.
ESI-HRMS: Calc'd for $C_{76}H_{57}O_8P_4Pd^+$ ($M + H^+$): 1327.203872; Found: 1327.2034.

*Preparation of cyclometallated SEGPHOS precatalyst **9***



The following procedure was adapted from the synthesis of a BINAP-ligated precatalyst prepared by Buchwald and co-workers.[56] To a 20 mL vial containing *N*-methyl-2-aminobiphenylpalladium methanesulfonate dimer (77.6 mg, 0.100 mmol, 0.500 equiv) and (*S*)-SEGHPOS (122.1 mg, 0.200 mmol, 1.00 equiv) was added dichloromethane (4 mL), and the reaction mixture was stirred at ambient temperature for 1 h. The solvent was removed under vacuum until ~100 μL remained, and the residue was treated with diethyl ether (4 mL). The slurry was stirred vigorously at ambient temperature for 30 min, and the precipitated solid was collected by filtration on a fine fritted glass funnel. The solid was washed with diethyl ether (3×1.5 mL) to afford complex **9** as an air-stable tan solid (153.1 mg, 77.0% yield).
^{1}H NMR (CD_3CN, 500 MHz): δ 8.04 (br s, 2 H), 7.85–7.58 (m, 7 H), 7.55–7.46 (m, 4 H), 7.35–7.03 (m, 11 H), 6.88 (apt q, 7.1 Hz, 1 H), 6.84 (t, *J* = 7.4 Hz, 1 H), 6.79 (d, *J* = 7.7 Hz, 1 H), 6.56–6.29 (m, 5 H), 5.82 (s, 1 H), 5.75 (s, 1 H), 5.73 (s, 1 H), 5.42 (s, 1 H), 4.30–4.17 (m, 1 H, N–H), and 2.41 (s, 3 H, sulfonate C*H*$_3$), and 2.27–2.24 (m, 3 H, N–C*H*$_3$, complexity due to stereogenic *N*) ppm.
^{31}P NMR (CD_3CN, 202 MHz): δ 33.5 (d, *J* = 43.5, 1 P) and 12.9 (d, *J* = 43.1, 1 P) ppm.
ESI-HRMS: calc'd $C_{51}H_{40}O_4NP_2Pd$ ($M - {}^-OSO_2Me$): 898.1462; found: 898.1475.

*Preparation of racemic arylated fluorooxindoles **4a–b***



To a 4 mL vial containing *N*-methyl-2-aminobiphenylpalladium methanesulfonate dimer (5.1 mg, 0.0066 mmol) and RuPhos (9.3 mg, 0.020 mmol) was added benzene (500 μL), and the mixture was stirred for 1 h. The mixture was then transferred quantitatively to a 1.00 mL volumetric flask and diluted to the mark with benzene to afford a stock solution of RuPhos-ligated precatalyst (0.0013 M Pd).

To a separate 4 mL vial was added the appropriate aryl triflate **7** (0.100 mmol, 1.00 equiv), *N*-methyl-3-fluorooxindole (**3**, 33.0 mg, 0.200 mmol, 2.00 equiv), K_3PO_4 (63.7 mg, 0.300 mmol, 3.00 equiv), the palladium precatalyst solution (300 μL, 0.0040 mmol Pd, 4 mol% Pd), and benzene (350 μL). A Teflon-coated magnetic stir bar was added, and the vial was sealed with a Teflon-lined cap and removed from the drybox. The reaction mixture was stirred vigorously at 65 °C for 18 h. The presence of arylated product **4** in an aliquot of the reaction mixture was confirmed by NMR spectroscopy. The reaction mixture was then filtered through a plug of silica and concentrated under vacuum. Compound **4b** was additionally purified by thin-layer chromatography (3:1 hexanes:ethylacetate, R_f = 0.2). The exact purity and isolated yields were not determined. The mixture thus obtained was used to determine the HPLC retention times of the two enantiomers of **4**.

HPLC Conditions:

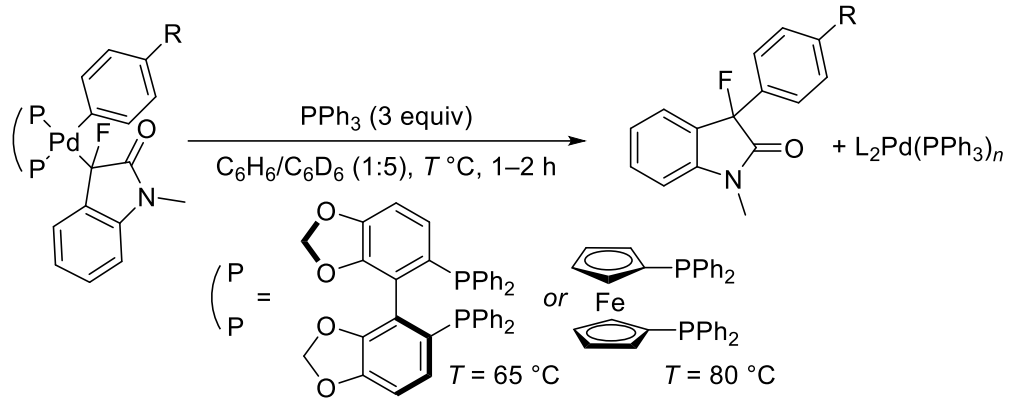
3 (for comparison to chromatograms that contain it as an impurity):
IF column, 4% *i*PrOH in hexane, 1.0 mL/min, 240 nm, t_R = 20.570, 21.735 min.
4a: IF column, 4% *i*PrOH in hexane, 1.0 mL/min, 240 nm, t_R = 29.9, 35.5 min.
4b: OD-H column, 1.5% *i*PrOH in hexane, 1.0 mL/min, 240 nm, t_R = 15.843, 23.601 min

3.8.3 Reactivity of Arylpalladium Fluoroenolate Complexes

*Sample preparation for tracking the thermolysis of complexes **2a–b** and **6a–g***

To a 1 mL vial containing the fluoroenolate complex (~0.01 mmol, exact loading determined by $^{19}F\{^{31}P\}$ NMR spectroscopy before thermolysis) was added 100 μL of a stock solution of triphenylphosphine (0.300 M, 0.0300 mmol, ~ 3 equiv) and 4,4'-difluorobiphenyl (0.0750 M, 0.00750 mmol, ~ 0.75 equiv), followed by C_6D_6 (500 μL). The mixture was quickly mixed with a pipette and transferred to a screw-top NMR tube, which was sealed with a Teflon-lined cap, removed from the drybox, and cooled to 0 °C in an ice bath until data collection began.

*Tracking the thermolysis of fluoroenolate complexes **2a–b** and **6a–g***



A 600 MHz Bruker NMR spectrometer equipped with a triple broadband probe was preheated to 65 °C (for **2a–b**) or 80 °C (for **6a–g**). The temperature was calibrated according to the spectral distance between glycol peaks in an 80% solution of ethylene glycol in DMSO-d_6. The ^{1}H channel of the probe was tuned to ^{19}F and the broadband probe was tuned to ^{31}P. The spectral centers for the two nuclei were set to –135.5 ppm and 20 ppm, respectively. An inverse-gated ^{19}F{^{31}P} pulse program was used for all subsequent acquisitions. Shimming and 90° pulse calibration were performed on the ^{19}F signals of a dummy sample (600 µL of a solution of triphenylphosphine (0.0500 M) and 4,4'-difluorobiphenyl (0.0125 M) in 1:5 C_6H_6:C_6D_6 (v/v)). The cold sample was then quickly warmed to ambient temperature and transferred to the instrument. After letting the sample thermally equilibrate for ~30 s, inverse-gated ^{19}F{^{31}P} NMR spectra were acquired every minute ((ns=3, d1=18.75, aq=0.25)×3+3.0 s = 60.0 s). First-order exponential fits of product formation were determined using LibreOffice Calc's Solver to minimize the total squared error between the exponential fit and the experimental data by varying *A*, *k*, and *c* in the first-order exponential equation $y = A\,(1 - \exp(-kt + c))$. Final yields were determined after heating at 65 °C (for **2a–b**) or 80 °C (for **6a–g**) overnight. In the case of the (*S*)-SEGPHOS-ligated complexes **2a–b**, the *ee* of the arylated product was determined by chiral HPLC.

*^{19}F NMR shifts of arylated fluorooxindoles **4a–g***

4a (R = CN): (565 MHz, C_6D_6, 65 °C): δ –152.6 ppm
4b (R = H): (565 MHz, C_6D_6, 65 °C): δ –151.1 ppm
4c (R = CF_3): (565 MHz, C_6D_6, 65 °C): δ –152.0 ppm
4d (R = $C(O)C_6H_5$): (565 MHz, C_6D_6, 65 °C): δ –152.3 ppm
4e (R = Cl): (565 MHz, C_6D_6, 65 °C): δ –150.2 ppm
4f (R = CH_3): (565 MHz, C_6D_6, 65 °C): δ –150.1 ppm
4g (R = OCH_3): (565 MHz, C_6D_6, 65 °C): δ –147.4 ppm

*Thermolysis of SEGPHOS-ligated complexes **2a–b***

See Table 3.2.1 for a table of averaged rate constants for **2a–b**

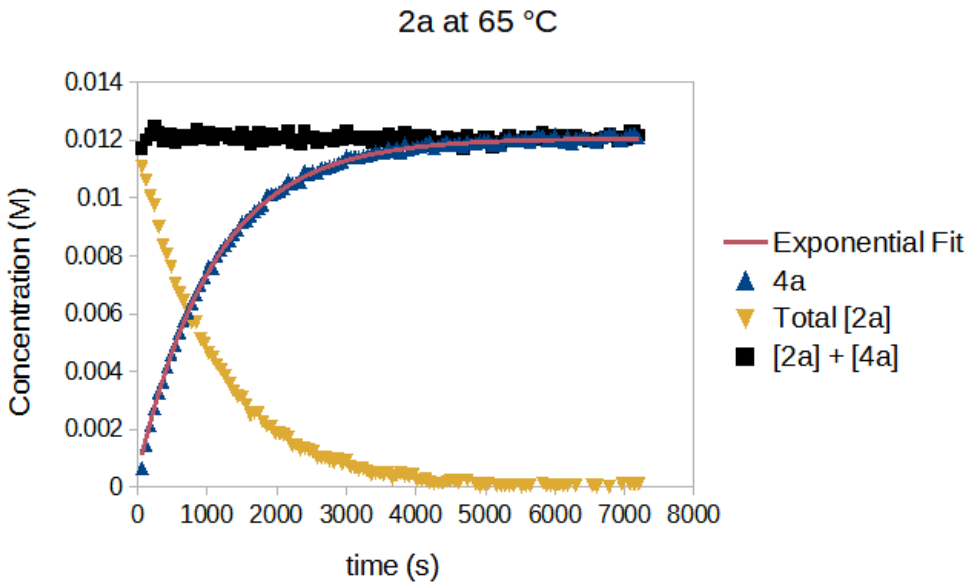


Figure 3.8.1 Fit: y = 1.20×10^{-2} (1 – exp(-9.05×10^{-4} *t* – 4.01×10^{-2}); Plot of the formation of **4a** and decomposition of both diastereomers of **2a** over time in the thermolysis of **2a**. Equivalent to Figure 3.2.2b.

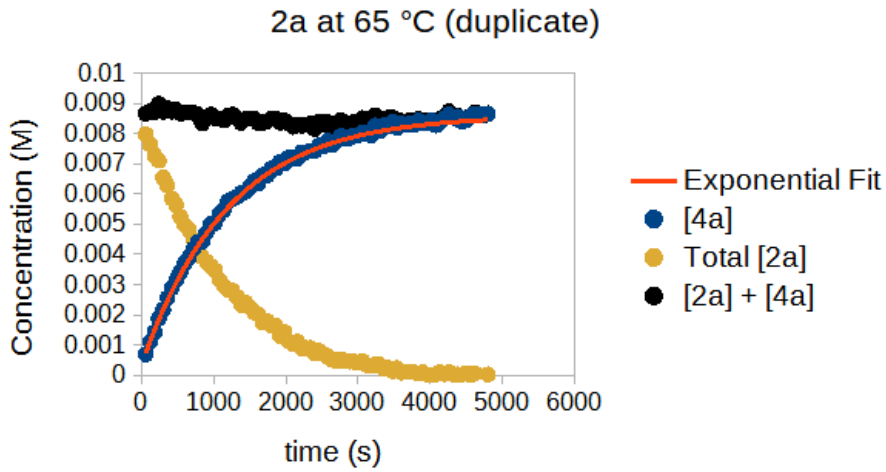


Figure 3.8.2 Fit: *y* = 8.61×10^{-3} (1 – exp(-8.30×10^{-4} *t* – 3.92×10^{-2})); Plot of the formation of **4a** over time in the thermolysis of **2a**. Replicate for estimate of error in k_{obs}.

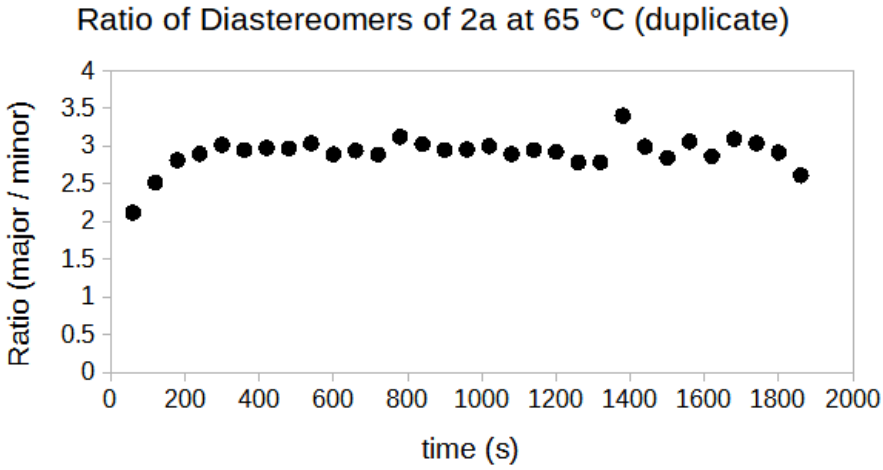


Figure 3.8.3 Ratio of diastereomers of **2a** across the reaction coordinate (major / minor). Later time points are omitted due to noise at low concentrations.

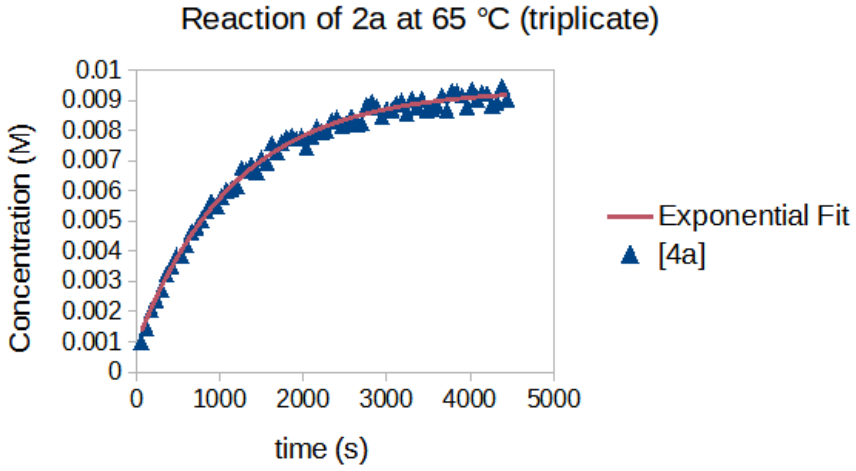


Figure 3.8.4 Fit: $y = 9.37\times10^{-3}\ (1 - \exp(-8.49\times10^{-4}\ t - 1.03\times10^{-1}))$; Plot of the formation of **4a** over time in the thermolysis of **2a**. Spectra were acquired without ^{31}P decoupling, so reliable integrals of the resonances corresponding to the diastereomers of **2a** could not be obtained. Replicate for estimate of error in k_{obs}.

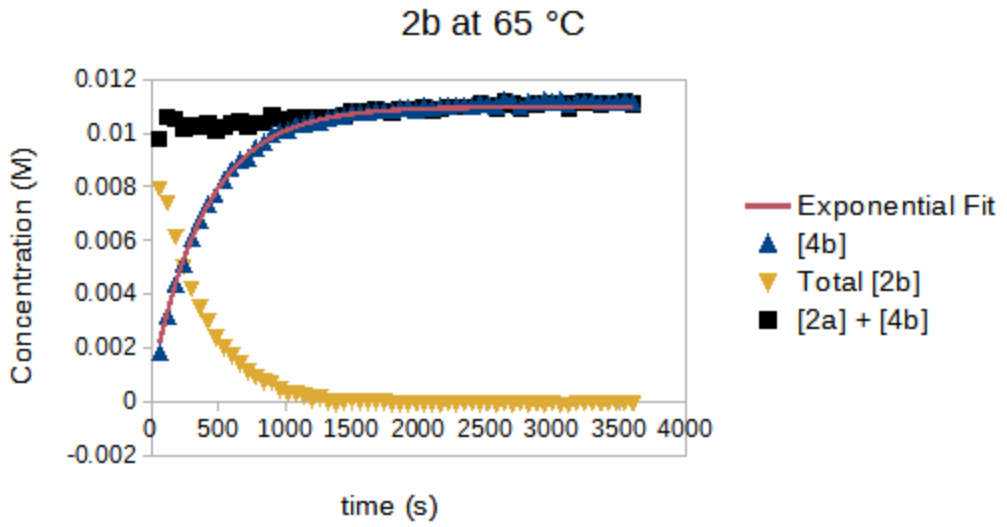


Figure 3.8.5 Fit: y = 1.10×10^{-3} (1 – exp(-2.43×10^{-3} *t* – 3.68×10^{-2}); Plot of the formation of **4b** and decomposition **2b** over time in the thermolysis of **2b**.

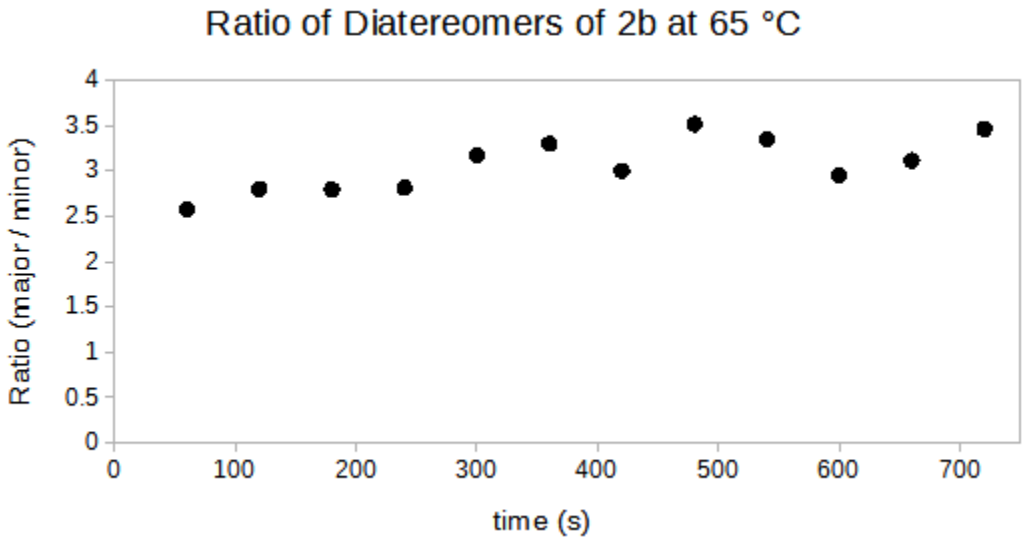


Figure 3.8.6 Ratio of diastereomers of **2b** across the reaction coordinate (major / minor). Later time points omitted due to noise at low concentrations.

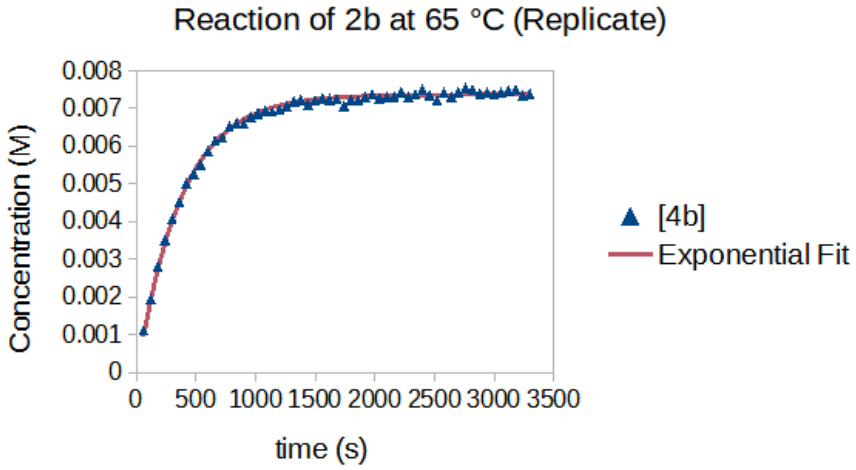
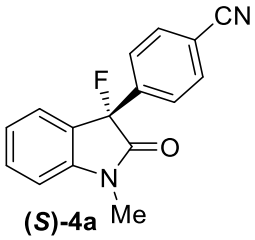


Figure 3.8.7 Fit: y = 7.37×10^{-3} (1 – exp(-2.70×10^{-3} *t* – 2.52×10^{-2}); Plot of the formation of **4b** over time in the thermolysis of **2b**. Spectra were acquired without ^{31}P decoupling, so reliable integrals of the resonances corresponding to the diastereomers of **2b** could not be obtained.

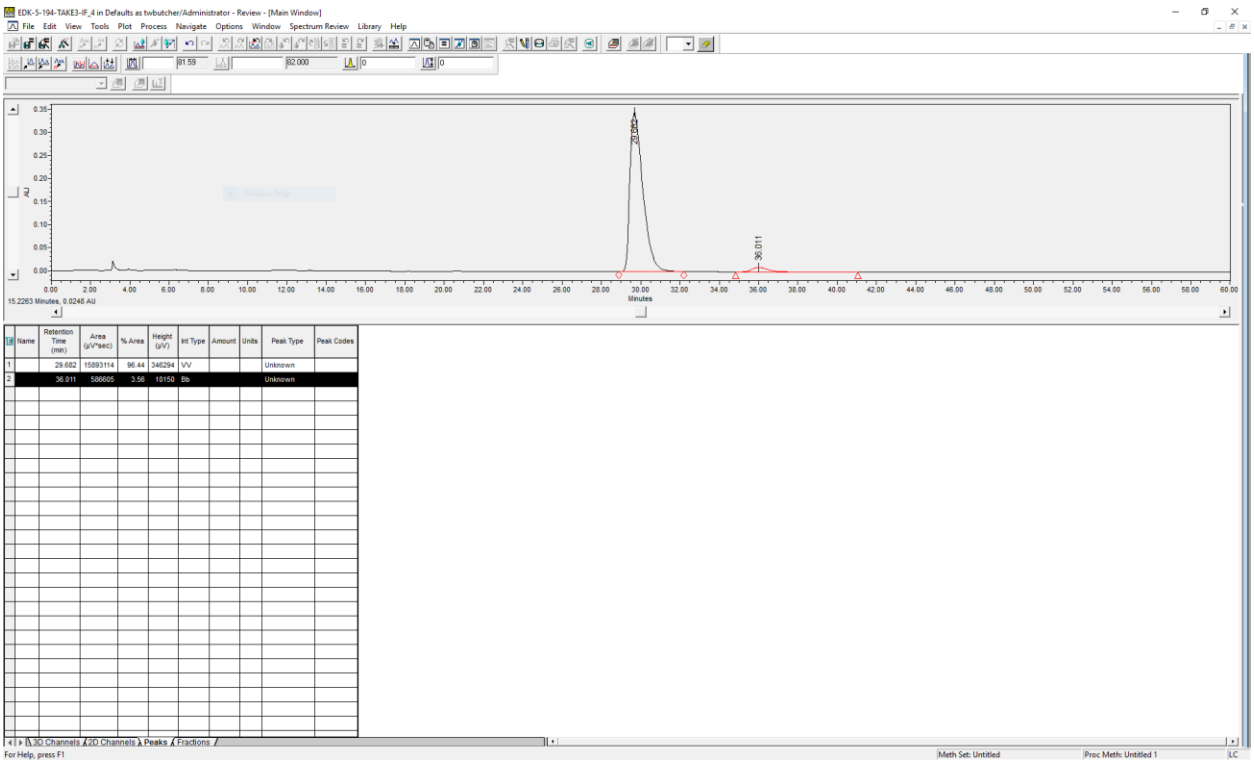
*ee of **4a** from the thermolysis of **2a***



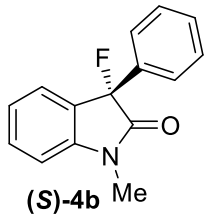
(*S*)-4a

IF column, 4% *i*PrOH in hexane, 1.0 mL/min, 240 nm, t_R = 29.9, 35.5 min.

92.9% ee

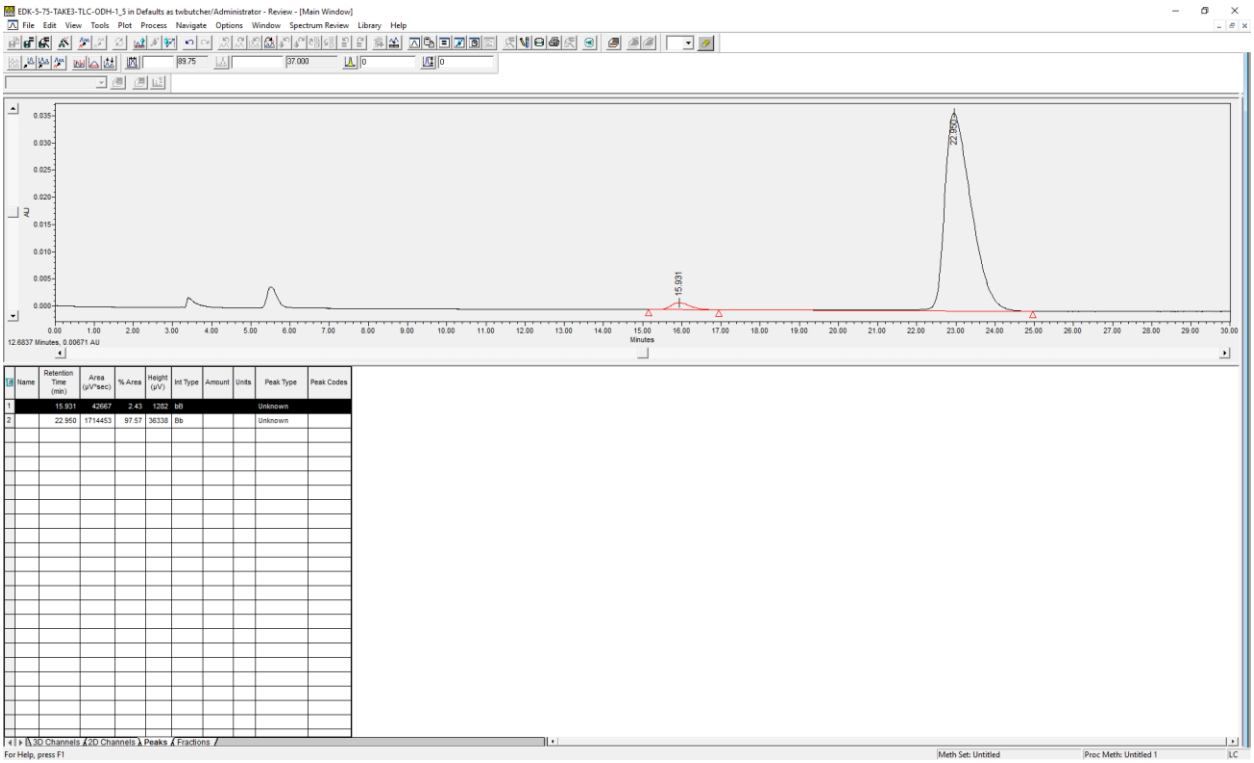


*ee of **4b** from the thermolysis of **2b***



(*S*)-4b

OD-H column, 1.5% *i*PrOH in hexane, 1.0 mL/min, 240 nm, t_R = 15.931, 22.950 min.
95% ee



*Thermolysis of DPPF-ligated complexes **6a–g***

Table 3.8.1 Rate constants for the reductive elimination of **6a–g**

Compound	R	k_{obs} ($s^{-1}\times10^4$)	Final Yield
6a	CN	2.2±0.3	> 99%
6c	CF_3	1.9±0.3	> 99%
6d	$C(O)C_6H_5$	6.9±0.8	> 99%
6e	Cl	3.1±0.4	99%
6b	H	13±2	> 99%
6f	CH_3	17±2	> 99%
6g	OCH_3	14±2	99%

In an attempt to increase the linearity of the Hammett plot in the main text (Figure 3.3.2), we also considered separating the inductive and resonance effects of the *para* substituent of the arene according to the equation $\bar{\sigma} = (\boldsymbol{F} + \boldsymbol{\lambda R})/(\mathbf{1} + |\boldsymbol{\lambda}|)$**,** where λ is an addition fit parameter and F and R are the Swain-Lupton constants[45] corresponding to the field (inductive) and resonance effects of the substituent. This kind of separation has generated very good linear fits for the reductive elimination from arylpalladium amide,[39] thiolate,[40] and alkoxide complexes.[41,46] λ was determined by maximizing the R^2 value of the linear least-squares fit of $\bar{\sigma}$. The resulting plot is shown in . The fit was slightly improved compared to the Hammett plot in Figure 3.8.8. In contrast to previous reports of the reductive elimination of aryl sulfides from arylpalladium sulfide (ρ_R / ρ_F = 5.0 / 1.7)[40] and arylpalladium amide (ρ_R / ρ_F = 2 / 1)[39] complexes, in which the resonance parameter had a greater influence on the rate of reaction than did the field parameter, the field parameter had a greater influence than the resonance parameter in the reductive elimination of fluoroenolate complexes **6a–g** (ρ_R / ρ_F ~ 1 / 2).

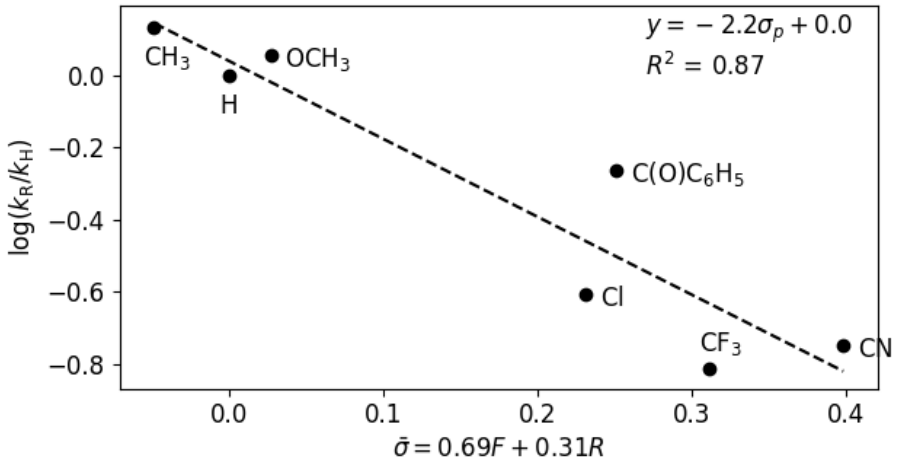
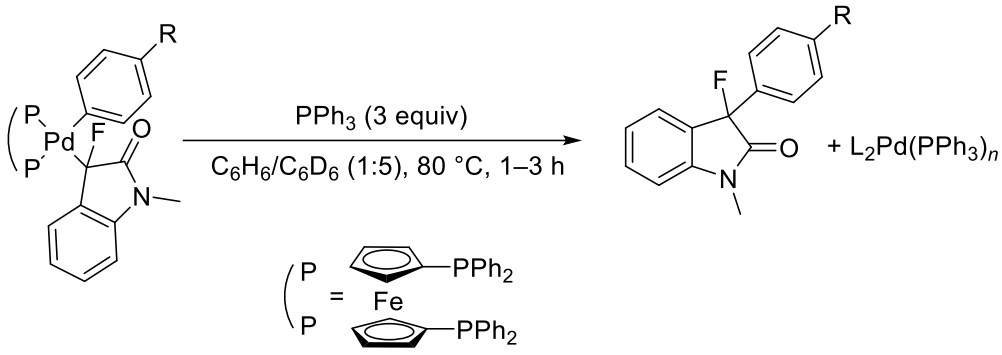


Figure 3.8.8 Plot of the relative rates of formation of arylated products **4a–g** in the reactions of DPPF-ligated arylpalladium fluoroenolate complexes **6a–g** *vs* the $\bar{\sigma}$ values of the *para* substituent of the eliminating aryl group. $\lambda = 0.448$. $\rho_F = \rho / (1 + |\lambda|) = -1.5$, $\rho_R = \lambda\rho / (1 + |\lambda|) = -0.7$.

Plots of time courses for the reductive elimination from DPPF-ligated complexes ***6a–g***



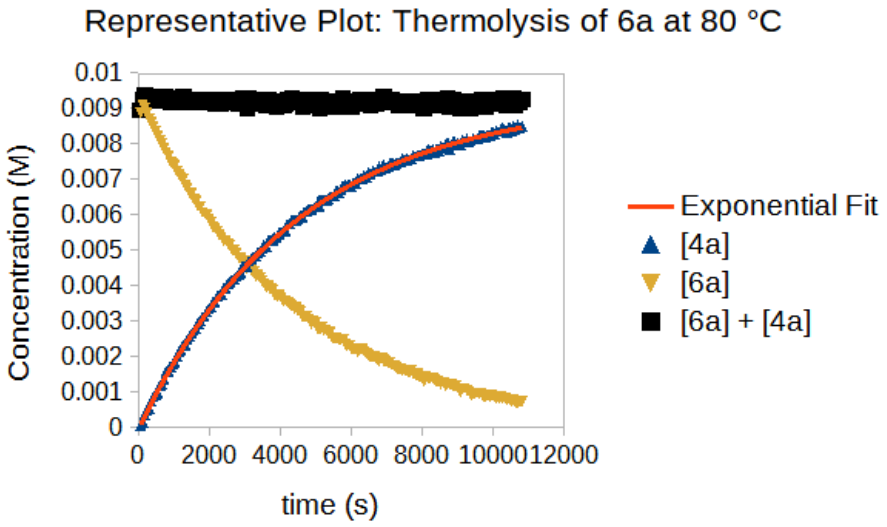


Figure 3.8.9 Fit: y = 9.29×10^{-3} (1 – exp(-2.24×10^{-4} *t* + 5.59×10^{-3}); Plot of the formation of **4a** and decomposition of **6a** over time in the thermolysis of **6a**.

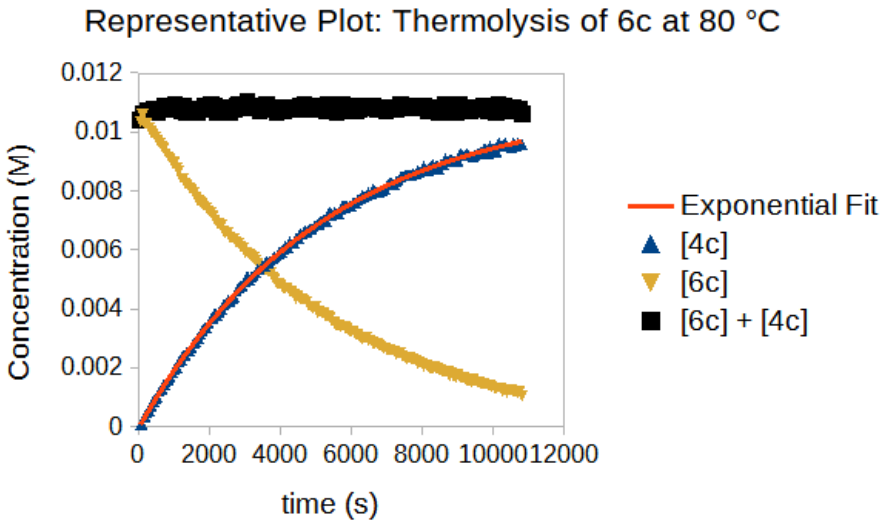


Figure 3.8.10 Fit: $y = 1.11\times10^{-2}\ (1 - \exp(-1.93\times10^{-4}\ t - 5.56\times10^{-3})$; Plot of the formation of **4c** and decomposition of **6c** over time in the thermolysis of **6c**.

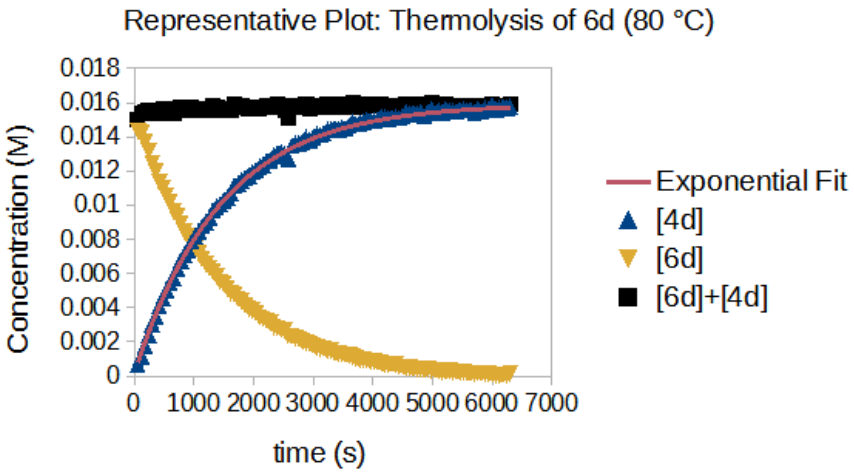


Figure 3.8.11 Fit: $y = 1.59\times10^{-2}\ (1 - \exp(-6.85\times10^{-4}\ t - 9.50\times10^{-3})$; Plot of the formation of **4d** and decomposition of **6d** over time in the thermolysis of **6d**.

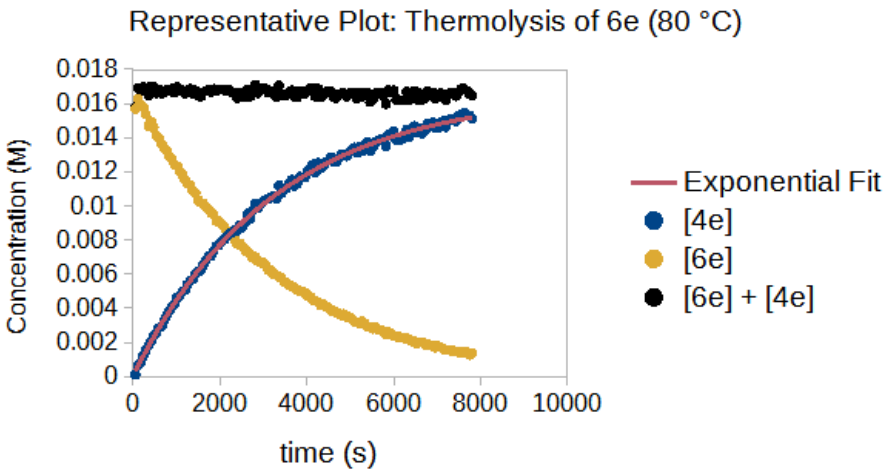


Figure 3.8.12 Fit: y = 1.67×10^{-2} (1 – exp(-3.10×10^{-4} *t* – 1.59×10^{-4}); Plot of the formation of **4e** and decomposition of **6e** over time in the thermolysis of **6e**.

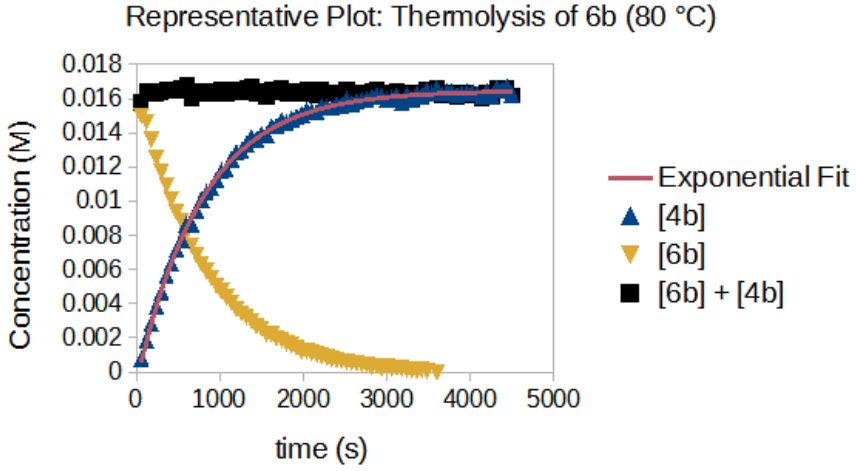


Figure 3.8.13 Fit: y = 1.65×10^{-2} (1 – exp(-1.26×10^{-3} *t* – 1.46×10^{-2}); Plot of the formation of **4b** and decomposition of **6b** over time in the thermolysis of **6b**.

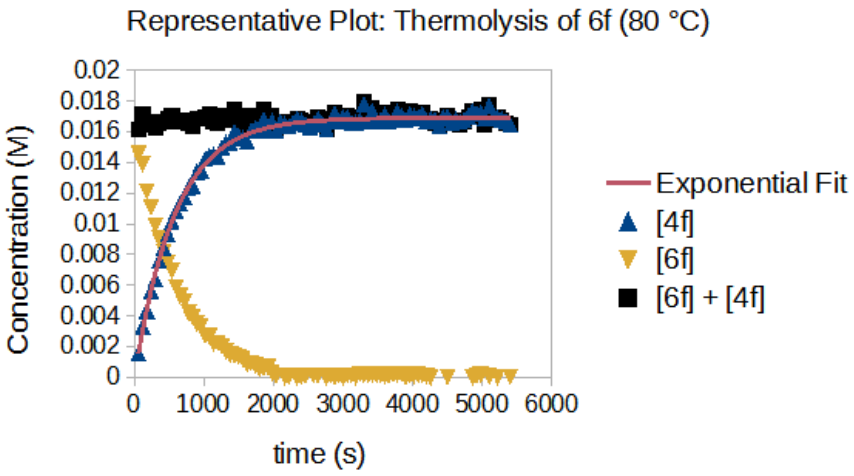


Figure 3.8.14 Fit: y = 1.69×10^{-2} (1 – exp(-1.71×10^{-3} *t* – 6.06×10^{-3}); Plot of the formation of **4f** and decomposition of **6f** over time in the thermolysis of **6f**.

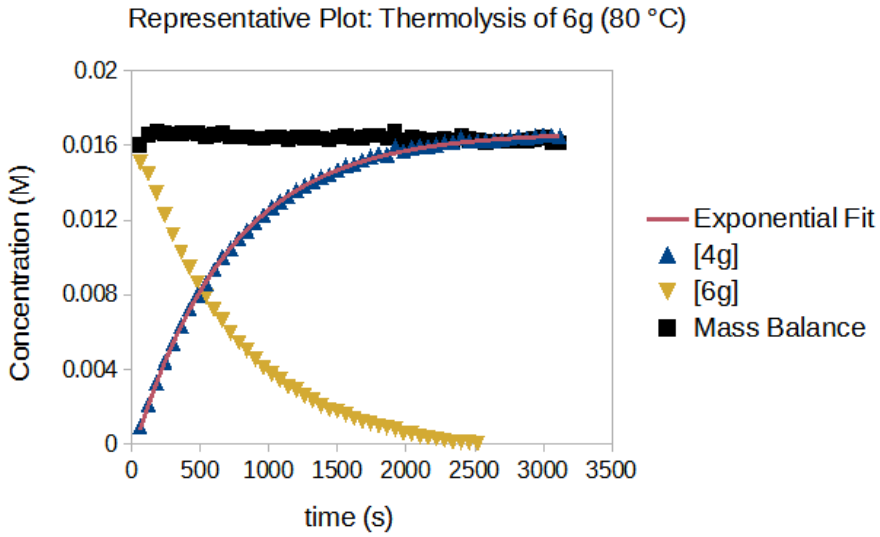
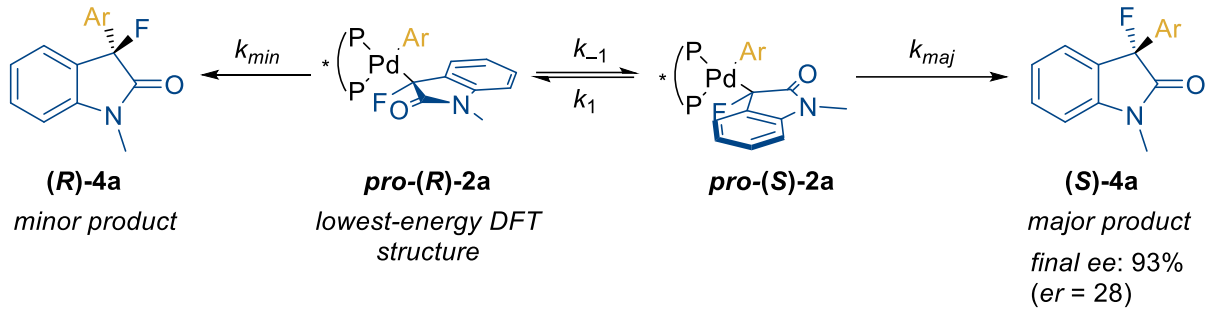


Figure 3.8.15 Fit: y = 1.67×10^{-2} (1 – exp(-1.43×10^{-3} *t* – 3.92×10^{-2}); Plot of the formation of **4g** and decomposition of **6g** over time in the thermolysis of **6g**.

*Determining the rate constants for the epimerization and reductive elimination of fluoroenolate complex **2a***

The reaction of **2a** was modeled as two elementary reactions: first-order epimerization between the two diastereomers of **2a**, and first-order reductive elimination from each of the two diastereomers (Scheme 3.8.1). However, we could not treat this system according to Curtin-Hammett kinetics because epimerization and reductive elimination (product formation) occurred with similar rates. In this section, the goal is to fit the values of each rate constant using COPASI's "Parameter Estimation" function with the data acquired while monitoring the reaction by $^{19}F\{^{31}P\}$ NMR spectroscopy (cf. Section 3.2).



Scheme 3.8.1 Modeled elementary reactions for the epimerization and reductive elimination of **2a**.

Relevant observables:

[***pro*-(*R*)-2a**] at all time points
[***pro*-(*S*)-2a**] at all time points
er_{final} (the measured *er* of arylated product **4a** after the reaction is run to completion)
k_{obs} = 8.6×10^{-4} s^{-1} (the rate constant derived from the exponential fit of product formation)

We could not measure the *ee* of **4a** at each NMR time point, so we could not provide COPASI with data to fit the instantaneous concentrations of [**(*S*)-4a**] and [**(*R*)-4a**]. While we knew the *ee* of the product **4a** at the end of the reaction as well as the total concentration of [**4a**] at each time point, COPASI does not support constraints on the sum of the concentrations of two species (i.e., the final concentrations of the two enantiomers of **4a**, representing the *er* of the reaction). To avoid this limitation, we applied an iterative scheme and present a supporting kinetic derivation below.

We fist considered the "steady-state" domain of the reaction (*i.e.*, the part of the reaction when the ratio of [***pro*-(*R*)-2a**] to [***pro*-(*S*)-2a**] is constant after some initial equilibration. In this regime, the *er* of any new product formed (er_{steady}) is also constant (Lemma 1). Furthermore, k_{maj} and k_{min} can be calculated in terms of er_{steady}, the steady-state *dr* of **2a** (below referred to as *K*), and the rate constant of the total concentration of **4a** ((*R*) + (*S*)) k_{obs} (Lemma 2). Note that k_{maj} and k_{min} are by construction valid over the duration of the reaction, not just in the steady-state regime. Thus, given a value of er_{steady}, we supplied our COPASI model with k_{maj} and k_{min} calculated from er_{steady} and fit the remaining parameters according to the concentrations of **2a** during the time course. However, er_{steady} was not known in advance, so we iteratively guessed its value and simulated the reaction with the estimated parameters until the final *er* of the arylated product **4a** given by the simulation matched the measured er_{final}. The rate constants in Scheme 3.2.1 were then extracted from COPASI.

Lemma 1 *er_{steady} is constant if [**pro-(R)-2a**] / [**pro-(S)-2a**] is constant*

Let *K* = [***pro*-(*R*)-2a**] / [***pro*-(*S*)-2a**] (the steady-state *dr* of **2a**)

Let [**2a**] = [***pro*-(*R*)-2a**] + [***pro*-(*S*)-2a**] (the total concentration of **2a**)

Then,

(1) [***pro*-(*R*)-2a**] = *K* [***pro*-(*S*)-2a**]

(2) [**2a**] = *K* [***pro*-(*S*)-2a**] + [***pro*-(*S*)-2a**] = [***pro*-(*S*)-2a**] (1 + *K*)

so

(3) $[\textbf{\textit{pro}-(\textit{S})-2a}] = \frac{[\mathbf{2a}]}{1+K}$

(4) $[(\textbf{\textit{pro}-(\textit{R})-2a})] = \frac{\boldsymbol{K}[\mathbf{2a}]}{1+K}$

The rates of product formation are then

(5) $rate_S = d[\textbf{(\textit{S})-4a}] / dt = k_{maj}\,[\textbf{\textit{pro}-(\textit{S})-2a}] = \frac{k_{maj}[\mathbf{2a}]}{1+K}$

(6) $rate_R = d[\textbf{(\textit{R})-4a}] / dt = k_{min}\,[\textbf{\textit{pro}-(\textit{R})-2a}] = \frac{k_{min}K[\mathbf{2a}]}{1+K}$

Note that the ratio of the rates of product formation is constant:

(7) $rate_S / rate_R = d[\textbf{(\textit{S})-4a}]/dt \,/\, d[\textbf{(\textit{R})-4a}]/dt = d[\textbf{(\textit{S})-4a}]/d[\textbf{(\textit{R})-4a}]$

(8) $= \frac{k_{maj}[\mathbf{2a}]}{1+K} / \frac{k_{min}K[\mathbf{2a}]}{1+K} = \frac{k_{maj}}{k_{min}\cdot K}$

Because the ratio of the rates of formation of the two enantiomers are constant over the domain currently in consideration, the *er* of the product is also constant:

(9) $[\textbf{(\textit{S})-4a}] = \int_0^{[(\textit{R})\text{-4a}]} \frac{d[(\textit{S})\text{-4a}]}{d[(\textit{R})\text{-4a}]'} d[(\textit{R})\text{-4a}]' = \int_0^{[(\textit{R})\text{-pdt}]} \frac{k_{maj}}{k_{min}\cdot K} d[(\textit{R})\text{-pdt}]'$

(10) $[\textbf{(\textit{S})-4a}] = \frac{k_{maj}}{k_{min}\cdot K}[(\textit{R})\text{-4a}]$

(11) $er_{steady} = [\textbf{(\textit{S})-4a}] / [\textbf{(\textit{R})-4a}] = \frac{k_{maj}}{k_{min}\cdot K}$, a constant value.

Lemma 2 *k_{maj} and k_{min} can be expressed in terms of K, k_{obs}, and er_{steady}*

The total rate of product formation is the sum of the rates of formation of the two enantiomers (from (5) and (6)):

(12) $rate_{total} = rate_S + rate_R = k_{obs}\,[\mathbf{2a}] = \frac{k_{maj}[\mathbf{2a}]}{1+K} + \frac{k_{min}K[\mathbf{2a}]}{1+K}$

(13) $k_{obs} = \frac{1}{1+K}\left(k_{maj} + k_{min}\cdot K\right)$

Rearranging (11), we find that

(14) $k_{min}\cdot K = \frac{k_{maj}}{er_{steady}}$

so, by (13),

(15) $k_{obs} = \frac{1}{1+K}\left(k_{maj} + \frac{k_{maj}}{er_{steady}}\right)$

(16) $= \frac{k_{maj}}{1+K}\left(1 + \frac{1}{er_{steady}}\right)$

We then solve (16) for k_{maj}:

(17) $k_{maj} = k_{obs}(1+K)\frac{1}{1+1/er_{steady}} = k_{obs}\frac{(1+K)\cdot er_{steady}}{er_{steady}+1}$

k_{min} can then be determined from (11) and (17):

(18) $k_{min} = \frac{k_{maj}}{er_{steady}\cdot K}$.

With the expressions for k_{maj} and k_{min}, we then defined an iterative algorithm to adjust er_{steady} until the simulated final *er* of the reaction (er_{final}) matches that determined experimentally.

*Algorithm for determining the rate constants for reductive elimination and epimerization for complex **2a***

$er_{steady} \leftarrow er_{final}$ *//initial guess for* er_{steady}

loop

calculate trial k_{maj} and k_{min} based on er_{steady} *// (17) and (18)*

k_1, k_{-1}, [***pro*-(*R*)-2a**]$_0$, [***pro*-(*S*)-2a**]$_0$ ← ParameterEstimation(k_{maj}, k_{min}, time course data)

[**(*S*)-4a**]^{sim}, [**(*R*)-4a**]^{sim} ← Simulate(k_{maj}, k_{min}, k_1, k_{-1}, [***pro*-(*R*)-2a**]$_0$, [***pro*-(*S*)-2a**]$_0$)

$er_{sim} \leftarrow$ [**(*S*)-4a**]$_{last}^{sim}$ / [**(*R*)-4a**]$_{last}^{sim}$

stop when $er_{sim} = er_{final}$

adjust er_{steady} to a new guess targeting $er_{sim} = er_{final}$

end loop

COPASI model setup

A model with four species and four rate constants was created according to Scheme 3.8.1. Initial estimates for the concentration of each diastereomer of **2a** were set to 0.005 M (approximately half of the final experimental yield of **4a**). The initial concentrations of **4a** were set to 0. All rate constants except for k_{maj} and k_{min} were initially set to 4.4×10^{-4} s^{-1} (approximately half of k_{obs}).

COPASI parameter estimation

Time points of the concentrations of the diastereomers of **2a** were loaded from a CSV file as "Experimental Data." k_{maj} and k_{min} were calculated according to the estimated er_{steady} (for the first iteration, this was set to 94% *ee*) and fixed in the parameter set. During parameter estimation ("Evolutionary Programming" method, 2000 generations, population size = 40), k_1, k_{-1}, [***pro*-(*R*)-2a**]$_0$ and [***pro*-(*S*)-2a**]$_0$ were allowed to vary between 1×10^{-6} and 1. As noted, the concentration of arylated product **4a** at each time point could not be constrained because it is the sum of the two species in consideration (*i.e.*, the two enantiomers of **4a**).

COPASI simulations with estimated parameters

Simulations were run for 7200 s, corresponding to > 99.9% conversion. The simulated *er* was calculated from the simulated concentrations of the two enantiomers of **4a** at t = 7200 s.

Table 3.8.2 Parameters determined by parameter estimation with COPASI

Parameter	Estimated Value
[***pro*-(*S*)-2a**]$_0$	0.007732 M
[***pro*-(*R*)-2a**]$_0$	0.004840 M
k_1	0.008732 s^{-1}
k_{-1}	0.003834 s^{-1}

Table 3.8.3 Final concentrations of the product enantiomers of **4a**

Species	Final Concentration (M)
(*S*)-4a	0.012154
(*R*)-4a	0.000416

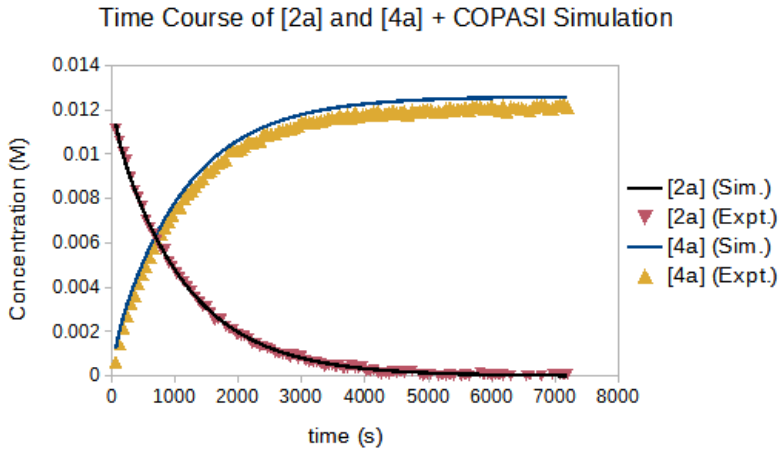
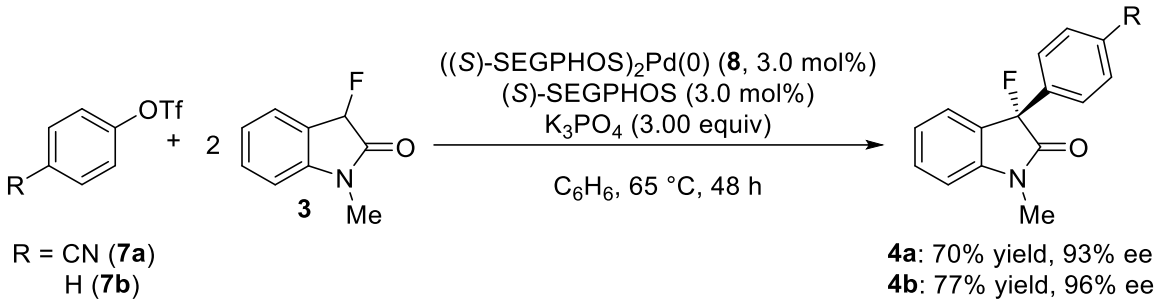


Figure 3.8.16 Plot of the simulated experimental concentrations of fluoroenolate complex **2a** and arylated product **4a**.

3.8.4 Investigations of the Catalytic Reaction

*Determining the yields, ee values, and resting states of the enantioselective Pd-catalyzed α-arylation of fluorooxindole **3** with aryl triflates **7a–b***



Scheme 3.8.2 Arylation reactions of aryl triflates **7a–b** catalyzed by precatalyst **8**

To a 4 mL vial containing ((*S*)-SEGPHOS)$_2$Pd(0) (**8**, 4.0 mg, 3.0 μmol, 3.0 mol%), (*S*)-SEGPHOS (1.8 mg, 3.0 μmol, 3.0 mol%), *N*-methyl-3-fluorooxindole (**3**, 33.0 mg, 0.200 mmol, 2.00 equiv), and K_3PO_4 (63.7 mg, 0.300 mmol, 3.00 equiv) was added aryl triflate (0.100 mmol, 1.00 equiv), 4,4'-difluorobiphenyl (variable, but measured exactly), and C_6H_6 (650 μL). A stir bar was added, and the vial was sealed with a Teflon-lined cap and removed from the glove box. The reaction mixture was heated at 65 °C with vigorous stirring. After ~1 h, the reaction mixture was removed from heating, pumped into the glove box, and an aliquot (100 μL) was diluted in C_6H_6 (500 μL) for analysis of the catalytic resting state. The reaction mixture was resealed and removed from the glove box, and heating and stirring were resumed. After 48 h, the reaction mixture was diluted with ethyl acetate (2 mL) and passed through a plug of silica, which was flushed with more ethyl acetate (3×1 mL). The filtrate was concentrated under vacuum, the residue was taken up in $CDCl_3$, and yields were determined by quantitative ^{19}F NMR spectroscopy (**4a**: 70%; **4b**: 77%). The reaction mixture was then concentrated, products **4a–b** were obtained *via* silica gel thin-layer chromatography (3:1 hexanes:ethyl acetate, R_f = 0.2 (**4a**), 0.3 (**4b**)). The *ee* values of **4a** and **4b** were determined by chiral HPLC.

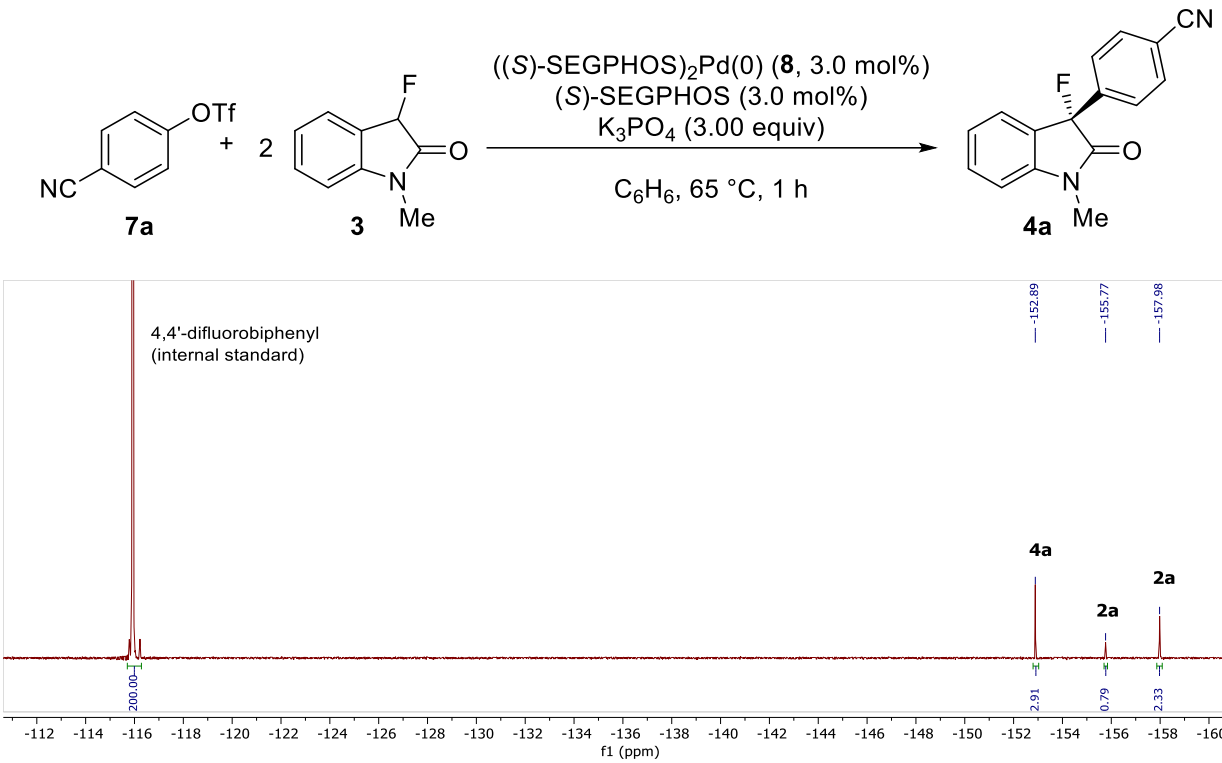


Figure 3.8.17 Inverse-gated $^{19}F\{^{31}P\}$ NMR spectrum of the resting state (1 h) of the reaction of aryl triflate **7a** with fluorooxindole **3** catalyzed by ((*S*)-SEGPHOS)$_2$Pd(0) (**8**) (Scheme 3.8.2). Complex **2a** accounts for 0.0016 mmol (~50% of the loading of Pd precatalyst **8**).

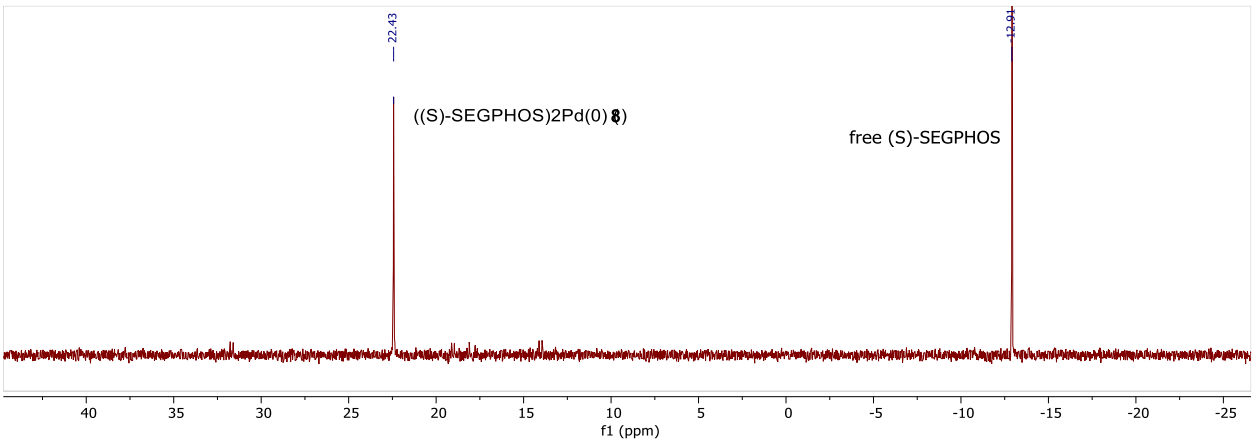
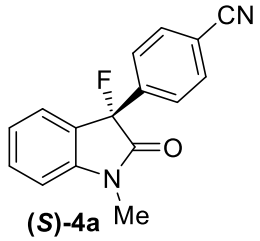


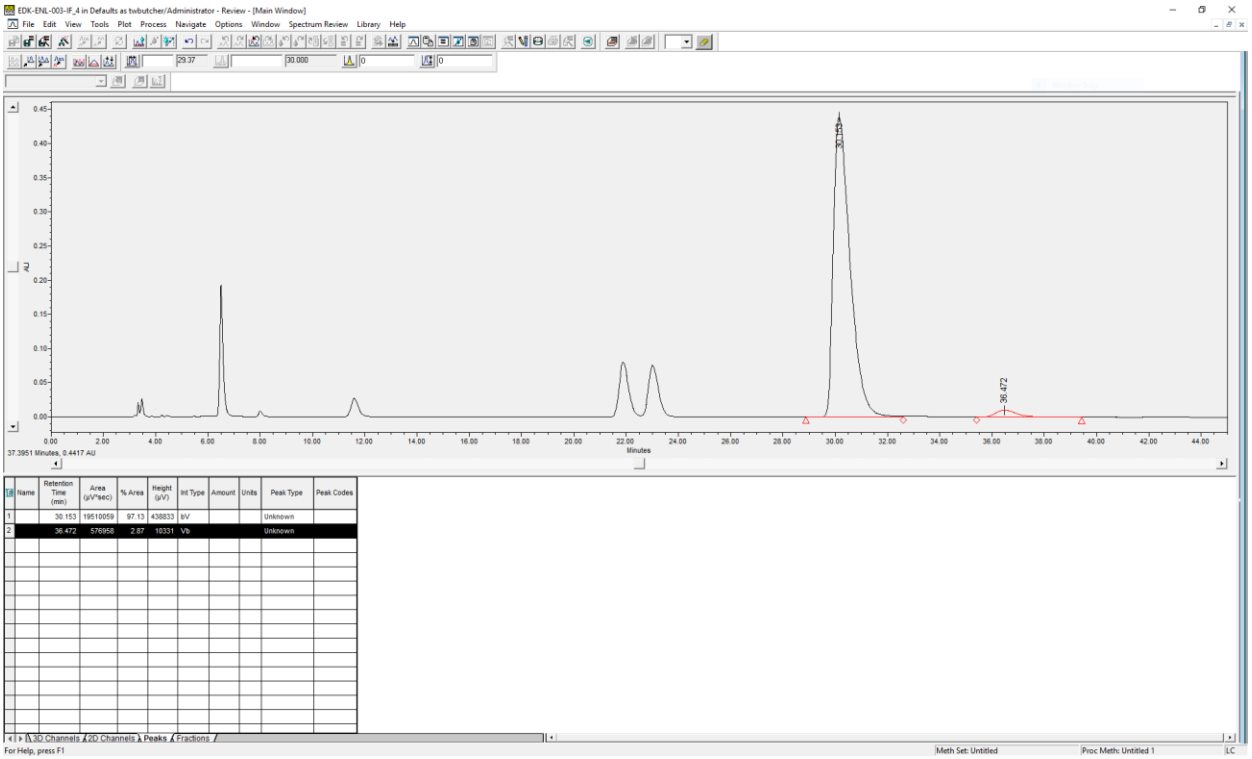
Figure 3.8.18 $^{31}P\{^{1}H\}$ NMR spectrum of the resting state (1 h) of the reaction of aryl triflate **7a** with fluorooxindole **3** catalyzed by ((*S*)-SEGPHOS)$_2$Pd(0) (**8**).



(***S***)-**4a**

IF column, 4% *i*PrOH in hexane, 1.0 mL/min, 240 nm, t_R = 30.153, 36.472 min.

94% ee



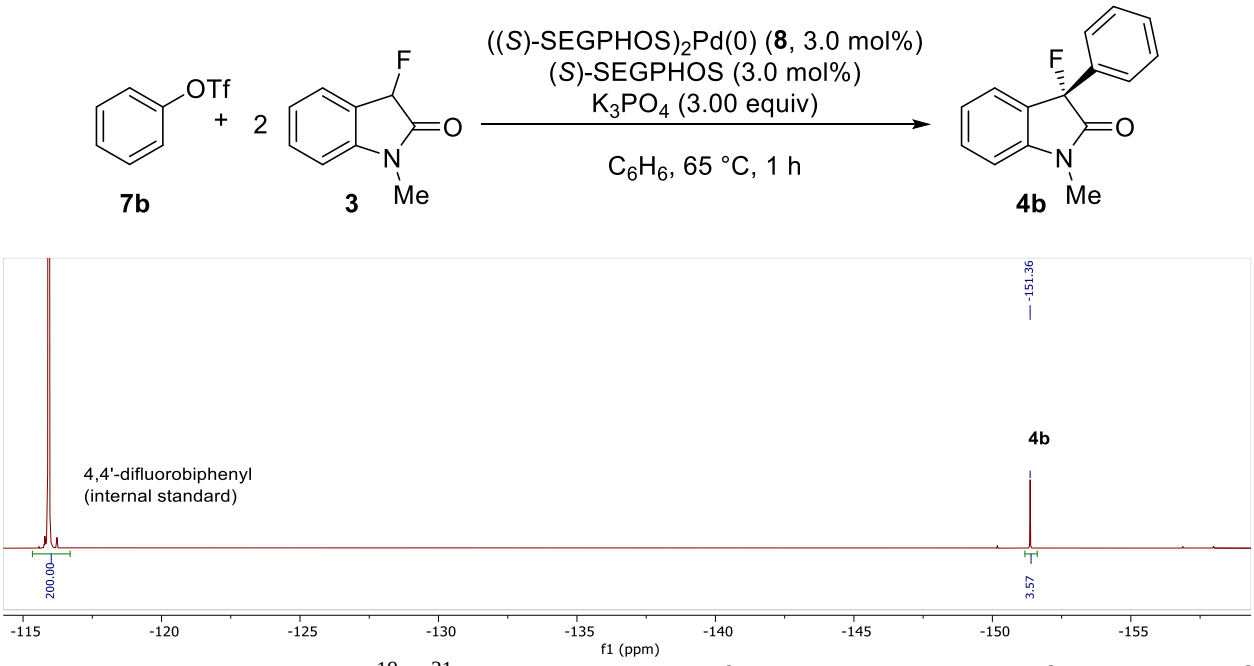


Figure 3.8.19 Inverse-gated $^{19}F\{^{31}P\}$ NMR spectrum of the resting state (1 h) of the reaction of aryl triflate **7b** with fluorooxindole **3** catalyzed by ((*S*)-SEGPHOS)$_2$Pd(0) (**8**) (Scheme 3.8.2). No phenylpalladium enolate complex **2b** was observed. Corresponds to 0.0038 mmol arylated product **4b** (3.8% yield).

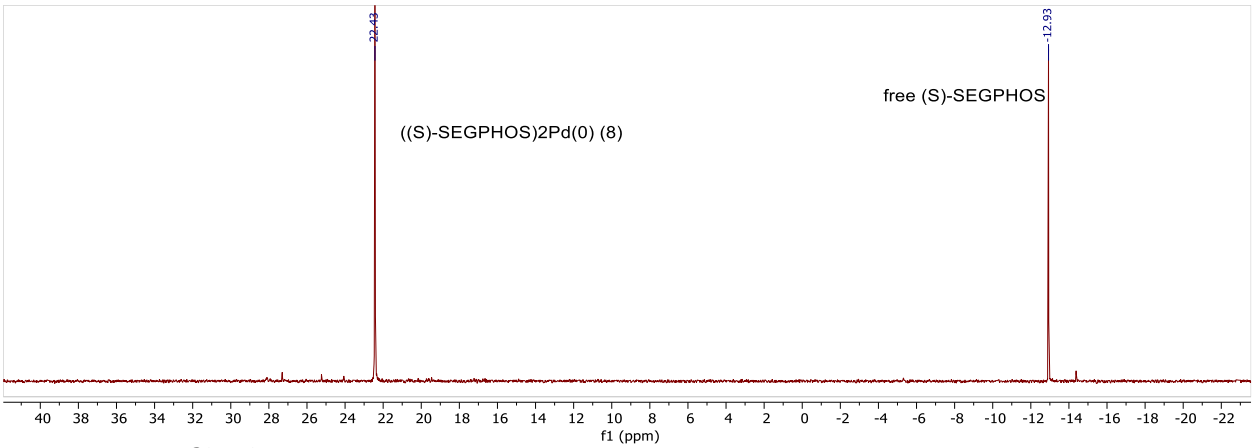
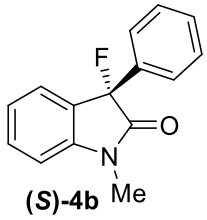
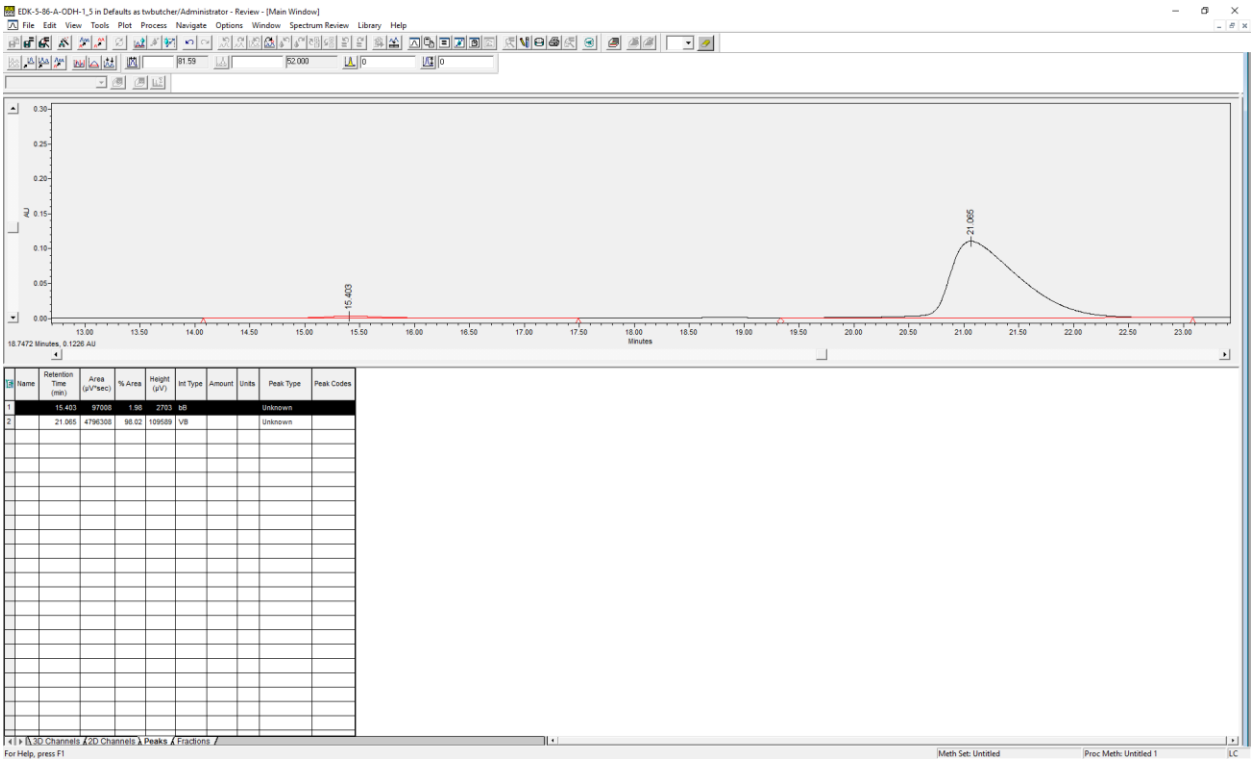


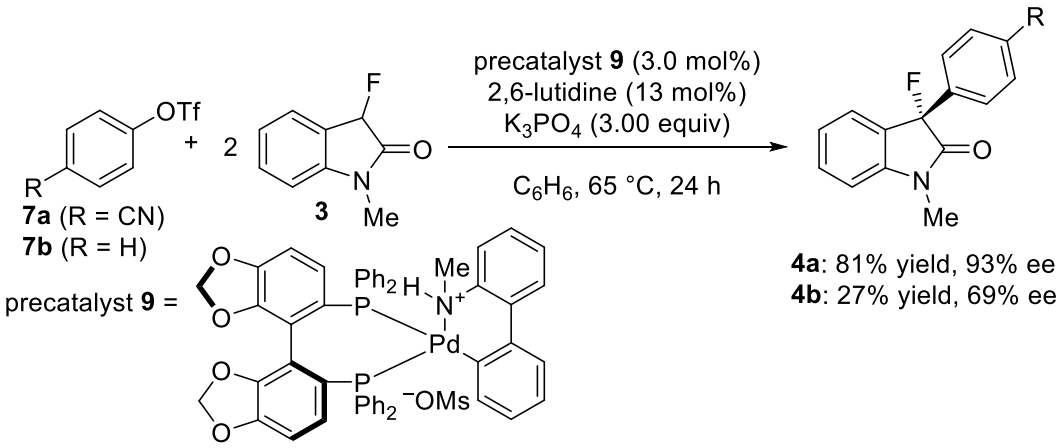
Figure 3.8.20 $^{31}P\{^{1}H\}$ NMR spectrum of the resting state (1 h) of the reaction of aryl triflate **7b** with fluorooxindole **3** catalyzed by ((*S*)-SEGPHOS)$_2$Pd(0) (**8**).



(*S*)-4b

OD-H column, 1.5% *i*PrOH in hexane, 1.0 mL/min, 240 nm, t_R = 15.403, 21.065 min.
96% ee





Scheme 3.8.3 Arylation reactions of aryl triflates **7a–b** catalyzed by precatalyst **8**.

To a 4 mL vial containing precatalyst **9** (3.0 mg, 3.0 μmol, 3.0 mol%), *N*-methyl-3-fluorooxindole (**3**, 33.0 mg, 0.200 mmol, 2.00 equiv), and K_3PO_4 (63.7 mg, 0.300 mmol, 3.00 equiv) was added aryl triflate (0.100 mmol, 1.00 equiv), 4,4'-difluorobiphenyl (variable, but measured exactly), 2,6-lutidine (1.5 μL, 0.013 mmol, 13 mol%), and C_6H_6 (650 μL). A stir bar was added, and the vial was sealed with a Teflon-lined cap and removed from the glove box. The reaction mixture was heated at 65 °C with vigorous stirring. After ~1 h, the reaction of aryl triflate **7a** was removed from heating, pumped into the glove box, and an aliquot (100 μL) was diluted in C_6H_6 (500 μL) for analysis of the catalytic resting state. The reaction mixture was resealed and removed from the glove box, and heating and stirring were resumed. After 48 h, the reaction mixture was diluted with ethyl acetate (2 mL) and passed through a plug of silica, which was flushed with more ethyl acetate (3×1 mL). The filtrate was concentrated under vacuum, the residue was taken up in $CDCl_3$, and yields were determined by quantitative ^{19}F NMR spectroscopy (**4a**: 81%; **4b**: 27%). The reaction mixture was then concentrated, and products **4a–b** were obtained *via* silica gel thin-layer chromatography (3:1 hexanes:ethyl acetate, R_f = 0.2 (**4a**), 0.3 (**4b**)). The *ee* values of **4a** and **4b** were determined by HPLC.

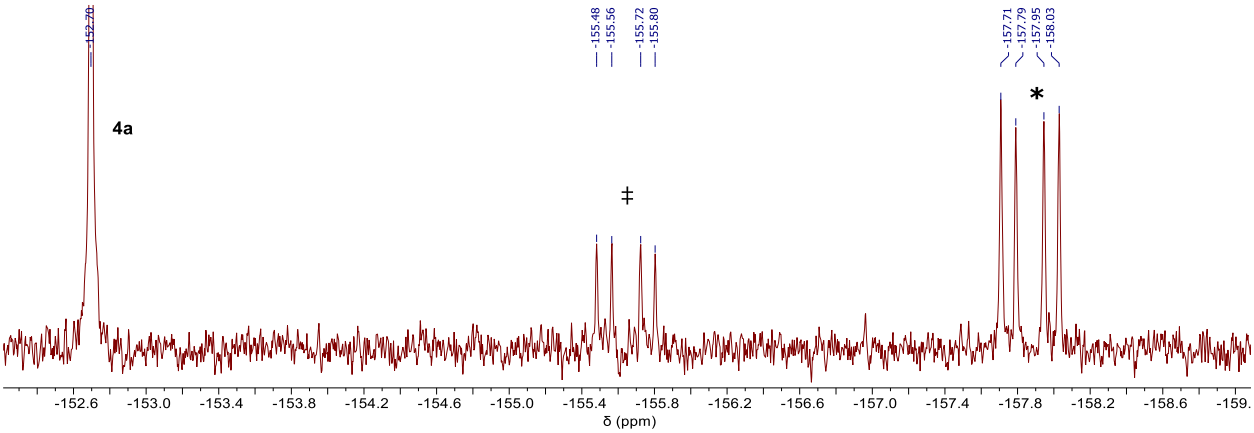


Figure 3.8.21 ^{19}F spectrum of the resting state (1 h) of the reaction of 4-cyanophenyl triflate **7a** with fluorooxindole **3** catalyzed by precatalyst **9** (Scheme 3.8.3). (*) and (‡) indicate resonances for the two diastereomers of **2a**.

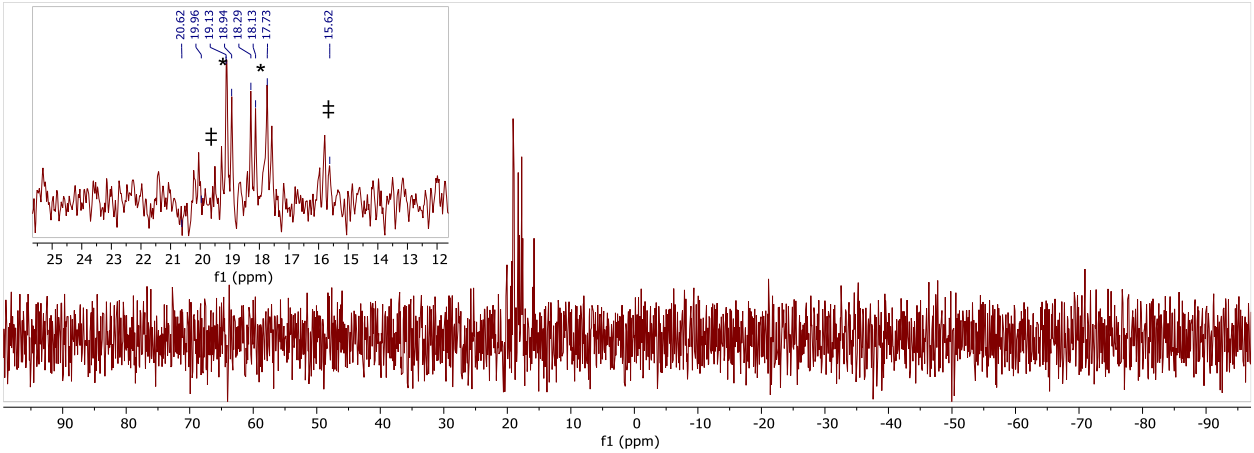
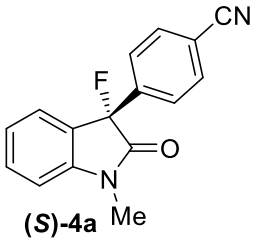
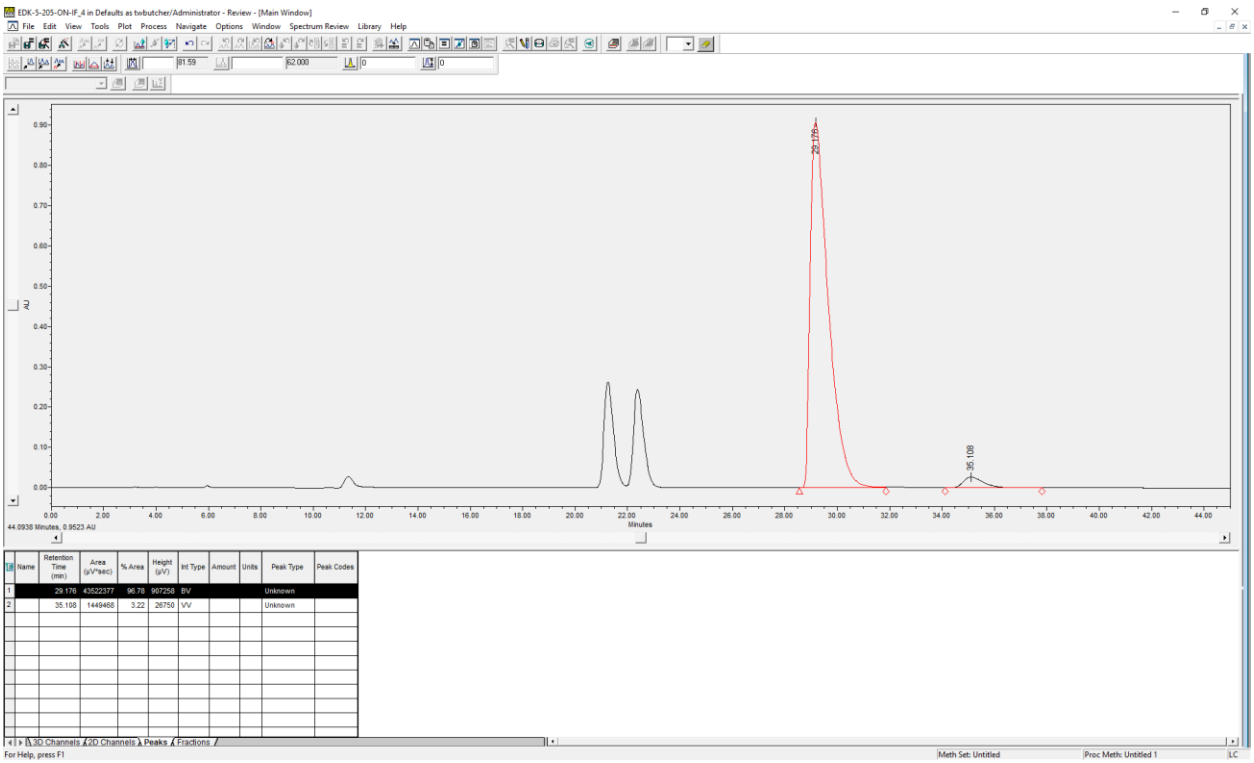


Figure 3.8.22 $^{31}P\{^{1}H\}$ NMR spectrum of the resting state (1 h) of the reaction of aryl triflate **7a** with fluorooxindole **3** catalyzed by precatalyst **9** (Scheme 3.8.3). (*) and (‡) indicate resonances for the two diastereomers of 4-cyanophenylpalladium fluoroenolate complex **2a**. Complex **2a** was the only detected P-containing species. Notably, ((*S*)-SEGPHOS)$_2$Pd(0) (complex **8**, 22.4 ppm) is absent from the spectrum.

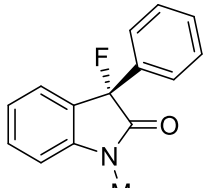


(*S*)-4a

IF column, 4% *i*PrOH in hexane, 1.0 mL/min, 240 nm, t_R = 29.176, 35.108 min. Also contains fluorooxindole **3**.
94% ee

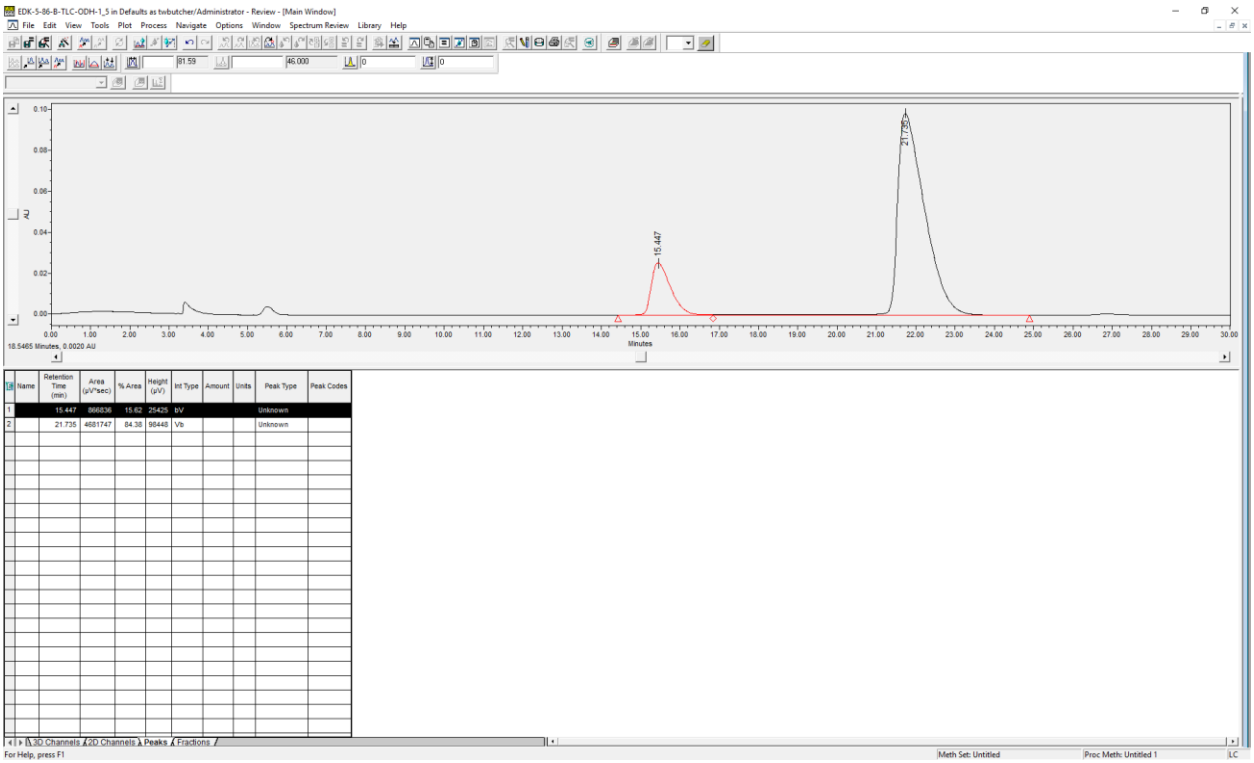


	Name	Retention Time (min)	Area (µV*sec)	% Area	Height (µV)	Int Type	Amount	Units	Peak Type	Peak Codes
1		29.176	43522377	96.78	967258	BV			Unknown	
2		35.108	1449468	3.22	26750	VV			Unknown	

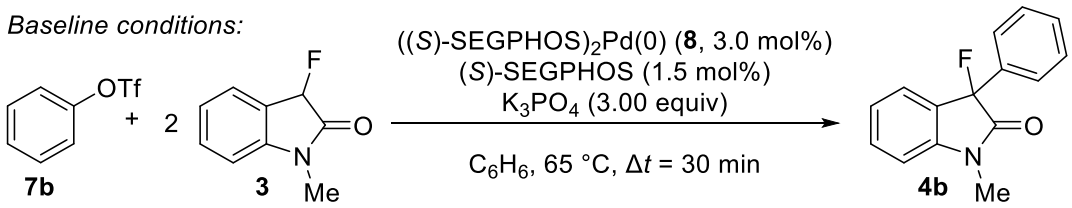


(*S*)-4b

OD-H column, 1.5% *i*PrOH in hexane, 1.0 mL/min, 240 nm, t_R = 15.447, 21.735 min.
69% ee



*Measuring the initial rates of the Pd-catalyzed enantioselective α-arylation of fluorooxindole **3** with aryl triflates **7a–b***



Scheme 3.8.4 Arylation of fluorooxindole **3** with phenyl triflate (**7b**) using $(SEGPHOS)_2Pd$ (**8**) as the precatalyst

*Order in [**8**] (1.5–6 mol%):*
The following stock solutions (C_6H_6) were prepared in 1.00 mL volumetric flasks:
Solution A: Phenyl triflate (**7b**) + (*S*)-SEGPHOS + 4,4'-difluorobiphenyl (internal standard):

- **7b**: 227.2 mg → 1.00 M
- (*S*)-SEGPHOS: 9.2 mg → 0.015 M
- 4,4'-difluorobiphenyl: 46.1 mg → 0.242 M

Solution B: 3-fluorooxindole (**3**):

- **3**: 247.8 mg → 1.50 M

Solution C: ((*S*)-SEGPHOS)$_2$Pd(0) (**8**)

- **8**: 29.7 mg → 0.0224 M

To 4 mL vials containing K_3PO_4 (63.7 mg, 0.300 mmol) were added Stock Solution A (100.0 μL; 0.100 mmol **7b**; 1.5 μmol (*S*)-SEGPHOS; 0.0242 mmol 4,4'-difluorobiphenyl), Stock Solution B (67.0 μL, 0.100 mmol **3**), Stock Solution C (67.0 μL; 133.0, 200.0, or 267.0 μL, 1.50, 3.00, 4.50, or 6.00 μmol **8**), and enough benzene to afford a total liquid volume of 650 μL. Magnetic stir bars were added to the vials, and the vials were sealed, removed from the glove box, and heated to 65 °C with vigorous stirring. Every ~30 min (actual time varied, but was recorded exactly by chronometer), the vials were cooled to 0 °C in an ice bath to pause the reaction, and the chronometer was also paused. The vials were quickly pumped into the glove box, and aliquots (50 μL) were taken from each vial. The vials and aliquots were then removed from the glove box, and the reaction vials were again heated to 65 °C with vigorous stirring at the same time that the chronometer was unpaused.

Aliquots were diluted with ethyl acetate (1.5 mL) and passed through silica plugs, which were flushed with more ethyl acetate (3×1 mL). The filtrates were then concentrated under vacuum and dissolved in $CDCl_3$, and quantitative ^{19}F NMR spectra were acquired. The extent of the reaction was determined by integrating the resonance corresponding to arylated product **4b** relative to that of the internal standard in each aliquot.

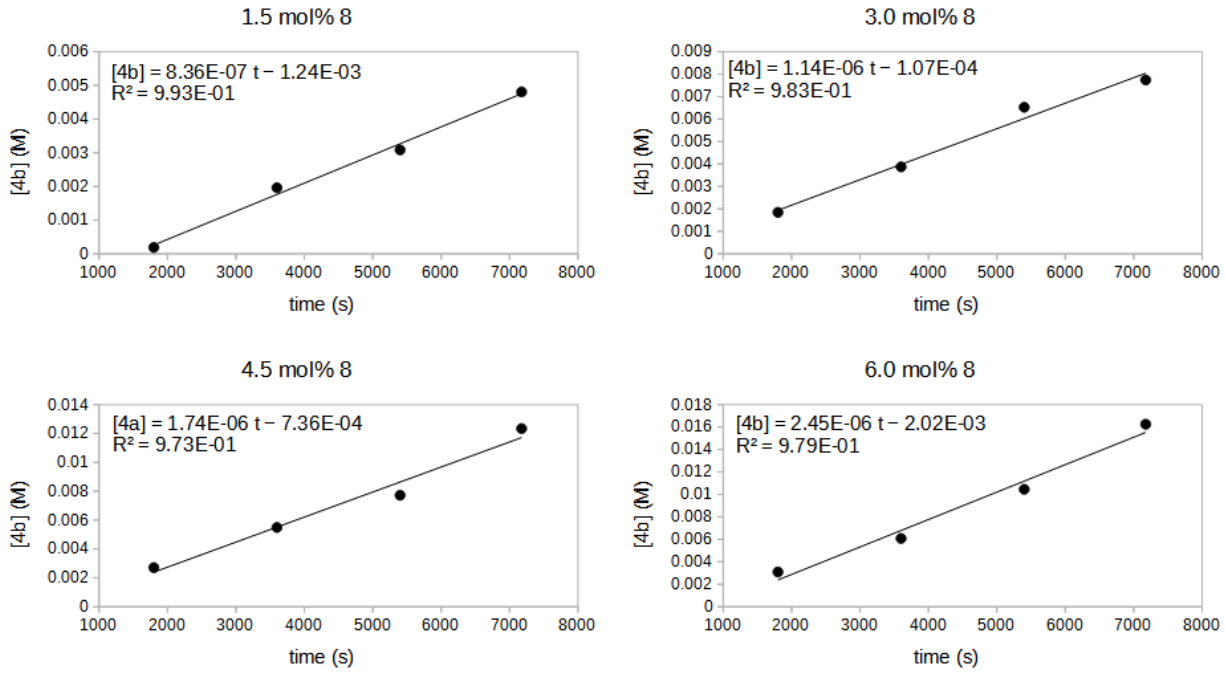


Figure 3.8.23 Formation of arylated product **4b** (Scheme 3.8.4) *vs* time varying the initial loading of precatalyst **8**

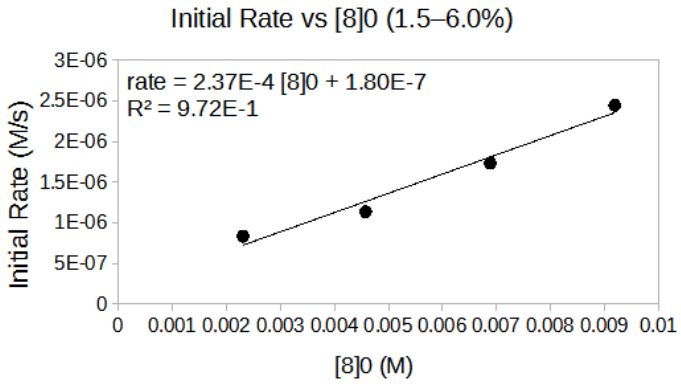


Figure 3.8.24 Plot of the initial rate of formation of **4b** (Scheme 3.8.4) varying the initial loading of precatalyst **8**. Linearity suggests first-order behavior. Equivalent to Figure 3.5.1a.

*Order in [**7b**] (0.505–2.02 equiv):*
The following stock solutions (C_6H_6) were prepared in 1.00 mL volumetric flasks:
Solution A: Phenyl triflate (**7b**):

- **7b**: 228.9 mg → 1.01 M

Solution B: 3-fluorooxindole (**3**) + 4,4'-difluorobiphenyl (internal standard):

- **3**: 165.2 mg → 1.00 M
- 4,4'-difluorobiphenyl: 32.1 mg → 0.169 M

Solution C: ((*S*)-SEGPHOS)$_2$Pd(0) (**8**) + (*S*)-SEGPHOS:

- **8**: 19.2 mg → 0.0145 M
- (*S*)-SEGPHOS: 4.5 mg → 0.0074 M

To 4 mL vials containing K_3PO_4 (63.7 mg, 0.300 mmol) were added Stock Solution A (50.0, 100.0, 150.0, or 200.0 μL, 0.0505, 0.101, 0.152, or 0.202 mmol **7b**), Stock Solution B (200.0 μL; 0.200 mmol **3**; 0.0338 mmol 4,4'-difluorobiphenyl), Stock Solution C (200.0 μL; 2.9 μmol **8**; 1.5 μmol (*S*)-SEGPHOS), and enough benzene to afford a total liquid volume of 650 μL. Magnetic stir bars were added to the vials, and the vials were sealed, removed from the glove box, and heated to 65 °C with vigorous stirring. Every ~30 min (actual time varied, but was recorded exactly by chronometer), the vials were cooled to 0 °C in an ice bath to pause the reaction, and the chronometer was also paused. The vials were quickly pumped into the glove box, and aliquots (50 μL) were taken from each vial. The vials and aliquots were then removed from the glove box, and the reaction vials were again heated to 65 °C with vigorous stirring at the same time that the chronometer was unpaused.

Aliquots were diluted with ethyl acetate (1.5 mL) and passed through silica plugs, which were flushed with more ethyl acetate (3×1 mL). The filtrates were then concentrated under vacuum and dissolved in $CDCl_3$, and quantitative ^{19}F NMR spectra were acquired. The extent of the reaction was determined by integrating the resonance corresponding to arylated product **4b** relative to that of the internal standard in each aliquot.

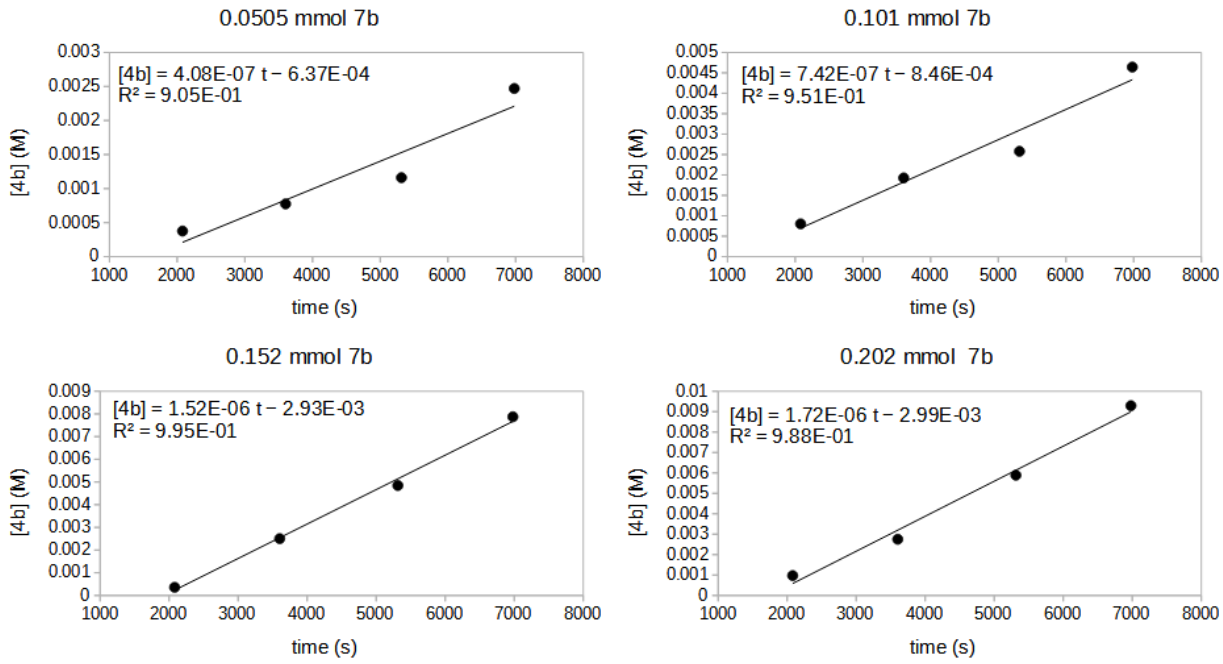


Figure 3.8.25 Formation of arylated product **4b** (**Scheme 3.8.4**) *vs* time varying the initial loading of phenyl triflate (**7b**).

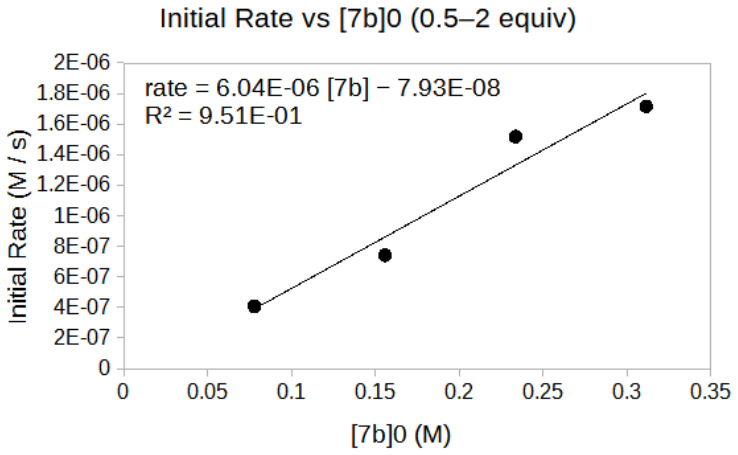


Figure 3.8.26 Plot of the initial rate of formation of product **4b** (**Scheme 3.8.4**) varying the initial loading of phenyl triflate (**7b**). Linearity suggests first-order behavior. Equivalent to Figure 3.5.1b.

*Order in [**3**] (1.00–4.00 equiv):*
The following stock solutions (C_6H_6) were prepared in 1.00 mL volumetric flasks:
Solution A: Phenyl triflate (**7b**)) + 4,4'-difluorobiphenyl (internal standard):

- **7b**: 226.2 mg → 1.00 M
- 4,4'-difluorobiphenyl: 44.7 mg → 0.235 M

Solution B: 3-fluorooxindole (**3**):

- **3**: 247.8 mg → 1.50 M

Solution C: ((*S*)-SEGPHOS)$_2$Pd(0) (**8**) + (*S*)-SEGPHOS:

- **8**: 20.0 mg → 0.0151 M
- (*S*)-SEGPHOS: 4.7 mg → 0.0077 M

To 4 mL vials containing K_3PO_4 (63.7 mg, 0.300 mmol) were added Stock Solution A (100.0 μL; 0.100 mmol **7b**; 0.0235 mmol 4,4'-difluorobiphneyl), Stock Solution B (67.0, 133.0, 200.0, or 267.0 μL; 0.100, 0.200, 0.300, or 0.400 mmol **3**), Stock Solution C (200.0 μL; 3.00 μmol **8**; 1.5 μmol (*S*)-SEGPHOS), and enough benzene to afford a total liquid volume of 650 μL. Magnetic stir bars were added to the vials, and the vials were sealed, removed from the glove box, and heated to 65 °C with vigorous stirring. Every ~30 min (actual time varied, but was recorded exactly by chronometer), the vials were cooled to 0 °C in an ice bath to pause the reaction, and the chronometer was also paused. The vials were quickly pumped into the glove box, and aliquots (50 μL) were taken from each vial. The vials and aliquots were then removed from the glove box, and the reaction vials were again heated to 65 °C with vigorous stirring at the same time that the chronometer was unpaused.

Aliquots were diluted with ethyl acetate (1.5 mL) and passed through silica plugs, which were flushed with more ethyl acetate (3×1 mL). The filtrates were then concentrated under vacuum and dissolved in $CDCl_3$, and quantitative ^{19}F NMR spectra were acquired. The extent of the reaction was determined by integrating the resonance corresponding to arylated product **4b** relative to that of the internal standard in each aliquot.

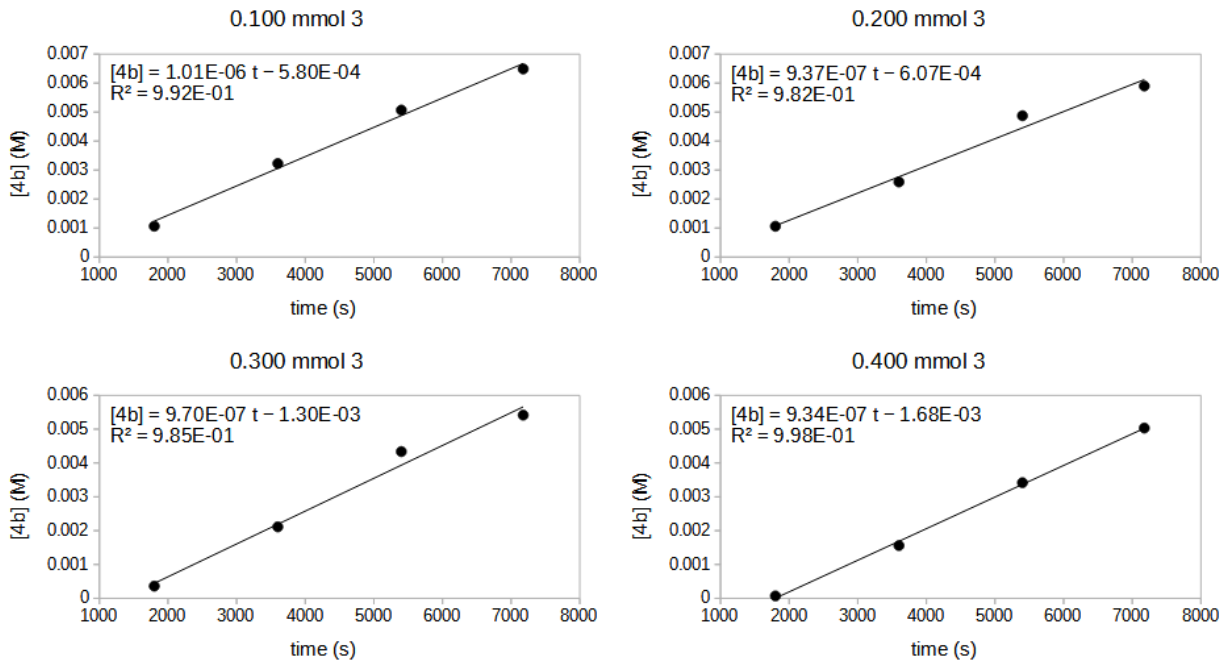


Figure 3.8.27 Formation of arylated product **4b** (Scheme 3.8.4) *vs* time varying initial loadings fluorooxindole **3**.

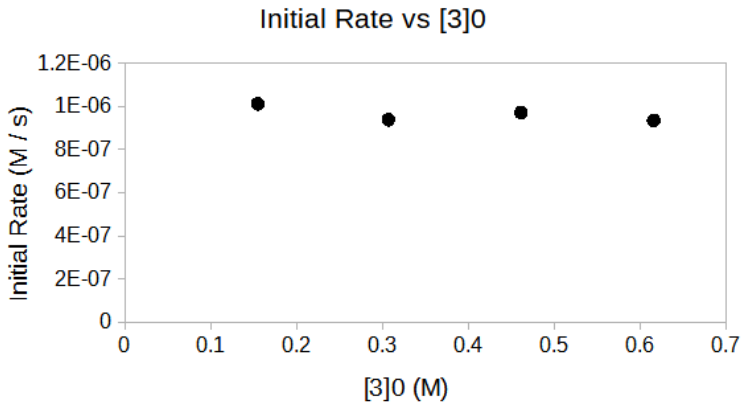


Figure 3.8.28 Plot of the initial rate of the formation of **4b** (**Scheme 3.8.4**) varying the initial loading of fluorooxindole **3**. Equivalent to Figure 3.5.1c.

Order in [(S)-SEGPHOS] (1.00–4.00 equiv):
The following stock solutions (C_6H_6) were prepared in 1.00 mL volumetric flasks:
Solution A: Phenyl triflate (**7b**)):

- **7b**: 229.9 mg → 1.02 M

Solution B: 3-fluorooxindole (**3**) + 4,4'-difluorobiphenyl (internal standard):

- **3**: 165.2 mg → 1.00 M
- 4,4'-difluorobiphenyl: 41.8 mg → 0.220 M

Solution C: ((*S*)-SEGPHOS)$_2$Pd(0) (**8**):

- **8**: 19.7 mg → 0.0148 M

Solution D: (*S*)-SEGPHOS:

- (*S*)-SEGPHOS: 24.4 mg → 0.0400 M

To 4 mL vials containing K_3PO_4 (63.7 mg, 0.300 mmol) were added Stock Solution A (100.0 μL; 0.100 mmol **7b**), Stock Solution B (200 μL; 0.200 mmol **3**; 0.044 mmol 4,4'-difluorobiphenyl), Stock Solution C (200.0 μL; 2.96 μmol **8**), Stock Solution D (37.5, 75.0, 112.5, or 150.0 μL; 1.50, 3.00, 4.50, or 6.00 μmol (*S*)-SEGPHOS), and enough benzene to afford a total liquid volume of 687.5 μL. Magnetic stir bars were added to the vials, and the vials were sealed, removed from the glove box, and heated to 65 °C with vigorous stirring. Every ~30 min (for the reactions containing 1.50 and 3.00 μmol (*S*)-SEGPHOS) or ~60 min (for the reactions containing 4.50 and 6.00 μmol (*S*)-SEGPHOS; actual times varied, but were recorded exactly by chronometer), the vials were cooled to 0 °C in an ice bath to pause the reaction, and the chronometer was also paused. The vials were quickly pumped into the glove box, and aliquots (50 μL) were taken from each vial. The vials and aliquots were then removed from the glove box, and the reaction vials were again heated to 65 °C with vigorous stirring at the same time that the chronometer was unpaused.

Aliquots were diluted with ethyl acetate (1.5 mL) and passed through silica plugs, which were flushed with more ethyl acetate (3×1 mL). The filtrates were then concentrated under vacuum and dissolved in $CDCl_3$, and quantitative ^{19}F NMR spectra were acquired. The extent of the reaction was determined by integrating the resonance corresponding to arylated product **4b** relative to that of the internal standard in each aliquot.

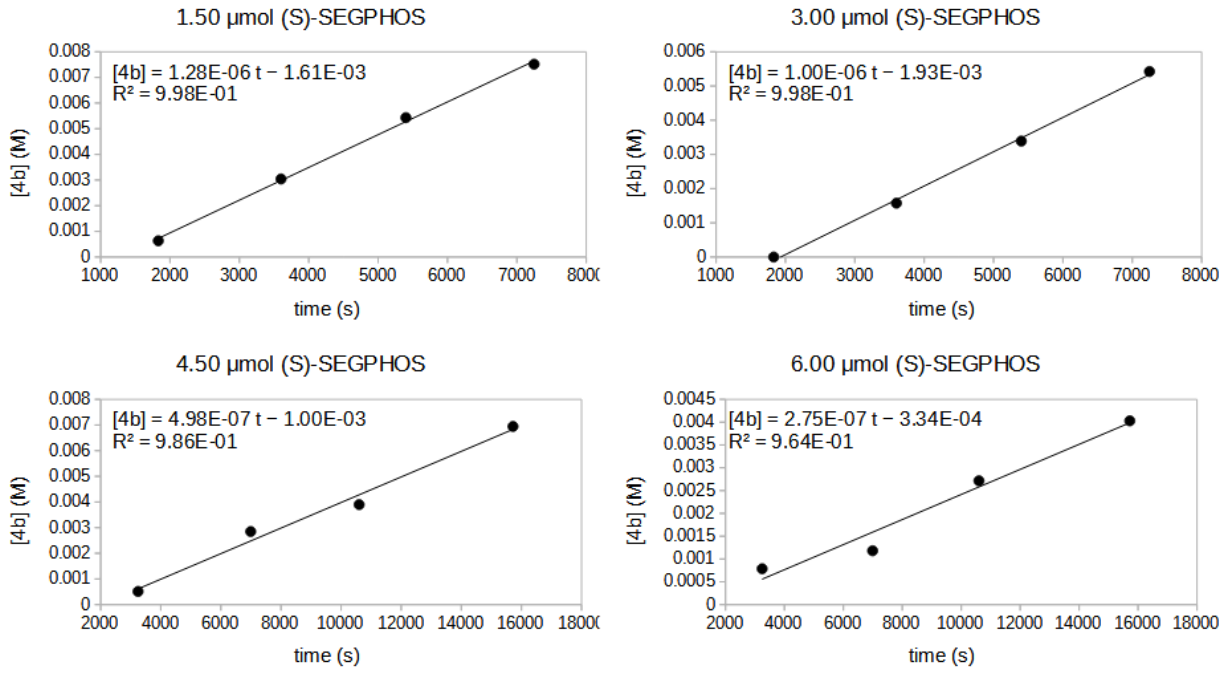


Figure 3.8.29 Formation of arylated product **4b** (Scheme 3.8.4) *vs* time varying the initial loading of (*S*)-SEGHPOS.

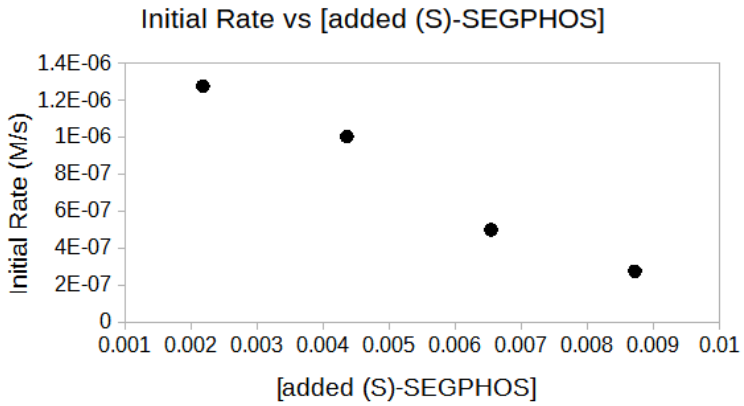
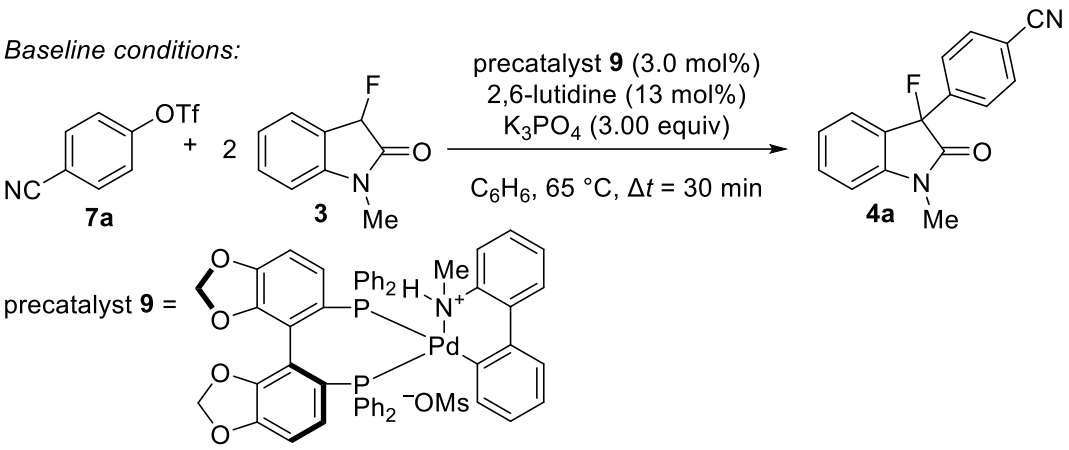


Figure 3.8.30 Plot of the initial rate of the formation of **4b** (**Scheme 3.8.4**) varying the initial loading of (*S*)-SEGPHOS. Equivalent to Figure 3.5.1d.



Scheme 3.8.5 Arylation of fluorooxindole **3** with 4-cyanophenyl triflate (**7a**) using palladacycle **9** as the precatalyst

*Order in [**9**] (2.0–5.0 μmol):*
The following stock solution (CH_3CN) was prepared in a 1.00 mL volumetric flask:
Solution A: Precatalyst **9**:

- **8**: 16.9 mg → 0.00170 M

The following stock solutions (C_6H_6) were prepared in 1.00 mL volumetric flasks:
Solution B: 4-cyanophenyl triflate (**7a**) 4,4'-difluorobiphenyl (internal standard):

- **7a**: 252.1 mg → 1.00 M
- 4,4'-difluorobiphenyl: 46.1 mg → 0.302 M

Solution C: 3-fluorooxindole (**3**):

- **3**: 165.2 mg → 1.00 M

To 4 mL vials was added Stock Solution C (117.5, 176.5, 235.0, or 294.0 μL; 1.99, 3.00, 3.99, or 5.00 μmol precatalyst **9**), and the solvent was removed under vacuum to leave thin films of precatalyst on the walls of the vials. To each of these vials was added K_3PO_4 (63.7 mg, 0.300 mmol), Stock Solution B (100.0 μL; 0.100 mmol **7a**; 0.0302 mmol 4,4'-difluorobiphenyl), Stock Solution C (200.0 μL; 0.200 mmol **3**), 2,6'-lutidine (1.5 μL, 0.013 mmol) and enough benzene to afford a total liquid volume of 650 μL. Magnetic stir bars were added to the vials, and the vials were sealed, removed from the glove box, and heated to 65 °C with vigorous stirring. Every ~30 min (actual time varied, but was recorded exactly by chronometer), the vials were cooled to 0 °C in an ice bath to pause the reaction, and the chronometer was also paused. The vials were quickly pumped into the glove box, and aliquots (50 μL) were taken from each vial. The vials and aliquots were then removed from the glove box, and the reaction vials were again heated to 65 °C with vigorous stirring at the same time that the chronometer was unpaused.

Aliquots were diluted with ethyl acetate (1.5 mL) and passed through silica plugs, which were flushed with more ethyl acetate (3×1 mL). The filtrates were then concentrated under vacuum and dissolved in $CDCl_3$, and quantitative ^{19}F NMR spectra were acquired. The extent of the reaction was determined by integrating the resonance corresponding to arylated product **4a** relative to that of the internal standard in each aliquot.

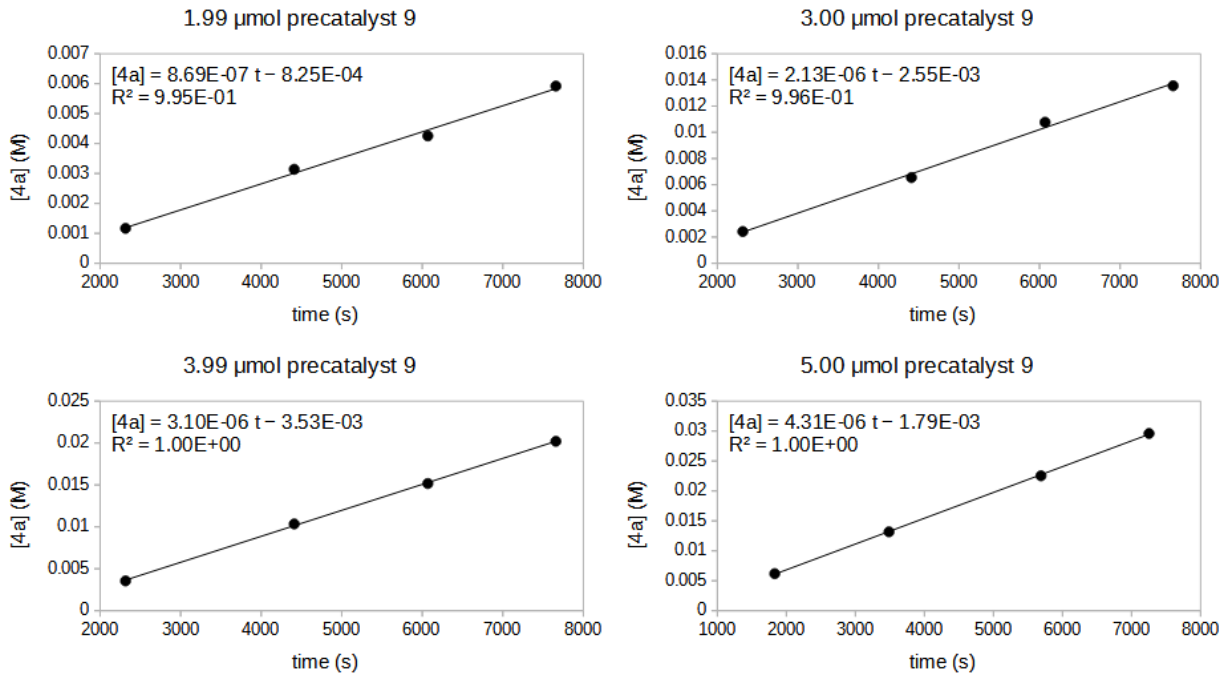


Figure 3.8.31 Formation of arylated product **4a** (Scheme 3.8.5) *vs* time varying the loading of precatalyst **9**.

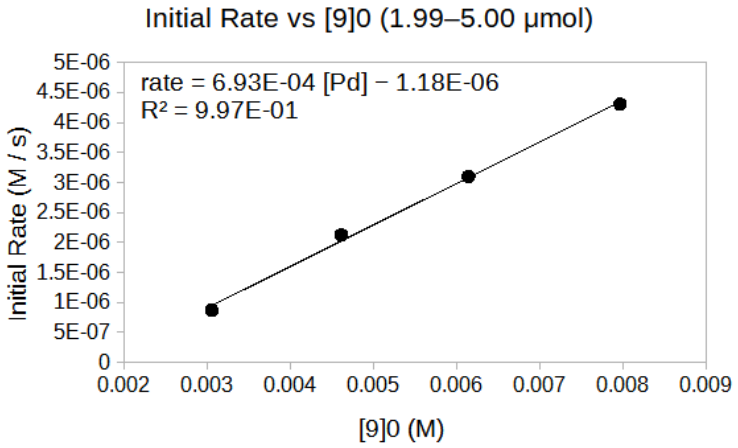


Figure 3.8.32 Plot of the initial rate of the formation of **4a** (**Scheme 3.8.5**) varying the initial loading of precatalyst **9**. Equivalent to Figure 3.5.2a.

*Order in [**7a**] (0.101–0.403 mmol):*
The following stock solution (CH_3CN) was prepared in a 1.00 mL volumetric flask:
Solution A: Precatalyst **9**:

- **8**: 14.9 mg → 0.0150 M

The following stock solutions (C_6H_6) were prepared in 1.00 mL volumetric flasks:
Solution B: 4-cyanophenyl triflate (**7a**):

- **7a**: 379.4 mg → 1.51 M

Solution C: 3-fluorooxindole (**3**) + 4,4'-difluorobiphenyl (internal standard):

- **3**: 167.1 mg → 1.01 M
- 4,4'-difluorobiphenyl: 44.8 mg → 0.236 M

To 4 mL vials was added Stock Solution C (200.0 μL; 3.00 μmol precatalyst **9**), and the solvent was removed under vacuum to leave thin films of precatalyst on the walls of the vials. To each of these vials was added K_3PO_4 (63.7 mg, 0.300 mmol), Stock Solution B (67.0, 133.0, 200.0, or 267 μL; 0.101, 0.201, 0.302, or 0.403 mmol **7a**), Stock Solution C (200.0 μL; 0.200 mmol **3**; 0.0472 mmol 4,4'-difluorobiphenyl), 2,6'-lutidine (1.5 μL, 0.013 mmol) and enough benzene to afford a total liquid volume of 650 μL. Magnetic stir bars were added to the vials, and the vials were sealed, removed from the glove box, and heated to 65 °C with vigorous stirring. Every ~30 min (actual time varied, but was recorded exactly by chronometer), the vials were cooled to 0 °C in an ice bath to pause the reaction, and the chronometer was also paused. The vials were quickly pumped into the glove box, and aliquots (50 μL) were taken from each vial. The vials and aliquots were then removed from the glove box, and the reaction vials were again heated to 65 °C with vigorous stirring at the same time that the chronometer was unpaused.

Aliquots were diluted with ethyl acetate (1.5 mL) and passed through silica plugs, which were flushed with more ethyl acetate (3×1 mL). The filtrates were then concentrated under vacuum and dissolved in $CDCl_3$, and quantitative ^{19}F NMR spectra were acquired. The extent of the reaction was determined by integrating the resonance corresponding to arylated product **4a** relative to that of the internal standard in each aliquot.

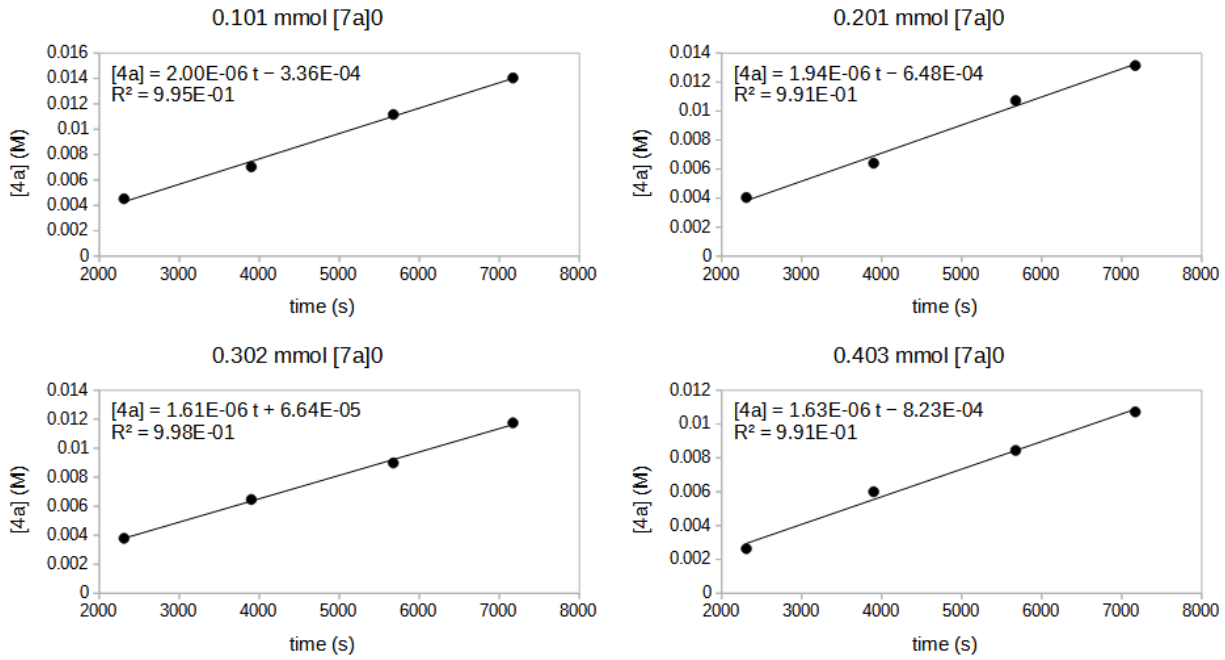


Figure 3.8.33 Formation of arylated product **4a** (Scheme 3.8.5) *vs* time varying the initial loading of 4-cyanophenyl triflate (**7a**).

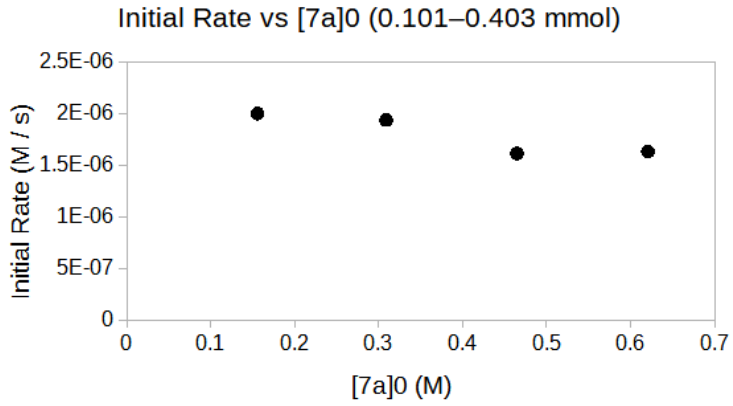


Figure 3.8.34 Plot of the initial rate of the formation of **4a** (Scheme 3.8.5) varying the initial loading of 4-cyanophenyl triflate (**7a**). Equivalent to Figure 3.5.2b.

*Order in [**3**] (0.101–0.403 mmol):*
The following stock solution (CH_3CN) was prepared in a 1.00 mL volumetric flask:
Solution A: Precatalyst **9**:

- **8**: 14.8 mg → 0.0149 M

The following stock solutions (C_6H_6) were prepared in 1.00 mL volumetric flasks:
Solution B: 4-cyanophenyl triflate (**7a**) + 4,4'-difluorobiphenyl (internal standard):

- **7a**: 260.6 mg → 1.04 M
- 4,4'-difluorobiphenyl: 42.7 mg → 0.225 M

Solution C: 3-fluorooxindole (**3**):

- **3**: 247.8 mg → 1.50 M

To 4 mL vials was added Stock Solution C (200.0 μL; 2.98 μmol precatalyst **9**), and the solvent was removed under vacuum to leave thin films of precatalyst on the walls of the vials. To each of these vials was added K_3PO_4 (63.7 mg, 0.300 mmol), Stock Solution B (100.0 μL; 0.104 mmol **7a**; 0.0225 mmol 4,4'-difluorobiphenyl), Stock Solution C (67.0, 133.0, 200.0, or 267 μL; 0.100, 0.200, 0.300, 0.401 mmol **3**), 2,6'-lutidine (1.5 μL, 0.013 mmol) and enough benzene to afford a total liquid volume of 650 μL. Magnetic stir bars were added to the vials, and the vials were sealed, removed from the glove box, and heated to 65 °C with vigorous stirring. Every ~30 min (actual time varied, but was recorded exactly by chronometer), the vials were cooled to 0 °C in an ice bath to pause the reaction, and the chronometer was also paused. The vials were quickly pumped into the glove box, and aliquots (50 μL) were taken from each vial. The vials and aliquots were then removed from the glove box, and the reaction vials were again heated to 65 °C with vigorous stirring at the same time that the chronometer was unpaused.

Aliquots were diluted with ethyl acetate (1.5 mL) and passed through silica plugs, which were flushed with more ethyl acetate (3×1 mL). The filtrates were then concentrated under vacuum and dissolved in $CDCl_3$, and quantitative ^{19}F NMR spectra were acquired. The extent of the reaction was determined by integrating the resonance corresponding to arylated product **4a** relative to that of the internal standard in each aliquot.

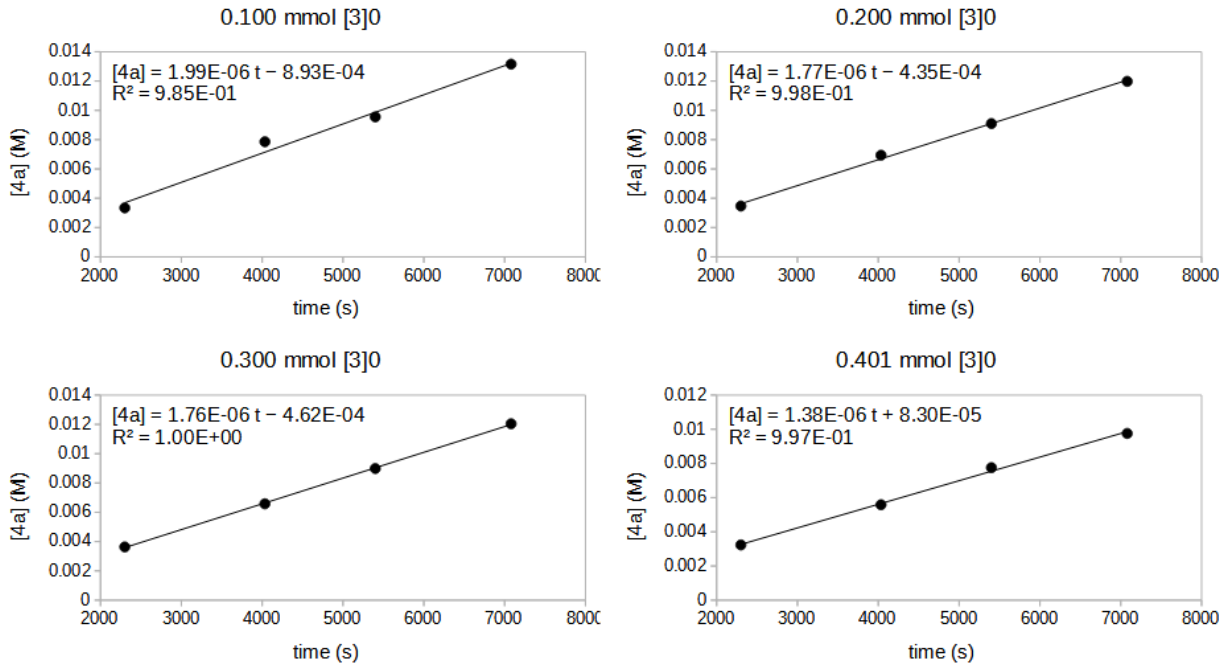


Figure 3.8.35 Formation of arylated product **4a** (Scheme 3.8.5) *vs* time varying the initial loading of fluorooxindole **3**.

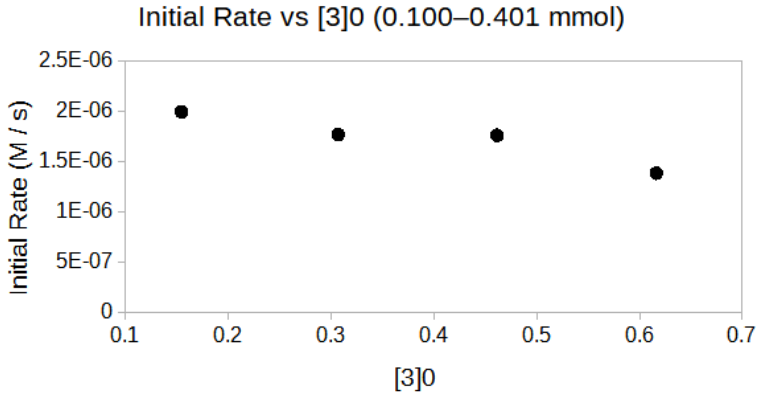


Figure 3.8.36 Plot of the initial rate of the formation of **4a** (Scheme 3.8.5) varying the initial loading of fluorooxindole **3**. Equivalent to Figure 3.5.2c.

3.8.5 Computational Methods

General considerations

DFT calculations were conducted at the Molecular Graphics and Computation Facility at the University of California, Berkeley using the Gaussian 16 software package.[63] All calculations, including geometry optimizations, were performed in benzene solvent using the SMD solvent continuum reported by Truhlar and co-workers according to the Solvent-Accessible Surface (scrf=sas).[64] Initial geometries were constructed in GaussView[65] and optimized to stationary points (either minima or first-order saddle points) using the PBE0 functional (the hybrid functional based on the Perdew-Burke-Ernzerhof functional [PBE][66,67] as described by Adamo[68]) with Grimme's D3 dispersion correction with Becke-Johnson damping (GD3-BJ)[69] and the basis sets def2-TZVP (with effective core potential) for Pd and def2-SVP for all light atoms (**BS1**).[70] The nature of each stationary point was verified by accompanying frequency calculations (all positive eigenvalues for minima and exactly one negative eigenvalue for transition states). Several rotomers for each ground state and transition state were considered, but only those lowest in energy or relevant to the reaction coordinate are presented here. Connectivity of transition states to ground-state minima was established by following the intrinsic reaction coordinate (IRC). Frequency calculations were performed at 1 atm at 338.15 K (65 °C). Further single point energy (SPE) calculations were performed on the optimized geometries with the larger def2-QZVP basis set (with ECP) on Pd (obtained through the Basis Set Exchange,[70–74] accessed October 2019) and Truhlar's minimally-augmented version of the def2-TZVP basis set ("ma-TZVP") on all light atoms (**BS2**).[70,75] Additional SPE calculations with other functionals (ωB97X-D and B3LYP-D3(BJ)) using **BS2** were conducted on a subset of these structures to validate the choice of functional (see **Error! Reference source not found.** below). In all cases, Gibbs free energies for calculations using **BS2** were approximated by summing the internal energy calculated with **BS2** and the thermal correction from the frequency calculation on the same structure with **BS1**. Coordinates for optimized geometries are given as a multi-structure XYZ file with titles matching the name of the structures given in **Figure 3.4.1** and Table 3.8.4, which is available from the publisher of the published manuscript.[51]

NBO analyses were conducted with the NBO 6.0 program.[53] Wiberg bond indices (NBO keyword: BNDIDX) along the intrinsic reaction coordinate for the Pd→π^* interaction (see main text) were calculated in **BS1**. The second-order NBO interactions in the transition states to reductive elimination ($TS_{H,minor}$ and $TS_{H,major}$) were calculated in both (unaugmented) **BS1** and (augmented) **BS2**. The energetic differences from the two basis sets were not found to be significantly different. The energies calculated using **BS2** are presented in the main text.

Grid data for NCI analyses[48] and NBO orbitals were generated using Multiwfn 3.7[49] and visualized using VMD.[50] RDG isosurfaces for NCI analyses were drawn at $s = 0.05$ au excluding $\rho > 0.05$ au, and an oversaturated color scale (range of $\text{sgn}(\lambda_2)\rho = -0.03 - 0.03$ au instead of the full –0.05 to 0.05) was used throughout for higher visual contrast.

Although we searched extensively, lower-energy transition states for the isomerization between the α-*C*-bound and *O*-bound forms of the enolate fragment were not found. Thus, the DFT calculations predict a slightly higher overall barrier for isomerization from ***pro*-(*S*)** to **κO2** than for reductive elimination from ***pro*-(*S*)** (through **pro-(*S*)-rot**). Nevertheless, the difference between these barriers is small (~1 kcal/mol), which is well within the error expected from DFT calculations.

Table 3.8.4 Energies of Computed Structures (PBE0-D3(BJ)/**BS2** + SMD(Benzene, SAS))

	Complex 2a (Ar = 4-CN-C_6H_4)		Complex 2b (Ar = C_6H_5)	
Structure	**E (Hartree)**	**G (Hartree)**	**E (Hartree)**	**G (Hartree)**
***pro*-(*R*)**	–3475.21999599	–3474.53206999	–3383.04053317	–3382.34869617
***pro*-(*R*)-rot**	–3475.20777148	–3474.51775548	–3383.02910238	–3382.33432438
RE-TS-(*R*)	–3475.17863159	–3474.49011859	–3382.99995517	–3382.30697817
pdt-(*R*)	–3475.24382234	–3474.55313534	–3383.06572986	–3382.37117786
isom-TS-(*R*)	–3475.1845392	–3474.4952172	–3383.00636512	–3382.31275712
κO1	–3475.2116716	–3474.5239276	–3383.03274568	–3382.34158468
κO2	–3475.20869412	–3474.52410512	–3383.02954204	–3382.34000504
isom-TS-(*S*)	–3475.1845392	–3474.4952172	–3383.0052219	–3382.3102949
***pro*-(*S*)**	–3475.21872522	–3474.53027422	–3383.03976739	–3382.34655639
***pro*-(*S*)-rot**	–3475.21517738	–3474.52466838	–3383.03640546	–3382.34195946
RE-TS-(*S*)	–3475.18353368	–3474.49450468	–3383.00519128	–3382.31199428
pdt-(*S*)	–3475.24382234	–3474.55307134	–3383.06488778	–3382.37073778

Table 3.8.5 Energies of Computed Structures (Functional/**BS2** + SMD(Benzene, SAS))

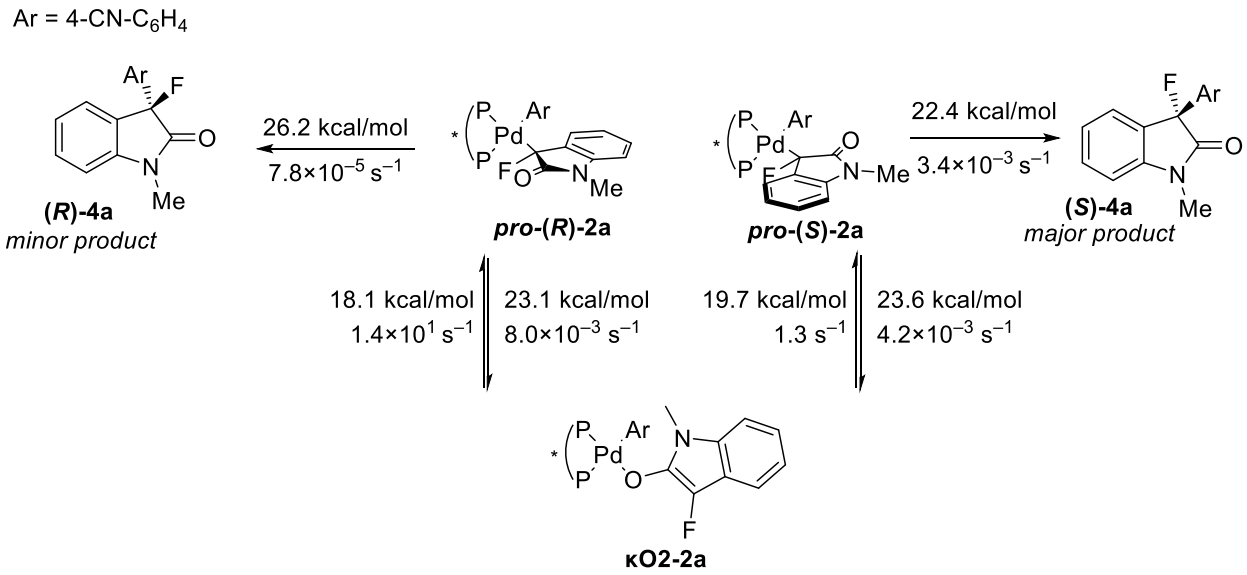
	B3LYP-D3(BJ)			ωB97X-D		
Structure	**E (Hartree)**	**G (Hartree)**	**ΔG (kcal/mol)**	**E (Hartree)**	**G (Hartree)**	**ΔG (kcal/mol)**
***pro*-(*R*)**	–3478.78667141	–3478.09874541	0.00	–3477.53298471	–3476.84505871	0.00
***pro*-(*R*)-rot**	–3478.77603435	–3478.08611435	7.93	–3477.52245198	–3476.83253198	7.86
RE-TS-(*R*)	–3478.74293423	–3478.05446823	27.78	–3477.49049032	–3476.80202432	27.00
isom-TS-(*R*)	–3478.75128212	–3478.06196012	23.08	–3477.49483574	–3476.80551374	24.81
κO1	–3478.77902002	–3478.09127602	4.69	–3477.52075122	–3476.83616222	5.58
κO2	–3478.77574807	–3478.09115907	4.76	–3477.52396675	–3476.83622275	5.54
isom-TS-(*S*)	–3478.74976258	–3478.05925058	24.78	–3477.49379529	–3476.80328329	26.21
***pro*-(*S*)**	–3478.78588553	–3478.09743453	0.82	–3477.53190832	–3476.84345732	1.00
***pro*-(*S*)-rot**	–3478.78217076	–3478.09166176	4.45	–3477.52790675	–3476.83739775	4.81
RE-TS-(*S*)	–3478.74560267	–3478.05657367	26.46	–3477.49347879	–3476.80444979	25.48

*Simulating the ee of arylated products **4a–b** using rate constants determined from DFT energies*

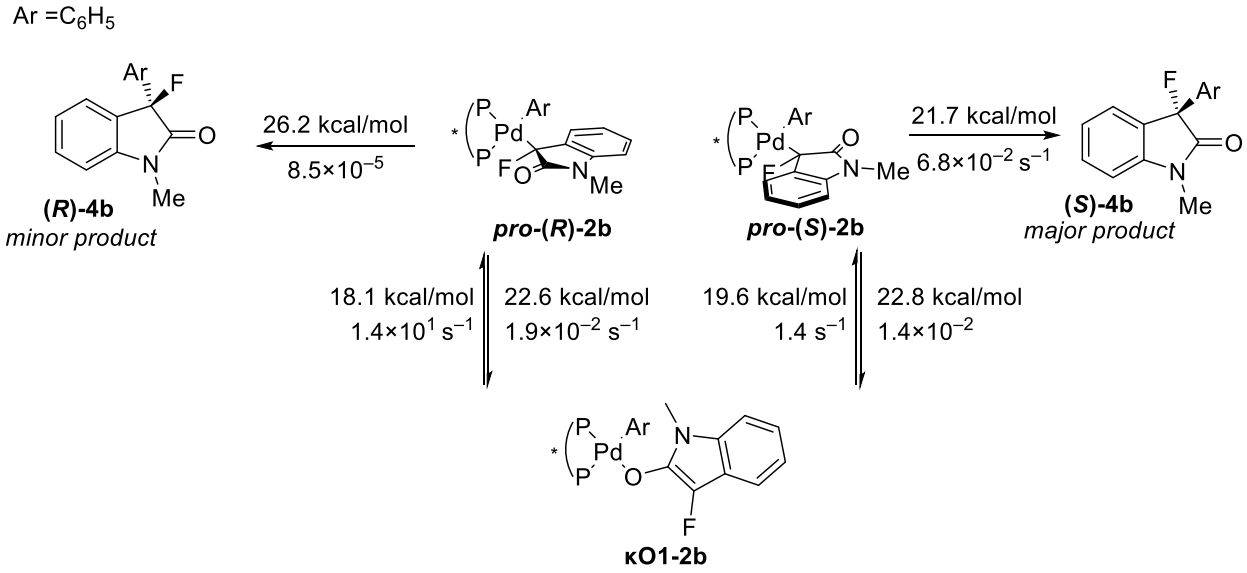
The reaction paths described in Scheme 3.8.6 and Scheme 3.8.7 (below) were entered into COPASI, and the rate constants were calculated from the free energies of each structure using the Eyring equation. The initial concentrations of ***pro*-(*S*)** and ***pro*-(*R*)** were each set to 1 M, and a time course was simulated for 7200 s (120 intervals of 60 s, max internal steps = 100000). At the end of the simulation, < 1% of ***pro*-(*S*)** and ***pro*-(*R*)** remained. The *ee* value was calculated as the ratio of product **(*S*)-4** to **(*R*)-4**.

Final amounts of **(*S*)-4a** and **(*R*)-4a** from the simulation of complex **2a** (Ar = 4-CN-C_6H_4): 1.8614 M, 0.1297 M (*ee* = 87.0%).

Final amounts of **(*S*)-4b** and **(*R*)-4b** from the simulation of complex **2b** (Ar = Ph): 1.9356 M, 0.0644 M (*ee* = 93.6%).



Scheme 3.8.6 Schematic of the simulation of the formation of **4a** from fluoroenolate complex **2a** using rate constants determined from DFT calculations. Energies are $\Delta G^{\ddagger}$ determined at PBE0-D3(BJ)/**BS2** + SMD(benzene, SAS) (T = 338.15 K).



Scheme 3.8.7 Schematic of the simulation of the formation of **4b** from fluoroenolate complex **2b** using rate constants determined from DFT calculations. Energies are $\Delta G^{\ddagger}$ determined at PBE0-D3(BJ)/**BS2** + SMD(benzene, SAS) (T = 338.15 K).

In order to evaluate the sensitivity of the calculated *ee* values to small differences in energy (*i.e.*, computational error), the energy of the highest transition state (**isom-TS-(*S*)**) was artificially adjusted by ±1 kcal/mol (+22.6 or +24.6 kcal/mol for **2a** and +23.8 or +21.8 kcal/mol for **2b**), and

the simulations were re-run. The results of these simulations are summarized in Table 3.8.6. The signs of the *ee* values do not change, consistent with our conclusion that the primary determinant of enantioselectivity for the formation of **4a–b** from complexes **2a–b** is the relative barriers to reductive elimination. However, with a difference of ±1 kcal/mol, a range well within the anticipated error from DFT calculations, the simulated *ee* values do vary moderately (70–93% for **2a** and 82–97% for **2b**), with lower barriers to isomerization leading to higher *ee* values. Thus, the free energies from DFT calculations produce rate constants that accurately reproduce the *ee* values measured experimentally (93% for **2a** and 95% for **2b**, respectively).

Table 3.8.6 Dependence of Simulated *ee* for the Thermolysis of Complexes **2a–b** on a 1 kcal/mol Difference to the Free Energy of **isom-TS-(*S*)**

Complex	$\Delta G^{\ddagger}$ for isom-TS-(*S*) (kcal/mol)[a]	Final Concentration of 4-(*S*) (M)	Final Concentration of 4-(*R*) (M)	*ee* (%)
2a	+22.6	1.9332	0.0668	93.3
	+24.6	1.5407	0.2749	69.7
2b	+21.8	1.9675	0.0325	96.8
	+23.8	1.7891	0.1781	81.9

[a]Relative to the free energy of ***pro*-(*S*)**

*Quantifying d(Pd) → π^* interactions in the transition state to reductive elimination of complex **2b** with second-order NBO analysis*

NBO analyses of both **RE-TS-(*S*)-2b** and **RE-TS-(*R*)-2b** generated localized wavefunctions such that the Pd center contained 5 lone-pair *d* orbitals. The delocalizations of all five of these orbitals into the C=O* antibonding orbital of the carbonyl on the fluorooxindole (**RE-TS-(*S*)-2b**) or a π^* orbital of the aromatic ring of the fluorooxindole (**RE-TS-(*R*)-2b**) were considered. Second-order interactions were examined using both **BS1** and **BS2**, as augmenting basis sets with diffuse orbitals can have large effects on population-based analyses.

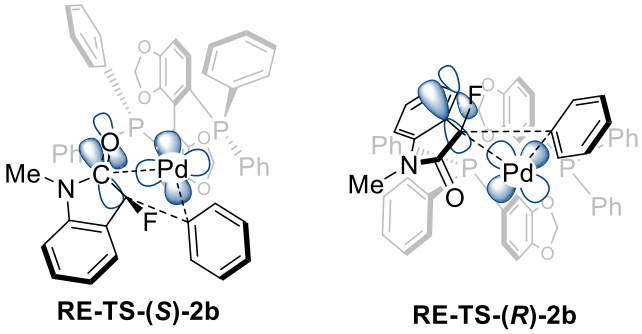


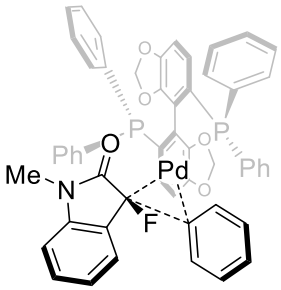
Table 3.8.7 NBO Second-Order Interactions for the Transition States to Reductive Elimination for Complex **2b** Using both **BS1** and **BS2**

NBO	E^2 in BS2 (kcal/mol)	
	d*(Pd) → C=O **(RE-TS-(*S*)-2b)**	***d*(Pd) → C=C*** **(RE-TS-(*R*)-2b)**
Pd LP(1)	< 0.05	0.41
Pd LP(2)	1.39	2.01
Pd LP(3)	1.30	0.06
Pd LP(4)	1.31	< 0.05
Pd LP(5)	4.74	0.89
Sum	8.74	3.37
NBO	**E^2 in BS1 (kcal/mol)**	
	d*(Pd) → C=O **(RE-TS-(*S*)-2b)**	***d*(Pd) → C=C*** **(RE-TS-(*R*)-2b)**
Pd LP(1)	0.01	0.40
Pd LP(2)	1.22	1.95
Pd LP(3)	1.09	0.02
Pd LP(4)	1.81	< 0.01
Pd LP(5)	4.34	0.80
Sum	8.47	3.17

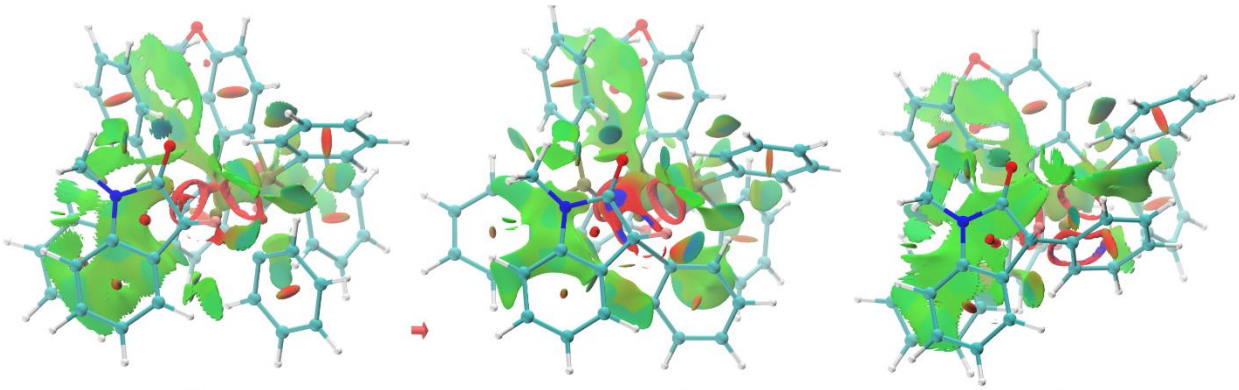
*Generation of NCI plots of the transition states to reductive elimination of complex **2b***

The formatted checkpoint files containing the electron density of **RE-TS-(*S*)-2b** and **RE-TS-(*R*)-2b** from the high-level SPE calculations (PBE0-D3(BJ)/**BS2** + SMD(Benzene, SAS)) were used as inputs for Multiwfn 3.7.[49] Gaussian Cube files were generated using the NCI plot module (menu navigation: 20 → 1). The density cutoff (`RDG_maxrho`) was left at the default value of 0.05 au. A grid spacing of 0.06 Å was used to generate the Cube files used for Figure 3.4.2. Plots in the Supporting Information were generated using a grid spacing of 0.15 Å. The isosurfaces were visualized using VMD.[50] Plots containing the LP(5) and C=O* NBOs (**RE-TS-(*S*)-2b**, main text Figure 3.4.2c) or LP(2) and C=C* NBOs (**RE-TS-(*R*)-2b**, main text Figure 3.4.2f) were generated by plotting the Cube files of the corresponding NBOs on top of the NCI plot in VMD.

The *d*(Pd)→π* interactions described in the main text were not present in the ground states corresponding to the transition states:

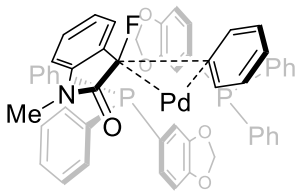


RE-TS-(*S*)-2b

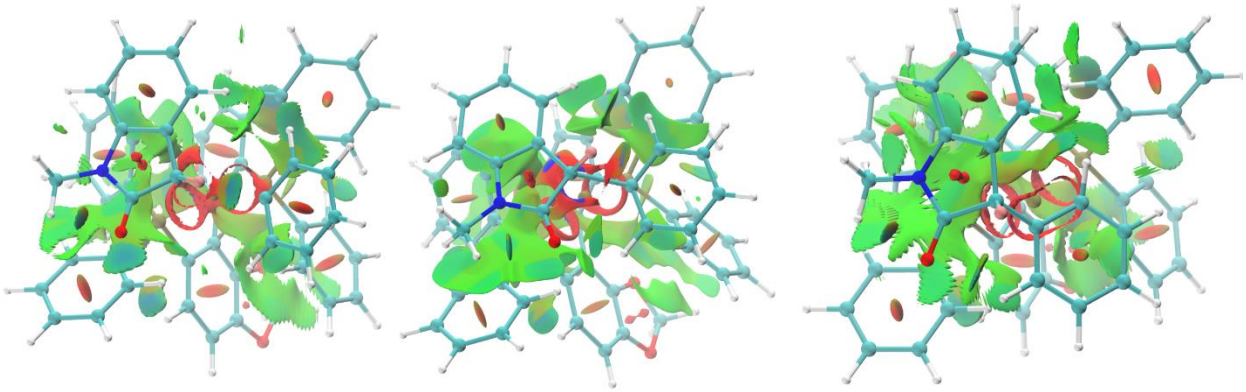


***pro*-(*S*)-rot-2b** **RE-TS-(*S*)-2b** **pdt-(*S*)**

Figure 3.8.37 NCI plots of the ground-state conformer of **2b** (left) leading to the transition state (center) to form the major product enantiomer (right). The blue region between the Pd center and the carbon atom of the C=O of the fluorooxindole fragment in **RE-TS-(*S*)-2b** is absent in the corresponding ground-state structure ***pro*-(*S*)-rot-2b** and in the product η^2-arene complex **pdt-(*S*)**.



RE-TS-(*R*)-2b



***pro*-(*R*)-rot-2b** **RE-TS-(*R*)-2b** **pdt-(*R*)**

Figure 3.8.38 NCI plots of the ground-state conformer of **2b** (left) leading to the transition state to form the minor product enantiomer (right). The blue region between the Pd center and the carbon atom of the arene ring of the fluorooxindole fragment in **RE-TS-(*R*)-2b** is absent in the corresponding ground-state structure ***pro*-(*R*)-rot-2b** and the product η^2-arene complex **pdt-(*R*)**.

3.9 References

Portions of this chapter were reprinted with permission from "Direct Observation of Diastereomeric α-C-Bound Enolates during Enantioselective α-Arylations: Synthesis, Characterization, and Reactivity of Arylpalladium Fluorooxindole Complexes," Kalkman, E. D. and Hartwig, J. F. *J. Am. Chem. Soc.* **2021**, *143*, 11741–11750.

(1) Palucki, M.; Buchwald, S. L. Palladium-Catalyzed α-Arylation of Ketones. *J. Am. Chem. Soc.* **1997**, *119*, 11108–11109.
(2) Hamann, B. C.; Hartwig, J. F. Palladium-Catalyzed Direct α-Arylation of Ketones. Rate Acceleration by Sterically Hindered Chelating Ligands and Reductive Elimination from a Transition Metal Enolate Complex. *J. Am. Chem. Soc.* **1997**, *119*, 12382–12383.
(3) Satoh, T.; Kawamura, Y.; Miura, M.; Nomura, M. Palladium-Catalyzed Regioselective Mono- and Diarylation Reactions of 2-Phenylphenols and Naphthols with Aryl Halides. *Angew. Chem. Int. Ed.* **1997**, *36*, 1740–1742.
(4) Muratake, H.; Natsume, M. Palladium-Catalyzed Intramolecular α-Arylation of Aliphatic Ketones. *Tetrahedron Lett.* **1997**, *38*, 7581–7582.
(5) Muratake, H.; Hayakawa, A.; Natsume, M. A Novel Phenol-Forming Reaction for Preparation of Benzene, Furan, and Thiophene Analogs of CC-1065/Duocarmycin Pharmacophores. *Tetrahedron Lett.* **1997**, *38*, 7577–7580.

(6) Culkin, D. A.; Hartwig, J. F. Palladium-Catalyzed α-Arylation of Carbonyl Compounds and Nitriles. *Acc. Chem. Res.* **2003**, *36*, 234–245.
(7) Prim, D.; Marque, S.; Gaucher, A.; Campagne, J.-M. Transition-Metal-Catalyzed α-Arylation of Enolates. **2011**, *76*, 49–280.
(8) Magano, J.; Dunetz, J. R. Large-Scale Applications of Transition Metal-Catalyzed Couplings for the Synthesis of Pharmaceuticals. *Chem. Rev.* **2011**, *111*, 2177–2250.
(9) Hao, Y.-J.; Hu, X.-S.; Zhou, Y.; Zhou, J.; Yu, J.-S. Catalytic Enantioselective α-Arylation of Carbonyl Enolates and Related Compounds. *ACS Catal.* **2019**, *10*, 955–993.
(10) Åhman, J.; Wolfe, J. P.; Troutman, M. V.; Palucki, M.; Buchwald, S. L. Asymmetric Arylation of Ketone Enolates. *J. Am. Chem. Soc.* **1998**, *120*, 1918–1919.
(11) Lee, S.; Hartwig, J. F. Improved Catalysts for the Palladium-Catalyzed Synthesis of Oxindoles by Amide α-Arylation. Rate Acceleration, Use of Aryl Chloride Substrates, and a New Carbene Ligand for Asymmetric Transformations. *J. Org. Chem.* **2001**, *66*, 3402–3415.
(12) Hamada, T.; Chieffi, A.; Ahman, J.; Buchwald, S. L. An Improved Catalyst for the Asymmetric Arylation of Ketone Enolates. *J. Am. Chem. Soc.* **2002**, *124*, 1261–1268.
(13) Liao, X.; Weng, Z.; Hartwig, J. F. Enantioselective α-Arylation of Ketones with Aryl Triflates Catalyzed by Difluorphos Complexes of Palladium and Nickel. *J. Am. Chem. Soc.* **2008**, *130*, 195–200.
(14) García-Fortanet, J.; Buchwald, S. L. Asymmetric Palladium-Catalyzed Intramolecular A-Arylation of Aldehydes. *Angew. Chem. Int. Ed.* **2008**, *47*, 8108–8111.
(15) Taylor, A. M.; Altman, R. A.; Buchwald, S. L. Palladium-Catalyzed Enantioselective α-Arylation and α-Vinylation of Oxindoles Facilitated by an Axially Chiral P-Stereogenic Ligand. *J. Am. Chem. Soc.* **2009**, *131*, 9900–9901.
(16) Zhou, J. Recent Developments in Asymmetric Coupling of Enolates. *Synlett* **2011**, *2012*, 1–5.
(17) Nareddy, P.; Mantilli, L.; Guenee, L.; Mazet, C. Atropoisomeric (P,N) Ligands for the Highly Enantioselective Pd-Catalyzed Intramolecular Asymmetric A-Arylation of A-Branched Aldehydes. *Angew. Chem. Int. Ed.* **2012**, *51*, 3826–3831.
(18) Jiao, Z.; Beiger, J. J.; Jin, Y.; Ge, S.; Zhou, J. S.; Hartwig, J. F. Palladium-Catalyzed Enantioselective α-Arylation of α-Fluoroketones. *J. Am. Chem. Soc.* **2016**, *138*, 15980–15986.
(19) Jin, Y.; Chen, M.; Ge, S.; Hartwig, J. F. Palladium-Catalyzed, Enantioselective α-Arylation of α-Fluorooxindoles. *Org. Lett.* **2017**, *19*, 1390–1393.
(20) Rao, X.; Li, N.; Bai, H.; Dai, C.; Wang, Z.; Tang, W. Efficient Synthesis of (−)-Corynoline by Enantioselective Palladium-Catalyzed A-Arylation with Sterically Hindered Substrates. *Angew. Chem. Int. Ed.* **2018**, *57*, 12328–12332.
(21) Jette, C. I.; Geibel, I.; Bachman, S.; Hayashi, M.; Sakurai, S.; Shimizu, H.; Morgan, J. B.; Stoltz, B. M. Palladium-Catalyzed Construction of Quaternary Stereocenters by Enantioselective Arylation of Gamma-Lactams with Aryl Chlorides and Bromides. *Angew. Chem. Int. Ed.* **2019**, *58*, 4297–4301.
(22) Chieffi, A.; Kamikawa, K.; Ahman, J.; Fox, J. M.; Buchwald, S. L. Catalytic Asymmetric Vinylation of Ketone Enolates. *Org. Lett.* **2001**, *3*, 1897–1900.
(23) Liu, X.; Hartwig, J. F. Palladium-Catalyzed α-Arylation of Azlactones to Form Quaternary Amino Acid Derivatives. *Org. Lett.* **2003**, *5*, 1915–1918.

(24) Jiao, Z.; Chee, K. W.; Zhou, J. S. Palladium-Catalyzed Asymmetric α-Arylation of Alkylnitriles. *J. Am. Chem. Soc.* **2016**, *138*, 16240–16243.
(25) Huang, X.; Oh, W.; Zhou, J. S. Palladium-Catalyzed Enantioselective Arylation of Racemic Ketones to Form Bridged Bicycles via Dynamic Kinetic Resolution. *Angew. Chem. Int. Ed.* **2018**, *57*, 7673–7677.
(26) Ostrowska, S.; Scattolin, T.; Nolan, S. P. N-Heterocyclic Carbene Complexes Enabling the α-Arylation of Carbonyl Compounds. *Chem. Commun.* **2021**, *57*, 4354–4375.
(27) Culkin, D. A.; Hartwig, J. F. C−C Bond-Forming Reductive Elimination of Ketones, Esters, and Amides from Isolated Arylpalladium(II) Enolates. *J. Am. Chem. Soc.* **2001**, *123*, 5816–5817.
(28) Culkin, D. A.; Hartwig, J. F. Carbon−Carbon Bond-Forming Reductive Elimination from Arylpalladium Complexes Containing Functionalized Alkyl Groups. Influence of Ligand Steric and Electronic Properties on Structure, Stability, and Reactivity. *Organometallics* **2004**, *23*, 3398–3416.
(29) Kawatsura, M.; Hartwig, J. F. Simple, Highly Active Palladium Catalysts for Ketone and Malonate Arylation: Dissecting the Importance of Chelation and Steric Hindrance. *J. Am. Chem. Soc.* **1999**, *121*, 1473–1478.
(30) Liu, X.; Hartwig, J. F. Palladium-Catalyzed Arylation of Trimethylsilyl Enolates of Esters and Imides. High Functional Group Tolerance and Stereoselective Synthesis of α-Aryl Carboxylic Acid Derivatives. *J. Am. Chem. Soc.* **2004**, *126*, 5182–5191.
(31) Huang, Z.; Liu, Z.; Zhou, J. S. An Enantioselective, Intermolecular Alpha-Arylation of Ester Enolates to Form Tertiary Stereocenters. *J. Am. Chem. Soc.* **2011**, *133*, 15882–15885.
(32) Huang, Z.; Chen, Z.; Lim, L. H.; Quang, G. C.; Hirao, H.; Zhou, J. S. Weak Arene C–H···O Hydrogen Bonding in Palladium-Catalyzed Arylation and Vinylation of Lactones. *Angew. Chem. Int. Ed.* **2013**, *52*, 5807–5812.
(33) Huang, Z. Y.; Lim, L. H.; Chen, Z. L.; Li, Y. X.; Zhou, F.; Su, H. B.; Zhou, J. R. Arene CH–O Hydrogen Bonding: A Stereocontrolling Tool in Palladium-Catalyzed Arylation and Vinylation of Ketones. *Angew. Chem. Int. Ed.* **2013**, *52*, 4906–4911.
(34) Yang, J.; Zhou, J. A General Method for Asymmetric Arylation and Vinylation of Silyl Ketene Acetals. *Org. Chem. Front.* **2014**, *1*, 365–367.
(35) Kirker, G. W.; Bakac, A.; Espenson, J. H. Homolysis and Acidolysis Reactions of (α-Hydroxyalkyl)- and (α-Alkoxyalkyl)Chromium(III) Complexes: Kinetics, Steric Effects, and Bond Energies. *J. Am. Chem. Soc.* **1982**, *104*, 1249–1255.
(36) Blau, R. J.; Espenson, J. H.; Bakac, A. Kinetic Study of the Reaction of Aquochromium(II) Ions with Benzyl Radicals in Aqueous Solutions: Thermodynamics of the Chromium–Carbon Bond. *Inorg. Chem.* **1984**, *23*, 3526–3528.
(37) Albéniz, A. C.; Casares, J. A. Chapter One - Palladium-Mediated Organofluorine Chemistry. In *Advances in Organometallic Chemistry*; Pérez, P. J., Ed.; Academic Press, 2014; Vol. 62, pp 1–110.
(38) Hoops, S.; Sahle, S.; Gauges, R.; Lee, C.; Pahle, J.; Simus, N.; Singhal, M.; Xu, L.; Mendes, P.; Kummer, U. COPASI—a COmplex PAthway SImulator. *Bioinformatics* **2006**, *22*, 3067–3074.
(39) Driver, M. S.; Hartwig, J. F. Carbon–Nitrogen-Bond-Forming Reductive Elimination of Arylamines from Palladium(II) Phosphine Complexes. *J. Am. Chem. Soc.* **1997**, *119*, 8232–8245.

(40) Mann, G.; Barañano, D.; Hartwig, J. F.; Rheingold, A. L.; Guzei, I. A. Carbon–Sulfur Bond-Forming Reductive Elimination Involving *Sp*-, Sp^2-, and Sp^3-Hybridized Carbon. Mechanism, Steric Effects, and Electronic Effects on Sulfide Formation. *J. Am. Chem. Soc.* **1998**, *120*, 9205–9219.
(41) Widenhoefer, R. A.; Buchwald, S. L. Electronic Dependence of C−O Reductive Elimination from Palladium (Aryl)Neopentoxide Complexes. *J. Am. Chem. Soc.* **1998**, *120*, 6504–6511.
(42) Hartwig, J. F. Electronic Effects on Reductive Elimination to Form Carbon-Carbon and Carbon-Heteroatom Bonds from Palladium(II) Complexes. *Inorg. Chem.* **2007**, *46*, 1936–1947.
(43) Gu, Y.; Leng, X.; Shen, Q. Cooperative Dual Palladium/Silver Catalyst for Direct Difluoromethylation of Aryl Bromides and Iodides. *Nat. Commun.* **2014**, *5*, 5405.
(44) Arlow, S. I.; Hartwig, J. F. Synthesis, Characterization, and Reactivity of Palladium Fluoroenolate Complexes. *J. Am. Chem. Soc.* **2017**, *139*, 16088–16091.
(45) Hansch, C.; Leo, A.; Taft, R. W. A Survey of Hammett Substituent Constants and Resonance and Field Parameters. *Chem. Rev.* **1991**, *91*, 165–195.
(46) Widenhoefer, R. A.; Zhong, H. A.; Buchwald, S. L. Direct Observation of C–O Reductive Elimination from Palladium Aryl Alkoxide Complexes to Form Aryl Ethers. *J. Am. Chem. Soc.* **1997**, *119*, 6787–6795.
(47) Bondi, A. Van Der Waals Volumes and Radii. *J. Phys. Chem.* **1964**, *68*, 441–451.
(48) Johnson, E. R.; Keinan, S.; Mori-Sanchez, P.; Contreras-Garcia, J.; Cohen, A. J.; Yang, W. Revealing Noncovalent Interactions. *J. Am. Chem. Soc.* **2010**, *132*, 6498–6506.
(49) Lu, T.; Chen, F. Multiwfn: A Multifunctional Wavefunction Analyzer. *J. Comput. Chem.* **2012**, *33*, 580–592.
(50) Humphrey, W.; Dalke, A.; Schulten, K. VMD: Visual Molecular Dynamics. *J. Mol. Graph.* **1996**, *14*, 33–38.
(51) Kalkman, E. D.; Hartwig, J. F. Direct Observation of Diastereomeric α-C-Bound Enolates during Enantioselective α-Arylations: Synthesis, Characterization, and Reactivity of Arylpalladium Fluorooxindole Complexes. *J. Am. Chem. Soc.* **2021**, *143*, 11741–11750.
(52) Reed, A. E.; Curtiss, L. A.; Weinhold, F. Intermolecular Interactions from a Natural Bond Orbital, Donor-Acceptor Viewpoint. *Chem. Rev.* **1988**, *88*, 899–926.
(53) Glendening, E. D.; Landis, C. R.; Weinhold, F. NBO 6.0: Natural Bond Orbital Analysis Program. *J. Comput. Chem.* **2013**, *34*, 1429–1437.
(54) Wiberg, K. B. Application of the Pople-Santry-Segal CNDO Method to the Cyclopropylcarbinyl and Cyclobutyl Cation and to Bicyclobutane. *Tetrahedron* **1968**, *24*, 1083–1096.
(55) Balaraman, K.; Wolf, C. Catalytic Enantioselective and Diastereoselective Allylic Alkylation with Fluoroenolates: Efficient Access to C3-Fluorinated and All-Carbon Quaternary Oxindoles. *Angew. Chem. Int. Ed.* **2017**, *56*, 1390–1395.
(56) Bruno, N. C.; Niljianskul, N.; Buchwald, S. L. *N* -Substituted 2-Aminobiphenylpalladium Methanesulfonate Precatalysts and Their Use in C–C and C–N Cross-Couplings. *J. Org. Chem.* **2014**, *79*, 4161–4166.
(57) Li, H.; Grasa, G. A.; Colacot, T. J. A Highly Efficient, Practical, and General Route for the Synthesis of (R3P)2Pd(0): Structural Evidence on the Reduction Mechanism of Pd(II) to Pd(0). *Org. Lett.* **2010**, *12*, 3332–3335.
(58) Kwong, F. Y.; Lai, C. W.; Yu, M.; Tian, Y.; Chan, K. S. Palladium-Catalyzed Phosphination of Functionalized Aryl Triflates. *Tetrahedron* **2003**, *59*, 10295–10305.

(59) Rosenau, C. P.; Jelier, B. J.; Gossert, A. D.; Togni, A. Exposing the Origins of Irreproducibility in Fluorine NMR Spectroscopy. *Angew. Chem. Int. Ed.* **2018**, *57*, 9528–9533.
(60) Neukom, J. D.; Perch, N. S.; Wolfe, J. P. Intramolecular Insertion of Alkenes into Pd−N Bonds. Effects of Substrate and Ligand Structure on the Reactivity of (P−P)Pd(Ar)[N(Ar ^{1})(CH $_{2}$) $_{3}$ CR═CHR′] Complexes. *Organometallics* **2011**, *30*, 1269–1277.
(61) Klinkenberg, J. L.; Hartwig, J. F. Reductive Elimination from Arylpalladium Cyanide Complexes. *J. Am. Chem. Soc.* **2012**, *134*, 5758–5761.
(62) Alcazar-Roman, L. M.; Hartwig, J. F.; Rheingold, A. L.; Liable-Sands, L. M.; Guzei, I. A. Mechanistic Studies of the Palladium-Catalyzed Amination of Aryl Halides and the Oxidative Addition of Aryl Bromides to Pd(BINAP)$_2$ and Pd(DPPF)$_2$: An Unusual Case of Zero-Order Kinetic Behavior and Product Inhibition. *J. Am. Chem. Soc.* **2000**, *122*, 4618–4630.
(63) Frisch, M. J.; Trucks, G. W.; Schlegel, H. B.; Scuseria, G. E.; Robb, M. A.; Cheeseman, J. R.; Scalmani, G.; Barone, V.; Petersson, G. A.; Nakatsuji, H.; Li, X.; Caricato, M.; Marenich, A. V.; Bloino, J.; Janesko, B. G.; Gomperts, R.; Mennucci, B.; Hratchian, H. P.; Ortiz, J. V.; Izmaylov, A. F.; Sonnenberg, J. L.; Williams-Young, D.; Ding, F.; Lipparini, F.; Egidi, F.; Goings, J.; Peng, B.; Petrone, A.; Henderson, T.; Ranasinghe, D.; Zakrzewski, V. G.; Gao, J.; Rega, N.; Zheng, G.; Liang, W.; Hada, M.; Ehara, M.; Toyota, K.; Fukuda, R.; Hasegawa, J.; Ishida, M.; Nakajima, T.; Honda, Y.; Kitao, O.; Nakai, H.; Vreven, T.; Throssell, K.; Montgomery, J. A.; Peralta, J. E.; Ogliaro, F.; Bearpark, M. J.; Heyd, J. J.; Brothers, E. N.; Kudin, K. N.; Staroverov, V. N.; Keith, T. A.; Kobayashi, R.; Normand, J.; Raghavachari, K.; Rendell, A. P.; Burant, J. C.; Iyengar, S. S.; Tomasi, J.; Cossi, M.; Millam, J. M.; Klene, M.; Adamo, C.; Cammi, R.; Ochterski, J. W.; Martin, R. L.; Morokuma, K.; Farkas, O.; Foresman, J. B.; Fox, D. J. *Gaussian 16, Revision A.03*; Gaussian, Inc.: Wallingford CT, 2016.
(64) Marenich, A. V.; Cramer, C. J.; Truhlar, D. G. Universal Solvation Model Based on Solute Electron Density and on a Continuum Model of the Solvent Defined by the Bulk Dielectric Constant and Atomic Surface Tensions. *J. Phys. Chem. B* **2009**, *113*, 6378–6396.
(65) Dennington, R.; Keith, T. A.; Millam, J. M. *GaussView, Version 6.1*; Semichem Inc.: Shawnee Mission, KS, 2016.
(66) Perdew, J. P.; Burke, K.; Ernzerhof, M. Generalized Gradient Approximation Made Simple. *Phys. Rev. Lett.* **1996**, *77*, 3865–3868.
(67) Perdew, J. P.; Burke, K.; Ernzerhof, M. Generalized Gradient Approximation Made Simple. *Phys. Rev. Lett.* **1997**, *78*, 1396–1396.
(68) Adamo, C.; Barone, V. Toward Reliable Density Functional Methods without Adjustable Parameters: The PBE0 Model. *J. Chem. Phys.* **1999**, *110*, 6158–6170.
(69) Grimme, S.; Ehrlich, S.; Goerigk, L. Effect of the Damping Function in Dispersion Corrected Density Functional Theory. *J. Comput. Chem.* **2011**, *32*, 1456–1465.
(70) Weigend, F.; Ahlrichs, R. Balanced Basis Sets of Split Valence, Triple Zeta Valence and Quadruple Zeta Valence Quality for H to Rn: Design and Assessment of Accuracy. *Phys. Chem. Chem. Phys.* **2005**, *7*, 3297–3305.
(71) Feller, D. The Role of Databases in Support of Computational Chemistry Calculations. *J. Comput. Chem.* **1996**, *17*, 1571–1586.

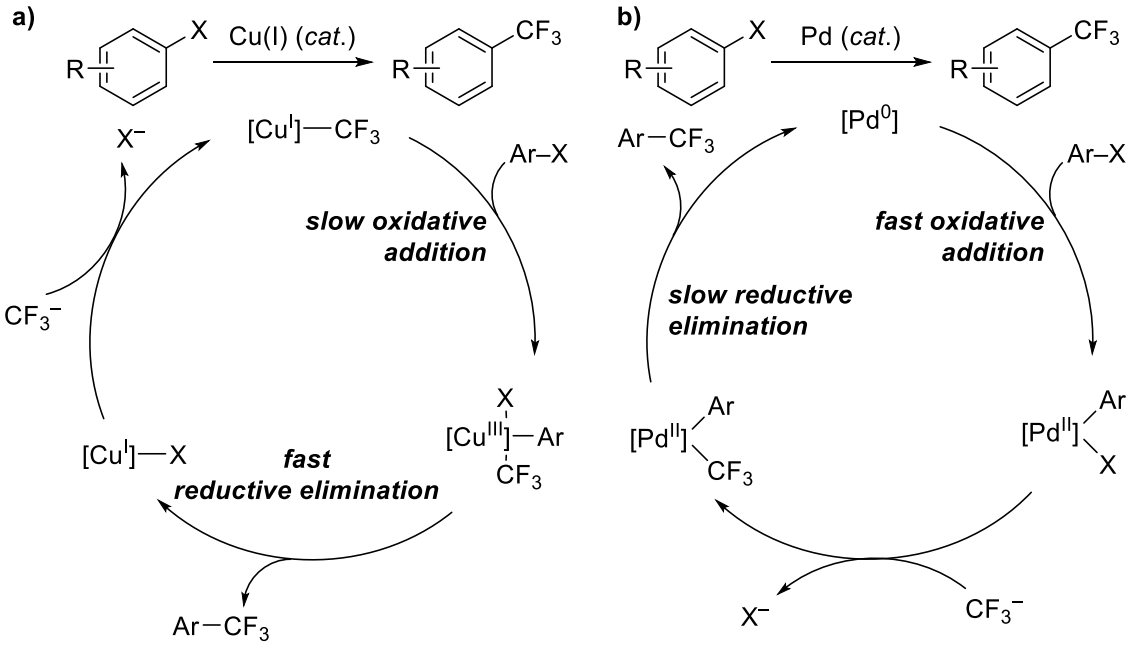
(72) Schuchardt, K. L.; Didier, B. T.; Elsethagen, T.; Sun, L.; Gurumoorthi, V.; Chase, J.; Li, J.; Windus, T. L. Basis Set Exchange: A Community Database for Computational Sciences. *J. Chem. Inf. Model.* **2007**, *47*, 1045–1052.
(73) Andrae, D.; Häußermann, U.; Dolg, M.; Stoll, H.; Preuß, H. Energy-Adjusted *Ab Initio* Pseudopotentials for the Second and Third Row Transition Elements. *Theor. Chim. Acta* **1990**, *77*, 123–141.
(74) Pritchard, B. P.; Altarawy, D.; Didier, B.; Gibson, T. D.; Windus, T. L. New Basis Set Exchange: An Open, Up-to-Date Resource for the Molecular Sciences Community. *J. Chem. Inf. Model.* **2019**, *59*, 4814–4820.
(75) Zheng, J.; Xu, X.; Truhlar, D. G. Minimally Augmented Karlsruhe Basis Sets. *Theor. Chem. Acc.* **2011**, *128*, 295–305.

Chapter 4

Investigations into the Formation, Speciation, and Reactivity of Aryl(trifluoromethyl)palladium Complexes toward the Development of a Robust Palladium-Catalyzed Trifluoromethylation of Aryl Bromides

4.1 Introduction

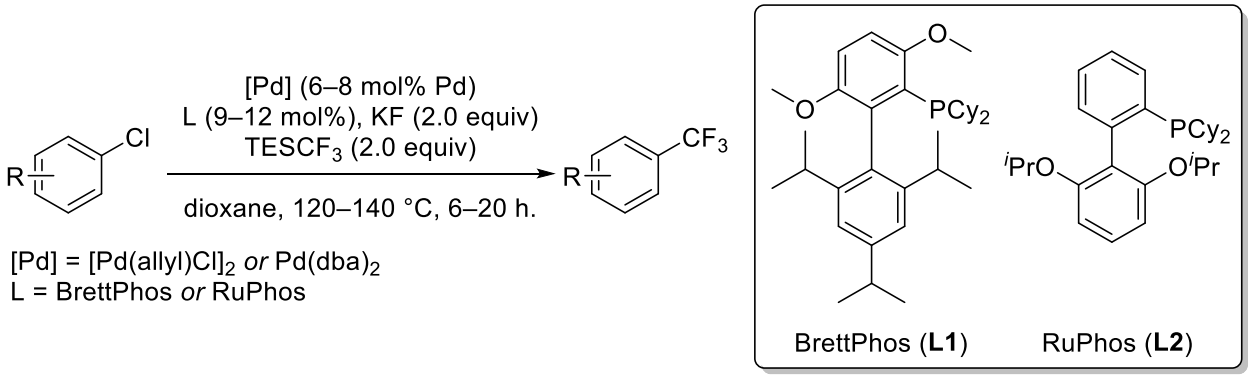
The past half century has seen extensive development of methods mediated by transition metals to introduce fluoroalkyl groups into organic compounds (see Chapter 1).[1–4] Particularly desirable are methods that form trifluoromethylarenes, which are of great interest for their unique physical and chemical properties in biologically active compounds.[5–14] While simple trifluoromethylarenes are accessible on large scales *via* the Swarts process,[1,15,16] the strongly acidic reaction conditions are incompatible with many functional groups, and as such the process is not feasible for the late-stage selective functionalization of complex molecules. To this end, trifluoromethylcopper species, first reported by McLouglin and Thrower in 1969,[17] have seen great success as reagents for the trifluoromethylation of aryl halides[1,18] and are intermediates in Cu-catalyzed trifluoromethylations of aryl iodides.[19–23] While the reagents for these processes are usually inexpensive, copper-mediated trifluoromethylations of aryl halides generally are limited in scope to aryl iodides and a few electron-poor aryl bromides. Copper-*catalyzed* methods typically form low yields of trifluoromethylarenes, even from aryl iodides, and when they do give high yields, they require high loadings of catalyst.[19–21,23] This limited scope in aryl halide is due to the prohibitively slow rate of the oxidative addition of aryl bromides and chlorides to the trifluoromethylcopper species, which is the rate-limiting step, and the instability of the trifluoromethylcopper species toward the CuX (X = Cl, Br) byproducts of these reactions.[24,25] A photocatalytic copper-catalyzed trifluoromethylation of aryl bromides was reported in 2018 by MacMillan; however this method was limited by the requirement of expensive trifluoromethylsulfonium oxidant, silanol reductant, and the oxidizing iridium photocatalyst.[26]



Scheme 4.1.1 General mechanisms for the trifluoromethylation of aryl halides catalyzed by a) copper or b) palladium.

Analogous reactions catalyzed by palladium complexes are a potential solution to the limited scope of the copper-mediated methods for trifluoromethylation. Whereas the slow oxidative addition of the aryl halide to trifluoromethylcopper species limits the scope of aryl

halides that undergo copper-mediated trifluoromethylation (Scheme 4.1.1a), the oxidative addition of a wide range of aryl electrophiles, including aryl chlorides, bromides, and sulfonates, to Pd catalysts, is well known.[27–29] The catalytic cycle for the Pd-catalyzed trifluoromethylation of aryl halides involves oxidative addition of the aryl halide to a Pd(0) species to form the corresponding arylpalladium halide, followed by transmetallation of a nucleophilic equivalent of CF_3 to form an aryl(trifluoromethyl)palladium complex, which then undergoes reductive elimination to furnish the trifluoromethylarene and regenerate the starting Pd(0) species (Scheme 4.1.1b). A system that follows this mechanism was reported by Buchwald in 2010 and is the only current example of a Pd-catalyzed trifluoromethylation of aryl halides with a broad range of substituents on the aryl ring.[30] While this report certainly represents a significant achievement, the method suffers from several drawbacks, including high reaction temperatures (> 120 °C) and catalyst loadings (> 6 mol%). Perhaps most surprising is that Buchwald's method is restricted in scope to aryl *chlorides*; the authors noted that applying similar reaction conditions to the trifluoromethylation of aryl bromides led to significantly diminished yields. The reason for this restriction remains unknown. Buchwald, Schoenebeck, and Sanford recently have reported Pd-catalyzed trifluoromethylations of other classes of sp^2-carbon electrophiles, such as vinyl sulfonates and aroyl halides,[31–33] but no further examples of Pd-catalyzed trifluoromethylations of aryl halides have been reported. Thus, aryl bromides constitute a significant gap in the scope of thermal trifluoromethylation reactions catalyzed by both Pd and Cu.



Scheme 4.1.2 The Pd-catalyzed trifluoromethylation of aryl chlorides.[30]

Several studies have uncovered some of the difficulties in developing trifluoromethylation reactions catalyzed by Pd. Early examples of aryl(trifluoromethyl)palladium complexes revealed their high thermal stability (Figure 4.1.1a), signaling the difficulty in achieving product-forming reductive elimination as part of a putative catalytic reaction.[34,35] While subsequent work by our group and others has identified several ligands that facilitate the reductive elimination of trifluoromethylarene from aryl(trifluoromethyl)palladium complexes (Figure 4.1.1b), the number of such ligands is only around a dozen, and reductive elimination from most complexes of these ligands still require high temperatures (> 120 °C).[30,36–40] Unfortunately, many of these ligands can be displaced by CF_3^- to form poly(trifluoromethyl)palladium species, a process that was first reported by Naumann and cited by Grushin and Arlow as setbacks during the preparation of isolated aryl(trifluoromethyl)palladium complexes for study.[36,40,41] Other documented side-reactions that can degrade the Pd catalyst include the well-precedented α-elimination from metal–CF_3 species to form difluorocarbene[30,38,39] and the bimolecular exchange of X-type ligands[35,36,41] (Figure 4.1.1c), both of which form stable, off-cycle species. It is unclear whether any of these side reactions are operative under the catalytic reaction conditions developed by Buchwald.[30]

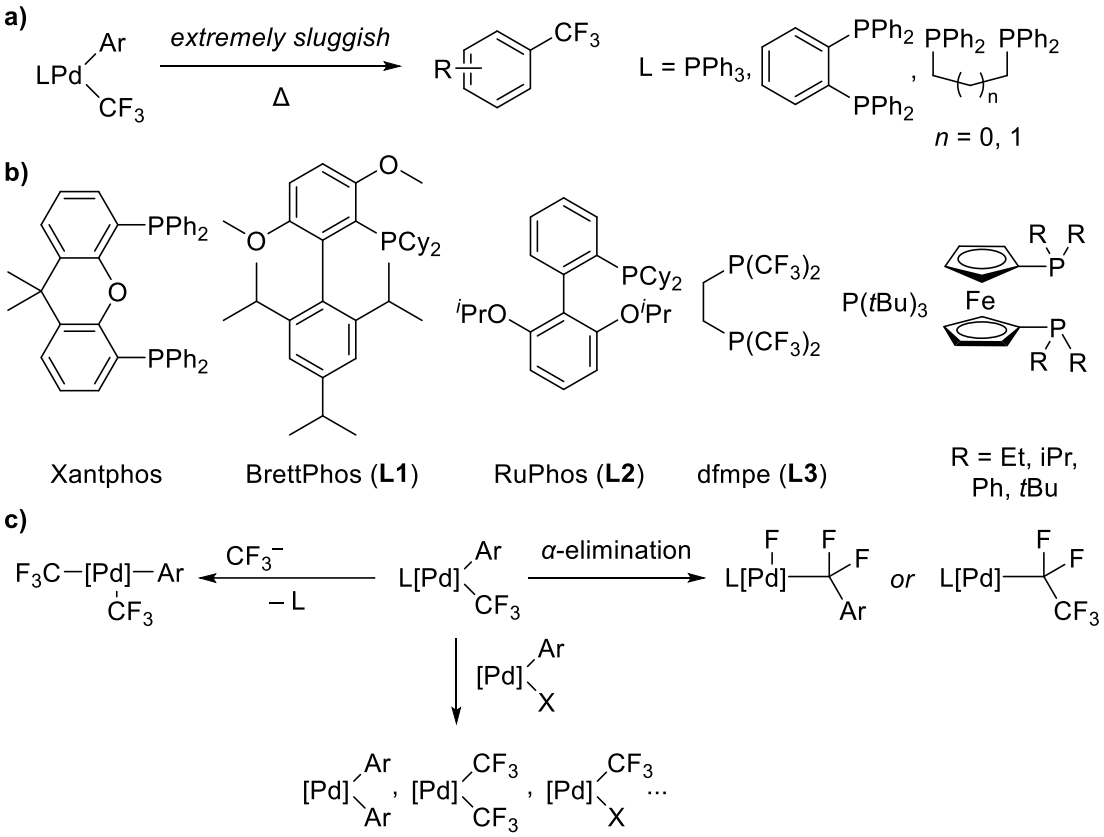


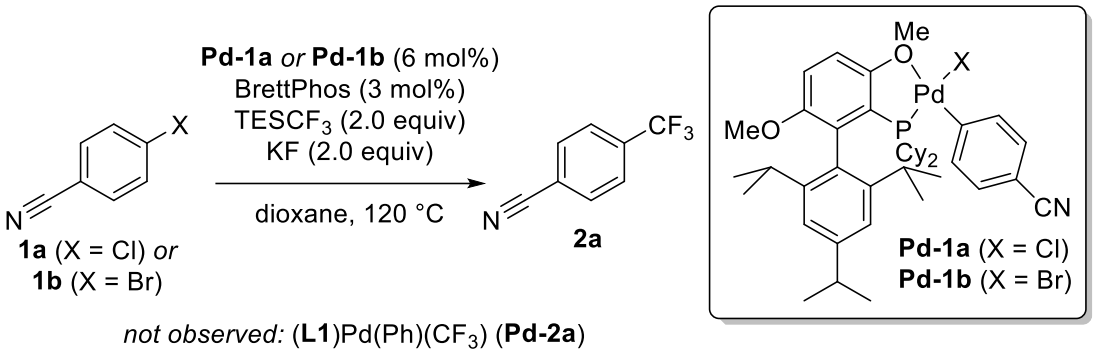
Figure 4.1.1 Challenges to Pd-catalyzed trifluoromethylation reactions. a) Difficult reductive elimination from aryl(trifluoromethyl)palladium complexes. b) Ligands that enable reductive elimination from aryl(trifluoromethyl)palladium complexes. c) Possible side-reactions involving aryl(trifluoromethyl)palladium complexes.

In this Chapter, we report preliminary investigations of these potential side reactions to reveal the origins of the limitations of Buchwald's Pd-catalyzed trifluoromethylation of aryl bromides and chlorides. We also describe efforts to identify other ligand scaffolds that facilitate reductive elimination from aryl(trifluoromethyl)palladium complexes and investigations into the application of trifluoromethylcopper species as sources of nucleophilic CF_3 to overcome some of the challenges encountered in the transmetallation step.

4.2 Investigations of the Trifluoromethylation of Aryl Halides Catalyzed by Pd Complexes Containing BrettPhos

To begin our investigations, we studied reactions catalyzed by Buchwald's $[Pd(allyl)Cl]_2$/L system (L = BrettPhos (**L1**), RuPhos (**L2**)) that gave high yields of trifluoromethylarene from aryl chlorides.[30] We first sought to examine the reactants, products and palladium complexes present in the catalytic trifluoromethylation of 4-chlorobenzonitrile (**1a**) or 4-bromobenzonitrile (**1b**) (Scheme 4.2.1). After 2.5 hours, aliquots of the reaction mixtures were analyzed by ^{19}F and $^{31}P\{^1H\}$ NMR spectroscopy. The ^{19}F NMR spectra contained $TESCF_3$, CHF_3, and 4-trifluoromethylbenzonitrile (**2**; ~2% and ~3% yield for X = Cl and Br, respectively). No (**L1**)Pd–CF_3 species were observed. The $^{31}P\{^1H\}$ NMR spectra of the reaction of **1a** contained only free **L1** and arylpalladium chloride complex **Pd-1a**. The presence of **Pd-1a** is consistent with the

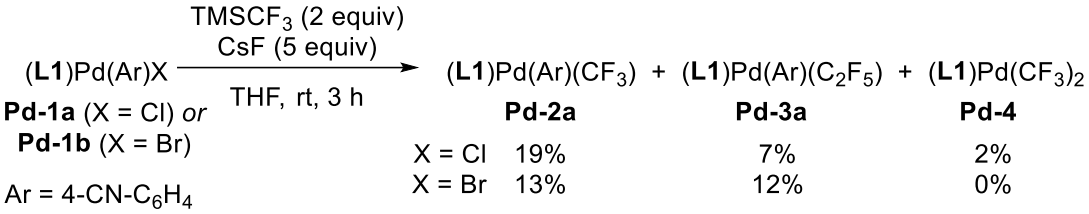
arylpalladium halide complex as the resting state and turnover-limiting activation of $TESCF_3$. A similar result was observed in the reaction of aryl bromide **1b** with **Pd-1b** as a catalyst, although a small quantity of an unidentified Pd–CF_3 species also was observed in the ^{19}F NMR spectrum. The identity of the resting state of the catalyst in these reactions is consistent with rapid oxidative addition of the aryl halides to (BrettPhos)Pd(0), even at room temperature (see Section 4.7.2 in the syntheses of **Pd-1a** and **Pd-1b**).[30,42,43]



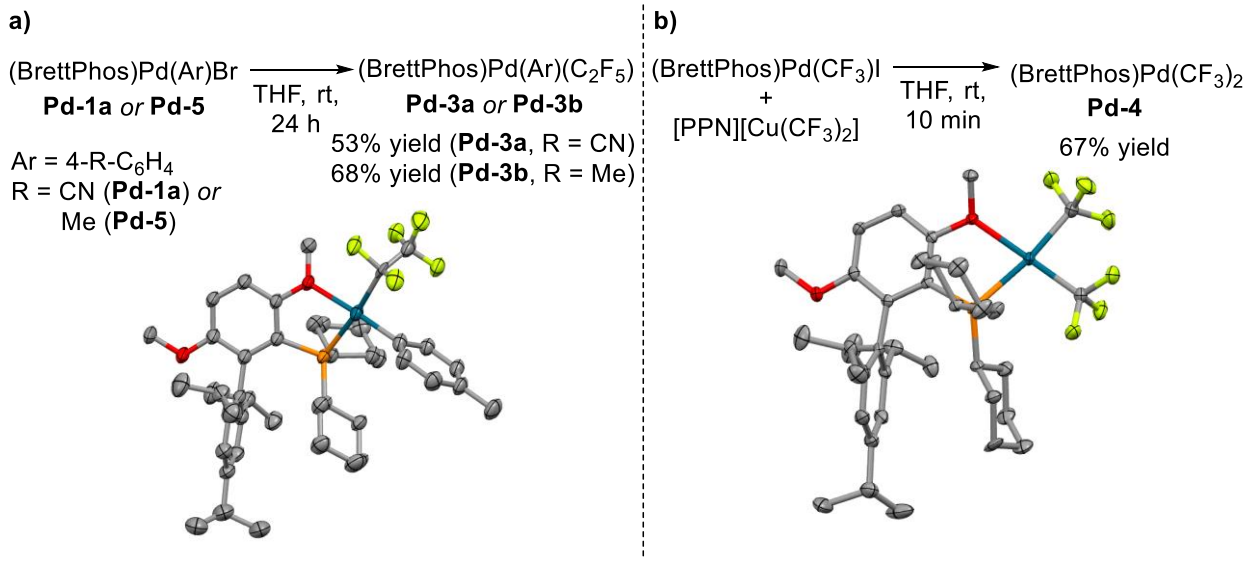
not observed: (**L1**)Pd(Ph)(CF_3) (**Pd-2a**)

Scheme 4.2.1 Pd-catalyzed trifluoromethylation of aryl halides **1a-b** catalyzed by arylpalladium halide complexes **Pd-1a-b**

We next conducted a series of stoichiometric reactions to model individual steps of the catalytic reaction. We first examined the transmetallation step by treating arylpalladium chloride (**Pd-1a**) and bromide (**Pd-1b**) complexes ligated by BrettPhos (**L1**) with a combination of $TMSCF_3$ and CsF in THF and analyzing the reaction mixture by ^{19}F and $^{31}P\{^1H\}$ NMR spectroscopy (Scheme 4.2.2). The reaction of the arylpalladium chloride complex **Pd-1a** for 3 hours at ambient temperature led to only ~30% conversion of **Pd-1a** and formed the corresponding aryl(trifluoromethyl)palladium complex **Pd-2a** in 19% yield.[30] Among many unidentified side products, we detected TMSF and CHF_3 in the reaction mixture, as well as (**L1**)Pd(4-CN-C_6H_4)(C_2F_5) (**Pd-3a**, 7% yield) and (**L1**)Pd(CF_3)$_2$ (**Pd-4**, 2% yield). The identities of complexes **Pd-3a** and **Pd-4** were confirmed by independent syntheses (Scheme 4.2.3). Free **L1** (~20% yield) was also observed in the $^{31}P\{^1H\}$ NMR spectrum of the reaction mixture. The corresponding reaction of arylpalladium bromide complex **Pd-1b** with $TMSCF_3$ and CsF formed fewer side products (see Section 4.7) but still led to only 30% conversion of **Pd-1b** and gave a lower yield of aryl(trifluoromethyl)palladium complex **Pd-2a** (13%) and free **L1** (~10%) and larger amounts of the pentafluoroethyl complex **Pd-3a** (12%). No *bis*(trifluoromethyl)palladium complex **Pd-4** was formed in this reaction, and no trifluoromethylarene **2a** was formed in reactions of either arylpalladium halide complex. **Pd-3a** likely formed from the reaction of the aryl(trifluoromethyl)palladium complex **Pd-2a** with $TMSCF_3$ to form a Pd=CF_2 species and TMSF,[44] or by reaction of free CF_3^- (generated from $TMSCF_3$ and CsF) with another equivalent of $TMSCF_3$ to form difluorocarbene and $Me_3Si(F)(CF_3)^-$, which reacts with the difluorocarbene to form $C_2F_5^-$ and TMSF.[45,46] ^{19}F NMR chemical shifts similar to those of aryl(pentafluoroethyl)palladium complexes **Pd-3a** and *bis*(trifluoromethyl)palladium complex **Pd-4** were also observed in minor amounts in the NMR spectra of the (BrettPhos)Pd(aryl)(CF_3) complexes reported by Buchwald.[30]

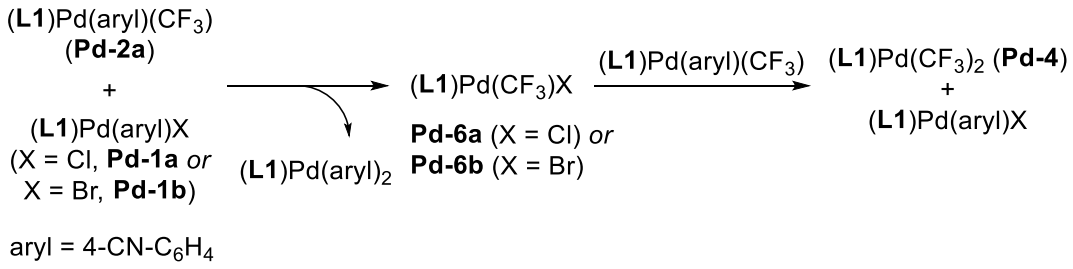


Scheme 4.2.2 Reaction of BrettPhos-ligated arylpalladium halide complexes **Pd-1a** and **Pd-1b** with $TMSCF_3$. Yields were determined by ^{19}F NMR spectroscopy relative to 4-(trifluoromethoxy)anisole as an internal standard.



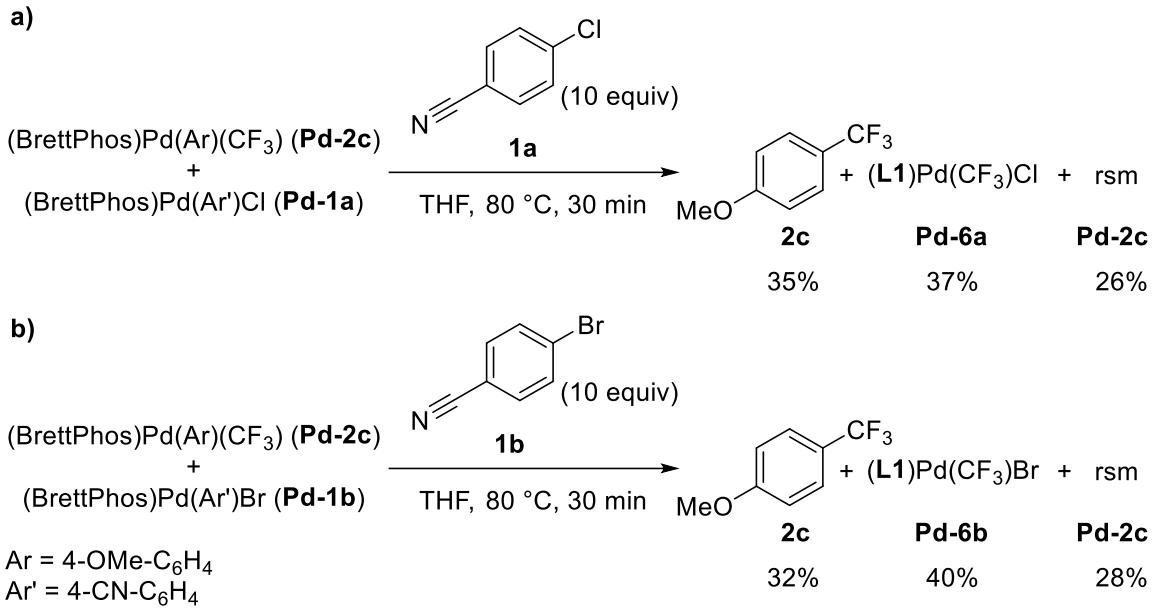
Scheme 4.2.3 a) Synthesis of (BrettPhos)Pd(4-R-C_6H_4)(C_2F_5) (**Pd-3a**, R = CN; **Pd-3b**, R = Me) and OTERP diagram of **Pd-3b**. b) Synthesis and OTERP diagram of (BrettPhos)Pd(CF_3)$_2$ (**Pd-4**). Thermal ellipsoids are drawn at 50% probability. Hydrogen atoms are omitted for clarity. Light gray = C, red = O, light green = F, orange = P, dark gray = Pd.

At this time, we are unsure of the process by which free Brettphos (**L1**) forms in this reaction. We initially considered that multiple additions of CF_3^- might displace **L1** to form poly(trifluoromethyl)palladate species.[36] Indeed, ^{19}F NMR resonances that did not exhibit ^{19}F–^{31}P coupling and whose chemical shifts (–15 to –25 ppm) are consistent with Pd(CF_3)$_n$ species[35,36,47] were detected in the reaction of arylpalladium chloride complex **Pd-1a**. However, similar resonances were *not* observed in the ^{19}F NMR spectrum of the reaction of arylpalladium *bromide* complex **Pd-1b** despite the formation of **L1** in ~10% yield, suggesting that free ligand also can accumulate by another mechanism.



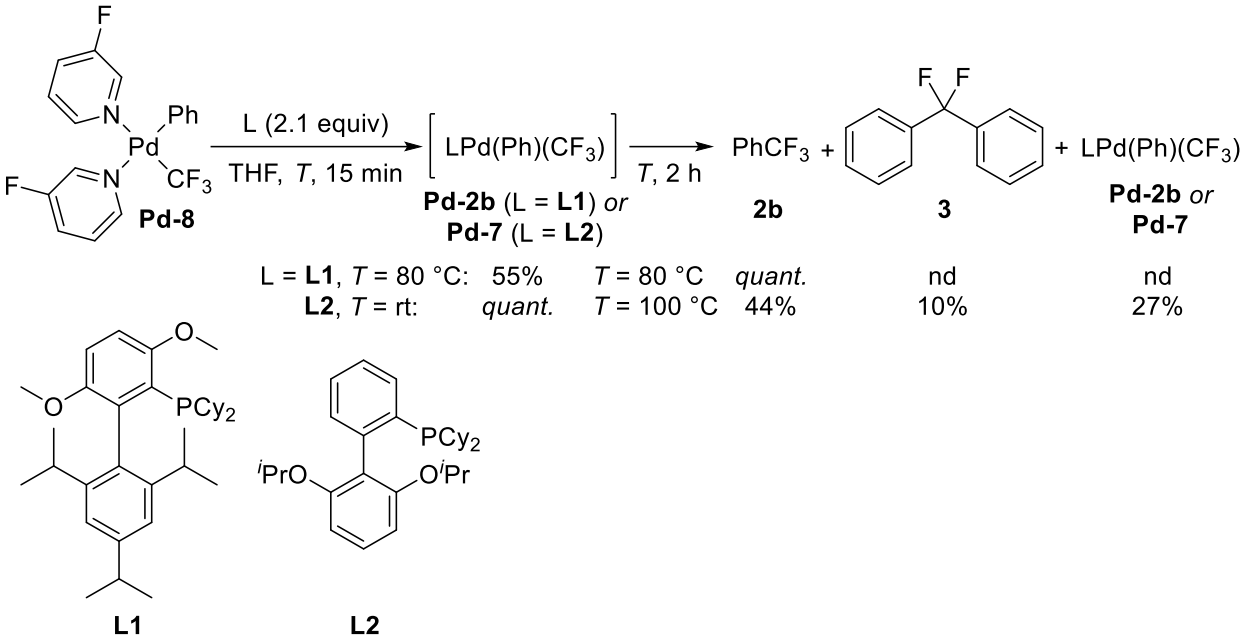
Scheme 4.2.4 Proposed exchange of anionic ligands between aryl(trifluoromethyl)palladium complex **Pd-2a** and arylpalladium halide complexes **Pd-1a** and **Pd-1b**

Given the accumulation of *bis*(trifluoromethyl) complex **Pd-4** in the reaction of BrettPhos-ligated arylpalladium chloride complex **Pd-1a**, we also considered that the BrettPhos-ligated arylpalladium trifluoromethyl complex **Pd-2a** might exchange its aryl or trifluoromethyl ligands with the aryl or halide ligands of arylpalladium halide complexes **Pd-1a** or **Pd-1b** (Scheme 4.2.4a or b, respectively).[35,36,48,49] To test this hypothesis, we treated (BrettPhos)Pd(4-OCH_3-C_6H_4)(CF_3) (**Pd-2c**)[30] with (BrettPhos)Pd(4-CN-C_6H_4)X complexes **Pd-1a** (X = Cl) or **Pd-1b** (X = Br) and excess aryl chloride (**1a**) or bromide (**1b**) to trap any generated Pd(0) species (Scheme 4.2.5). While no reaction occurred at ambient temperature over 15 minutes, new broad features at 1.4 (X = Cl) or 5.6 ppm (X = Br) appeared in the ^{19}F NMR spectra of the reaction mixtures after 30 minutes at 80 °C in 37% (X = Cl) or 40% (X = Br) yield relative to **Pd-2c**. These signals were accompanied by new quartets in the $^{31}P\{^1H\}$ NMR spectra at 62.2 (X = Cl, J = 35.3 Hz) or 61.1 (X = Br, J = 34.7 Hz) ppm. These signals are consistent with previously reported spectral data for (BrettPhos)Pd(CF_3)X species **Pd-6a** (X = Cl) and **Pd-6b** (X = Br),[50,*Note 1*] indicating that the exchange of aryl and halide ligands between Pd centers can occur at elevated temperatures. Nevertheless, *bis*(trifluoromethyl) complex **Pd-4** was not observed in these reactions, suggesting that the **Pd-4** formed from the reaction of (**L1**)Pd(aryl)Cl complex **Pd-1a**, $TMSCF_3$ and CsF (Scheme 4.2.2) did not arise from further reaction of (BrettPhos)Pd(CF_3)Cl (**Pd-6a**) with (**L1**)Pd(aryl)(CF_3) complex **Pd-2a**. Neither *bis*(trifluoromethyl)palladium complex **Pd-4** nor (BrettPhos)Pd(CF_3)Br (**Pd-6b**)[50] were detected in the reactions of arylpalladium bromide complex **Pd-1b** with $TMSCF_3$ or in the catalytic trifluoromethylation reactions. Thus, the mechanism of formation of (BrettPhos)Pd(CF_3)X complexes **Pd-6a** and **Pd-6b** and *bis*(trifluoromethyl)palladium complex **Pd-4** is unknown.



Scheme 4.2.5 Reaction of aryl(trifluoromethyl)palladium complex **Pd-2c** with arylpalladium halide complexes a) **Pd-1a** or b) **Pd-1b**. Conditions: **Pd-2c** (4.9 μmol, 1.0 equiv), **Pd-1a** or **Pd-1b** (4.9 μmol, 1.0 equiv), **1a** or **1b** (49 μmol, 10 equiv), THF (600 μL). Yields were determined by ^{19}F NMR spectroscopy relative to 4-(trifluoromethoxy)anisole as an internal standard.

Finally, we sought to establish whether the putative phenyl(trifluoromethyl)palladium intermediates ligated by **L1** (**Pd-2b**) or **L2** (**Pd-7**) engaged in side-reactions, such as α-fluoride elimination or the exchange of X-type ligands (**Error! Reference source not found.**). Complexes **Pd-2b** and **Pd-7** were generated independently from a route involving transmetallation by treating aryl(trifluoromethyl)palladium precursor Pd(3-fluoropyridine)$_2$(Ph)(CF$_3$) (**Pd-8**)[37] with BrettPhos (**L1**) or RuPhos (**L2**) in THF (**Error! Reference source not found.**). While the reaction of **L1** with **Pd-8** did not occur at room temperature, according to ^{19}F NMR spectroscopy, heating the mixture at 80 °C for 15 minutes formed the BrettPhos-ligated phenyl(trifluoromethyl)palladium complex **Pd-2b** and trifluoromethylbenzene (**2b**) in 55% and 8% yield, respectively, with 36% **Pd-8** remaining. After further heating at 80 °C for 2 hours, **2b** formed in quantitative yields, and no other fluorine-containing species besides 3-fluoropyridine was observed by ^{19}F NMR spectroscopy, demonstrating that neither α-fluoride elimination nor the exchange of X-type ligands between two equivalents of **Pd-2b** occurred during the thermolysis of **Pd-2b**.



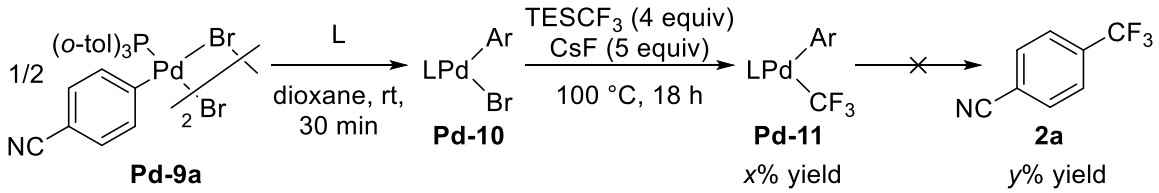
Scheme 4.2.6 Reductive elimination of *in situ*-generated complexes **Pd-2a** and **Pd-7**. nd = not detected. Yields were determined by ^{19}F NMR spectroscopy relative to 4-(trifluoromethoxy)anisole as an internal standard.

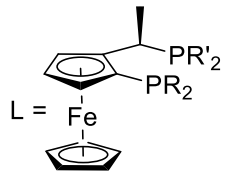
In contrast to the sluggish reaction of precursor **Pd-8** and **L1** to form **Pd-2b**, the reaction of **Pd-8** and RuPhos (**L2**) formed aryl(trifluoromethyl)palladium complex **Pd-7** in quantitative yields after 15 minutes at ambient temperature. Heating the mixture containing **Pd-7** at 100 °C for 2 hours formed trifluoromethylarene **2b** in only 44% yield, with 27% of **Pd-7** remaining. Difluorodiphenylmethane (**3**) also formed in 10% yield, indicating that side-reactions involving α-fluoride elimination had occurred.[38,51] These results demonstrate that reductive elimination of trifluoromethylbenzene from RuPhos-ligated **Pd-7** requires higher temperatures and proceeds with slower rates than that from BrettPhos-ligated **Pd-2b** and that **Pd-7** is more prone to side-reactions than **Pd-2b**. It was observed previously that catalytic reactions containing RuPhos (**L2**) only gave high yields of trifluoromethylarene in reactions of sterically hindered aryl chlorides.[30] In these cases, the extra steric crowding around the metal center likely decreases the barrier to reductive elimination, allowing product formation to outpace the deleterious side reactions.[51]

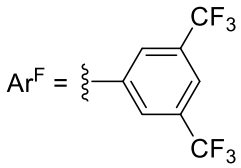
4.3 Investigations of Other Ligand Scaffolds

Concurrently, we have sought to identify other ligands that facilitate both the challenging reductive elimination step and that enable the selective transmetallation of CF_3^- for halide in the corresponding arylpalladium halide complexes. Most previous examples of ligands for which the corresponding aryl(trifluoromethyl)palladium complexes undergo reductive elimination of trifluoromethylarene are bidentate, either as chelating diphosphines or *via* κ^2-C,C or κ^2-C,O binding in dialkylbiarylphosphines.[30,35–37,39–41] Most of these ligands also bond with wide bite angles or contain bulky alkyl groups on phosphorus, and these properties tend to facilitate reductive elimination. Consistent with this pattern, Arlow identified the bulky diphosphine CyPF-*t*Bu (**L4**) as a ligand for which the corresponding phenyl(trifluoromethyl)palladium complex

undergoes reductive elimination in high yield at 100 °C. Thus, we evaluated the propensity of the arylpalladium bromide complexes bound by a series of related Josiphos derivatives **L4–L12**, which contain a variety of alkyl- and arylphosphino moieties to undergo transmetallation of CF_3^- for bromide and reductive elimination from the corresponding aryl(trifluoromethyl)palladium complexes. (Scheme 4.3.1).







	R	R'	*x*%	*y*%
L4	Cy	*t*Bu	0	0
L5	Cy	Cy	13	0
L6	Ph	Cy	25	0
L7	2-furyl	*o*-tolyl	29	0
L8	Ar^F	Ar^F	34	2
L9	2-naphthyl	3,5-xylyl	~3[a]	0
L10	Ar^F	Cy	31	0
L11	Ar^F	3,5-xylyl	35	0
L12	Ph	tBu	12	8

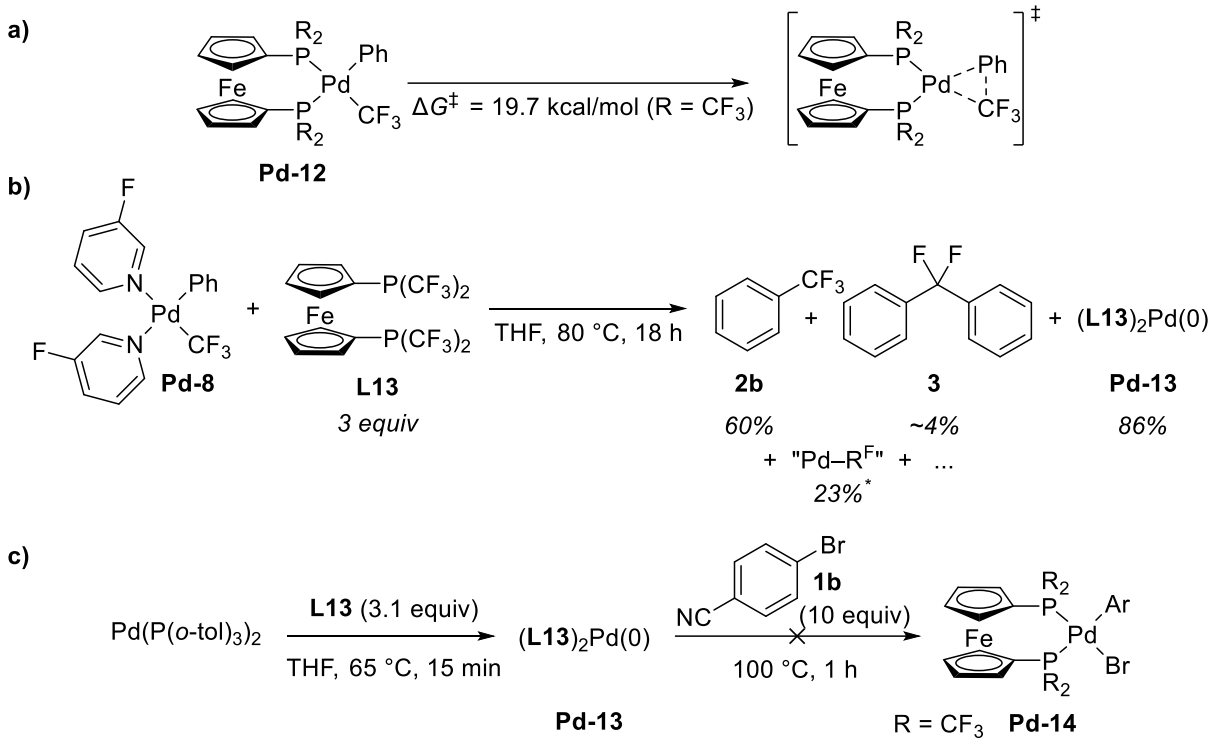
Scheme 4.3.1 Reactions of arylpalladium halide complexes ligated by Josiphos derivatives with $TESCF_3$ and CsF. Conditions: dimer **Pd-9a** (2.5 μmol, 0.50 equiv), ligand (5.0 μmol, 1.0 equiv), CsF (25 μmol, 5.0 equiv) in dioxane (500 μL) for 30 min, followed by $TESCF_3$ (20 μmol, 4.0 equiv), 100 °C, 18 h. Reaction yields were determined by ^{19}F NMR spectroscopy relative to 4-(trifluoromethoxy)anisole as an internal standard. Aryl(trifluoromethyl)palladium complexes **Pd-11** were identified by their characteristic ^{19}F–^{31}P coupling. [a]Broad resonances were detected, leading to uncertain quantification.

To evaluate the reactivity of complexes containing these ligands, we generated LPd(aryl)Br complexes **Pd-10** *in situ* by the reaction of the arylpalladium bromide dimer {((*o*-tol)$_3$P)Pd(4-CN-C$_6$H$_4$)Br}$_2$ **Pd-9a** and ligands **L4–L12** and treated the resulting complexes with $TESCF_3$ and CsF at 100 °C for 18 hours (Scheme 4.3.1). Although the desired aryl(trifluoromethyl)palladium complexes **Pd-11** containing ligands **L5-L12** were detected in the reaction mixtures by ^{19}F NMR spectroscopy, these complexes generally did not form trifluoromethylarene **2a** under the reaction conditions. The arylpalladium bromide complex of ligand **L4**, which is the ligand that has been reported to enable the reductive elimination of trifluoromethylbenzene in high yields at these temperatures,[40] did not undergo transmetallation of CF_3 to form **Pd-11-L4**, presumably due the severe steric crowding around the Pd center in this complex. Aryl(trifluoromethyl)palladium complexes of ligands that contained electron-poor 3,5-*bis*(trifluoromethyl)phenyl groups (**Pd-11-L8**, **Pd-11-L10**, and **Pd-11-L11**) did not form trifluoromethylarene **2a**, nor did complexes of ligands containing bulky *o*-tolyl or naphthyl groups (**Pd-11-L7**, **Pd-11-L9**). Three Josiphos ligands (**L5**, **L6**, **L12**) containing a bulky alkylphosphine moiety connected to the stereogenic carbon of the ligand reacted with arylpalladium bromide dimer **Pd-9a** to form the corresponding arylpalladium bromide complexes **Pd-10-L5**, **Pd-10-L6**, and **Pd-10-L12**, which reacted with $TMSCF_3$ and CsF to form the corresponding aryl(trifluoromethyl)palladium complexes **Pd-11-L5**,

Pd-11-L6, and **Pd-11-L12**, albeit in low yields. Of these aryl(trifluoromethyl)palladium complexes, only **Pd-11-L12** underwent subsequent reductive elimination of trifluoromethylarene **2a**; however more than half of the aryl(trifluoromethyl)palladium complex **Pd-11-L12** remained after 18 hours at 100 °C, indicating that reductive elimination from this complex is extremely slow.[40] Overall, aryl(trifluoromethyl)palladium complexes containing Josiphos ligands require much higher temperatures to form trifluoromethylarene than complexes containing BrettPhos or Xantphos.

We sought to identify other classes of ligands that enabled reductive elimination of trifluoromethylarene at lower temperatures. Schoenebeck identified 1,2-*bis*(*bis*(trifluoromethyl)phosphino)ethane (dfmpe, **L3**) as a ligand that facilitated the reductive elimination of trifluoromethylarene from the corresponding palladium complexes within one hour at 80 °C.[37,52] The electrostatic repulsion of the *bis*(trifluoromethyl)phosphines of **L3** and the trifluoromethyl ligand of the complex was cited as the driving force for this reaction, although we note that perfluoroalkylphosphines are also strong π-acceptors and thus likely lower the barrier for reductive elimination by stabilizing the nascent Pd(0) character of the transition state.[53–56] However, the preparation and handling of **L3** are inconvenient due to its high volatility.

We hypothesized that arylpalladium trifluoromethyl complexes containing the ligand 1,1'-*bis*(*bis*(trifluoromethyl)phosphino)ferrocene[55] (dfmpf, **L13**), which is an air-stable solid, might undergo reductive elimination at an even lower temperature than analogous complexes containing **L3** due to the larger bite angle of **L13** than of **L3**. This hypothesis was supported by DFT calculations (Scheme 4.3.2a). The free energy barrier for reductive elimination from (**L13**)Pd(Ph)(CF_3) (**Pd-12**) was calculated to be only 19.7 kcal/mol, suggesting that this reaction might proceed rapidly, even at room temperature. For comparison, the barriers for reductive eliminations from (BrettPhos)Pd(Ph)(CF_3), (dfmpe)Pd(Ph)(CF_3), and (CyPF-*t*Bu)Pd(Ph)(CF_3) were calculated to be 22,[30] 24.0, and 27.6 kcal/mol, respectively. In addition, Arlow showed that (dppf)Pd(Ph)I reacted with $TMSCF_3$ and CsF to form (dppf)Pd(Ph)(CF_3) in 46% isolated yield, suggesting that the transmetallation step also could occur and the fluoroalkyl ligand **L13** and a palladium precursor could catalyze the trifluoromethylation of aryl halides.



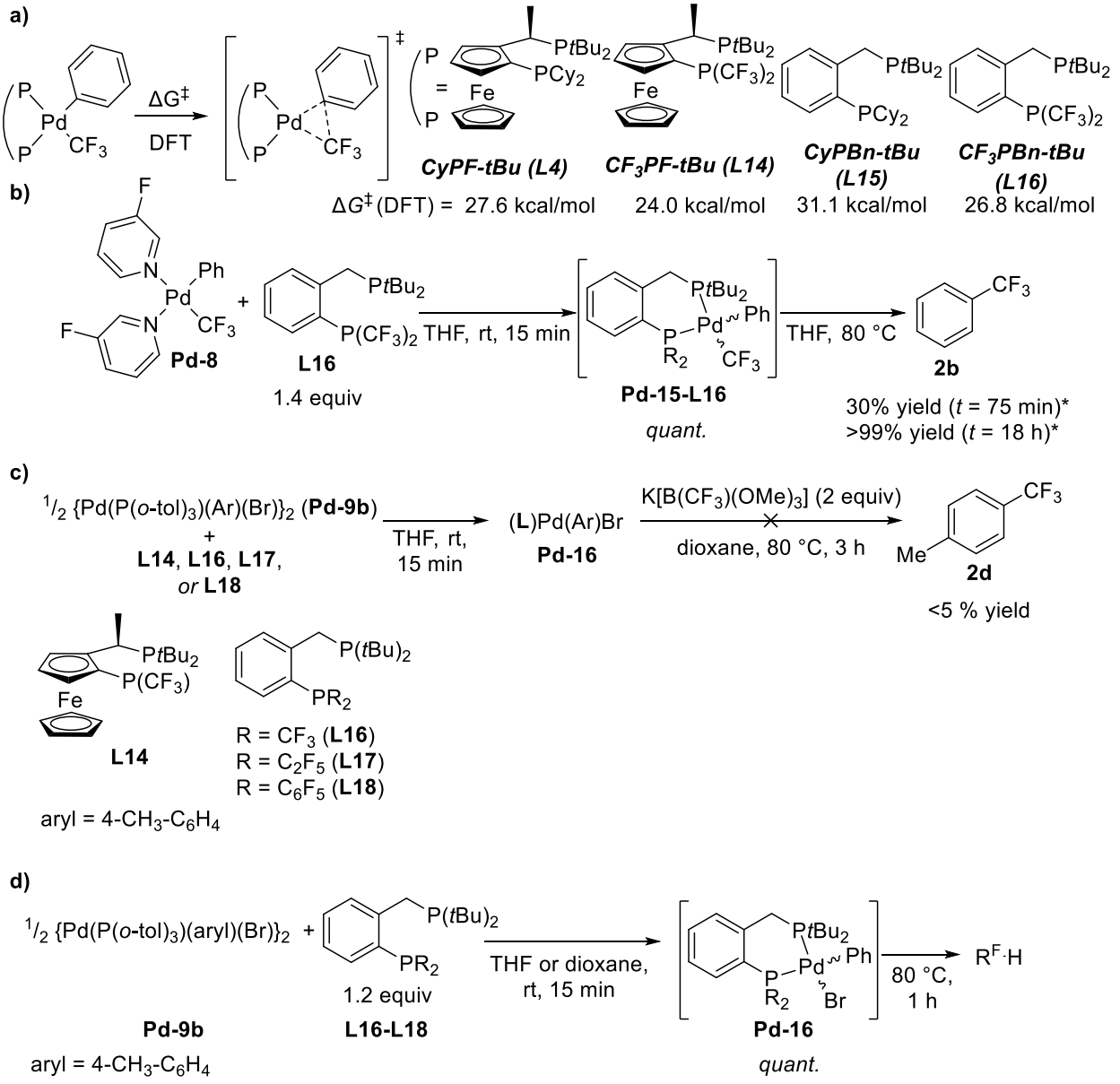
Scheme 4.3.2 a) Computed barriers for reductive elimination from (L)Pd(Ph)(R^F) containing *bis*(*bis*(perfluoroalkyl)phosphino)ferrocene ligands; see Section 4.7 for computational methods). b) Reaction of **L13** with complex **Pd-8**. Reaction conditions: **Pd-8** (5.0 μmol, 1.0 equiv), **L13** (15 μmol, 3.0 equiv), THF (600 μL). c) Formation of (**L13**)Pd(0) (**Pd-13**) and reaction with aryl halide **1b**. *The yield of "Pd–R^F" was calculated assuming $R^F = CF_3$.

Thus, a mixture of phenyl(trifluoromethyl)palladium complex **Pd-8** and an excess of the fluorinated ferrocenyl ligand **L13** were combined in THF at ambient temperature, and the mixture was analyzed by ^{19}F NMR spectroscopy for the formation of trifluoromethylarene (Scheme 4.3.2b). However, after 15 minutes, only resonances corresponding to the starting compounds were observed, suggesting that **L13** undergoes slow substitution for 3-fluoropyridine in complex **Pd-8**. However, upon heating the reaction mixture at 80 °C for 30 minutes, trifluoromethylbenzene (**2b**) formed in 44% yield, along with another species that we assigned as (**L13**)$_2$Pd(0) (**Pd-13**) and 49% of remaining **Pd-8**. No other Pd–CF_3 resonances were observed, consistent with rate-limiting ligand substitution to form **Pd-12** and fast reductive elimination. Further heating of the mixture at 80 °C for 18 hours led to full conversion of **Pd-8** and generated trifluoromethylarene **2b** in 60% yield. The other products included unidentified Pd–CF_3 species and difluorodiphenylmethane (**3**), indicating that side-reactions involving α-fluoride elimination had occurred. Furthermore, treating (**L13**)$_2$Pd(0) (**Pd-13**) generated from Pd(P(*o*-tol)$_3$)$_2$ and **L13** with aryl bromide **1b** at 100 °C to form (**L13**)Pd(aryl)Br complex **Pd-14** resulted in no conversion of complex **Pd-13** (Scheme 4.3.2c), suggesting that ligand dissociation to form a coordinatively unsaturated Pd(0) complex and subsequent oxidative addition of the aryl bromide is too slow to achieve catalysis under mild conditions.

We also considered that a non-symmetrical *bis*-phosphine ligand in which one phosphine contained alkyl substituents while the other contained perfluoroalkyl substituents might enable both oxidative addition of aryl halide to Pd(0) and reductive elimination of trifluoromethylarene

from Pd(II). We chose ligands **L14** and **L16–L18** (Scheme 4.3.3) as targets because synthetic routes to Josiphos and PBn-type ligands containing two different phosphine moieties are well precedented.[57]

We first conducted DFT calculations to evaluate the free energy barriers to reductive elimination from phenyl(trifluoromethyl)palladium complexes containing these ligands



Scheme 4.3.3 a) Calculated barriers for reductive elimination of trifluoromethylbenzene for complexes containing diphosphine ligands **L4**, **L14–L16** (see Section 4.7.4 for details). b) Conditions: **Pd-8** (4.3 μmol, 1.0 equiv), **L16** (5.9 μmol, 1.4 equiv) in 700 μL THF. c) Conditions: **Pd-9b** (2.5 μmol, 0.50 equiv), ligand (6.0 μmol, 1.2 equiv) in 700 μL dioxane. d) Conditions: **Pd-9b** (2.3 μmol, 0.50 equiv), **L14** or **L15–L18** (7.0 μmol, 1.5 equiv), K[B(CF$_3$)(OMe)$_3$] (9.3 μmol, 2.0 equiv) in 700 μL dioxane *Yields determined by ^{19}F NMR spectroscopy relative to 4-(trifluoromethoxy)anisole as an internal standard.

(Scheme 4.3.3a). The computed barriers to reductive elimination from complexes of ligands **L14** and **L16** were 24.0 and 26.8 kcal/mol respectively, and these barriers are significantly lower than those of complexes containing the similar non-fluorinated ligands CyPF-*t*Bu (**L4**) and CyPBn-*t*Bu (**L15**) (27.6 and 31.1 kcal/mol, respectively). Thus, we evaluated the reactivity of complexes containing these ligands experimentally.

Treating aryl(trifluoromethyl)palladium precursor **Pd-8** with 1.4 equivalents of fluoroalkylphosphine **L16** at ambient temperature rapidly formed the complex (**L16**)Pd(Ph)(CF_3) (**Pd-15-L16**) in quantitative yields (Scheme 4.3.3b). Heating the reaction mixture at 80 °C formed trifluoromethylarene **2b** in 30% yield after 75 minutes and in quantitative yield after 18 hours, in agreement with the barrier to reductive elimination predicted by DFT calculations (predicted $t_{1/2}$ at 80 °C = 60 min).

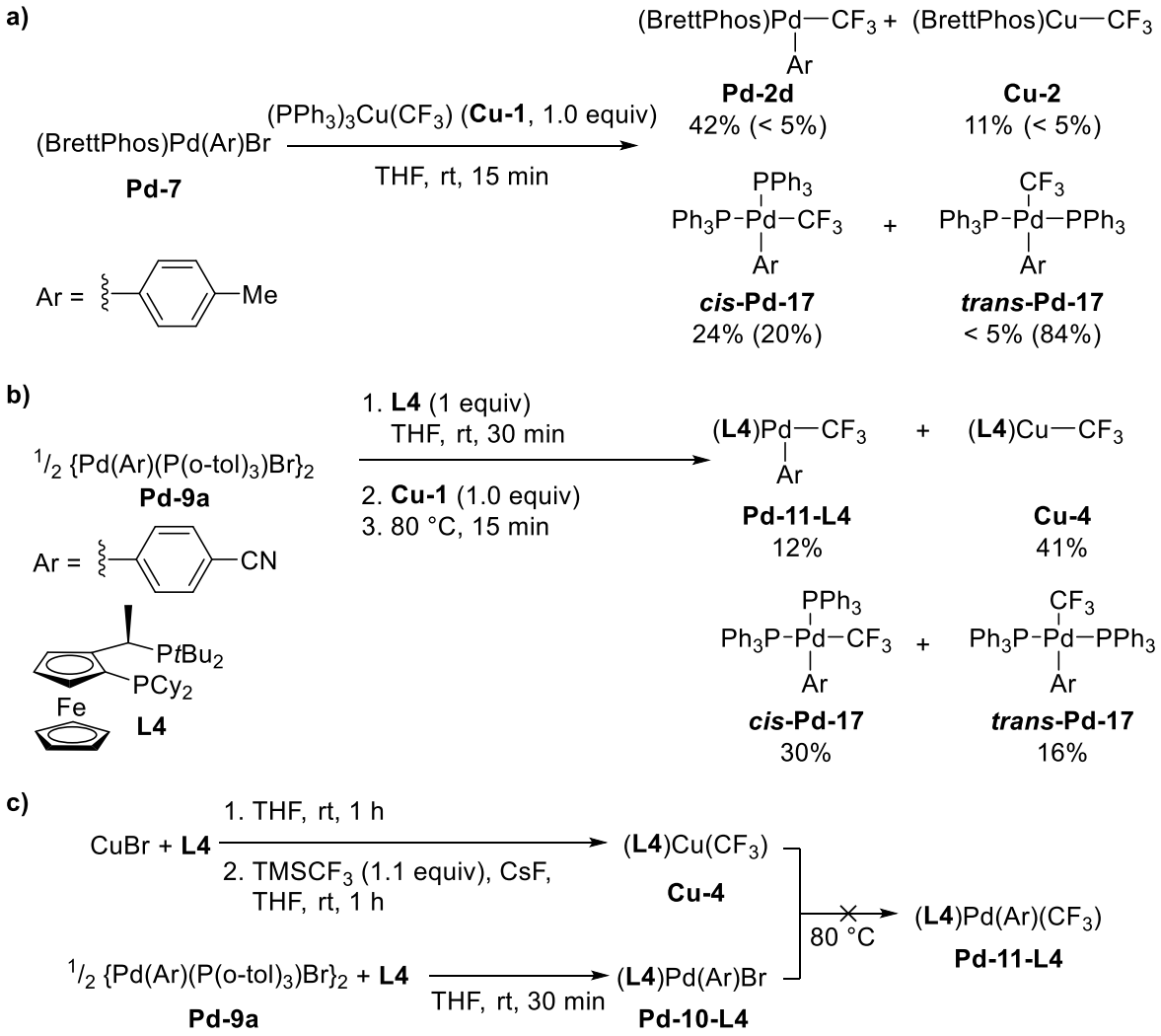
To evaluate whether the arylpalladium bromide complexes of these ligands could react with CF_3^- to form the corresponding aryl(trifluoromethyl)palladium complexes, we treated arylpalladium bromide complexes **Pd-16** containing ligands **L14** or **L16-18** with K[B(CF_3)(OMe)$_3$] in THF at 80 °C (Scheme 4.3.3c). However, no signals consistent with aryl(trifluoromethyl)palladium complexes were detected by ^{19}F NMR spectroscopy, and less than 5% of trifluoromethylarene had **2d** formed. In addition, we found that simply heating the same arylpalladium bromide complexes **Pd-16** in THF in the absence of any source of CF_3^- formed R^F–H (R^F = CF_3, C_2F_5, C_6F_5) due to decomposition of the fluoroalkylphosphine moieties (Scheme 4.3.3d). Due the instability of the fluoroalkylphosphines **L14** and **L16–L18** ligated to arylpalladium bromide complexes, we did not evaluate the reactivity of palladium complexes containing ligands **L14** and **L16–L18** further.

4.4 Trifluoromethylcopper Reagents as Sources of Nucleophilic CF_3

One attractive approach to temper the high reactivity and instability of CF_3^- and to facilitate the transmetallation to an arylpalladium halide complex is incorporate the CF_3 moiety into a separate organometallic complex. Many stable fluoroalkyl complexes of Group 11[48,58–62] and Group 12[63–68] metals undergo transmetallation with arylpalladium halide complexes to form the corresponding aryl(trifluoromethyl)palladium complexes. Pérez-Temprano reported a single example of the Pd-catalyzed trifluoromethylation of iodobenzene in which $Ag(CF_3)_2^-$ species served as the source of nucleophilic CF_3; however, the method required high loadings of Pd catalyst (20 mol%) and slow addition of the temperature-sensitive reagent and proceeded to less than 3 turnovers of the catalyst.[66] Pd-catalyzed cross-couplings of a wider scope of aryl halides with trifluoromethylmetal reagents have not been reported.

We considered that trifluoromethylcopper reagents might be suitable alternatives to the trifluoromethysilver reagents reported by Pérez-Temprano because trifluoromethylcopper species are easy to access from inexpensive copper(I) precursors and are often stable at elevated temperatures.[69–71] Thus, we began our investigations by combining (BrettPhos)Pd(aryl)Br (aryl = 4-Me-C_6H_4, **Pd-5**) with 1 equivalent of the discrete Cu–CF_3 species (PPh_3)$_3$Cu(CF_3)[25] (**Cu-1**) in THF at ambient temperature (Scheme 4.4.1a). ^{19}F NMR spectroscopy revealed the presence of (BrettPhos)Pd(Ar)(CF_3) complex **Pd-2d** and *cis*-(PPh_3)$_2$Pd(Ar)(CF_3) (***cis*-Pd-17**) in the reaction mixture, demonstrating that trifluoromethylcopper species are capable of delivering an equivalent of CF_3 to arylpalladium halide complexes containing an ancillary ligand. A new doublet at –31.9 ppm also was observed and was assigned as (BrettPhos)Cu(CF_3) (**Cu-2**). However, upon heating at 65 °C for 20 min, the aryl(trifluoromethyl)palladium complex **Pd-2d** decayed completely and converted into a mixture of ***cis*-** and ***trans*-Pd-17** (20 and 84% yield, respectively) ligated by PPh_3,

likely forming from the exchange of ancillary phosphine ligands between the Pd and Cu centers. The $^{31}P\{^{1}H\}$ NMR spectrum of the reaction mixture contained a broad feature at ~11 ppm assigned to (BrettPhos)CuBr (**Cu-3**). While PPh_3-ligated complexes **Pd-17** did not undergo reductive elimination to form trifluoromethylarene,[36] we considered that **Pd-17** and BrettPhos-ligated **Cu-3** might be in equilibrium with PPh_3-ligated Cu(I) and the BrettPhos-ligated aryl(trifluoromethyl)palladium complex **Pd-2d**, which could form trifluoromethylarene upon heating. However, no trifluoromethylarene formed after heating the mixture at 80 °C overnight, suggesting that the formation of (BrettPhos)Pd(aryl)(CF_3) (**Pd-2d**) in such an equilibrium is prohibitively unfavorable.

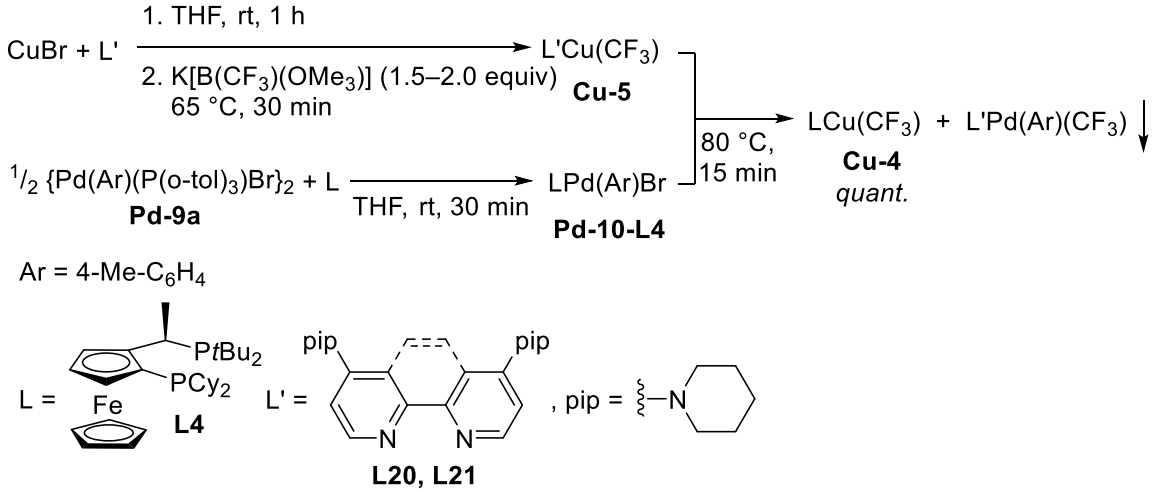


Scheme 4.4.1 Reactions of several arylpalladium halide complexes with trifluoromethylcopper complex **Cu-1** Yields were determined by ^{19}F NMR spectroscopy relative to 4-(trifluoromethoxy)anisole as an internal standard. Yields in parentheses represent those after heating the mixture for 20 min at 65 °C.

We next considered that a chelating diphosphine ligand might bind more strongly to the Pd center and prevent the deleterious exchange of ancillary ligands between the starting Pd and Cu complexes (Scheme 4.4.1b). Treating arylpalladium bromide dimer **Pd-9a** with CyPF-*t*Bu (**L4**) in

THF formed (**L4**)Pd(aryl)Br (**Pd-10-L4**) instantaneously, as determined by $^{31}P\{^{1}H\}$ NMR spectroscopy. However, when **Pd-10-L4** was treated with $(PPh_3)_3Cu(CF_3)$ (**Cu-1**) at room temperature (Scheme 4.4.1b), the only fluorine-containing species detected in the ^{19}F NMR spectrum of the reaction mixture was (**L4**)Cu(CF_3) (**Cu-4**). Heating the reaction mixture at 80 °C for 15 minutes formed a mixture of the trifluoromethylpalladium complexes ***cis***- and ***trans***-**Pd-17** and a small amount of (**L4**)Pd(aryl)(CF_3) (**Pd-11-L4**); however, continued heating formed trifluoromethylarene **2a** in only 10% yield. We also investigated whether (**L4**)Cu(CF_3) (**Cu-4**) would undergo transmetallation with the arylpalladium bromide complex **Pd-10-L4** containing the same ligand in the absence of PPh_3; however, the reaction of **Cu-4** with **Pd-10-L4** at 80 °C formed no Pd–CF_3 species or trifluoromethylarene product, likely due to the large steric bulk of **L4** preventing transmetallation (Scheme 4.4.1c).

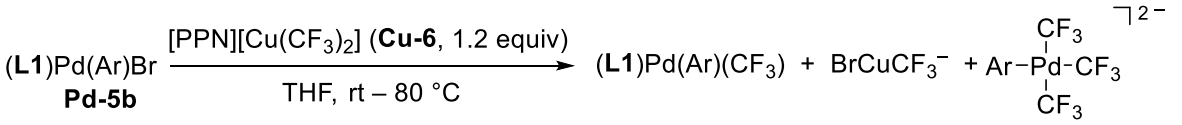
To circumvent the exchange of ancillary ligands, we investigated systems in which the trifluoromethylcopper species contained the chelating pyridine-based ligands 4,4'-di(piperidin-1-yl)-2,2'-bipyridine (pip_2bpy, **L19**) or 4,7-di(piperidin-1-yl)-1,10-phenanthroline (pip_2bpy, **L20**, Scheme 4.4.2). We reasoned that the harder *N*,*N* ligands would bind preferentially to the harder first-row transition metal Cu, while the softer phosphine ligands would bind preferentially to the softer Pd center. The trifluoromethylcopper species **Cu-5** containing ligands **L19** and **L20** were generated *in situ* by first combining copper(I) bromide and **L19** or **L20** in THF,[70,71] followed by treatment with $K[B(CF_3)(OMe)_3]$ and heating at 65 °C for 30 minutes. However, treating a solution of arylpalladium bromide **Pd-10-L4** with solutions of these copper reagents and heating at 80 °C for 15 minutes formed CyPF-*t*Bu-ligated trifluoromethylcopper complex **Cu-4** in quantitative yields, in addition to insoluble precipitates. Again, heating the mixture at 80 °C for 18 hours did form any trifluoromethylarene **2d**.



Scheme 4.4.2 Reaction of *in situ*-generated (CyPF-*t*Bu)Pd(Ar)Br (**Pd-10-L4**) with L'Cu(CF_3) complexes **Cu-5** containing ligands **L19** and **L20**. See Section 4.7.3 for reaction conditions.

Lastly, we hypothesized that the ancillary phosphine ligand of an arylpalladium bromide complex would remain bound to Pd in reactions with $Cu(CF_3)_2^-$ because $Cu(CF_3)_2^-$ does not form complexes with ancillary ligands.[65,72–74] Thus, we treated (BrettPhos)Pd(4-Me-C_6H_4)Br (**Pd-5**) with 1.2 equivalents of [PPN][$Cu(CF_3)_2$] (**Cu-6**)[75] in THF and analyzed the mixture by NMR spectroscopy (Scheme 4.4.3). After 15 minutes, aryl(trifluoromethyl)palladium complex **Pd-2d** and the heteroleptic cuprate $BrCu(CF_3)^-$ (**Cu-7**) had formed in 86 and 85% yield, respectively. The

complex (**L1**)Cu(CF_3) (**Cu-2**) was present in only trace amounts (< 1% yield), demonstrating that transmetallation had occurred without transfer of **L1** from the Pd center to Cu. After heating the mixture at 80 °C for 18 hours, both aryl(trifluoromethyl)palladium complex **Pd-2d** and cuprate **Cu-7** were consumed completely, but no trifluoromethylarene had formed. Instead, a new trifluoromethyl complex that was characterized by two new mutually coupled resonances in the ^{19}F NMR spectrum of the mixture in a 1:2 ratio, was observed, and this complex was tentatively assigned as Pd(aryl)$(CF_3)_3^{2-}$ (**Pd-18**). We propose that such a species forms by the sequential reaction of arylpalladium bromide **Pd-5b** with multiple equivalents nucleophilic CF_3, displacing the ancillary ligand **L1**.[47] Ongoing work in our lab seeks to characterize this and other side-products of the reaction and to develop other trifluoromethylmetal reagents for the Pd-catalyzed trifluoromethylation of aryl halides.



		Pd-2d	Cu-7	Pd-18
Ar = 4-Me-C_6H_4	rt, 15 min	86%	85%	6%
PPN = $Ph_3P{=}N{=}PPh_3^+$	80 °C, 15 min	0%	0%	37%

Scheme 4.4.3 Reaction of arylpalladium bromide complex **Pd-5b** with [PPN][Cu$(CF_3)_2$] (**Cu-6**). Conditions: **Pd-5b** (5.0 μmol, 1.0 equiv), **Cu-6** (5.8 μmol, 1.2 equiv), THF (600 μL). Yields were determined by ^{19}F NMR spectroscopy relative to 4-(trifluoromethoxy)anisole as an internal standard.

4.5 Conclusions

In summary, we have conducted investigations into the Pd-catalyzed trifluoromethylation of aryl halides reported by Buchwald and found that, while (BrettPhos)Pd(aryl)(CF_3) complexes formed trifluoromethylarene in quantitative yields in the absence of side-products, the reaction of the corresponding arylpalladium halide complexes (BrettPhos)Pd(aryl)X with $TMSCF_3$ and CsF occurred in low yields and formed several side-products, including aryl(pentafluoroethyl)- and *bis*(trifluoromethyl)palladium complexes **Pd-3** and **Pd-4**. These two side-products suggest that α-fluoride elimination and exchange of X-type ligands between Pd centers both occurred during the reaction. We also have shown that arylpalladium halide and aryl(trifluoromethyl)palladium complexes undergo exchange of X-type ligands to form the trifluoromethylpalladium halide species (BrettPhos)Pd(CF_3)X (X = Cl, Br), which would lie off the catalytic cycle of trifluoromethylation.

We also evaluated several Josiphos derivatives as ancillary ligands on trifluoromethylpalladium complexes. We found many arylpalladium bromide complexes containing these ligands underwent transmetallation with CF_3^- to form the corresponding aryl(trifluoromethyl)palladium species, but most of the resulting arylpalladium trifluoromethyl complexes of these ligands did not form trifluoromethylarene, even at 100 °C for 18 hours. We did identify, with the aid of DFT calculations, several perfluoroalkylphosphine ligands that should form aryl(trifluoromethyl)palladium complexes that undergo reductive elimination, and experimental studies confirmed that complexes containing these ligands undergo reductive elimination of trifluoromethylarene at 80 °C. However, the ligands did not form catalysts for the

trifluoromethylation of aryl halides because they either formed stable Pd(0) complexes that did not undergo oxidative addition or decomposed in the presence of trace water.

Finally, we evaluated trifluoromethylcopper species as reagents to transfer equivalents of nucleophilic CF_3 to arylpalladium bromide complexes. Trifluoromethylcopper complexes generally underwent transmetallation with arylpalladium bromide complexes containing BrettPhos or CyPF-*t*Bu as ancillary ligands to form high yields of the trifluoromethylpalladium complexes. However, exchange of ancillary ligands between the Pd and Cu centers occurred when the copper species contained phosphines or bidentate pyridine-based ligands, thereby forming aryl(trifluoromethyl)palladium species that did not undergo reductive elimination of trifluoromethylarene. Reactions in which *bis*(trifluoromethyl)cuprate served as the source of CF_3^- initially formed aryl(trifluoromethyl)palladium complexes that did not transfer the ancillary ligand to Cu. However, upon heating to induce reductive elimination, these species formed a poly(trifluoromethyl)metal species without forming trifluoromethylarene. Future work will focus on identifying ligand scaffolds for both Cu and Pd that facilitate transmetallation to Pd, without displacement of its ancillary ligand, and on trifluoromethylation reactions with other trifluoromethylmetal reagents.

4.6 Footnotes

1. The chemical shift of (BrettPhos)Pd(CF_3)Cl (**Pd-6a**) was reported previously, though it differs somewhat from that observed in our experiments (^{19}F: –0.07 ppm; ^{31}P{^{1}H}: 65.0 ppm). This difference is likely explained by the difference in solvent (THF *vs* $CDCl_3$) or inconsistent referencing of chemical shifts.[76] Removal of the THF solvent and dissolution in $CDCl_3$ resulted smaller differences in chemical shift (^{19}F: 0.27 ppm; ^{31}P{^{1}H}: 64.7 ppm).

4.7 Supplementary Experimental Information

4.7.1 General Experimental Procedures and Reagent Availability

All experiments were conducted in a nitrogen-atmosphere drybox unless otherwise specified. All glassware and Teflon-coated stir bars were dried in a glassware oven for at least 2 h or flame-dried and cooled under vacuum directly before use. Reaction conducted in vials were sealed with Teflon-lined caps. Toluene, tetrahydrofuran (THF), diethyl ether, hexane, dichloromethane, and pentane were dried with an Innovative Pure-Solv solvent purification system. THF was additionally dried over activated 4 Å molecular sieves. Alumina was dried at 200 °C overnight under high vacuum for 3 d. Anhydrous dioxane was purchased from Acros Organics and dried over NaK alloy and was pass through a short plug of alumina directly before use. Deuterated solvents were purchased from Cambridge Isotope Laboratories, degassed *via* three freeze-pump-thaw cycles, and stored over molecular sieves. NMR spectra were acquired on Bruker 400, 500, or 600 MHz spectrometers at the UC Berkeley NMR facility. ^{1}H and ^{13}C NMR spectra are referenced to the residual solvent signals. ^{19}F NMR signals in proteated solvents (*e.g.*, dioxane, THF) were referenced to the internal standard 4-(trifluoromethoxy)anisole, which was set to δ –59.0 ppm. Elemental analyses were performed by the UC Berkeley Microanalytical Laboratory. GC/MS analyses were conducted with a system consisting of an Agilent 6890N GC and an Agilent 5973 Mass Selective Detector.

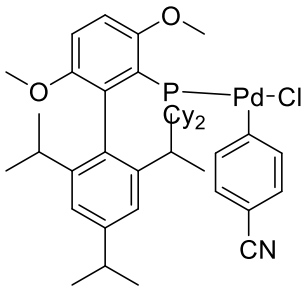
N-methyl-2-aminobiphenylpalladium methanesulfonate,[43] aryl(trifluoromethyl)palladium complex **Pd-8**,[37] dimers **9**,[77] trifluoromethylcopper complex **Cu-1**,[25] Pd(P(*o*-

tol)$_3$)$_2$(CF$_3$)(OTFA),[44] **L5**,[55] **L13**,[55] and K[B(CF$_3$)(OMe)$_3$][20] were prepared according to reported procedures. All other reagents were purchased from commercial suppliers and used as received.

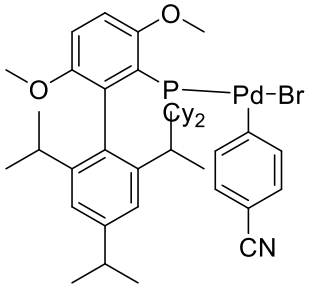
4.7.2 Synthetic Methods

*General preparation of (BrettPhos)Pd(aryl)X complexes **Pd-1a-b** (X = Cl, Br)*

N-methyl-2-aminobiphenylpalladium methanesulfonate[43] (1.00 equiv), BrettPhos (1.05 equiv), and aryl halide (5 equiv) were dissolved in THF (0.050 M) and stirred until homogeneous. Potassium *tert*-butoxide (1.05 equiv) was added in one portion as a 0.20 M solution in THF. The mixture was allowed to stir for 1 h, and then was filtered through a syringe filter. The filtrate was concentrated under vacuum to an oil, and diethyl ether or hexane was added to precipitate the product, which was collected *via* filtration through a fine-fritted glass funnel. The solid obtained thereby was dried under vacuum for 4 h to afford the product as a pale powder. Compounds **Pd-1** consisted of a mixture of isomers, complicating spectroscopic analysis.



Pd-1a
Spectroscopic characterization matched that reported in the literature.[51]



Pd-1b consists of a ~1:1 ratio of isomers, complicating assignment. Reported integrals will total 2× the number of protons.
^{1}H NMR (500 MHz, CDCl$_3$): δ 7.54 (dd, *J* = 8.4, 2.0 Hz, 2H), 7.27 (dd, *J* = 7.4, 1.9 Hz, 2H), 7.15 (d, *J* = 8.1 Hz, 2H), 7.12 (d, *J* = 8.0 Hz, 2H), 7.10 – 6.98 (m, 6 H), 6.89 (dd, *J* = 8.9, 2.9 Hz, 1H), 6.83 (d, *J* = 8.8 Hz, 1H), 4.93 (s, 3H), 3.83 (s, 3H), 3.60 (s, 3H), 3.35 (s, 3H), 3.07 (hept, *J* = 7.0 Hz, 1H), 2.92 (hept, *J* = 6.9 Hz, 1H), 2.78 – 2.63 (m, 2H), 2.47 (hept, *J* = 6.8 Hz, 2H), 2.31 (hept, 6.8 Hz, 2H), and 1.81 – 0.54 (m, 78H) ppm.
^{31}P{^{1}H} (202 MHz, CDCl$_3$): δ 46.24, 36.14 ppm.
Anal Calc'd for C$_{42}$H$_{57}$BrNO$_2$PPd: C, 61.13; H, 6.96; N: 1.70. Found: C, 60.75; H: 6.92; N: 1.70.

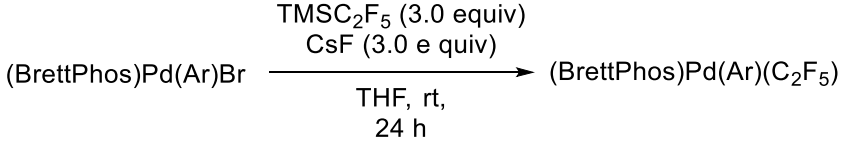
*Preparation of (BrettPhos)Pd(4-OMe-C$_6$H$_4$)(CF$_3$) (**Pd-2c**)*

Although compound **Pd-2c** has been reported previously,[30] we present a new synthesis here

that avoids the generation of Pd–C_2F_5 and Pd$(CF_3)_n$ species. To a 20-mL vial were added Pd(P(*o*-tol)$_3$)$_2$(CF_3)(OTFA)[44] (50.0 mg, 55.7 μmol, 1.0 equiv), BrettPhos (**L1**, 32.9 mg, 61.3 μmol, 1.10 equiv), and benzene (2 mL). The vial was sealed with a Teflon-lined cap, removed from the glove box, and stirred at 65 °C for 1 h. After cooling to ambient temperature, the vial was returned to the glove box (**Mixture A**). To a separate 4 mL vial was added 2-(4-methoxyphenyl)-5,5-dimethyl-1,3,2-dioxaborinane (14.7 mg, 66.9 μmol, 1.20 equiv) and a THF solution of potassium trimethylsilanolate (0.10 M, 585 μL, 58.5 μmol, 1.05 equiv) (**Mixture B**). **Mixture B** was mixed by pipette until homogeneous and transferred with the aid of 500 μL THF to rapidly stirring **Mixture A**. The combined reaction mixture was allowed to stir for 30 min at ambient temperature, over which time it darkened slightly from yellow to orange. The mixture then was filtered through a short plug of alumina (eluting with THF) to remove any unreacted palladium trifluoroacetate species, palladium black, and other salt byproducts. Under air, the filtrate was concentrated to a brown oil (no heating was applied to assist in the removal of solvent), and this oil was treated with a minimal amount (~150 μL) of diethyl ether, resulting in the immediate formation of a light-colored precipitate. The suspension was stored overnight at –20 °C to complete the precipitation of a light tan solid, from which the mother liquor was decanted. The solid was washed once with cold diethyl ether (300 μL) and twice with pentane (400 μL), and the tan solid was dried on high vacuum overnight to afford the product (30.6 mg, 67% yield). The product contained a small amount (~3%) of P(*o*-tol)$_3$.

Spectroscopic characterization closely matches that reported in the literature.[30]
^{1}H NMR (500 MHz, $CDCl_3$): δ 7.27 ppm (d, *J* = 8.4 Hz, 2H), 7.04 – 6.97 (m, 3H), 6.59 (*J* = 8.2 Hz, 2H), 4.24 (s, 3H), 3.69 (s, 3H), 3.59 (s, 3H), 2.93 (sept, *J* = 6.9 Hz, 1H), 2.36 (sept, *J* = 6.7 Hz, 2H), and 2.07 – 0.55 (m, 40H) ppm.
^{19}F NMR (564 MHz, $CDCl_3$): δ –30.4 (d, $^3J_{F–P}$ = 44.9 Hz, 3F) ppm.
^{31}P NMR (243 MHz, $CDCl_3$): δ 31.7 (q, $^3J_{P–F}$ = 45.0 Hz, 1P) ppm.

*Preparation of (BrettPhos)Pd(4-R-C_6H_4)(C_2F_5) (**Pd-3a-b**, R = CN, Me)*



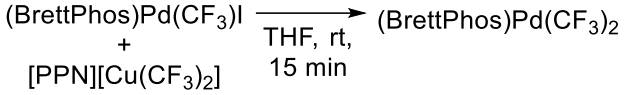
To a 1-dram vial were added (BrettPhos)Pd(4-R-C_6H_5)Br (**Pd-1b** or **Pd-5**, 25 μmol, 1.00 equiv), CsF (11.2 mg, 73.7 μmol, 3.00 equiv), followed by THF (1.0 mL). To this mixture was added $TMSC_2F_5$ (13.0 μL, 73.7 μmol, 3.00 equiv), and the mixture was stirred for 18 h at ambient temperature. The mixture then was passed through a plug of dry basic alumina, concentrated to ~100 μL, layered with pentane, and stored at –35 °C for a week. The liquor then was decanted, and the precipitate washed with pentane (3×1 mL). The needles obtained from the reaction of **Pd-5** forming **Pd-3b** were suitable for characterization by single-crystal X-ray diffraction.

Pd-3a: Brown solid (14.4 mg, 168 μmol, 68.1% yield).
^{1}H NMR (600 MHz, C_6D_6): δ 7.71 (d, *J* = 7.9 Hz, 2H), 7.05 (s, 2H), 6.96 (d, *J* = 7.9 Hz, 2H), 6.33 (dd, *J* = 9.2, 4.5 Hz, 1H), 6.25 (d, J = 9.2 Hz, 1H), 3.78 (s, 3H), 2.88 (s, 3H), 2.73 (hept, J = 7.1 Hz, 1H), and 2.42 (d, J = 6.7 Hz, 2H), and 1.85 – 0.54 (m, 40H) ppm.
^{19}F NMR (565 MHz, Benzene-d_6): δ –79.88 (s, 3F), –104.97 (d, *J* = 27.3 Hz, 2F).

$^{31}P\{^{1}H\}$ NMR (243 MHz, Benzene-d_6): δ 30.07 (t, J = 27.7 Hz) ppm.

Pd-3b: colorless needles, (11.2 mg, 13.1 μmol, 53.2% yield).
^{1}H NMR (600 MHz, C_6D_6): δ 7.75 (d, J = 7.7 Hz, 2H), 7.07 (s, 2H), 6.92 (d, J = 7.7 Hz, 2H), 6.38 (dd, J = 9.2, 4.5 Hz, 1H), 6.27 (d, J = 9.2 Hz, 1H), 3.85 (s, 3H), 2.90 (s, 3H), 2.73 (hept, J = 6.8 Hz, 1H), 2.49 (hept, J = 6.6 Hz, 2H), 2.18 (s, 3H), 1.87 – 1.67 (m, 5H), 1.62 – 1.32 (m, 10H), 1.31 – 1.23 (m, 1H), 1.19 (d, J = 6.7 Hz, 6H), 1.14 (d, J = 6.9 Hz, 6H), 1.09 (d, J = 14.4 Hz, 1H), 1.05 (d, J = 6.6 Hz, 6H), 1.02 – 0.93 (m, 1H), 0.86 – 0.79 (m, 2H), and 0.73 – 0.62 (m, 2H) ppm.
^{19}F NMR (565 MHz, C_6D_6): δ –79.68 (s, 3 F) and –105.28 (d, $^{3}J_{F–P}$ = 26.5 Hz) ppm.
$^{31}P\{^{1}H\}$ NMR (243 MHz, C_6D_6): δ 28.9 (br t, $^{3}J_{P–F}$ = 26.3 Hz) ppm.

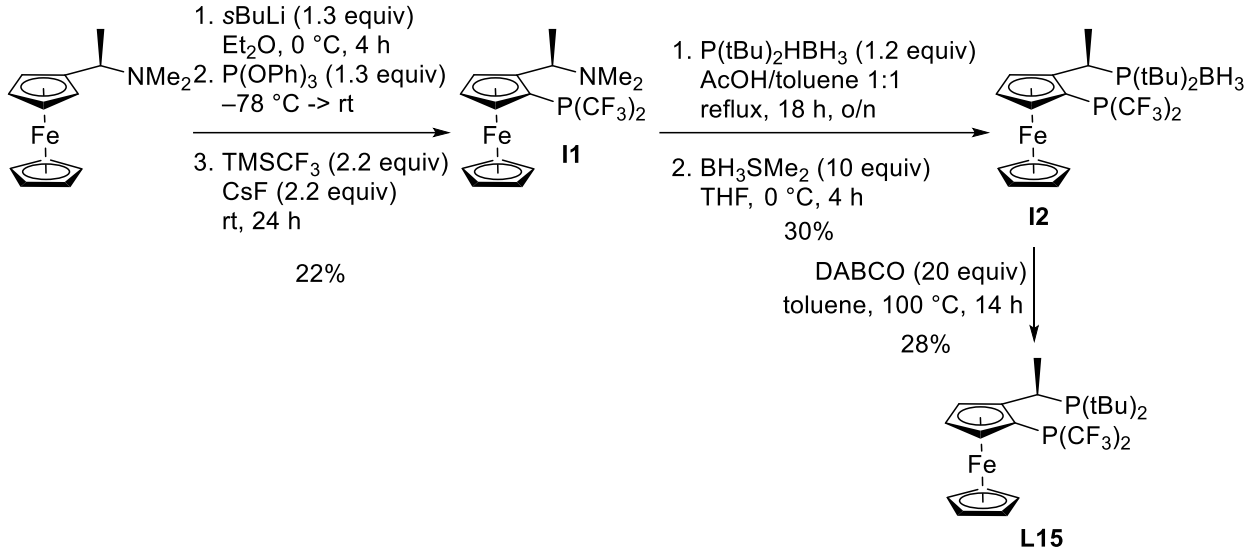
*Preparation of (BrettPhos)Pd(CF_3)$_2$ (**Pd-4**)*



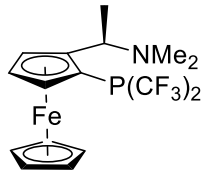
To a 1-dram vial containing (BrettPhos)Pd(CF_3)I[51] (8.4 mg, 10 μmol, 1.0 equiv) and [PPN][Cu(CF_3)$_2$] (8.9 mg, 12 μmol, 1.2 equiv) was added THF (700 μL), and the mixture was stirred by pipette until homogeneous. The reaction mixture was allowed to stand at room temperature for 15 min, after which it was passed through a plug of dry basic alumina. The mixture was concentrated to ~100 μL, layered with pentane (2 mL), and cooled to –35 °C overnight, affording colorless plates suitable for X-ray diffraction. The **Pd-4** thus obtained contained two molecules of THF (31.4 mg, 66.5% yield).

^{1}H NMR (600 MHz, C_6D_6) δ 7.09 (s, 2H), 6.29 (dd, J = 9.2, 4.3 Hz, 1H), 6.22 (d, J = 9.2 Hz, 1H), 3.84 (s, 3H), 2.86 (s, 3H), 2.74 (hept, J = 6.9 Hz, 1H), 2.36 (hept, J = 6.8 Hz, 2H), and 1.96 – 0.67 (m, 40H) ppm.
^{19}F NMR (565 MHz, C_6D_6) δ –5.89 (br s, 3F), –31.65 (dq, J = 53.2, 6.9 Hz, 3F).
$^{31}P\{^{1}H\}$ NMR ($CDCl_3$, 243 MHz): δ 43.5 – 42.4 (m) ppm.
Anal. Calcd for $C_{37}H_{53}F_6O_2PPd$ + 2×C_4H_8O: C, 58.40; H, 7.52. Found: C, 58.20; H, 7.25.

*Preparation of CF_3PF-t*Bu (**L15**)*



Author's note: recent experience by other members of our lab found that Josiphos scaffolds in which both arms are bulky alkylphosphines are generally stable to air, potentially obviating the need for the BH_3 protection/deprotection sequence.

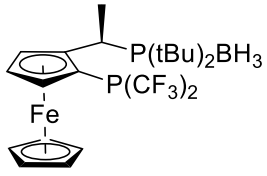


I1

The following method was adapted from a literature procedure.[56] To a 25 mL round-bottom flask equipped with a rubber stopper was added Ugi amine (150 mg, 583 μmol, 1.0 equiv) and diethyl ether (1.0 mL). The flask was removed from the glove box, equipped with a N_2 balloon, and cooled to 0 °C in an ice bath. A solution of *s*BuLi (1.0 M in cyclohexane, 760 μL, 760 μmol, 1.3 equiv) was added dropwise at this temperature, and the solution was stirred at 0 °C for 4 h. The solution then was cooled to –100 °C in a liquid nitrogen/ethanol bath, and triphenylphosphite (200 μL, 758 μmol, 1.30 equiv) was added dropwise with vigorous stirring (Note: triphenylphosphite isn't very soluble in Et_2O and at this temperature tends to freeze solid as chips in the bottom of the flask. Vigorous stirring helps prevent jamming). The solution then was allowed to warm slowly to room temperature overnight. The solvent was removed under vacuum without exposure to air, CsF (195 mg, 1.28 mmol, 2.20 equiv) was added under an N_2 cone, followed by diethyl ether (3 mL) and $TMSCF_3$ (190 μL, 1.28 mmol, 2.2 equiv). The mixture was allowed to stir overnight at ambient temperature, and then exposed to air, and the solvent was removed under vacuum. The brown tarry residue was purified by flash column chromatography (basic alumina, 9:1:0.1 :: hexane:DCM:triethylamine, R_f ~ 0.3) yielding the product as an impure brown solid (53.6 mg, 21.6% yield). The material was carried forward without further purification.

^{1}H NMR (400 MHz, $CDCl_3$): δ 4.55 – 4.45 (m, 3H), 4.24 (s, 5H), 3.95 (q, *J* = 6.7 Hz), 2.04 (s, 6H), and 1.23 (d, *J* = 6.6 Hz, 3H) ppm.

^{19}F NMR (376 MHz, $CDCl_3$): δ –50.4 (dq, *J* = 70.2, 8.9 Hz, 3F) and –53.75 (dq, *J* = 57.8, 9.1 Hz, 3F) ppm.



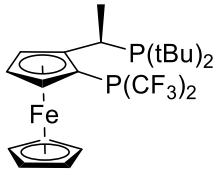
I2

The following procedure was adapted from the literature.[78] To a 10 mL Schlenk bomb was added **I1** (53.6 mg, 126 μmol, 1.0 equiv), P(*t*Bu)$_2$H·BH$_3$ (24.2 mg, 151 μmol, 1.2 equiv), toluene (500 μL), and acetic acid (500 μL). The bomb was removed from the glove box and sparged 3× with dry argon. The mixture then was heated at 95 °C for 18 h with vigorous stirring under flow of argon. The mixture then was concentrated under vacuum to a messy foam, which was treated with toluene (3 mL), and the solvent was again removed under vacuum. Once dry, the Schlenk bomb was backfilled with argon and THF (1 mL) was added. The mixture was cooled to 0 °C and BH$_3$·SMe$_2$ (109 μL, 1.26 mmol, 10 equiv) was added dropwise. The mixture was stirred for 4 h at this temperature and was quenched by the dropwise addition of methanol (3 mL). The solvent was removed under vacuum and the residue was purified under air by flash column chromatography (silica gel, 4:1 :: hexane:ethyl acetate, R_f ~ 0.3) to afford the product as an orange foam (20.3 mg, 29.8% yield).

^{1}H NMR (400 MHz, CDCl$_3$): δ 4.90 – 4.59 (m, 2H), 4.67 (s, 1H), 4.33 (s, 5H), 4.14 – 4.04 (m, 1H), and 2.45 – 0.61 (m, 21H) ppm.

^{19}F NMR (376 MHz, CDCl$_3$): δ –51.6 (dq, *J* = 81.0, 9.0 Hz, 3F) and –53.1 (dq, *J* = 69.6, 8.8 Hz, 3F) ppm.

^{31}P{^{1}H} NMR (162 MHz, CDCl$_3$): δ –2.8 (qqd, *J* = 82, 70, 11.5 Hz, 1P). Phosphine borane is invisible due to excessive splitting.



L15

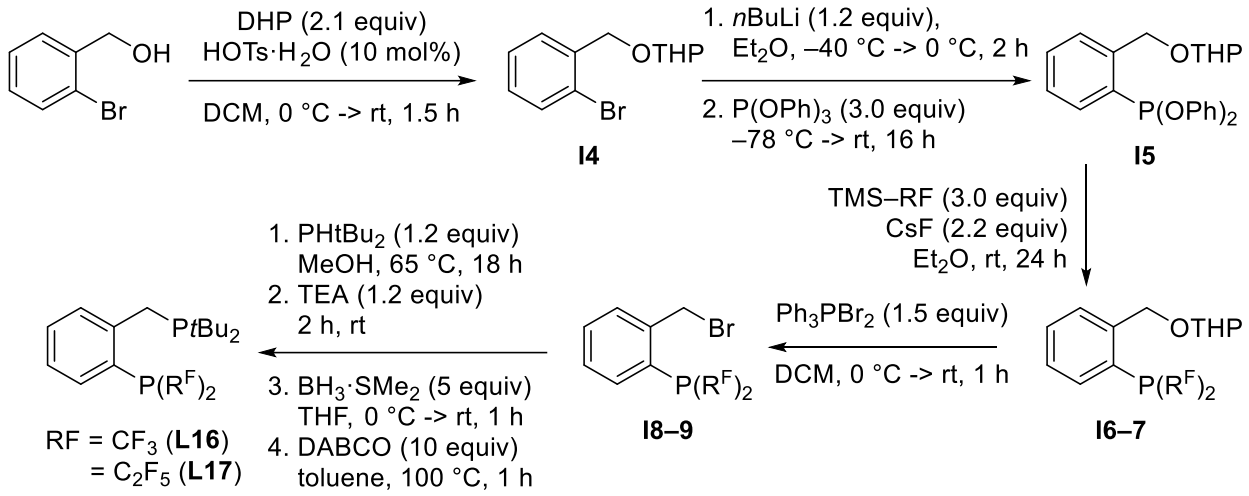
To a 1-dram vial were added **I2** (20.3 mg, 37.6 μmol, 1.00 equiv), DABCO (84.3 mg, 752 μmol, 20.0 equiv), and toluene (500 μL). The vial was sealed, removed from the glove box, and heated at 100 °C for 14 h. The mixture then was passed through a plug of silica gel and all colored fractions were collected, eluting with 19:1 :: pentane : diethyl ether. The solvent was removed to afford the product as an impure yellow solid (5.5 mg, 28% yield).

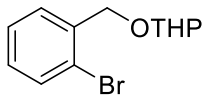
^{1}H NMR (400 MHz, CDCl$_3$): δ 4.56 – 4.49 (m, 2H), 4.45 (s, 1H), 4.23 (s, 1H), 3.19 (q, *J* = 5.7 Hz, 1H), 1.87 – 1.75 (m, 3H), 1.31 (d, *J* = 10.5 Hz, 9H), and 1.03 (d, *J* = 10.8 Hz, 9H) ppm.

^{19}F NMR (376 MHz, CDCl$_3$): δ –51.4 (dq, *J* = 75.5 Hz, 7.5 Hz, 3F) and –52.2 (ddq, *J* = 48.9, 33.7, 7.5 Hz, 3F).

^{31}P{^{1}H} NMR (162 MHz, CDCl$_3$): δ 61.9 – 59.8 (m, 1P) and –5.7 – –9.9 (m, 1P) ppm.

*Preparation of alkyl-fluoroalkyl ligands **L16**–**L17***

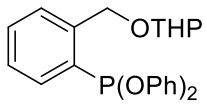




I4

To a 100 mL round-bottom flask was added 4-bromobenzyl alcohol (5.00 g, 26.7 mmol, 1.00 equiv), *p*-toluenesulfonic acid monohydrate (508 mg, 2.67 mmol, 10 mol%), and dichloromethane (25 mL) under air. The mixture was cooled to 0 °C in an ice bath and 3,4-dihydro-2*H*-pyran (5.12 mL, 56.1 mmol, 2.1 equiv) in dichloromethane (25 mL) was added over 1 min. The reaction was allowed to warm to ambient temperature over 1 h. The mixture then was transferred to a separation funnel and treated with saturated aqueous $NaHCO_3$ (100 mL), which was extracted with diethyl ether (3×50 mL). The combined organic extracts were dried over $MgSO_4$ and concentrated to a viscous oil, which was purified by flash column chromatography (silica gel, 50:1 :: pentane : diethyl ether, $R_f \sim 0.4$) to afford the product as a colorless oil (6.2382 g, 86.1% yield).

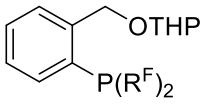
Spectroscopic characterization matched that reported in the literature. [79]
^{1}H NMR (400 MHz, $CDCl_3$) δ 7.53 (t, *J* = 8.1 Hz, 2H), 7.32 (t, *J* = 7.5 Hz, 1H), 7.15 (t, *J* = 7.8 Hz, 1H), 4.83 (d, *J* = 13.3 Hz, 1H), 4.78 (t, *J* = 3.6 Hz, 1H), 4.58 (d, *J* = 13.3 Hz, 1H), 4.01 – 3.87 (m, 1H), 3.69 – 3.43 (m, 1H), 2.01 – 1.48 (m, 6H).



I5

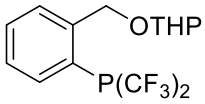
An oven-dried 50 mL round-bottom flask was charged with **I4** (1.00 g, 3.69 mmol, 1.0 equiv), sealed with a rubber septum equipped with a N_2 balloon, and placed under an atmosphere of N_2. To the flask then was added diethyl ether (10 mL), and the mixture was cooled to –40 °C in a dry ice/acetonitrile bath. To the stirring reaction mixture then was added *n*-butyllithium (2.61 M in hexane, 1.70 mL, 4.43 mmol, 1.20 equiv) dropwise. The mixture was allowed to stir for 15 min at –40 °C, and then the dry ice bath was replaced with a water ice bath, and the mixture was stirred

for another 2 h. The mixture then was cooled to –78 °C in a dry ice/acetone bath, and a solution of triphenylphosphite (2.90 mL, 11.1 mmol, 3.00 equiv) in diethyl ether (10 mL) was added dropwise. The mixture was allowed to warm to room temperature overnight. The mixture then was opened to air, diluted with pentane (20 mL), and filtered through a pad of Celite to remove most of the lithium phenoxide. The filtrate was concentrated under vacuum and subjected to flash column chromatography (silica gel, 19:1 :: pentane : diethyl ether, R_f ~ 0.25; R_f of remaining $P(OPh)_3$: ~0.6) to afford the product as a colorless oil (1.0397 g, 69.0% yield). The material obtained was found to degrade slowly under air and was used without further purification.



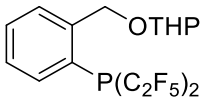
I6–7

To a 20 mL vial were added **I5** (550 mg, 1.34 mmol, 1.00 equiv), CsF (448 mg, 2.96 mmol, 2.2 equiv), diethyl ether (5.0 mL), and TMS–R^F (R^F = CF_3, C_2F_5, 4.00 mmol, 4.0 equiv). The mixture was stirred at ambient temperature for 24 h. Under air, the mixture was filtered through a plug of Celite and concentrated to an oil, which was purified by flash column chromatography (silica gel, 20:1 :: hexanes : ethyl acetate) to afford the product as a colorless oil.



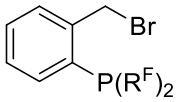
I6

Colorless oil, 333.3 mg, 69% yield.
^{1}H NMR (500 MHz, $CDCl_3$): δ 7.96 (dd, *J* = 7.9, 3.9 Hz, 1H), 7.62 – 7.55 (m, 1H), 7.53 (ddd, *J* = 7.5, 5.3, 1.5 Hz, 1H), 7.47 (td, *J* = 7.6, 1.6 Hz, 1H), 4.97 (d, *J* = 11.4 Hz, 1H), 4.76 (t, *J* = 3.5 Hz, 1H), 4.71 (d, *J* = 11.7 Hz, 1H), 3.90 (ddd, *J* = 11.8, 9.1, 2.9 Hz, 1H), 3.63 – 3.54 (m, 1H), and 1.91 – 1.42 (m, 6H) ppm.
^{19}F NMR (470 MHz, $CDCl_3$): δ –52.4 ppm (dq, *J* = 81.3, 7.2 Hz, 3F) and –52.6 (dq, *J* = 80.7, 7.6 Hz, 3F) ppm.
^{31}P NMR (202 MHz, $CDCl_3$): δ 9.82 (approx. hept, *J* = 81.6 Hz) ppm.



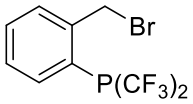
I7

Colorless oil, 328.7 mg, 97.2% yield.
^{1}H NMR (400 MHz, $CDCl_3$) δ 7.98 (d, *J* = 7.9 Hz, 1H), 7.65 – 7.49 (m, 2H), 7.45 (td, *J* = 7.5, 1.8 Hz, 1H), 4.94 (d, *J* = 11.9 Hz, 1H), 4.72 (t, *J* = 3.4 Hz, 1H), 4.69 (d, *J* = 12.0 Hz, 1H), 3.95 – 3.81 (m, 1H), 3.57 (dd, *J* = 11.2, 5.3 Hz, 1H), and 1.87 – 1.49 (m, 6H) ppm.
^{19}F NMR (376 MHz, $CDCl_3$): δ –81.3 – –81.5 (m, 6F) and –109.7 – –110.6 (m, 4F) ppm.
^{31}P NMR (202 MHz, $CDCl_3$): δ –11.6 – –12.9 (m) ppm.



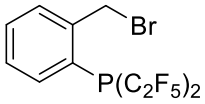
I8–9

To a round-bottom flask under Ar were triphenylphosphine (260 mg, 0.992 mmol, 1.60 equiv) and DCM (5 mL). The mixture was cooled to 0 °C in an ice bath, and Br_2 (48 μL, 0.93 mmol, 1.5 equiv) was added dropwise, producing a white precipitate. The mixture was allowed to stir for 30 min at 0 °C, and then **I6** or **I7** (620 μmol, 1.00 equiv) was added with the aid of DCM (1 mL). The reaction mixture was allowed to warm to room temperature over 30 min, and then was quenched by the addition of water (20 mL). The mixture was extracted with pentane (3×15 mL) and the organic layers were dried over $MgSO_4$ and carefully concentrated to an oil, which was passed through a silica plug eluting with 20:1 hexane:diethyl ether to remove any remaining triphenylphosphine oxide. The product was carried forward without further purification after removing the solvent under vacuum.



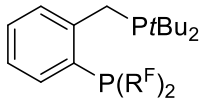
I8

The reaction was conducted on a 1 mmol scale. Colorless oil, 298.6 mg, 95.2% yield.
^{1}H NMR (400 MHz, $CDCl_3$): δ 8.01 – 7.85 (m, 1H), 7.61 (t, *J* = 7.6 Hz, 1H), 7.54 (t, *J* = 6.8 Hz, 1H), 7.51 – 7.43 (m, 1H), and 4.79 (s, 2H) ppm.
^{19}F NMR (376 MHz, $CDCl_3$): δ –51.50 (d, *J* = 83.5 Hz) ppm.
^{31}P NMR (202 MHz, $CDCl_4$): δ –11.83 (hept, *J* = 83.8 Hz) ppm.



I9

Colorless oil, 229.1 mg, 84.2% yield.
^{1}H NMR (500 MHz, $CDCl_3$) δ 8.02 – 7.94 (m, 1H), 7.60 (tt, *J* = 7.7, 1.1 Hz, 1H), 7.53 (ddd, *J* = 7.8, 6.3, 1.4 Hz, 1H), 7.46 (td, *J* = 7.7, 1.4 Hz, 1H), and 4.74 (s, 2H) ppm.
^{19}F NMR (470 MHz, $CDCl_3$) δ –81.35 (d, *J* = 16.7 Hz) and –109.73 – –110.08 (m) ppm.
^{31}P NMR (202 MHz, $CDCl_3$) δ -13.91 (d, *J* = 17.2 Hz).

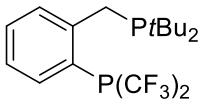


RF = CF_3 (**L16**)
= C_2F_5 (**L17**)

To a 20 mL vial were added **I8** or **I9** (342 μmol, 1.0 equiv), $PH(tBu)_2$ (820 μL, 410 μmol, 1.20 equiv), and degassed methanol (1 mL). The vial was sealed, removed from the glove box, and heated at 65 °C for 18 h. The mixture then was returned to the glove box and triethylamine (58 μL, 410 μmol, 1.2 equiv) was added. The mixture was stirred at ambient temperature for 2 h and then concentrated to dryness. Hexane (3 mL) was added, and the mixture was stirred vigorously for 1 h, and then was filtered through a syringe filter into a round-bottom flask equipped with a septum. THF (5 mL) was added, and the mixture was cooled to 0 °C. At this temperature, BH_3SMe_2 (162 μL, 1.71 mmol, 5 equiv) was added dropwise, and the mixture was allowed to warm to ambient temperature over 2.5 h. The mixture was quenched with saturated aqueous $NaHCO_3$ and extracted with diethyl ether (3×15 mL). The combined organic layers were dried over $MgSO_4$ and

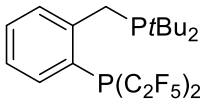
concentrated under vacuum and purified by flash column chromatography (25:1 :: pentane : diethyl ether, R_f ~ 0.3).

The material thus obtained placed in a 1 mL vial containing DABCO (72.2 mg, 644 μmol, 1.88 equiv), and toluene was added. The vial was sealed and heated at 100 °C for 1 h. The mixture then was passed through a plug of silica and eluted with 20:1 :: hexane : diethyl ether (3 column volumes) and concentrated to afford the product as a colorless oil that solidified upon standing for 2 d.



L16

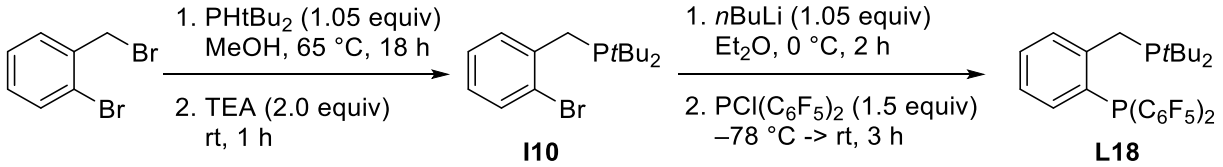
The reaction was conducted on a 300 μmol scale. Colorless solid, 29.1 mg, 24.0% yield.
^{1}H NMR (600 MHz, $CDCl_3$) δ 7.85 (dd, J = 8.0, 3.4 Hz, 1H), 7.67 (ddt, J = 7.7, 5.9, 1.7 Hz, 1H), 7.47 (t, J = 7.61 Hz, 1H), 7.28 (7.69 Hz, 1H), 3.24 (t, J = 2.2 Hz, 2H), and 1.13 (d, J = 10.8 Hz, 18H) ppm.
^{19}F NMR (565 MHz, $CDCl_3$) δ –52.19 (dd, J = 79.1, 6.8 Hz, 6F) ppm.
^{31}P NMR (243 MHz, $CDCl_3$) δ 43.11 (d(hept), J = 49.9, 7.2 Hz), -12.40 ((hept)d, J = 78.6, 56.0 Hz).
HRMS (ESI+): calc'd for $C_{17}H_{25}F_6P_2^+$ $[M+H]^+$: 405.1330; found: 405.1330.



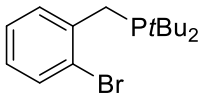
L17

Colorless solid, 69.9 mg, 40.6% yield.
^{1}H NMR (600 MHz, $CDCl_3$): δ 7.90 – 7.84 (m, 1H), 7.68 – 7.63 (m, 1H), 7.46 (td, J = 7.5, 1.2 Hz, 1H), 7.29 – 7.25 (m, 1H), 3.19 (t, J = 2.4 Hz, 2H), and 1.12 (d, J = 10.8 Hz, 18H) ppm.
^{19}F NMR (565 MHz, $CDCl_3$): δ –81.7 (dd, J = 17.0, 5.8 Hz, 6F) and –108.73 – –111.00 (m, 4F) ppm.
^{31}P{^{1}H} NMR (242 MHz, $CDCl_3$): δ 41.7 (d, J = 58.1 Hz, 1P) and –14.13 – –15.63 (m, 1P) ppm.
HRMS (ESI+): calc'd for $C_{19}H_{25}F_{10}OP_2^+$ $[M+OH]^+$: 521.122096; found: 521.1218.

*Preparation of **L18***



I10 **L18**

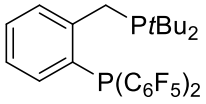


I10

The following procedure was adapted from the literature.[57] To a 1-dram vial containing 2-bromobenzyl bromide (250 mg, 1.00 mmol, 1.00 equiv) was added degassed methanol (2 mL) and

di-*tert*-butylphosphine (194.3 μL, 1.05 mmol, 1.05 equiv). The vial was sealed and heated at 65 °C for 18 h. The mixture then was cooled to room temperature, and triethylamine (278 μL, 2.00 mmol, 2.00 equiv), and the mixture was stirred for 1 h. The solvent then was removed under reduce pressure, and pentane (10 mL) was added. The mixture was filtered through a syringe filter and concentrated to a colorless oil (281.3 mg, 89% yield).

Spectroscopic characterization matched that reported in the literature.[57]
^{1}H NMR (400 MHz, $CDCl_3$) δ 7.67 (dt, *J* = 7.8, 2.2 Hz, 1H), 7.50 (dd, *J* = 7.9, 1.4 Hz, 1H), 7.22 (td, *J* = 7.6, 1.4 Hz, 1H), 6.99 (td, *J* = 7.7, 1.7 Hz, 1H), 3.01 (d, *J* = 3.4 Hz, 2H), and 1.16 (d, *J* = 11.0 Hz, 18H) ppm.
^{31}P{^{1}H} NMR (162 MHz, $CDCl_3$): δ 34.6 ppm.



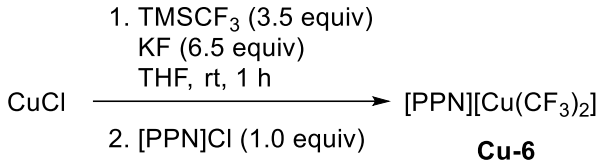
L18

To a round-bottom flask were added **I10** (100.0 mg, 317.2 μmol, 1.00) and diethyl ether (2 mL). The flask was sealed with a rubber septum, removed from the glove box, and cooled to 0 °C in an ice bath. To the stirring solution then was added *n*BuLi (2.5 M in hexane, 133 μL, 333 mmol, 1.05 equiv) dropwise. The mixture was allowed to stir at 0 °C for 2 h, and then the ice bath was removed and replaced with a dry ice/acetone cold bath. At –78 °C then was added $PCl(C_6F_5)_2$[80], and the mixture was allowed to warm to ambient temperature overnight. The mixture was again cooled to 0 °C and BH_3SMe_2 (2.0 M in THF, 1.3 mL, 2.5 mmol, 8.0 equiv) was added dropwise. The stirring mixture was allowed to warm to ambient temperature over 3 h, after which saturated aqueous $NaHCO_3$ (50 mL) was added (caution: gas evolution). The mixture was transferred to a separatory funnel and extracted with diethyl ether (2×20 mL). The combined organic extracts were dried over Na_2SO_4 and concentrated. The residue was purified by flash column chromatography (silica gel, 100% hexanes -> 10:1 :: hexanes : diethyl ether, R_f ~ 0.5) to afford the borane adduct of **L18** as a light-yellow solid.

In the glove box, this solid then was transferred using toluene (1 mL) to a 4 mL vial containing DABCO (81.0 mg, 722 mg, 2.28 equiv). The vial was sealed and heated at 100 °C for 24 h. The reaction mixture was filtered through a plug of silica gel (eluted with 19:1 :: pentane : diethyl ether) and concentrated to a colorless oil, from which colorless plates formed after standing at ambient temperature for 1 wk. The crystals were washed with 400 μL cold pentane (this was a mistake) and dried under vacuum to afford the product as a yellow solid (21.1 mg, 11% yield).

^{1}H NMR (600 MHz, $CDCl_3$): δ 7.67 (t, *J* = 7.2 Hz, 1H), 7.34 (dd, *J* = 7.6, 1.4 Hz, 1H), 7.29 (t, *J* = 6.1 Hz, 1H), 7.16 – 7.10 (m, 1H), 3.11 (t, *J* = 2.9 Hz, 2H), 1.12 and (d, *J* = 10.9 Hz, 18H) ppm.
^{19}F NMR (565 MHz, $CDCl_3$): δ –129.05 – –129.34 (m, 4F), –150.08 (t, *J* = 20.7 Hz, 2F), and –160.38 (td, *J* = 22.7, 8.2 Hz, 2F) ppm.
^{31}P NMR (243 MHz, $CDCl_3$) δ 36.55 (d, *J* = 41.1 Hz, 1P) and –54.33 – –55.51 (m, 1P) ppm.
HRMS (ESI+): anal. calc'd for $C_{27}H_{25}F_{10}P_2^+$ $[M+H]^+$: 601.1266; found: 601.1265.

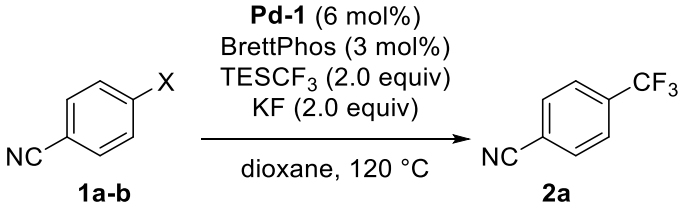
*Preparation of [PPN][Cu(CF$_3$)$_2$] (**Cu-6**)*



This procedure was adapted from the reported synthesis of [PPh$_4$][Cu(CF$_3$)$_2$] by Shen.[75] To a 20-mL vial were added CuCl (100 mg, 1.00 mmol), KF (380 mg, 6.50 mmol, 6.50 equiv), TMSCF$_3$ (0.52 mL, 3.5 mmol, 3.5 equiv), and THF (7.5 mL), and the mixture was stirred vigorously for 2 h at ambient temperature. [PPN]Cl (580 mg, 1.00 mmol, 1.00 equiv) then was added as a solid and stirred for 30 min at ambient temperature, resulting in a fine suspension. The mixture was filtered through a syringe filter and concentrated under vacuum to a thin film. The residue was recrystallized 4 times from diethyl ether by dissolving the residue in a minimal amount of solvent and cooling to –35 °C for 15 min, affording the product as large colorless needles. NMR spectroscopy revealed the presence of ~5% Cu(CF$_3$)Cl$^-$.

^{1}H NMR (500 MHz, THF-d_8) δ 7.68 (td, J = 7.4, 1.5 Hz, 6H), 7.61 (dd, J = 13.3, 7.8 Hz, 12H), and 7.51 (td, J = 7.7, 3.1 Hz, 12H) ppm.
^{19}F NMR: δ –32.0 ppm.
^{31}P NMR: δ 21.1 ppm.
Anal. Calc'd for $C_{38}H_{30}CuF_6NP_2$: C, 61.67; H, 4.09; N, 1.89. Found: C, 61.72; H, 3.99; N, 1.95.

*General procedure for the catalytic trifluoromethylation of aryl halides **1a-b***



The following was adapted from literature procedure.[30] To a 1 dram vial were added arylpalladium halide complex **Pd-1a-b** (30 μmol, 6.0 mol%), BrettPhos (8.0 mg, 15 μmol, 3.0 mol%), 4-halobenzonitrile (**1a-b**, 0.500 mmol, 1.00 equiv), KF (58.1 mg, 1.00 mmol, 2.00 equiv), TESCF$_3$ (190 μL, 1.0 mmol, 2.0 equiv), 4-(trifluoromethoxy)anisole as an internal standard (~0.25 equiv, determined exactly), and dioxane (2.00 mL). The vial was sealed with a Teflon-lined cap, and the mixture was stirred vigorously at 120 °C for 2.5 h before being allowed to cool to ambient temperature. An aliquot of the reaction mixture was taken in the glove box at this point to monitor the reaction. The vial was resealed and returned to heating for another 16 h, after which the vial was opened to air and transferred to an NMR tube for analysis by unlocked ^{19}F NMR spectroscopy. We note that this setup is frustratingly sensitive to stirring; identical reactions prepared from identical batches of reagents regularly gave different results depending on minute differences in position on the stir plate and the angle of the reaction vessel. In some cases, no activation of the TESCF$_3$ was observed even overnight, while in others using identical setups all silane was consumed within 3 h.

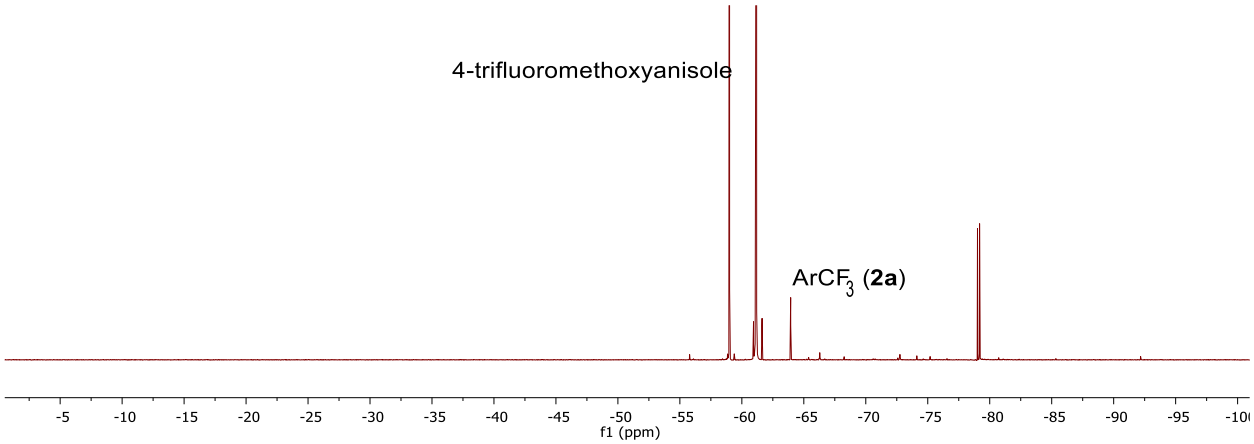


Figure 4.7.1 ^{19}F NMR spectrum of the catalytic trifluoromethylation of **1a** catalyzed by **Pd-1a**.

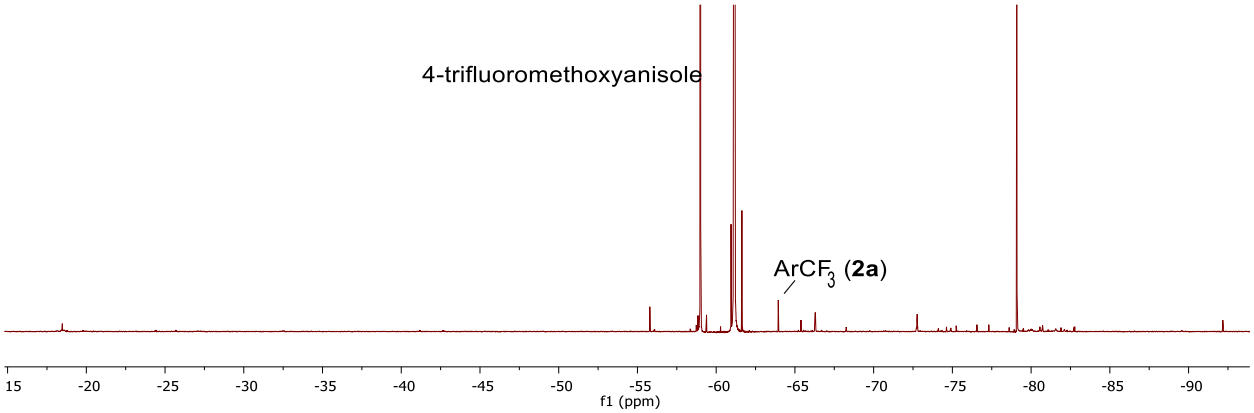


Figure 4.7.2 ^{19}F NMR spectrum of the catalytic trifluoromethylation of **1b** catalyzed by **Pd-1b**.

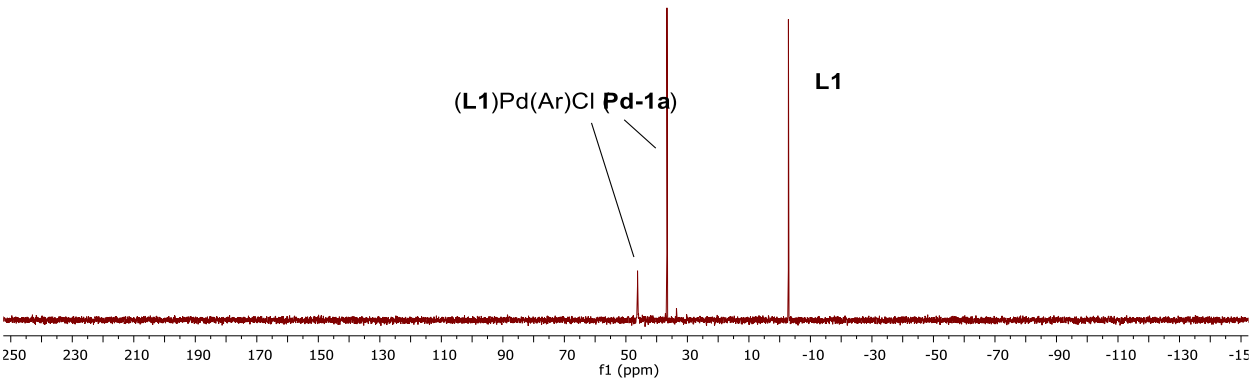


Figure 4.7.3 ^{31}P{^{1}H} NMR spectrum of the catalytic trifluoromethylation of **1a** catalyzed by **Pd-1a**.

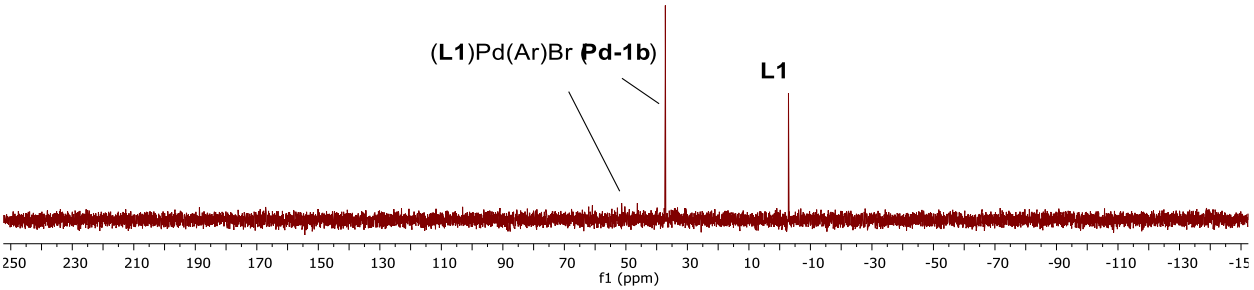


Figure 4.7.4 $^{31}P\{^{1}H\}$ NMR spectrum of the catalytic trifluoromethylation of **1b** catalyzed by **Pd-1b**.

4.7.3 Stoichiometric Reactions

*Reaction of $(py^F)_2Pd(Ph)(CF_3)$ (**Pd-8**) with BrettPhos (**L1**) and RuPhos (**L2**)*

To a 1-dram vial was added complex **Pd-8** (2.1 mg, 4.7 μmol, 1.0 equiv), **L1** (5.1 mg, 9.9 μmol, 2.1 equiv) or **L2** (4.6 mg, 9.9 μmol, 2.1 equiv), 4-(trifluoromethoxy)anisole (variable, but determined exactly) and THF (700 μL). The mixture was mixed by pipette until homogeneous, and transferred to an NMR tube, and heated at 80 °C for 15 min. The mixture was cooled to ambient temperature and ^{19}F NMR spectra were acquired, and then returned to heating for a total reaction time of 2 h. The reaction containing **L2** was returned to heating at 100 °C instead of 80 °C due to a lack of conversion at this temperature. The mixtures were then analyzed by ^{19}F NMR spectroscopy to determine yields.

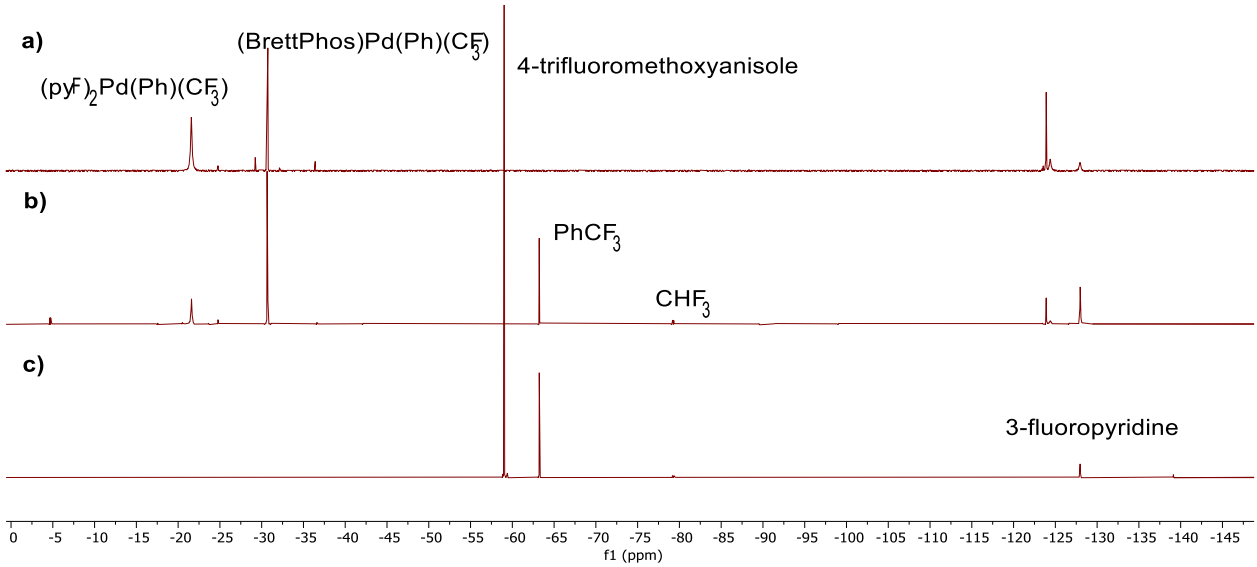


Figure 4.7.5 Reaction of $(py^F)_2Pd(Ph)(CF_3)$ (**Pd-8**) with BrettPhos (**L1**) a) after 15 min at rt; b) after 15 min at 80 °C; and c) after another 1.75 h at 80 °C.

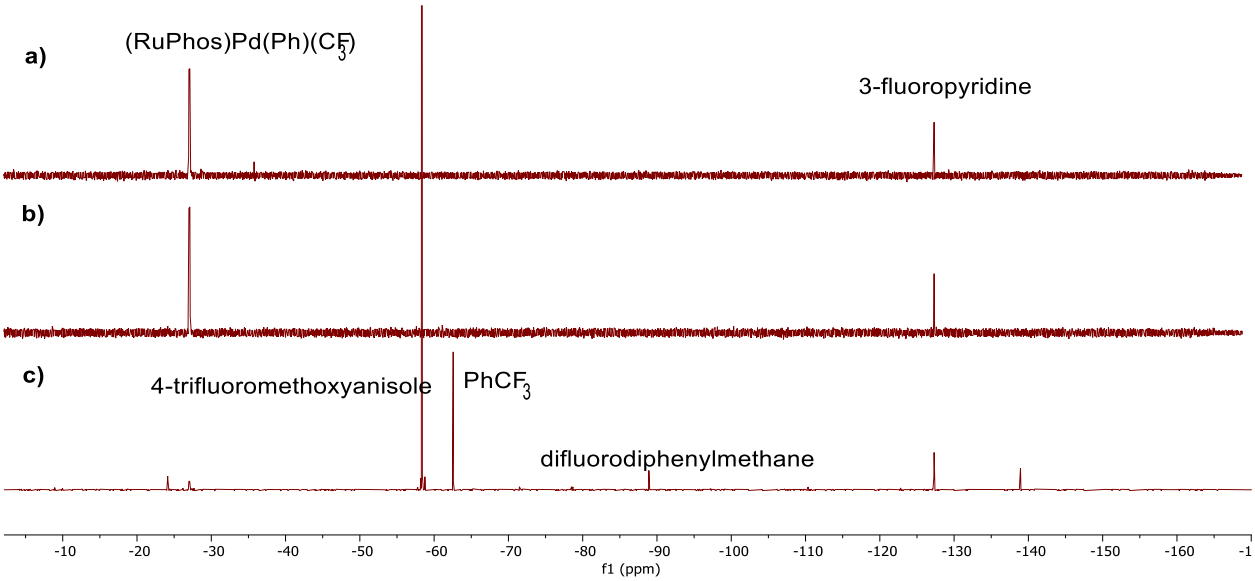


Figure 4.7.6 ^{19}F NMR spectrum of the reaction of $(py^F)_2Pd(Ph)(CF_3)$ (**Pd-8**) with RuPhos (**L2**) a) after 15 min at rt; b) after 15 min at 80 °C; and c) after another 1.75 h at 100 °C.

*Reaction of arylpalladium halide complexes **Pd-1a** and **Pd-1b** with $TMSCF_3$*

To a 1-dram vial were added (BrettPhos)Pd(Ar)X (**Pd-1**, Ar = 4-CN-C_6H_4) (12 μmol, 1.0 equiv), $TMSCF_3$ (4.7 μL, 32 μmol, 2.6 equiv), CsF (3.7 mg, 25 μmol, 2.0 equiv), and 4-(trifluoromethoxy)anisole as an internal standard (exact amount varied but was determined exactly). The vial was sealed with a Teflon-lined cap and stirred vigorously for 3 h at ambient temperature. The mixture then was transferred to an NMR tube and was analyzed by ^{19}F NMR spectroscopy.

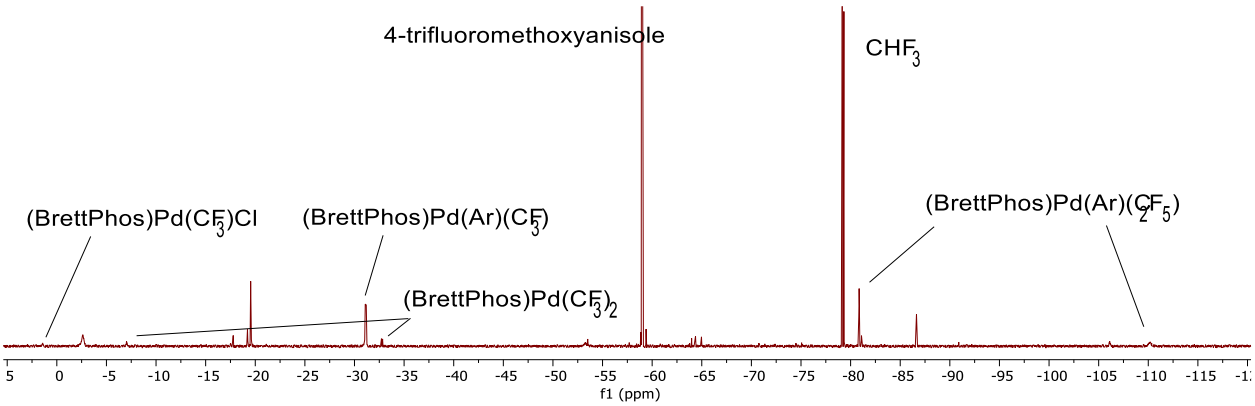


Figure 4.7.7 ^{19}F NMR spectrum of the reaction of **Pd-1a** with $TMSCF_3$ and KF. Identified species are marked.

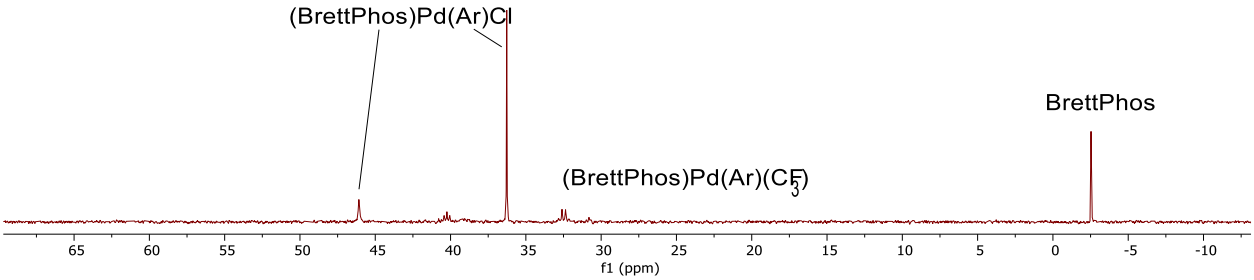


Figure 4.7.8 $^{31}P\{^{1}H\}$ NMR spectrum of the reaction of **Pd-1a** with $TMSCF_3$ and KF. Identified species are marked.

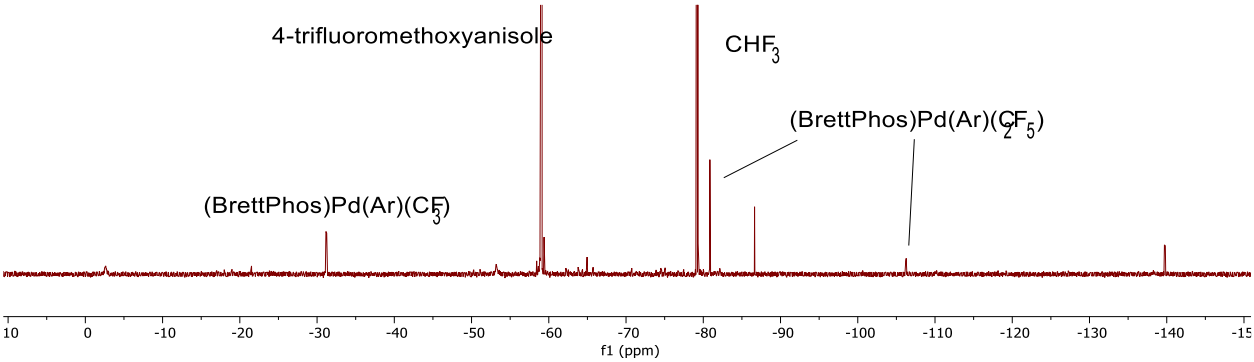


Figure 4.7.9 ^{19}F NMR spectrum of the reaction of **Pd-1b** with $TMSCF_3$ and KF. Identified species are marked.

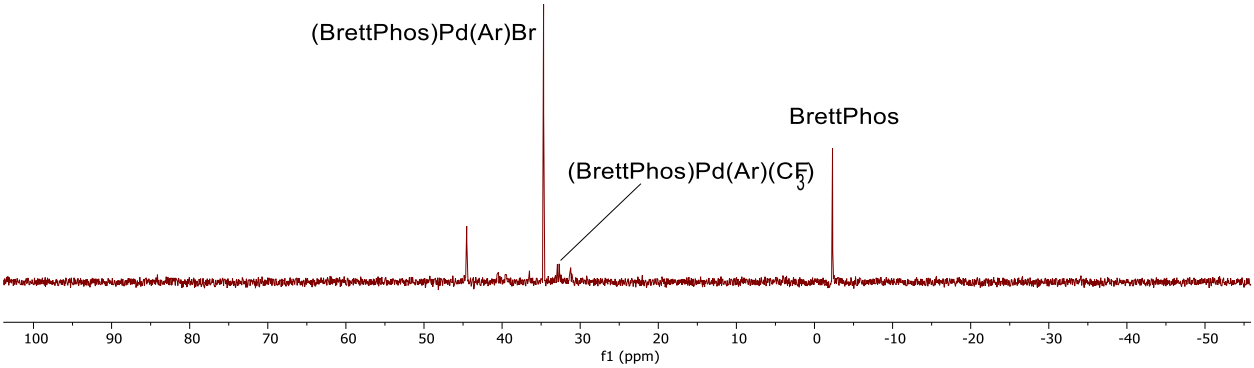
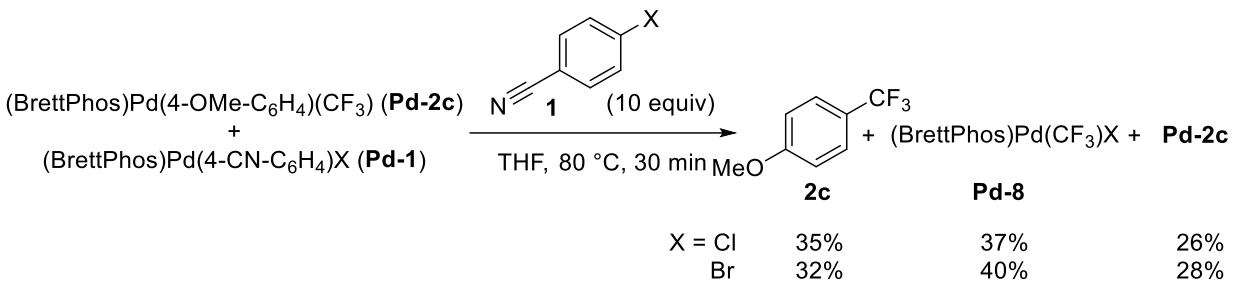


Figure 4.7.10 $^{31}P\{^{1}H\}$ NMR spectrum of the reaction of **Pd-1b** with $TMSCF_3$ and KF. Identified species are marked.

*Reaction of (BrettPhos)Pd(4-OMe-C_6H_4)(CF_3) (**Pd-2c**) with Arylpalladium Halides **1a** and **1b***



To a 1-dram vial was added **Pd-2c**, triphenylphosphine oxide (6.4 mg, 23 μmol) and 4-(trifluoromethoxy)anisole (3.6 mg, 19 μmol) as internal standards, and THF (1400 μL). Into separate vials were then added **Pd-1a** (3.8 mg, 4.9 μmol, 1.0 equiv) and 4-chlorobenzonitrile (**1a**, 6.7 mg, 49 μmol, 10 equiv) or **Pd-1b** (4.0 mg, 4.9 μmol, 1.0 equiv) and 4-bromobenzonitrile (**1b**, 8.9 mg, 49 μmol, 10 equiv). To each of the vials containing arylpalladium halide complexes was added 600 μL of the solution containing **Pd-2c**. The reaction solutions were mixed by pipette, transferred to NMR tubes, and analyzed by ^{19}F NMR spectroscopy. The reactions were then heated at 80 °C for 30 min, and then allowed to cool to ambient temperature and analyzed by ^{19}F and ^{31}P{^{1}H} NMR spectroscopy.

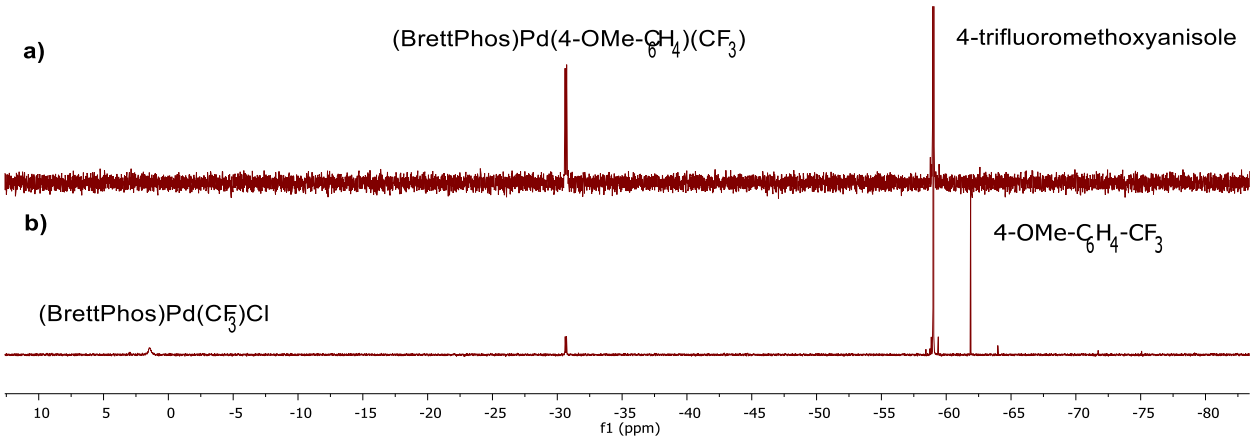


Figure 4.7.11 ^{19}F NMR spectra of the reaction of (BrettPhos)Pd(4-OMe-C_6H_4)(CF_3) (**Pd-2c**) and (BrettPhos)Pd(4-CN-C_6H_4)Cl (**Pd-2a**) a) after 15 min at ambient temperature and b) after 30 min at 80 °C.

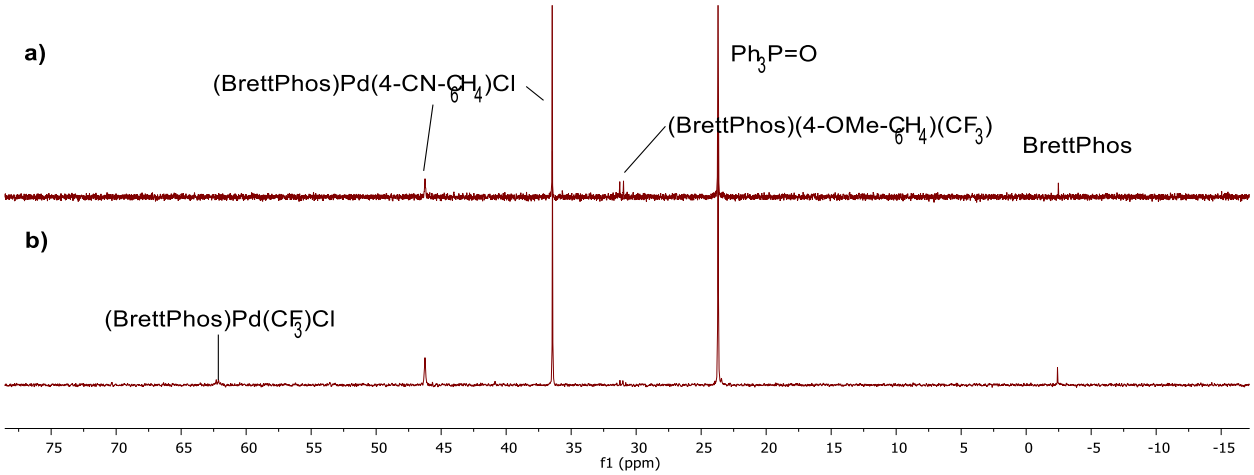


Figure 4.7.12 $^{31}P\{^{1}H\}$ NMR spectra of the reaction of (BrettPhos)Pd(4-OMe-C_6H_4)(CF_3) (**Pd-2c**) and (BrettPhos)Pd(4-CN-C_6H_4)Cl (**Pd-2a**) a) after 15 min at ambient temperature and b) after 30 min at 80 °C.

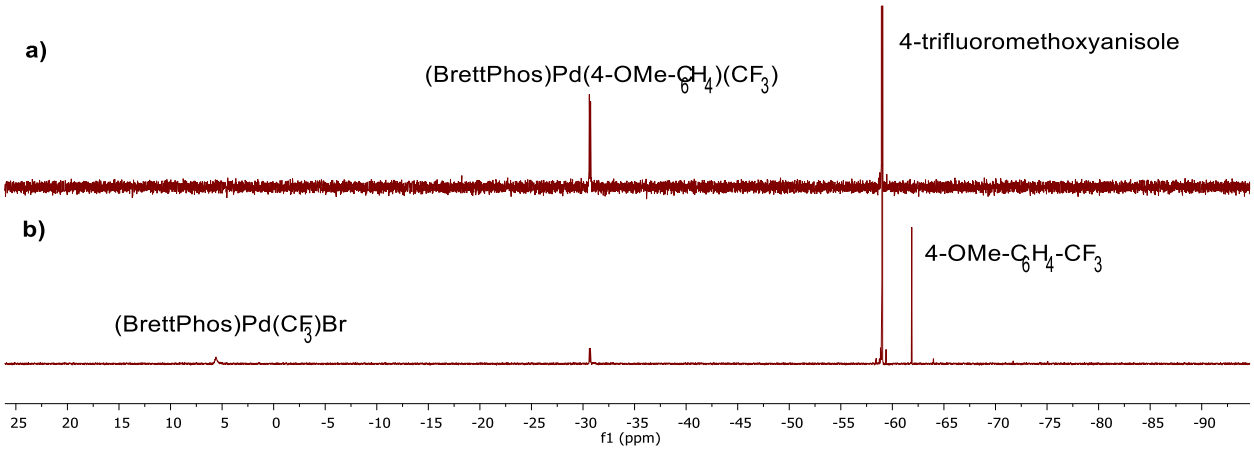


Figure 4.7.13 ^{19}F NMR spectra of the reaction of (BrettPhos)Pd(4-OMe-C_6H_4)(CF_3) (**Pd-2c**) and (BrettPhos)Pd(4-CN-C_6H_4)Br (**Pd-1b**) a) after 15 min at ambient temperature and b) after 30 min at 80 °C.

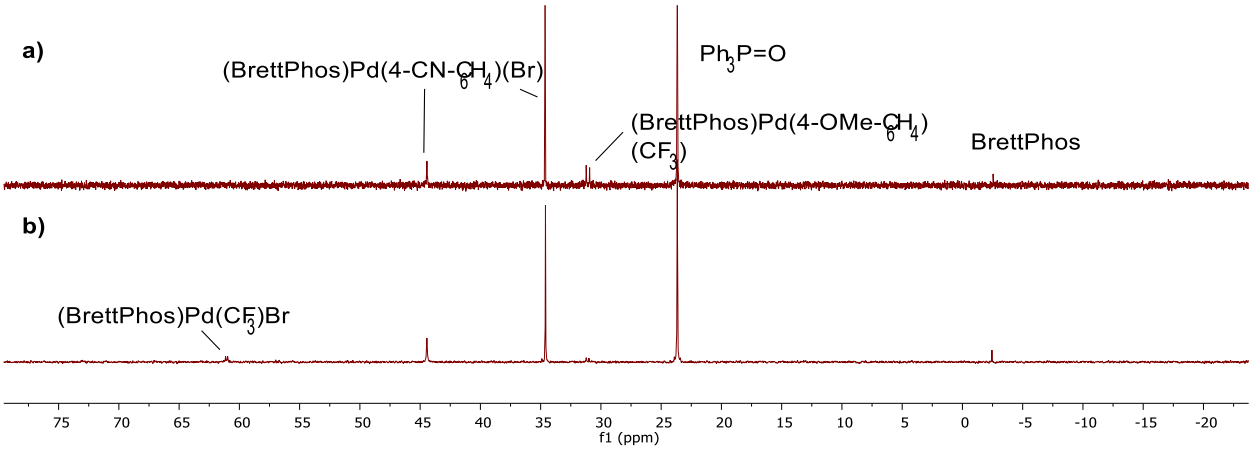


Figure 4.7.14 $^{31}P\{^{1}H\}$ NMR spectra of the reaction of (BrettPhos)Pd(4-OMe-C_6H_4)(CF_3) (**Pd-2c**) and (BrettPhos)Pd(4-CN-C_6H_4)Br (**Pd-1b**) a) after 15 min at ambient temperature and b) after 30 min at 80 °C.

*General procedure for the reaction of arylpalladium bromide dimer **Pd-9a** with a variety of Josiphos ligands **L5-L12***

To a 1-dram vial containing dimer **Pd-9a** (3.0 mg, 2.5 μmol, 0.50 equiv), CsF (3.8 mg, 25 μmol, 5.0 equiv), and ligand (5.0 μmol, 1.0 equiv) was added 500 μL of a stock solution of 4-(trifluoromethoxy)anisole in dioxane. The mixture was stirred magnetically at ambient temperature for 30 min, and then sealed with a Teflon-lined cap and heated at 100 °C for 18 h with vigorous stirring. The mixture was allowed to cool to ambient temperature and transferred to an NMR tube. The mixture then was analyzed by unlocked ^{19}F NMR spectroscopy. See main text for yields.

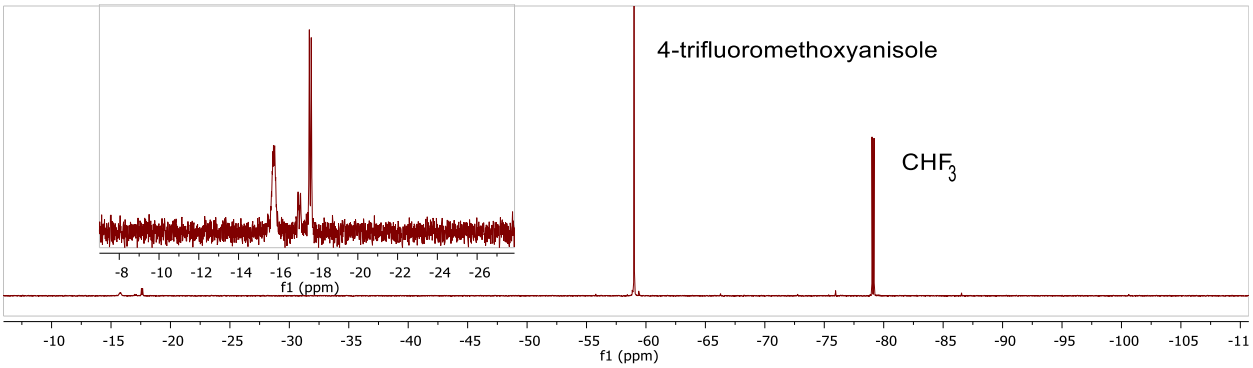


Figure 4.7.15 ^{19}F NMR spectrum from the reaction of dimer **Pd-9a**, **L5**, $TESCF_3$, and CsF.

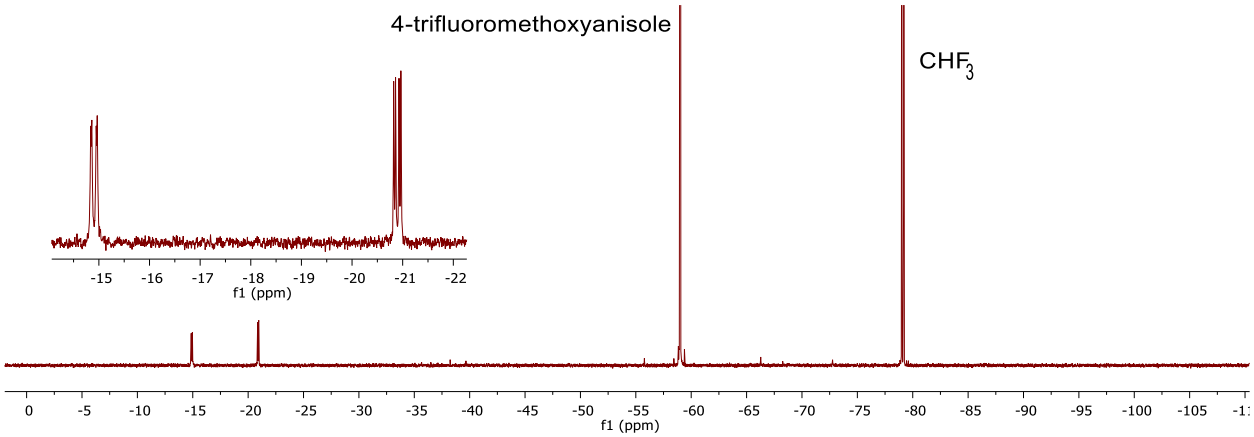


Figure 4.7.16 ^{19}F NMR spectrum for the reaction of dimer **Pd-9a**, **L6**, $TESCF_3$, and CsF.

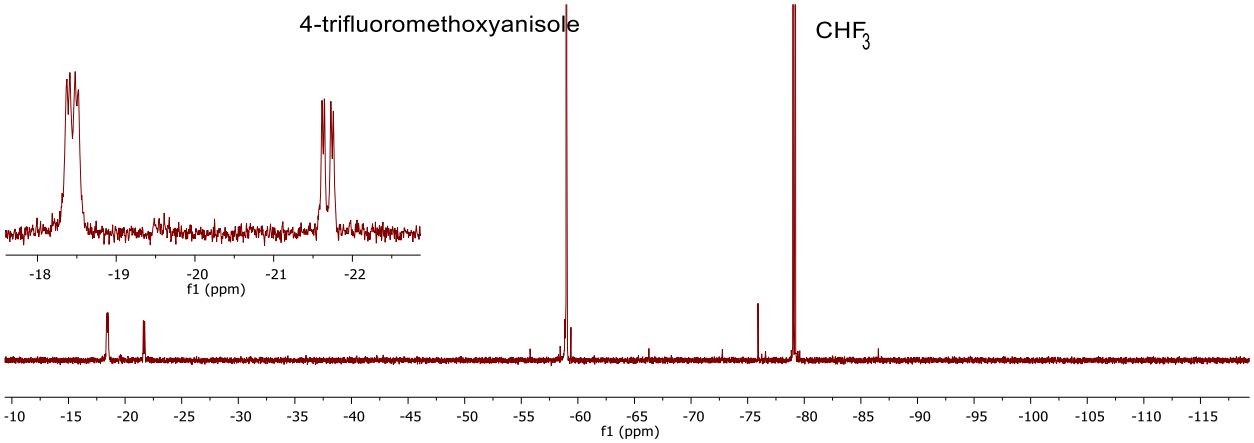


Figure 4.7.17 ^{19}F NMR spectrum for the reaction of dimer **Pd-9a**, **L7**, $TESCF_3$, and CsF.

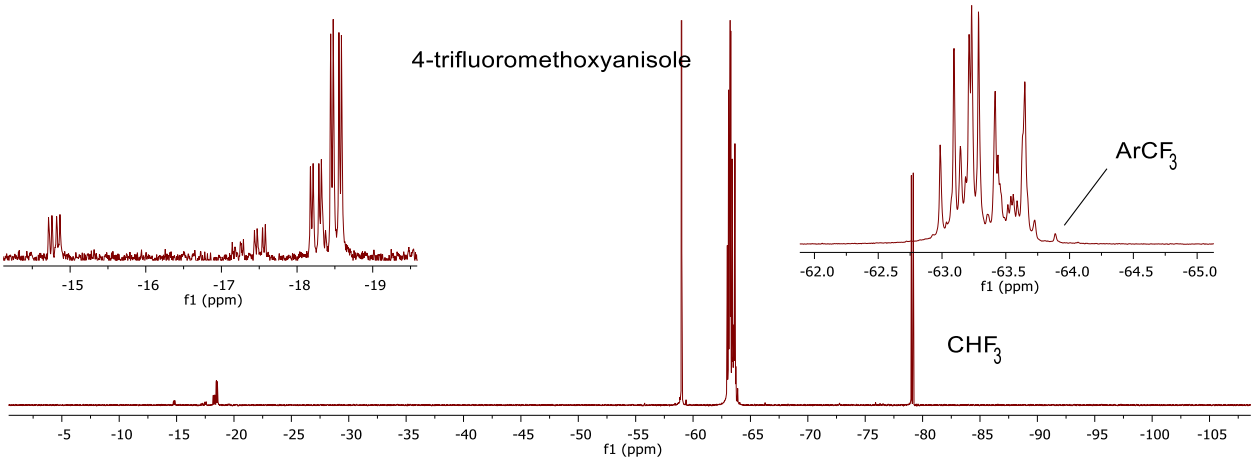


Figure 4.7.18 ^{19}F NMR spectrum for the reaction of dimer **Pd-9a**, **L8**, $TESCF_3$, and CsF.

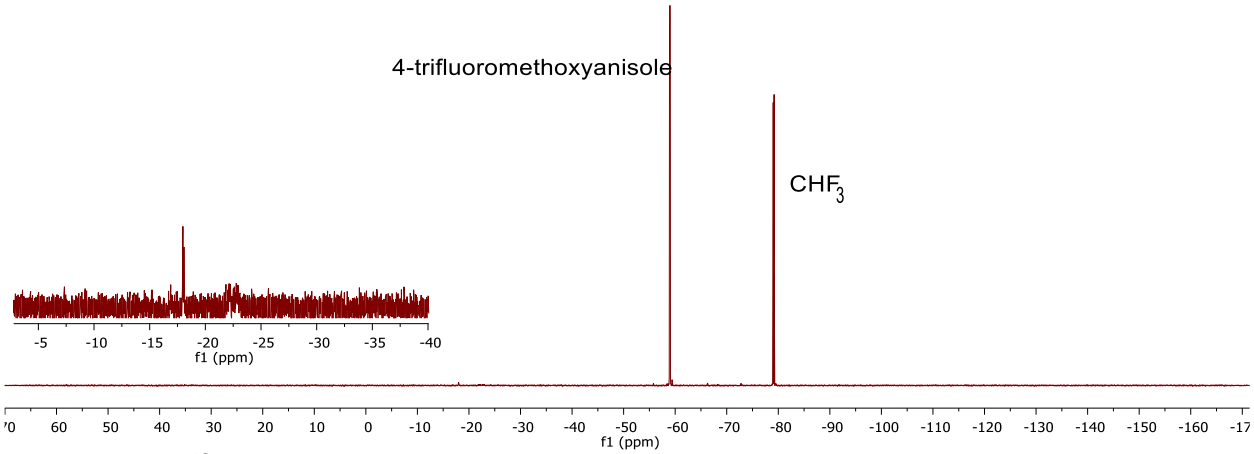


Figure 4.7.19 ^{19}F NMR spectrum for the reaction of dimer **Pd-9a**, **L9**, $TESCF_3$, and CsF.

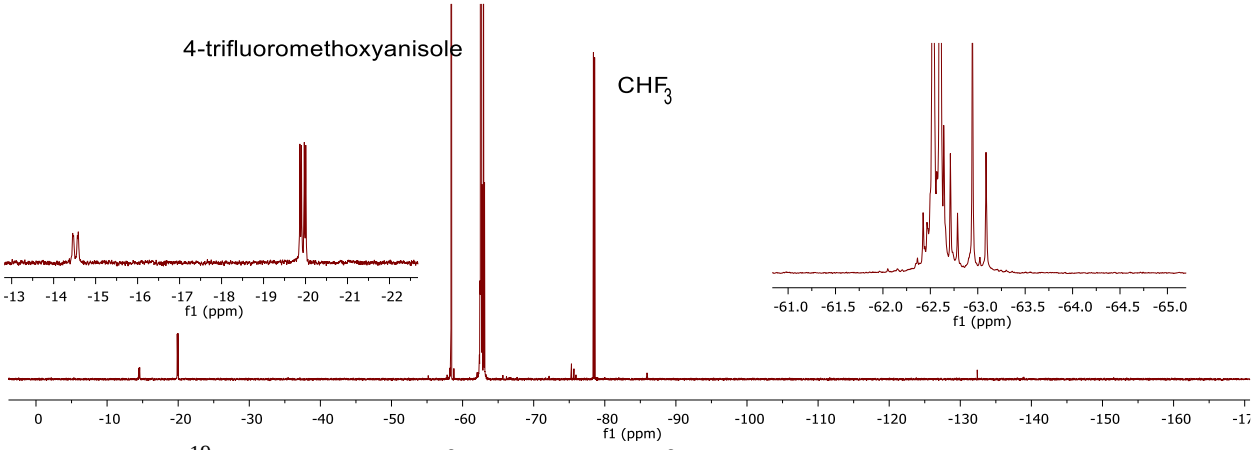


Figure 4.7.20 ^{19}F NMR spectrum for the reaction of dimer **Pd-6a**, **L10**, $TESCF_3$, and CsF.

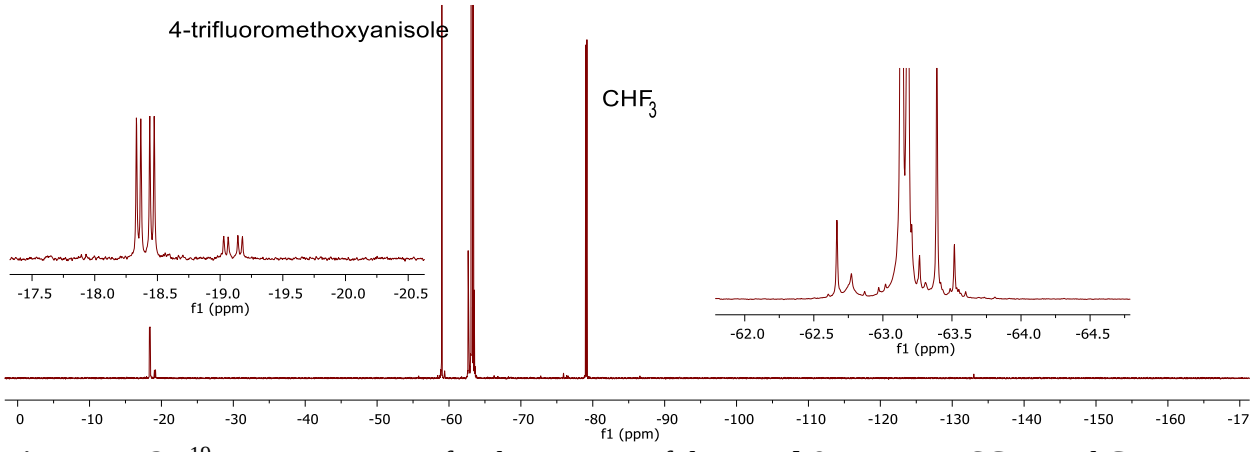


Figure 4.7.21 ^{19}F NMR spectrum for the reaction of dimer **Pd-9a**, **L11**, $TESCF_3$, and CsF.

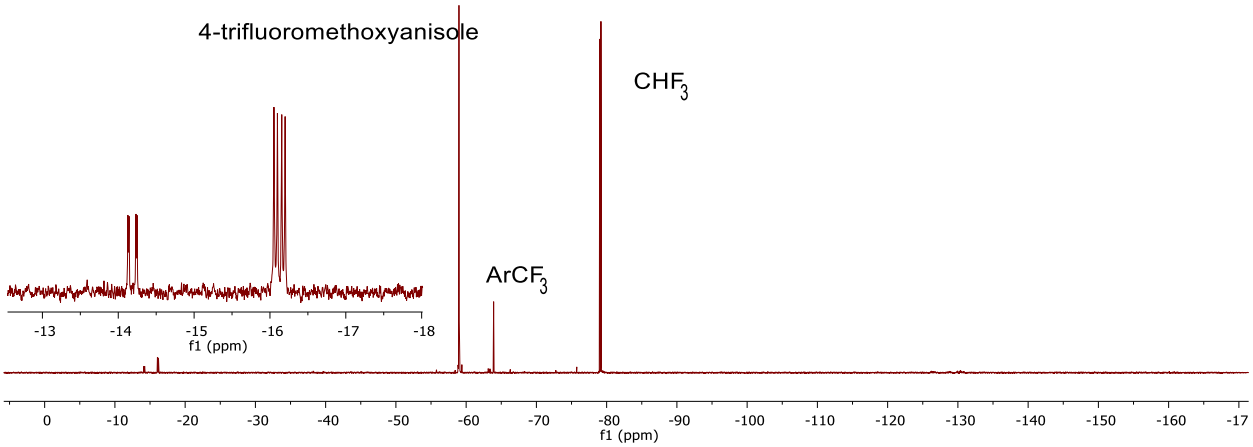


Figure 4.7.22 ^{19}F NMR spectrum for the reaction of dimer **Pd-9a**, **L11**, $TESCF_3$, and CsF.

*Reaction of aryl(trifluoromethyl)palladium complex **Pd-8** with dfmpf (**L13**)*

To a 1-dram vial were added **Pd-8** (2.2 mg, 5.0 μmol, 1.0 equiv), **L13** (7.6 mg, 15 μmol, 2.9 equiv), 4-(trifluoromethoxy)anisole (1.9 mg, 10 μmol, 2.0 equiv), and THF (600 μL). The mixture was mixed by pipette, transferred to an NMR tube, and heated for 18 h. The progress of the reaction was monitored by ^{19}F NMR spectroscopy. Yields were determined after 18 h relative to 3-fluoropyridine (2 mol per mol **Pd-8**).

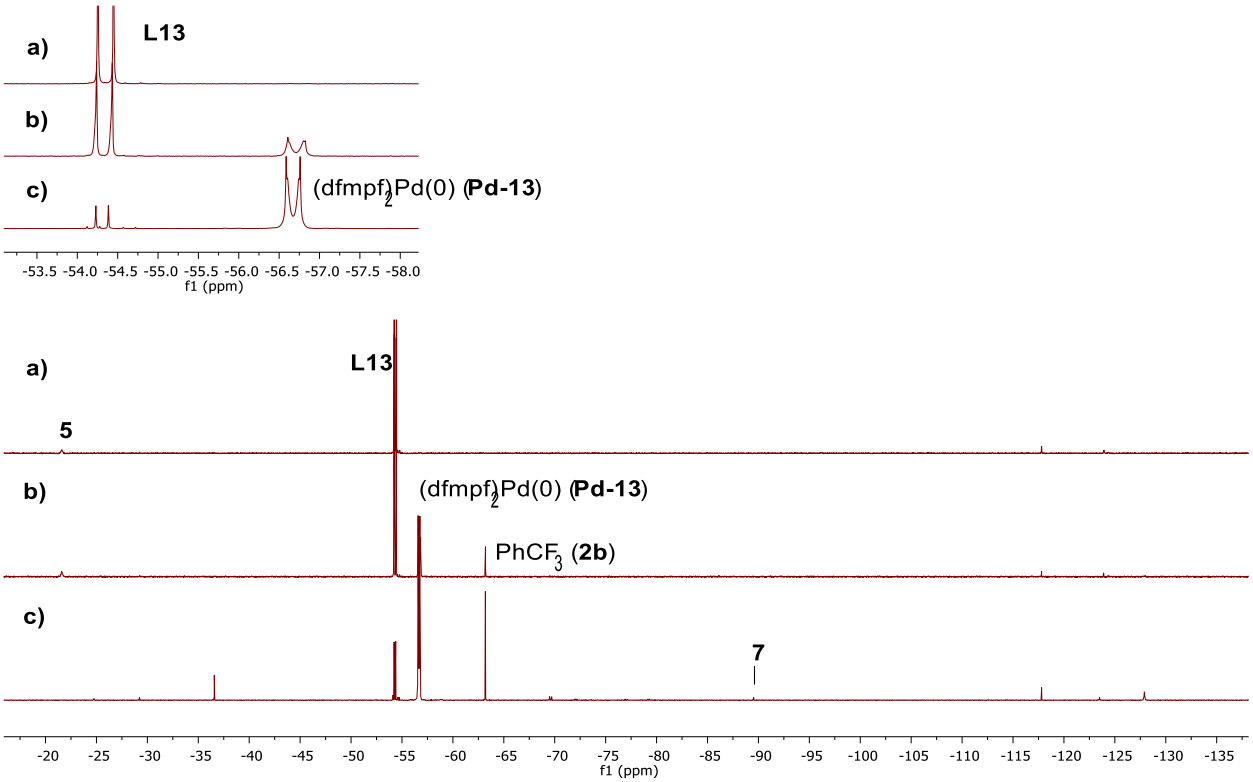


Figure 4.7.23 Reaction of complex **Pd-8** with **L14** at 80 °C after a) 0 min; b) 30 min; c) 18 h.

*Confirmation of spectral assignment of complex **Pd-13** and its lack of reactivity aryl halide*

To two separate 1-dram vials were added $Pd(P(o\text{-tol})_3)_2$ (3.5 mg, 4.9 μmol, 1.0 equiv), **L15**

(7.9 mg, 15 μmol, 3.1 equiv), 4-(trifluoromethoxy)anisole (~1.3 mg, measured exactly) 6.8 μmol, 1.4 equiv), and THF (500 μL). The vials were sealed with a Teflon-lined cap and heated at 80 °C for 1 h. The contents of one of the reaction vials then was analyzed by NMR spectroscopy. To the other was added 4-bromobenzonitrile (**1b**, 20 mg), and the mixture was heated at 100 °C for 1 h. Analysis by ^{19}F and $^{31}P\{^{1}H\}$ NMR spectroscopy followed. The matching broad feature at –57.7 in this reaction and in the reaction with **Pd-8** (*vide supra*) suggest the assignment $(dfmpf)_2Pd(0)$ (**Pd-13**).

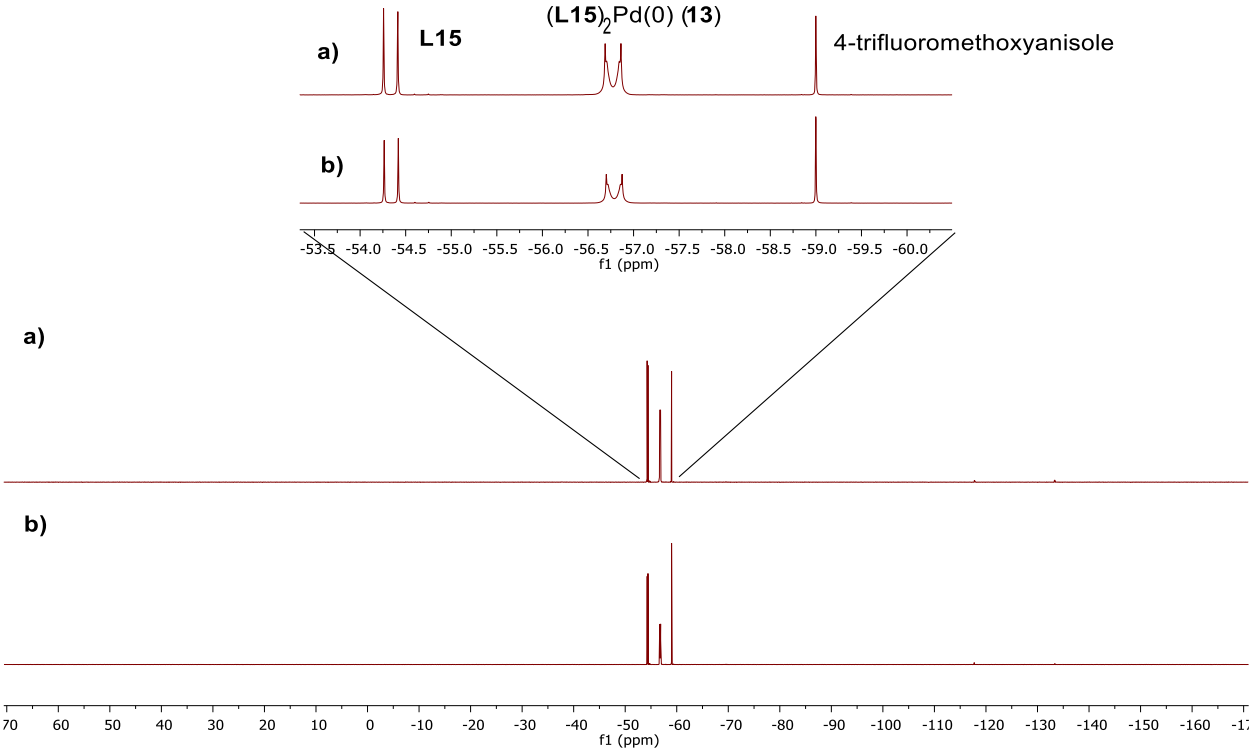


Figure 4.7.24 ^{19}F NMR spectra of the reaction of $Pd(P(o\text{-tol})_3)_2$ and **L15** a) after 1 h at 80 °C; b) a separate reaction after adding **1b** and heating at 100 °C for 1 h.

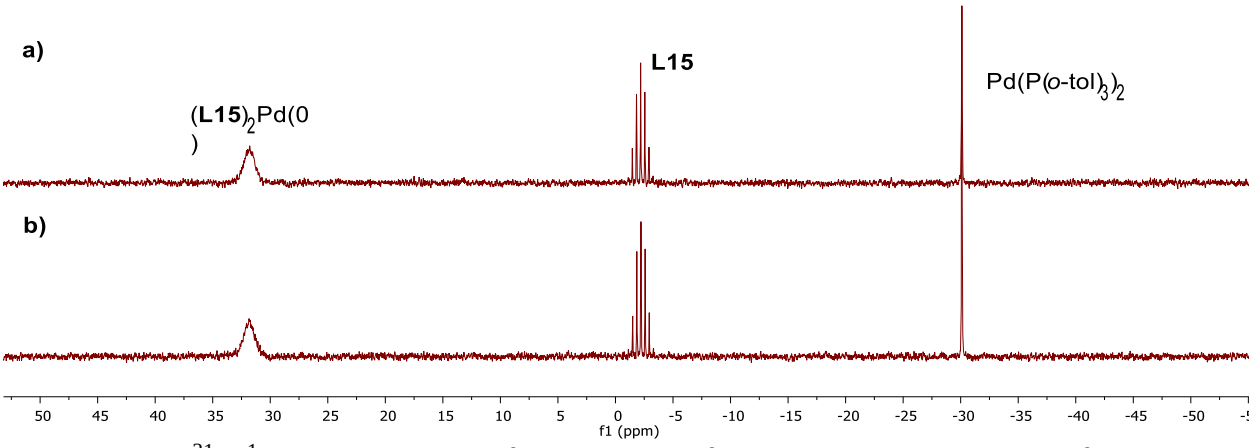


Figure 4.7.25 $^{31}P\{^{1}H\}$ NMR spectra of the reaction of $Pd(P(o\text{-tol})_3)_2$ and **L15** a) after 1 h at 80 °C; b) after adding **1b** and heating at 100 °C for 1 h.

*Reaction of **Pd-9b** with **L14** and K[B(CF$_3$)(OMe)$_3$]*

To a 1-dram vial was added dimer **Pd-9b** (2.7 mg, 2.3 μmol, 0.50 equiv), K[B(CF$_3$)(OMe)$_3$] (2.0 mg, 9.3 μmol, 2.0 equiv), 4-(trifluoromethoxy)anisole as an internal standard (5.4 mg, 28 μmol, 6.1 equiv), and dioxane 700 μL. The mixture was mixed by pipette, transferred to an NMR tube, and heated at 80 °C for 15 min, after which the mixture was allowed to cool to ambient temperature and a ^{19}F NMR spectrum was acquired. The tube then was returned to heating at 80 °C for an additional 3 h, and then analyzed again by ^{19}F NMR spectroscopy.

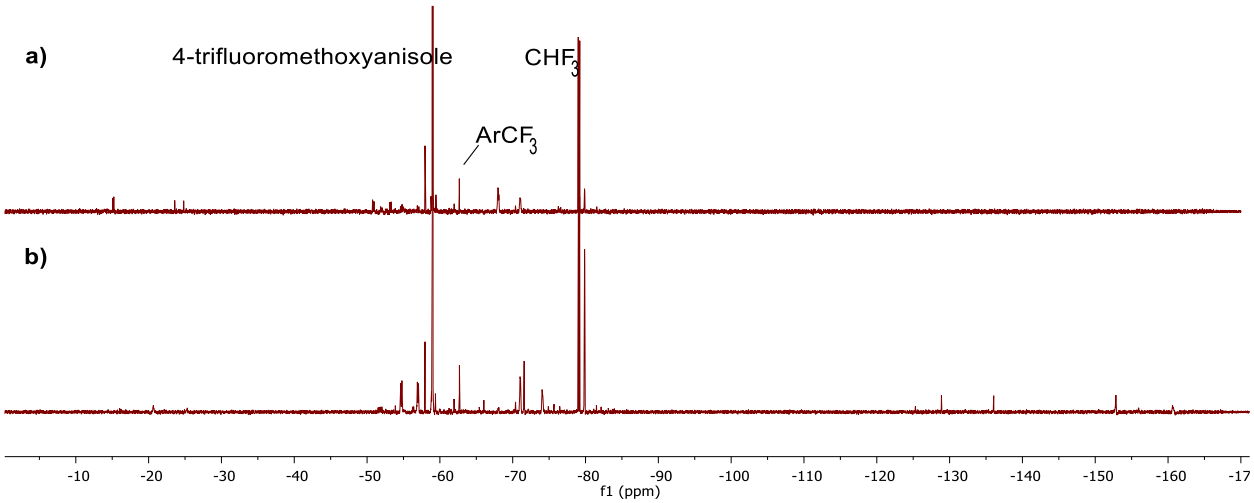


Figure 4.7.26 Reaction of dimer **Pd-9b**, ligand **L14**, and K[B(CF$_3$)(OMe)$_3$] after a) 15 min or b) 3 h at 80 °C.

*Reaction of aryl(trifluoromethyl)palladium complex **Pd-8** with **L16***

To a 1-dram vial were added complex **Pd-8** (1.9 mg, 4.3 μmol, 1.0 equiv), **L16** (2.4 mg, 1.4 equiv, 5.9 μmol), 4,4'-difluorobiphenyl as an internal standard (2.1 mg, 11 μmol, 2.6 equiv), and THF (700 μL). The mixture was mixed by pipette until homogeneous and then transferred to an NMR tube. The mixture was heated for 18 h at 80 °C and monitored by ^{19}F NMR spectroscopy.

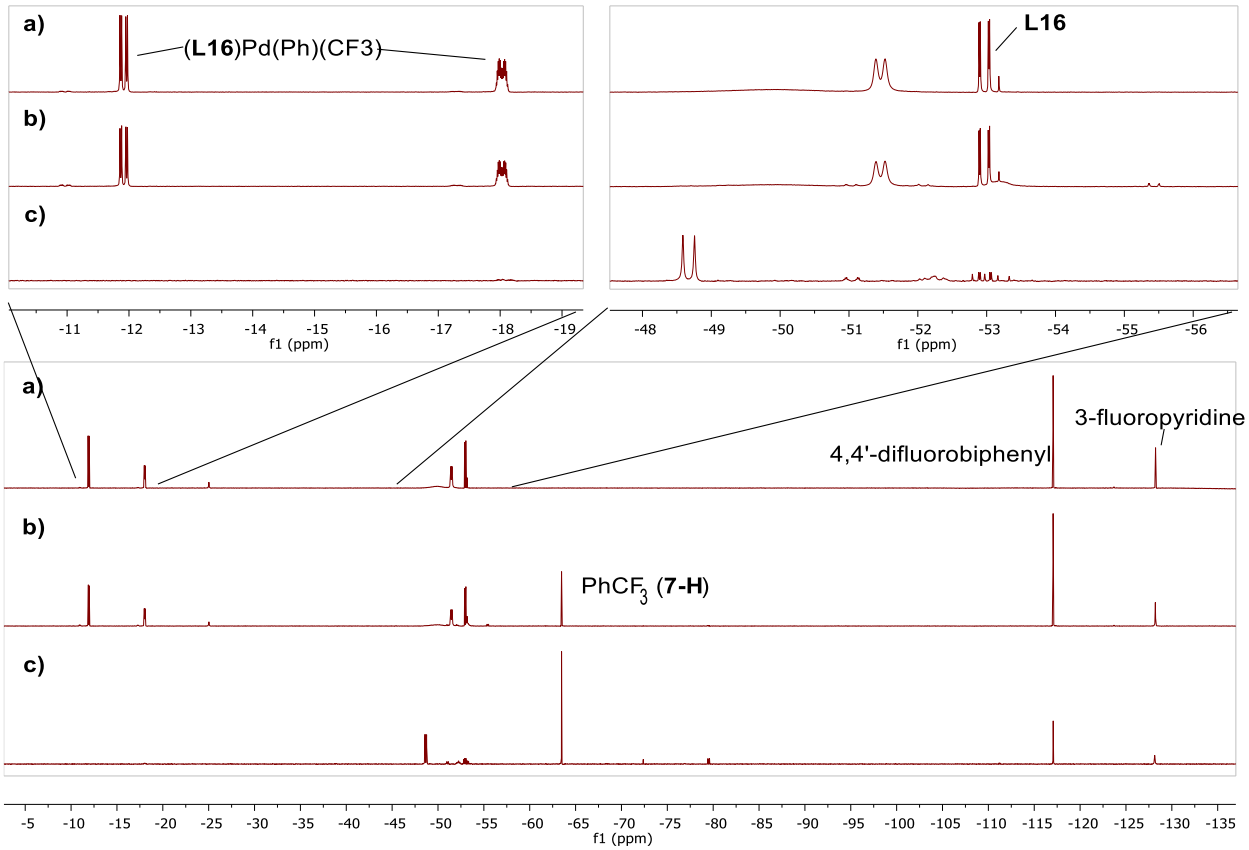


Figure 4.7.27 Reaction of **Pd-8** and **L16** at 80 °C after a) 0 min; b) 75 min; c) 18 h.

*Ligand decomposition in the reaction of arylpalladium bromide dimer **Pd-9b** and ligand **L16***

To a 1-dram vial were added dimer **Pd-9b** (2.9 mg, 2.5 μmol, 0.50 equiv), **L16** (~2 mg, ~5 μmol, ~1 equiv), 4-(trifluoromethoxy)anisole, and dioxane (700 μL). The mixture was heated at 80 °C overnight, and then analyzed by ^{19}F NMR spectroscopy. The NMR spectrum revealed the formation of CHF_3, indicating P–CF_3 cleavage.

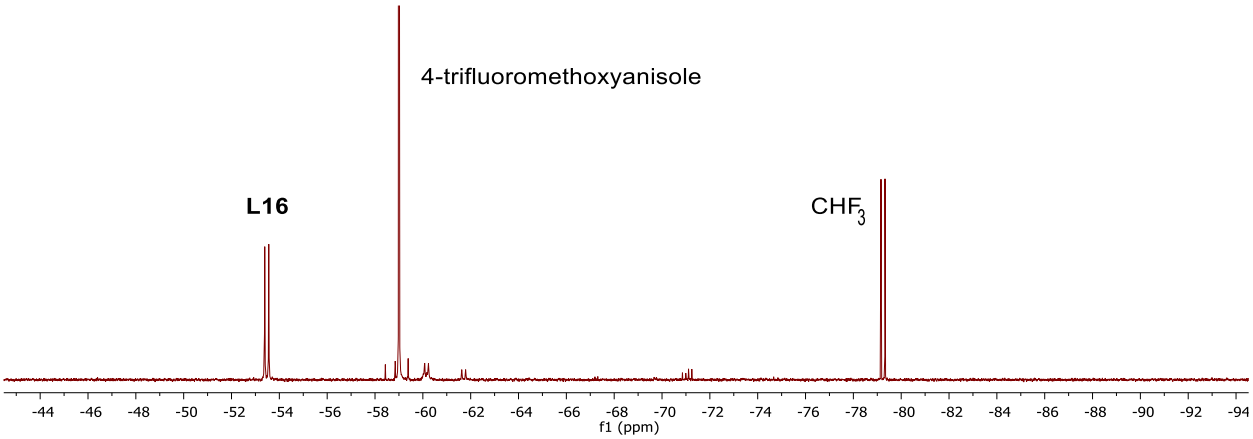


Figure 4.7.28 Reaction of **L16** and dimer **Pd-9b** in dioxane for 18 h

*Ligand decomposition in the reaction of arylpalladium bromide dimer **Pd-9b**, ligands **L17–L18**, and K[B(CF$_3$)(OMe)$_3$]*

To a 1-dram vial were added **Pd-9b** (2.9 mg, 2.5 μmol, 0.50 equiv), ligand (6.0 μmol, 1.2 equiv), K[B(CF$_3$)(OMe)$_3$] (1.4 mg, 6.5 μmol, .3 equiv), 4-(trifluoromethoxy)anisole, and dioxane (700 μL). The mixture was mixed by pipette until homogeneous and transferred to an NMR tube. The mixture was heated at 65 °C for 20 min, then 80 °C for 4 h while monitoring by ^{19}F NMR spectroscopy. The ^{19}F NMR spectra revealed the formation of H–R^F (R^F = C_2F_5, C_6F_5 for **L17** and **L18**, respectively).

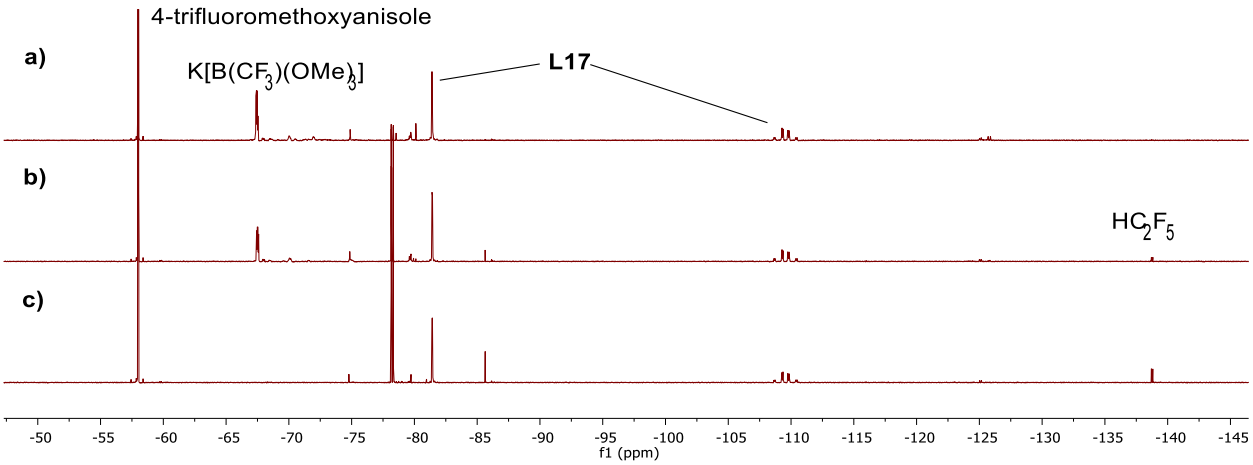


Figure 4.7.29 Reaction of dimer **Pd-9b**, **L17**, and K[B(CF$_3$)(OMe)$_3$] a) upon mixing; b) after 20 min at 65 °C; c) after another 4 h at 80 °C.

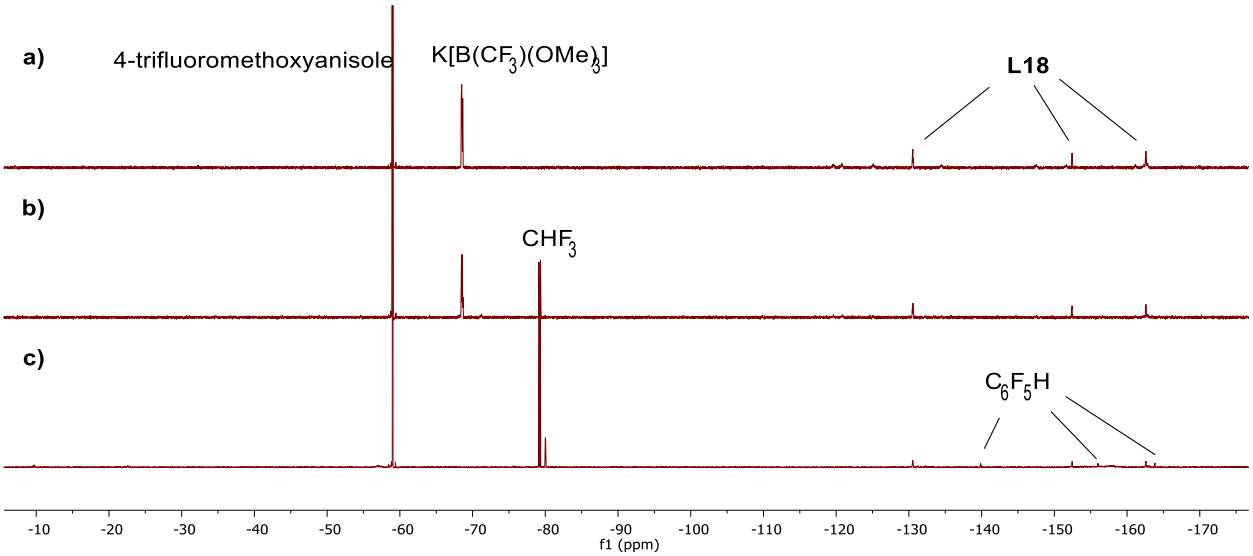


Figure 4.7.30 Reaction of dimer **Pd-9b**, **L18**, and K[B(CF$_3$)(OMe)$_3$] a) upon mixing; b) after 20 min at 65 °C; c) after another 4 h at 80 °C.

*Reaction of arylpalladium bromide complex **Pd-5** with (PPh$_3$)$_3$Cu(CF$_3$) **(Cu-1)***

A 1-dram vial was charged with arylpalladium bromide complex **Pd-5** (4.1 mg, 5.0 μmol, 1.0 equiv) and **15** (4.8 mg, 5.0 μmol, 1.0 equiv), THF (700 μL), and 4-(trifluoromethoxy)anisole

as an internal standard (2.7 mg, 14 μmol, 2.8 equiv). The mixture was mixed by pipette and transferred to an NMR tube. After 15 min, unlocked ^{19}F NMR spectra were acquired. The mixture then was heated at 65 °C for 20 min, and ^{19}F and ^{31}P NMR spectra were acquired.

Separately, **Cu-1** (4.8 mg, 5.0 μmol, 1.0 equiv) and **L1** (4.0 mg, 7.5 μmol, 1.5 equiv) were combined in THF (700 μL), and an unquantified amount of 4-(trifluoromethoxy)anisole was added as an internal standard. This solution was used to determine the chemical shifts of the putative species (BrettPhos)Cu(CF_3) (**Cu-2**) (^{19}F (376 MHz, THF): δ –32.0 ppm (d, $^3J_{F–P}$ = 13.5 Hz); ^{31}P{^{1}H} (162 MHz, THF): δ 6.4 ppm (br s)).

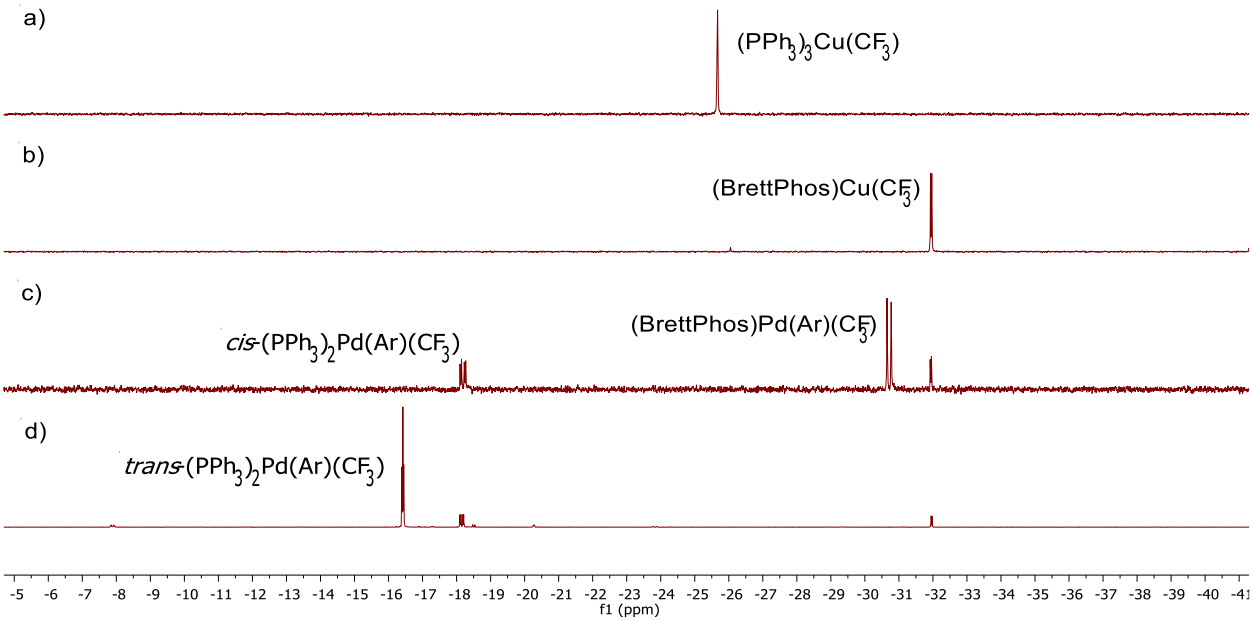


Figure 4.7.31 ^{19}F NMR spectra in THF of a) (PPh_3)$_3$Cu(CF_3) (**Cu-1**); b) a mixture of **Cu-1** and **L1**; c) the reaction of **Pd-5** with **Cu-1** after 15 min at room temperature; d) the same mixture after heating at 65 °C for 20 min.

*Reaction of arylpalladium bromide dimer **Pd-9a**, CyPF-tBu (**L4**), and (PPh_3)$_3$Cu(CF_3) (**Cu-1**)*

A 4 mL vial was charged with arylpalladium bromide dimer **Pd-9a** (2.6 mg, 2.5 μmol, 0.50 equiv) and CyPF-tBu (2.8, 5.0 μmol, 1.0 equiv) and THF (600 μL), and the mixture was stirred magnetically for 30 min. During this time, the solid dissolved the mixture darkened slightly. To the reaction then was added **15** (4.8 mg, 5.0 μmol, 1.0 equiv) and 4-(trifluoromethoxy)anisole as an internal standard (2.7 mg, 14 μmol, 2.8 equiv). The mixture was mixed by pipette and transferred to an NMR tube and heated at 80 °C. After 15 min at this temperature, unlocked ^{19}F NMR spectra were acquired.

Separately, **Cu-1** (4.8 mg, 5.0 μmol, 1.0 equiv) and CyPF-tBu (4.0 mg, 7.5 μmol, 1.5 equiv) were combined in THF (700 μL), and an unquantified amount of 4-(trifluoromethoxy)anisole was added as an internal standard. This solution was used to determine the chemical shift of the putative species (BrettPhos)Cu(CF_3) (**Cu-2**) (^{19}F (376 MHz, THF): δ –32.0 ppm (d, $^3J_{F–P}$ = 13.5 Hz); ^{31}P{^{1}H} (162 MHz, THF): δ 6.4 ppm (br s)).

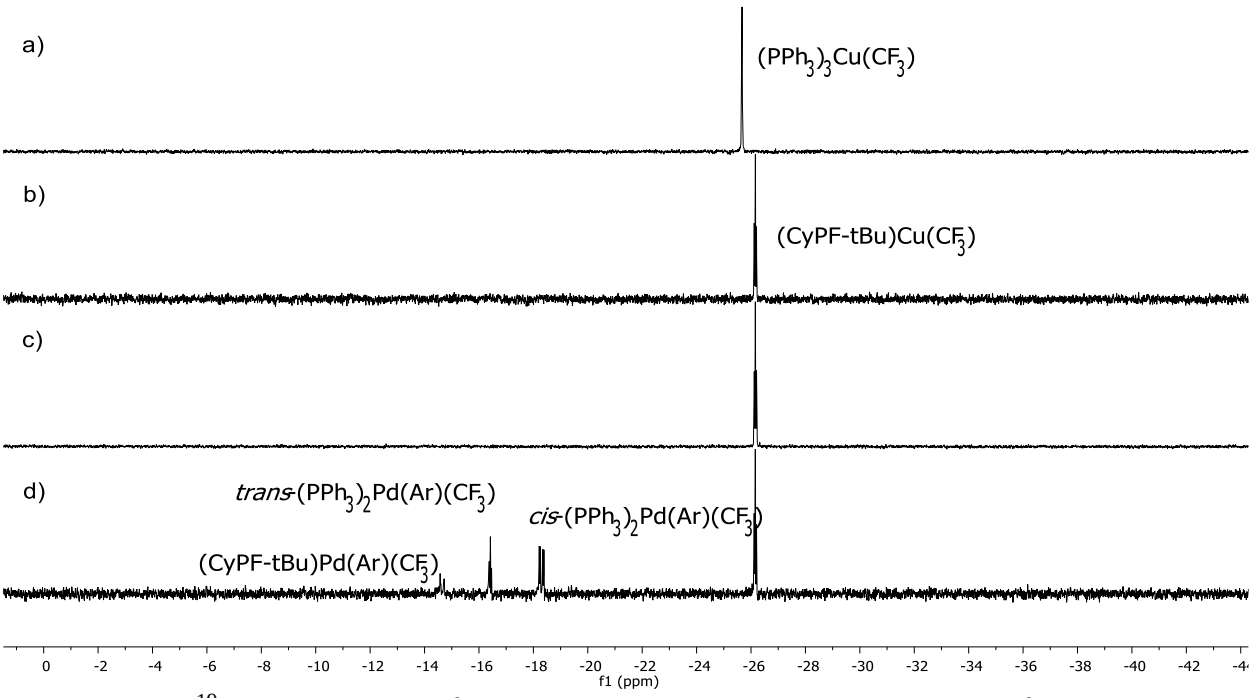


Figure 4.7.32 ^{19}F NMR spectra of a) $(PPh_3)_3Cu(CF_3)$ (**Cu-1**); b) a mixture of **Cu-1** and **L4** at ambient temperature; c) the reaction of dimer **Pd-9a**, **L4**, and **Cu-1** after 15 min at ambient temperature; d) the same reaction mixture after heating at 80 °C for 20 min.

*Reaction of arylpalladium bromide dimer **Pd-9a**, CyPF-tBu (**L4**), and L'Cu(CF_3) complexes **Cu-5** (L' = pip_2bpy, pip_2phen)*

To a 1-dram vial were added pip_2bpy (**L19**) or pip_2phen (**L20**) (5.0 μmol, 1.0 equiv) and CuBr (0.7 mg, 5 μmol, 1 equiv), and THF (500 μL). The mixture was stirred for 1 h at rt, and then $K[B(CF_3)(OMe)_3]$ (2.2 mg, 10 μmol, 2.0 equiv) was added as a solid. The vial was sealed and removed from the glove box, and the mixture was stirred for 10 min at 80 °C. The mixture was allowed to cool to rt, pumped back into the glove box, and transferred to an NMR tube for analysis. After acquisition, a mixture of **Pd-9a** (2.6 mg, 5.0 μL, 1.0 equiv) and **L14** (2.8 mg, 5.0 μL, 1.0 equiv) in THF (500 μL) was added to the NMR tube in the glove box. The mixture then was heated at 80 °C for 15 minutes, and then analyzed by ^{19}F NMR spectroscopy.

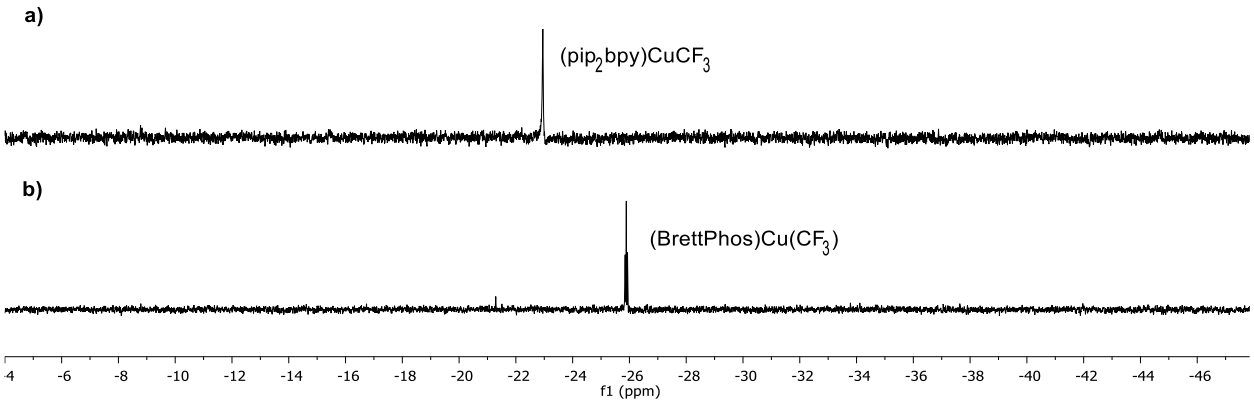


Figure 4.7.33 ^{19}F NMR spectra of a) the reaction of pip$_2$bpy (**L19**), CuBr, and K[B(CF$_3$)(OMe)$_3$] in THF after 10 min at 80 °C; b) the same reaction after addition of *in situ*-generated (**L4**)Pd(aryl)Br (**Pd-10-L4**) and heating at 80 °C for 15 min.

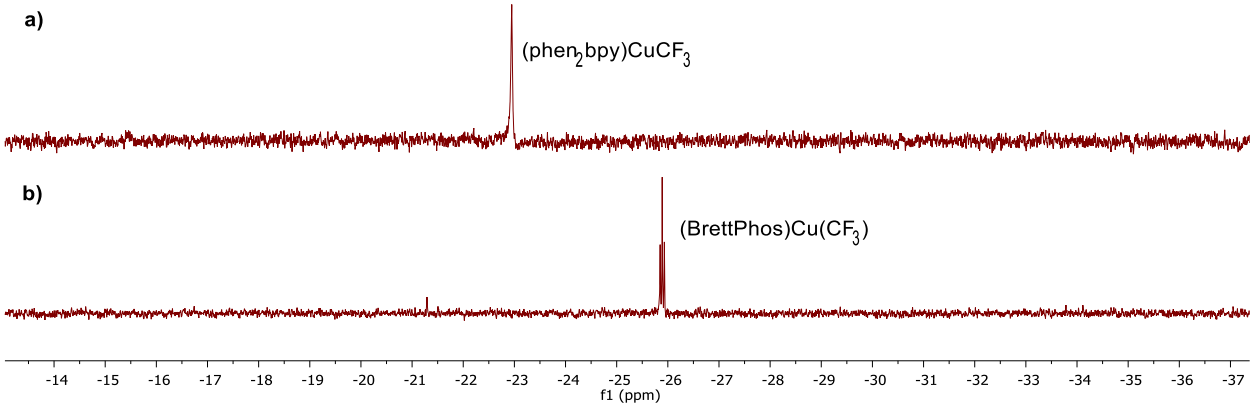


Figure 4.7.34 ^{19}F NMR spectra of a) the reaction of pip$_2$phen (**L20**), CuBr, and K[B(CF$_3$)(OMe)$_3$] in THF after 10 min at 80 °C; b) the same reaction after addition of *in situ*-generated (**L4**)Pd(aryl)Br (**Pd-10-L4**) and heating at 80 °C for 15 min.

4.7.4 Computational Details

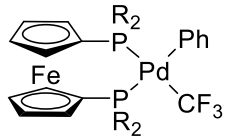
General Considerations

DFT calculations were conducted at the Molecular Graphics and Computation Facility (MGCF) at the University of California, Berkeley using the Gaussian 16[81] software package. All calculations, including geometry optimizations, were performed in THF solvent using the SMD solvent continuum model reported by Truhlar and co-workers according to the Solvent-Accessible Surface (scrf=sas).[82] Initial geometries were constructed in GaussView[83] and optimize to stationary points (either minima or first-order saddle points) using the PBE0 functional (the hybrid functional based on the Perdew-burke-Ernzerhof functional [PBE][84,85] as described by Adamo[86]) with Grimme's D3 dispersion correction with Becke-Johnson damping (GD3BJ)[87] and the basis sets def2-TZVP (with ECP) for Pd and def2-SVP for all light atoms (**BS1**). The nature of each stationary point was evaluated by accompanying frequency calculations (all positive eigenvalues for minima and exactly one negative eigenvalue for transition states). Several isomers were considered, but only those representing the minimum-energy path are presented here. Transition

states were connected to ground states by following the intrinsic reaction coordinate downhill from the transition state. Further single-point energy calculations were performed on the optimized geometries with the larger def2-QZVP basis set (with ECP) on Pd (obtained through the Basis Set Exchange,[88] accessed October 2019) and Truhlar's minimally-augmented version of the def2-TZVP basis set ("ma-TZVP") on all light atoms (**BS2**).[89] In all cases, Gibbs free energies for **BS2** were approximated by adding the thermal corrections obtained from frequency calculations using **BS1** to the **BS2** electronic energies.

Optimized Geometries

Geometries are given in the XYZ file format with the name of the compound as the title

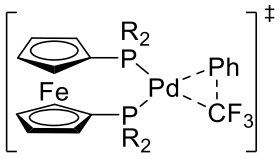


R = CF_3

E(**BS1**): -4375.45808635 Eh
Thermal correction: 0.249453 Eh
E(**BS2**): -4378.35644153 Eh
G(**BS2**): -4378.10698853 Eh

```
   53
(dfmpf)Pd(Ph)(CF3)
C       0.49138300      2.37844700     -0.54730000
C       1.12695700      1.98110700     -1.77380800
H       0.85146200      1.12244300     -2.38362500
C       2.19601400      2.88003100     -2.01657800
H       2.89438700      2.82419600     -2.84969800
C       2.23163800      3.82802200     -0.95626000
H       2.96440500      4.62417700     -0.83550400
C       1.17870100      3.53427900     -0.05119700
H       0.95421700      4.06803900      0.86860300
C       2.66779300      0.01464700      0.36217700
C       2.58915200      0.87152200      1.51131900
H       1.83753800      0.81949100      2.29494100
C       3.64760500      1.81098400      1.42708000
H       3.83570100      2.61870900      2.13218700
C       4.38298600      1.54815300      0.23899100
H       5.23204300      2.12206300     -0.12849700
C       3.79355600      0.43680800     -0.41869500
H       4.11731900      0.01186800     -1.36526100
Fe      2.41412000      1.91942400     -0.21454100
Pd     -0.88178000     -0.90872100      0.03359400
P      -0.89285900      1.43168400      0.09182100
P       1.45768100     -1.28885400      0.07722300
C      -2.90221400     -0.79468800     -0.14487700
```

```
C       -3.48514400     -0.76346000     -1.41464500
C       -3.72563900     -0.74663700      0.98253100
C       -4.86879900     -0.65409700     -1.55405200
H       -2.86252900     -0.82643200     -2.31082000
C       -5.10927900     -0.63657500      0.84134400
H       -3.29425800     -0.79773900      1.98497900
C       -5.68406900     -0.58421600     -0.42652600
H       -5.31109000     -0.62662100     -2.55359300
H       -5.74170200     -0.59442800      1.73226600
H       -6.76786000     -0.49611700     -0.53597900
C        2.07411300     -1.98898900     -1.57420700
C        2.16275900     -2.61644700      1.27432900
C       -1.15718600      2.10220300      1.84533900
C       -2.29096800      2.40342700     -0.76601400
F        3.35164600     -2.36296000     -1.52532300
F        1.97058900     -1.02941000     -2.50400100
F        1.35375400     -3.01837500     -1.97231300
F        3.33614100     -2.22537700      1.76674900
F        1.32508100     -2.75656900      2.29645300
F        2.34415300     -3.79254700      0.69550700
F       -2.31055300      2.05140100     -2.04936500
F       -2.04593500      3.71280400     -0.70885500
F       -3.47920200      2.19123100     -0.23413900
F       -2.34082000      1.71837100      2.29842700
F       -1.10149800      3.43052000      1.91915900
F       -0.22455800      1.61156000      2.66608000
C       -1.29354700     -2.92709000      0.01712300
F       -0.17143600     -3.69706600      0.13784700
F       -2.08127600     -3.32235800      1.03095300
F       -1.87520300     -3.35351100     -1.11599800
```



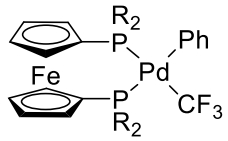
R = CF_3

E(**BS1**): -4375.42316515Eh
Thermal correction: 0.246982 Eh
E(**BS2**): -4378.32325299 Eh
G(**BS2**): -4378.07627099 Eh

```
    53
 (dfmpf)Pd(Ph)(CF3) RE transition state
C        0.83381000     -2.36369100      0.51464800
C        1.49962500     -1.91028900      1.70268200
H        1.14982600     -1.12009600      2.36329800
```

C	2.70319300	-2.64875300	1.83510000
H	3.44593900	-2.51624800	2.61978200
C	2.79477800	-3.55068600	0.73852700
H	3.62256700	-4.22807700	0.53511400
C	1.64321500	-3.38694100	-0.07660600
H	1.43209600	-3.91926600	-1.00089300
C	2.64450300	0.33292500	-0.45381700
C	2.52688300	-0.49243200	-1.62260400
H	1.68385700	-0.49948200	-2.31083400
C	3.68073900	-1.31418800	-1.69154900
H	3.87489200	-2.07354000	-2.44696800
C	4.50928000	-1.01257000	-0.57457500
H	5.44842900	-1.50338900	-0.32442500
C	3.88209800	0.00703200	0.18950600
H	4.25795500	0.43975400	1.11342500
Fe	2.65398300	-1.61979300	0.05865900
Pd	-0.90263200	0.73409400	-0.09763700
P	-0.67980500	-1.56730000	-0.04433900
P	1.31614400	1.45852400	-0.00333000
C	-2.94982500	0.90776800	0.03444100
C	-3.43724400	0.89426000	1.34738500
C	-3.76527500	0.46209400	-1.01485900
C	-4.69852200	0.36375400	1.61403800
H	-2.82779800	1.29464400	2.16187900
C	-5.02484200	-0.05781300	-0.73767400
H	-3.40761500	0.51128900	-2.04595200
C	-5.49441400	-0.11418100	0.57570900
H	-5.06298200	0.33457200	2.64399300
H	-5.64722300	-0.42532500	-1.55754700
H	-6.48605200	-0.52084700	0.78647600
C	1.85631000	2.09188200	1.69720900
C	1.85482200	2.97340300	-1.01489000
C	-1.00516200	-2.44748800	-1.68811600
C	-1.93674400	-2.52456700	1.00824000
F	3.10959600	2.54425800	1.73577800
F	1.75937100	1.10942500	2.59939700
F	1.05572100	3.07777900	2.07910900
F	3.16542000	3.19883200	-0.95502900
F	1.54171200	2.74819900	-2.29072900
F	1.23083600	4.07174000	-0.60814200
F	-1.93338300	-1.99462500	2.23308900
F	-1.64449700	-3.81714100	1.12822500
F	-3.16015700	-2.42448500	0.50465200
F	-2.17041400	-2.05337200	-2.18777300
F	-1.02847000	-3.77668200	-1.59730900
F	-0.05080700	-2.12422600	-2.56837000

C	-2.06377400	2.65937500	-0.34620500
F	-1.37504000	3.00386000	-1.46221000
F	-3.26654100	3.22238300	-0.54389700
F	-1.54803500	3.32412100	0.70257800



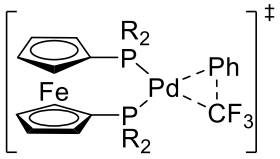
R = CF_2H

E(**BS1**): -3979.12591993 Eh
Thermal correction: 0.284158 Eh
E(**BS2**): -3981.54849987 Eh
G(**BS2**): -3981.26434187 Eh

53
(df2mpf)Pd(Ph)(CF3)

C	0.96809000	2.13354200	-0.60805400
C	1.60709100	1.58389200	-1.77256300
H	1.22309200	0.77163800	-2.38833300
C	2.85314900	2.24337600	-1.93383200
H	3.59062300	2.02615300	-2.70450600
C	2.99555800	3.19039100	-0.88105100
H	3.86309600	3.82457300	-0.70592000
C	1.83516900	3.13663700	-0.06509000
H	1.64604800	3.72068700	0.83146700
C	2.53335200	-0.61234800	0.46406600
C	2.52683000	0.25386700	1.60817100
H	1.70624100	0.37186200	2.31140100
C	3.75848400	0.95763400	1.62483100
H	4.04419200	1.71734200	2.35024000
C	4.52862800	0.53729100	0.50491200
H	5.50766200	0.91995700	0.22131100
C	3.78415700	-0.43699000	-0.21199000
H	4.09006600	-0.93458900	-1.12860400
Fe	2.72906300	1.30095600	-0.11885300
Pd	-1.07514800	-0.77001000	-0.14204500
P	-0.61340200	1.50446200	-0.03975100
P	1.10870600	-1.61270200	0.00791000
C	-3.01982000	-0.18532100	-0.10081700
C	-3.75773000	0.05004700	-1.26659400
C	-3.64629400	0.00975800	1.13620100
C	-5.07487900	0.50556300	-1.19757900
H	-3.30958700	-0.13706400	-2.24713200
C	-4.96538700	0.46158800	1.20620700
H	-3.10634400	-0.20330200	2.06461300

```
C      -5.68037000      0.71987800      0.03897100
H      -5.63474300      0.68752600     -2.11913000
H      -5.43747000      0.60835400      2.18159400
H      -6.71106200      1.07871000      0.09253900
C       1.68083800     -2.51209200     -1.53440700
C       1.25205100     -2.97103000      1.30540700
C      -0.89290800      2.17815600      1.68872800
C      -1.80781100      2.66821700     -0.94578900
F       2.87987700     -3.10057300     -1.37509700
F       1.78894800     -1.61089000     -2.53969500
F       2.52440900     -3.37717500      1.43945500
F       0.85751700     -2.42454600      2.47703700
F      -1.19554200      3.82993700     -1.23309300
F      -2.86881400      2.93774900     -0.16321700
F      -0.48999000      3.45757600      1.81201500
F      -0.22412400      1.43666400      2.59835300
C      -1.85934100     -2.66951500     -0.26345800
F      -0.91692000     -3.64498900     -0.57160600
F      -2.39021000     -3.09095500      0.89926600
F      -2.80152600     -2.84635600     -1.20125800
H       0.61057000     -3.83485900      1.07248400
H       0.93604200     -3.27302200     -1.81610200
H      -2.16164900      2.20220700     -1.88047100
H      -1.97093400      2.11981600      1.90930400
```

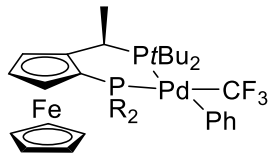


R = CF_2H

E(**BS1**): -3979.07716908 Eh
Thermal correction: 0.281382 Eh
E(**BS2**): Eh
G(**BS2**): Eh

```
    53
 (df2mpf)Pd(Ph)(CF3) RE transition state
C       1.08164700      2.02413900     -0.75098900
C       1.39460200      1.23428200     -1.91213300
H       0.78720300      0.41950200     -2.30482400
C       2.65486700      1.65986900     -2.40439700
H       3.18285300      1.23045600     -3.25401100
C       3.12992500      2.70424500     -1.56141000
H       4.08821000      3.21307200     -1.65389800
C       2.16566800      2.94052700     -0.54638300
H       2.24596200      3.65713700      0.26543700
```

C	2.53342600	-0.82920900	0.35781700
C	2.75467600	0.15365500	1.37955600
H	2.05523100	0.41426700	2.17087200
C	4.02586400	0.74090200	1.14971100
H	4.46889600	1.54303900	1.73734000
C	4.59390100	0.13617400	-0.00655100
H	5.54890400	0.39538200	-0.46072500
C	3.68228300	-0.83748500	-0.49699800
H	3.81346800	-1.45538000	-1.38153100
Fe	2.79241600	0.99627500	-0.47065100
Pd	-1.08929300	-0.54855100	0.09918400
P	-0.40444300	1.66142600	0.19590600
P	0.95520400	-1.68550700	0.19380000
C	-3.10807900	-0.37567400	-0.21203300
C	-3.50340500	0.04735200	-1.49068700
C	-3.89792100	-0.03865800	0.89907300
C	-4.61741400	0.87124300	-1.63817200
H	-2.92810000	-0.26098400	-2.36783300
C	-5.00825800	0.78286700	0.73906200
H	-3.62673900	-0.40766800	1.89192200
C	-5.36988800	1.24735300	-0.52634800
H	-4.90491400	1.21464700	-2.63555800
H	-5.60028200	1.06398600	1.61382000
H	-6.24586300	1.88845500	-0.64669500
C	1.21242000	-2.78879800	-1.29940000
C	1.10454000	-2.99325200	1.53360000
C	-0.17100200	2.36731500	1.92440400
C	-1.56117000	3.01182400	-0.40804600
F	2.37641500	-3.46790600	-1.27616200
F	1.20444200	-2.02421700	-2.41709000
F	2.32264800	-3.56094900	1.56487600
F	0.89758600	-2.38015100	2.72004500
F	-0.98175800	4.23018500	-0.34623200
F	-2.65271500	3.03486500	0.38880200
F	0.79087800	3.30545900	2.02351100
F	0.14241000	1.37165200	2.78786400
C	-2.57034000	-2.24041400	-0.23242100
F	-2.06216500	-2.99171400	0.78863400
F	-3.84723000	-2.65328900	-0.28816600
F	-2.02501800	-2.69316100	-1.38678100
H	0.34062600	-3.78036900	1.40273400
H	0.38099000	-3.51235500	-1.36587000
H	-1.87966600	2.81581200	-1.44679700
H	-1.13104400	2.80588100	2.24726700



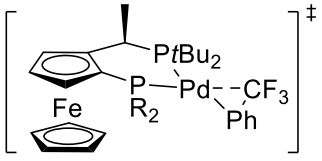
R = Cy

E(**BS1**): -3890.53953286 Eh
Thermal correction: 0.809701 Eh
E(**BS2**): Eh
G(**BS2**): Eh

```
   103
 (CyPF-tBu)Pd(Ph)(CF3)
Pd      1.66830800      0.35107300      0.05448600
Fe     -3.70309500      0.04120400      0.17435400
P       0.46077300      2.44581300     -0.14167500
P      -0.24951300     -1.03832400      0.23137100
C      -4.21651400     -1.35526500     -1.25077400
H      -3.57809300     -2.12745300     -1.67073900
C      -5.03642100     -1.48854200     -0.09695300
H      -5.11563700     -2.37269300      0.53345000
C      -5.71593800     -0.25267900      0.10102300
H      -6.40186500     -0.02197800      0.91457900
C      -5.30972800      0.64398800     -0.92805700
H      -5.63738700      1.67656700     -1.03960700
C      -4.37872300     -0.03721000     -1.76314800
H      -3.88209800      0.37337200     -2.64103000
C      -1.72982600     -0.10906000      0.76471900
C      -2.63167900     -0.39125100      1.84662600
H      -2.69776600     -1.31698700      2.40725200
C      -3.45637000      0.74270400      2.06207300
H      -4.25697400      0.81945900      2.79557800
C      -3.09336800      1.73275000      1.11014500
H      -3.58406100      2.69542500      0.98685400
C      -2.01811300      1.22881400      0.31827600
C      -1.28205200      1.97775800     -0.74989100
H      -1.00174700      1.24224000     -1.51815800
C      -2.18177700      3.01357400     -1.41823900
H      -3.14605600      2.53765600     -1.65101900
H      -1.76524400      3.37718100     -2.36425200
H      -2.39085900      3.88570400     -0.78769500
C       0.25947000      3.55281400      1.39185500
C       1.49674800      4.42055200      1.62667600
H       1.37952000      4.92801200      2.59900800
H       1.61058400      5.20769700      0.86854600
H       2.41749900      3.83146900      1.66691600
```

C	-0.95977400	4.47211500	1.35403100
H	-0.97753900	5.07327300	2.27884100
H	-1.90257700	3.91622500	1.31897200
H	-0.93008800	5.17759700	0.51217000
C	0.13606400	2.57016600	2.56378800
H	0.00438400	3.13433800	3.50253100
H	1.04516500	1.95765200	2.65830200
H	-0.72289500	1.89279900	2.45875500
C	1.16754900	3.41586700	-1.62152000
C	0.58305600	4.81704600	-1.81269200
H	0.96907100	5.23792200	-2.75660700
H	0.89560100	5.50051500	-1.01124400
H	-0.51036700	4.84272200	-1.87001600
C	0.91559900	2.54590700	-2.86000800
H	1.48246900	2.95736400	-3.71100400
H	-0.13837500	2.50099300	-3.16533100
H	1.27297300	1.51614600	-2.69479000
C	2.68607000	3.54873900	-1.48553200
H	3.06144400	4.11921600	-2.35182000
H	3.18360900	2.57163300	-1.48975000
H	2.99614800	4.07956700	-0.57859200
C	2.74313500	-1.29202900	-0.46309600
C	3.23922200	-2.29601400	0.37558200
H	3.11467700	-2.21193500	1.45798500
C	3.91937400	-3.40251500	-0.13855500
H	4.28257200	-4.17814000	0.54199500
C	4.14594900	-3.51664800	-1.50838400
H	4.67684600	-4.38261200	-1.91170800
C	3.70935700	-2.49817700	-2.35516500
H	3.90224900	-2.55800000	-3.43019200
C	3.02056600	-1.40196300	-1.83543300
H	2.69112400	-0.61752200	-2.52413400
C	0.12489700	-2.19825300	1.62432400
H	1.02974400	-2.69215700	1.22933700
C	-0.87658100	-3.30956400	1.94657100
H	-1.81511700	-2.89526000	2.34188800
H	-1.15136700	-3.86805800	1.03956100
C	-0.29276600	-4.25731500	2.99124400
H	-1.02120200	-5.04981400	3.22818000
H	0.59205700	-4.76501100	2.56650700
C	0.11162400	-3.50733000	4.25498400
H	0.54520700	-4.20248000	4.99209800
H	-0.79290100	-3.08181900	4.72717900
C	1.09308100	-2.38384000	3.94400200
H	2.04270900	-2.82183700	3.58814100
H	1.33918600	-1.82032200	4.85835000

C	0.55516300	-1.43336800	2.87881500
H	1.32151300	-0.68656300	2.60908600
H	-0.30083100	-0.86585300	3.28372900
C	-0.77400800	-2.15146200	-1.16176900
H	-1.76950600	-2.53070400	-0.87447000
C	0.16509000	-3.34352500	-1.37364700
H	1.18835900	-2.98137400	-1.54192400
H	0.20646000	-3.97608400	-0.47603900
C	-0.26707500	-4.18347000	-2.57093900
H	-1.25504400	-4.63928000	-2.37233500
H	0.43985600	-5.01820100	-2.70251200
C	-0.34431300	-3.34645400	-3.84037300
H	0.66511700	-2.97098600	-4.08534000
H	-0.66574200	-3.96359300	-4.69497300
C	-1.28848900	-2.16711500	-3.65235600
H	-2.31880900	-2.54627700	-3.52402700
H	-1.30771700	-1.53393300	-4.55439900
C	-0.90007900	-1.32373300	-2.44267200
H	0.07287900	-0.83648600	-2.63090800
H	-1.63575800	-0.51805100	-2.29399400
C	3.54468300	1.03056700	0.56179800
F	3.61894000	2.30240100	1.06336600
F	4.03840700	0.27849100	1.58285600
F	4.50214400	1.00425000	-0.39690500



R = Cy

E(**BS1**): -3890.49306893 Eh
Thermal correction: 0.80709 Eh
E(**BS2**): -3892.66091335 Eh
G(**BS2**): -3891.85382335 Eh

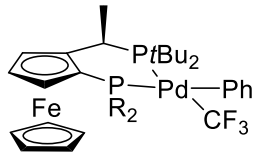
103
(CyPF-tBu)Pd(Ph)(CF3) (transition state to RE)

Pd	-1.57884600	0.39540900	-0.07688400
Fe	3.72882100	-0.05583900	-0.21471300
P	-0.36317700	2.47173700	0.03467600
P	0.24704100	-1.07298500	-0.12815800
C	4.19959800	-1.30838000	1.34642500
H	3.52306100	-1.98902400	1.85670500
C	4.98319500	-1.61676500	0.20015700
H	4.99681200	-2.56876300	-0.32809800
C	5.72458000	-0.45183400	-0.14967900

H	6.40157400	-0.35403800	-0.99689000
C	5.39384500	0.57666900	0.77830700
H	5.77954200	1.59501700	0.76613200
C	4.44815800	0.04760400	1.70281200
H	3.99528500	0.58438400	2.53514600
C	1.74091300	-0.21215100	-0.73673200
C	2.60658200	-0.61663900	-1.80912900
H	2.63252300	-1.59585000	-2.27615000
C	3.45026300	0.47014700	-2.15567800
H	4.23148100	0.45702000	-2.91366100
C	3.13223600	1.55637000	-1.29723400
H	3.63802900	2.51932800	-1.28613200
C	2.07081100	1.15902500	-0.42884600
C	1.40638900	2.04924200	0.58151500
H	1.17093000	1.42090700	1.45191100
C	2.34396000	3.15588900	1.05463800
H	3.31980700	2.71474200	1.30913600
H	1.97023700	3.65333600	1.95714500
H	2.52009100	3.93102400	0.29904700
C	-0.26431900	3.40115400	-1.61566000
C	-1.60104300	4.10211700	-1.86527000
H	-1.62887800	4.45266500	-2.91080300
H	-1.74112300	4.98510500	-1.22587900
H	-2.45187500	3.42124300	-1.72397000
C	0.87346800	4.41075100	-1.74512400
H	0.79473200	4.92089100	-2.72061600
H	1.85621200	3.92242900	-1.72136300
H	0.84803400	5.18809300	-0.96946900
C	-0.09959300	2.31337300	-2.68638800
H	-0.06846200	2.78844400	-3.68194900
H	-0.94474100	1.61035700	-2.66937400
H	0.82676100	1.73640400	-2.56410100
C	-0.99415900	3.60601600	1.43072700
C	-0.44982000	5.03448800	1.43853600
H	-0.82997800	5.56230100	2.33011200
H	-0.79103100	5.60543200	0.56349400
H	0.64473700	5.08975000	1.47126300
C	-0.66257200	2.89250400	2.74699700
H	-1.18193700	3.40054500	3.57632000
H	0.40837400	2.88840300	2.99097500
H	-1.01698400	1.84889300	2.72735200
C	-2.52161400	3.66679200	1.34671100
H	-2.90341000	4.26804400	2.18939200
H	-2.96662700	2.66628300	1.41183000
H	-2.88596600	4.12826200	0.42109900
C	-3.09962800	-0.90873000	0.20955300

C	-3.30370300	-2.14659300	-0.43727500
H	-3.07249700	-2.24279000	-1.50051900
C	-3.79701200	-3.24072200	0.26100100
H	-3.91990200	-4.19591600	-0.25751200
C	-4.13537600	-3.13353900	1.61385600
H	-4.52318800	-3.99797800	2.15721400
C	-4.01170500	-1.89739500	2.24611400
H	-4.30500600	-1.78543600	3.29353800
C	-3.53563100	-0.78929900	1.54707400
H	-3.49116300	0.18407600	2.04373400
C	-0.04904900	-2.45919400	-1.31916100
H	-0.99320100	-2.86635700	-0.91165600
C	0.95042400	-3.61718800	-1.35509300
H	1.94170700	-3.27283400	-1.68963500
H	1.10129000	-4.02506900	-0.34380100
C	0.46443500	-4.72245700	-2.28938700
H	1.21059300	-5.53253200	-2.33482800
H	-0.45405800	-5.17096600	-1.86899200
C	0.16629800	-4.18960600	-3.68561500
H	-0.19737300	-5.00135200	-4.33635300
H	1.10398800	-3.82408900	-4.14337300
C	-0.84634700	-3.05164900	-3.63798600
H	-1.81422100	-3.44652300	-3.27905900
H	-1.03178500	-2.65524800	-4.64938500
C	-0.38756300	-1.92812300	-2.71457100
H	-1.16528100	-1.15026600	-2.62793500
H	0.48929200	-1.42620800	-3.15630200
C	0.67739400	-1.95476500	1.44847000
H	1.59962300	-2.53517700	1.27136600
C	-0.45936000	-2.90550800	1.83463800
H	-1.40126100	-2.33534300	1.87319200
H	-0.60352000	-3.67995800	1.06718700
C	-0.21605400	-3.56952900	3.18517000
H	0.66152400	-4.23854400	3.11564800
H	-1.07688400	-4.21044000	3.43535900
C	0.02182500	-2.54231000	4.28345500
H	-0.89787400	-1.94644800	4.42497500
H	0.22286300	-3.04124700	5.24541300
C	1.16831600	-1.61098100	3.91373100
H	2.10980100	-2.18944600	3.87575500
H	1.31232500	-0.84220300	4.69057400
C	0.92569300	-0.94229400	2.56582900
H	0.03813800	-0.28824200	2.63814200
H	1.77640900	-0.29739400	2.30065100
C	-3.78765300	0.60303600	-0.81883100
F	-4.33262200	1.56201800	-0.04990800

F	-3.32603000	1.20992500	-1.95522800
F	-4.84191300	-0.09784500	-1.28474100



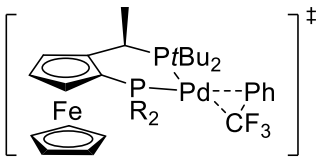
R = CF_3

E(**BS1**): -4094.77417244 Eh
Thermal correction: 0.519605 Eh
E(**BS2**): -4097.43964255 Eh
G(**BS2**): -4096.92003755 Eh

77
(CF3PF-tBu)Pd(Ph)(CF3)

Pd	-1.54800200	-0.60077900	0.22093400
Fe	3.53999200	0.65205300	-0.77752900
P	0.68253700	-1.26516600	0.21103600
P	-0.96512200	1.76093800	0.45804900
C	5.43375400	1.40410300	-0.92633600
H	5.74033400	2.17882400	-1.62756800
C	4.92696900	1.61659400	0.38674100
H	4.79653300	2.58404500	0.86872000
C	4.60709100	0.34873600	0.94746200
H	4.18147700	0.17400200	1.93281500
C	4.92194300	-0.65076700	-0.01881300
H	4.76203500	-1.72051700	0.09219000
C	5.43355200	0.00179400	-1.17368800
H	5.73431200	-0.48409700	-2.10078100
C	2.61437800	0.99480600	-2.55890900
H	3.13539800	1.18544700	-3.49575000
C	2.22326800	1.97558800	-1.60453500
H	2.38932300	3.04767400	-1.69123100
C	1.60019900	1.31550000	-0.50864200
C	1.64954200	-0.09957000	-0.77033400
C	2.26929000	-0.28489600	-2.05488900
H	2.46159600	-1.23367900	-2.54723000
C	0.91315400	1.92724300	0.66979000
H	1.05454300	1.22854200	1.50509100
C	1.53445700	3.24926600	1.09974600
H	2.60653000	3.08564000	1.28335600
H	1.09812200	3.62578500	2.03228100
H	1.44625200	4.04101200	0.34780300
C	-1.63103100	2.28106800	2.16481000
C	-1.68801600	3.78775500	2.41611500
H	-2.02877800	3.96289300	3.45046100

H	-2.40596900	4.29118300	1.75463100
H	-0.71755300	4.28833300	2.30762700
C	-0.75318900	1.60374700	3.22383300
H	-1.23947900	1.70799200	4.20737300
H	0.24846000	2.04678700	3.31249800
H	-0.64383400	0.52429200	3.03101800
C	-3.03808000	1.70056200	2.31617600
H	-3.44359200	1.99062800	3.29985000
H	-3.01597600	0.60157200	2.27019900
H	-3.73456300	2.05721400	1.54800800
C	-1.53502600	2.93329600	-0.91485300
C	-3.05428700	3.10223400	-0.83303500
H	-3.39683900	3.62435400	-1.74150900
H	-3.36678700	3.71197300	0.02634700
H	-3.57785000	2.13785600	-0.79359000
C	-0.86785300	4.30816500	-0.91502400
H	-1.35641800	4.93410900	-1.68042800
H	0.19377600	4.24741600	-1.18857000
H	-0.95431900	4.83861400	0.04220200
C	-1.20110400	2.22285700	-2.23089400
H	-1.54035200	2.84900700	-3.07303900
H	-1.71670900	1.25798600	-2.30436700
H	-0.12437700	2.05019000	-2.35612300
C	-3.37992000	-0.34547900	-0.64085000
C	-4.60742400	-0.11138400	-0.01109600
C	-3.38523700	-0.48925100	-2.03655900
C	-5.77921900	0.05669100	-0.75073800
H	-4.67115200	-0.06987300	1.07690300
C	-4.55435300	-0.32226700	-2.78104700
H	-2.46317100	-0.75058200	-2.56442800
C	-5.75652200	-0.03057600	-2.14116400
H	-6.72125200	0.25056000	-0.22993100
H	-4.52238700	-0.43082200	-3.86875900
H	-6.67380800	0.10415600	-2.71971800
C	-2.25059000	-2.49878400	0.48710400
F	-2.30074800	-3.27107300	-0.61425100
F	-1.43510400	-3.15892000	1.36183900
F	-3.46583700	-2.57908800	1.06011800
C	1.69657400	-1.68684300	1.76835100
C	1.03160100	-2.87487200	-0.74008900
F	0.99448500	-2.50540400	2.53734600
F	1.92496300	-0.56780100	2.47355300
F	2.87554900	-2.25872200	1.53747000
F	0.66690700	-3.94441400	-0.05668400
F	0.36719700	-2.84406100	-1.89126400
F	2.33147700	-3.01546900	-1.03053000

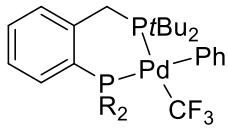


R = CF_3

E(**BS1**): -4094.73486113 Eh
Thermal correction: 0.518277 Eh
E(**BS2**): -4097.40009262 Eh
G(**BS2**): -4096.88181562 Eh

```
     77
 (CF3PF-tBu)Pd(Ph)(CF3) RE transition state
Pd     -1.49050800     -0.48503700     -0.12906900
Fe      3.76089600      0.48841000     -0.15379700
P       0.65553600     -1.30147700     -0.04543400
P      -0.87554200      1.84420400     -0.04974900
C       5.63392200      1.17751600      0.28885800
H       6.16319300      1.94646500     -0.27196400
C       4.76132800      1.39650600      1.39218600
H       4.52239400      2.36198900      1.83481600
C       4.24740500      0.13633600      1.80658200
H       3.53844800     -0.03110600      2.61405900
C       4.80741700     -0.86582900      0.96202500
H       4.58404500     -1.92959100      0.99885000
C       5.66429700     -0.22209800      0.02694800
H       6.21550900     -0.71063100     -0.77528800
C       3.40428600      0.81201700     -2.13447200
H       4.17946500      0.95280700     -2.88587400
C       2.80143000      1.83586000     -1.35306700
H       3.04615000      2.89446000     -1.40695100
C       1.85680800      1.24317200     -0.46397000
C       1.91701400     -0.18279600     -0.67430000
C       2.86859600     -0.43423400     -1.72251800
H       3.14531600     -1.40830800     -2.11654300
C       0.95248300      1.97310100      0.48920500
H       0.91518700      1.37510700      1.41111300
C       1.53001500      3.33701200      0.85539300
H       2.59450600      3.21476400      1.10320000
H       1.04219200      3.76458600      1.73828500
H       1.46074000      4.07195400      0.04450200
C      -1.79378700      2.92203800      1.22026500
C      -1.60830000      4.43453500      1.09410900
H      -2.13173100      4.92861400      1.93051400
H      -2.05897800      4.82108500      0.16892700
H      -0.56397700      4.76414800      1.12472000
```

C	-1.32695700	2.41821600	2.59206200
H	-1.97173100	2.84920800	3.37534500
H	-0.29232100	2.69644600	2.83519800
H	-1.41371100	1.32143700	2.66101200
C	-3.29134500	2.61814800	1.12511400
H	-3.81174800	3.15010800	1.93903700
H	-3.49558700	1.54886200	1.24138400
H	-3.73917100	2.95012300	0.18186700
C	-1.00673800	2.56818100	-1.79945800
C	-2.47669000	2.87073200	-2.09422600
H	-2.59268000	3.06485000	-3.17369100
H	-2.83789600	3.76297600	-1.56432500
H	-3.12916100	2.02513900	-1.83455900
C	-0.16881800	3.81850100	-2.05663200
H	-0.36731200	4.18122100	-3.07977200
H	0.90674500	3.60847900	-1.99701700
H	-0.40653600	4.64089200	-1.36852900
C	-0.55659500	1.45546700	-2.75525900
H	-0.65599000	1.80869300	-3.79565400
H	-1.17734000	0.55193600	-2.64195800
H	0.49130200	1.16446800	-2.60367600
C	-3.53491500	-0.68584600	0.05770300
C	-3.94705500	-0.88379300	1.38739500
C	-4.44243400	-0.11292800	-0.85128700
C	-5.18891200	-0.41914400	1.81796800
H	-3.28522400	-1.40157500	2.08674300
C	-5.67913600	0.34539700	-0.41434900
H	-4.17244200	-0.02825300	-1.90689900
C	-6.05605600	0.20646400	0.92453100
H	-5.48249400	-0.55692100	2.86187400
H	-6.36251200	0.81394100	-1.12769700
H	-7.03203400	0.56309200	1.26110800
C	-2.72609100	-2.33399900	-0.58105800
F	-2.01501400	-2.55904500	-1.71880700
F	-2.25381200	-3.14119300	0.38371000
F	-3.93323200	-2.84771000	-0.88879400
C	1.12268500	-1.72443100	1.74454100
C	1.19796100	-2.94538600	-0.81949700
F	0.19758300	-2.53559600	2.25109600
F	1.12520000	-0.60626400	2.48581200
F	2.30473400	-2.31469700	1.91452000
F	0.50559700	-3.94659700	-0.28972300
F	0.95942400	-2.90874600	-2.12988200
F	2.49670400	-3.23033400	-0.66207100



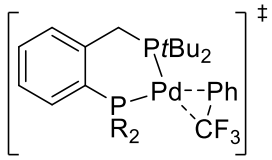
R = Cy

E(**BS1**): -2433.21811107 Eh
Thermal correction: 0.714541 Eh
E(**BS2**): -2435.18857119 Eh
G(**BS2**): -2434.47403019 Eh

```
    91
 (CyPBn-tBu)Pd(Ph)(CF3)
Pd      0.74726000     -0.57086300      0.37678000
C       0.43727500     -2.32595100      1.40154100
C       2.65039500     -1.28955500      0.20982900
C       3.60971600     -1.45998800      1.21504700
C       2.98529200     -1.74087000     -1.07751100
C       4.85772000     -2.02477200      0.94383200
H       3.38735300     -1.16014600      2.24170800
C       4.22786300     -2.31225500     -1.35516700
H       2.26128100     -1.65136200     -1.89427400
C       5.17662100     -2.44935200     -0.34386900
H       5.58585200     -2.13731700      1.75245300
H       4.45380600     -2.65147300     -2.37024700
H       6.15283100     -2.89278700     -0.55587700
F      -0.84291000     -2.51501400      1.86523400
F       0.73466600     -3.48834600      0.77400700
F       1.17241300     -2.33644200      2.54420900
C      -3.04311500      1.44783300     -1.86063500
C      -1.98879800      1.40993200     -0.93443600
C      -1.28518300      2.60689000     -0.67707900
C      -1.67512200      3.77812800     -1.34307200
C      -2.71841800      3.79363100     -2.25963000
C      -3.40707400      2.61474500     -2.52321700
H      -3.60824800      0.54231600     -2.07901000
H      -1.13880800      4.70594800     -1.12749100
H      -2.99186900      4.72387000     -2.76266600
H      -4.23316900      2.59913400     -3.23752600
P      -1.55050400     -0.17703100     -0.09068600
C      -0.14071300      2.71753300      0.28441800
H       0.15773500      3.77170400      0.34642000
H      -0.46019500      2.42272800      1.29588200
P       1.36946600      1.67268500     -0.00119300
C      -2.77497500     -0.27293000      1.29952400
C      -2.33763900      0.63232800      2.45180500
C      -4.23306800     -0.02666000      0.92250500
H      -2.66375000     -1.31344200      1.64313200
```

C	-3.25337600	0.46800800	3.65979400
H	-2.36660200	1.68632800	2.11864400
H	-1.29434500	0.40225100	2.72349200
C	-5.14400700	-0.19609300	2.13639300
H	-4.34388000	0.99683900	0.52465900
H	-4.54987400	-0.71275900	0.12019000
C	-4.71349900	0.70104700	3.29067600
H	-2.94333900	1.15490800	4.46397400
H	-3.13348900	-0.55411200	4.06074000
H	-6.18807500	0.01452400	1.85310700
H	-5.11802800	-1.25073800	2.46444800
H	-5.36220400	0.53703000	4.16628400
H	-4.85016300	1.75809100	2.99797800
C	-2.11851100	-1.43853000	-1.33628600
C	-1.22647700	-1.37350200	-2.57883600
C	-2.18528100	-2.86868800	-0.80030300
H	-3.14614400	-1.16418300	-1.62796400
C	-1.69484200	-2.34434100	-3.65685900
H	-0.19510500	-1.62533900	-2.27218800
H	-1.19392200	-0.34916300	-2.98087600
C	-2.68530400	-3.82182900	-1.88178300
H	-1.18642100	-3.18980400	-0.47409000
H	-2.83636000	-2.92668600	0.08479300
C	-1.80436600	-3.76682200	-3.12350200
H	-1.00781700	-2.30413400	-4.51773100
H	-2.68101000	-2.01705100	-4.03426600
H	-2.71998300	-4.84745700	-1.48059000
H	-3.72420200	-3.56122400	-2.15642900
H	-2.19186000	-4.44162600	-3.90401200
H	-0.79549800	-4.13481700	-2.86449700
C	2.40781900	2.27348700	1.48060700
C	2.06330100	2.23465900	-1.66780500
C	3.88429000	1.92156300	1.29492000
H	4.39006700	1.98214300	2.27297100
H	4.03587900	0.90604400	0.90888300
H	4.38990700	2.63306300	0.62824600
C	1.85636400	1.51353400	2.69368900
H	1.93102700	0.42322000	2.57271800
H	2.42729400	1.80167100	3.59218000
H	0.80065400	1.75274400	2.89433700
C	2.29957300	3.77439300	1.75947400
H	2.99459200	4.02991500	2.57647200
H	2.57926400	4.39326000	0.89527200
H	1.29771000	4.07832700	2.09372700
C	3.47338300	1.67791200	-1.87922100
H	3.72664200	1.75938500	-2.94937300

```
H       4.23515500      2.23791300     -1.32436900
H       3.55108600      0.61807700     -1.59923300
C       2.07326200      3.74882800     -1.85480800
H       2.43644500      3.98586200     -2.86905800
H       1.07262300      4.19399300     -1.76190300
H       2.74770100      4.25276000     -1.14788800
C       1.14476000      1.58748600     -2.71167200
H       1.12777300      0.49406200     -2.59726700
H       0.11133200      1.95499500     -2.65871400
H       1.52725000      1.81683500     -3.72009900
```



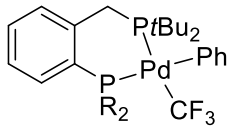
R = Cy

E(**BS1**): -2433.16489005 Eh
Thermal correction: 0.711702 Eh
E(**BS2**): -2435.13485883 Eh
G(**BS2**): -2434.42315683 Eh

```
    91
 (CyPBn-tBu)Pd(Ph)(CF3) RE transition state
Pd      0.70289700     -0.52259100      0.31362900
C       0.97430100     -2.46913200      1.56297800
C       2.33519700     -1.72660700      0.43514400
C       3.55739200     -1.46797800      1.08594200
C       2.37353400     -2.40905900     -0.79765300
C       4.76354000     -1.75736200      0.46330700
H       3.55525300     -1.02121900      2.08200600
C       3.58917500     -2.67291300     -1.42863900
H       1.43930800     -2.73647000     -1.26123200
C       4.79045600     -2.34078600     -0.80829100
H       5.70095300     -1.51970500      0.97381100
H       3.59180600     -3.16517900     -2.40473700
H       5.74378700     -2.56413600     -1.29227500
F      -0.07927900     -2.03062200      2.33294500
F       0.52603900     -3.56406100      0.92739700
F       1.82564600     -2.91331500      2.50985600
C      -3.08874400      1.49515000     -1.88412100
C      -2.00296100      1.45307000     -0.99480100
C      -1.22557400      2.62496800     -0.83273400
C      -1.57721700      3.76701900     -1.56993700
C      -2.64968000      3.78409000     -2.45212200
C      -3.41611300      2.63490300     -2.60978100
H      -3.70645000      0.60756900     -2.02152800
```

H	-0.97950800	4.67332800	-1.44066400
H	-2.88517800	4.69346600	-3.00981800
H	-4.26951000	2.62116100	-3.29149600
P	-1.59649600	-0.12782800	-0.12303300
C	-0.06041100	2.77949700	0.10587200
H	0.25941000	3.82928200	0.06765700
H	-0.39276800	2.59873700	1.14026400
P	1.43746600	1.67886500	-0.03017500
C	-2.71794400	-0.11967200	1.36010600
C	-2.23117600	0.90204100	2.38869800
C	-4.20680200	0.05525800	1.07509600
H	-2.54652600	-1.12218300	1.79235200
C	-3.05209500	0.83475300	3.67176400
H	-2.32114300	1.91637000	1.95836300
H	-1.16335000	0.72958200	2.60031200
C	-5.02787500	-0.00844000	2.36104900
H	-4.36867900	1.03175600	0.58568100
H	-4.56202400	-0.71224500	0.36863300
C	-4.54043800	1.00353000	3.39099000
H	-2.70375000	1.60152600	4.38291500
H	-2.87783900	-0.14158100	4.15838300
H	-6.09423500	0.15487600	2.13469900
H	-4.95402100	-1.02550300	2.78675200
H	-5.12129000	0.91269000	4.32321700
H	-4.72395000	2.02471100	3.01001900
C	-2.33362000	-1.42014500	-1.24046400
C	-1.52589900	-1.49253400	-2.53885800
C	-2.37203500	-2.78204900	-0.54534300
H	-3.37395900	-1.14627800	-1.48538200
C	-2.03574300	-2.58863200	-3.46708100
H	-0.47053600	-1.69038700	-2.27658900
H	-1.53657300	-0.51831800	-3.05305200
C	-2.88503000	-3.87205300	-1.48141900
H	-1.35929500	-3.03963700	-0.19901900
H	-3.00528200	-2.73917700	0.35476100
C	-2.06997400	-3.94083800	-2.76643900
H	-1.40611300	-2.63540200	-4.37054800
H	-3.05317900	-2.33038900	-3.81344300
H	-2.86803400	-4.84370600	-0.96173800
H	-3.94327900	-3.67360100	-1.73201700
H	-2.47457200	-4.71445700	-3.43916400
H	-1.03721700	-4.24978200	-2.52306700
C	2.46587500	2.44390200	1.38299400
C	2.19509300	2.04469500	-1.72356000
C	3.93691300	2.06451100	1.21759400
H	4.47152900	2.25754700	2.16316000

H	4.06770300	1.00290000	0.96929300
H	4.43048200	2.66556300	0.44060400
C	1.92786300	1.78726700	2.65937400
H	2.01740800	0.69137900	2.62354800
H	2.49160100	2.15496400	3.53353600
H	0.86700000	2.02356300	2.83577400
C	2.35816900	3.96246100	1.53041200
H	3.05541400	4.29754400	2.31709400
H	2.62532200	4.50163300	0.61077500
H	1.35528700	4.28845700	1.84094300
C	3.44699000	1.17798500	-1.89312500
H	3.75765400	1.19834400	-2.95124300
H	4.29879200	1.52800000	-1.29857900
H	3.25145400	0.12945400	-1.62325900
C	2.51641900	3.51279800	-1.97856900
H	2.85947600	3.64376400	-3.01933400
H	1.63803300	4.16311800	-1.84614000
H	3.32149100	3.88184200	-1.32669100
C	1.16482600	1.55007700	-2.74660300
H	0.87501800	0.50753600	-2.54274300
H	0.25306800	2.16058000	-2.76837700
H	1.61306700	1.58509400	-3.75368500



R = CF_3

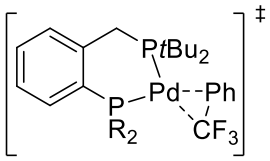
E(**BS1**): -2637.61143233 Eh
Thermal correction: 0.403914 Eh
E(**BS2**): -2639.91299116 Eh
G(**BS2**): -2639.50907716 Eh

65
(CF3PBn-tBu)Pd(Ph)(CF3)

C	-4.72513500	2.00671100	-0.49160800
C	-4.18805800	3.20495600	-0.03027400
C	-3.95981600	0.85030400	-0.43639600
C	-2.64606600	0.87037300	0.05887500
C	-2.09894500	2.07811600	0.53969900
C	-2.89788600	3.22899600	0.48334000
H	-5.74246200	1.96696500	-0.88588700
H	-4.77806300	4.12372900	-0.05971900
H	-4.40117300	-0.08371000	-0.78264800
H	-2.49142000	4.16808700	0.86690500
P	-1.64859700	-0.65859700	0.08486000
C	-2.28142300	-1.51350200	-1.50403100

F	-1.47107600	-2.47757700	-1.89469600
F	-2.32160200	-0.60002500	-2.47843100
F	-3.50720400	-2.03113800	-1.38573400
C	-2.55218900	-1.64009800	1.46725500
F	-2.91705500	-2.85915300	1.11111600
F	-3.64620400	-0.99797700	1.87784500
F	-1.72735500	-1.72282000	2.50964000
C	-0.74413700	2.20341600	1.17627800
P	0.78641800	1.70722500	0.23472500
C	2.11367200	2.37538400	1.42090700
C	0.72146900	2.65334500	-1.39891600
C	2.12291500	2.74049400	-2.00562900
C	0.12709800	4.05456700	-1.27538500
C	-0.15844600	1.80679200	-2.32565400
C	1.94176000	3.84619300	1.79966400
C	3.52009400	2.19506700	0.83969500
C	1.97973600	1.50425900	2.67715400
H	-0.19819000	2.27884500	-3.32134300
H	-1.19196100	1.72411600	-1.96411900
H	0.24281700	0.78893900	-2.44943700
H	2.66737600	1.78700000	-1.95388600
H	2.73409200	3.51417900	-1.52258800
H	2.03200000	3.01708000	-3.06893600
H	0.68230600	4.69290100	-0.57457500
H	-0.92673200	4.03414000	-0.96752900
H	0.16304700	4.54785800	-2.26117300
H	2.02134900	0.43175000	2.43556700
H	1.04818600	1.69644600	3.22992000
H	2.81215600	1.72668500	3.36397200
H	3.76541300	2.97176800	0.10592300
H	3.66996800	1.21457000	0.37529000
H	4.25094100	2.28456900	1.65976400
H	2.72737600	4.11515600	2.52500600
H	0.98026400	4.07137600	2.28318900
H	2.06395600	4.51613600	0.93698400
Pd	0.68436800	-0.67434300	0.08172300
C	2.67678700	-0.90046200	-0.22767700
C	3.58920300	-1.23285100	0.78123300
C	3.16940500	-0.74472500	-1.53041100
C	4.53285800	-0.86275500	-1.80675400
C	5.43313300	-1.15413100	-0.78384800
C	4.95266400	-1.35138900	0.50927700
H	3.23842100	-1.41099400	1.80027100
H	5.64496000	-1.60225200	1.31788700
H	4.89145900	-0.72787400	-2.83113100
H	6.50143000	-1.24240100	-0.99655500

H	2.48267600	-0.53328100	-2.35521600
C	0.74800100	-2.72650300	0.18987200
F	1.48901100	-3.17916600	1.22410100
F	1.21310400	-3.34941800	-0.90687700
F	-0.48531700	-3.28797600	0.40781300
H	-0.70701400	1.57106200	2.07805400
H	-0.62830600	3.23940500	1.51998000



R = CF_3

E(**BS1**): -2637.56584809 Eh
Thermal correction: 0.401223 Eh
E(**BS2**): -2639.86753245 Eh
G(**BS2**): -2639.46630945 Eh

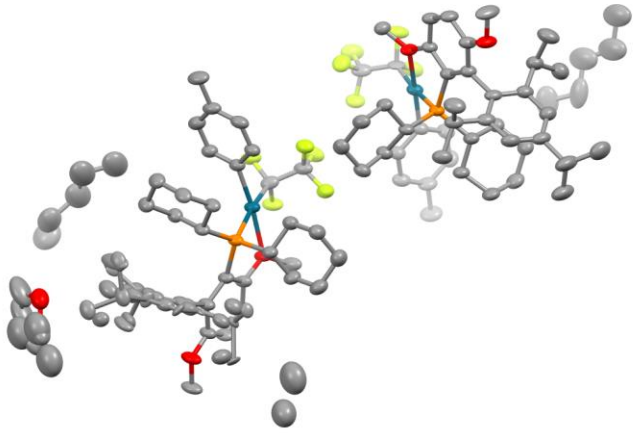
65
(CF3PBn-tBu)Pd(Ph)(CF3) (transition state to RE)

C	-2.25789200	4.58932100	-0.14893700
C	-3.43338700	3.97504000	-0.56597000
C	-1.10119100	3.83096800	-0.02161500
C	-1.09304200	2.45281500	-0.29421200
C	-2.27696000	1.82921800	-0.75855600
C	-3.42885900	2.62020100	-0.87410700
H	-2.23425200	5.65809400	0.07338200
H	-4.35471700	4.55263200	-0.67076700
H	-0.18511200	4.32598400	0.29197300
H	-4.34693700	2.15355700	-1.23979900
P	0.43503900	1.46429400	-0.07075500
C	1.18397000	2.10401800	1.57189600
F	0.93046900	1.21628000	2.53708500
F	0.73819100	3.27989600	2.01332900
F	2.50555600	2.20011300	1.44514100
C	1.58336800	2.38426800	-1.26862000
F	2.78450000	1.82848900	-1.30009900
F	1.74833900	3.68638000	-1.00564800
F	1.04508200	2.28577500	-2.48821800
C	-2.37952400	0.40820800	-1.24675000
P	-1.93534200	-1.02720200	-0.14017500
C	-2.59506100	-2.46419900	-1.19776800
C	-2.96527400	-0.79046200	1.42968500
C	-4.36747700	-0.23615500	1.19026400
C	-2.17410900	0.19474400	2.29740900
C	-3.04409500	-2.11955100	2.18160500

C	-1.84785000	-2.35831100	-2.53349400
C	-4.10088700	-2.44487600	-1.44689100
C	-2.20653400	-3.79722300	-0.55334300
H	-3.41263600	-1.93370700	3.20412200
H	-2.05904600	-2.60387700	2.26591900
H	-3.74309000	-2.82483400	1.71083700
H	-4.98008800	-0.88083800	0.54673400
H	-4.34173500	0.76976500	0.74955800
H	-4.89283800	-0.14765600	2.15642900
H	-1.16625700	-0.18491300	2.51931300
H	-2.70200800	0.34196900	3.25468900
H	-2.07515000	1.18389700	1.82799600
H	-1.13471800	-3.84852100	-0.33061300
H	-2.44174900	-4.61328400	-1.25689200
H	-2.75911300	-3.99979800	0.37163700
H	-4.45994700	-1.49440200	-1.86975700
H	-4.67381800	-2.65331400	-0.53226100
H	-4.35986500	-3.23372300	-2.17315200
H	-2.02306600	-3.27431200	-3.12087500
H	-0.75995700	-2.26634100	-2.38098100
H	-2.18764200	-1.51234100	-3.14835600
Pd	0.44731800	-0.83258100	0.03767300
C	2.45013700	-1.26039700	-0.01475400
C	2.97436400	-1.40762100	-1.30880600
C	3.28646900	-0.78279800	1.00945200
C	4.58240700	-0.37683100	0.71935800
C	5.08329100	-0.47695300	-0.58074100
C	4.27646200	-0.99905800	-1.58878800
H	2.35607800	-1.83944700	-2.09967800
H	4.66346700	-1.09550200	-2.60654500
H	5.21103700	0.02530500	1.51810500
H	6.10582700	-0.16229300	-0.80134300
H	2.90723000	-0.71249500	2.03180200
C	1.45219100	-2.84319500	0.45682500
F	0.54490100	-3.12594700	1.43956800
F	2.55410100	-3.47220600	0.90899100
F	1.08891500	-3.53479800	-0.64307300
H	-1.69141300	0.28776200	-2.09857400
H	-3.39414800	0.26213600	-1.64444200

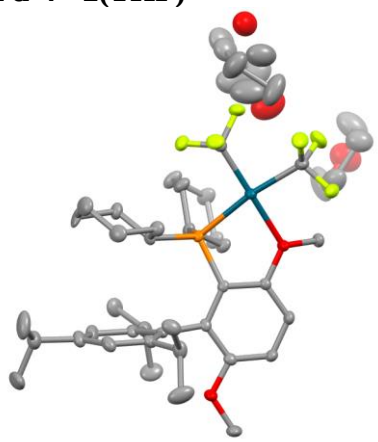
4.7.5 Data for Single-Crystal X-Ray Diffraction of Complexes **Pd-3b** and **Pd-4**

Pd-3b



Identification code	JFH2022004
Empirical formula	$C_{48.77}H_{71.08}F_5O_{2.23}PPd$
Formula weight	925.42
Temperature/K	100
Crystal system	monoclinic
Space group	$P2_1/c$
a/Å	16.89560(10)
b/Å	25.3734(3)
c/Å	23.7603(3)
α/°	90
β/°	91.2690(10)
γ/°	90
Volume/Å^3	10183.51(19)
Z	8
ρ_{calc}g/cm^3	1.207
μ/mm^{-1}	3.667
F(000)	3900.0
Crystal size/mm^3	0.21 × 0.05 × 0.04
Radiation	CuKα (λ = 1.54184)
2Θ range for data collection/°	6.286 to 149.006
Index ranges	$-13 \leq h \leq 20$, $-31 \leq k \leq 31$, $-29 \leq l \leq 28$
Reflections collected	109774
Independent reflections	20731 [R_{int} = 0.0695, R_{sigma} = 0.0490]
Data/restraints/parameters	20731/407/1224
Goodness-of-fit on F^2	1.042
Final R indexes [I>=2σ (I)]	R_1 = 0.0570, wR_2 = 0.1588
Final R indexes [all data]	R_1 = 0.0718, wR_2 = 0.1707
Largest diff. peak/hole / e Å^{-3}	1.46/-1.59

Pd-4 · 2(THF)



Identification code	JFH2022003
Empirical formula	$C_{45}H_{69}F_6O_4PPd$
Formula weight	925.37
Temperature/K	100
Crystal system	monoclinic
Space group	$P2_1/c$
a/Å	10.6584(6)
b/Å	29.6587(8)
c/Å	18.5819(10)
α/°	90
β/°	129.161(9)
γ/°	90
Volume/Å^3	4554.5(6)
Z	4
ρ_{calc}g/cm^3	1.350
μ/mm^{-1}	0.507
F(000)	1944.0
Crystal size/mm^3	0.202 × 0.108 × 0.075
Radiation	Mo Kα (λ = 0.71073)
2Θ range for data collection/°	5.628 to 52.742
Index ranges	$-13 \leq h \leq 11$, $-37 \leq k \leq 36$, $-20 \leq l \leq 23$
Reflections collected	58942
Independent reflections	9314 [R_{int} = 0.0489, R_{sigma} = 0.0318]
Data/restraints/parameters	9314/372/562
Goodness-of-fit on F^2	1.139
Final R indexes [I>=2σ (I)]	R_1 = 0.0494, wR_2 = 0.1208
Final R indexes [all data]	R_1 = 0.0573, wR_2 = 0.1273

Largest diff. peak/hole / e $Å^{-3}$ 1.53/-0.84

4.8 References

(1) Tomashenko, O. A.; Grushin, V. V. Aromatic Trifluoromethylation with Metal Complexes. *Chem. Rev.* **2011**, *111*, 4475–4521.

(2) Liang, T.; Neumann, C. N.; Ritter, T. Introduction of Fluorine and Fluorine-Containing Functional Groups. *Angew. Chem. Int. Ed. Engl.* **2013**, *52*, 8214–8264.

(3) Burton, D. J.; Yang, Z.-Y. Fluorinated Organometallics: Perfluoroalkyl and Functionalized Perfluoroalkyl Organometallic Reagents in Organic Synthesis. *Tetrahedron* **1992**, *48*, 189–275.

(4) McClinton, M. A.; McClinton, D. A. Trifluoromethylations and Related Reactions in Organic Chemistry. *Tetrahedron* **1992**, *48*, 6555–6666.

(5) Jeschke, P. The Unique Role of Fluorine in the Design of Active Ingredients for Modern Crop Protection. *ChemBioChem* **2004**, *5*, 570–589.

(6) Böhm, H.-J.; Banner, D.; Bendels, S.; Kansy, M.; Kuhn, B.; Müller, K.; Obst-Sander, U.; Stahl, M. Fluorine in Medicinal Chemistry. *ChemBioChem* **2004**, *5*, 637–643.

(7) Purser, S.; Moore, P. R.; Swallow, S.; Gouverneur, V. Fluorine in Medicinal Chemistry. *Chem. Soc. Rev.* **2008**, *37*, 320–330.

(8) Kirk, K. L. Fluorination in Medicinal Chemistry: Methods, Strategies, and Recent Developments. *Org. Process Res. Dev.* **2008**, *12*, 305–321.

(9) Gillis, E. P.; Eastman, K. J.; Hill, M. D.; Donnelly, D. J.; Meanwell, N. A. Applications of Fluorine in Medicinal Chemistry. *J. Med. Chem.* **2015**, *58*, 8315–8359.

(10) Dolbier, W. R. Fluorine Chemistry at the Millennium. *J. Fluor. Chem.* **2005**, *126*, 157–163.

(11) Yamazaki, T.; Taguchi, T.; Ojima, I. Unique Properties of Fluorine and Their Relevance to Medicinal Chemistry and Chemical Biology. In *Fluorine in Medicinal Chemistry and Chemical Biology*; John Wiley & Sons, Ltd, 2009; pp 1–49.

(12) Wang, J.; Sanchez-Rosello, M.; Acena, J. L.; del Pozo, C.; Sorochinsky, A. E.; Fustero, S.; Soloshonok, V. A.; Liu, H. Fluorine in Pharmaceutical Industry: Fluorine-Containing Drugs Introduced to the Market in the Last Decade (2001-2011). *Chem. Rev.* **2014**, *114*, 2432–2506.

(13) Inoue, M.; Sumii, Y.; Shibata, N. Contribution of Organofluorine Compounds to Pharmaceuticals. *ACS Omega* **2020**, *5*, 10633–10640.

(14) Meanwell, N. A. Synopsis of Some Recent Tactical Application of Bioisosteres in Drug Design. *J. Med. Chem.* **2011**, *54*, 2529–2591.

(15) Swarts, F. Fluorine Derivatives of Toluene. *Bull Acad R Belg* **1898**, *35*, 375.

(16) Daudt, H. W.; Youker, M. A. Preparation of Carbon Compounds Containing Fluorine. U.S. Patent 2005705, 1935.

(17) McLoughlin, V. C. R.; Thrower, J. A Route to Fluoroalkyl-Substituted Aromatic Compounds Involving Fluoroalkylcopper Intermediates. *Tetrahedron* **1969**, *25*, 5921–5940.

(18) Wang, H.; Vicic, D. A. Organometallic Aspects of Fluoroalkylation Reactions with Copper and Nickel. *Synlett* **2013**, *24*, 1887–1898.

(19) Oishi, M.; Kondo, H.; Amii, H. Aromatic Trifluoromethylation Catalytic in Copper. *Chem. Commun.* **2009**, No. 14, 1909–1911.

(20) Knauber, T.; Arikan, F.; Roschenthaler, G. V.; Goossen, L. J. Copper-Catalyzed Trifluoromethylation of Aryl Iodides with Potassium (Trifluoromethyl)Trimethoxyborate. *Chem. Eur. J.* **2011**, *17*, 2689–2697.
(21) Aikawa, K.; Nakamura, Y.; Yokota, Y.; Toya, W.; Mikami, K. Stable but Reactive Perfluoroalkylzinc Reagents: Application in Ligand-Free Copper-Catalyzed Perfluoroalkylation of Aryl Iodides. *Chem. Eur. J.* **2015**, *21*, 96–100.
(22) Nakamura, Y.; Fujiu, M.; Murase, T.; Itoh, Y.; Serizawa, H.; Aikawa, K.; Mikami, K. Cu-Catalyzed Trifluoromethylation of Aryl Iodides with Trifluoromethylzinc Reagent Prepared in Situ from Trifluoromethyl Iodide. *Beilstein J. Org. Chem.* **2013**, *9*, 2404–2409.
(23) Kondo, H.; Oishi, M.; Fujikawa, K.; Amii, H. Copper-Catalyzed Aromatic Trifluoromethylation via Group Transfer from Fluoral Derivatives. *Adv. Synth. Catal.* **2011**, *353*, 1247–1252.
(24) Konovalov, A. I.; Lishchynskyi, A.; Grushin, V. V. Mechanism of Trifluoromethylation of Aryl Halides with $CuCF_3$ and the Ortho Effect. *J. Am. Chem. Soc.* **2014**, *136*, 13410–13425.
(25) Tomashenko, O. A.; Escudero-Adan, E. C.; Belmonte, M. M.; Grushin, V. V. Simple, Stable, and Easily Accessible Well-Defined $CuCF_3$ Aromatic Trifluoromethylating Agents. *Angew. Chem. Int. Ed.* **2011**, *50*, 7655–7659.
(26) Le, C.; Chen, T. Q.; Liang, T.; Zhang, P.; MacMillan, D. W. C. A Radical Approach to the Copper Oxidative Addition Problem: Trifluoromethylation of Bromoarenes. *Science* **2018**, *360*, 1010–1014.
(27) Johansson Seechurn, C. C. C.; Kitching, M. O.; Colacot, T. J.; Snieckus, V. Palladium-Catalyzed Cross-Coupling: A Historical Contextual Perspective to the 2010 Nobel Prize. *Angew. Chem. Int. Ed.* **2012**, *51*, 5062–5085.
(28) Heravi, M. M.; Kheilkordi, Z.; Zadsirjan, V.; Heydari, M.; Malmir, M. Buchwald-Hartwig Reaction: An Overview. *J. Organomet. Chem.* **2018**, *861*, 17–104.
(29) Dorel, R.; Grugel, C. P.; Haydl, A. M. The Buchwald–Hartwig Amination After 25 Years. *Angew. Chem. Int. Ed.* **2019**, *58*, 17118–17129.
(30) Cho, E. J.; Senecal, T. D.; Kinzel, T.; Zhang, Y.; Watson, D. A.; Buchwald, S. L. The Palladium-Catalyzed Trifluoromethylation of Aryl Chlorides. *Science* **2010**, *328*, 1679–1681.
(31) Cho, E. J.; Buchwald, S. L. The Palladium-Catalyzed Trifluoromethylation of Vinyl Sulfonates. *Org. Lett.* **2011**, *13*, 6552–6555.
(32) Keaveney, S. T.; Schoenebeck, F. Palladium-Catalyzed Decarbonylative Trifluoromethylation of Acid Fluorides. *Angew. Chem. Int. Ed. Engl.* **2018**, *57*, 4073–4077.
(33) Malapit, C. A.; Ichiishi, N.; Sanford, M. S. Pd-Catalyzed Decarbonylative Cross-Couplings of Aroyl Chlorides. *Org. Lett.* **2017**, *19*, 4142–4145.
(34) Culkin, D. A.; Hartwig, J. F. Carbon−Carbon Bond-Forming Reductive Elimination from Arylpalladium Complexes Containing Functionalized Alkyl Groups. Influence of Ligand Steric and Electronic Properties on Structure, Stability, and Reactivity. *Organometallics* **2004**, *23*, 3398–3416.
(35) Grushin, V. V.; Marshall, W. J. Unexpected H2O-Induced Ar−X Activation with Trifluoromethylpalladium(II) Aryls. *J. Am. Chem. Soc.* **2006**, *128*, 4632–4641.
(36) Grushin, V. V.; Marshall, W. J. Facile Ar-CF3 Bond Formation at Pd. Strikingly Different Outcomes of Reductive Elimination from [(Ph3P)2Pd(CF3)Ph] and [(Xantphos)Pd(CF3)Ph]. *J. Am. Chem. Soc.* **2006**, *128*, 12644–12645.

(37) Nielsen, M. C.; Bonney, Karl. J.; Schoenebeck, F. Computational Ligand Design for the Reductive Elimination of ArCF3 from a Small Bite Angle PdII Complex: Remarkable Effect of a Perfluoroalkyl Phosphine. *Angew. Chem. Int. Ed.* **2014**, *53*, 5903–5906.
(38) Ferguson, D. M.; Bour, J. R.; Canty, A. J.; Kampf, J. W.; Sanford, M. S. Stoichiometric and Catalytic Aryl-Perfluoroalkyl Coupling at Tri-Tert-Butylphosphine Palladium(II) Complexes. *J. Am. Chem. Soc.* **2017**, *139*, 11662–11665.
(39) Ferguson, D. M.; Bour, J. R.; Canty, A. J.; Kampf, J. W.; Sanford, M. S. Aryl–CF3 Coupling from Phosphinoferrocene-Ligated Palladium(II) Complexes. *Organometallics* **2019**, *38*, 519–526.
(40) Arlow, S. I. The Development of Transition Metal-Catalyzed Fluoroalkylation and Fluoroenolate Arylation Reactions. Ph.D. Thesis, University of California, Berkeley, 2018.
(41) Bakhmutov, V. I.; Bozoglian, F.; Gómez, K.; González, G.; Grushin, V. V.; Macgregor, S. A.; Martin, E.; Miloserdov, F. M.; Novikov, M. A.; Panetier, J. A.; Romashov, L. V. CF3–Ph Reductive Elimination from [(Xantphos)Pd(CF3)(Ph)]. *Organometallics* **2012**, *31*, 1315–1328.
(42) Olsen, E. P. K.; Arrechea, P. L.; Buchwald, S. L. Mechanistic Insight Leads to a Ligand Which Facilitates the Palladium-Catalyzed Formation of 2-(Hetero)Arylaminooxazoles and 4-(Hetero)Arylaminothiazoles. *Angew. Chem. Int. Ed.* **2017**, *56*, 10569–10572.
(43) Bruno, N. C.; Niljianskul, N.; Buchwald, S. L. N-Substituted 2-Aminobiphenylpalladium Methanesulfonate Precatalysts and Their Use in C–C and C–N Cross-Couplings. *J. Org. Chem.* **2014**, *79*, 4161–4166.
(44) Lee, G. M.; Korobkov, I.; Baker, R. T. D8 Nickel and Palladium Difluorocarbenes Derived from Trifluoromethyl POCOP-Type Pincer Complexes. *J. Organomet. Chem.* **2017**, *847*, 270–277.
(45) Johnston, C. P.; West, T. H.; Dooley, R. E.; Reid, M.; Jones, A. B.; King, E. J.; Leach, A. G.; Lloyd-Jones, G. C. Anion-Initiated Trifluoromethylation by TMSCF3: Deconvolution of the Siliconate-Carbanion Dichotomy by Stopped-Flow NMR/IR. *J. Am. Chem. Soc.* **2018**, *140*, 11112–11124.
(46) García-Domínguez, A.; West, T. H.; Primozic, J. J.; Grant, K. M.; Johnston, C. P.; Cumming, G. G.; Leach, A. G.; Lloyd-Jones, G. C. Difluorocarbene Generation from TMSCF3: Kinetics and Mechanism of NaI-Mediated and Si-Induced Anionic Chain Reactions. *J. Am. Chem. Soc.* **2020**, *142*, 14649–14663.
(47) Naumann, D.; Kirij, N. V.; Maggiarosa, N.; Tyrra, W.; Yagupolskii, Y. L.; Wickleder, M. S. Synthesen und Charakterisierungen der ersten Tris- und Tetrakis(trifluormethyl)palladate(II) und -platinate(II), [M(CF3)3(PPh3)]— und [M(CF3)4]2— (M = Pd, Pt). *Z. Für Anorg. Allg. Chem.* **2004**, *630*, 746–751.
(48) Aikawa, K.; Serizawa, H.; Ishii, K.; Mikami, K. Palladium-Catalyzed Negishi Cross-Coupling Reaction of Aryl Halides with (Difluoromethyl)Zinc Reagent. *Org. Lett.* **2016**, *18*, 3690–3693.
(49) Zhang, S.-L.; Deng, Z.-Q. Synthesis and Reductive Elimination of ArylPd(II) Trifluoromethyl Complexes: A Remarkable Concentration Effect on Chemoselectivity. *Phys. Chem. Chem. Phys.* **2016**, *18*, 32664–32667.
(50) King, R. P.; Buchwald, S. L. Synthesis of (MeCN)2Pd(CF3)OTs, a General Precursor to Palladium(II) Trifluoromethyl Complexes LPd(CF3)X. *Organometallics* **2019**, *38*, 3490–3493.

(51) Maleckis, A.; Sanford, M. S. Catalytic Cycle for Palladium-Catalyzed Decarbonylative Trifluoromethylation Using Trifluoroacetic Esters as the CF3 Source. *Organometallics* **2014**, *33*, 2653–2660.
(52) Anstaett, P.; Schoenebeck, F. Reductive Elimination of ArCF3 from Bidentate PdII Complexes: A Computational Study. *Chem. – Eur. J.* **2011**, *17*, 12340–12346.
(53) Apel, J.; Grobe, J. Perfluormethyl-Element-Liganden. XIX. Koordinationsfähigkeit von Liganden des Typs MenP(CF3)3−n (n = 0–3). *Z. Für Anorg. Allg. Chem.* **1979**, *453*, 53–67.
(54) Fernandez, A. L.; Wilson, M. R.; Prock, A.; Giering, W. P. Evaluation of the Stereoelectronic Parameters of Fluorinated Phosphorus(III) Ligands. The Quantitative Analysis of Ligand Effects (QALE). *Organometallics* **2001**, *20*, 3429–3435.
(55) Velazco, E. J.; Caffyn, A. J. M.; Le Goff, X. F.; Ricard, L. Synthesis, Structure, and Coordination Properties of 1,1′-Bis(Bis(Trifluoromethyl)Phosphino)Ferrocene, Dfmpf. *Organometallics* **2008**, *27*, 2402–2404.
(56) Hu, Z.; Li, Y.; Liu, K.; Shen, Q. Bis(Perfluoroalkyl) Phosphino-Oxazoline: A Modular, Stable, Strongly π-Accepting Ligand for Asymmetric Catalysis. *J. Org. Chem.* **2012**, *77*, 7957–7967.
(57) Bodé, N. E.; Tassone, J. P.; Ferguson, M. J.; Stradiotto, M. Structural and Reactivity Comparisons of JosiPhos CyPF-Cy and a Simplified Variant ("CyPBn-Cy") in Nickel-Catalyzed C(Sp2)-N Cross-Couplings. *Organometallics* **2021**, *40*, 2915–2922.
(58) Krause, L. J.; Morrison, J. A. Trifluoromethyl Group 2B Compounds: Bis(Trifluoromethyl)Cadmium.Base. New, More Powerful Ligand-Exchange Reagents and Low-Temperature Difluorocarbene Sources. *J. Am. Chem. Soc.* **1981**, *103*, 2995–3001.
(59) Morrison, J. A. Trifluoromethyl-Containing Transition Metal Complexes. In *Advances in Organometallic Chemistry*; Stone, F. G. A., West, R., Eds.; Academic Press, 1993; Vol. 35, pp 211–239.
(60) Kremlev, M. M.; Tyrra, W.; Mushta, A. I.; Naumann, D.; Yagupolskii, Y. L. The Solid Complex Zn(CF3)Br·2DMF as an Alternative Reagent for the Preparation of Both, Trifluoromethyl and Pentafluoroethyl Copper, CuCF3 and CuC2F5. *J. Fluor. Chem.* **2010**, *131*, 212–216.
(61) Hori, K.; Motohashi, H.; Saito, D.; Mikami, K. Precatalyst Effects on Pd-Catalyzed Cross-Coupling Difluoromethylation of Aryl Boronic Acids. *ACS Catal.* **2019**, *9*, 417–421.
(62) Serizawa, H.; Ishii, K.; Aikawa, K.; Mikami, K. Copper-Catalyzed Difluoromethylation of Aryl Iodides with (Difluoromethyl)Zinc Reagent. *Org. Lett.* **2016**, *18*, 3686–3689.
(63) Gu, Y.; Leng, X.; Shen, Q. Cooperative Dual Palladium/Silver Catalyst for Direct Difluoromethylation of Aryl Bromides and Iodides. *Nat. Commun.* **2014**, *5*, 5405.
(64) Chang, D.; Gu, Y.; Shen, Q. Pd-Catalyzed Difluoromethylation of Vinyl Bromides, Triflates, Tosylates, and Nonaflates. *Chem. – Eur. J.* **2015**, *21*, 6074–6078.
(65) Martínez de Salinas, S.; Mudarra, Á. L.; Odena, C.; Martínez Belmonte, M.; Benet-Buchholz, J.; Maseras, F.; Pérez-Temprano, M. H. Exploring the Role of Coinage Metalates in Trifluoromethylation: A Combined Experimental and Theoretical Study. *Chem. – Eur. J.* **2019**, *25*, 9390–9394.
(66) Martínez de Salinas, S.; Mudarra, Á. L.; Benet-Buchholz, J.; Parella, T.; Maseras, F.; Pérez-Temprano, M. H. New Vistas in Transmetalation with Discrete "AgCF3" Species: Implications in Pd-Mediated Trifluoromethylation Reactions. *Chem. – Eur. J.* **2018**, *24*, 11895–11898.

(67) Lishchynskyi, A.; Grushin, V. V. Cupration of C2F5H: Isolation, Structure, and Synthetic Applications of [K(DMF)2][(t-BuO)Cu(C2F5)]. Highly Efficient Pentafluoroethylation of Unactivated Aryl Bromides. *J. Am. Chem. Soc.* **2013**, *135*, 12584–12587.
(68) García-Domínguez, P. Synthesis of L–Au(I)–CF2H Complexes and Their Application as Transmetalation Shuttles to the Difluoromethylation of Aryl Iodides. *Organometallics* **2021**, *40*, 2923–2928.
(69) Zanardi, A.; Novikov, M. A.; Martin, E.; Benet-Buchholz, J.; Grushin, V. V. Direct Cupration of Fluoroform. *J. Am. Chem. Soc.* **2011**, *133*, 20901–20913.
(70) Morimoto, H.; Tsubogo, T.; Litvinas, N. D.; Hartwig, J. F. A Broadly Applicable Copper Reagent for Trifluoromethylations and Perfluoroalkylations of Aryl Iodides and Bromides. *Angew. Chem. Int. Ed.* **2011**, *50*, 3793–3798.
(71) Litvinas, N. D.; Fier, P. S.; Hartwig, J. F. A General Strategy for the Perfluoroalkylation of Arenes and Arylbromides by Using Arylboronate Esters and [(Phen)CuR^F]. *Angew. Chem. Int. Ed.* **2012**, *51*, 536–539.
(72) Dubinina, G. G.; Ogikubo, J.; Vicic, D. A. Structure of Bis(Trifluoromethyl)Cuprate and Its Role in Trifluoromethylation Reactions. *Organometallics* **2008**, *27*, 6233–6235.
(73) Dubinina, G. G.; Furutachi, H.; Vicic, D. A. Active Trifluoromethylating Agents from Well-Defined Copper(I)-CF_3 Complexes. *J. Am. Chem. Soc.* **2008**, *130*, 8600–8601.
(74) Lu, Z.; Liu, H.; Liu, S.; Leng, X.; Lan, Y.; Shen, Q. A Key Intermediate in Copper-Mediated Arene Trifluoromethylation, [NBu4N][Cu(Ar)(CF3)3]: Synthesis, Characterization, and C(Sp2)−CF3 Reductive Elimination. *Angew. Chem. Int. Ed.* **2019**, *58*, 8510–8514.
(75) Liu, H.; Shen, Q. Bistrifluoromethylated Organocuprate $[Ph_4P]^+[Cu(CF_3)_2]^-$: Synthesis, Characterization and Its Application for Trifluoromethylation of Activated Heteroaryl Bromides, Chlorides and Iodides. *Org. Chem. Front.* **2019**, *6*, 2324–2328.
(76) Rosenau, C. P.; Jelier, B. J.; Gossert, A. D.; Togni, A. Exposing the Origins of Irreproducibility in Fluorine NMR Spectroscopy. *Angew. Chem. Int. Ed.* **2018**, *57*, 9528–9533.

Chapter 5

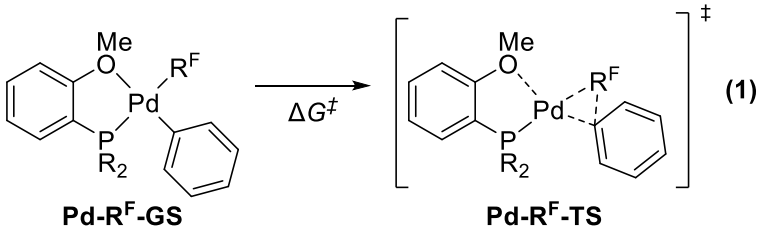
Computational Studies of the Electronic Effects of the Participating Ligands on the Reductive Elimination of Fluoroalkylarenes from Several Aryl(fluoroalkyl)palladium Complexes

5.1 Introduction

The construction of organic molecules containing fluorine is important for the development of biologically active molecules, including pharmaceuticals and agrochemicals, because fluorinated functional groups can drastically alter the lipophilicity, acidity, and metabolic stability of these molecules, compared to non-fluorinated analogues.[1–10] Pd-catalyzed fluoroalkylations of aryl halides are valuable reactions to introduce fluorinated motifs at late stages in the synthesis of these molecules, owing to the high selectivity and functional group tolerance of Pd catalysts.[11] Key to the formation of fluoroalkylarenes in these reactions is the reductive elimination from an intermediate aryl(fluoroalkyl)palladium complex. While many studies have investigated this step experimentally and computationally for complexes containing perfluoroalkylarenes, difluoromethylarenes, and *α*-aryl-*α*-fluorocarboxylic acid derivatives (see Chapter 1),[12–30] a more comprehensive study of the effect of the fluoroalkyl ligand on the rate of reductive elimination of fluoroalkylarenes has not been reported. To this end, we report in this Chapter computational investigations into reductive elimination of fluoroalkylarenes from (L)Pd(Ph)(R^F) complexes (L = di-*tert*-butyl(2-methoxyphenyl)phosphine) containing a series of alkyl ligands (R^F = CF_3, CF_2H, CFH_2, CH_3, CF_2Ph,[27,28] or CF_2CN[26]) and present a rationale for the relative barriers to reductive elimination of fluoroalkylarenes from these complexes.

5.2 Results and Discussion

To begin, we conducted DFT calculations to obtain optimized ground-state and transition-state geometries of complexes **Pd-R^F** (eq 1, **Pd-R^F-GS** and **Pd-R^F-TS**, respectively). Complexes of di-*tert*-butyl(2-methoxyphenyl)phosphine were chosen for this study because recent work in our group has shown that the coupling of aryl halides with aryldifluoromethylsilanes catalyzed by palladium complexes of this ligand form high yields of diaryldifluoromethanes.[27] The calculated free energy barriers to reductive elimination and some selected geometric parameters are shown in Table 5.2.1. Overall, the calculated barriers indicate that the reductive elimination from all **Pd-R^F** complexes except for **Pd-CF_3** would proceed quickly, even at 25 °C ($t_{1/2}$ < 5 min for $R^F \neq CF_3$ according to the Eyring equation), while reductive elimination from **Pd-CF_3** likely would require heating to proceed with a reasonable rate ($t_{1/2}$ = 49 min at 100 °C).



Pd-R^F-GS **Pd-R^F-TS** **(1)**

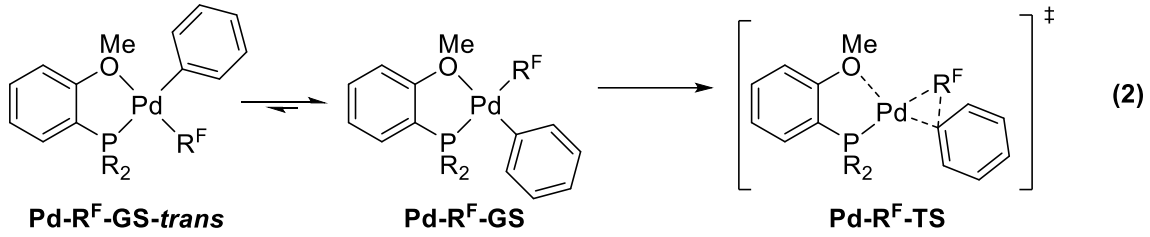
R = *t*Bu

R^F = CF_3, CF_2H, CFH_2, CH_3, CF_2CN, CF_2Ph

For all fluoroalkyl ligands, we found that the lowest-energy ground-state structures **Pd-R^F-GS** were distorted square-planar species in which both the phosphine and methoxy fragments of **L2** were bound to the Pd center (eq 2). Structures in which the aryl group was *cis* to the phosphino group was generally slightly lower in energy than that with the aryl group trans to the phosphino group (ΔG = 0.2 – 2.0 kcal/mol). The corresponding lowest-energy transition-state structures for reductive elimination **Pd-R^F-TS** also were distorted square planar species, except for **Pd-CF_2Ph-**

TS, in which the methoxy group of the ligand twisted significantly out of the plane defined by the other ligands (φ(C(aryl), Pd, P, O) = 123°, Figure 5.2.1). We attribute the greater distortion of the complex containing the CF_2Ph fragment, relative to the complexes containing other fluoroalkyl ligands, to the larger size of the CF_2Ph group than that of the other fluoroalkyl ligands. Nevertheless, the Pd–O bond was significantly longer for all R^F in **Pd-R^F-TS** than in **Pd-R^F-GS** (Δr(Pd–O) = 0.179 – 0.612 Å). A similar lengthening of the Pd–O bond in the transition state for reductive elimination from alkylpalladium amido complexes containing similar ligands was computed by DFT.[31] The Pd–O distances in the structures **Pd-R^F-TS** were all shorter than the sum of the van der Waals radii of Pd and O (r_{vdW}(Pd) + r_{vdW}(O) = 3.15 Å, r(Pd–O) = 2.469 – 2.918 Å),[32] suggesting that the oxygen atom of **L2** is still partially bound to the Pd center in the transition state.

Table 5.2.1 Barriers to Reductive Elimination and Selected Bond Lengths for Complexes **Pd-R^F**



Pd-R^F-GS-*trans* **Pd-R^F-GS** **Pd-R^F-TS**

R = *t*Bu

R^F = CF_3, CF_2H, CFH_2, CH_3, CF_2CN, CF_2Ph

R^F	**$\Delta G^‡$ (kcal/mol)**	***r*(Pd–P) (Å, GS*)**	***r*(Pd–P) (Å, TS*)**	***r*(Pd–O) (Å, GS*)**	***r*(Pd–O) (Å, TS*)**	**φ(C(aryl), Pd, P, O) (°, GS*)|**	**φ(C(aryl), Pd, P, O) (°, TS*)|**
CF_3	28.2	2.389	2.326	2.290	2.469	175	176
CF_2H	18.5	2.396	2.336	2.286	2.664	176	156
CFH_2	16.0	2.390	2.333	2.303	2.603	173	154
CH_3	14.0	2.370	2.331	2.299	2.588	180	166
CF_2CN	21.0	2.363	2.342	2.286	2.773	179	147
CF_2Ph	17.3	2.391	2.326	2.306	2.918	171	123

*GS = lowest-energy ground state, TS = lowest-energy transition state |Torsion angles (see Figure 5.2.1b)

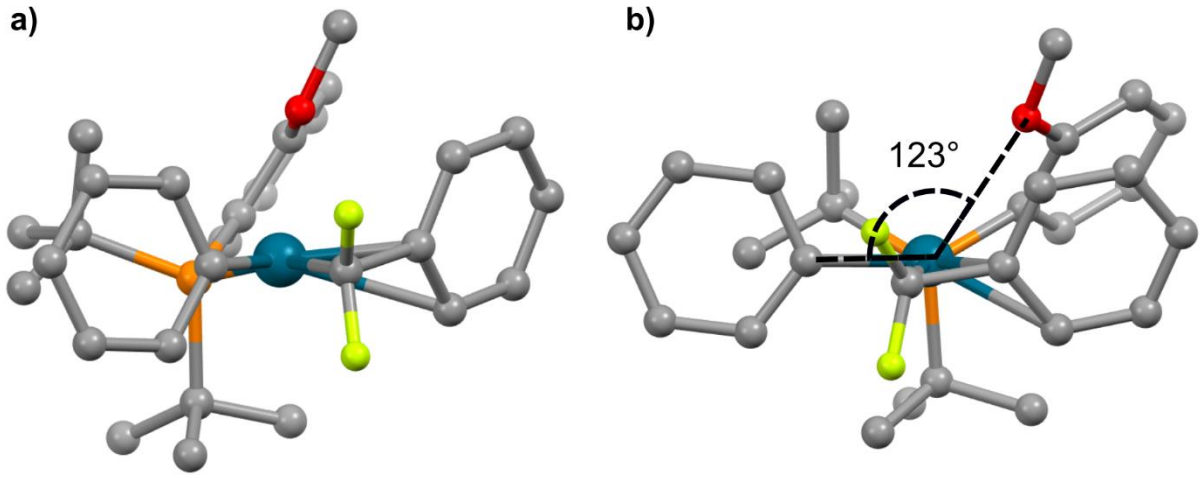


Figure 5.2.1 Different views of **Pd-CF$_2$Ph-TS** showing the unbound methoxy fragment of the **L2** and highlighting the torsion angle φ(C(aryl),Pd,P,O). Hydrogens atoms have been omitted for clarity. Light gray = C, red = O, light green = F, orange = P, dark gray = Pd.

The rates of reductive eliminations of alkylarenes from Pd complexes containing alkyl groups that are more electron-withdrawing (*i.e.*, more electronegative) are generally slower than those from complexes containing alkyl groups that are less electron-withdrawing (less electronegative; *e.g.*, the rate of elimination of aryl–R for R = CH_2Ph > $CH_2C(O)Ph$ > CH_2CN).[12,33–35] We considered that the overall charge of the fluoroalkyl fragments in complexes **Pd-R^F** would serve as a quantitative measure of the electronegativity of these fragments, with more electronegative fragments carrying a greater negative charge. Thus, we compared the free-energy barriers for reductive elimination from complexes **Pd-R^F** with the electronegativity of their R^F fragments by plotting these barriers *vs* the summed QTAIM atomic charges[36] of the R^F fragments in **Pd-R^F-GS** (Figure 5.2.2a). The plot revealed that, overall, the computed barriers to reductive elimination from complexes containing more electronegative fluoroalkyl ligands (*e.g.*, **Pd-CF$_3$**, **Pd-CF$_2$CN**) were generally higher than those from complexes containing less electronegative fluoroalkyl ligands (*e.g.*, **Pd-CFH$_2$**, **Pd-CH$_3$**). This result is consistent with both the preceding discussion of the electronic effects of alkyl ligands and with literature reports of reductive elimination from aryl(fluoroalkyl)palladium complexes. For example, the reductive elimination of fluoroalkylarene from (DPPF)Pd(Ph)(CF_3)[26] containing the more electronegative CF_3 group occurred at a significantly higher temperature (140 °C) than the elimination from the related complex (DPPF)Pd(Ph)(CF_2H) containing the less electronegative CF_2H group (DPPF)Pd(Ph)(CF_2H)[23] (47 °C), despite both reactions proceeding with similar rates ($t_{1/2}$ = 77 min for (DPPF)Pd(Ph)(CF_3), 160 min for (DPPF)Pd(Ph)(CF_2H)).

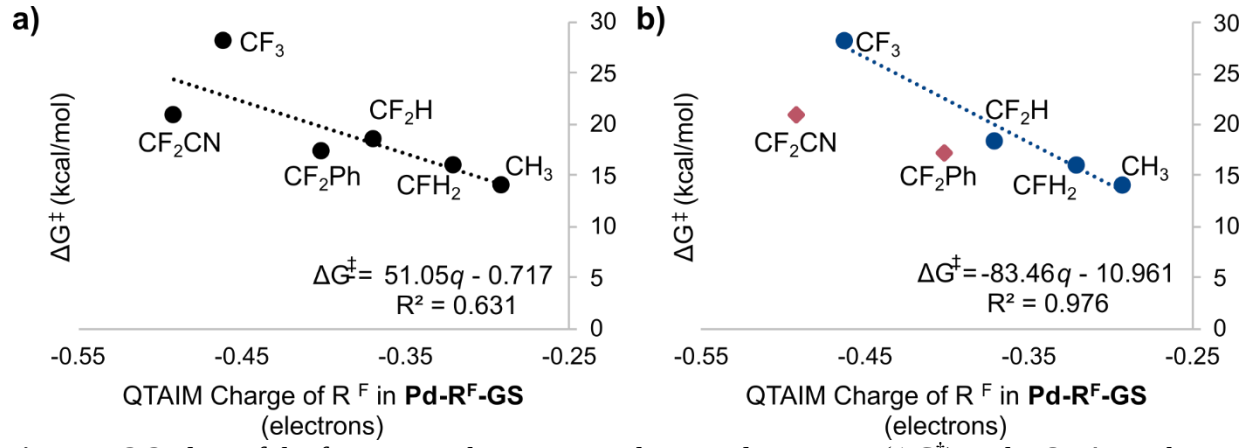


Figure 5.2.2 Plots of the free energy barriers to reductive elimination ($\Delta G^{\ddagger}$) *vs* the QTAIM charges (q) of the R^F fragments of complexes **Pd-R^F**. a) Correlation between $\Delta G^{\ddagger}$ and q for all data points. b) Correlation between $\Delta G^{\ddagger}$ and q considering only unsubstituted perfluoroalkyl ligands (R^F = CF_3, CF_2H, CFH_2, and CH_3, blue circles).

While the correlation between $\Delta G^{\ddagger}$ and the charges of the fragments was modestly linear when all data points were considered (R^2 = 0.63, Figure 5.2.2a), we found a much more linear correlation among the subset of unsubstituted fluoroalkyl ligands (R^F = CF_nH_{3-n}, R^2 = 0.98, Figure 5.2.2b). The difference between these two correlations suggests that interactions of the CN or Ph fragments with the Pd center in **Pd-CF$_2$CN-TS** and **Pd-CF$_2$Ph-TS** lead to a stabilization of these structures that is absent in the transition-state structures of the complexes **Pd-CF$_n$H$_{3-n}$** lacking the π systems of the cyano or phenyl groups (Figure 5.2.3).

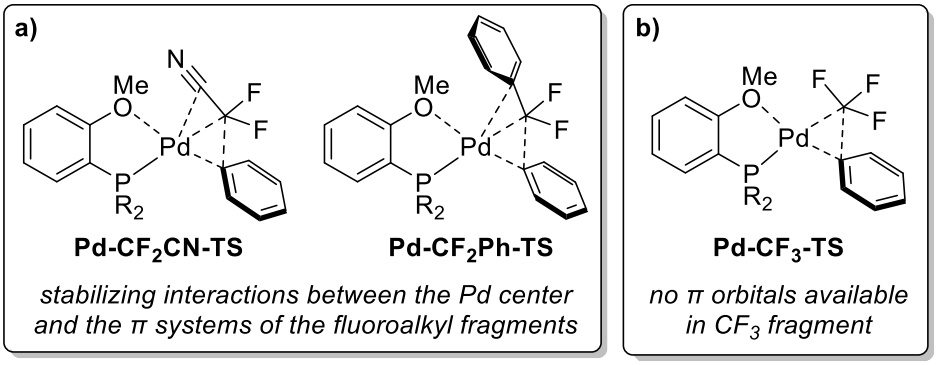


Figure 5.2.3 a) Putative interactions between the Pd center and the π systems of **Pd-CF$_2$CN-TS** and **Pd-CF$_2$Ph-TS**; b) **Pd-CF$_3$-TS**, which cannot experience such interactions

Indeed, a close examination of the transition-state geometries of **Pd-CF$_2$CN** and **Pd-CF$_2$Ph** revealed that the phenyl (for **Pd-CF$_2$Ph-TS**) and nitrile fragments (for **Pd-CF$_2$-CN**) are oriented such that the π orbitals of these fragments could interact with the Pd center (see Figure 5.2.4 for 3D structures). To probe the contacts between these fragments and the Pd center, we conducted IGMH analyses of **Pd-R^F-TS** (R^F = CF_2CN, CF_2Ph).[37,38] Similar to the Noncovalent Interaction (NCI) analysis described by Wang,[39] IGMH analysis is a visual method that classifies interactions in specific regions of space in a molecule according to the sign of the second eigenvalue λ_2 of the Hessian of the calculated electron density (ρ). Regions in which λ_2 is negative are considered bonding-like and stabilizing, while regions in which λ_2 is positive are considered

non-bonded and destabilizing. These two regimes ($\lambda_2 < 0$ and $\lambda_2 > 0$) traditionally are colored blue and red, respectively, in the resulting plots, with stronger interactions (larger ρ) denoted by brighter colors. Regions with low electron density and λ_2 close to zero correspond to van der Waals interactions and are colored green. While a detailed description of IGMH analysis is beyond the scope of this section, we note that the primary advantages of IGMH analysis over NCI analysis in the context of this work are that a) IGMH analyses inherently focus on regions between predefined fragments of interest, whereas NCI analyses are nonspecific and highlight interactions across the entire molecule; and b) IGMH analyses include regions of space with high covalency that would be excluded in conventional NCI analyses.

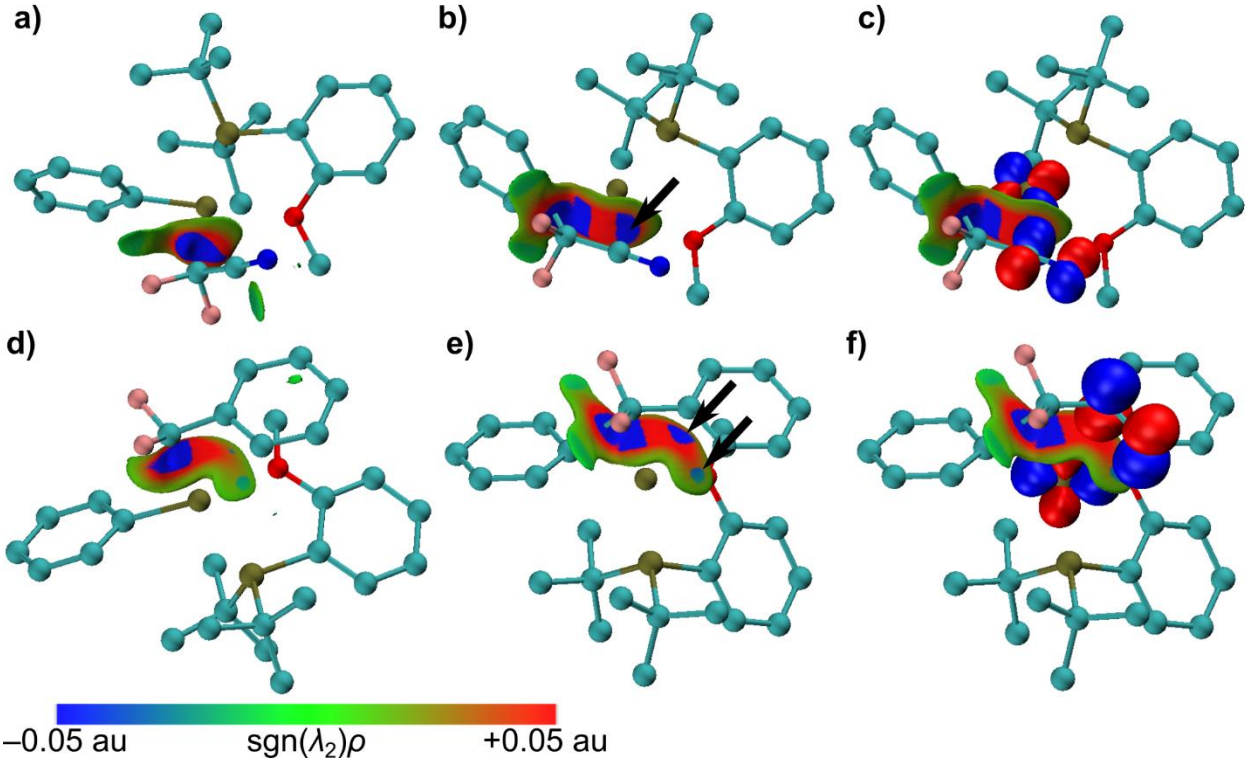


Figure 5.2.4 IGMH plots of a) **Pd-CF$_2$CN-GS'**; b) **Pd-CF$_2$CN-TS**; c) **Pd-CF$_2$CN-TS** overlayed with the leading NBOs responsible for the *d*(Pd)→π^* interaction (see text); d) **Pd-CF$_2$Ph-GS'**; e) **Pd-CF$_2$Ph-TS**; f) **Pd-CF$_2$Ph-TS** overlayed with the leading NBOs responsible for the *d*(Pd)→π^* interaction. Black arrows indicate the regions of space corresponding to the *d*(Pd)→π^* interactions. Hydrogen atoms have been omitted for clarity. Blue isosurfaces = bonding like, stabilizing interactions; green isosurfaces = van der Waals interactions; red isosurfaces = nonbonded, destabilizing interactions.

IGMH plots probing interactions between the R^F ligand and the rest of the molecule are presented for **Pd-CF$_2$CN-TS** and **Pd-CF$_2$Ph-TS**, along with the connected ground-state structures **Pd-CF$_2$CN-GS'** and **Pd-CF$_2$Ph-GS'** in Figure 5.2.4. In the transition-state structures of both complexes, IGMH plots clearly display blue isosurfaces between the Pd center and the electrophilic carbon of the R^F that is α to the difluoromethylene unit (black arrows in Figure 5.2.4b and e, respectively), indicative of stabilizing, bonding interactions. These regions are strongly reminiscent of the stabilizing interaction of occupied *d* orbitals of the Pd center into the π^* orbitals of a fluoroenolate fragment ("*d*(Pd)→π^* interactions") observed in the transition states to reductive

elimination from arylpalladium fluorooxindole complexes (see Chapter 3).[40] Indeed, examination of the second-order perturbations in NBO analyses of the transition-state structures revealed significant donor–acceptor interactions from the mostly-filled *d* orbitals of the Pd center into the mostly-vacant π^* antibonding orbitals of the nitrile (R^F = CF_2CN, E_2^{pert} = 16.6 kcal/mol) or the phenyl ring (R^F = CF_2Ph, E_2^{pert} = 14.0 kcal/mol).[41] The leading *d* and π^* orbitals involved in these interactions are plotted in Figure 5.2.4c and f for **Pd-CF₂CN** and **Pd-CF₂Ph**, respectively. These $d(Pd)\rightarrow\pi^*$ interactions were absent (R^F = CF_2CN) or were significantly reduced (R^F = CF_2Ph) in the connected ground-state structures (red and green isosurfaces in Figure 5.2.4a and d, respectively), demonstrating that the $d(Pd)\rightarrow\pi^*$ are present only in the transition-state structures.

To probe the effect of removing these interactions on the calculated free energy barriers to reductive elimination, the Fock matrix elements corresponding to the $d\rightarrow\pi^*$ interactions were set to zero artificially using the `$NBODEL` keyword list. Subsequent reorthogonalization of the modified wavefunction led to an increase in energy of 13.2 and 8.7 kcal/mol for **Pd-CF₂CN-TS** and **Pd-CF₂Ph-TS**, respectively ($\Delta G^{\ddagger *}$ = 34.2, 26.0 kcal/mol, respectively). Plotting these new energetic barriers and those of the complexes containing CF_nH_{3-n} ligands *vs* the QTAIM charges of the R^F fragment in **Pd-R^F-GS** revealed a strong linear correlation for all data points (Figure 5.2.5, R^2 = 0.95) in an extension of the linear relationship observed for R^F = CF_nH_{3-n} in Figure 5.2.2b. Thus, in the absence of the $d(Pd)\rightarrow\pi^*$ interactions in **Pd-CF₂CN-TS** and **Pd-CF₂Ph-TS**, the barriers to reductive elimination from **Pd-R^F** correlate linearly with the electronegativity of the R^F ligand, with higher barriers for complexes containing more electronegative fluoroalkyl ligands and lower barriers for complexes containing less electronegative fluoroalkyl ligands.

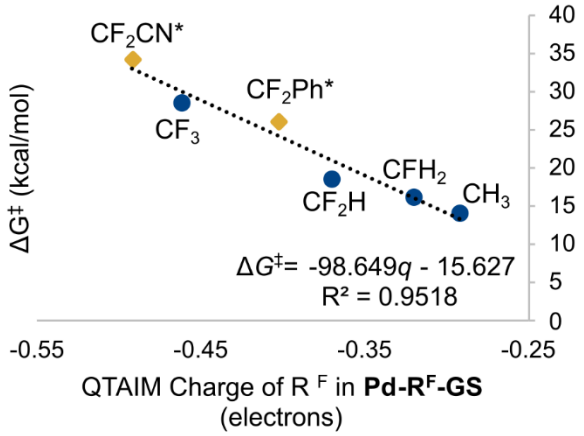
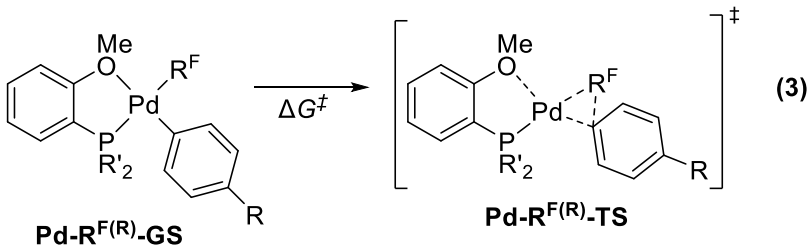


Figure 5.2.5 Plot of the energetic barriers to reductive elimination ($\Delta G^{\ddagger}$) *vs* the QTAIM charge of R^F in **Pd-R^F-GS**. All data points are considered for the linear regression. *Yellow diamonds correspond to transition-state energies resulting from the deletion of $d\rightarrow\pi^*$ interactions.

Finally, we evaluated the effect of modifying the electronic properties of the aryl ligand in complexes **Pd-R^F** on the barriers for reductive elimination from these complexes. The computed free energy barriers to reductive elimination from (**L2**)Pd(aryl)R^F complexes containing 4-cyanophenyl, phenyl, or 4-(dimethylamino)phenyl fragments as the aryl ligands (**Pd-R$^{F(CN)}$**, **Pd-R^F**, and **Pd-R$^{F(NMe2)}$**, respectively; eq 3) are shown in Figure 5.2.6 (see Section 5.6 for a numerical list of energies).[*Note 1*] The electronic properties of the aryl group of complexes containing trifluoromethyl or monofluoromethyl ligands (**Pd-CF$_3^{(R)}$** and **Pd-CFH$_2^{(R)}$**, respectively) did not measurably affect the calculated barriers to reductive elimination. However, the barriers to

reductive elimination from complexes containing difluoromethylene units (**Pd-CF$_2$H$^{(R)}$**, **Pd-CF$_2$CN$^{(R)}$**, and **Pd-CF$_2$Ph$^{(R)}$**) were lower from complexes containing more electron-rich aryl ligands than from complexes containing less electron-rich aryl ligands, a trend that is consistent with the rates of elimination measured experimentally for aryl(difluoromethyl)palladium complexes.[23] In contrast, the trend in barriers to reductive elimination from complexes aryl(methyl)palladium complexes **Pd-CH$_3$$^{(R)}$**, in which the alkyl ligand does not contain fluorine, were the opposite, *i.e.*, the barrier to reductive elimination from aryl(methyl)palladium complexes containing *more* electron-rich aryl ligands was lower than that from complexes containing less electron-rich aryl ligands. This opposite trend in barriers for reductive elimination from complexes containing fluorinated and non-fluorinated alkyl ligands has been observed experimentally for arylpalladium (fluoro)enolate complexes.[12,25,40] While we currently do not have an explanation for the correlation between the electronic properties of the aryl ligand and the barriers to reductive elimination from complexes containing some fluoroalkyl ligands (R^F = CF_2CN, CF_2Ph, CF_2H) but not others (R^F = CF_3, CFH_2), we note that a previous computational study investigating the rates of reductive elimination from several aryl(trifluoromethyl)palladium complexes also revealed no systematic effect of the electronic properties of the arene on the barriers for reductive elimination of trifluoromethylarene.[42]



R^F = CF_3, CF_2H, CFH_2, CH_3, CF_2CN, CF_2Ph
R = CN, H, NMe_2
R' = *t*Bu

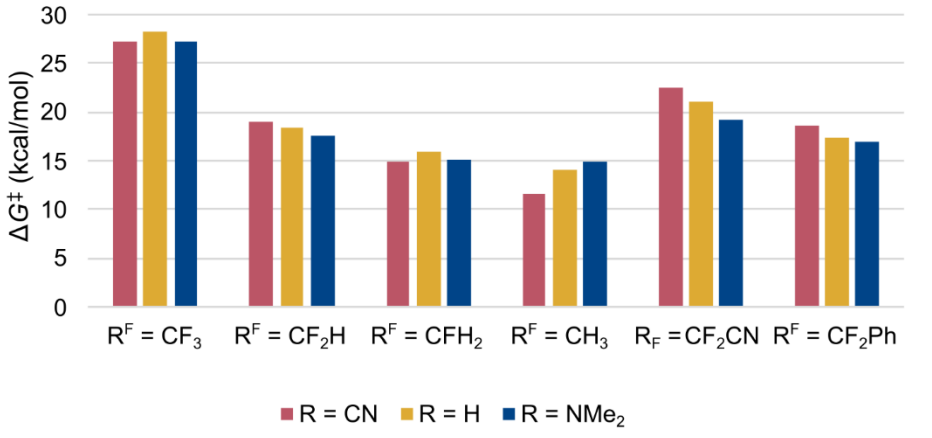


Figure 5.2.6 Free energy barriers to reductive elimination ($\Delta G^{‡}$) for complexes **Pd-R$^{F(R)}$** containing substituted aryl ligands (eq 3)

5.3 Conclusions

In summary, we have conducted DFT calculations to investigate the reductive elimination of fluoroalkylarenes from a series of aryl(fluoroalkyl)palladium complexes containing the dialkyl 2-methoxyphenylphosphine ligand **L2**. In agreement with previous studies of arylpalladium complexes containing 2-alkoxyphenylphosphines, the ligand was found to bind to all species through both the phosphine and methoxy moieties, and the Pd–O bond was found to lengthen significantly in the transition states to reductive elimination.[31] While the calculated free energy barriers to reductive elimination from complexes containing more electronegative fluoroalkyl ligands was higher than those from complexes containing less electronegative fluoroalkyl ligands for $R^F = CF_nH_{3-n}$, the barriers to reductive elimination from **Pd-CF$_2$CN** and **Pd-CF$_2$Ph** were lower than would be predicted from the electronegativities of the CF_2CN and CF_2Ph fragments. IGMH and NBO analyses predict that the transition states to reductive elimination for **Pd-CF$_2$CN** and **Pd-CF$_2$Ph** are stabilized by $d(Pd)\rightarrow\pi^*$ interactions in which occupied *d* orbitals of the Pd center interact with the π^* antibonding orbitals of the CN and Ph fragments. The computed transition-state energies after specifically deleting these interactions by NBO analysis were higher than those for reductive elimination from **Pd-CF$_2$CN** and **Pd-CF$_2$Ph** with inclusion of these interactions, demonstrating that the $d(Pd)\rightarrow\pi^*$ interactions are the origin of the lower barriers to reductive elimination from **Pd-CF$_2$CN** and **Pd-CF$_2$Ph** than would be expected based solely on the electronegativities of the fluoroalkyl fragments. Finally, while the barriers for reductive elimination from (**L2**)Pd(aryl)(R^F) (R^F = CF_3 and CFH_2) complexes containing electron-rich aryl ligands were similar to those for complexes containing electron-poor aryl ligands, the barriers to elimination from (**L2**)Pd(aryl)(R^F) complexes containing other fluoroalkyl ligands (R^F = CF_2H, CF_2CN, CF_2Ph) and more electron-rich aryl ligands were lower than those of complexes containing more electron-poor aryl ligands. In contrast, the barriers for elimination of methylarenes from aryl(methyl)palladium complexes containing electron-rich aryl ligands were *higher* than those for complexes containing less electron-rich ligands. Future work in our group will seek to evaluate these results experimentally.

Overall, our results suggest that reductive eliminations of fluoroalkylarenes from (**L2**)Pd(aryl)(R^F) complexes containing moderately electronegative fluoroalkyl groups (*e.g.*, R^F = CF_2H and CFH_2) or more strongly electronegative fluoroalkyl groups containing electrophilic π^* orbitals (R^F = CF_2CN and CF_2Ph) are generally facile ($\Delta G^{\ddagger} < 25$ kcal/mol). Thus, developing Pd-catalyzed fluoroalkylation reactions that form fluoroalkylarenes containing these or similar fluoroalkyl groups will depend only on identifying suitable reaction conditions and aryl and fluoroalkyl coupling partners. However, fluoroalkylation reactions involving more highly electronegative groups that do not contain electrophilic π^* orbitals (*e.g.*, R^F = perfluoroalkyl) likely will require other ancillary ligands that form aryl(fluoroalkyl)palladium complexes with lower barriers to reductive elimination. Ongoing work in our group seeks to evaluate by DFT calculations whether other functional groups besides those containing electrophilic C=X π^* bonds can lower the barrier to reductive elimination of fluoroalkylarenes (*e.g.*, the SO_2R or $P(O)(OR)_2$ fragments in R^F = CF_2SO_2R or $CF_2P(O)(OR)_2$) and to develop reaction conditions for new Pd-catalyzed fluoroalkylation reactions.

5.4 Footnotes

1. While we are confident in our assessment of the relative barriers to reductive elimination for complexes containing different fluoroalkyl ligands due to the large differences in $\Delta G^{\ddagger}$ ($|\Delta\Delta G^{\ddagger}|$

= 2 – 14 kcal/mol), we note that the differences in energy between complexes containing the same fluoroalkyl ligand but different aryl ligands (*e.g.*, **Pd-CF$_3^{(CN)}$** and **Pd-CF$_3^{(NMe2)}$**) are much closer to the level of error expected for DFT calculations ($|\Delta\Delta G^{\ddagger}|$ = 0.1 – 3 kcal/mol). In ongoing work, we are calculating $\Delta G^{\ddagger}$ for complexes containing a wider range of aryl groups with a wider range of functionals in order to evaluate the accuracy of the results in this report.

5.5 Computational Methods

DFT calculations were conducted at the Molecular Graphics and Computation Facility (MGCF) at the University of California, Berkeley using the Gaussian 16[43] software package. All calculations, including geometry optimizations, were performed in THF solvent using the SMD solvent continuum model reported by Truhlar and co-workers according to the Solvent-Accessible Surface (scrf=sas).[44] Initial geometries were constructed in GaussView[45] and optimize to stationary points (either minima or first-order saddle points) using the PBE0 functional (the hybrid functional based on the Perdew-burke-Ernzerhof functional [PBE][46,47] as described by Adamo[48]) with Grimme's D3 dispersion correction with Becke-Johnson damping (GD3BJ)[49] and the basis sets def2-TZVP (with ECP) for Pd and def2-SVP for all light atoms (**BS1**). The nature of each stationary point was evaluated by accompanying frequency calculations (all positive eigenvalues for minima and exactly one negative eigenvalue for transition states). Several isomers were considered, but only those representing the minimum-energy paths are presented here. Transition states were connected to ground states by following the intrinsic reaction coordinate downhill from the transition state. While in most cases this corresponded to **Pd-R^F-GS**, intermediate ground state structures that were slightly higher in energy than **Pd-R^F-GS** were connected to the transition state **Pd-R^F-TS** for R^F = CF_2CN, CF_2Ph. These structures were labeled **Pd-R^F-GS'**.

Further single-point energy calculations were performed on the optimized geometries with the larger def2-QZVP basis set (with ECP) on Pd (obtained through the Basis Set Exchange,[50] accessed October 2019) and Truhlar's minimally-augmented version of the def2-TZVP basis set ("ma-TZVP") on all light atoms (**BS2**).[51] In all cases, Gibbs free energies for **BS2** were approximated by adding the thermal corrections obtained from frequency calculations using **BS1** to the **BS2** electronic energies.

NBO analyses were conducted with the NBO 6.0 program.[52] d(Pd)→π^* interactions (see main text) were calculated evaluated by summing the E_2^{pert} delocalizations from the five localized lone pairs on the Pd center into π^* orbital of the nitrile fragment that faced the Pd center (C–N(3)*) (for **Pd-CF$_2$CN**) or the nearest localized C=C* bond of the phenyl ring (for **Pd-CF$_2$Ph**). Deletions of the corresponding matrix elements were accomplished using the $NBODEL keyword list.

IGMH analysis[38] was conducted with Multiwfn 3.8(dev)[53] using the default parameters and a grid resolution of 0.1 Bohr. Complexes **Pd-R^F** were partitioned into fragments corresponding to the fluoroalkyl ligand (CF_3, CF_2H, CFH_2, CH_3, CF_2CN, or CF_2Ph) and the rest of the molecule. Grid data were visualized with VMD.[54]

AIM analyses were conducted on **BS2** wavefunctions using AIMAll[55] with Simple connectivity searching and the VeryFine integration mesh. All other parameters were left as their defaults.

5.6 Optimized Structures and Energies

Table 5.6.1 Energies of Optimized Structures

Structure	E(BS1) (Hartree)	Thermal Correction to Free Energy (Hartree)	G(BS1) (Hartree)	E(BS2) (Hartree)	G(BS2) (Hartree)	QTAIM Charge on R^F
Pd-CF_3-GS	-1698.01917984	0.416122	-1697.60305784	-1699.4812436	-1699.0651216	-0.46194
Pd-CF_3-GS-*trans*	-1698.01924144	0.41721	-1697.60203144	-1699.48056496	-1699.06335496	
Pd-CF_3-TS	-1697.97296375	0.413891	-1697.55907275	-1699.43404082	-1699.02014982	
Pd-$CF_3^{(CN)}$-GS	-1790.09297239	0.412966	-1789.68000639	-1791.65900602	-1791.24604002	
Pd-$CF_3^{(CN)}$-TS	-1790.04766994	0.41005	-1789.63761994	-1791.61267497	-1791.20262497	
Pd-$CF_3^{(NMe2)}$-GS	-1831.74135814	0.483613	-1831.25774514	-1833.34419781	-1832.86058481	
Pd-$CF_3^{(NMe2)}$-TS	-1831.6960795	0.480578	-1831.2155015	-1833.29772966	-1832.81715166	
Pd-CF_2H-GS	-1598.92540373	0.425659	-1598.49974473	-1600.26785113	-1599.84219213	-0.370227
Pd-CF_2H-GS-*trans*	-1598.92687099	0.425998	-1598.50087299	-1600.26864855	-1599.84265055	
Pd-CF_2H-TS	-1598.88990875	0.420455	-1598.46945375	-1600.23361337	-1599.81315837	
Pd-CF_2H-TS-*trans*	-1598.89033169	0.422637	-1598.46769469	-1600.23383574	-1599.81119874	
Pd-$CF_2H^{(CN)}$-GS	-1690.99922488	0.421851	-1690.57737388	-1692.44566866	-1692.02381766	
Pd-$CF_2H^{(CN)}$-TS	-1690.9640133	0.417923	-1690.5460903	-1692.41141704	-1691.99349404	
Pd-$CF_2H^{(NMe2)}$-GS	-1732.64737074	0.492358	-1732.15501274	-1734.13055305	-1733.63819505	
Pd-$CF_2H^{(NMe2)}$-TS	-1732.61328882	0.487434	-1732.12585482	-1734.0977065	-1733.6102725	
Pd-CFH_2-GS	-1499.83866046	0.431896	-1499.40676446	-1501.06160835	-1500.62971235	-0.320609
Pd-CFH_2-GS-*trans*	-1499.83885753	0.434013	-1499.40484453	-1501.06127298	-1500.62725998	
Pd-CFH_2-TS	-1499.8124755	0.430428	-1499.3820475	-1501.03467236	-1500.60424436	
Pd-CFH_2-TS-*trans*	-1499.81069384	0.430827	-1499.37986684	-1501.03320315	-1500.60237615	
Pd-$CFH_2^{(CN)}$-GS	-1591.91321654	0.429768	-1591.48344854	-1593.24019838	-1592.81043038	
Pd-$CFH_2^{(CN)}$-TS	-1591.88821652	0.42758	-1591.46063652	-1593.21419093	-1592.78661093	
Pd-$CFH_2^{(NMe2)}$-GS	-1633.56069991	0.500318	-1633.06038191	-1634.92434609	-1634.42402809	
Pd-$CFH_2^{(NMe2)}$-TS	-1633.53447007	0.497438	-1633.03703207	-1634.89748371	-1634.40004571	
Pd-CH_3-GS	-1400.77013308	0.438211	-1400.33192208	-1401.87249526	-1401.43428426	-0.292233
Pd-CH_3-GS-*trans*	-1400.77058701	0.440447	-1400.33014001	-1401.87298367	-1401.43253667	
Pd-CH_3-TS	-1400.74710362	0.437442	-1400.30966162	-1401.84933713	-1401.41189513	
Pd-CH_3-TS-*trans*	-1400.74608615	0.438647	-1400.30743915	-1401.84813045	-1401.40948345	
Pd-$CH_3^{(CN)}$-GS	-1492.8453811	0.437598	-1492.4077831	-1494.05183709	-1493.61423909	
Pd-$CH_3^{(CN)}$-TS	-1492.82415079	0.434304	-1492.38984679	-1494.03000186	-1493.59569786	
Pd-$CH_3^{(NMe2)}$-GS	-1534.49129711	0.504449	-1533.98684811	-1535.73450086	-1535.23005186	
Pd-$CH_3^{(NMe2)}$-TS	-1534.46841356	0.50482	-1533.96359356	-1535.71105774	-1535.20623774	
Pd-CF_2CN-GS	-1690.99013764	0.420518	-1690.56961964	-1692.43488837	-1692.01437037	-0.491634
Pd-CF_2CN-GS'	-1690.98893894	0.42169	-1690.56724894	-1692.43360756	-1692.01191756	

Structure	E(BS1) (Hartree)	Thermal Correction to Free Energy (Hartree)	G(BS1) (Hartree)	E(BS2) (Hartree)	G(BS2) (Hartree)	QTAIM Charge on R^F
Pd-CF_2CN-GS-*trans*	-1690.9886694	0.421971	-1690.5666984	-1692.43302078	-1692.01104978	
Pd-CF_2CN-TS	-1690.95421954	0.418819	-1690.53540054	-1692.39968294	-1691.98086394	
Pd-CF_2CN-TS-*trans*	-1690.95165145	0.420908	-1690.53074345	-1692.39588271	-1691.97497471	
Pd-$CF_2CN^{(CN)}$-GS	-1783.06310284	0.417129	-1782.64597384	-1784.61180975	-1784.19468075	
Pd-$CF_2CN^{(CN)}$-TS	-1783.02519909	0.415536	-1782.60966309	-1784.57428785	-1784.15875185	
Pd-$CF_2CN^{(NMe2)}$-GS	-1824.71273392	0.487287	-1824.22544692	-1826.29821627	-1825.81092927	
Pd-$CF_2CN^{(NMe2)}$-TS	-1824.67976005	0.485588	-1824.19417205	-1826.26590396	-1825.78031596	
Pd-CF_2Ph-GS	-1829.56765022	0.501121	-1829.06652922	-1831.14484737	-1830.64372637	-0.401886
Pd-CF_2Ph-GS'	-1829.56049309	0.499557	-1829.06093609	-1831.13956335	-1830.64000635	
Pd-CF_2Ph-GS-*trans*	-1829.56743184	0.500749	-1829.06668284	-1831.14410393	-1830.64335493	
Pd-CF_2Ph-TS	-1829.53662346	0.499538	-1829.03708546	-1831.11567441	-1830.61613641	
Pd-CF_2Ph-TS-*trans*	-1829.52037907	0.497414	-1829.02296507	-1831.09736497	-1830.59995097	
Pd-CF_2Ph-CN-GS	-1921.64253949	0.497157	-1921.14538249	-1923.32371844	-1922.82656144	
Pd-$CF_2Ph^{(CN)}$-TS	-1921.61024786	0.496388	-1921.11385986	-1923.29316482	-1922.79677682	
Pd-$CF_2Ph^{(NMe2)}$-GS	-1963.29094662	0.568868	-1962.72207862	-1965.00916054	-1964.44029254	
Pd-$CF_2Ph^{(NMe2)}$-TS	-1963.26026177	0.566656	-1962.69360577	-1964.97999326	-1964.41333726	

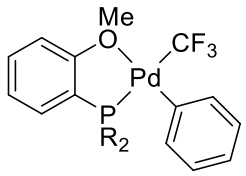
Table 5.6.2 Free Energy Barriers to Reductive Elimination for complexes **Pd-R$^{F(R)}$** (TS – GS)

Complex	$\Delta G^{\ddagger}$ (kcal/mol)
Pd-CF_3	28.2
Pd-$CF_3^{(CN)}$	27.2
Pd-$CF_3^{(NMe2)}$	27.3
Pd-CF_2H	18.5
Pd-$CF_2H^{(CN)}$	19.0
Pd-$CF_2H^{(NMe2)}$	17.5
Pd-CFH_2	16.0
Pd-$CFH_2^{(CN)}$	14.9
Pd-$CFH_2^{(NMe2)}$	15.0
Pd-CH_3	14.0
Pd-$CH_3^{(CN)}$	11.6
Pd-$CH_3^{(NMe2)}$	14.9
Pd-CF_2CN	21.0
Pd-$CF_2CN^{(CN)}$	22.5
Pd-$CF_2CN^{(NMe2)}$	19.2
Pd-CF_2Ph	17.3
Pd-$CF_2Ph^{(CN)}$	18.7
Pd-$CF_2Ph^{(NMe2)}$	16.9

Table 5.6.3 Energies Resulting from the Deletion of d(Pd)→π^* Interactions

Complex	E^* Hartree	$\Delta G^{\ddagger *}$ (kcal/mol)
Pd-CF_2CN-TS	-1692.37868598	34.2
Pd-CF_2Ph-TS	-1831.10187718	26.0

$\Delta G^{\ddagger *}$ was calculated by adding the thermal correction of the corresponding structures in Table 5.6.1 to E^* and subtracting the corresponding unmodified ground-state energies.



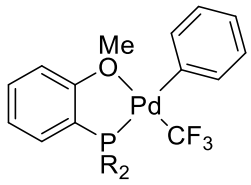
Pd-CF_3-GS

58

Pd-CF3-GS

C	2.38723100	1.41225500	0.14370000
C	2.45068300	0.01211400	0.28686400
C	3.68043500	-0.54011000	0.66425600
C	4.80000500	0.24846900	0.91320400
C	4.70589900	1.62874400	0.77609700
C	3.50492400	2.21342900	0.38706300
H	3.77360800	-1.62002400	0.75998200
H	5.74114900	-0.21826000	1.20965700
H	5.57235700	2.26469300	0.97094400
H	3.43997400	3.29627000	0.28638000
P	0.93034500	-0.97304700	-0.06566100
O	1.20065100	1.95349000	-0.25293500
C	1.18941000	3.26262000	-0.80153700
H	1.98321300	3.35983800	-1.55849800
C	0.84797200	-2.34045100	1.24037000
C	1.25857200	-1.63103200	-1.80680100
C	2.65854700	-2.20275400	-2.01320100
H	2.87094600	-3.06076200	-1.36122900
H	2.75238900	-2.55554600	-3.05411700
H	3.43999800	-1.44602500	-1.85420600
C	0.20062100	-2.68105800	-2.14650300
H	-0.81678600	-2.33948100	-1.90573600
H	0.23625900	-2.89665900	-3.22729400
H	0.37777900	-3.63110200	-1.62212600
C	1.07921500	-0.41399500	-2.72052000
H	0.07256100	0.02320500	-2.62868200
H	1.81193200	0.37702600	-2.49762500
H	1.22983800	-0.71688900	-3.77002900
C	-0.55535300	-2.95285600	1.17817100
H	-1.34378800	-2.20017100	1.29201600
H	-0.74372100	-3.49229600	0.24090600
H	-0.65801400	-3.68001600	2.00064600
C	1.00030800	-1.61396100	2.58033800
H	0.30690600	-0.75990600	2.65133400
H	0.76117700	-2.30877700	3.40193800
H	2.01988900	-1.23635400	2.74310500
C	1.85984600	-3.47978600	1.12584000
H	2.90713700	-3.16407400	1.21015800

H	1.67978400	-4.18897900	1.95088100
H	1.74262000	-4.04538600	0.19091300
Pd	-0.72605100	0.74611000	0.01740200
C	-2.39064400	-0.30590100	0.07152300
C	-2.90876200	-0.86834400	-1.10188800
C	-3.07728400	-0.53101700	1.27311300
C	-4.05037800	-1.67235100	-1.06838500
H	-2.42570900	-0.67570600	-2.06371800
C	-4.21426800	-1.33792200	1.30634900
H	-2.72072700	-0.07401600	2.19955100
C	-4.70208900	-1.92022800	0.13729000
H	-4.43298600	-2.10481000	-1.99732500
H	-4.72633800	-1.50930000	2.25746800
H	-5.59293200	-2.55258700	0.16438200
C	-1.90178900	2.40173900	0.13609800
F	-1.23034500	3.34873000	0.86834500
F	-3.12555500	2.36044600	0.68094000
F	-2.07559700	2.98621100	-1.08925300
H	0.21083600	3.39468800	-1.27311900
H	1.31349700	4.02402200	-0.01757400



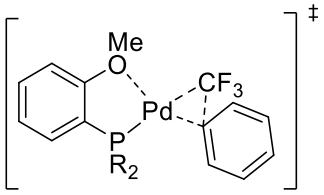
Pd-CF_3-GS-*trans*

58

Pd-CF3-GS-trans

C	-1.03254200	2.32797800	-0.13928400
C	-2.01928500	1.33133200	-0.00102100
C	-3.34230000	1.75440300	0.18390900
C	-3.69166500	3.09975800	0.23695900
C	-2.69853600	4.06293200	0.10310800
C	-1.37391000	3.68333800	-0.08510500
H	-4.12844000	1.00962400	0.29107400
H	-4.73372100	3.38945600	0.38403000
H	-2.94784300	5.12557500	0.14644300
H	-0.60926600	4.45226900	-0.18045500
P	-1.51934200	-0.44391600	-0.00826700
O	0.25928700	1.93180300	-0.32515000
C	1.23491800	2.91591200	-0.63810700
H	0.90944100	3.51144500	-1.50478200
C	-2.35735800	-1.15096500	-1.55228200
C	-2.20533800	-1.12751200	1.62361100

C	-3.71141500	-1.37511600	1.66648900
H	-3.97836200	-1.76861100	2.66165000
H	-4.30617700	-0.46378800	1.52151300
H	-4.03360600	-2.12476900	0.92995600
C	-1.47849700	-2.44074300	1.92710100
H	-1.84064900	-2.82799300	2.89404700
H	-1.65748700	-3.21536600	1.17046300
H	-0.39311700	-2.29609300	2.00614500
C	-1.80579400	-0.10752400	2.69428300
H	-2.37179300	0.83146600	2.61745600
H	-1.99542800	-0.53654200	3.69191200
H	-0.73116500	0.13312300	2.63653900
C	-1.47962600	-0.64846500	-2.70385400
H	-0.44745300	-1.02169100	-2.61793300
H	-1.89424900	-0.99755600	-3.66431600
H	-1.44185000	0.45216000	-2.74002900
C	-3.79505700	-0.69585900	-1.78993700
H	-3.86716300	0.38770900	-1.95607200
H	-4.17363100	-1.18861800	-2.70116800
H	-4.47384900	-0.97253400	-0.97113600
C	-2.30474200	-2.67789000	-1.50611300
H	-2.97546200	-3.09461100	-0.74037400
H	-2.63937100	-3.07542400	-2.47871100
H	-1.28963500	-3.04939100	-1.32126100
Pd	0.87011000	-0.26010900	-0.06880700
C	2.81437100	0.24658900	0.05245200
C	3.68205900	0.25743800	-1.04886800
C	3.27096000	0.81103800	1.25337700
C	4.94345700	0.85058000	-0.96666000
H	3.37120400	-0.20601700	-1.98911500
C	4.53398500	1.39932800	1.34104100
H	2.62955900	0.80132700	2.14061900
C	5.37233300	1.42795800	0.22768300
H	5.59920200	0.85652000	-1.84226300
H	4.86615700	1.83663100	2.28714900
H	6.36075500	1.89010400	0.29326900
C	1.53396300	-2.12593400	-0.00225700
F	2.08475600	-2.46747400	1.18146500
F	2.44897800	-2.42549600	-0.94542700
F	0.55131300	-3.05445500	-0.20010300
H	1.42408700	3.57016000	0.22674900
H	2.15475900	2.37613200	-0.88365700



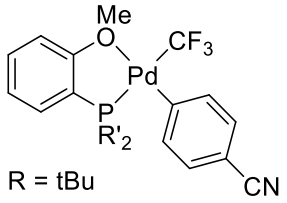
Pd-CF_3-TS

58

Pd-CF3-TS

C	-2.46084100	-1.57327300	0.26946600
C	-2.57076200	-0.16342600	0.29362700
C	-3.80789100	0.38230700	0.65299100
C	-4.89847700	-0.41273700	0.99658800
C	-4.76226500	-1.79590000	0.97715700
C	-3.55117700	-2.37817800	0.61425900
H	-3.92633200	1.46508300	0.66524900
H	-5.84724800	0.04972300	1.27531500
H	-5.60495300	-2.43818800	1.24363300
H	-3.46250400	-3.46407200	0.60178100
P	-1.08466900	0.83956200	-0.13332000
O	-1.27100400	-2.09942400	-0.10748700
C	-1.09583800	-3.49625200	-0.14707800
H	-1.80241800	-3.96860500	-0.84955400
C	-1.00771600	2.27656100	1.10016800
C	-1.46539900	1.41238500	-1.89703500
C	-2.85752000	2.00418300	-2.09826600
H	-3.03169300	2.90531400	-1.49544500
H	-2.97977000	2.29304600	-3.15616700
H	-3.64839700	1.27589100	-1.86759900
C	-0.38884300	2.41046900	-2.32298100
H	0.62208300	2.03418700	-2.10165900
H	-0.45660200	2.58311400	-3.41021400
H	-0.50844400	3.38740100	-1.83246000
C	-1.33723400	0.14794300	-2.75216000
H	-0.33080600	-0.29290200	-2.67058600
H	-2.06887300	-0.62148600	-2.46105400
H	-1.52166400	0.39863600	-3.81039300
C	0.41056900	2.85162700	0.99980500
H	1.17515000	2.07732000	1.14327400
H	0.60493400	3.33698300	0.03424000
H	0.54505800	3.61512400	1.78431900
C	-1.16439000	1.63138300	2.47967400
H	-0.47680000	0.77757000	2.59646200
H	-0.91731900	2.37024500	3.25990000
H	-2.18665600	1.27191800	2.66522000
C	-2.00561200	3.41925400	0.92728600

H	-3.05573100	3.10872900	1.00893400
H	-1.83410100	4.16393600	1.72294500
H	-1.87409100	3.94251400	-0.03043900
Pd	0.71482800	-0.63241700	-0.05984500
C	2.59295100	0.00772000	0.12729800
C	3.13627200	0.73031900	-0.95632300
C	3.03054300	0.32540200	1.42943400
C	3.98221900	1.80875700	-0.72814100
H	2.86712700	0.45367700	-1.97885500
C	3.88576800	1.40320100	1.64319100
H	2.67512100	-0.26699000	2.27583400
C	4.35592000	2.16061600	0.57145900
H	4.36032900	2.38276300	-1.57859300
H	4.18672100	1.65405900	2.66399600
H	5.02640700	3.00552800	0.74325100
C	2.57948400	-1.87022500	-0.09934300
F	2.31461000	-2.58094300	1.01859700
F	3.90701000	-1.97370400	-0.27152400
F	2.07972400	-2.58861900	-1.15455500
H	-0.07242400	-3.66511400	-0.50120300
H	-1.21082400	-3.94566900	0.85331100



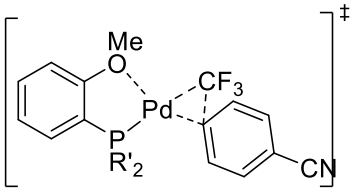
Pd-CF_3-CN-GS

59

Generated by Multiwfn

C	-2.95041900	0.90941400	-0.16181500
C	-2.70456800	-0.47065700	-0.29549400
C	-3.78068300	-1.28285700	-0.67314400
C	-5.04469400	-0.76030600	-0.92973800
C	-5.25649100	0.60788900	-0.80123000
C	-4.21506100	1.44474800	-0.41318900
H	-3.63371700	-2.35738600	-0.76359500
H	-5.85929800	-1.42362100	-1.22598700
H	-6.24061800	1.03666200	-1.00282300
H	-4.38968800	2.51611800	-0.32010300
P	-1.00851900	-1.09576500	0.06805300
O	-1.91201600	1.70158100	0.23405400
C	-2.19488100	2.97329400	0.80128400
H	-2.99432700	2.87923900	1.55224800
C	-0.61954400	-2.41581600	-1.23041500

C	-1.18359500	-1.79737100	1.81357900
C	-2.41810200	-2.67091000	2.01935500
H	-2.42454600	-3.56129100	1.37667400
H	-2.43665700	-3.02498400	3.06371500
H	-3.35005400	-2.11350100	1.84822800
C	0.08414900	-2.57679500	2.16313900
H	0.99758100	-2.01034500	1.92984400
H	0.09136100	-2.79426500	3.24393100
H	0.13501600	-3.54230200	1.63978200
C	-1.28982900	-0.56594500	2.71937600
H	-0.40654300	0.08626500	2.63289200
H	-2.18038900	0.03828800	2.48724100
H	-1.37619100	-0.88958700	3.76976000
C	0.88779300	-2.68440100	-1.17648200
H	1.47539200	-1.77392500	-1.33753500
H	1.21063800	-3.12531300	-0.22435400
H	1.14741100	-3.40023700	-1.97365000
C	-0.94558900	-1.76015800	-2.57588300
H	-0.47593400	-0.76633300	-2.66051500
H	-0.55100900	-2.38675400	-3.39222700
H	-2.02597400	-1.63761500	-2.73656700
C	-1.33985400	-3.75662800	-1.09382100
H	-2.43319200	-3.68948300	-1.15356900
H	-1.02038600	-4.40944900	-1.92296000
H	-1.07592700	-4.27574600	-0.16189300
Pd	0.22708700	0.94967800	-0.01823400
C	2.08438100	0.30987200	-0.04979000
C	2.71815800	-0.08841600	1.13695100
C	2.81792200	0.23562300	-1.24560700
C	4.01589800	-0.58888700	1.12983000
H	2.19720600	-0.00204000	2.09359400
C	4.11233700	-0.26676000	-1.26662500
H	2.37015200	0.57580800	-2.18196500
C	4.72245800	-0.69442900	-0.07680400
H	4.49163700	-0.89991700	2.06248100
H	4.66400600	-0.32922600	-2.20713100
C	1.00435100	2.82747400	-0.14263700
F	0.13675300	3.59790300	-0.86956500
F	2.20390700	3.04850400	-0.69950400
F	1.05770800	3.43317700	1.08017200
H	-1.27330100	3.31249900	1.28405400
H	-2.48072200	3.69947700	0.02657500
C	6.05176600	-1.22054400	-0.09315200
N	7.12932100	-1.65046600	-0.10666800



R' = tBu

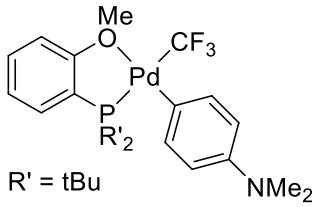
Pd-CF_3-CN-TS

59

Generated by Multiwfn

C	-3.02248900	1.04581600	-0.34025000
C	-2.80901000	-0.35087400	-0.31567400
C	-3.88906700	-1.17687100	-0.64671800
C	-5.13144400	-0.66200500	-1.00720900
C	-5.31348600	0.71578500	-1.03407100
C	-4.26670000	1.57054500	-0.70084300
H	-3.75893100	-2.25806700	-0.62207600
H	-5.95028300	-1.33690600	-1.26314100
H	-6.28018200	1.14011100	-1.31482800
H	-4.42772000	2.64774400	-0.72608700
P	-1.13878800	-0.97730100	0.14157100
O	-1.98032700	1.84419100	0.00626600
C	-2.14122500	3.24575400	0.02807700
H	-2.94303400	3.54276500	0.72339000
C	-0.71390800	-2.37686700	-1.05973300
C	-1.38278500	-1.57388400	1.91980300
C	-2.59802200	-2.47216600	2.13373600
H	-2.55107600	-3.40351600	1.55416000
H	-2.65416900	-2.75563400	3.19837300
H	-3.53699200	-1.95651500	1.88618900
C	-0.10541600	-2.28013000	2.37417000
H	0.79265100	-1.68494800	2.14749400
H	-0.14107300	-2.43577400	3.46524300
H	0.01092800	-3.27050600	1.91075000
C	-1.56589100	-0.29271200	2.73941400
H	-0.69335600	0.37392000	2.64975400
H	-2.45794600	0.27169100	2.42670000
H	-1.69406500	-0.55231300	3.80349800
C	0.79639600	-2.60894900	-0.93571500
H	1.36491800	-1.68386800	-1.09420400
H	1.08517700	-3.01558600	0.04246200
H	1.11202100	-3.33832800	-1.70004900
C	-1.00172700	-1.81234100	-2.45337400
H	-0.52965500	-0.82508100	-2.58736100
H	-0.58382800	-2.48987800	-3.21596000
H	-2.07763100	-1.70323200	-2.65096500

C	-1.42662300	-3.71324200	-0.86608800
H	-2.51861200	-3.65170100	-0.96218600
H	-1.08067000	-4.41448700	-1.64394400
H	-1.18952300	-4.17315900	0.10356500
Pd	0.22695200	0.89722200	0.04000800
C	2.18787300	0.68436100	-0.03596800
C	2.85127400	0.19104300	1.11471500
C	2.77210200	0.41636200	-1.29849000
C	3.95168100	-0.63796600	0.99933800
H	2.47115300	0.44611300	2.10669800
C	3.87878900	-0.40716200	-1.41141100
H	2.32657800	0.84645800	-2.19838800
C	4.47620700	-0.96230800	-0.26639300
H	4.42303900	-1.04728000	1.89551300
H	4.29202400	-0.63400200	-2.39654700
C	1.78159900	2.53866300	0.07805900
F	1.32971500	3.14351700	-1.04262600
F	3.05648100	2.92897400	0.19468300
F	1.16153200	3.13254800	1.13623200
H	-1.18981300	3.65753700	0.38315900
H	-2.35398300	3.64121100	-0.97857600
C	5.60700800	-1.82342500	-0.38318400
N	6.52547600	-2.52756000	-0.47778200



Pd-CF_3-NMe_2-GS

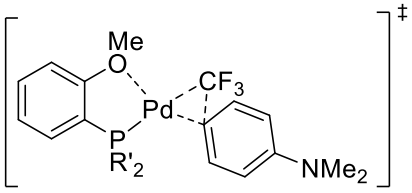
66

Generated by Multiwfn

C	-3.30611300	0.69420000	-0.15228600
C	-2.93003400	-0.65631200	-0.29599700
C	-3.92653700	-1.56328300	-0.67581500
C	-5.23520700	-1.16231000	-0.92898000
C	-5.57537800	0.17878300	-0.79316900
C	-4.61713100	1.10763700	-0.40019100
H	-3.67935900	-2.61888800	-0.76829500
H	-5.98369500	-1.89875100	-1.22727000
H	-6.59596000	0.51395400	-0.99143400
H	-4.89281100	2.15681000	-0.29964700
P	-1.17817900	-1.12044500	0.05737800
O	-2.34968800	1.57746900	0.24964300
C	-2.74872900	2.82676600	0.79147700

H	-3.53725400	2.67528600	1.54517100
C	-0.66305900	-2.36172200	-1.27602100
C	-1.29325400	-1.88555200	1.78159100
C	-2.45048600	-2.86276200	1.96808500
H	-2.39330900	-3.72668300	1.29206100
H	-2.42686100	-3.25533000	2.99875400
H	-3.42667100	-2.37747500	1.82655800
C	0.03471200	-2.56878000	2.10860700
H	0.89985000	-1.93153400	1.87373100
H	0.06889200	-2.80042400	3.18622600
H	0.15198400	-3.52025600	1.57005800
C	-1.49619200	-0.68983600	2.71827400
H	-0.67069100	0.03511000	2.64182300
H	-2.43427300	-0.15531400	2.50158700
H	-1.55115600	-1.04385100	3.76124500
C	0.85815400	-2.52792600	-1.19041800
H	1.38602000	-1.56751100	-1.22288700
H	1.17680400	-3.05273400	-0.28059900
H	1.19388900	-3.13123800	-2.05017800
C	-1.00208700	-1.66865100	-2.59944700
H	-0.58226100	-0.64990000	-2.63312600
H	-0.56452900	-2.24009600	-3.43438600
H	-2.08572600	-1.59481800	-2.77131900
C	-1.28952000	-3.75415400	-1.22185700
H	-2.37842400	-3.76306800	-1.35603900
H	-0.86935100	-4.35642700	-2.04468800
H	-1.04873200	-4.28220700	-0.28849700
Pd	-0.13894100	1.02925800	0.00455100
C	1.76936100	0.52984200	-0.02181800
C	2.41809800	0.11466100	1.14450200
C	2.52994600	0.54573600	-1.19627700
C	3.74183400	-0.32438300	1.13692000
H	1.89287900	0.13608000	2.10363600
C	3.85040500	0.10463800	-1.22331000
H	2.08891600	0.90845200	-2.12828000
C	4.48835400	-0.36642300	-0.05723100
H	4.19139800	-0.63294700	2.08111400
H	4.38813800	0.13648300	-2.17122900
C	0.47163700	2.96355700	-0.10699300
F	-0.45457400	3.65934700	-0.84689700
F	1.65160200	3.30392600	-0.64371900
F	0.44680400	3.57596700	1.11754800
H	-1.86193600	3.25815000	1.26579500
H	-3.09948800	3.50930400	0.00342500
N	5.78986000	-0.83648200	-0.08269300
C	6.45226800	-1.14891400	1.15033200

H	7.45425800	-1.54419200	0.93769400
H	6.57050700	-0.27227700	1.81906000
H	5.91130600	-1.92583200	1.71835700
C	6.56509000	-0.70734700	-1.28255200
H	6.08970900	-1.22638500	-2.13302900
H	6.72915400	0.34601600	-1.58751100
H	7.54998200	-1.16899400	-1.13311900



R' = tBu

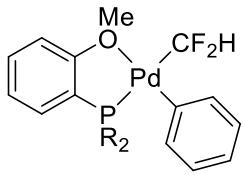
Pd-CF_3-NMe_2-TS

66

Generated by Multiwfn

C	-3.39443700	0.74950500	-0.48788800
C	-3.00498800	-0.60752700	-0.39457700
C	-3.94027800	-1.57573900	-0.77567700
C	-5.20588100	-1.24075000	-1.25094200
C	-5.56129100	0.09972400	-1.34541500
C	-4.66385300	1.09331400	-0.96518100
H	-3.67380000	-2.62915800	-0.69870800
H	-5.90713700	-2.02512200	-1.54225300
H	-6.54894600	0.38514700	-1.71543200
H	-4.96017600	2.13904800	-1.04171700
P	-1.30291900	-0.99055700	0.20059100
O	-2.50023100	1.68298700	-0.09035900
C	-2.81692300	3.05061900	-0.18830900
H	-3.69135700	3.30622400	0.43349200
C	-0.63358600	-2.38428500	-0.89884500
C	-1.61181300	-1.56025900	1.98074900
C	-2.72936100	-2.58516600	2.15164600
H	-2.53571500	-3.52417500	1.61624000
H	-2.83210100	-2.83675200	3.22124000
H	-3.69957600	-2.19077500	1.81668800
C	-0.29915400	-2.09697300	2.55146200
H	0.53705900	-1.40604400	2.36165600
H	-0.39600100	-2.22166400	3.64318100
H	-0.03478200	-3.08031700	2.13577900
C	-1.99447000	-0.28177600	2.73285600
H	-1.19741100	0.47620400	2.66756500
H	-2.91962500	0.16569100	2.33787300
H	-2.16608500	-0.51637600	3.79709100

C	0.88294100	-2.41755600	-0.67059500
H	1.34029800	-1.43358000	-0.83697700
H	1.15225300	-2.74271800	0.34311100
H	1.33764500	-3.13205400	-1.37747400
C	-0.88767100	-1.91990700	-2.33539500
H	-0.53050800	-0.88756900	-2.48438200
H	-0.33584700	-2.57028000	-3.03434700
H	-1.95191200	-1.95402300	-2.60924500
C	-1.18484100	-3.79209700	-0.68651500
H	-2.26658700	-3.87580500	-0.85573700
H	-0.69963500	-4.47638500	-1.40325800
H	-0.96243200	-4.17642100	0.31902900
Pd	-0.08130900	0.99528200	0.11314400
C	1.92065300	1.04770600	0.02588700
C	2.61875400	0.57657400	1.15316300
C	2.50973800	0.83399400	-1.23065600
C	3.77608400	-0.17503600	1.02373800
H	2.22935300	0.78062100	2.15386700
C	3.67556500	0.08833300	-1.36797100
H	2.03029400	1.23677500	-2.12568700
C	4.33793500	-0.44895700	-0.24507100
H	4.25385100	-0.54985000	1.92895800
H	4.06965600	-0.07435100	-2.37103500
C	1.21657000	2.79158100	0.14619300
F	0.96493200	3.29878600	-1.07670500
F	2.37229700	3.35910400	0.54207500
F	0.30874500	3.39289900	1.00162700
H	-1.93990200	3.59222500	0.18383400
H	-3.00776600	3.34700300	-1.23342700
N	5.49140800	-1.19441800	-0.37430100
C	5.96576500	-1.54468300	-1.68254000
H	5.24084700	-2.15758700	-2.25408500
H	6.19536200	-0.65158600	-2.29032700
H	6.89412300	-2.12307600	-1.59291300
C	6.07042300	-1.81733300	0.78172300
H	6.98379600	-2.35145300	0.49034600
H	6.35745800	-1.07696900	1.54924700
H	5.39224900	-2.54938500	1.26330000



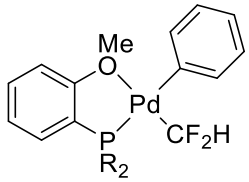
Pd-CF_2H-GS

58

Pd-CF2H-GS

C	2.42480200	-1.27867000	0.11363100
C	2.38099300	0.12707700	0.21192500
C	3.57671600	0.79016800	0.51305600
C	4.76800600	0.10535400	0.73429500
C	4.78007500	-1.28206400	0.64814100
C	3.61571100	-1.97587200	0.33432900
H	3.58194100	1.87704600	0.57123900
H	5.67990000	0.65662500	0.97109700
H	5.70296300	-1.83942300	0.82399200
H	3.63931000	-3.06301000	0.27287400
P	0.76944500	0.97820600	-0.06846900
O	1.27358900	-1.92867700	-0.21562700
C	1.34056800	-3.28855500	-0.61853200
H	0.35831200	-3.53812300	-1.02988500
C	0.98180500	1.73893600	-1.78479400
C	0.59973100	2.26838400	1.30668500
C	0.85527200	1.49293400	2.60275300
H	1.90890800	1.19994800	2.71711700
H	0.58266100	2.12232500	3.46577900
H	0.24143300	0.57811700	2.64703100
C	1.50352000	3.49726000	1.23120100
H	1.27716200	4.15241000	2.08913600
H	2.57464500	3.26593800	1.29048600
H	1.32424200	4.09045400	0.32339700
C	-0.85630600	2.74576100	1.30681500
H	-1.11321700	3.32515600	0.41042200
H	-1.56656500	1.91312800	1.37800700
H	-1.01300500	3.40367800	2.17779000
C	2.30862100	2.45667700	-2.01524600
H	2.46228300	3.30291300	-1.33190000
H	3.16658500	1.77580700	-1.92224200
H	2.32418700	2.86190300	-3.04119500
C	-0.18635500	2.68984000	-2.04649200
H	-0.08483300	3.63171300	-1.48798800
H	-0.21190800	2.94998700	-3.11782300
H	-1.15540300	2.23856900	-1.78722500
C	0.89170000	0.54397100	-2.73999200
H	0.97857200	0.89599200	-3.78149800
H	1.70457400	-0.17863100	-2.56679500
H	-0.06383600	0.00655600	-2.63473600
Pd	-0.74289900	-0.87847500	0.01974200
C	-2.51520300	-0.01142500	0.08856700
C	-3.23423800	0.09574400	1.29014900
C	-3.09880600	0.52469800	-1.06899600
C	-4.45995500	0.76113100	1.34252600

H	-2.82747500	-0.33898800	2.20818700
C	-4.32866100	1.18399500	-1.01922800
H	-2.59333900	0.42398600	-2.03339300
C	-5.01087600	1.31559400	0.18861500
H	-4.99010500	0.84316300	2.29581100
H	-4.75754000	1.59597900	-1.93734000
H	-5.97104000	1.83592500	0.22809000
C	-1.80601700	-2.59444600	0.18656700
F	-1.83695100	-3.28029600	-1.01198900
F	-1.13161400	-3.42601500	1.05869900
H	2.11231400	-3.41398200	-1.39392500
H	1.54947600	-3.94549700	0.23885200
H	-2.84777100	-2.54565800	0.54429900



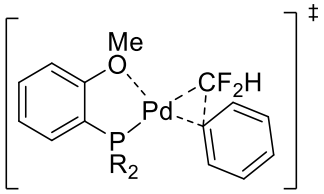
Pd-CF_2H-GS-*trans*

58

Pd-CF2H-GS-trans

C	0.83343000	2.31067100	0.04084100
C	1.86290200	1.36014100	-0.11188800
C	3.14834100	1.84218500	-0.38889200
C	3.41929900	3.20040100	-0.52314500
C	2.38441000	4.11641600	-0.37422900
C	1.09507900	3.67789200	-0.09087800
H	3.96778700	1.13478100	-0.50184700
H	4.43430900	3.53686800	-0.74236200
H	2.57333200	5.18724500	-0.47886800
H	0.29440700	4.40801100	0.01732100
P	1.46021000	-0.43507600	0.04147300
O	-0.41838600	1.85277200	0.32294100
C	-1.42192200	2.78070400	0.70218300
H	-2.28230500	2.18891300	1.03112900
C	2.30585400	-0.92883400	1.66205000
C	2.22913800	-1.24811100	-1.48941200
C	1.80592200	-0.37428900	-2.67376500
H	2.32396300	0.59502100	-2.69214600
H	2.03803300	-0.90052600	-3.61430600
H	0.72010200	-0.18305900	-2.65992500
C	3.74555400	-1.42935100	-1.47855500
H	4.04995000	-1.91183800	-2.42250500
H	4.30198000	-0.48497800	-1.41797000

H	4.08190300	-2.08486100	-0.66291200
C	1.57337900	-2.62259000	-1.65452800
H	1.76441400	-3.29292700	-0.80648600
H	0.48636500	-2.54456500	-1.77835900
H	1.98540200	-3.10240000	-2.55813800
C	3.72077200	-0.38861800	1.85129400
H	4.41814800	-0.73164600	1.07480300
H	3.74524000	0.70952800	1.88284100
H	4.11159500	-0.74958700	2.81761400
C	2.30844100	-2.45236100	1.78340200
H	3.01702100	-2.92349900	1.08640000
H	2.62455700	-2.73103800	2.80254000
H	1.31187700	-2.87728300	1.60789200
C	1.39842600	-0.33795000	2.74631500
H	1.81149500	-0.57192400	3.74184000
H	1.32579500	0.75851600	2.66767900
H	0.37962500	-0.75142000	2.68842600
Pd	-0.92825000	-0.36732600	0.08013200
H	-1.06326600	3.41290800	1.52939500
H	-1.72640300	3.40646000	-0.15100200
C	-1.50795800	-2.25747900	0.01671900
H	-2.42831700	-2.44849400	0.59272900
F	-0.56236700	-3.11192200	0.53272200
F	-1.73390900	-2.69025800	-1.25811100
C	-2.90506300	0.02596900	-0.02154700
C	-3.78891600	-0.16966400	1.05071800
C	-3.40969200	0.66838500	-1.16480100
C	-5.10946000	0.28355900	1.00089400
H	-3.44302100	-0.68199900	1.95540500
C	-4.73075700	1.11454100	-1.22530000
H	-2.75886000	0.82915700	-2.03063200
C	-5.58501500	0.92941200	-0.13862700
H	-5.77179700	0.12835900	1.85769400
H	-5.09748600	1.60922200	-2.12960700
H	-6.61891900	1.28144800	-0.18292700



Pd-CF_2H-TS

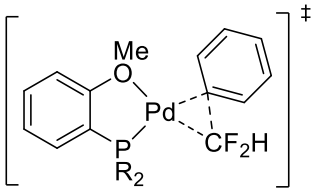
58

Generated by Multiwfn

C	-2.60872700	-1.52431000	0.19183900

C	-2.60937100	-0.11497300	0.07072800
C	-3.84907700	0.53452100	0.05481700
C	-5.05242700	-0.15914900	0.15380600
C	-5.02737600	-1.54373900	0.27669500
C	-3.81502500	-2.22660400	0.29627500
H	-3.87807700	1.61987200	-0.03761000
H	-6.00043600	0.38187200	0.13691400
H	-5.95945000	-2.10805600	0.35783900
H	-3.81499200	-3.31241700	0.38909300
P	-1.00209500	0.77130200	-0.07696900
O	-1.41152900	-2.14865400	0.20124300
C	-1.33907200	-3.53440600	0.40341300
H	-0.27014600	-3.78563200	0.43302000
C	-0.86486500	1.72086500	1.55420700
C	-1.17956600	1.90975600	-1.58563200
C	-1.81500900	1.05195900	-2.68283500
H	-2.87791700	0.84530700	-2.49402500
H	-1.73783100	1.57723700	-3.64934700
H	-1.29462200	0.08542500	-2.78609200
C	-1.97669600	3.19774100	-1.39738700
H	-2.00904300	3.74260600	-2.35613400
H	-3.01950600	3.02493400	-1.09858400
H	-1.51197900	3.87089200	-0.66311900
C	0.24498000	2.26729800	-2.02396100
H	0.79923500	2.83012000	-1.26040200
H	0.82677600	1.36138100	-2.24658000
H	0.20175600	2.88879600	-2.93442100
C	-2.09111300	2.52935100	1.96718100
H	-2.35822200	3.30968600	1.24255200
H	-2.96931200	1.88845700	2.12976900
H	-1.88008200	3.03570800	2.92439800
C	0.36832600	2.62142400	1.46806800
H	0.20841700	3.48181000	0.80138900
H	0.59734100	3.02504000	2.46847500
H	1.25453700	2.06814200	1.12085600
C	-0.62126700	0.63069300	2.60265600
H	-0.48115400	1.09570800	3.59296300
H	-1.47457700	-0.06182500	2.67689600
H	0.27874100	0.04225600	2.36692000
Pd	0.78140400	-0.72049400	-0.29746100
C	2.71375100	-0.21559700	0.00627600
C	3.37201300	0.58209100	-0.94449200
C	3.11755400	-0.12172200	1.34863000
C	4.33241400	1.50898200	-0.54987300
H	3.12194500	0.47992200	-2.00244900
C	4.07836500	0.80949500	1.73923500

H	2.67206200	-0.78391700	2.09424600
C	4.68299800	1.63702200	0.79492800
H	4.81518100	2.13743300	-1.30329300
H	4.36004700	0.88244900	2.79321100
H	5.43796500	2.36504500	1.10128800
C	2.35366400	-2.05919900	-0.55988600
F	3.25304200	-2.10402400	-1.57150400
F	2.85638500	-2.74543500	0.49475000
H	-1.79569400	-3.83016400	1.36301500
H	-1.81519300	-4.09650500	-0.41811400
H	1.48160600	-2.66297500	-0.93220700



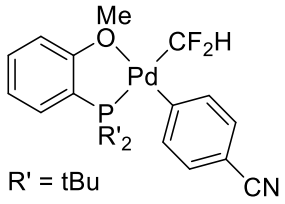
Pd-CF_2H-TS-*trans*

58

Pd-CF2H-TS-trans

C	1.18000000	2.29182000	-0.06025700
C	2.07222100	1.19595500	-0.13894500
C	3.41902900	1.47478200	-0.39602600
C	3.88621500	2.77271100	-0.58833200
C	2.98876900	3.83240900	-0.52018900
C	1.64244800	3.59822400	-0.25718100
H	4.12968700	0.65063800	-0.45213200
H	4.94421600	2.95037000	-0.79062600
H	3.33326000	4.85848700	-0.67013000
H	0.95228400	4.43985500	-0.20355400
P	1.40239100	-0.50981100	0.06783000
O	-0.11204900	2.02229600	0.21867100
C	-1.07118300	3.04954300	0.23121400
H	-2.03103400	2.56950200	0.46026200
C	2.03801000	-1.00809900	1.78005400
C	2.16105200	-1.55033000	-1.32787900
C	1.98291300	-0.72138500	-2.60236500
H	2.65831400	0.14499100	-2.64145600
H	2.18872700	-1.35302100	-3.48262800
H	0.94833300	-0.35058700	-2.69123000
C	3.61609800	-1.98694600	-1.17744400
H	3.91061600	-2.56718900	-2.06846800
H	4.32112800	-1.14818500	-1.10161000
H	3.76488200	-2.64242800	-0.30752500
C	1.28332400	-2.80220200	-1.44899600

H	1.32130200	-3.43415400	-0.55095700
H	0.22994900	-2.54253300	-1.62436500
H	1.63771600	-3.41108300	-2.29821300
C	3.52370400	-0.77037300	2.03291700
H	4.17172600	-1.34173700	1.35522800
H	3.78736700	0.29378300	1.94974100
H	3.77155000	-1.08613700	3.06080600
C	1.68033500	-2.47667400	2.00901900
H	2.30885000	-3.15564200	1.41382400
H	1.84011100	-2.73392300	3.06974700
H	0.62525100	-2.67702300	1.76513000
C	1.22833500	-0.14123500	2.74975000
H	1.50267900	-0.39308100	3.78818900
H	1.42674500	0.93202800	2.60345100
H	0.14601900	-0.30610900	2.62585100
Pd	-0.92725300	-0.38553100	0.00099700
H	-0.84932300	3.79901600	1.00971200
H	-1.14433100	3.54728700	-0.75027500
C	-2.45940500	-1.99889300	-0.19924300
H	-3.52309000	-2.22691600	-0.02026500
F	-1.80780800	-2.87324300	0.64013600
F	-2.21931600	-2.37598100	-1.48521700
C	-2.89504500	-0.15024200	-0.02378200
C	-3.46301000	0.23837200	1.20556000
C	-3.40172400	0.40578700	-1.21244800
C	-4.45492000	1.21518000	1.24350800
H	-3.11309900	-0.22334800	2.13335600
C	-4.39502800	1.38291600	-1.16353900
H	-3.00308100	0.07255700	-2.17422600
C	-4.92201300	1.79410500	0.06096000
H	-4.87049900	1.52730400	2.20547900
H	-4.76253800	1.82689900	-2.09271200
H	-5.70618200	2.55408000	0.09450600



Pd-CF_2H-CN-GS

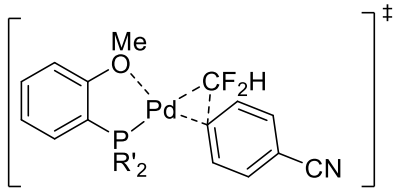
59

Generated by Multiwfn

C	2.92223400	0.91485300	-0.15560800
C	2.65291100	-0.46555200	-0.24441500
C	3.72057800	-1.31287300	-0.56490300

C	5.00110700	-0.82699300	-0.81134600
C	5.23650500	0.54088400	-0.73168900
C	4.20426100	1.41290000	-0.40053700
H	3.55157900	-2.38692100	-0.61926900
H	5.80858500	-1.51707200	-1.06266600
H	6.23319300	0.94290300	-0.92695500
H	4.40217800	2.48251100	-0.34531500
P	0.93430400	-1.04583700	0.07740800
O	1.89407800	1.74229300	0.18902100
C	2.18853400	3.06713700	0.61023600
H	1.26666000	3.46751800	1.04168500
C	1.05001700	-1.79040200	1.80905700
C	0.53425800	-2.32084400	-1.26292300
C	0.91215100	-1.64086600	-2.58241800
H	1.99972900	-1.54775900	-2.71250800
H	0.51971800	-2.23374300	-3.42474400
H	0.47489000	-0.63100100	-2.65127800
C	1.21036600	-3.68590100	-1.14959500
H	0.88485700	-4.31011600	-1.99841100
H	2.30604800	-3.64562400	-1.19426800
H	0.91933600	-4.21911800	-0.23364800
C	-0.98249100	-2.53714500	-1.24784000
H	-1.33809300	-3.00450500	-0.32008600
H	-1.53393300	-1.59893000	-1.37989200
H	-1.25336300	-3.21008000	-2.07812700
C	2.24394600	-2.71468100	2.03031300
H	2.23726700	-3.58888900	1.36559100
H	3.20063000	-2.18865300	1.90220400
H	2.21730900	-3.09432300	3.06561500
C	-0.25446700	-2.52644200	2.11462800
H	-0.32923700	-3.47985900	1.57200300
H	-0.29681500	-2.76272000	3.19075800
H	-1.13950300	-1.92100600	1.86975300
C	1.18144200	-0.57787200	2.73679600
H	1.23123800	-0.91873700	3.78423100
H	2.09941700	-0.00507800	2.53250900
H	0.32653500	0.10963900	2.63838500
Pd	-0.26178100	1.03132800	-0.02106500
C	-2.14929300	0.47583600	-0.06117200
C	-2.89152200	0.47154900	-1.25654200
C	-2.80985000	0.07597800	1.11317600
C	-4.21062500	0.03571300	-1.29288400
H	-2.42582700	0.80838300	-2.18682000
C	-4.13142200	-0.35554400	1.09316100
H	-2.28649000	0.10564200	2.07204100
C	-4.84334400	-0.39159300	-0.11537400

H	-4.76288800	0.02516700	-2.23523100
H	-4.62363900	-0.66705200	2.01720300
C	-1.02641400	2.90159500	-0.19475100
F	-0.95141600	3.57855400	1.00341500
F	-0.21600500	3.60199800	-1.06155600
H	2.98101100	3.05065700	1.37428200
H	2.48988100	3.69503500	-0.24107100
H	-2.05898800	3.02671200	-0.56127600
C	-6.19840300	-0.84627300	-0.14466500
N	-7.29751400	-1.21722900	-0.16856300



R' = tBu

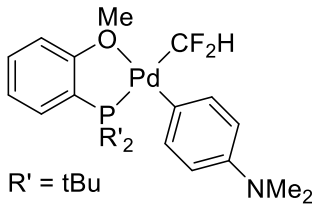
Pd-CF_3-CN-TS

59

Generated by Multiwfn

C	-3.11994100	1.11441100	-0.22500300
C	-2.87592600	-0.27101800	-0.08883900
C	-3.98307800	-1.12767500	-0.07104600
C	-5.28757400	-0.65558500	-0.18599700
C	-5.50308000	0.71061900	-0.32637300
C	-4.42853900	1.59455000	-0.34618500
H	-3.82277400	-2.19991200	0.03635400
H	-6.12693000	-1.35319400	-0.16745000
H	-6.51835700	1.10294700	-0.42029600
H	-4.61903700	2.66216000	-0.45131600
P	-1.14222400	-0.86210200	0.07898100
O	-2.04927500	1.94374200	-0.23031000
C	-2.23128000	3.31718100	-0.46139100
H	-1.22814600	3.76338300	-0.49107200
C	-0.83151600	-1.83274100	-1.51338900
C	-1.11699600	-1.94286000	1.63680400
C	-1.88307500	-1.15193400	2.70046300
H	-2.96543300	-1.13007900	2.51040500
H	-1.72126700	-1.61519100	3.68777100
H	-1.52713200	-0.10996700	2.75891100
C	-1.69510200	-3.34961800	1.50945800
H	-1.63689700	-3.85000800	2.49074800
H	-2.75289100	-3.35978700	1.21377500
H	-1.12886400	-3.97048200	0.80086800
C	0.34736200	-2.04228400	2.07562600

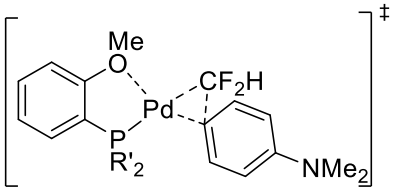
H	0.98543800	-2.54121700	1.33342400
H	0.77303200	-1.04579400	2.25637500
H	0.40863500	-2.62163700	3.01209600
C	-1.89447400	-2.85922000	-1.89477100
H	-2.03017100	-3.64297400	-1.13787600
H	-2.86844800	-2.38908800	-2.09070900
H	-1.58642900	-3.36137500	-2.82737400
C	0.53784700	-2.50279600	-1.39213000
H	0.52302100	-3.35489000	-0.69688800
H	0.84242700	-2.89416400	-2.37695900
H	1.31226600	-1.79440600	-1.06067200
C	-0.77583700	-0.75791400	-2.60389800
H	-0.55735500	-1.22936200	-3.57661300
H	-1.73444100	-0.22410200	-2.70031400
H	0.00938600	-0.01410500	-2.39701800
Pd	0.29106900	0.97602300	0.21272500
C	2.28086700	0.79279600	0.11396800
C	2.99801200	0.28706400	1.21801800
C	2.82227300	0.58275600	-1.17166000
C	4.13525600	-0.48340300	1.04238500
H	2.64748200	0.49715300	2.23006100
C	3.95961400	-0.18911300	-1.35502300
H	2.33538700	1.02870900	-2.04103300
C	4.62371600	-0.74501800	-0.24972700
H	4.65955500	-0.89211800	1.90872900
H	4.34575700	-0.36588700	-2.36106700
C	1.63408000	2.59969500	0.36697200
F	2.43013500	2.93193300	1.40961800
F	2.10684300	3.19957500	-0.74950900
H	-2.72464700	3.50298600	-1.42969200
H	-2.80945700	3.79609800	0.34647600
H	0.65515800	3.09368400	0.59370000
C	5.78995400	-1.54795600	-0.43405200
N	6.73591000	-2.20371700	-0.58388100



Pd-CF_2H-NMe_2-GS

```
    66
 Generated by Multiwfn
C       3.28122400      0.72381800     -0.16406400
C       2.88997300     -0.62762700     -0.26138500
C       3.87671800     -1.56103300     -0.60071700
C       5.19262400     -1.18828700     -0.85931300
C       5.54817500      0.15272100     -0.77239100
C       4.60004700      1.10853300     -0.42153200
H       3.61317900     -2.61540100     -0.65922900
H       5.93322600     -1.94486300     -1.12524400
H       6.57404700      0.46776500     -0.97664300
H       4.89208500      2.15596800     -0.35988600
P       1.12699200     -1.05889900      0.07067100
O       2.33614900      1.63403400      0.20053500
C       2.74433600      2.93705500      0.58760300
H       1.86448700      3.41965800      1.02288900
C       1.20305300     -1.87242500      1.77478900
C       0.59937100     -2.24973900     -1.30361800
C       0.97530200     -1.52981300     -2.60244300
H       2.06319500     -1.48110400     -2.75606100
H       0.53528600     -2.06615800     -3.45926300
H       0.58351000     -0.49930400     -2.61313400
C       1.19178400     -3.65720000     -1.28206000
H       0.76915900     -4.22855300     -2.12566000
H       2.28210400     -3.68210800     -1.40497300
H       0.93019900     -4.20502300     -0.36565000
C      -0.92712200     -2.37291700     -1.24157500
H      -1.27187700     -2.91855700     -0.35353900
H      -1.42400800     -1.39481600     -1.24475100
H      -1.27204900     -2.93544700     -2.12516400
C       2.32708700     -2.88759300      1.96060000
H       2.25653800     -3.73566700      1.26573900
H       3.31965500     -2.42888800      1.84782500
H       2.27310900     -3.30065500      2.98222800
C      -0.14861100     -2.52370200      2.06836200
H      -0.28629800     -3.45871600      1.50606600
H      -0.20521300     -2.77889700      3.13980400
H      -0.99128800     -1.85599100      1.83659700
C       1.42581800     -0.70187200      2.73843000
H       1.46110700     -1.07708100      3.77496600
H       2.37908900     -0.18687600      2.54060600
H       0.61995400      0.04539800      2.66691800
Pd      0.11651600      1.11385000      0.02582500
C      -1.81492100      0.69187100     -0.00379200
C      -2.58001300      0.78719600     -1.17390100
C      -2.48568800      0.24860600      1.14226800
```

C	-3.91964800	0.40531800	-1.21993800
H	-2.12026800	1.15367700	-2.09712900
C	-3.82742300	-0.12944100	1.11882500
H	-1.95699000	0.18965600	2.09799600
C	-4.58329900	-0.06582000	-0.06911500
H	-4.45038500	0.48372500	-2.16929900
H	-4.28586500	-0.47437300	2.04619800
C	-0.50093800	3.03363500	-0.12392300
F	-0.33014800	3.70946000	1.06978400
F	0.32963100	3.67957700	-1.02084700
H	3.54578800	2.87345300	1.34026300
H	3.08199800	3.52078000	-0.28175900
H	-1.53336300	3.23818800	-0.45195600
N	-5.91528700	-0.43989400	-0.10189400
C	-6.50720400	-1.04740900	1.05444800
H	-6.02083600	-2.00114700	1.34329300
H	-6.47030600	-0.38007900	1.93351900
H	-7.56575800	-1.25965700	0.85537500
C	-6.60167800	-0.49883800	-1.35971700
H	-6.15430000	-1.22617800	-2.06706600
H	-7.64596800	-0.79396900	-1.19363500
H	-6.61887500	0.48303600	-1.86475800

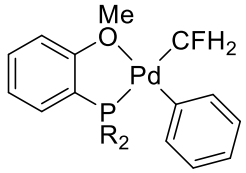


R' = tBu

Pd-CF_3-NMe_2-TS

```
    66
 Generated by Multiwfn
C      -3.46315100      0.91304300     -0.53084600
C      -3.12841800     -0.42842400     -0.22972800
C      -4.16197600     -1.37190500     -0.23548800
C      -5.48071800     -1.02796900     -0.52239400
C      -5.78591200      0.29572700     -0.81823600
C      -4.78630200      1.26394500     -0.82403200
H      -3.93127100     -2.41262600     -0.00884400
H      -6.26064500     -1.79183200     -0.51628900
H      -6.81344400      0.58751300     -1.04836200
H      -5.04416300      2.29727800     -1.05533500
P      -1.37794700     -0.84346000      0.16538100
O      -2.46410900      1.81924500     -0.52261500
C      -2.71329400      3.15225100     -0.87593500
H      -1.74283400      3.66563400     -0.83944600
C      -0.81975100     -1.85874400     -1.33170800
C      -1.43648300     -1.86098800      1.76730300
C      -2.39211300     -1.11480000      2.70185900
H      -3.44354300     -1.21452400      2.39738500
H      -2.29498300     -1.51787200      3.72377900
H      -2.15165600     -0.03956800      2.74300500
C      -1.84928400     -3.32618300      1.65384000
H      -1.85330500     -3.77700300      2.66087700
H      -2.85870100     -3.46475200      1.24321700
H      -1.14436900     -3.91030000      1.04544500
C      -0.02813800     -1.78906500      2.36908600
H       0.73592800     -2.24554100      1.72490800
H       0.27297100     -0.74515600      2.53987400
H      -0.01611700     -2.32144100      3.33543600
C      -1.74510800     -2.99498100     -1.75647800
H      -1.87699800     -3.75861800     -0.97870500
H      -2.73683600     -2.62656900     -2.05544900
H      -1.31077900     -3.50097300     -2.63556300
C       0.58512600     -2.38915900     -1.04083700
H       0.57626700     -3.20254600     -0.29999100
H       1.02050000     -2.79942900     -1.96738700
H       1.25528400     -1.59306500     -0.68131100
C      -0.74613400     -0.83549800     -2.46956900
H      -0.37519700     -1.32723300     -3.38463100
H      -1.73506400     -0.40748800     -2.69771400
H      -0.06343400     -0.00887400     -2.21983900
Pd     -0.03099900      1.05572100      0.38077400
C       1.98860200      1.02033000      0.22886400
C       2.74591600      0.45478700      1.26355800
C       2.52383200      0.95494600     -1.06437800
```

C	3.93007000	-0.22653900	1.01147900
H	2.39858400	0.53530400	2.29595700
C	3.70692000	0.27431000	-1.33279300
H	2.00134000	1.44237500	-1.89082400
C	4.44026700	-0.34667300	-0.30014000
H	4.46483500	-0.66684700	1.85323300
H	4.06255900	0.23719100	-2.36251100
C	1.11306000	2.75436500	0.63315800
F	1.87972900	3.07823600	1.70324800
F	1.53270600	3.48119600	-0.43271100
H	-3.11668400	3.23455200	-1.89958600
H	-3.40425100	3.64427400	-0.16989100
H	0.09112500	3.15441100	0.88906900
N	5.61156800	-1.02846800	-0.55707900
C	6.29128600	-1.70673100	0.50885800
H	5.67406400	-2.49876600	0.97625600
H	7.20092300	-2.18163000	0.11958600
H	6.60189200	-1.01368300	1.31161000
C	6.05535800	-1.19557500	-1.91103200
H	6.24646800	-0.22757200	-2.40890400
H	6.99751400	-1.75833700	-1.92126600
H	5.32724200	-1.74992000	-2.53495500



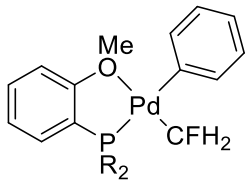
Pd-CFH$_2$-GS

58

Pd-CFH2-GS

C	2.50554300	-1.17334300	-0.00498800
C	2.34043900	0.22260900	0.10495300
C	3.49254900	1.00056100	0.28006900
C	4.76057600	0.43368800	0.37117600
C	4.89481200	-0.94693500	0.28164600
C	3.77571700	-1.75061800	0.08867800
H	3.39975800	2.08326300	0.33898300
H	5.63627300	1.07066200	0.50953800
H	5.87986700	-1.41314200	0.35747000
H	3.89932200	-2.83038900	0.01898700
P	0.63931000	0.91491400	-0.01891500
O	1.39693700	-1.93657800	-0.22066200
C	1.57878500	-3.25724600	-0.70865400
H	0.59108900	-3.62149200	-0.99800200
C	0.66506400	1.87451300	-1.64797600

C	0.42179400	1.97784900	1.53278200
C	1.46658200	3.05527700	1.81247400
H	1.57923800	3.76840600	0.98348300
H	1.14379700	3.63693800	2.69242800
H	2.45112100	2.63525200	2.05681700
C	-0.96105200	2.63209500	1.47137400
H	-1.74288200	1.93712800	1.13586200
H	-1.23655800	2.98063300	2.48068500
H	-0.97176200	3.51131900	0.81332400
C	0.44544900	0.95253300	2.67220600
H	-0.33027100	0.18203300	2.53883200
H	1.41886500	0.44255700	2.74480500
H	0.26290100	1.46503600	3.63145700
C	-0.68329900	2.57468000	-1.82647900
H	-1.53092700	1.92385700	-1.56723000
H	-0.75588700	3.48967600	-1.22333400
H	-0.79842300	2.87307800	-2.88191300
C	0.80257300	0.77474500	-2.70702200
H	-0.02103500	0.04638100	-2.64204200
H	0.78375800	1.22781800	-3.71223700
H	1.75209500	0.22559000	-2.60808400
C	1.79729600	2.88098700	-1.82422000
H	2.78660400	2.40278800	-1.81160200
H	1.68974900	3.37295300	-2.80583100
H	1.78042100	3.67586100	-1.06501200
Pd	-0.71694100	-1.05229200	0.00675400
C	-2.53955800	-0.29612100	-0.00343400
C	-3.25617300	-0.04505600	1.17802000
C	-3.17473800	0.00107400	-1.22046600
C	-4.53208400	0.51974900	1.14667700
H	-2.81254800	-0.29096300	2.14704000
C	-4.45259400	0.56279700	-1.25365700
H	-2.66676400	-0.20775700	-2.16629600
C	-5.13570800	0.83308400	-0.06969700
H	-5.05996300	0.71287600	2.08510900
H	-4.91780700	0.78867800	-2.21761100
H	-6.13493000	1.27488300	-0.09505100
C	-1.76096500	-2.79217100	0.18227200
F	-0.89137200	-3.82134000	0.57637000
H	2.25811900	-3.24894800	-1.57537100
H	1.97209900	-3.91935000	0.07754500
H	-2.55182200	-2.73529300	0.94724200
H	-2.22307900	-3.10243100	-0.77339000



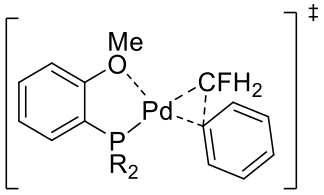
Pd-CFH_2-GS-*trans*

58

Pd-CFH2-GS-trans

C	0.92424000	2.22624000	-0.25835900
C	1.91800600	1.23025500	-0.15387700
C	3.25681100	1.63979400	-0.19907700
C	3.61873600	2.97443500	-0.35313200
C	2.62182100	3.93672100	-0.46498200
C	1.28081800	3.56975200	-0.41757400
H	4.04417300	0.89294700	-0.10905800
H	4.67266900	3.25686600	-0.38462200
H	2.88166800	4.99078300	-0.58682200
H	0.51624000	4.34072800	-0.49737900
P	1.40264200	-0.51883900	0.09626400
O	-0.38120300	1.84257400	-0.19177700
C	-1.39076800	2.80680600	-0.43990000
H	-2.34204100	2.26433000	-0.43630800
C	2.22189800	-1.01792100	1.73344800
C	2.08137800	-1.44756000	-1.40463500
C	1.90418500	-2.94794500	-1.16292800
H	0.86415800	-3.20103800	-0.91561000
H	2.15630500	-3.49069900	-2.08922500
H	2.57045500	-3.32987000	-0.37541500
C	1.15898000	-1.01661000	-2.55099200
H	1.48499700	-1.50393800	-3.48534100
H	0.11664500	-1.30941500	-2.35511500
H	1.19332600	0.07217300	-2.71620000
C	3.52719600	-1.14868700	-1.79132400
H	3.66197800	-0.10437300	-2.10508800
H	4.24598300	-1.37137000	-0.99092400
H	3.79967800	-1.78011800	-2.65377100
C	3.71395000	-1.33169400	1.67452900
H	4.06984900	-1.58016100	2.68875700
H	3.93470300	-2.19896100	1.03605500
H	4.31696900	-0.48127800	1.32848200
C	1.46714100	-2.24132400	2.26209500
H	1.89409700	-2.53936400	3.23426100
H	0.40267300	-2.01164300	2.41510200
H	1.53896200	-3.11017000	1.59286600
C	1.96742400	0.14514000	2.69649300

H	2.23036300	-0.16604200	3.72110200
H	2.56539500	1.03366500	2.44983100
H	0.90445500	0.43797100	2.70024800
Pd	-0.95713700	-0.36679700	0.14593900
C	-2.94395500	-0.03622500	0.16597600
C	-3.76908700	-0.37109100	-0.92060800
C	-3.53928400	0.65239900	1.23778900
C	-5.11522200	-0.00297400	-0.95435600
H	-3.35103500	-0.94040600	-1.75685500
C	-4.88815500	1.01477600	1.21413000
H	-2.93819800	0.92489900	2.11219900
C	-5.68058100	0.69364600	0.11313900
H	-5.73044600	-0.26719400	-1.81983100
H	-5.32353000	1.55090800	2.06289400
H	-6.73581600	0.97852600	0.09049400
C	-1.46080200	-2.30279800	0.17356600
F	-1.44713800	-2.78455900	-1.13627900
H	-1.40654500	3.57180300	0.35247100
H	-1.23902600	3.28177100	-1.42176500
H	-0.72164500	-2.88919400	0.74148100
H	-2.46331000	-2.49728400	0.58016400



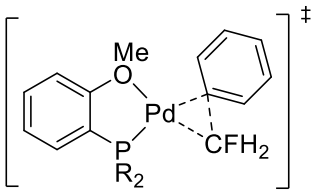
Pd-CFH$_2$-TS

58

Pd-CFH2-TS

C	-2.54231700	1.44009900	0.09714900
C	-2.47947300	0.02670600	0.10060100
C	-3.68506200	-0.67587600	0.20568000
C	-4.91461700	-0.02926600	0.30574100
C	-4.95124800	1.36065900	0.30617600
C	-3.77409200	2.09585300	0.20272600
H	-3.66538000	-1.76550000	0.21037300
H	-5.83511500	-0.61076400	0.38536700
H	-5.90501900	1.88775200	0.38609800
H	-3.82061200	3.18477600	0.19871600
P	-0.83306500	-0.78843500	-0.04383700
O	-1.37736200	2.11243400	-0.01284100
C	-1.34395300	3.51114400	0.10312500
H	-0.28242200	3.79153700	0.08293600
C	-1.01794600	-2.08986700	-1.41332200

C	-0.56884000	-1.55305300	1.66766500
C	-1.72226200	-2.38664000	2.21813500
H	-1.96268900	-3.25772500	1.59456200
H	-1.44345200	-2.76974200	3.21458100
H	-2.63510700	-1.78800000	2.34850200
C	0.71617900	-2.38092800	1.61654100
H	1.54994000	-1.81453400	1.17351500
H	1.01105100	-2.66257900	2.64123900
H	0.58577500	-3.31484400	1.04981200
C	-0.35439000	-0.34671600	2.58746100
H	0.49113400	0.27088300	2.24768000
H	-1.24997300	0.29260200	2.63666300
H	-0.13796500	-0.69744200	3.61061800
C	0.40339600	-2.41432800	-1.88635700
H	0.91974500	-1.50486500	-2.22564200
H	1.02308300	-2.86584600	-1.09938400
H	0.35560800	-3.12709300	-2.72718500
C	-1.75347100	-1.38925600	-2.55838500
H	-1.29590900	-0.41267600	-2.78762700
H	-1.69146600	-2.00944100	-3.46817000
H	-2.81651200	-1.22047600	-2.33561000
C	-1.72793500	-3.39122000	-1.05068400
H	-2.76150600	-3.24277000	-0.70955000
H	-1.77925300	-4.03410300	-1.94590400
H	-1.18672400	-3.95879000	-0.28052900
Pd	0.81692900	0.79855700	-0.49453100
C	2.77868200	0.45589000	-0.20350500
C	3.24721900	0.56009500	1.11858900
C	3.46170400	-0.41628100	-1.07591600
C	4.29249500	-0.24348800	1.57353100
H	2.78180900	1.27937700	1.79647400
C	4.50584100	-1.21195400	-0.61656000
H	3.15731300	-0.48301400	-2.12397800
C	4.92327700	-1.14083500	0.71480400
H	4.61821600	-0.16088000	2.61434400
H	5.00069100	-1.89979800	-1.30816200
H	5.74302800	-1.76840700	1.07207200
C	2.28468300	2.22762600	-0.89552400
F	2.38370000	3.12475300	0.14310500
H	-1.86668400	4.00531100	-0.73367500
H	-1.78098500	3.84811300	1.05821200
H	3.21838700	2.25026600	-1.47075800
H	1.47663500	2.57916700	-1.59083000



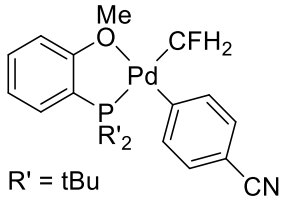
Pd-CFH$_2$-TS-*trans*

58

Pd-CFH2-TS-trans

C	-1.05039900	2.24792800	0.11441300
C	-1.99553100	1.19849200	0.02193600
C	-3.34895500	1.54733800	-0.04639500
C	-3.77575100	2.87298200	-0.03455200
C	-2.82908500	3.88793900	0.05099100
C	-1.47358600	3.58247800	0.12545100
H	-4.09748000	0.75817700	-0.11505900
H	-4.84047900	3.10716300	-0.09217000
H	-3.14188300	4.93487800	0.06112700
H	-0.74444600	4.38957200	0.19220400
P	-1.38516800	-0.53921100	-0.03370400
O	0.25032400	1.90565200	0.19548500
C	1.24978900	2.89222600	0.26522200
H	2.20526400	2.35609400	0.32956900
C	-2.29063200	-1.35162500	-1.49420100
C	-1.92065500	-1.23876300	1.64322500
C	-1.58891000	-2.73117600	1.65890000
H	-0.54720100	-2.91358900	1.35106300
H	-1.71074500	-3.12515400	2.68188200
H	-2.25509100	-3.31527800	1.00642900
C	-1.02005500	-0.51849100	2.65238900
H	-1.22361400	-0.89994200	3.66727300
H	0.04633600	-0.68202700	2.42746800
H	-1.20386000	0.56730000	2.66131500
C	-3.37675100	-1.01028400	2.03748700
H	-3.61634000	0.05991200	2.11411300
H	-4.08978300	-1.47773600	1.34580700
H	-3.55473500	-1.45219500	3.03276600
C	-3.73816200	-1.78294700	-1.27420100
H	-4.13254200	-2.21394400	-2.21021600
H	-3.82764900	-2.56046400	-0.50215000
H	-4.40384100	-0.95174500	-1.00521600
C	-1.46180700	-2.58370300	-1.87567500
H	-1.92141800	-3.08099100	-2.74657500
H	-0.43478700	-2.29572100	-2.14483400
H	-1.40135300	-3.32336900	-1.06460100
C	-2.20579400	-0.34962600	-2.64830400

H	-2.49165100	-0.84786200	-3.58979700
H	-2.87104500	0.51350800	-2.50658300
H	-1.17834600	0.03182700	-2.76946800
Pd	0.96161000	-0.52788500	-0.20716400
C	2.93415700	-0.31815100	-0.22047000
C	3.55318800	-0.05882300	1.01452800
C	3.45280400	0.30396700	-1.37435000
C	4.61575400	0.84103500	1.10034500
H	3.19233900	-0.57002700	1.91013600
C	4.51027800	1.20509600	-1.28016500
H	3.01549900	0.08138900	-2.35226800
C	5.09519600	1.48147400	-0.04211100
H	5.07406300	1.04374500	2.07242600
H	4.88505100	1.69553800	-2.18296000
H	5.92977900	2.18319400	0.02811600
C	2.32052200	-2.18158100	-0.36068300
F	2.54262900	-2.71730600	0.88411000
H	1.25395400	3.52759300	-0.63633300
H	1.12951200	3.52360700	1.16162800
H	1.47644300	-2.72465100	-0.82712400
H	3.20356400	-2.37208500	-0.98643900



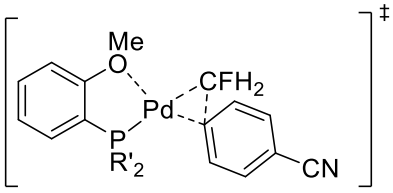
Pd-CFH$_2$-CN-GS

59

Generated by Multiwfn

C	2.91041400	0.94692800	-0.11991000
C	2.60264900	-0.41791800	-0.28106400
C	3.64180300	-1.27267500	-0.66789300
C	4.93135800	-0.80579600	-0.90471400
C	5.20641800	0.54802100	-0.74557800
C	4.20228400	1.42565000	-0.34931800
H	3.44373800	-2.33717500	-0.78132200
H	5.71648600	-1.50059400	-1.20861000
H	6.21175400	0.93341200	-0.92979400
H	4.42701700	2.48540600	-0.23314600
P	0.87311600	-0.95567500	0.05732800
O	1.90640600	1.78071300	0.27804600
C	2.25242300	3.00953800	0.89866400
H	1.33998500	3.39440600	1.36142800
C	1.00719800	-1.72963500	1.77752800

C	0.42517800	-2.21649900	-1.28268100
C	1.05721100	-3.60341500	-1.17689600
H	0.74365500	-4.13385700	-0.26688500
H	0.71678600	-4.21056400	-2.03231200
H	2.15396900	-3.59978800	-1.21272200
C	-1.09756800	-2.38500100	-1.25407200
H	-1.61968000	-1.43123700	-1.39379400
H	-1.39635500	-3.05932300	-2.07371000
H	-1.46111700	-2.82849500	-0.31763800
C	0.80954600	-1.55014200	-2.60722500
H	0.40666600	-0.52587900	-2.67096300
H	1.89757100	-1.49458200	-2.75304300
H	0.38533000	-2.12922400	-3.44382500
C	-0.30953300	-2.43532600	2.10212300
H	-1.18260600	-1.79920700	1.89378500
H	-0.42698000	-3.37412200	1.54193800
H	-0.33105500	-2.69383300	3.17385200
C	1.18834400	-0.53755300	2.72294000
H	0.35172400	0.17475600	2.64734000
H	1.24321000	-0.89777600	3.76370400
H	2.12024400	0.01091900	2.51515700
C	2.18211100	-2.68622700	1.95938800
H	3.14793000	-2.18434800	1.80450400
H	2.17684500	-3.07112600	2.99318300
H	2.13342500	-3.55595500	1.29097000
Pd	-0.26860700	1.15809900	-0.00103400
C	-2.16786900	0.65415300	-0.04217100
C	-2.92252000	0.66021300	-1.23008000
C	-2.82747200	0.26737600	1.13846700
C	-4.25148200	0.25479100	-1.25254300
H	-2.45798600	0.98100400	-2.16608300
C	-4.15813400	-0.13501100	1.13273900
H	-2.29264300	0.28023800	2.09151900
C	-4.88332600	-0.15526700	-0.06841400
H	-4.81250700	0.25457300	-2.18978600
H	-4.64709400	-0.43678000	2.06177500
C	-1.03135200	3.03677600	-0.15519700
F	0.00411300	3.90597600	-0.51029100
H	3.02309200	2.83670500	1.66608600
H	2.60333000	3.74527300	0.16095600
H	-1.80716200	3.12316500	-0.93300400
H	-1.45336300	3.39524800	0.80211300
C	-6.24878000	-0.57785500	-0.08348600
N	-7.35666700	-0.92269900	-0.09563000



R' = tBu

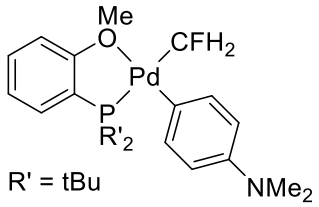
Pd-CFH$_2$-CN-TS

59

Generated by Multiwfn

C	3.03246000	1.09492900	-0.11702200
C	2.76382200	-0.29242400	-0.09383400
C	3.85469000	-1.16648400	-0.16389500
C	5.16622100	-0.70746400	-0.25300800
C	5.40544100	0.66201200	-0.27768600
C	4.34697000	1.56317000	-0.21063000
H	3.67602600	-2.24138400	-0.14999400
H	5.99324800	-1.41804700	-0.30483900
H	6.42703700	1.04273300	-0.34823000
H	4.55295800	2.63320900	-0.22483000
P	1.01490300	-0.85266300	0.03577100
O	1.97430600	1.93658800	-0.04409800
C	2.15313500	3.32015800	-0.22675800
H	1.14657700	3.75706700	-0.26063700
C	0.97654700	-2.13340800	1.43256300
C	0.65595600	-1.59455400	-1.66623800
C	1.68332100	-2.59494200	-2.18767700
H	1.78707600	-3.48071600	-1.54759900
H	1.36397000	-2.95051200	-3.18191600
H	2.67458100	-2.13672900	-2.31373100
C	-0.73523300	-2.22777200	-1.61908500
H	-1.48402600	-1.53857900	-1.19898400
H	-1.05518300	-2.48471500	-2.64261600
H	-0.74908500	-3.15900800	-1.03375400
C	0.62868000	-0.38514900	-2.60644900
H	-0.12365900	0.35400500	-2.29006300
H	1.60656300	0.11960700	-2.65106500
H	0.37865200	-0.71774500	-3.62777200
C	-0.48484200	-2.23488300	1.88187200
H	-0.86626500	-1.25679000	2.20540500
H	-1.15265900	-2.59982700	1.08952400
H	-0.55803300	-2.93602600	2.73016700
C	1.78844700	-1.52505300	2.57888300
H	1.47741400	-0.48702800	2.78232800
H	1.61917500	-2.11038700	3.49781700
H	2.86846800	-1.52075000	2.37503400

C	1.49312000	-3.53189900	1.10502900
H	2.54262300	-3.54401300	0.78128200
H	1.43458100	-4.15644700	2.01239100
H	0.88661000	-4.02975300	0.33532400
Pd	-0.30971200	1.02907900	0.41976400
C	-2.29856300	0.95485500	0.33272500
C	-2.87999600	0.95340600	-0.95543800
C	-3.03436300	0.34086700	1.37580600
C	-4.07012600	0.28864600	-1.20986400
H	-2.37850000	1.48142800	-1.76922000
C	-4.22320900	-0.32026800	1.12688400
H	-2.64979400	0.37301700	2.39850200
C	-4.75538900	-0.36999500	-0.17599300
H	-4.48222900	0.27528400	-2.22138100
H	-4.75597500	-0.81333800	1.94306500
C	-1.55219200	2.70380800	0.73453900
F	-1.56227600	3.46838700	-0.40753700
H	2.71922200	3.77225000	0.60486600
H	2.66261600	3.53580700	-1.18028300
H	-2.44991400	2.93533100	1.32098900
H	-0.68291100	3.01233400	1.36728900
C	-5.97560700	-1.06134400	-0.43615600
N	-6.96795200	-1.62620400	-0.64764700



Pd-CFH_2-NMe_2-GS

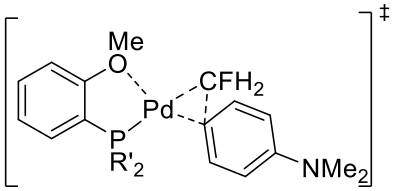
66

Generated by Multiwfn

C	3.26768000	0.83920000	-0.13613800
C	2.88258200	-0.50625000	-0.30200400
C	3.87023400	-1.41433400	-0.70130200
C	5.18268900	-1.02039200	-0.94632000
C	5.53492500	0.31438500	-0.78068100
C	4.58435400	1.24410000	-0.37137400
H	3.61197700	-2.46547800	-0.81629600
H	5.92491200	-1.75695100	-1.25990400
H	6.55928000	0.64397200	-0.96906100
H	4.87040700	2.28816300	-0.24897700
P	1.12667100	-0.94889700	0.05086300
O	2.31666500	1.72549900	0.27167800
C	2.73540500	2.94136200	0.86906000

H	1.84397500	3.39399400	1.30990200
C	1.24691900	-1.75289000	1.75992800
C	0.59858200	-2.17498400	-1.29391100
C	1.17920500	-3.58674200	-1.23246800
H	0.88883900	-4.11488600	-0.31339200
H	0.77257300	-4.16990200	-2.07593100
H	2.27211400	-3.62723300	-1.32399200
C	-0.92858500	-2.28874600	-1.22907300
H	-1.42085600	-1.31069600	-1.29228400
H	-1.27405000	-2.90252300	-2.07779200
H	-1.27956200	-2.77614300	-0.31002200
C	0.97464700	-1.49723300	-2.61501500
H	0.59680600	-0.46223000	-2.65158400
H	2.06130600	-1.46745800	-2.78022200
H	0.51954500	-2.05086400	-3.45286000
C	-0.09517200	-2.40698800	2.08914000
H	-0.94372400	-1.73748100	1.88415100
H	-0.25000100	-3.33941300	1.52713200
H	-0.12176000	-2.66690400	3.16070700
C	1.48494800	-0.58011400	2.71675800
H	0.67684200	0.16553300	2.65421700
H	1.53561200	-0.95325500	3.75349000
H	2.43566500	-0.06641800	2.50438000
C	2.38152100	-2.76030700	1.92174100
H	3.36708700	-2.29676700	1.77162300
H	2.36322400	-3.16319500	2.94880300
H	2.29501900	-3.61527600	1.23782600
Pd	0.09232500	1.21746800	0.01809700
C	-1.83253300	0.77250100	-0.02065700
C	-2.60466000	0.83121200	-1.18855700
C	-2.49755200	0.35250600	1.13861100
C	-3.94153000	0.43753400	-1.21903600
H	-2.15473100	1.18420100	-2.12128600
C	-3.83564100	-0.03873100	1.13043200
H	-1.96677800	0.32815300	2.09492700
C	-4.59104900	-0.03050000	-0.05938400
H	-4.48011700	0.50148200	-2.16505000
H	-4.29050200	-0.35274500	2.07048500
C	-0.62513100	3.11104300	-0.11744000
F	0.43652800	3.99873200	-0.35395000
H	3.49024300	2.73829900	1.64528700
H	3.13756800	3.63785600	0.11848700
H	-1.33112100	3.22684500	-0.95597500
H	-1.12726000	3.44274200	0.80944100
N	-5.90982500	-0.45309600	-0.08522700
C	-6.57847800	-0.75499300	1.14690400

H	-6.06434700	-1.55772700	1.70363900
H	-6.66235000	0.11732500	1.82680000
H	-7.59501200	-1.11127100	0.93396000
C	-6.68716900	-0.26666200	-1.27582500
H	-6.23659300	-0.78247000	-2.14156100
H	-7.68758700	-0.69527300	-1.13063200
H	-6.81410600	0.79911600	-1.55543500



R' = tBu

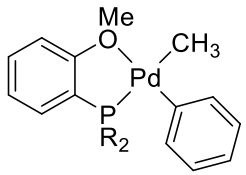
Pd-CFH_2-NMe_2-TS

66

Generated by Multiwfn

C	-3.35920500	0.98443100	0.45680900
C	-3.02546500	-0.38189700	0.29768500
C	-4.04760900	-1.32247300	0.46445300
C	-5.35450500	-0.95233000	0.77375100
C	-5.65832900	0.39560100	0.92859900
C	-4.66940800	1.36245900	0.77241800
H	-3.81749600	-2.38166300	0.35016700
H	-6.12630300	-1.71487400	0.89519700
H	-6.67651100	0.70735500	1.17383700
H	-4.92416000	2.41533600	0.89358100
P	-1.28672800	-0.82447600	-0.12472100
O	-2.36959400	1.88399800	0.29265200
C	-2.59257300	3.24929300	0.52278300
H	-1.61861900	3.73967400	0.39161700
C	-1.39553600	-2.07303900	-1.55130400
C	-0.64036500	-1.60175100	1.47721400
C	-1.51997700	-2.68212600	2.09938600
H	-1.65787900	-3.55554400	1.44871300
H	-1.04344400	-3.04251600	3.02710500
H	-2.51083500	-2.29444700	2.37671400
C	0.76491200	-2.14061900	1.20480000
H	1.39939700	-1.39057000	0.70766200
H	1.24724100	-2.40572500	2.16059700
H	0.74746500	-3.05138100	0.58774500
C	-0.54584500	-0.42551200	2.45413600
H	0.10503700	0.36974900	2.06016900
H	-1.53526700	0.01016100	2.66474900
H	-0.12436500	-0.77580600	3.41148800

C	-0.01863200	-2.06101900	-2.22616000
H	0.24241700	-1.04663400	-2.56218800
H	0.78622400	-2.39954800	-1.55907500
H	-0.03447200	-2.73088700	-3.10291500
C	-2.41331500	-1.49556200	-2.53816400
H	-2.20702700	-0.43276400	-2.74660800
H	-2.34953600	-2.04251100	-3.49376900
H	-3.44692000	-1.57308600	-2.17246600
C	-1.75970600	-3.51417000	-1.20351200
H	-2.74029800	-3.61234600	-0.71810200
H	-1.80560700	-4.10752300	-2.13270200
H	-1.00632500	-3.98865900	-0.55886000
Pd	-0.02127800	1.06329700	-0.66148400
C	1.99313300	1.11029400	-0.51547000
C	2.54803900	1.30153000	0.75746500
C	2.76155700	0.37824100	-1.43624100
C	3.75611000	0.71646700	1.12867600
H	2.01687500	1.91786700	1.48678100
C	3.97045800	-0.20700000	-1.07980700
H	2.39754100	0.23600600	-2.45748500
C	4.50269300	-0.05971900	0.22019100
H	4.11780100	0.87720400	2.14450500
H	4.50435700	-0.78983400	-1.83083100
C	1.06787600	2.76359000	-1.12752000
F	1.12354500	3.64698500	-0.07290600
H	-3.31309600	3.67581800	-0.19636600
H	-2.94919600	3.43489100	1.55035600
H	1.90293900	2.97186300	-1.80770200
H	0.12336700	2.96901300	-1.70419400
N	5.70593500	-0.64096400	0.57876900
C	6.12839200	-0.59659000	1.94877200
H	7.10570900	-1.08688700	2.04688900
H	6.24870800	0.44081300	2.30690300
H	5.42438700	-1.10493300	2.63844700
C	6.35141900	-1.54716100	-0.32662800
H	5.74068400	-2.44364100	-0.55685200
H	6.59840100	-1.06110700	-1.28665300
H	7.29710500	-1.89112300	0.11218500



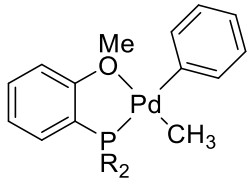
Pd-CH_3-GS

58

Pd-CH3-GS

C	2.52900400	1.20488100	-0.00004300
C	2.29789500	-0.18686400	-0.00003300
C	3.41764200	-1.02891700	0.00000200
C	4.71874900	-0.53397500	0.00005000
C	4.91976900	0.84071400	0.00007300
C	3.83326600	1.71017800	0.00002400
H	3.27053700	-2.10698400	-0.00000600
H	5.56656700	-1.22164900	0.00007500
H	5.93159000	1.25255400	0.00012700
H	4.01493000	2.78353900	0.00004400
P	0.56140900	-0.80474900	-0.00002500
O	1.44718900	2.03543500	-0.00012100
C	1.66573600	3.43271500	-0.00044700
H	0.67740900	3.90141500	-0.00069400
C	0.42612100	-1.81463200	1.59585200
C	0.42607700	-1.81471700	-1.59582900
C	0.54770500	-0.75594100	-2.69769200
H	-0.22393900	0.02322100	-2.59558200
H	1.53213500	-0.26205300	-2.68491400
H	0.42751800	-1.23571800	-3.68341700
C	1.47483800	-2.89777000	-1.83064200
H	1.23129100	-3.42941200	-2.76613600
H	2.48518300	-2.48471000	-1.95368300
H	1.49500000	-3.65241100	-1.03140600
C	-0.96958000	-2.44032300	-1.65246800
H	-1.04467100	-3.33736600	-1.02323700
H	-1.75866400	-1.73770700	-1.34922800
H	-1.18061800	-2.75388500	-2.68855100
C	-0.96953300	-2.44023200	1.65259500
H	-1.75863200	-1.73763100	1.34936000
H	-1.04467200	-3.33729800	1.02340200
H	-1.18050800	-2.75375200	2.68870400
C	0.54779900	-0.75580400	2.69766000
H	-0.22383700	0.02336500	2.59553000
H	0.42762500	-1.23553500	3.68341000
H	1.53223800	-0.26193700	2.68483900
C	1.47488500	-2.89768200	1.83065400
H	2.48524400	-2.48463200	1.95360100
H	1.23140200	-3.42927400	2.76619500
H	1.49497700	-3.65236700	1.03145800
Pd	-0.69625100	1.20418500	0.00006100
C	-2.54379400	0.53768500	0.00003000
C	-3.22789600	0.28559800	-1.20024000
C	-3.22800300	0.28552500	1.20021800
C	-4.51981500	-0.24300800	-1.20081300

H	-2.74702400	0.50586400	-2.15728600
C	-4.51992100	-0.24308700	1.20064100
H	-2.74721800	0.50574300	2.15732000
C	-5.17137100	-0.51883900	-0.00012300
H	-5.02252300	-0.43719400	-2.15292100
H	-5.02271300	-0.43733700	2.15269200
H	-6.18264900	-0.93320100	-0.00018000
C	-1.60232400	3.04230400	0.00032900
H	2.21579700	3.74437100	0.90166300
H	2.21603900	3.74390100	-0.90257100
H	-1.26574000	3.58592100	-0.90316700
H	-1.26514700	3.58591500	0.90360800
H	-2.70153500	3.05463200	0.00068700



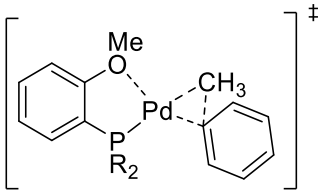
Pd-CH_3-GS-*trans*

58

Pd-CH3-GS-trans

C	-0.77442100	2.17948900	0.03106900
C	-1.81364100	1.22526800	0.00359700
C	-3.13031400	1.69914300	-0.05295400
C	-3.42893800	3.05816100	-0.07469600
C	-2.38867200	3.97946900	-0.03788200
C	-1.06718700	3.54771500	0.01422200
H	-3.95120100	0.98416100	-0.08378800
H	-4.46755300	3.39103800	-0.12015400
H	-2.59859900	5.05147800	-0.05286000
H	-0.26748100	4.28621400	0.03570400
P	-1.37607700	-0.56376100	-0.00267100
O	0.50860600	1.72778000	0.06929600
C	1.56652200	2.66765700	0.14443800
H	1.46538800	3.29578000	1.04356300
C	-2.21455000	-1.26196300	-1.55392400
C	-2.10779400	-1.22277800	1.61355900
C	-1.96875900	-2.74555300	1.61274900
H	-0.94312300	-3.06177000	1.37316200
H	-2.21070200	-3.13343000	2.61635000
H	-2.65909600	-3.22843900	0.90526200
C	-1.19775100	-0.63638000	2.69822300
H	-1.23831100	0.46440800	2.71243200
H	-1.52581200	-0.99424500	3.68865200

H	-0.14819900	-0.93494700	2.54836500
C	-3.55079800	-0.83127200	1.92011300
H	-4.26208100	-1.16492800	1.15268300
H	-3.85381200	-1.30540700	2.86907200
H	-3.66273300	0.25340300	2.05484300
C	-1.52388000	-2.58986700	-1.87960500
H	-0.44102500	-2.45509100	-2.01028900
H	-1.67878400	-3.35141500	-1.10249600
H	-1.93842300	-2.99134800	-2.81953300
C	-1.88786900	-0.27093900	-2.67470900
H	-2.43281800	0.67780700	-2.56913500
H	-0.80930800	-0.04456000	-2.70623400
H	-2.16428100	-0.71448000	-3.64562600
C	-3.72142300	-1.48858300	-1.47518200
H	-3.99162600	-2.23904700	-0.71854900
H	-4.28611100	-0.56875000	-1.27147200
H	-4.07824300	-1.87028800	-2.44682700
Pd	0.98014000	-0.53052900	-0.02788100
C	2.97395600	-0.28017100	-0.03481500
C	3.66451500	-0.03756200	-1.23495800
C	3.71340900	-0.19388700	1.15732100
C	5.01807500	0.30555500	-1.24389600
H	3.13437400	-0.11319200	-2.19000400
C	5.06698600	0.14988600	1.15590200
H	3.22244500	-0.39490600	2.11521200
C	5.72517400	0.40493300	-0.04636200
H	5.52594400	0.49412500	-2.19466600
H	5.61323200	0.21599900	2.10178400
H	6.78504000	0.67298400	-0.05055200
C	1.47049800	-2.48881500	-0.02060300
H	2.49157000	2.08460300	0.20752700
H	1.59384100	3.29967900	-0.75734700
H	0.57577300	-3.12677900	-0.04622000
H	2.04766700	-2.72104000	0.88886900
H	2.10110100	-2.73614900	-0.88913600



Pd-CH_3-TS

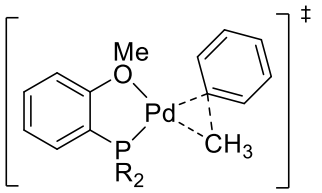
58

Generated by Multiwfn

C	2.62958800	-1.29147700	0.07967600

C	2.39895700	0.10359700	0.07187700
C	3.51669500	0.94444100	0.12484900
C	4.81710800	0.45031800	0.19005800
C	5.01848800	-0.92496500	0.20630700
C	3.93377300	-1.79496600	0.15120300
H	3.36895800	2.02360300	0.11449100
H	5.66391900	1.13822700	0.22945300
H	6.02982800	-1.33506500	0.25995700
H	4.11150500	-2.86999400	0.15920700
P	0.66388400	0.71818400	-0.03952700
O	1.55131000	-2.10376500	0.01170700
C	1.71562300	-3.49503100	0.07499800
H	0.70613700	-3.92594500	0.04030300
C	0.65994700	1.90761100	-1.52097600
C	0.39470800	1.60816900	1.61109000
C	0.32522200	0.47531400	2.64007800
H	-0.47906600	-0.23612000	2.39721700
H	1.27233700	-0.08479400	2.69401600
H	0.12807900	0.89603700	3.64065600
C	1.47734200	2.59161400	2.04743400
H	1.17815300	3.04820600	3.00635700
H	2.44167000	2.09259100	2.21802100
H	1.62986500	3.41317000	1.33500500
C	-0.96277800	2.30975800	1.54327000
H	-0.93585000	3.20375000	0.90274700
H	-1.75327900	1.63759200	1.17576200
H	-1.25212800	2.64460200	2.55361000
C	-0.80356800	2.07115600	-1.94210400
H	-1.25659600	1.09821200	-2.17649300
H	-1.42381700	2.53832000	-1.16504900
H	-0.85602600	2.70843700	-2.84128900
C	1.39973200	1.17244100	-2.64148100
H	1.01611800	0.14618100	-2.76510300
H	1.24419700	1.70482400	-3.59473000
H	2.48244100	1.11110100	-2.46082700
C	1.27337800	3.28847300	-1.30759600
H	2.33224600	3.25263100	-1.01750800
H	1.22372900	3.85351300	-2.25407600
H	0.72567900	3.87533700	-0.55664900
Pd	-0.80739700	-1.07584800	-0.26304300
C	-2.78695500	-0.82027100	-0.09363800
C	-3.30639700	-0.65709200	1.20749800
C	-3.50185500	-0.21408000	-1.14980300
C	-4.42860400	0.13518700	1.44646900
H	-2.81346900	-1.15023700	2.04945500
C	-4.62001100	0.57554800	-0.90612600

H	-3.16519200	-0.36219000	-2.17936900
C	-5.09021600	0.76621900	0.39532300
H	-4.78839700	0.25746500	2.47220700
H	-5.13486700	1.04863400	-1.74738400
H	-5.97006100	1.38590400	0.58314100
C	-2.18344100	-2.66003700	-0.42911500
H	2.29581100	-3.87906600	-0.78125600
H	2.20079900	-3.80480800	1.01599500
H	-1.30104500	-3.13982400	-0.92247700
H	-3.02784900	-2.82776300	-1.10650500
H	-2.38273700	-3.16774200	0.52460000



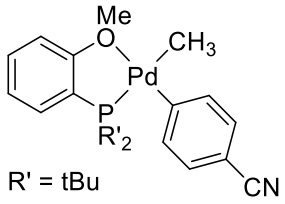
Pd-CH_3-TS-*trans*

58

Pd-CH3-TS-trans

C	-0.73243000	2.21337400	0.03928300
C	-1.77120400	1.26319800	-0.10456600
C	-3.05658400	1.74381200	-0.37723900
C	-3.32597900	3.10203800	-0.52657100
C	-2.28641000	4.01648300	-0.39783000
C	-0.99572200	3.57965200	-0.11583100
H	-3.87709900	1.03443300	-0.48138100
H	-4.34150600	3.43916500	-0.74312800
H	-2.47479800	5.08654700	-0.51403500
H	-0.19252200	4.30892500	-0.01370400
P	-1.35470200	-0.52667400	0.04162100
O	0.49606400	1.74686200	0.33876500
C	1.59649900	2.62128400	0.39907200
H	1.46868300	3.37167600	1.19743700
C	-2.26403200	-1.39760100	-1.38325800
C	-2.06796000	-0.97810300	1.73810900
C	-1.94563900	-2.48987200	1.92472000
H	-0.92657700	-2.84008100	1.69749500
H	-2.16656400	-2.75265500	2.97297000
H	-2.65350200	-3.04873400	1.29489000
C	-1.13800800	-0.27729500	2.73386500
H	-1.17666100	0.81793100	2.62799500
H	-1.44535400	-0.52409900	3.76426500
H	-0.09153500	-0.59355100	2.59631400
C	-3.50046300	-0.52193700	1.99918500

H	-4.22821500	-0.97363100	1.31209300
H	-3.79441300	-0.81644700	3.02125400
H	-3.59816300	0.57144400	1.93763800
C	-1.57097500	-2.75432400	-1.55785200
H	-0.49285500	-2.62802100	-1.73401000
H	-1.69133200	-3.40697000	-0.68159300
H	-2.00795200	-3.27911100	-2.42432300
C	-1.97973700	-0.55891900	-2.63185900
H	-2.53225800	0.39101200	-2.63776300
H	-0.90525000	-0.32586700	-2.71598100
H	-2.27178700	-1.12723500	-3.53077400
C	-3.76463000	-1.63489500	-1.23286900
H	-3.99822300	-2.29616500	-0.38624300
H	-4.34582500	-0.71038300	-1.11682000
H	-4.14288000	-2.13363500	-2.14150900
Pd	0.98707900	-0.74199000	-0.05582200
C	2.96032900	-0.66088600	-0.13805900
C	3.51023200	-0.09392500	-1.30375600
C	3.62684100	-0.43036900	1.08435400
C	4.64837000	0.71026500	-1.24171000
H	3.03013800	-0.27685600	-2.26890300
C	4.76238100	0.37392000	1.13993900
H	3.24261600	-0.88773000	2.00051200
C	5.27916100	0.95227800	-0.02204500
H	5.04560900	1.15401700	-2.15911200
H	5.25152800	0.55141300	2.10202300
H	6.17330700	1.57856800	0.02351000
C	2.19863000	-2.47585900	-0.41833100
H	2.47099500	1.99882100	0.62683400
H	1.76067100	3.13034000	-0.56511600
H	1.40897000	-3.08897700	0.05345400
H	3.15318500	-2.83754700	-0.01699000
H	2.19993300	-2.64373000	-1.50441800



Pd-CH_3-CN-GS

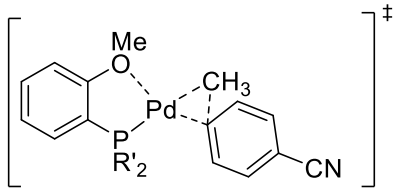
59

Generated by Multiwfn

C	-2.95864900	-1.04544700	-0.00011000
C	-2.62959600	0.32588500	-0.00000500
C	-3.68579100	1.24668300	0.00028500

C	-5.01846000	0.84543300	0.00044600
C	-5.31665100	-0.51154100	0.00033100
C	-4.29520100	-1.45659200	0.00005900
H	-3.46217700	2.31162000	0.00039900
H	-5.81526800	1.59150100	0.00066900
H	-6.35515900	-0.85025700	0.00046800
H	-4.55378200	-2.51395300	-0.00000800
P	-0.85622000	0.81934400	-0.00017000
O	-1.93753900	-1.95235000	-0.00037500
C	-2.26023700	-3.33084300	-0.00067000
H	-1.31079400	-3.87341600	-0.00099300
C	-0.64413600	1.81263500	1.59692400
C	-0.64435100	1.81254500	-1.59735500
C	-0.85253700	0.76688500	-2.69876600
H	-0.14455200	-0.07116500	-2.60114800
H	-1.87267300	0.35214400	-2.68319900
H	-0.69827600	1.23611800	-3.68462100
C	-1.60654500	2.97421600	-1.82756300
H	-1.32674100	3.48482800	-2.76442400
H	-2.64635400	2.64095200	-1.94593900
H	-1.56417300	3.72828500	-1.02885000
C	0.79522500	2.32816800	-1.65811000
H	0.94406700	3.21254900	-1.02424200
H	1.52844600	1.56462800	-1.36300600
H	1.02544200	2.63036100	-2.69327800
C	0.79544200	2.32828600	1.65744100
H	1.52863400	1.56474400	1.36227200
H	0.94417800	3.21263600	1.02350700
H	1.02580200	2.63053500	2.69256000
C	-0.85215200	0.76703500	2.69842300
H	-0.14416100	-0.07100600	2.60075800
H	-0.69776700	1.23632800	3.68423000
H	-1.87228200	0.35227000	2.68301600
C	-1.60631600	2.97430700	1.82719100
H	-2.64610700	2.64103600	1.94571800
H	-1.32639900	3.48497500	2.76398700
H	-1.56405800	3.72833100	1.02843000
Pd	0.24934800	-1.27927300	-0.00018400
C	2.13722700	-0.76891400	0.00016400
C	2.84434800	-0.57704500	-1.20134500
C	2.84404200	-0.57745000	1.20191800
C	4.17214900	-0.16746000	-1.20853700
H	2.34738600	-0.75315200	-2.15844900
C	4.17184100	-0.16786700	1.20958500
H	2.34683700	-0.75388300	2.15883500
C	4.85033900	0.05168800	0.00064700

H	4.69684800	-0.01611900	-2.15463800
H	4.69630000	-0.01684500	2.15587100
C	1.01675900	-3.18191800	-0.00015200
H	-2.83171700	-3.59933400	0.90167500
H	-2.83206700	-3.59885700	-0.90293400
H	0.63711500	-3.69398900	-0.90424000
H	0.63661800	-3.69412700	0.90364900
H	2.11111200	-3.28547600	0.00013900
C	6.21390900	0.47902800	0.00089300
N	7.32076600	0.82809000	0.00109200



R' = tBu

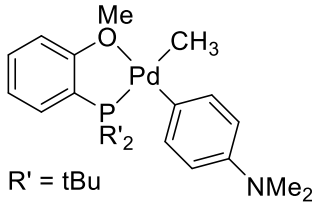
Pd-CH_3-CN-TS

59

Generated by Multiwfn

C	-3.03145900	-1.05651100	0.15647900
C	-2.68111300	0.31215200	0.15184000
C	-3.71158700	1.24426700	0.32202800
C	-5.03815500	0.85996500	0.49836000
C	-5.35739500	-0.49280500	0.50069700
C	-4.36219900	-1.45056500	0.32982900
H	-3.47264200	2.30677000	0.31617400
H	-5.81458900	1.61576100	0.63085700
H	-6.39203100	-0.81655300	0.63577500
H	-4.63254000	-2.50592300	0.33360600
P	-0.90839900	0.77037500	-0.05582700
O	-2.03437800	-1.96057000	-0.01562000
C	-2.32681800	-3.33590800	0.00833000
H	-1.37210800	-3.85794400	-0.13457000
C	-0.50933000	1.96375700	1.36254800
C	-0.86372500	1.59921600	-1.75697300
C	-1.07200300	0.44914900	-2.74730300
H	-0.29546900	-0.32415400	-2.63561100
H	-2.05305800	-0.03334500	-2.61282400
H	-1.03103100	0.83744300	-3.77885900
C	-1.92978800	2.66090700	-2.01372300
H	-1.78064400	3.08128900	-3.02278400
H	-2.94448700	2.23918200	-1.98843200
H	-1.88306400	3.49942400	-1.30622000
C	0.53228900	2.19012400	-1.95751000

H	0.68280300	3.10604800	-1.36761600
H	1.32426600	1.47291500	-1.69156400
H	0.66561000	2.46311200	-3.01771100
C	1.01746900	2.05783500	1.44566700
H	1.48494400	1.06637000	1.51283500
H	1.45883100	2.57164300	0.58125200
H	1.29539800	2.63189400	2.34540400
C	-1.02003900	1.26290500	2.62433500
H	-0.64890000	0.22623700	2.68145900
H	-0.65456800	1.79946700	3.51548100
H	-2.11825000	1.23453500	2.67319300
C	-1.08401200	3.37495600	1.27510200
H	-2.18158400	3.39891900	1.25084300
H	-0.77630400	3.94046600	2.17089800
H	-0.70200800	3.92699200	0.40467800
Pd	0.30172800	-1.21874800	-0.03969300
C	2.28167800	-1.19346100	-0.01515300
C	2.96126200	-0.75523900	-1.18269000
C	2.95381000	-1.00758600	1.22026400
C	4.18327900	-0.11179300	-1.11219800
H	2.50406600	-0.91991700	-2.16147200
C	4.17931600	-0.36739600	1.29200800
H	2.48734400	-1.36459500	2.14159600
C	4.81335400	0.10329700	0.12864400
H	4.66777200	0.23917700	-2.02639400
H	4.65963000	-0.21785300	2.26179700
C	1.50422200	-2.96759300	-0.13470200
H	-2.75729700	-3.64133800	0.97635400
H	-3.01260800	-3.61751600	-0.80768200
H	1.22362500	-3.42763300	0.82803800
H	2.51976200	-3.30324700	-0.36870400
H	0.86891800	-3.34318900	-0.96235500
C	6.06957000	0.77236700	0.20172400
N	7.09285300	1.31924000	0.26074300



Pd-CH_3-NMe_2-GS

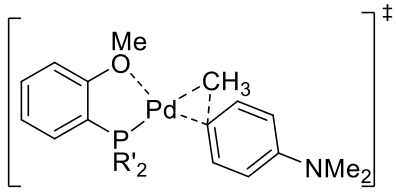
66

Generated by Multiwfn

C	3.31498600	-0.97015000	-0.00226300
C	2.93063300	0.38765600	-0.00229800

C	3.95025600	1.34843600	-0.00429900
C	5.29843400	1.00111100	-0.00672300
C	5.65081000	-0.34276900	-0.00709300
C	4.66744200	-1.32740300	-0.00479300
H	3.68405700	2.40354000	-0.00381700
H	6.06470400	1.77866700	-0.00828400
H	6.70211600	-0.63980200	-0.00910100
H	4.96679800	-2.37411700	-0.00507900
P	1.13522600	0.80818900	0.00104400
O	2.33251700	-1.91525800	0.00061000
C	2.70249300	-3.27963900	0.00515000
H	1.77078900	-3.85304300	0.01001200
C	0.88762500	1.80284600	-1.59141700
C	0.89343100	1.79618500	1.59853700
C	1.13365300	0.75592100	2.69847500
H	0.45167900	-0.10282200	2.59584500
H	2.16637000	0.37302300	2.68252700
H	0.96388200	1.21823600	3.68534000
C	1.81634900	2.98839600	1.83268200
H	1.51853800	3.48847200	2.77000200
H	2.86668300	2.68951900	1.95154500
H	1.75039900	3.74182700	1.03471600
C	-0.56318500	2.26230700	1.65956300
H	-0.73932000	3.14581600	1.03131400
H	-1.26971700	1.47615800	1.35707100
H	-0.80489000	2.54977500	2.69661700
C	-0.56889200	2.27036800	-1.64381300
H	-1.27455200	1.48373300	-1.34052600
H	-0.74109400	3.15206500	-1.01191100
H	-0.81542100	2.56132900	-2.67875200
C	1.12205300	0.76692900	-2.69667500
H	0.43866400	-0.09080700	-2.59557700
H	0.94995100	1.23395400	-3.68092200
H	2.15403500	0.38184800	-2.68582500
C	1.81030100	2.99534600	-1.82522700
H	2.85951900	2.69600900	-1.95240200
H	1.50701700	3.50044100	-2.75808800
H	1.75028800	3.74480000	-1.02307000
Pd	0.10681600	-1.32662600	-0.00144300
C	-1.80265100	-0.84947600	-0.00136900
C	-2.52134100	-0.67016700	1.18779100
C	-2.52111100	-0.66690300	-1.19016500
C	-3.85668600	-0.26863900	1.19820100
H	-2.03493200	-0.84953000	2.15096500
C	-3.85644300	-0.26533500	-1.19976400
H	-2.03449700	-0.84357700	-2.15372900

C	-4.55700800	-0.02954700	-0.00052600
H	-4.35313500	-0.14519000	2.16130500
H	-4.35268200	-0.13923300	-2.16263200
C	-0.59414800	-3.24987200	-0.00465300
H	3.28108800	-3.53332000	-0.89742900
H	3.28605700	-3.52574400	0.90661200
H	-0.20769100	-3.75564300	0.90126300
H	-0.19578500	-3.75633400	-0.90500600
H	-1.68616300	-3.37611000	-0.01169900
N	-5.87441900	0.40592400	-0.00004900
C	-6.60316300	0.43636000	1.23441100
H	-6.11445500	1.08923900	1.97787900
H	-7.60639000	0.84649800	1.05708300
H	-6.72406900	-0.56308000	1.70114300
C	-6.60296800	0.43975400	-1.23453500
H	-6.11419900	1.09473800	-1.97611000
H	-6.72372700	-0.55839000	-1.70406500
H	-7.60626100	0.84930800	-1.05622600



R' = tBu

Pd-CH_3-NMe_2-TS

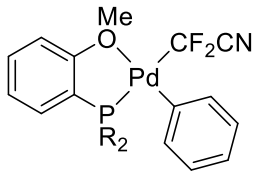
66

Generated by Multiwfn

C	3.42742800	-0.85654700	-0.41709700
C	2.91980100	0.46340600	-0.38972000
C	3.77689900	1.49094900	-0.79756800
C	5.07599100	1.24805700	-1.23763200
C	5.54773200	-0.05881900	-1.26821100
C	4.73125900	-1.10895800	-0.85852800
H	3.42072000	2.51954200	-0.76993600
H	5.71237800	2.07806600	-1.55076200
H	6.56340400	-0.27291800	-1.60947100
H	5.11828700	-2.12726600	-0.88384800
P	1.17873800	0.72250600	0.16506500
O	2.60896200	-1.84374200	0.00844700
C	3.05337500	-3.17253400	0.00003900
H	2.22096900	-3.77880100	0.38204600
C	0.44267600	2.06358000	-0.96331000
C	1.41810300	1.34728700	1.93978500
C	1.86544300	0.11263300	2.72842900

H	1.12044300	-0.69637000	2.66014600
H	2.82688800	-0.28070500	2.36387300
H	1.99621400	0.38022800	3.79082500
C	2.46699400	2.44282900	2.10805600
H	2.53721800	2.71820800	3.17447100
H	3.46494300	2.10470700	1.79351900
H	2.22386200	3.35895800	1.55372800
C	0.06482200	1.81361800	2.47634000
H	-0.25039500	2.77091000	2.03624900
H	-0.72490400	1.07044300	2.28530100
H	0.13365200	1.96488200	3.56694400
C	-1.07793100	2.00886600	-0.76975600
H	-1.47823200	1.00282800	-0.94941700
H	-1.38965000	2.31237400	0.23848500
H	-1.55418700	2.70164900	-1.48409900
C	0.75440400	1.60607200	-2.39086000
H	0.47006600	0.55091200	-2.53633900
H	0.17293600	2.21202600	-3.10564300
H	1.81857500	1.70912400	-2.64701600
C	0.89414900	3.50788300	-0.75449100
H	1.97053800	3.66796100	-0.89993200
H	0.37893600	4.14946100	-1.48954300
H	0.62219800	3.88599700	0.24114100
Pd	0.02097300	-1.30908000	0.11966400
C	-1.98279900	-1.40109900	0.04028600
C	-2.70468800	-0.96633800	1.16609300
C	-2.62434700	-1.25133700	-1.20114100
C	-3.94511700	-0.34773200	1.05641200
H	-2.27518200	-1.09590800	2.16347600
C	-3.86753600	-0.63767400	-1.32476600
H	-2.12543500	-1.60079900	-2.10927200
C	-4.56622700	-0.16305900	-0.19676700
H	-4.43469800	-0.00723200	1.96928900
H	-4.29321500	-0.53033300	-2.32280400
C	-1.02602100	-3.12320500	0.21623000
H	3.30166400	-3.51635600	-1.01852900
H	3.92694900	-3.31413100	0.65889200
H	-1.61348900	-3.45873400	1.07923900
H	0.01787200	-3.50327800	0.37315800
H	-1.41510500	-3.59751800	-0.69340900
N	-5.80732700	0.44359900	-0.31061700
C	-6.30442700	0.78099800	-1.61298700
H	-7.30196000	1.23017600	-1.51910000
H	-5.65823400	1.50079400	-2.15649700
H	-6.41184100	-0.11240000	-2.25190800
C	-6.38562400	1.07894900	0.83791800

H	-7.37263600	1.48184800	0.57495800
H	-6.53920500	0.36422800	1.66462200
H	-5.77273400	1.91528600	1.23284200



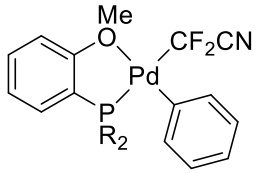
Pd-CF_2CN-GS

59

Pd-CF2CN-GS

C	-2.34950500	1.49181800	-0.25290900
C	-2.49436500	0.09244200	-0.31602700
C	-3.75020800	-0.40677000	-0.68065000
C	-4.81649100	0.43335300	-0.98884700
C	-4.64175000	1.81156000	-0.92822000
C	-3.41149200	2.34471700	-0.55672700
H	-3.90803400	-1.48274600	-0.71931600
H	-5.78077200	0.00775300	-1.27253200
H	-5.46635800	2.48508100	-1.17197400
H	-3.27707600	3.42569000	-0.51897300
P	-1.03413600	-0.94853700	0.12172000
O	-1.13424600	1.98205500	0.12536200
C	-1.06290500	3.27224100	0.71177100
H	-1.89768400	3.41239100	1.41554800
C	-1.06466100	-2.46048100	-1.01600100
C	-1.36377200	-1.38424800	1.93241100
C	-2.79147800	-1.84797700	2.20921900
H	-3.05592000	-2.76715100	1.67012900
H	-2.89722400	-2.06157200	3.28611500
H	-3.53102600	-1.07466900	1.95607000
C	-0.35898100	-2.44740800	2.37620000
H	0.67259500	-2.18420200	2.09931200
H	-0.39697900	-2.54691600	3.47356200
H	-0.58756600	-3.43656700	1.95456900
C	-1.10463100	-0.09000600	2.71076300
H	-0.08124900	0.28739500	2.55765900
H	-1.80875700	0.70664200	2.42672700
H	-1.24182200	-0.27955100	3.78813000
C	0.30157000	-3.14727500	-0.91135600
H	1.12790200	-2.47008100	-1.15487200
H	0.49550700	-3.56373600	0.08541500
H	0.32741000	-3.98547600	-1.62712900
C	-1.21074300	-1.89415200	-2.43192400
H	-0.47104300	-1.09942300	-2.62203600

H	-1.03254500	-2.69764400	-3.16501700
H	-2.21002000	-1.47865500	-2.62367700
C	-2.13646900	-3.51491200	-0.74014000
H	-3.16708400	-3.14449400	-0.80327700
H	-2.04186700	-4.31182000	-1.49631800
H	-2.00280900	-3.99207200	0.24071700
Pd	0.71628900	0.64741200	-0.15341600
C	2.31211100	-0.50866900	-0.19129100
C	2.86797400	-0.97410800	1.00620300
C	2.91541200	-0.88396500	-1.39904400
C	3.96977100	-1.83262400	0.99456400
H	2.45102200	-0.65909800	1.96676000
C	4.01337700	-1.74386700	-1.40833800
H	2.52733900	-0.50279700	-2.34689800
C	4.54004000	-2.22977700	-0.21232500
H	4.38621100	-2.18783800	1.94130500
H	4.46359900	-2.03330000	-2.36199900
H	5.40004900	-2.90385600	-0.22118800
C	2.02379200	2.21073900	-0.43036700
F	1.30898700	3.25577900	-0.98293900
F	3.09607300	2.04042200	-1.23887500
H	-0.11726300	3.32064200	1.26349700
H	-1.07325100	4.06102400	-0.05408000
C	2.47443300	2.64588200	0.90000800
N	2.71710300	2.92326100	1.99953100



Pd-CF_2CN-GS'

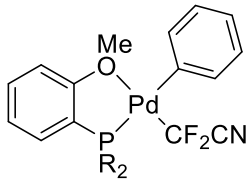
59

Pd-CF2CN-GS’

C	-2.36095700	1.39582100	0.12913300
C	-2.43302400	0.00271200	0.32632200
C	-3.64154400	-0.51706600	0.80459800
C	-4.73026400	0.29643400	1.10371200
C	-4.62568500	1.66977900	0.91718800
C	-3.44705000	2.22182300	0.42583400
H	-3.74280700	-1.59103900	0.94467200
H	-5.65461900	-0.14583700	1.47965800
H	-5.46617200	2.32639700	1.15267600
H	-3.37511300	3.29974000	0.28804700
P	-0.95188700	-1.01872100	-0.08049100
O	-1.20070800	1.90493600	-0.37800700

C	-1.21447500	3.21862000	-0.91839000
H	-1.28391600	3.97399700	-0.12195100
C	-1.35826100	-1.66893000	-1.80957700
C	-0.85164900	-2.39441800	1.21721400
C	-1.89150000	-3.51149000	1.12381000
H	-1.79826900	-4.08534600	0.19129600
H	-1.71358200	-4.21877700	1.95071600
H	-2.93173000	-3.17723100	1.21865700
C	0.53230400	-3.04496600	1.11011400
H	1.34363200	-2.32287800	1.25144600
H	0.61852000	-3.80909600	1.90013200
H	0.69528000	-3.54991800	0.14951500
C	-0.94280900	-1.67662300	2.56740200
H	-0.23032200	-0.83752100	2.62120500
H	-1.94736400	-1.28033000	2.77193100
H	-0.68724000	-2.38370000	3.37329400
C	-0.34474200	-2.74778300	-2.19093400
H	0.69104200	-2.42953600	-2.00267900
H	-0.51802300	-3.69031500	-1.65229400
H	-0.43768300	-2.96851900	-3.26714700
C	-1.18453200	-0.46262800	-2.73834500
H	-0.16216200	-0.05471200	-2.69512800
H	-1.38831000	-0.76928200	-3.77764400
H	-1.88382500	0.35067400	-2.49176300
C	-2.78154600	-2.20182700	-1.95300500
H	-3.53345500	-1.42477300	-1.75426700
H	-2.93288100	-2.54635600	-2.98978700
H	-2.98716700	-3.05683900	-1.29537500
Pd	0.72824200	0.66571500	-0.11153300
C	2.34846600	-0.42785000	0.09529000
C	2.97395500	-0.54620500	1.34370800
C	2.90008800	-1.10617200	-0.99697200
C	4.09345600	-1.36279800	1.50273200
H	2.58370400	-0.00126400	2.20739600
C	4.02182700	-1.92206500	-0.83525600
H	2.46032100	-0.99809100	-1.99196800
C	4.61694400	-2.06234600	0.41634200
H	4.56145900	-1.45065500	2.48719000
H	4.43392000	-2.44985400	-1.69995000
H	5.49235800	-2.70396900	0.54257700
C	2.00052600	2.29582700	-0.16044500
F	1.88721700	2.92245300	-1.38893700
F	3.33009500	2.15298900	0.04895600
H	-0.26609000	3.34387600	-1.44949900
H	-2.05067000	3.32617400	-1.62662200
C	1.47134500	3.21978700	0.85892100

N	0.94784900	3.86551700	1.66729700



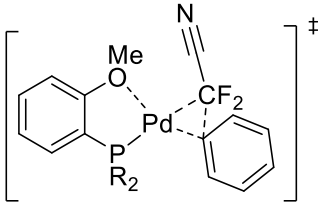
Pd-CF_2CN-GS-*trans*

59

Pd-CF2CN-GS-trans

C	-1.19287100	2.32377000	-0.13989900
C	-2.12959100	1.27054700	-0.15045900
C	-3.48276100	1.61082700	-0.28304000
C	-3.90692400	2.92720900	-0.43168500
C	-2.96049400	3.94432300	-0.45314700
C	-1.60952600	3.64884600	-0.30522900
H	-4.23326400	0.82359000	-0.26899700
H	-4.97027000	3.15155900	-0.53334700
H	-3.26762700	4.98488400	-0.57995100
H	-0.88580100	4.46155500	-0.31765200
P	-1.54728500	-0.46424400	0.06808700
O	0.12340700	2.01697800	0.05173000
C	1.05276300	3.08460900	0.18100200
H	1.14573600	3.63754300	-0.76625300
C	-2.15500800	-1.36656300	-1.48609900
C	-2.38242300	-1.02569000	1.67362200
C	-3.87724800	-1.31525700	1.57364900
H	-4.25124600	-1.61162200	2.56802400
H	-4.46408700	-0.43965000	1.26511500
H	-4.09683500	-2.14646800	0.88853900
C	-1.65739600	-2.27612200	2.17590100
H	-2.09232600	-2.57319600	3.14467100
H	-1.75419300	-3.12974200	1.49272500
H	-0.58542600	-2.09016400	2.32506300
C	-2.13169100	0.10614900	2.67477400
H	-2.70277500	1.01448900	2.43560900
H	-2.43288100	-0.22718500	3.68143600
H	-1.06295500	0.37318700	2.72112800
C	-1.19827300	-0.89828800	-2.58859400
H	-0.15848200	-1.19972600	-2.39347700
H	-1.50237500	-1.34461100	-3.54996700
H	-1.22049200	0.19659200	-2.71136400
C	-3.58609200	-1.06490500	-1.92738400
H	-3.71187700	-0.02312500	-2.25102900
H	-3.82121400	-1.70096500	-2.79696000

H	-4.33510400	-1.29018300	-1.15556200
C	-2.00321200	-2.87411700	-1.28228700
H	-2.74239800	-3.27194400	-0.57112300
H	-2.17586900	-3.38174500	-2.24552800
H	-1.00141500	-3.15135200	-0.93391300
Pd	0.83400200	-0.17193800	0.14977700
C	2.76395400	0.40396500	0.09996800
C	3.36457900	0.74186600	-1.11977700
C	3.46783800	0.66729000	1.28372800
C	4.61226100	1.36813600	-1.15466600
H	2.85994500	0.50882000	-2.06273800
C	4.71385200	1.29561800	1.25093400
H	3.04056900	0.37977700	2.24898400
C	5.28653000	1.65446700	0.03093200
H	5.06231700	1.62839500	-2.11685200
H	5.24410600	1.50090500	2.18528200
H	6.26311800	2.14461900	0.00455700
C	1.60094200	-2.01753000	0.19126000
F	2.55825100	-2.22325400	1.12970800
F	0.66128700	-2.98914000	0.44591600
H	0.74420200	3.76312000	0.99093700
H	2.01708500	2.63178900	0.42914900
C	2.14655100	-2.30973600	-1.14650900
N	2.50848100	-2.48101300	-2.23342400



Pd-CF_2CN-TS

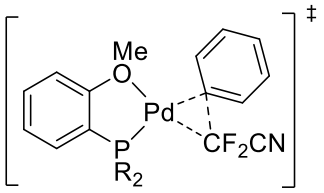
59

Pd-CF2CN-TS

C	2.58407600	-1.40837500	-0.66213200
C	2.64193000	-0.07645300	-0.18768100
C	3.90536000	0.48539200	0.02866000
C	5.08069300	-0.22966700	-0.18392900
C	5.00097700	-1.54600400	-0.62550200
C	3.76375900	-2.13522600	-0.86478500
H	3.97627000	1.51435000	0.38051600
H	6.04902800	0.24000200	-0.00140900
H	5.91062800	-2.12796900	-0.79203900
H	3.72005800	-3.16619200	-1.21485500
P	1.07655500	0.81944500	0.16263100
O	1.36709200	-1.92121100	-0.91869100

C	1.23251300	-3.27157700	-1.28022500
H	1.60461600	-3.94369200	-0.49011100
C	0.92738900	2.02384800	-1.28718500
C	1.31586000	1.69368900	1.83115200
C	2.12327000	2.98973400	1.83336900
H	1.64187400	3.77963100	1.23970800
H	2.19425800	3.36454700	2.86835200
H	3.15284300	2.86697200	1.47173300
C	-0.09260900	1.99622800	2.35825400
H	-0.67442000	1.06989200	2.47864800
H	-0.01547300	2.48674600	3.34320100
H	-0.66376000	2.66168000	1.69617700
C	1.95825500	0.66335300	2.76412600
H	1.43069300	-0.30381600	2.72035000
H	3.01550400	0.47954100	2.52858100
H	1.90117900	1.02771700	3.80325600
C	-0.27087200	2.93874000	-1.03489600
H	-1.17493700	2.36807500	-0.77504600
H	-0.07672800	3.66851600	-0.23493800
H	-0.49248600	3.51266600	-1.94988800
C	0.63408300	1.12905900	-2.49531900
H	-0.28024500	0.53668500	-2.34523700
H	0.49163200	1.75764500	-3.39021300
H	1.46397600	0.43611200	-2.70251500
C	2.18151500	2.84303800	-1.57738800
H	3.04181900	2.20269000	-1.81988100
H	1.99586600	3.48364000	-2.45612200
H	2.46423700	3.50618600	-0.74953000
Pd	-0.77647300	-0.63438100	0.29912400
C	-2.64881900	0.03454900	-0.17314900
C	-3.24228900	0.97614400	0.68146600
C	-2.92969100	0.09115200	-1.54657400
C	-4.02395200	2.00238100	0.15879000
H	-3.07903700	0.91239200	1.75870300
C	-3.71037600	1.12349000	-2.06301700
H	-2.53019300	-0.67485100	-2.21433100
C	-4.25255900	2.08749000	-1.21520100
H	-4.46041200	2.74314800	0.83370100
H	-3.89961400	1.16889900	-3.13851300
H	-4.86691800	2.89436800	-1.62126200
C	-2.56356800	-1.75761900	0.51751100
F	-3.10627000	-2.43815100	-0.51866200
F	-3.49821400	-1.62340800	1.48678700
H	0.15806700	-3.44867900	-1.41163700
H	1.74765800	-3.48881500	-2.23154400
C	-1.47476300	-2.59378200	1.07701700

N	-0.64486300	-3.29600300	1.50474300



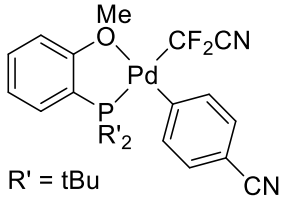
Pd-CF_2CN-TS-*trans*

59

Pd-CF2CN-TS-trans

C	1.34206000	2.30457800	0.08356500
C	2.19462100	1.19976900	-0.13922200
C	3.51679200	1.46793900	-0.51236100
C	3.99275400	2.76470700	-0.68370300
C	3.13101100	3.83536800	-0.47399600
C	1.81252600	3.61118400	-0.09104200
H	4.20041800	0.63626500	-0.67708200
H	5.03000100	2.93304300	-0.97931100
H	3.48215800	4.86164900	-0.60498000
H	1.15149800	4.46137000	0.07326900
P	1.52622300	-0.50804200	0.04416800
O	0.07475300	2.04582200	0.47608200
C	-0.83920900	3.10447300	0.64186200
H	-0.50641900	3.79837600	1.43152600
C	2.28910900	-1.08368600	1.67817600
C	2.16352200	-1.48232600	-1.45505900
C	3.61675400	-1.95064500	-1.41444500
H	3.84145000	-2.49665200	-2.34614000
H	4.34264600	-1.12928800	-1.35023900
H	3.80752300	-2.64443400	-0.58386600
C	1.25583600	-2.71108700	-1.58458800
H	1.58249800	-3.31109700	-2.45053400
H	1.27944700	-3.36109000	-0.69947000
H	0.21037900	-2.41654400	-1.75253800
C	1.92515900	-0.58800500	-2.67442300
H	2.62272900	0.25960500	-2.72353800
H	2.04967100	-1.18395600	-3.59371000
H	0.89942900	-0.18320000	-2.67642300
C	1.49925300	-0.32174000	2.74730800
H	0.42566000	-0.56355900	2.70180300
H	1.87194700	-0.59755400	3.74802900
H	1.60775200	0.76895400	2.64058300
C	3.77367900	-0.77000000	1.84214400
H	3.97379500	0.31057600	1.81725900
H	4.11097900	-1.14153200	2.82462100

H	4.40020400	-1.25700800	1.08256500
C	2.04223800	-2.58225000	1.84594100
H	2.65581200	-3.18495900	1.16038000
H	2.32075600	-2.88012600	2.87085200
H	0.98760700	-2.85679900	1.69610400
Pd	-0.83833100	-0.27936400	0.08895300
C	-2.75715000	0.22758600	-0.06282300
C	-3.40939100	0.56774600	1.13381900
C	-3.07891300	0.90458100	-1.24600000
C	-4.31525600	1.62504500	1.15380800
H	-3.20241300	0.00400900	2.04704900
C	-3.98621100	1.96397000	-1.21538400
H	-2.61396000	0.60078500	-2.18692200
C	-4.60117600	2.32867500	-0.01860600
H	-4.80686000	1.89966700	2.09065100
H	-4.21930800	2.50334000	-2.13707200
H	-5.31843100	3.15262100	-0.00050300
C	-2.45592900	-1.68424200	-0.33607100
F	-3.74569500	-1.95869200	0.03761100
F	-2.39872900	-1.88735500	-1.67433300
H	-0.99129200	3.65760800	-0.29925600
H	-1.78875200	2.64780100	0.94411800
C	-1.65484100	-2.69167700	0.36677900
N	-1.11124000	-3.54406300	0.94088400



Pd-CF_2CN-CN-GS

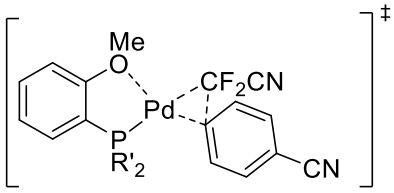
60

Generated by Multiwfn

C	-2.95205600	0.92699700	-0.27250000
C	-2.74682900	-0.46465600	-0.31781600
C	-3.84098000	-1.26503300	-0.66756800
C	-5.08249200	-0.71836800	-0.97861300
C	-5.25349600	0.66121800	-0.93663300
C	-4.19230300	1.48723200	-0.58004800
H	-3.72774100	-2.34715200	-0.69206200
H	-5.91281600	-1.37257600	-1.25044700
H	-6.21980100	1.10640600	-1.18349200
H	-4.32914300	2.56832600	-0.55658200
P	-1.07568000	-1.10744700	0.12231900
O	-1.89409200	1.70921200	0.09320000

C	-2.14908600	2.97202700	0.69207700
H	-2.99315000	2.89083400	1.39361000
C	-0.72767700	-2.58023000	-1.01274100
C	-1.27732000	-1.59985600	1.93618700
C	-2.53814300	-2.41208800	2.22010200
H	-2.55777500	-3.37316200	1.68995300
H	-2.58496300	-2.63586000	3.29893200
H	-3.45134200	-1.85640000	1.96289200
C	-0.03283300	-2.36730000	2.38240300
H	0.89640900	-1.84679400	2.10739900
H	-0.04511100	-2.47208400	3.47968700
H	0.00312300	-3.38244800	1.96221100
C	-1.35852000	-0.27686500	2.70522100
H	-0.46725700	0.35094100	2.54770400
H	-2.24494300	0.30930600	2.41914000
H	-1.44040300	-0.48781300	3.78406300
C	0.76999800	-2.89117600	-0.92147200
H	1.38887900	-2.03171500	-1.20114400
H	1.08099000	-3.21383100	0.08061300
H	1.00120800	-3.71448700	-1.61704800
C	-1.03046900	-2.08159800	-2.42925400
H	-0.53094800	-1.12002100	-2.63156900
H	-0.65173200	-2.81375600	-3.16072100
H	-2.10556800	-1.94781800	-2.61299500
C	-1.49052000	-3.87179500	-0.71809400
H	-2.58226800	-3.77507500	-0.76376000
H	-1.20917600	-4.62174300	-1.47566500
H	-1.22407800	-4.29467400	0.26054900
Pd	0.22270000	0.87538500	-0.15832000
C	2.05875700	0.17179000	-0.16581000
C	2.71327200	-0.09461600	1.04537000
C	2.75652400	-0.05531800	-1.36264300
C	4.00216600	-0.61784100	1.06601200
H	2.22021000	0.12015800	1.99674600
C	4.04239200	-0.58011200	-1.35422800
H	2.29050400	0.18268500	-2.32144400
C	4.67467800	-0.87732600	-0.13657700
H	4.49709200	-0.82471000	2.01723700
H	4.56940200	-0.76190200	-2.29328100
C	1.10012400	2.71811500	-0.43550100
F	0.15268400	3.54994900	-0.99049400
F	2.18256000	2.80958800	-1.24346500
H	-1.24737300	3.25168600	1.24839100
H	-2.35629800	3.73925700	-0.06739200
C	1.43297300	3.24601200	0.89571000
N	1.60995500	3.56030200	1.99764900

C	5.99494800	-1.42662800	-0.12269900
N	7.06461100	-1.87553400	-0.11177300



R' = tBu

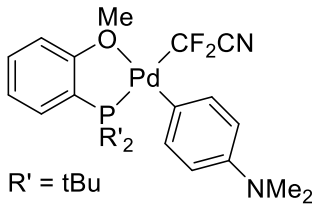
Pd-CF_2CN-CN-TS

60

Generated by Multiwfn

C	-3.04841600	0.80976100	-0.88011500
C	-2.83140600	-0.45681100	-0.28880600
C	-3.93974000	-1.29186700	-0.10481300
C	-5.22665800	-0.90404100	-0.46580800
C	-5.42121000	0.35316800	-1.02757700
C	-4.34302700	1.20718700	-1.23555700
H	-3.79565800	-2.27654200	0.33913900
H	-6.06854100	-1.57997700	-0.30537800
H	-6.42373800	0.68048300	-1.31305200
H	-4.51515400	2.18751500	-1.67868600
P	-1.13765700	-0.92608600	0.24175000
O	-1.97066700	1.59016900	-1.09158600
C	-2.13248700	2.88370400	-1.61821800
H	-2.72804900	3.52452200	-0.94828100
C	-0.60452300	-2.20400400	-1.04376500
C	-1.30081700	-1.64322900	1.99143800
C	-1.79506300	-3.08328800	2.10754700
H	-1.10351300	-3.79927000	1.64157500
H	-1.86305200	-3.35157200	3.17513600
H	-2.79415800	-3.23991400	1.67971900
C	0.09233400	-1.55111200	2.62533000
H	0.43505200	-0.50647400	2.66869800
H	0.05048700	-1.94259600	3.65545700
H	0.85032800	-2.12916600	2.07863500
C	-2.23276300	-0.69668000	2.75298600
H	-1.93570500	0.35672600	2.61922700
H	-3.28123500	-0.79213200	2.43896600
H	-2.17992800	-0.92323300	3.83064600
C	0.74912600	-2.77585900	-0.62264500
H	1.47218000	-1.98240000	-0.38315100
H	0.66659600	-3.44522000	0.24625600
H	1.17026100	-3.37027700	-1.45006000
C	-0.43712500	-1.39583000	-2.33419600

H	0.29582200	-0.58505100	-2.21204500
H	-0.08148600	-2.06002700	-3.13931300
H	-1.38890800	-0.95178400	-2.66415100
C	-1.60705800	-3.32611500	-1.29712400
H	-2.56813200	-2.94127500	-1.66687500
H	-1.20471500	-3.99490700	-2.07650800
H	-1.79668100	-3.94366700	-0.40973200
Pd	0.28903200	0.94763400	0.28106300
C	2.28104500	0.66875600	0.04551400
C	2.99784800	0.00826700	1.06081800
C	2.70646700	0.51308000	-1.28684100
C	4.03122900	-0.86000000	0.74745000
H	2.72760900	0.16385300	2.10614700
C	3.73821000	-0.35800900	-1.60614400
H	2.21474200	1.07591400	-2.08220700
C	4.40382600	-1.06381500	-0.59231300
H	4.55959700	-1.39196000	1.54101700
H	4.03738800	-0.49561300	-2.64696300
C	1.80000200	2.47075100	0.46137800
F	2.25603000	3.11606200	-0.63445600
F	2.67444800	2.66063000	1.47467100
H	-1.12569400	3.30954400	-1.70487100
H	-2.59392800	2.85510300	-2.61967600
C	0.52498500	3.10159000	0.86255100
N	-0.46309400	3.64367400	1.16672000
C	5.45897000	-1.97099100	-0.91753200
N	6.31254600	-2.71077600	-1.18177700



Pd-CF_2CN-NMe_2-GS

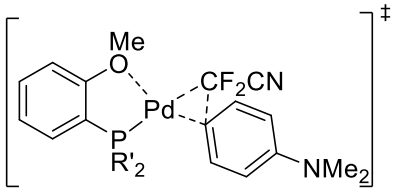
67

Generated by Multiwfn

C	-3.30640600	0.66810100	-0.28973800
C	-2.94480100	-0.69232200	-0.34533100
C	-3.93553800	-1.60362700	-0.72874500
C	-5.22420400	-1.19596600	-1.06236900
C	-5.55031000	0.15463800	-1.00818900
C	-4.59595900	1.08901300	-0.61826600
H	-3.70174000	-2.66589500	-0.76140300
H	-5.96952500	-1.93576600	-1.36022800
H	-6.55528400	0.49230600	-1.27105900

H	-4.85413100	2.14740300	-0.58512300
P	-1.21830500	-1.14702600	0.12748800
O	-2.35147400	1.55704500	0.10620900
C	-2.75112900	2.79402400	0.67333600
H	-3.59165800	2.63665300	1.36678800
C	-0.68561600	-2.57057200	-1.00025200
C	-1.41320400	-1.67482000	1.93334100
C	-2.59212000	-2.61144400	2.18390700
H	-2.50771900	-3.56134700	1.63956500
H	-2.63544000	-2.85574100	3.25869400
H	-3.55130400	-2.14518600	1.91639000
C	-0.10861500	-2.31761100	2.40429200
H	0.77063400	-1.71131700	2.14109900
H	-0.13024200	-2.42040800	3.50187500
H	0.03108200	-3.32565600	1.98852700
C	-1.64123700	-0.37277500	2.70836800
H	-0.81261300	0.33985200	2.57147000
H	-2.57396100	0.12638900	2.40491900
H	-1.72547300	-0.59892500	3.78420300
C	0.83157000	-2.73464400	-0.85492800
H	1.37301200	-1.80479400	-1.06356300
H	1.12987700	-3.07580100	0.14460600
H	1.17107300	-3.49654500	-1.57602700
C	-0.98196900	-2.08444200	-2.42243200
H	-0.55362800	-1.08420300	-2.59798700
H	-0.52146800	-2.77624900	-3.14648700
H	-2.05824700	-2.03537200	-2.64049900
C	-1.32627600	-3.93538200	-0.74905600
H	-2.41837700	-3.95207200	-0.85184400
H	-0.92979000	-4.64693600	-1.49234400
H	-1.06819700	-4.33581200	0.24121800
Pd	-0.14194100	0.96514800	-0.13438700
C	1.75801500	0.43144800	-0.13914100
C	2.42405000	0.15814400	1.05818700
C	2.49123300	0.29921500	-1.32258700
C	3.74486300	-0.28821000	1.07809100
H	1.91774100	0.30390100	2.01672700
C	3.80917000	-0.14977800	-1.32024600
H	2.03253100	0.54972300	-2.28260100
C	4.46745500	-0.47914100	-0.11678900
H	4.21219200	-0.48168800	2.04383700
H	4.32866700	-0.23732900	-2.27469700
C	0.54106600	2.88098600	-0.41499200
F	-0.49220000	3.61373200	-0.97123300
F	1.60557000	3.09264300	-1.22443900
H	-1.89171800	3.18082400	1.23249800

H	-3.02930200	3.52008000	-0.10417500
C	0.80975600	3.45313300	0.91278300
N	0.93630500	3.80846800	2.00945500
N	5.76526800	-0.95524000	-0.10946700
C	6.51286200	-0.99553700	-1.33311700
H	7.50037900	-1.43622600	-1.14405000
H	6.01755400	-1.62336900	-2.09449200
H	6.67133900	0.00574700	-1.78146600
C	6.44635500	-1.13604700	1.13995900
H	6.57692200	-0.19242600	1.70680000
H	5.91292300	-1.84472100	1.79764000
H	7.44412000	-1.55512800	0.95563700



R' = tBu

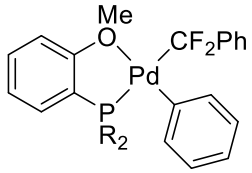
Pd-CF_2CN-NMe_2-TS

67

Generated by Multiwfn

C	-3.32508700	0.49382800	-1.04990700
C	-3.01897400	-0.70039400	-0.35464300
C	-4.05382300	-1.61998000	-0.15063000
C	-5.35549400	-1.37906100	-0.58212400
C	-5.64099200	-0.18642600	-1.23801500
C	-4.63589500	0.74625600	-1.47318900
H	-3.84006700	-2.55449000	0.36771400
H	-6.13853900	-2.11807100	-0.40215100
H	-6.65727300	0.02632100	-1.57844500
H	-4.87544500	1.67329800	-1.99348100
P	-1.31182800	-0.94954900	0.27874800
O	-2.31118200	1.34291800	-1.29287500
C	-2.56436500	2.60251100	-1.85853700
H	-3.23411400	3.20628200	-1.22493900
C	-0.57455500	-2.19321400	-0.94062200
C	-1.48029400	-1.65206600	2.03509900
C	-1.80979400	-3.13682800	2.17133500
H	-1.01776500	-3.77686200	1.75746300
H	-1.89753300	-3.38698500	3.24217700
H	-2.76098100	-3.42155600	1.70212400
C	-0.13674200	-1.38648200	2.72670700
H	0.08898400	-0.30948100	2.74674900
H	-0.18449500	-1.75027200	3.76706000

H	0.70582800	-1.89032300	2.23320600
C	-2.54570900	-0.80219200	2.73333200
H	-2.36362200	0.27458700	2.58151600
H	-3.56259800	-1.02302500	2.38087000
H	-2.51370500	-0.99669000	3.81829200
C	0.81132200	-2.59920100	-0.43943100
H	1.42934100	-1.72297100	-0.19245000
H	0.75995900	-3.25166300	0.44477500
H	1.33500900	-3.16387300	-1.22868800
C	-0.42560200	-1.40420600	-2.24500700
H	0.20778900	-0.51590100	-2.10686100
H	0.04535800	-2.04583600	-3.00854300
H	-1.39972000	-1.07590000	-2.63864200
C	-1.43675800	-3.42349600	-1.20708800
H	-2.42010300	-3.15294500	-1.61834700
H	-0.93476600	-4.05866700	-1.95664300
H	-1.59254900	-4.04180000	-0.31344400
Pd	-0.05726500	1.05040100	0.35154200
C	1.97754700	0.98768700	0.14073700
C	2.73007700	0.41290000	1.17291200
C	2.45946500	0.85496300	-1.16738900
C	3.86392100	-0.34190600	0.90543700
H	2.41779900	0.54151900	2.21118900
C	3.59175200	0.10065200	-1.44925200
H	1.93556300	1.34495300	-1.99108900
C	4.32047500	-0.53318900	-0.41890500
H	4.40164100	-0.78488500	1.74344000
H	3.91172500	0.01267500	-2.48718200
C	1.19846100	2.72556700	0.52359700
F	1.63469100	3.41140600	-0.56079100
F	1.98258900	3.04064000	1.58245300
H	-1.59412400	3.11018600	-1.92315700
H	-2.98756900	2.51289100	-2.87386300
C	-0.16683700	3.21885900	0.83543000
N	-1.24039000	3.62260800	1.05902200
N	5.43338100	-1.29326200	-0.68995400
C	5.85467200	-1.48594700	-2.04921500
H	6.11638000	-0.53389400	-2.54638500
H	6.74802400	-2.12247400	-2.06885000
H	5.07985100	-1.98064800	-2.66458500
C	6.13883000	-1.93927000	0.38124400
H	6.54099500	-1.21660600	1.11470200
H	5.50250300	-2.65564200	0.93409700
H	6.98921700	-2.49984400	-0.02647200



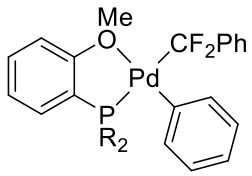
Pd-CF_2Ph-GS

68

Pd-CF2Ph-GS

C	-2.56243100	-1.86969400	0.06243900
C	-2.95472000	-0.55555900	0.38444200
C	-4.24776900	-0.37538600	0.89020700
C	-5.11749800	-1.44268000	1.09402800
C	-4.70037700	-2.73137500	0.77954400
C	-3.42860600	-2.94810200	0.25946500
H	-4.59344300	0.62954800	1.12431800
H	-6.11750500	-1.26345800	1.49334300
H	-5.36695700	-3.58247900	0.93629800
H	-3.10872700	-3.96155400	0.01923000
P	-1.75264800	0.81129400	0.08434200
O	-1.31748200	-2.04919500	-0.45869100
C	-1.05781700	-3.21968900	-1.21911500
H	-0.92456400	-4.09638200	-0.56850800
C	-1.88993700	1.98141600	1.56714100
C	-2.38390000	1.57641600	-1.52407600
C	-3.88842200	1.82888400	-1.56448300
H	-4.46459900	0.89852400	-1.45844300
H	-4.22564600	2.53385400	-0.79281500
H	-4.15317100	2.26693200	-2.54171900
C	-1.61702500	2.87392800	-1.78074400
H	-1.79760900	3.20487000	-2.81706000
H	-1.94986500	3.68756400	-1.12010100
H	-0.53145900	2.74662400	-1.65327600
C	-2.02463300	0.55093100	-2.60468200
H	-2.54759900	-0.40573300	-2.45043300
H	-2.32674600	0.93682800	-3.59250400
H	-0.94316200	0.34463200	-2.62982600
C	-0.68563100	2.92604500	1.51590600
H	-0.67698200	3.53939600	2.43227800
H	0.26556200	2.38529700	1.45907600
H	-0.72208800	3.61494400	0.66196000
C	-1.74401100	1.07693300	2.79473500
H	-1.60613900	1.69950700	3.69394400
H	-2.62480500	0.43932300	2.95683300
H	-0.86298900	0.42046400	2.70284100
C	-3.15031200	2.83827200	1.67593100
H	-3.25486100	3.52966000	0.82801600

H	-4.08006500	2.26362800	1.77106200
H	-3.07215000	3.45900100	2.58421700
Pd	0.28384500	-0.41114900	-0.19062800
C	1.62152900	1.04031000	-0.24755500
C	1.89972700	1.67430500	-1.46632000
C	2.34996900	1.44036300	0.88207300
C	2.86199700	2.68400400	-1.54917400
H	1.37659800	1.36886300	-2.37697200
C	3.30745600	2.45015500	0.80096500
H	2.18936800	0.94149600	1.84104800
C	3.56813500	3.07911500	-0.41580500
H	3.06307500	3.15961700	-2.51354800
H	3.86494100	2.73700500	1.69677500
H	4.32451500	3.86514200	-0.48147500
C	1.84658500	-1.73233700	-0.40354400
F	1.94661900	-2.07990000	-1.74095600
F	1.39194100	-2.88723900	0.22116700
H	-1.87997300	-3.39375300	-1.93089500
H	-0.12574500	-3.03860500	-1.76249100
C	3.20793500	-1.42080900	0.12550200
C	3.49413300	-1.62938200	1.47777300
C	4.17714700	-0.83942400	-0.69691900
C	4.72593200	-1.24797000	2.00262100
H	2.73636600	-2.08430300	2.11906500
C	5.40505500	-0.45445200	-0.16849200
H	3.95154700	-0.66991500	-1.75036800
C	5.68357600	-0.65281700	1.18309900
H	4.93876700	-1.41396700	3.06188500
H	6.14912500	0.01348100	-0.81767200
H	6.64617100	-0.34317100	1.59751300



Pd-CF_2Ph-GS'

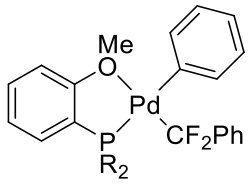
68

Pd-CF2Ph-GS’

C	2.48681200	0.09109500	-1.16030500
C	2.30018900	-0.97819500	-0.25490800
C	3.43738300	-1.67040700	0.17469100
C	4.71835500	-1.32262300	-0.24721300
C	4.87831000	-0.26358800	-1.13435200
C	3.76962400	0.43913700	-1.59582600
H	3.32315100	-2.51590800	0.85231300

H	5.58301500	-1.88515800	0.10997100
H	3.90522000	1.26584000	-2.29318900
P	0.58264600	-1.41068000	0.25152300
O	1.38048300	0.73432800	-1.58015700
C	1.42938900	1.54454500	-2.72259500
H	2.03746900	2.44994600	-2.56770200
C	0.68077000	-2.04164000	2.04114500
C	0.14279500	-2.79123800	-0.96643000
C	1.20423900	-3.88106400	-1.09182800
H	2.17898600	-3.47321500	-1.39687800
H	1.34343700	-4.45588300	-0.16748000
H	0.89052600	-4.59496300	-1.87214400
C	-1.20448300	-3.39410900	-0.56755700
H	-1.54353900	-4.07833700	-1.36293700
H	-1.13982400	-3.98438700	0.35828100
H	-1.97837700	-2.62369500	-0.43950400
C	-0.00048200	-2.09214400	-2.32163300
H	0.95942000	-1.68664600	-2.67442600
H	-0.34634600	-2.82448600	-3.06997400
H	-0.73314300	-1.27528900	-2.28107700
C	-0.74296400	-1.91894200	2.59852000
H	-0.75588400	-2.26218500	3.64662000
H	-1.08673100	-0.87384200	2.57197200
H	-1.47317500	-2.51930900	2.03904400
C	1.56968900	-1.06292500	2.81379100
H	1.43921400	-1.23105200	3.89568100
H	2.63710700	-1.17598300	2.58287300
H	1.29346500	-0.01869700	2.60278800
C	1.16316300	-3.47459400	2.25890000
H	0.48330700	-4.21292600	1.81177200
H	2.17350400	-3.66668600	1.87377200
H	1.19049600	-3.67905500	3.34253000
Pd	-0.79631600	0.56657100	0.21275500
C	-2.60858600	-0.12618100	-0.25521300
C	-3.02820500	-0.12764900	-1.59392100
C	-3.48978900	-0.63714500	0.70734200
C	-4.25646100	-0.67710200	-1.96442700
H	-2.39162000	0.30857400	-2.36864300
C	-4.72054000	-1.18305900	0.33795900
H	-3.22113400	-0.61534400	1.76569800
C	-5.10564400	-1.21740600	-1.00078700
H	-4.55233700	-0.67683700	-3.01754300
H	-5.38534700	-1.58347900	1.10895200
H	-6.06708800	-1.64943000	-1.28958300
C	-1.63801700	2.38567100	0.42138000
F	-2.41752800	2.52388000	1.52712900

F	-2.31493100	2.94789200	-0.60818800
H	1.81921100	0.98601400	-3.59138500
H	0.39500400	1.84971200	-2.92618700
C	-0.27998600	2.97564700	0.59163900
C	0.31894100	3.76224900	-0.40584500
C	0.49836800	2.55308400	1.68824500
C	1.65855300	4.11284400	-0.30729100
H	-0.28861400	4.09242000	-1.25028800
C	1.85124100	2.89032600	1.76372500
H	0.01857900	1.99704800	2.49808300
C	2.43481300	3.66316300	0.76562300
H	2.11094800	4.74502400	-1.07601300
H	2.44718600	2.55121500	2.61419400
H	3.49319200	3.92663000	0.82435300
H	5.87497300	0.02123100	-1.47969000



Pd-CF_2Ph-GS-*trans*

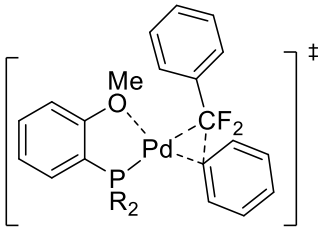
68

Pd-CF2Ph-GS-trans

C	2.24326500	2.03602300	-0.53682900
C	2.87287300	0.79208500	-0.32924100
C	4.27216700	0.75802800	-0.39589900
C	5.03350500	1.89197800	-0.65933900
C	4.38863300	3.10542100	-0.86592100
C	3.00142600	3.18147800	-0.80533500
H	4.78836900	-0.18589000	-0.23447900
H	6.12210700	1.82346300	-0.70123400
H	4.96362000	4.01054700	-1.07449600
H	2.51717200	4.14305700	-0.96425100
P	1.84930600	-0.68972300	0.07072200
O	0.88370100	2.08952600	-0.46372300
C	0.24591900	3.33766600	-0.68574600
H	0.48644200	3.72086800	-1.68964100
C	2.55613000	-1.29891600	1.72516300
C	2.18160200	-1.85993800	-1.38519300
C	3.63665200	-1.98622200	-1.83129900
H	4.29994200	-2.35794700	-1.03823400
H	3.68670300	-2.71402300	-2.65863500
H	4.03981900	-1.03865700	-2.21337000
C	1.63287600	-3.24721200	-1.05259900

H	1.67107300	-3.87419000	-1.95903700
H	2.23386900	-3.75580100	-0.28409200
H	0.59310700	-3.20939100	-0.70717600
C	1.37193100	-1.24933000	-2.53413700
H	1.72607000	-0.23775300	-2.78962900
H	1.47699600	-1.87557300	-3.43587700
H	0.30223200	-1.17623800	-2.28513200
C	3.90066400	-2.01898300	1.65821600
H	4.71165100	-1.39269100	1.26416900
H	4.19781000	-2.31082400	2.67958400
H	3.85018500	-2.94298500	1.06477700
C	1.52839400	-2.23447200	2.36690900
H	1.91323300	-2.55711100	3.34890700
H	0.56455000	-1.73459300	2.52653000
H	1.33924700	-3.13621700	1.77044500
C	2.66899000	-0.04824700	2.60243600
H	2.88508500	-0.35220200	3.63990700
H	3.47068700	0.62852400	2.27471400
H	1.72312600	0.51839100	2.61353900
Pd	-0.35881900	0.24486500	0.18985200
C	-2.04520300	1.33931900	0.31770400
C	-2.41832100	1.92764600	1.53418700
C	-2.81620900	1.63534500	-0.81768900
C	-3.51229900	2.79295300	1.61189200
H	-1.85680800	1.69693300	2.44449300
C	-3.90711600	2.50165900	-0.74546700
H	-2.57726400	1.16411100	-1.77643600
C	-4.25934900	3.08446200	0.47194800
H	-3.78589600	3.23892900	2.57272200
H	-4.49475600	2.71241900	-1.64354800
H	-5.11875000	3.75726200	0.53301500
C	-1.54494000	-1.27295500	0.74888800
F	-1.82578700	-1.16231100	2.08478200
F	-0.86072100	-2.46945700	0.64140100
H	-0.83030200	3.15450100	-0.61237800
H	0.54349700	4.06903900	0.08178400
C	-2.82143900	-1.43538200	-0.02991100
C	-4.05739300	-1.10530000	0.52892200
C	-2.76657300	-1.89311800	-1.34947300
C	-5.21955400	-1.21352600	-0.22984700
H	-4.09772300	-0.73698600	1.55442800
C	-3.92931200	-2.00015900	-2.10640700
H	-1.80115100	-2.15739300	-1.78669200
C	-5.16084600	-1.65573700	-1.54988100
H	-6.18010700	-0.94032700	0.21371500
H	-3.87404300	-2.35472500	-3.13874700

H	-6.07359200	-1.73219100	-2.14584400



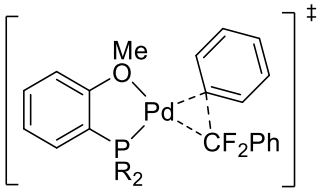
Pd-CF_2Ph-TS

68

Pd-CF2Ph-TS

C	2.60415800	0.91569300	-1.08217600
C	2.67451000	-0.18848400	-0.20040300
C	3.93915900	-0.56687300	0.26209300
C	5.09845500	0.11692300	-0.09655600
C	5.00392300	1.20884800	-0.95149600
C	3.76590800	1.60624600	-1.44729600
H	4.02803200	-1.42952200	0.92114900
H	6.06705100	-0.20900400	0.28736100
H	3.70789300	2.45990600	-2.12220900
P	1.11690300	-1.05589300	0.26776300
O	1.38852000	1.24647300	-1.55441500
C	1.26908300	2.22243400	-2.55021800
H	1.59767300	3.21501300	-2.20058200
C	1.34230600	-1.64407100	2.06480000
C	1.09435400	-2.50574400	-0.95323700
C	2.41078700	-3.27037300	-1.05521300
H	3.24202800	-2.61709300	-1.35817000
H	2.69000600	-3.77243300	-0.11997400
H	2.31291500	-4.05362400	-1.82614300
C	-0.05183500	-3.44421800	-0.57909300
H	-0.19539300	-4.18448100	-1.38366800
H	0.15185500	-4.00688000	0.34397500
H	-0.99991900	-2.90096600	-0.45550400
C	0.78824200	-1.86909400	-2.31191100
H	1.59271900	-1.19402600	-2.63955500
H	0.68885300	-2.66363600	-3.07043800
H	-0.15287400	-1.30150400	-2.28521600
C	-0.06953500	-1.93342700	2.59153900
H	-0.00662600	-2.25256100	3.64573300
H	-0.70231800	-1.03452300	2.53638500
H	-0.57888900	-2.72815600	2.02975800
C	1.89613500	-0.45092800	2.84964200
H	1.79816400	-0.64828600	3.93022400
H	2.95583800	-0.25380800	2.63946700

H	1.33414500	0.46935100	2.62296600
C	2.20064900	-2.88482500	2.30658400
H	1.76785200	-3.78260900	1.84360300
H	3.23602700	-2.78777200	1.95439300
H	2.25137400	-3.07704900	3.39174700
Pd	-0.75747800	0.31983100	0.19256800
C	-2.53407700	-0.59924000	-0.28966800
C	-2.76665400	-0.72081900	-1.66999500
C	-3.10475600	-1.54940800	0.56834100
C	-3.46558000	-1.81208100	-2.18064400
H	-2.38887500	0.04533300	-2.35249100
C	-3.81760700	-2.63188800	0.05525700
H	-2.98201300	-1.44686600	1.64800600
C	-3.98933700	-2.77757900	-1.32082100
H	-3.60899800	-1.90394700	-3.26068600
H	-4.24038400	-3.37128800	0.74097000
H	-4.54324800	-3.63016800	-1.72078200
C	-2.70170300	1.27502600	0.41616500
F	-3.30243700	1.01255800	1.59953100
F	-3.65639600	1.62797500	-0.47343500
H	1.83768400	1.94623700	-3.45578900
H	0.20245000	2.27767600	-2.80072000
C	-1.70151500	2.37111700	0.54875500
C	-1.49491300	3.28785900	-0.50305800
C	-0.89069100	2.46270300	1.70523700
C	-0.51016800	4.25983300	-0.39899700
H	-2.13287800	3.23054500	-1.38635600
C	0.11087400	3.43393500	1.77929000
H	-1.10039700	1.81960300	2.56197800
C	0.30661100	4.33041900	0.73394600
H	-0.37712600	4.97899300	-1.21133200
H	0.73255500	3.49282200	2.67580200
H	1.08554600	5.09292100	0.80319300
H	5.90036400	1.75947100	-1.24640000



Pd-CF_2Ph-TS-*trans*

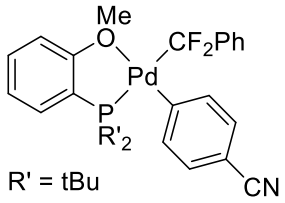
68

Pd-CF2Ph-TS-trans

C	2.68279600	1.92703600	-0.25312700
C	3.16901500	0.60697100	-0.09471800

C	4.55214200	0.43705300	0.03402400
C	5.43827000	1.51137700	0.02363000
C	4.93710000	2.80020800	-0.12139500
C	3.56876700	3.01143000	-0.25926400
H	4.95353600	-0.56913800	0.15173000
H	6.51101700	1.33881600	0.12994100
H	5.61373100	3.65820700	-0.13010900
H	3.19223200	4.02751000	-0.37476500
P	1.96346400	-0.78613500	-0.02271900
O	1.35314800	2.08723900	-0.40308400
C	0.78971600	3.37305200	-0.45939900
H	1.14862400	3.93404800	-1.33907500
C	2.45842700	-1.82174200	1.49148100
C	2.25542000	-1.69303200	-1.65924000
C	3.70845700	-2.00224300	-2.00676100
H	4.19658500	-2.65630000	-1.27202000
H	3.74533200	-2.52339900	-2.97875500
H	4.30795900	-1.08639500	-2.10910900
C	1.42161500	-2.97422400	-1.64290200
H	1.39952100	-3.41278300	-2.65489600
H	1.84143200	-3.73621100	-0.96953100
H	0.38356800	-2.77430900	-1.33488900
C	1.68681500	-0.74348100	-2.71874600
H	2.22847000	0.21510100	-2.74318600
H	1.77764700	-1.20456400	-3.71689800
H	0.62290300	-0.52673900	-2.53071400
C	3.66950700	-2.74056700	1.35476600
H	4.59971600	-2.20557900	1.12035800
H	3.83717700	-3.26026100	2.31353800
H	3.51678200	-3.51870300	0.59335000
C	1.23186900	-2.67139700	1.84522200
H	1.44124600	-3.24524900	2.76409900
H	0.34587000	-2.04477600	2.02161900
H	0.97219100	-3.39085300	1.05666800
C	2.68049300	-0.81604000	2.62395300
H	2.74397700	-1.35358000	3.58482300
H	3.60532800	-0.23535900	2.49844500
H	1.83986100	-0.10582600	2.69314400
Pd	-0.20477200	0.07940500	0.12100200
C	-1.96582800	0.95283400	0.22463100
C	-2.13426400	1.71281100	1.39528600
C	-2.43934500	1.46704900	-0.99831100
C	-2.71484400	2.97979600	1.33201900
H	-1.80876600	1.30171500	2.35378500
C	-3.01569300	2.73188800	-1.05096600
H	-2.36470500	0.86360900	-1.90630900

C	-3.15878900	3.49175400	0.11353800
H	-2.82573400	3.56978100	2.24586300
H	-3.36712200	3.12656200	-2.00791700
H	-3.62831000	4.47733900	0.07038000
C	-2.23593900	-0.95955300	0.56005000
F	-2.19319800	-1.06287900	1.91461500
F	-1.68842100	-2.13819700	0.07599300
H	-0.29449800	3.22864200	-0.54637900
H	1.00275400	3.94888600	0.45692200
C	-3.67101100	-0.97441700	0.09587600
C	-4.68753200	-0.45451200	0.90039100
C	-3.98306300	-1.48144400	-1.16788700
C	-6.00010900	-0.43466900	0.44030000
H	-4.44135400	-0.05637300	1.88606800
C	-5.29685800	-1.45185200	-1.62836600
H	-3.18896600	-1.89925900	-1.78944700
C	-6.30878200	-0.92668500	-0.82745900
H	-6.78979500	-0.02801500	1.07669200
H	-5.53210700	-1.84722500	-2.61958000
H	-7.33931800	-0.90255800	-1.18973800



Pd-CF_2Ph-CN-GS

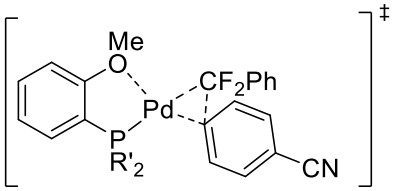
69

Generated by Multiwfn

C	-3.08024300	-1.51625700	0.02533500
C	-3.23571900	-0.16286100	0.38200900
C	-4.47273000	0.22689000	0.90936300
C	-5.51250400	-0.67863200	1.09807600
C	-5.32882800	-2.01149300	0.74652200
C	-4.11830400	-2.43285000	0.20597800
H	-4.63628600	1.26965900	1.17456600
H	-6.46249100	-0.33936500	1.51504200
H	-3.98121200	-3.47995300	-0.06226700
P	-1.81810300	0.97894300	0.09279600
O	-1.88693000	-1.89590900	-0.51307300
C	-1.84299200	-3.06545200	-1.31863100
H	-1.86224400	-3.97505600	-0.70108000
C	-1.76079100	2.16072700	1.57054600
C	-2.29462600	1.83743000	-1.52205500
C	-3.73388700	2.34287000	-1.56794700

H	-4.46016600	1.52540600	-1.45353700
H	-3.94592800	3.10276900	-0.80438500
H	-3.91968400	2.80943700	-2.54998600
C	-1.31598800	2.98408200	-1.77666500
H	-1.44011200	3.34586300	-2.81077000
H	-1.49836100	3.84074100	-1.11200600
H	-0.26844900	2.67004300	-1.65566900
C	-2.11196300	0.76617800	-2.60246200
H	-2.79405700	-0.08513800	-2.45461100
H	-2.33675400	1.20042800	-3.59064300
H	-1.08228200	0.37588700	-2.62385200
C	-0.39946400	2.86199400	1.54039700
H	-0.30980300	3.50167100	2.43390700
H	0.43218300	2.14927300	1.54990900
H	-0.26987200	3.50762200	0.66183100
C	-1.81037500	1.25808400	2.80724400
H	-1.56123800	1.85101000	3.70239000
H	-2.80092500	0.80894300	2.96522700
H	-1.07621200	0.43884600	2.73359700
C	-2.84087100	3.23919000	1.64467400
H	-2.78102100	3.94247600	0.80242400
H	-3.86540100	2.85028300	1.69597700
H	-2.68252700	3.82868300	2.56306900
Pd	-0.02704200	-0.58397000	-0.18727500
C	1.55408300	0.58783800	-0.17318600
C	1.98506400	1.19024500	-1.36607000
C	2.31992700	0.80687600	0.98434300
C	3.12749500	1.98306000	-1.40548700
H	1.43492200	1.02293900	-2.29558900
C	3.46114200	1.59648400	0.95990600
H	2.03776100	0.32827700	1.92459000
C	3.87741400	2.19531800	-0.23985900
H	3.45113300	2.43714100	-2.34475800
H	4.04803500	1.74427100	1.86865000
C	1.27253400	-2.16517000	-0.43102400
F	1.32690300	-2.47490400	-1.77787400
F	0.60481900	-3.23314900	0.14840200
H	-2.68769600	-3.06483200	-2.02492500
H	-0.89742800	-3.03185200	-1.86787900
C	2.65863200	-2.11874700	0.12310600
C	2.87608200	-2.39814600	1.47558300
C	3.73219500	-1.70825500	-0.67252000
C	4.14527100	-2.24970900	2.02816900
H	2.03757300	-2.72311800	2.09517000
C	4.99819500	-1.55461800	-0.11585000
H	3.56316000	-1.49117000	-1.72799900

C	5.20895700	-1.81871300	1.23682100
H	4.30465400	-2.46933800	3.08693400
H	5.82741900	-1.21872800	-0.74315800
H	6.20245400	-1.69047300	1.67314300
H	-6.13222700	-2.73732200	0.89085100
C	5.05946300	2.99810200	-0.27616600
N	6.01935600	3.64944200	-0.30607700



R' = tBu

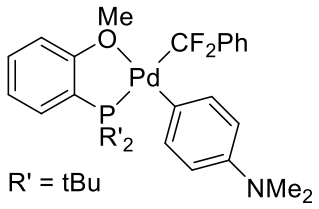
Pd-CF_2Ph-CN-TS

69

Generated by Multiwfn

C	2.89500200	-0.19812800	-1.27202600
C	2.60463500	-1.18420300	-0.30045300
C	3.65003900	-2.01929900	0.10798200
C	4.94362000	-1.88903500	-0.39089900
C	5.20981500	-0.90374200	-1.33467500
C	4.19294200	-0.06410100	-1.77860600
H	3.45057200	-2.80462500	0.83588200
H	5.73319700	-2.55933800	-0.04613300
H	4.41564100	0.69936700	-2.52363000
P	0.88562800	-1.32468900	0.34493400
O	1.87419600	0.57584600	-1.68673200
C	2.05380300	1.43997900	-2.77399500
H	2.78477300	2.23577800	-2.55578100
C	1.02641300	-1.83863800	2.17151700
C	0.16788700	-2.70671400	-0.73364100
C	1.05055400	-3.94652300	-0.84547300
H	2.04216100	-3.70846000	-1.25703900
H	1.18907500	-4.46431800	0.11223700
H	0.57473900	-4.66421100	-1.53501400
C	-1.21737100	-3.07387100	-0.20380500
H	-1.72088500	-3.73933700	-0.92430800
H	-1.17054500	-3.61244500	0.75405100
H	-1.85176400	-2.18560900	-0.07314200
C	0.01976400	-2.08279400	-2.12437000
H	0.99459100	-1.82318400	-2.56313100
H	-0.46656800	-2.80831900	-2.79755400
H	-0.59935400	-1.17491300	-2.09454700
C	-0.32548200	-1.49708500	2.81156400

H	-0.29501800	-1.75170100	3.88433200
H	-0.54591500	-0.42299900	2.71563800
H	-1.16174300	-2.04826700	2.36010200
C	2.08427300	-0.92790600	2.80219600
H	2.02109000	-1.00284000	3.90047900
H	3.10843700	-1.19149300	2.50652100
H	1.91851600	0.12628400	2.52719900
C	1.33616800	-3.30425000	2.47224300
H	0.53832100	-3.97471600	2.12369000
H	2.28498300	-3.65663900	2.04709600
H	1.41009100	-3.43532400	3.56494700
Pd	-0.27342900	0.68962000	0.25131500
C	-2.29000000	0.54124200	-0.00128000
C	-2.70619900	0.42392400	-1.34244600
C	-3.10756200	-0.02033100	0.99489100
C	-3.82842600	-0.31525000	-1.68362100
H	-2.13057300	0.91306300	-2.13200900
C	-4.24110700	-0.74866500	0.66403400
H	-2.84226900	0.10430900	2.04562200
C	-4.60572200	-0.92001900	-0.68151900
H	-4.11665500	-0.42703800	-2.73089700
H	-4.85244800	-1.19877200	1.44902700
C	-1.65689700	2.37299100	0.49142000
F	-2.20507100	2.46745100	1.72304300
F	-2.46911300	3.00347600	-0.38426200
H	2.36975500	0.88964600	-3.67751100
H	1.07850400	1.90558200	-2.96222900
C	-0.29690900	2.98268700	0.45791800
C	0.15788500	3.65984300	-0.69123800
C	0.57735400	2.83644400	1.55993000
C	1.44846200	4.16892400	-0.73507200
H	-0.52426000	3.79369600	-1.53221100
C	1.87934700	3.33549900	1.48635200
H	0.20821900	2.39126300	2.48573300
C	2.31937100	3.99812900	0.34473600
H	1.78175000	4.71265500	-1.62259900
H	2.54740600	3.21459700	2.34220600
H	3.33597000	4.39455500	0.29822400
H	6.21731400	-0.78461600	-1.74025800
C	-5.75891600	-1.68910600	-1.02624600
N	-6.69373500	-2.31699300	-1.30674100



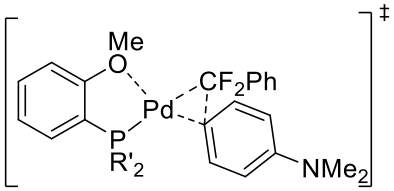
Pd-CF_2Ph-NMe_2-GS

76

Generated by Multiwfn

C	-3.52859600	-1.18699600	-0.22742900
C	-3.50778200	0.16379300	0.17780200
C	-4.72902200	0.75156000	0.53361400
C	-5.92433600	0.03811600	0.52053800
C	-5.91366500	-1.29953100	0.14206500
C	-4.72347300	-1.91258300	-0.23603000
H	-4.75105000	1.80023500	0.82293700
H	-6.85704100	0.52867700	0.80534300
H	-4.72938000	-2.96126400	-0.53091800
P	-1.89888800	1.06187900	0.17350300
O	-2.35672100	-1.75376400	-0.62456900
C	-2.40179800	-2.93495500	-1.41150400
H	-2.63468700	-3.81494800	-0.79356900
C	-1.72387600	1.77700300	1.91614000
C	-2.09356500	2.33705700	-1.20663600
C	-3.29023500	3.27473600	-1.08919100
H	-4.24867600	2.73788400	-1.11667800
H	-3.25501000	3.88977700	-0.17833900
H	-3.28644600	3.96999800	-1.94572600
C	-0.80326800	3.15304700	-1.31077800
H	-0.79053200	3.68090100	-2.27895900
H	-0.73096200	3.91698400	-0.52576400
H	0.09585600	2.52232800	-1.25884200
C	-2.24024200	1.47606800	-2.46666600
H	-3.15707300	0.86663400	-2.44551800
H	-2.29433100	2.12954000	-3.35305700
H	-1.38105300	0.79806800	-2.59301700
C	-0.48636000	2.67754800	1.93981600
H	-0.17370700	2.82894500	2.98643700
H	0.36537800	2.24279300	1.39820500
H	-0.69723200	3.67086000	1.51981300
C	-1.47517000	0.53856300	2.78531200
H	-1.32380800	0.84867800	3.83277100
H	-2.33056900	-0.15522900	2.76215200
H	-0.58382600	-0.01723700	2.45512800
C	-2.91097900	2.54759000	2.48922200
H	-3.22497400	3.38868000	1.85457600

H	-3.77874900	1.90195700	2.67879800
H	-2.61345200	2.97459400	3.46180100
Pd	-0.34631000	-0.68381000	-0.24294100
C	1.35143300	0.33103700	-0.22368100
C	1.90081000	0.78841800	-1.42690000
C	2.10590800	0.55253600	0.93358500
C	3.13170600	1.44258500	-1.47737800
H	1.37551000	0.61603900	-2.37103300
C	3.33460400	1.20550800	0.90232200
H	1.75569400	0.17812300	1.89909800
C	3.88125100	1.67639500	-0.30823000
H	3.50953700	1.76089500	-2.44935800
H	3.87957100	1.32544200	1.83848700
C	0.79418700	-2.38347000	-0.45400700
F	0.87697000	-2.72213000	-1.79458200
F	0.00565400	-3.38485600	0.10634500
H	-3.14780100	-2.82375000	-2.21386100
H	-1.40601700	-3.05883600	-1.84647900
C	2.15325700	-2.46506700	0.16158200
C	2.28239000	-2.74147200	1.52615300
C	3.29778300	-2.17853900	-0.58772900
C	3.53439800	-2.71634800	2.13429300
H	1.38771900	-2.96517400	2.11106500
C	4.54708700	-2.14753300	0.02415600
H	3.19808200	-1.95617200	-1.65054600
C	4.67140000	-2.41255600	1.38717000
H	3.62277600	-2.93248200	3.20224500
H	5.43241800	-1.90630700	-0.56957800
H	5.65294900	-2.38129700	1.86677300
H	-6.83937000	-1.87957300	0.13428900
N	5.10688900	2.32397800	-0.34551600
C	5.71530900	2.59472100	-1.61583400
H	6.65164000	3.14782000	-1.46281900
H	5.95278000	1.67880400	-2.19598300
H	5.06791100	3.22607800	-2.24743200
C	5.93941100	2.30717500	0.82357300
H	5.44356900	2.79069100	1.68225500
H	6.22878400	1.28422600	1.14042200
H	6.85967900	2.87240800	0.62481200



R' = tBu

Pd-CF_2Ph-NMe_2-TS

76

Generated by Multiwfn

C	3.02901400	-0.57270600	-1.36888400
C	2.65330200	-1.48309600	-0.35280600
C	3.59580600	-2.43949200	0.03830700
C	4.87213700	-2.49815300	-0.51689700
C	5.22523400	-1.58320400	-1.50191900
C	4.30981400	-0.62711300	-1.93149400
H	3.32645900	-3.17066600	0.79941500
H	5.57991600	-3.25924700	-0.18269600
H	4.59782900	0.07940100	-2.70967000
P	0.96412000	-1.35408800	0.37483600
O	2.10122300	0.31532200	-1.76802800
C	2.35497600	1.14593800	-2.86465600
H	3.19651100	1.83355600	-2.67886700
C	1.12178200	-1.86073500	2.20387800
C	0.00705400	-2.64505100	-0.63222600
C	0.70251800	-3.99727300	-0.75861400
H	1.69594800	-3.90586000	-1.22169600
H	0.81712400	-4.51356400	0.20328300
H	0.09820300	-4.65362300	-1.40796000
C	-1.38651000	-2.80466100	-0.02642000
H	-2.01407100	-3.40374600	-0.70726300
H	-1.36556300	-3.33093200	0.93935100
H	-1.88277700	-1.83360000	0.11501400
C	-0.13035000	-2.02924300	-2.02753600
H	0.84483400	-1.91408700	-2.52345100
H	-0.74984700	-2.69063200	-2.65645700
H	-0.61660300	-1.04427600	-1.98296100
C	-0.13750300	-1.32179900	2.89574300
H	-0.08895900	-1.55385300	3.97332800
H	-0.21554100	-0.23028900	2.77601400
H	-1.06246000	-1.76119600	2.49821200
C	2.32408400	-1.09708400	2.76747900
H	2.30165900	-1.14307800	3.86918500
H	3.28711000	-1.50649100	2.43428200
H	2.29316500	-0.03560600	2.47356400
C	1.23798200	-3.34979800	2.52567100

```
H       0.33864400     -3.90685600      2.22816000
H       2.10666300     -3.84006500      2.06664000
H       1.34420000     -3.47201600      3.61704600
Pd      0.06594400      0.79360600      0.29481600
C      -1.98593400      0.89673500      0.10672600
C      -2.47581200      0.81481400     -1.20411700
C      -2.82528600      0.44563600      1.13063400
C      -3.69869700      0.22054100     -1.49274400
H      -1.88174500      1.21404000     -2.03102200
C      -4.05823300     -0.13910800      0.86026100
H      -2.50723900      0.53626500      2.17123000
C      -4.52570700     -0.28039000     -0.46396500
H      -4.01310300      0.15659200     -2.53447800
H      -4.66042000     -0.49057500      1.69818300
C      -1.04255400      2.63217900      0.55691600
F      -1.51194500      2.80998200      1.81473200
F      -1.80104700      3.37015800     -0.28568000
H       2.55663300      0.55840600     -3.77796300
H       1.44620800      1.74172000     -3.01531100
C       0.38334100      3.04700400      0.44743700
C       0.87197600      3.64642100     -0.73302700
C       1.29309600      2.76205500      1.49456100
C       2.21945600      3.95166300     -0.85664500
H       0.16963400      3.88109100     -1.53438500
C       2.65068200      3.05626500      1.33952500
H       0.91554000      2.38510300      2.44698500
C       3.11869100      3.64702900      0.17090200
H       2.57857700      4.43912600     -1.76682800
H       3.34244800      2.82940400      2.15430900
H       4.17968000      3.88194400      0.06071000
H       6.22078300     -1.61122600     -1.95147000
N      -5.74100300     -0.87201100     -0.74070400
C      -6.50253300     -1.46231800      0.32251100
H      -5.96680700     -2.28956800      0.82878000
H      -6.77396500     -0.72224100      1.09617200
H      -7.43923100     -1.86884400     -0.07985200
C      -6.12783700     -1.09754900     -2.10393300
H      -7.11999000     -1.56603000     -2.13034300
H      -6.19710400     -0.15483600     -2.67539400
H      -5.42734300     -1.76301200     -2.64620500
```

5.7 References

(1) Jeschke, P. The Unique Role of Fluorine in the Design of Active Ingredients for Modern Crop Protection. *ChemBioChem* **2004**, *5*, 570–589.

(2) Böhm, H.-J.; Banner, D.; Bendels, S.; Kansy, M.; Kuhn, B.; Müller, K.; Obst-Sander, U.; Stahl, M. Fluorine in Medicinal Chemistry. *ChemBioChem* **2004**, *5*, 637–643.
(3) Purser, S.; Moore, P. R.; Swallow, S.; Gouverneur, V. Fluorine in Medicinal Chemistry. *Chem. Soc. Rev.* **2008**, *37*, 320–330.
(4) Kirk, K. L. Fluorination in Medicinal Chemistry: Methods, Strategies, and Recent Developments. *Org. Process Res. Dev.* **2008**, *12*, 305–321.
(5) Gillis, E. P.; Eastman, K. J.; Hill, M. D.; Donnelly, D. J.; Meanwell, N. A. Applications of Fluorine in Medicinal Chemistry. *J. Med. Chem.* **2015**, *58*, 8315–8359.
(6) Dolbier, W. R. Fluorine Chemistry at the Millennium. *J. Fluor. Chem.* **2005**, *126*, 157–163.
(7) Yamazaki, T.; Taguchi, T.; Ojima, I. Unique Properties of Fluorine and Their Relevance to Medicinal Chemistry and Chemical Biology. In *Fluorine in Medicinal Chemistry and Chemical Biology*; John Wiley & Sons, Ltd, 2009; pp 1–49.
(8) Wang, J.; Sanchez-Rosello, M.; Acena, J. L.; del Pozo, C.; Sorochinsky, A. E.; Fustero, S.; Soloshonok, V. A.; Liu, H. Fluorine in Pharmaceutical Industry: Fluorine-Containing Drugs Introduced to the Market in the Last Decade (2001-2011). *Chem. Rev.* **2014**, *114*, 2432–2506.
(9) Inoue, M.; Sumii, Y.; Shibata, N. Contribution of Organofluorine Compounds to Pharmaceuticals. *ACS Omega* **2020**, *5*, 10633–10640.
(10) Meanwell, N. A. Synopsis of Some Recent Tactical Application of Bioisosteres in Drug Design. *J. Med. Chem.* **2011**, *54*, 2529–2591.
(11) Albéniz, A. C.; Casares, J. A. Chapter One - Palladium-Mediated Organofluorine Chemistry. In *Advances in Organometallic Chemistry*; Pérez, P. J., Ed.; Academic Press, 2014; Vol. 62, pp 1–110.
(12) Culkin, D. A.; Hartwig, J. F. Carbon−Carbon Bond-Forming Reductive Elimination from Arylpalladium Complexes Containing Functionalized Alkyl Groups. Influence of Ligand Steric and Electronic Properties on Structure, Stability, and Reactivity. *Organometallics* **2004**, *23*, 3398–3416.
(13) Grushin, V. V.; Marshall, W. J. Facile Ar-CF3 Bond Formation at Pd. Strikingly Different Outcomes of Reductive Elimination from [(Ph3P)2Pd(CF3)Ph] and [(Xantphos)Pd(CF3)Ph]. *J. Am. Chem. Soc.* **2006**, *128*, 12644–12645.
(14) Grushin, V. V.; Marshall, W. J. Unexpected H2O-Induced Ar−X Activation with Trifluoromethylpalladium(II) Aryls. *J. Am. Chem. Soc.* **2006**, *128*, 4632–4641.
(15) Cho, E. J.; Senecal, T. D.; Kinzel, T.; Zhang, Y.; Watson, D. A.; Buchwald, S. L. The Palladium-Catalyzed Trifluoromethylation of Aryl Chlorides. *Science* **2010**, *328*, 1679–1681.
(16) Bakhmutov, V. I.; Bozoglian, F.; Gómez, K.; González, G.; Grushin, V. V.; Macgregor, S. A.; Martin, E.; Miloserdov, F. M.; Novikov, M. A.; Panetier, J. A.; Romashov, L. V. CF3–Ph Reductive Elimination from [(Xantphos)Pd(CF3)(Ph)]. *Organometallics* **2012**, *31*, 1315–1328.
(17) Nielsen, M. C.; Bonney, Karl. J.; Schoenebeck, F. Computational Ligand Design for the Reductive Elimination of ArCF3 from a Small Bite Angle PdII Complex: Remarkable Effect of a Perfluoroalkyl Phosphine. *Angew. Chem. Int. Ed.* **2014**, *53*, 5903–5906.
(18) Maleckis, A.; Sanford, M. S. Synthesis of Fluoroalkyl Palladium and Nickel Complexes via Decarbonylation of Acylmetal Species. *Organometallics* **2014**, *33*, 3831–3839.

(19) Maleckis, A.; Sanford, M. S. Catalytic Cycle for Palladium-Catalyzed Decarbonylative Trifluoromethylation Using Trifluoroacetic Esters as the CF3 Source. *Organometallics* **2014**, *33*, 2653–2660.
(20) Zhang, S.-L.; Deng, Z.-Q. Synthesis and Reductive Elimination of ArylPd(II) Trifluoromethyl Complexes: A Remarkable Concentration Effect on Chemoselectivity. *Phys. Chem. Chem. Phys.* **2016**, *18*, 32664–32667.
(21) Ferguson, D. M.; Bour, J. R.; Canty, A. J.; Kampf, J. W.; Sanford, M. S. Stoichiometric and Catalytic Aryl-Perfluoroalkyl Coupling at Tri-Tert-Butylphosphine Palladium(II) Complexes. *J. Am. Chem. Soc.* **2017**, *139*, 11662–11665.
(22) Ferguson, D. M.; Bour, J. R.; Canty, A. J.; Kampf, J. W.; Sanford, M. S. Aryl–CF3 Coupling from Phosphinoferrocene-Ligated Palladium(II) Complexes. *Organometallics* **2019**, *38*, 519–526.
(23) Gu, Y.; Leng, X.; Shen, Q. Cooperative Dual Palladium/Silver Catalyst for Direct Difluoromethylation of Aryl Bromides and Iodides. *Nat. Commun.* **2014**, *5*, 5405.
(24) Lu, C.; Gu, Y.; Wu, J.; Gu, Y.; Shen, Q. Palladium-Catalyzed Difluoromethylation of Heteroaryl Chlorides, Bromides and Iodides. *Chem. Sci.* **2017**, *8*, 4848–4852.
(25) Arlow, S. I.; Hartwig, J. F. Synthesis, Characterization, and Reactivity of Palladium Fluoroenolate Complexes. *J. Am. Chem. Soc.* **2017**, *139*, 16088–16091.
(26) Arlow, S. I. The Development of Transition Metal-Catalyzed Fluoroalkylation and Fluoroenolate Arylation Reactions. Ph.D. Thesis, University of California, Berkeley, 2018.
(27) Mormino, M. The Development of Transition Metal-Catalyzed Fluoroalkylation Reactions of Aryl Electrophiles. Ph.D. Thesis, University of California, Berkeley, 2017.
(28) Wade Wolfe, M. M.; Shanahan, J. P.; Kampf, J. W.; Szymczak, N. K. Defluorinative Functionalization of Pd(II) Fluoroalkyl Complexes. *J. Am. Chem. Soc.* **2020**, *142*, 18698–18705.
(29) Anstaett, P.; Schoenebeck, F. Reductive Elimination of ArCF3 from Bidentate PdII Complexes: A Computational Study. *Chem. – Eur. J.* **2011**, *17*, 12340–12346.
(30) Feng, Z.; Min, Q.-Q.; Zhang, X. Access to Difluoromethylated Arenes by Pd-Catalyzed Reaction of Arylboronic Acids with Bromodifluoroacetate. *Org. Lett.* **2016**, *18*, 44–47.
(31) Peacock, D. M.; Jiang, Q.; Hanley, P. S.; Cundari, T. R.; Hartwig, J. F. Reductive Elimination from Phosphine-Ligated Alkylpalladium(II) Amido Complexes To Form Sp ^{3} Carbon–Nitrogen Bonds. *J. Am. Chem. Soc.* **2018**, *140*, 4893–4904.
(32) Bondi, A. Van Der Waals Volumes and Radii. *J. Phys. Chem.* **1964**, *68*, 441–451.
(33) Culkin, D. A.; Hartwig, J. F. C−C Bond-Forming Reductive Elimination of Ketones, Esters, and Amides from Isolated Arylpalladium(II) Enolates. *J. Am. Chem. Soc.* **2001**, *123*, 5816–5817.
(34) Culkin, D. A.; Hartwig, J. F. Palladium-Catalyzed α-Arylation of Carbonyl Compounds and Nitriles. *Acc. Chem. Res.* **2003**, *36*, 234–245.
(35) Hartwig, J. F. Electronic Effects on Reductive Elimination to Form Carbon-Carbon and Carbon-Heteroatom Bonds from Palladium(II) Complexes. *Inorg. Chem.* **2007**, *46*, 1936–1947.
(36) Bader, R. F. W. Atoms in Molecules. *Acc. Chem. Res.* **1985**, *18*, 9–15.
(37) Lefebvre, C.; Rubez, G.; Khartabil, H.; Boisson, J.-C.; Contreras-García, J.; Hénon, E. Accurately Extracting the Signature of Intermolecular Interactions Present in the NCI Plot of the Reduced Density Gradient versus Electron Density. *Phys. Chem. Chem. Phys.* **2017**, *19*, 17928–17936.

(38) Lu, T.; Chen, Q. *Independent Gradient Model Based on Hirshfeld Partition (IGMH): A New Method for Visual Study of Interactions in Chemical Systems*; preprint; Chemistry, 2021.
(39) Johnson, E. R.; Keinan, S.; Mori-Sanchez, P.; Contreras-Garcia, J.; Cohen, A. J.; Yang, W. Revealing Noncovalent Interactions. *J. Am. Chem. Soc.* **2010**, *132*, 6498–6506.
(40) Kalkman, E. D.; Hartwig, J. F. Direct Observation of Diastereomeric α-C-Bound Enolates during Enantioselective α-Arylations: Synthesis, Characterization, and Reactivity of Arylpalladium Fluorooxindole Complexes. *J. Am. Chem. Soc.* **2021**, *143*, 11741–11750.
(41) Weinhold, F.; Landis, C. R.; Glendening, E. D. What Is NBO Analysis and How Is It Useful?, 2016.
(42) Zhang, S.-L.; Huang, L.; Sun, L.-J. The Mechanism, Electronic and Ligand Effects for Reductive Elimination from ArylPd(II) Trifluoromethyl Complexes: A Systematic DFT Study. *Dalton Trans.* **2015**, *44*, 4613–4622.
(43) Frisch, M. J.; Trucks, G. W.; Schlegel, H. B.; Scuseria, G. E.; Robb, M. A.; Cheeseman, J. R.; Scalmani, G.; Barone, V.; Petersson, G. A.; Nakatsuji, H.; Li, X.; Caricato, M.; Marenich, A. V.; Bloino, J.; Janesko, B. G.; Gomperts, R.; Mennucci, B.; Hratchian, H. P.; Ortiz, J. V.; Izmaylov, A. F.; Sonnenberg, J. L.; Williams-Young, D.; Ding, F.; Lipparini, F.; Egidi, F.; Goings, J.; Peng, B.; Petrone, A.; Henderson, T.; Ranasinghe, D.; Zakrzewski, V. G.; Gao, J.; Rega, N.; Zheng, G.; Liang, W.; Hada, M.; Ehara, M.; Toyota, K.; Fukuda, R.; Hasegawa, J.; Ishida, M.; Nakajima, T.; Honda, Y.; Kitao, O.; Nakai, H.; Vreven, T.; Throssell, K.; Montgomery, J. A.; Peralta, J. E.; Ogliaro, F.; Bearpark, M. J.; Heyd, J. J.; Brothers, E. N.; Kudin, K. N.; Staroverov, V. N.; Keith, T. A.; Kobayashi, R.; Normand, J.; Raghavachari, K.; Rendell, A. P.; Burant, J. C.; Iyengar, S. S.; Tomasi, J.; Cossi, M.; Millam, J. M.; Klene, M.; Adamo, C.; Cammi, R.; Ochterski, J. W.; Martin, R. L.; Morokuma, K.; Farkas, O.; Foresman, J. B.; Fox, D. J. *Gaussian 16, Revision A.03*; Gaussian, Inc.: Wallingford CT, 2016.
(44) Marenich, A. V.; Cramer, C. J.; Truhlar, D. G. Universal Solvation Model Based on Solute Electron Density and on a Continuum Model of the Solvent Defined by the Bulk Dielectric Constant and Atomic Surface Tensions. *J. Phys. Chem. B* **2009**, *113*, 6378–6396.
(45) Dennington, R.; Keith, T. A.; Millam, J. M. *GaussView, Version 6.1*; Semichem Inc.: Shawnee Mission, KS, 2016.
(46) Perdew, J. P.; Burke, K.; Ernzerhof, M. Generalized Gradient Approximation Made Simple. *Phys. Rev. Lett.* **1996**, *77*, 3865–3868.
(47) Perdew, J. P.; Burke, K.; Ernzerhof, M. Generalized Gradient Approximation Made Simple. *Phys. Rev. Lett.* **1997**, *78*, 1396–1396.
(48) Adamo, C.; Barone, V. Toward Reliable Density Functional Methods without Adjustable Parameters: The PBE0 Model. *J. Chem. Phys.* **1999**, *110*, 6158–6170.
(49) Grimme, S.; Ehrlich, S.; Goerigk, L. Effect of the Damping Function in Dispersion Corrected Density Functional Theory. *J. Comput. Chem.* **2011**, *32*, 1456–1465.
(50) Pritchard, B. P.; Altarawy, D.; Didier, B.; Gibson, T. D.; Windus, T. L. New Basis Set Exchange: An Open, Up-to-Date Resource for the Molecular Sciences Community. *J. Chem. Inf. Model.* **2019**, No. Manuscript in preparation.
(51) Zheng, J.; Xu, X.; Truhlar, D. G. Minimally Augmented Karlsruhe Basis Sets. *Theor. Chem. Acc.* **2011**, *128*, 295–305.
(52) Glendening, E. D.; Landis, C. R.; Weinhold, F. NBO 6.0: Natural Bond Orbital Analysis Program. *J. Comput. Chem.* **2013**, *34*, 1429–1437.

(53) Lu, T.; Chen, F. Multiwfn: A Multifunctional Wavefunction Analyzer. *J. Comput. Chem.* **2012**, *33*, 580–592.
(54) Humphrey, W.; Dalke, A.; Schulten, K. VMD: Visual Molecular Dynamics. *J. Mol. Graph.* **1996**, *14*, 33–38.
(55) Keith, T. A. *AIMALL*; TK Gristmill Software: Overland Park KS, USA, 2019.